**THÈSE DE DOCTORAT DE**

**L'UNIVERSITÉ PIERRE ET MARIE CURIE**

Spécialité

**Océanographie Biologique**

Présentée par

**Sakina-Dorothée Ayata**

Pour obtenir le grade de

**DOCTEUR DE L'UNIVERSITÉ PIERRE ET MARIE CURIE**

# Importance relative des facteurs hydroclimatiques et des traits d'histoire de vie sur la dispersion larvaire et la connectivité à différentes échelles spatiales (Manche, Golfe de Gascogne)

Soutenue le 8 janvier 2010, à la Station Biologique de Roscoff,

Devant le jury composé de :

| | |
|---|---|
| Pr Jean-Marc Guarini, Université Pierre et Marie Curie, Banyuls | Président |
| Pr Claire Paris, Université de Miami, USA | Rapporteur |
| Dr François Carlotti, CNRS, Marseille | Rapporteur |
| Dr Xabier Irigoien, AZTI, Espagne | Examinateur |
| Dr Pierre Petitgas, IFREMER, Nantes | Examinateur |
| Pr Dominique Davoult, Université Pierre et Marie Curie, Roscoff | Directeur |
| Dr Éric Thiébaut, Université Pierre et Marie Curie, Roscoff | Co-directeur |

# Résumé

En assurant la **dispersion**, la **phase larvaire** joue un rôle fondamental dans la dynamique des populations d'invertébrés marins à cycle de vie bentho-pélagique et détermine la **connectivité** au sein des **métapopulations marines**. La connectivité en milieu marin influence ainsi directement la dynamique des métapopulations et la persistance des populations locales, les potentialités d'expansion des espèces en réponse à des changements des conditions environnementales ou les limites biogéographiques d'aire de distribution des espèces. Dans ce contexte, le but du présent travail a été de mieux comprendre les rôles relatifs joués par les **processus hydrodynamiques et hydroclimatiques**, et les **traits d'histoire de vie** des invertébrés sur la dispersion larvaire et la connectivité en milieu côtier dans le Golfe de Gascogne et la Manche occidentale. Pour répondre à cette question, une **approche couplée** a été mise en œuvre, alliant l'**observation *in situ*** et la **modélisation biologie-physique** à deux échelles spatiales : régionale et locale.

Dans le Nord du Golfe de Gascogne, la description de la distribution larvaire de trois espèces côtières de polychètes (*Pectinaria koreni*, *Owenia fusiformis*, et *Sabellaria alveolata*) a mis en évidence le rôle prépondérant de l'organisation spatiale des **structures hydrologiques à méso-échelle** (*i.e.* plumes estuariennes) dans la variabilité de la distribution des abondances larvaires. À l'échelle régionale du Golfe de Gascogne et de la Manche occidentale, la simulation lagrangienne de la dispersion larvaire en conditions hydroclimatiques réalistes a souligné l'importance de la variabilité saisonnière des conditions hydroclimatiques et des traits d'histoire de vie (mois de ponte, durée de vie larvaire, comportement natatoire) dans le transport larvaire et la connectivité entre populations. Ces résultats ont suggéré de possibles échanges larvaires depuis les populations côtières du Golfe de Gascogne vers celles de la Manche occidentale, *i.e.* à travers une **zone de transition biogéographique**. Ils ont aussi permis de tester plusieurs hypothèses sur les conséquences possibles du **changement climatique** sur la dispersion et la connectivité entre populations marines, *i.e. via* une période de ponte précoce et une durée de vie larvaire raccourcie. À l'échelle locale du Golfe Normand-Breton, un modèle eulérien de dispersion a permis d'estimer la connectivité entre les récifs biogéniques construits par une espèce à forte valeur patrimoniale, *Sabellaria alveolata*. Ce modèle a permis de déterminer les influences relatives de la variabilité intra- et inter-annuelle des conditions hydroclimatiques sur la connectivité, dans un contexte de gestion et de **conservation d'un patrimoine naturel**.



*Mot-clés :* Océanographie biologique, écologie, dynamique des populations, métapopulation, connectivité, dispersion larvaire, modélisation couplée biologie-physique.

# Abstract

By ensuring the **dispersal**, the **larval phase** plays a fundamental role in the population dynamics of benthic invertebrates with a complex life cycle and determines the **connectivity** within **marine metapopulations**. Hence, the connectivity influences directly the dynamics of metapopulations and the persistence of local populations, the expansion abilities of species in response to changes in environmental conditions or biogeographic range limits. In this context, the aim of the present work was to better understand the relative roles played by **hydrodynamics and hydroclimatic processes** and **life history traits** of coastal invertebrates on the larval dispersal and the connectivity in the Bay of Biscay and in the western English Channel. To answer this question, a **coupled approach** was used, joining ***in situ* observation** and **bio-physical modelling** at two spatial scales, a regional one and a local one.

In the northern Bay of Biscay, the description of larval distribution of three coastal species of polychaetes (*Pectinaria koreni*, *Owenia fusiformis*, and *Sabellaria alveolata*) highlighted the major role of the spatial organization of the **mesoscale hydrological structures** (*i.e.*, river plumes) in the variability of larval abundance distributions. At the regional scale of the Bay of Biscay and the western English Channel, the Lagrangian simulation of the larval dispersal under realistic hydroclimatic forcing underlined the importance of the seasonal variability of the hydroclimatic conditions and the life history traits (spawning month, planktonic larval duration, larval swimming behaviour) in the larval transport and connectivity between populations. These results suggested possible larval exchanges from the Bay of Biscay to the western English Channel, *i.e.* through a **biogeographic transition zone**. They allowed to test several hypotheses about the potential consequences of **climate change** on the dispersal and connectivity of marine populations, *i.e.* through an earlier spawning period and a shortened planktonic larval duration. At the local scale of the Gulf of Saint-Malo, western English Channel, an Eulerian dispersal model permitted to estimate the connectivity between the biogenic reefs built by *Sabellaria alveolata*, a species with a high patrimonial value. This model allowed to determine the relative influences of the intra- and inter-annual variability of the hydroclimatic conditions on connectivity, in a context of management and **conservation of natural heritage**.



*Key-words:* Biologic oceanography, ecology, population dynamics, metapopulation, connectivity, larval dispersal, bio-physical modelling.

# Table des matières

# Table des figures

# Liste des tableaux

# Chapitre I

# Introduction générale

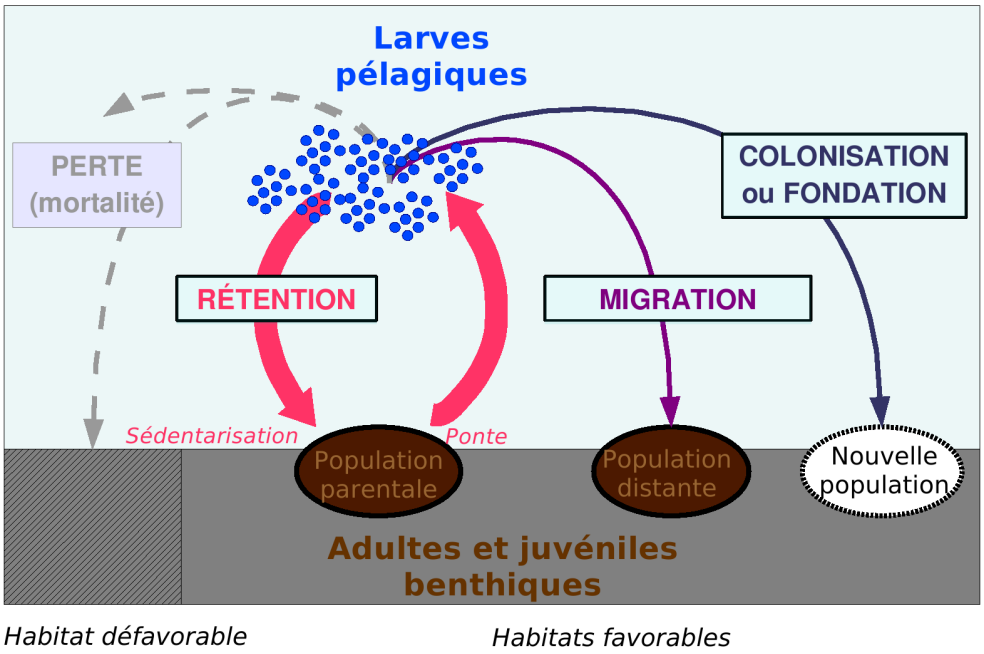


Figure I.1 – Cycle de vie bentho-pélagique des invertébrés marins. Les phases benthiques adulte et juvénile sont représentées en marron, la phase larvaire pélagique en bleu. Le cycle de vie représenté en rose inclut les évènements de ponte et de sédentarisation (retour à la vie benthique). Les devenirs possibles des larves sont indiqués dans des rectangles : perte par mortalité (en gris), rétention au sein de la population parentale, *i.e.* autorecrutement (en rose), migration vers une population distante, *i.e.* allorecrutement (en violet), et fondation d'une nouvelle population, *i.e.* colonisation (en bleu foncé).

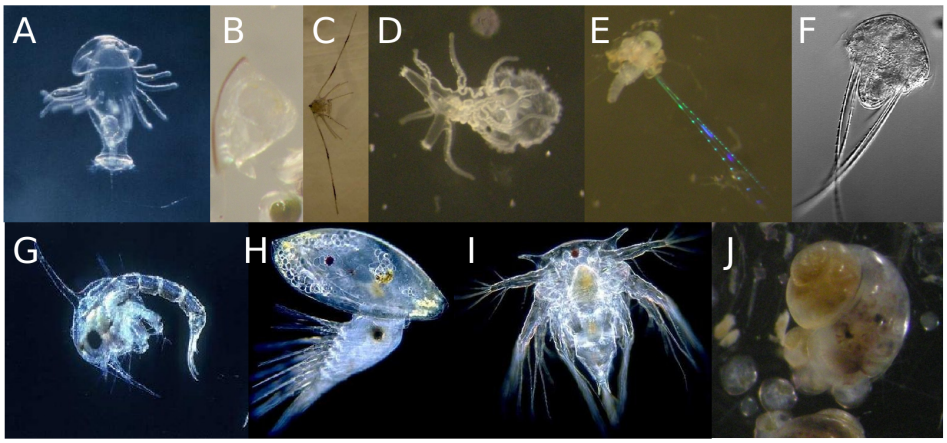


Figure I.2 – Diversité des formes de vie larvaires des invertébrés à cycle de vie bentho-pélagique. A) larve actinotroche de phoronidien, B) larve cyphonaute de bryozoaire, C) larve ophiopluteus d'ophiure, D) larve brachioloria d'étoile de mer, E) larve mitraria de polychète owenidé, F) larve métatrochophore de polychète sabellaridé, G) larve zoé de crustacé décapode, H) larve cypris de crustacé cirripède, I) larve nauplius de crustacé cirripède, J) larves véligères de gastéropode et bivalves.

# I.1 La dispersion en milieu marin

## I.1.1 Les invertébrés à cycle de vie bentho-pélagique

La plupart des invertébrés marins possèdent une **phase larvaire planctonique** (Eckman, 1996; Thorson, 1950), tandis que les phases juvéniles et les adultes sont benthiques et plus ou moins sédentaires, inféodées au substrat. Le cycle de vie de ces organismes est alors qualifié de **cycle de vie bentho-pélagique** (Figure I.1). La phase juvénile, qui assure tout ou partie de la croissance de l'organisme, est sexuellement immature, mais possède les mêmes comportements et les mêmes organes que la phase adulte. La phase adulte caractérise les individus ayant acquis la maturité sexuelle. Ceux-ci peuvent produire des gamètes et assurer la reproduction. La phase larvaire pélagique, qui résulte de la fécondation d'un gamète mâle et d'un gamète femelle puis du développement du zygote, est une phase de transition critique. Elle correspond à un stade immature, libre, morphologiquement et physiologiquement distinct du juvénile et de l'adulte, et dont l'écologie est radicalement différente (différence d'habitat, de nourriture) (Bachelet, 1990). A l'issue de la phase larvaire, la larve devient compétente (*i.e.* acquisition irréversible de la capacité à se métamorphoser), se sédentarise (*i.e.* fin de la vie planctonique et début de la vie benthique sous contrôle nerveux) et se métamorphose en juvénile (changement irréversible de morphologie et de physiologie sous contrôle endocrinien).

Chez ces organismes, la **dispersion**, qui correspond à la dissémination d'individus à partir d'un point d'émission, est principalement assurée par la phase larvaire planctonique (Thorson, 1950), bien que, dans une moindre mesure, la dispersion des gamètes mâles, la dispersion post-larvaire et les migrations des adultes peuvent aussi y contribuer.

Une très grande diversité existe parmi les larves d'invertébrés marins (Figure I.2), celles-ci se distinguant par leur morphologie, leur durée de vie larvaire, leur comportement natatoire, et leur mode de nutrition. Deux types de larves sont couramment définis selon ce dernier critère : les larves lécitotrophes, dont la croissance dépend des réserves maternelles contenues dans l'oeuf, et les larves planctotrophes, qui se nourrissent d'organismes planctoniques. Au regard de leur durée de vie, Levin et Bridges (1995) ont proposé de distinguer trois catégories de larves : (i) les larves anchiplaniques dont la durée de vie

varie entre quelques heures et quelques jours, (ii) les larves actaeplaniques d'une durée de vie comprise entre une semaine et deux mois, (iii) les larves téléplaniques dont la durée de vie excède deux mois. Les larves planctoniques d'organismes à cycle bentho-pélagique constituent le méroplancton.

### I.1.2 Pourquoi la phase larvaire est-elle importante dans la dynamique des populations marines ?

Plusieurs scénarios sont possibles concernant le devenir d'une larve pélagique (Figure I.1) : (i) celle-ci peut mourir au cours de sa vie larvaire –par exemple par prédation– ou à l'issue de son développement si elle n'a pas rencontré d'habitat favorable pour sa sédentarisation, (ii) à l'issue de son développement, la larve peut se sédentariser au niveau de la population parentale –on parle alors de rétention ou d'autorecrutement– ou (iii) au sein d'une population distante –on parle alors de migration et d'échanges larvaires entre populations–, ou encore (iv) dans un nouvel habitat favorable à son installation –on parle alors de colonisation. Pour de telles espèces, le recrutement, c'est-à-dire l'apport de nouveaux individus au sein des populations adultes, et le maintien de ces dernières dépendent donc en partie des apports larvaires et de la survie ultérieure des premiers stades de développement benthiques.

Dès 1946, Thorson a souligné l'importance du transport et de la survie larvaire dans la dynamique des populations d'invertébrés marins et leur variabilité spatio-temporelle. Cette idée fût reprise et formalisée plus tard dans la **théorie du 'supply-side ecology'**, qui met en exergue le rôle majeur des apports larvaires et de la dispersion dans la dynamique des populations marines (Gaines et Roughgarden, 1985; Lewin, 1986). Selon cette théorie, ce sont les processus affectant la phase larvaire qui sont responsables de la variabilité spatio-temporelle du nombre d'individus dans une population en déterminant les conditions initiales du recrutement (Caley *et al.*, 1996). Ainsi, Gaines et Bertness (1992) ont démontré que le taux de sédentarisation de la balane *Semibalanus balanoides* était corrélé positivement et significativement aux flux larvaires et au temps de résidence des masses d'eau dans la baie de Narragansett. D'autre part, Carroll (1996) a démontré que les

densités adultes des balanes *Semibalanus spp.* et *Balanus glandula* dans une baie d'Alaska étaient significativement corrélées à la densité initiale de jeunes recrues. Dans ce contexte, l'étude de la phase larvaire des organismes à cycle bentho-pélagique est devenu un point central de l'étude de la dynamique des populations marines. Il convient cependant de souligner que certains auteurs ont remis en cause ce rôle clef des apports larvaires dans la dynamique des populations benthiques, mettant l'accent sur les processus impliqués dans la régulation des effectifs des individus benthiques (*e.g.* Eckman, 1996; Hughes *et al.*, 2000; Ólafsson *et al.*, 1994).

### I.1.3 Quels sont les avantages et les désavantages de la phase larvaire ?

Les organismes à cycle de vie bentho-pélagique ont généralement une fécondité élevée, mais les oeufs produits en très grand nombre sont le plus souvent de petite taille, fait interprété comme un compromis lié au coût d'une fécondité élevée. Cette fécondité élevée contrebalancerait les fortes pertes démographiques au cours de la phase larvaire. Si d'un point de vue écologique et évolutif, de telles pertes sont potentiellement désavantageuses de part le gaspillage qu'elles entraînent, le cycle de vie bentho-pélagique demeure prépondérant chez les organismes marins (Eckman, 1996; Thorson, 1950)(*cf.* Figure I.2). L'avantage évolutif de l'existence d'une phase larvaire planctonique a donc été discuté, en particulier par Pechenik (1999) et Bonhomme et Planes (2000), respectivement chez les invertébrés marins et les poissons récifaux. Ces travaux ont souligné l'importance relative des forces sélectives agissant à court et à long terme pour expliquer le maintien d'une phase larvaire planctonique.

Ainsi, il existe de nombreux désavantages au maintien de la phase larvaire pélagique chez les invertébrés marins (Pechenik, 1999) :

- la dispersion peut entraîner la larve loin de l'habitat favorable de la population parentale,

- la dispersion augmente la vulnérabilité face aux prédateurs planctoniques,

- la dispersion pourrait entraîner d'importants flux géniques sur de grandes distances, ce qui réduit les possibilités d'adaptation locale et augmente la probabilité de perte de valeur sélective du fait de croisements entre individus issus de populations très éloignées ('outbreeding depression'),
- étant donné la spécificité du substrat pour la sédentarisation et la métamorphose, la dispersion peut conduire la larve à se métamorphoser sur un substrat non-optimal ou dans des conditions désavantageuses, ce qui limiterait la capacité des adultes à se développer et à se reproduire dans des conditions optimales,
- le délai à la métamorphose observé chez certaines espèces en l'absence de substrat favorable peut réduire par la suite la survie des juvéniles et leur succès reproducteur,
- les stress subis par la larve au cours de sa vie planctonique peuvent réduire son succès post-métamorphose.

En revanche, les principaux avantages que confèrent l'existence d'une phase larvaire planctonique sont liés à son potentiel de dispersion loin des populations parentales (Eckert, 2003; Pechenik, 1999; Ronce, 2007), permettant ainsi :

- une réduction de la compétition pour la nourriture entre larves apparentées dans le cas des larves planctotrophes,
- une réduction indirecte de la compétition entre les parents benthiques et leur progéniture planctonique,
- une augmentation de la probabilité que le juvénile occupe un habitat favorable dans le cas où la métamorphose est déclenchée par des molécules produites par des adultes conspécifiques,
- une réduction des risques liés à la dépression de consanguinité (croisements entre individus apparentés),
- le maintien d'une aire de répartition géographique étendue,

- une augmentation des probabilités de recolonisation après une extinction locale, et donc un avantage évolutif dans le cas où l'habitat est instable ou éphémère,
- une réduction du risque d'extinction et une augmentation de la persistence des espèces à l'échelle des temps géologiques.

## I.2 Définition et description de la dispersion larvaire

### I.2.1 Du transport larvaire à la dispersion

Selon les définitions proposées par Cowen *et al.* (2007) et Pineda *et al.* (2007), le **transport larvaire** est la résultante de deux phénomènes (Figure I.3A) : (i) le transport physique des larves par advection et diffusion turbulente, et (ii) le comportement natatoire des larves (ces deux phénomènes seront présentés en détail aux Sections I.3.1 et I.3.2). Le transport larvaire correspond donc au déplacement des larves dans la masse d'eau.

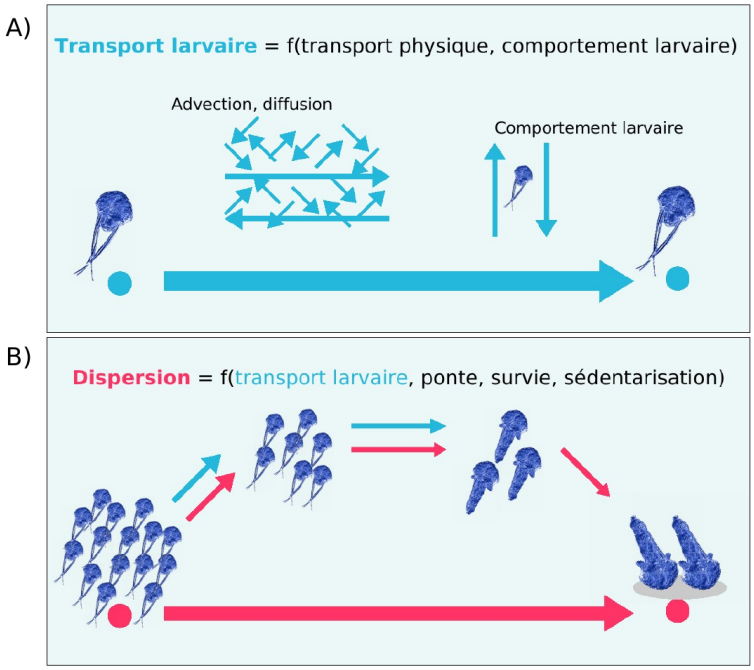


Figure I.3 – Définitions du transport (A) et de la dispersion larvaire (B) d'après Pineda *et al.* (2007). Les processus impliqués dans le transport larvaire sont indiqués par des flèches bleues, les processus impliqués dans la dispersion larvaire sont indiqués par des flèches roses.

Le terme de **dispersion larvaire** désigne quant à lui l'ensemble des processus régulant la dissémination des larves, depuis la ponte au sein de la population parentale jusqu'à la sédentarisation au sein d'un habitat benthique (Figure I.3B). La dispersion est donc la résultante des caractéristiques de la reproduction (*e.g.* lieu et période de ponte), de la survie larvaire, du transport larvaire, et de la sédentarisation (*e.g.* choix de l'habitat)[a]. Les larves ainsi dispersées pourront jouer un rôle dans la dynamique à court terme des

[a]Lorsque la phase de sédentarisation n'est pas inclue, on utilise parfois le terme de dispersion potentielle.

populations et des communautés. Néanmoins, elles ne contribueront sur le long terme à la pérennité d'une population que si elles survivent jusqu'au stade adulte et participent à la reproduction de la génération suivante. Dans ce cas, nous parlerons de **dispersion efficace**.

### I.2.2 Comment décrire la dispersion ?

La dispersion peut être décrite par une **courbe de dispersion** représentant le nombre de larves dispersées $N$ en fonction de la distance parcourue $x$ depuis leur point d'émission. Une autre manière de représenter la dispersion est de décrire un **noyau de dispersion** ('dispersal kernel' en anglais) représentant la densité de probabilité de dispersion, c'est-à-dire la courbe de distribution des probabilités de rencontrer une larve à une distance $x$ de son point d'émission (Figure I.4). Autrement dit, il s'agit de la probabilité qu'une larve émise d'une population donnée soit dispersée sur une distance $x$ et se sédentarise. Les noyaux de dispersion sont donc des **fonctions continues représentant la distribution spatiale des larves dispersées**. Ils sont en général représentés sur une dimension spatiale (distance parcourue $x$ depuis le point d'émission), mais peuvent aussi être décrits en deux dimensions (Edwards *et al.*, 2007). Étant donné la probabilité non nulle que la larve meurt au cours de la dispersion, l'intégrale du noyau par rapport à l'espace est strictement inférieure à un (et égale à un si la mortalité est nulle).

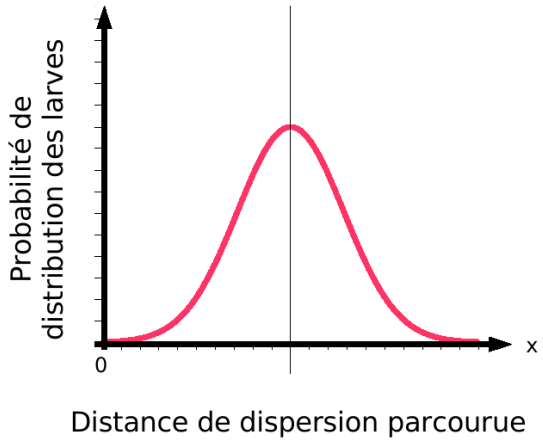


Figure I.4 – Noyau de dispersion : probabilité de distribution des larves en fonction de la distance parcourue $x$ depuis leur point d'émission. La distance de dispersion moyenne est indiquée par un trait fin vertical.

Les noyaux de dispersion décrivant la dispersion sont généralement représentés par des courbes gaussiennes sous l'hypothèse d'une diffusion turbulente isotrope et peuvent varier de différentes façons (Botsford *et al.*, 2009) : (i) selon leur magnitude en fonction de la probabilité de survie des larves (Figure I.5A), (ii) selon leur mode en fonction de la distance de dispersion moyenne (Figure I.5B), ou (iii) selon leur variance en fonction de la variabilité de la distance de dispersion autour de la valeur moyenne (Figure I.5C). La position du mode et la variance dépendent de l'importance relative des processus d'advection et de diffusion (voir Section I.3.1).

L'allure des noyaux de dispersion peut aussi différer d'une courbe gaussienne, en particulier lorsque leur forme n'est pas symétrique (Figure I.5D), par exemple lorsqu'il existe des zones de rétention où la probabilité de rencontrer des larves est plus importante. Ils peuvent également varier dans l'espace et dans le temps (Figure I.5E), par exemple pour différents sites d'émission ou pour différents évènements de ponte. Enfin, les noyaux de dispersion, peuvent être multi-modaux (Figure I.5F), par exemple dans le cas où les courants divergent.

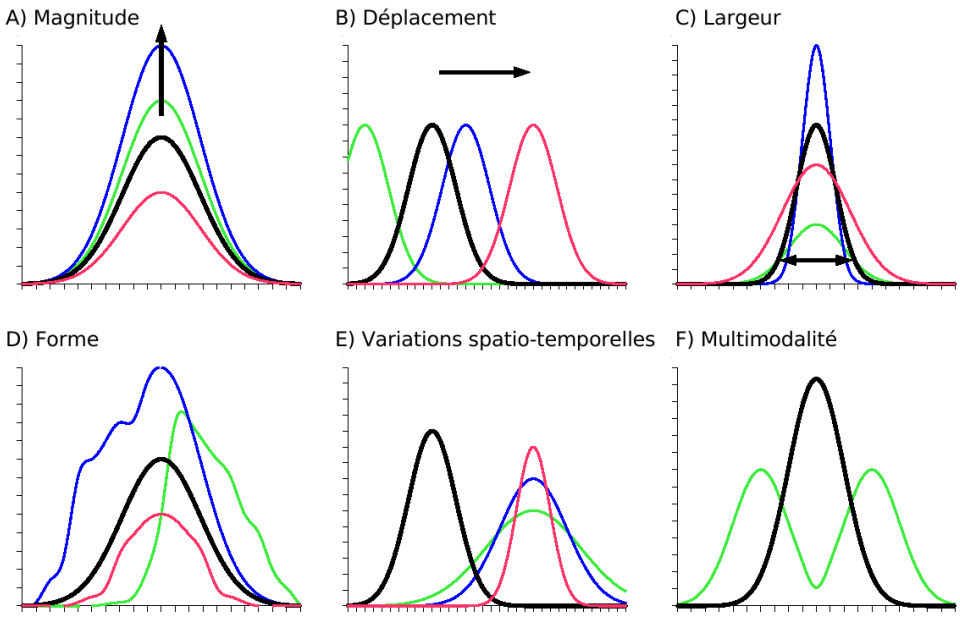


Figure I.5 – Principaux paramètres caractéristiques des noyaux de dispersion. Pour chaque paramètre, les courbes colorées représentent des exemples de variabilité par rapport au noyau de dispersion représenté par la courbe noire.

## I.3 La dispersion larvaire, un problème biophysique

Le transport et la dispersion larvaire sont la résultante d'interactions entre des **processus physiques** et des **processus biologiques**, faisant de l'étude de la dispersion un problème biophysique (Sponaugle *et al.*, 2002).

### I.3.1 Comment les processus physiques influencent-ils la dispersion ?

L'hydrodynamisme agit directement sur le transport larvaire à travers deux processus (Figure I.6) :

1. l'**advection**, c'est-à-dire par le transport moyen des larves par les courants marins dans une direction donnée et à une vitesse donnée (le transport de graines de pissenlit par le souffle de la semeuse est un exemple d'advection),

2. la **diffusion turbulente**, qui résulte des instabilités du courant moyen et engendre un transport aléatoire des larves dans les différentes directions de l'espace (par analogie avec la diffusion d'une goutte d'encre dans un verre d'eau).

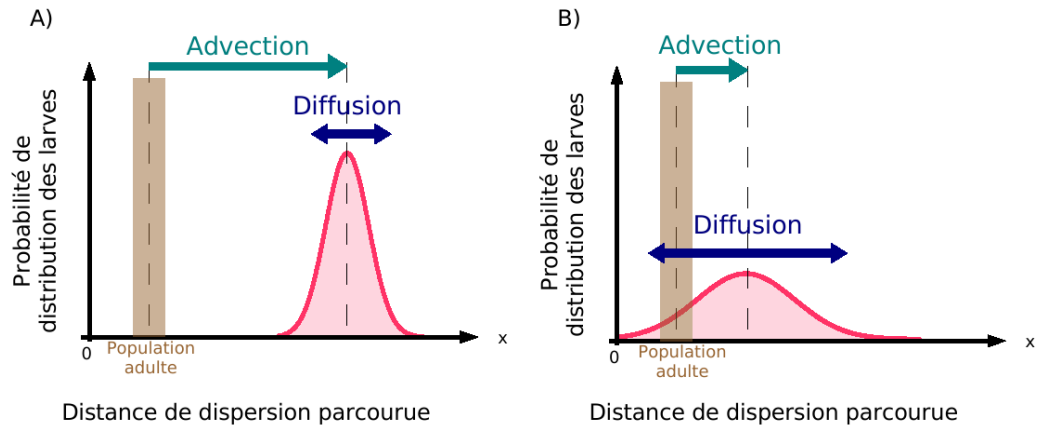


Figure I.6 – Conséquences de l'advection et de la diffusion turbulente sur la distribution des larves. (A) Conséquences d'une advection forte et d'une diffusion faible sur le noyau de dispersion. (B) Conséquences d'une diffusion forte et d'une advection faible sur le noyau de dispersion. Les processus d'advection sont représentés par une flèche turquoise et les processus de diffusion par une double flèche bleue. La localisation du site d'émission des larves au-dessus de la population adulte est représentée en marron et les noyaux de dispersion en rose.

Dans un modèle idéalisé et simplifié du milieu côtier tel que proposé par Siegel *et al.* (2003), où le courant côtier est stationnaire avec une vitesse moyenne $U$ et un écart-type $\sigma$, la distance moyenne parcourue par advection $L_{\mathrm{Adv}}$ pendant une durée $T$ par des larves issues d'un unique évènement de ponte est donnée par :

$$L_{\mathrm{Adv}} = UT \qquad \text{(Eq. I.1)}$$

Dans ce modèle, la variabilité autour de cette distance moyenne $L_{\mathrm{Diff}}$ induite par la diffusion turbulente est donnée par :

$$L_{\mathrm{Diff}} = \sqrt{\kappa T} = \sqrt{\sigma^2 \tau T} \qquad \text{(Eq. I.2)}$$

où $\kappa$ est le coefficient de diffusion turbulente défini par $\kappa = \sigma^2\tau$, avec $\tau$ l'échelle temporelle des fluctuations du courant.

Ce modèle a été utilisé par Byers et Pringle (2006) pour étudier chez une espèce semelpare, espèce pour laquelle chaque individu se reproduit une fois dans sa vie puis meurt, la dispersion et ses conséquences sur le maintien d'une population adulte pendant plusieurs générations. L'utilisation de ce modèle met alors en évidence que la combinaison de ces deux forces physiques résulte en des schémas de dispersion très différents qui se répercutent de générations en générations (Figure I.7). Alors que la diffusion turbulente tend à favoriser la rétention d'une partie de la population larvaire à proximité du lieu de ponte, l'advection induit un transport des larves en aval du lieu de ponte et un déplacement progressif, de générations en générations, de la zone où les apports larvaires sont maximaux.

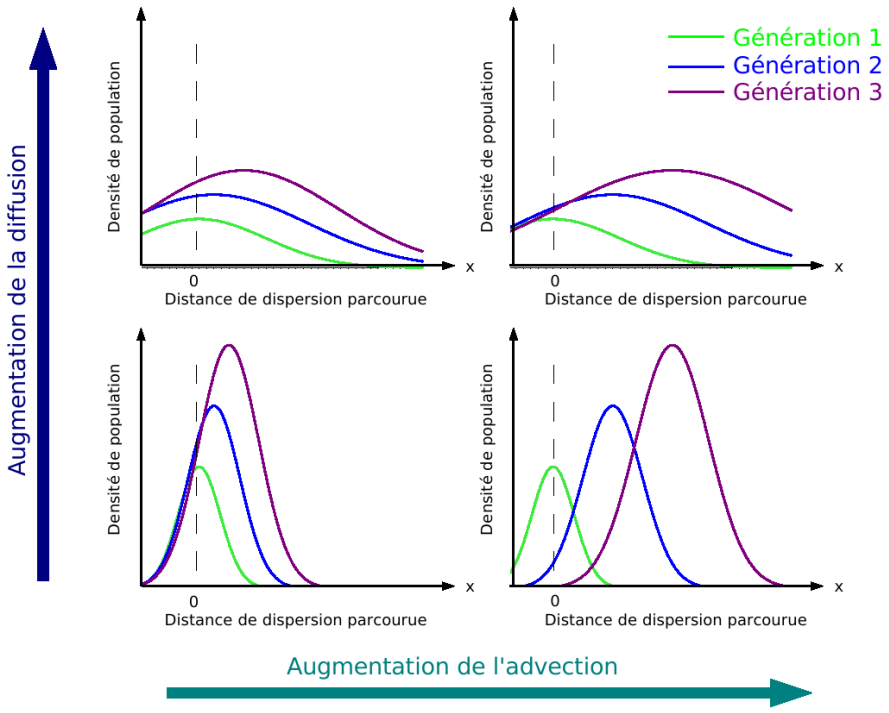


Figure I.7 – Conséquences de l'advection et de la diffusion turbulente sur la dispersion larvaire et la localisation d'une population benthique initialement localisée en $x$=0 (ligne pointillée) pendant trois générations successives, d'après Byers et Pringle (2006). Quatre cas sont présentés, avec de gauche à droite et de haut en bas : forte diffusion et faible advection, forte diffusion et forte advection, faible diffusion et faible advection, et faible diffusion et forte advection.

Les effets relatifs de l'advection et de la diffusion turbulente, c'est à dire l'importance relative de la valeur moyenne du courant et des fluctuations autour de cette valeur moyenne, peuvent être simplement appréhendés par le calcul du nombre de Peclet $P_e$ (Bird *et al.*, 2001). Ce nombre est défini comme le carré du rapport de l'échelle spatiale de l'advection ($L_{\mathrm{Adv}}$) sur l'échelle spatiale de la diffusion ($L_{\mathrm{Diff}}$), c'est à dire :

$$\begin{aligned} P_e &= \left( \frac{\text{Échelle des processus advectifs}}{\text{Échelle des processus diffusifs}} \right)^2 \\ &= \left( \frac{L_{\mathrm{Adv}}}{L_{\mathrm{Diff}}} \right)^2 = \left( \frac{UT}{\sqrt{\sigma^2 \tau T}} \right)^2 \\ &= \frac{U^2 T}{\kappa} = \frac{U^2 T}{\sigma^2 \tau} \end{aligned} \qquad \text{(Eq. I.3)}$$

Un nombre de Peclet supérieur à un caractérise les écoulements dans lesquels l'advection domine ($P_e \gg 1 \Rightarrow L_{\mathrm{Adv}} \gg L_{\mathrm{Diff}}$), tandis qu'un nombre de Peclet inférieur à

un caractérise les écoulements dans lesquels les processus de diffusion sont prépondérants ($P_e \ll 1 \Rightarrow L_{\mathrm{Diff}} \gg L_{\mathrm{Adv}}$).

Puisque la **circulation océanique** influence le transport larvaire par advection et diffusion turbulente, le transport va ainsi dépendre de nombreux paramètres hydrodynamiques qui détermineront les caractéristiques de ces deux variables. Il est ainsi possible de mentionner à titre d'exemple la circulation induite par la marée, les conditions de vent qui influencent les conditions de mélange et le transport advectif (*e.g.* transport d'Ekman), les gradients horizontaux de densité, les ondes internes, les structures frontales, la stratification verticale de la colonne d'eau, ou la turbulence (Cowen, 2002; Gawarkiewicz *et al.*, 2007; Largier, 2003). Les processus hydrodynamiques vont donc contraindre le transport larvaire **à toutes les échelles spatiales**, de la micro-échelle de la turbulence ($10^{-3}$ m), jusqu'à la macro-échelle de la circulation océanique globale ($10^{6}$ m), en passant par la méso-échelle de l'hydrodynamisme côtier ($10^{3}$ m).

Pour les organismes côtiers, il convient de souligner que la dispersion larvaire sera fortement influencée par l'**hydrodynamisme spécifique des régions côtières** qui se caractérise par la présence d'une couche limite côtière et de nombreuses **structures hydrodynamiques à méso-échelle** ; celles-ci tendent le plus souvent à favoriser la rétention locale (Largier, 2003). La couche limite côtière ('coastal boundary layer') résulte des forces de friction exercées par le fond dans les zones de faible bathymétrie et par le trait de côte. La résistance aux écoulements ainsi provoquée réduit dans les zones littorales l'intensité du transport advectif. Les tourbillons, généralement formés à proximité des îles, des caps ou d'accidents topographiques (Ménesguen et Gohin, 2006), augmentent quant à eux le temps de résidence des masses d'eau et, en corollaire, la probabilité que les larves soient retenues localement (Dubois *et al.*, 2007; Limouzy-Paris et al, 1997; Lobel et Robinson, 1986). Par ailleurs, les structures frontales formées par le contact de masses d'eau aux caractéristiques hydrologiques différentes peuvent agir comme des barrières physiques à la dispersion. La circulation convergente associée à ces structures peut également favoriser la concentration des organismes planctoniques dont les larves (Largier, 1993; Le Fèvre, 1986; Shanks *et al.*, 2003c). Dans le cas où le transport des larves est sous la seule dépendance des processus hydrodynamiques (*i.e.* larves passives), leur distribution dépend directement

de la distribution des masses d'eau telles que les plumes estuariennes (Shanks *et al.*, 2002; Thiébaut, 1996). Si les larves sont initialement exportées vers le large à la suite de leur émission, différents mécanismes pourront toutefois favoriser leur retour dans les régions côtières. Tel est le cas par exemple des phénomènes de relâchement d'upwelling observés le long des côtes californiennes et qui se traduisent par un courant orienté du large vers la côte (Wing *et al.*, 1998).

### I.3.2 De quels paramètres biologiques dépend la dispersion larvaire ?

Selon la définition proposée par Pineda *et al.* (2007), la dispersion larvaire repose sur les paramètres biologiques suivants : la ponte, la survie/mortalité des larves, la durée de vie larvaire, les comportements des larves et les mécanismes impliqués dans la sédentarisation (Figure I.3). Ces paramètres biologiques interagiront alors fortement avec les processus hydrodynamiques mentionnés précédemment (Metaxas, 2001).

La ponte des invertébrés marins peut être provoquée par des facteurs hydrodynamiques, tels que la marée ou les vagues (McCarthy *et al.*, 2003), et par des facteurs biologiques ou hydrologiques, tels que la présence de blooms phytoplanctoniques ou la température de l'eau (Lawrence et Soame, 2004; Olive, 1984; Olive *et al.*, 1990; Starr *et al.*, 1990). En réponse à ces différents paramètres, **le comportement de ponte des adultes** va influencer la dispersion larvaire en déterminant les conditions de vie initiales des larves. La ponte conditionne ainsi de par sa localisation et sa période (*e.g.* saisonnalité) l'environnement biotique et abiotique dans lequel seront présentes les larves. D'autre part, la fréquence plus ou moins élevée des événements de ponte sera à même d'accroître la variabilité des conditions environnementales rencontrées par différentes cohortes larvaires et la variabilité du devenir des larves émises par un individu au cours de sa vie (Byers et Pringle, 2006). Enfin, les modalités de la ponte influenceront le taux de rencontre des gamètes des espèces à fécondation externe, et de là, la quantité de larves produites (Levitan *et al.*, 1992).

Le taux de **mortalité larvaire** est affecté à la fois par l'environnement biotique de la larve en matière de conditions trophiques et de pression de prédation, et par l'environne-

ment abiotique des larves telles que les caractéristiques hydrologiques de la masse d'eau dans laquelle elles se développent. A titre d'exemple, selon la théorie du 'match-mismatch' de Cushing (1975) (*i.e.* synchronisme entre ponte et blooms phytoplanctoniques), la disponibilité en nourriture au moment de la ponte va fortement influencer la survie des larves planctotrophes (Edwards et Richardson, 2004). Le taux de mortalité larvaire est généralement très élevé mais fortement variable selon les espèces d'invertébrés (Pedersen *et al.*, 2008; Rumrill, 1990). À partir d'une étude basée sur 23 espèces d'invertébrés marins, Rumrill (1990) a ainsi estimé un taux moyen de mortalité larvaire de 0,229 ± 0,228 $j^{-1}$, pour une gamme de mortalité s'étalant entre 0,016 et 0,820 $j^{-1}$. Cette forte mortalité peut être responsable de goulots d'étranglement démographiques au cours de la phase larvaire (Schneider *et al.*, 2003). Une mortalité élevée, *i.e.* une faible probabilité de survie, diminuera les chances de succès de la dispersion.

La **durée de vie larvaire** est très variable entre espèces marines (*i.e.* de quelques heures à plusieurs dizaines de mois), voire entre populations d'une même espèce. Ses conséquences sur le succès de la dispersion sont fortes. Une relation établie par Shanks *et al.* (2003a) indique que plus la durée de vie larvaire est longue, plus la distance observée de dispersion est élevée (Figure I.8).

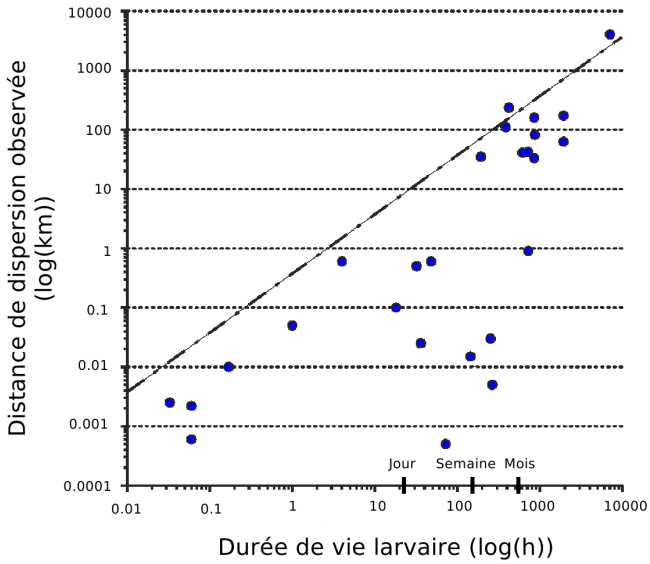


Figure I.8 – Relation entre la durée de vie larvaire et la distance de dispersion observée (échelle logarithmique). D'après Shanks *et al.* (2003a).

Cependant, il existe des exceptions à cette règle et on constate en particulier une distribution bimodale des distances de dispersion observée (Shanks, 2009; Shanks *et al.*, 2003a). Ainsi, de nombreuses espèces ayant des durées de vie larvaire de moins d'un jour se dispersent sur des distances de moins d'un kilomètre, alors que les autres se dispersent sur des distances de plusieurs dizaines voire centaines de kilomètres. Plus la durée de vie larvaire sera longue, plus la probabilité que la larve rencontre un habitat favorable distant de son point d'émission sera élevée, mais plus le taux de survie des larves sera faible.

Par ailleurs, les **taux métaboliques** et par conséquent de croissance étant influencés par la température, la durée de vie larvaire est fonction de la température rencontrée par la larve au cours de son développement (Dawirs, 1985). À l'issue d'une méta-analyse regroupant des espèces d'invertébrés marins et de poissons (Figure I.9), une relation entre la durée de vie larvaire ($PLD$) et la température ($T$) a ainsi été proposée par O'Connor *et al.* (2007) :

$$ln(PLD) = 3.17 - 1.34ln\left(\frac{T}{T_c}\right) - 0.28\left(ln\left(\frac{T}{T_c}\right)\right)^2 \text{ with } T_c = 15^\circ \text{ C.} \qquad \text{(Eq. I.4)}$$

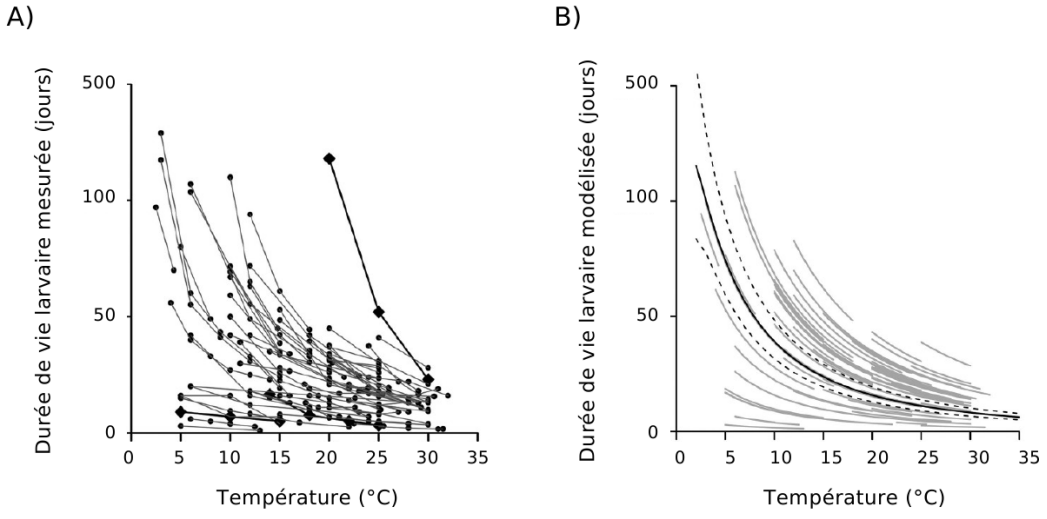


Figure I.9 – Lien entre la température et la durée de vie larvaire (A) mesurée et (B) calculée à partir de l'équation Eq. I.4, d'après O'Connor *et al.* (2007).

Le **comportement natatoire** des larves sur la verticale influence fortement le transport et donc la dispersion larvaire en raison des variations de la direction et la vitesse des courants selon cet axe (Garland *et al.*, 2002; Metaxas, 2001). Malgré des vitesses de nage de l'ordre du millimètre au centimètre par seconde (Chia *et al.*, 1984), l'interaction du comportement natatoire des larves avec l'hydrodynamisme a des conséquences sur les distances parcourues par les larves et sur le succès de la dispersion. Plusieurs types de **comportements natatoires sur la verticale** ont été observés chez les larves d'invertébrés marins, incluant en particulier un contrôle de la position des larves à une profondeur donnée ou différents comportements migratoires : la migration tidale, *i.e.* en fonction du cycle lunaire de la marée, la migration ontogénique, *i.e.* en fonction des stades de développement, et la migration nycthémérale, *i.e.* en fonction du cycle jour/nuit.

La **migration tidale** se caractérise le plus souvent par des larves qui nagent vers la surface pendant la marée montante (*i.e.* le flot) et vers le fond pendant la marée descendante (*i.e.* le jusant) (Figure I.10). Elle permet alors un transport sélectif des larves vers la côte et donc favorise la rétention larvaire ou la recolonisation de sites côtiers suite à un transport vers le large (Chen *et al.*, 1997; Hill, 1991a,b). Une migration tidale a par exemple été observée chez les larves du crabe de vase *Rhithropanopeus harrisii* (Chen *et al.*, 1997) ou du crabe rayé *Pachygrapsus crassipes* (DiBacco *et al.*, 2001).

De même, dans les estuaires, des **migrations ontogéniques** avec de jeunes larves situées dans les eaux de surface et des larves plus âgées localisées à proximité du fond peuvent interagir avec la circulation en double couche pour favoriser l'export vers le large des jeunes larves par les courants de surface et le retour vers la côte des larves plus âgées par les courants de fond (Figure I.11). Ce type de migration a été observé par exemple pour les larves des polychètes *Pectinaria koreni* (Lagadeuc, 1992b) et *Owenia fusiformis* (Thiébaut *et al.*, 1992) en baie de Seine orientale, où les gradients horizontaux de densité engendrés par les apports d'eaux douces de la Seine engendrent une circulation estuarienne résiduelle à deux couches.

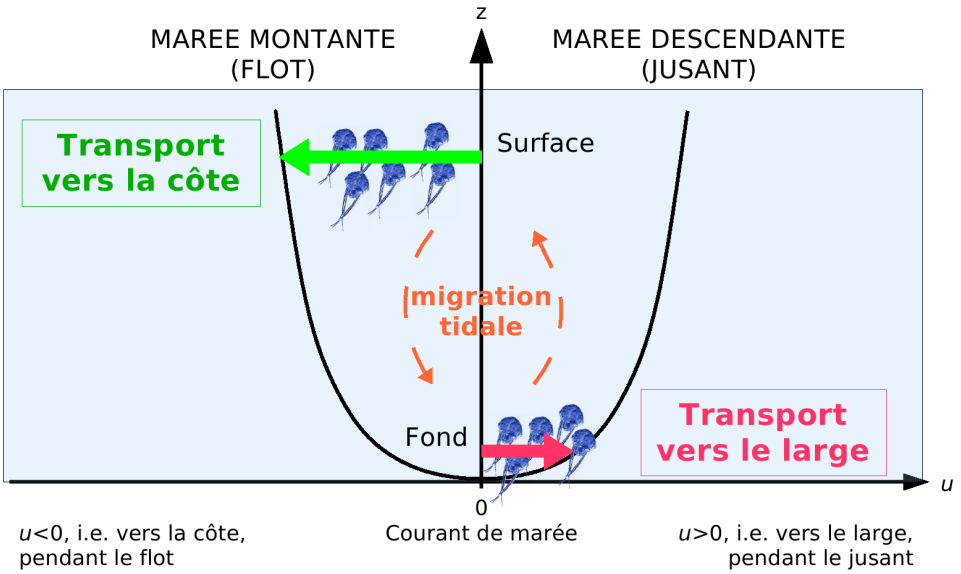


Figure I.10 – Un exemple d'interaction entre un comportement natatoire et la variabilité de la circulation sur la verticale : la migration tidale (en orange) et le transport sélectif par la marée. En noir est représenté le profil vertical du courant de marée moyen pendant le flot (courant négatif, *i.e.* vers la côte) et pendant le jusant (courant positif, *i.e.* vers le large). À marée montante, les larves migrent vers la surface où elles sont tansportées vers la côte par le courant de flot (vert). À marée descendante, les larves migrent vers le fond où elles sont légèrement exportées vers le large par le courant de jusant (rose). Le différentiel de transport entre le flot et le jusant explique le transport net vers la côte des larves.

Une **migration nycthémérale**, avec des larves situées prés du fond le jour pour diminuer les risques de prédation et à proximité de la surface la nuit, a par exemple été observée chez les larves mégalopes du crabe vert *Carcinus maenas* et les larves cypris des balanes *Chthamalus spp.* (Queiroga *et al.*, 2007). De plus, à partir d'observations *in situ* de ces larves le long des côtes ouest du Portugal, Queiroga *et al.* (2007) ont aussi suggéré une interaction entre la migration tidale chez ces espèces et la structure à deux couches du système de circulation d'upwelling et de downwelling de la péninsule ibérique, favorisant la rétention larvaire dans les eaux du plateau continental pendant les évènements d'upwelling (Marta-Almeida *et al.*, 2006; Peliz *et al.*, 2007). Hill (1991a,b, 1994) a par ailleurs constaté que la migration nycthémérale était en phase avec les ondes de marées S2 au-dessus du plateau continental du nord-ouest de l'Europe, permettant ainsi un transport différentiel par la marée.

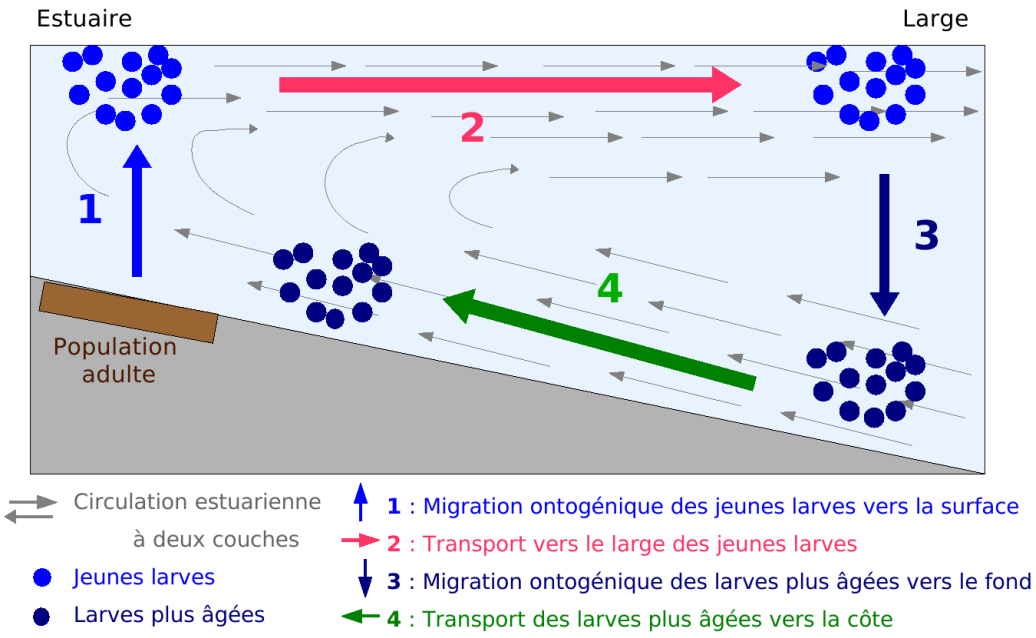


Figure I.11 – Un deuxième exemple d'interaction entre un comportement natatoire et la variabilité de la circulation sur la verticale : la migration ontogénique et la circulation estuarienne en double couche. La migration des jeunes larves vers la surface (1) favorise leur export vers le large par les courants de surface (2), tandis que la migration des larves plus âgées vers le fond (3) permet leur retour à la côte (4), *i.e.* vers l'habitat des populations adultes génitrices. D'après Lagadeuc (1992b).

Enfin, le **comportement des larves lors de la sédentarisation**, qui seront amenées à accepter ou à rejeter un substrat, ainsi que la distribution des habitats favorables influencent en partie la dispersion en déterminant les conditions du passage de la vie planctonique à la vie benthique (Butman, 1987; Gaines et Roughgarden, 1985). Cette étape peut être facilitée lorsque la sédentarisation et la métamorphose sont induites par des substances chimiques produites par exemple par des adultes conspécifiques ou par des biofilms microbiens spécifiques de l'habitat de l'espèce (Jensen et Morse, 1990; Qian, 1999), ou encore par des comportements larvaires de prospection (Woodson et McManus, 2007). En l'absence de signaux propices à la sédentarisation, les larves compétentes de certaines espèces sont ainsi capables de prolonger leur durée de vie planctonique et d'accroître leur potentiel de dispersion (Pechenik, 1999).

## I.4 La connectivité au sein de métapopulations marines

### I.4.1 Qu'est-ce qu'une population ?

De nombreuses définitions ont été proposées pour définir ce qu'est **une population** (Waples et Gaggiotti, 2006). D'un point de vue évolutif, une population désigne un groupe d'individus de la même espèce vivant suffisamment à proximité les uns des autres pour que n'importe quel individu puisse potentiellement se reproduire avec n'importe quel autre individu. D'un point de vue écologique, une population désigne un groupe d'individus de la même espèce occupant un espace particulier à un temps donné et qui vivent en interaction. C'est cette définition que nous utiliserons au cours de ce travail de thèse.

En milieu marin, la délimitation des populations peut parfois s'avérer difficile (Grimm *et al.*, 2003). Dans le cas d'espèces marines à cycle bentho-pélagique et vivant au sein d'un habitat fragmenté, la population est alors formée des individus adultes d'un fragment d'habitat benthique (ou patch) donné.

### I.4.2 Qu'est-ce qu'une métapopulation ?

Bien que l'importance des phénomènes d'extinction-recolonisation dans la persistence des populations locales fut soulignée par Wright (1940) et Andrewartha et Birch (1954) dès le milieu du vingtième siècle, le concept de **métapopulation** ne fut défini pour la première fois par Levins qu'en 1969 comme "une population de populations soumises à une alternance d'extinction et de colonisation". Il s'agit donc dans cette définition initiale d'un ensemble de populations structurées spatialement qui persiste malgré des extinctions locales (Figure I.12). Dans ce modèle d'extinction/recolonisation, les populations locales occupent un maillage infini composé de fragments d'habitat (ou 'patchs') équidistants et de même caractéristiques (*i.e.* taille, qualité, probabilité d'extinction). Le modèle de Levins fut initialement développé pour le contrôle des populations d'insectes nuisibles. Les objectifs de ces travaux étaient alors d'expliquer la persistence ou l'extinction des espèces lorsque les populations locales sont instables du fait de déplacement au sein de l'habitat fragmenté. La dynamique d'un tel modèle est rapide puisque chaque fragment d'habitat

ne peut avoir que deux états : occupé ou vide. En considérant des taux de migration entre populations locales faibles et indépendants de la distance les séparant, un tel modèle permet d'expliquer la pérennité d'une espèce à une échelle régionale supérieure à celle des populations locales.

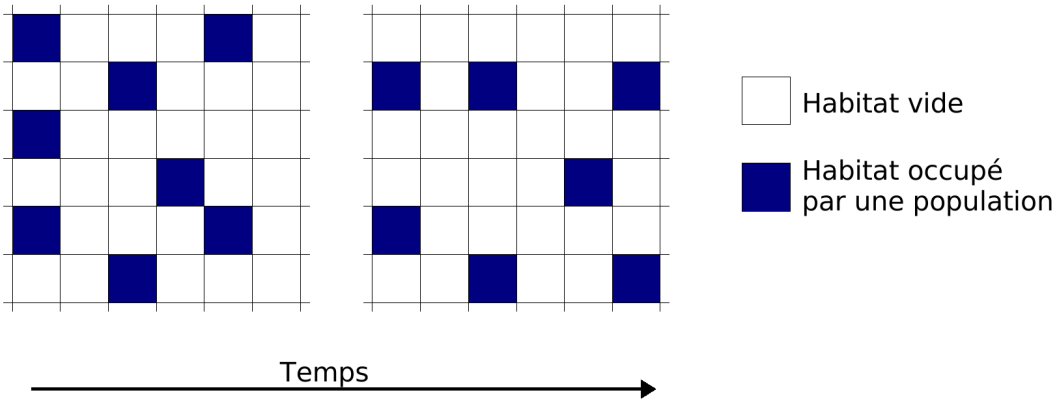


Figure I.12 – Modèle de métapopulation de Levins (1969), composé d'un maillage infini de fragments d'habitat (carrés) équidistants et de mêmes caractéristiques. Les fragments d'habitat sont vides (en blanc) ou occupés par une population locale (en bleu).

Par la suite, le modèle de métapopulations de Levins fut repris et développé dans des cas plus réalistes où les fragments d'habitat diffèrent en taille, en qualité et en probabilité d'extinction, devenant ainsi un paradigme majeur en écologie des populations et en biologie de la conservation (Hanski, 1999; Harrison, 1991). Plusieurs types de métapopulations furent ainsi décrits (Harrison, 1991) :

- le modèle classique de Levins composé d'une matrice d'habitats occupés ou vides (Figure I.13A) ;
- le modèle îles-continent (Figure I.13B) dans lequel il existe une population persistante (*i.e.* le continent) et des populations satellites (*i.e.* les îles) soumises à des phénomènes d'extinction et de recolonisation ; les échanges d'individus sont faibles et ont lieu aussi bien entre le continent et les îles qu'entre les îles ;
- le modèle source-puits (Figure I.13C), mentionné dès 1940 par Wright, dans lequel le maintien de la métapopulation dépend uniquement de la population source d'où sont issus tous les migrants et dont la probabilité de s'éteindre est nulle.

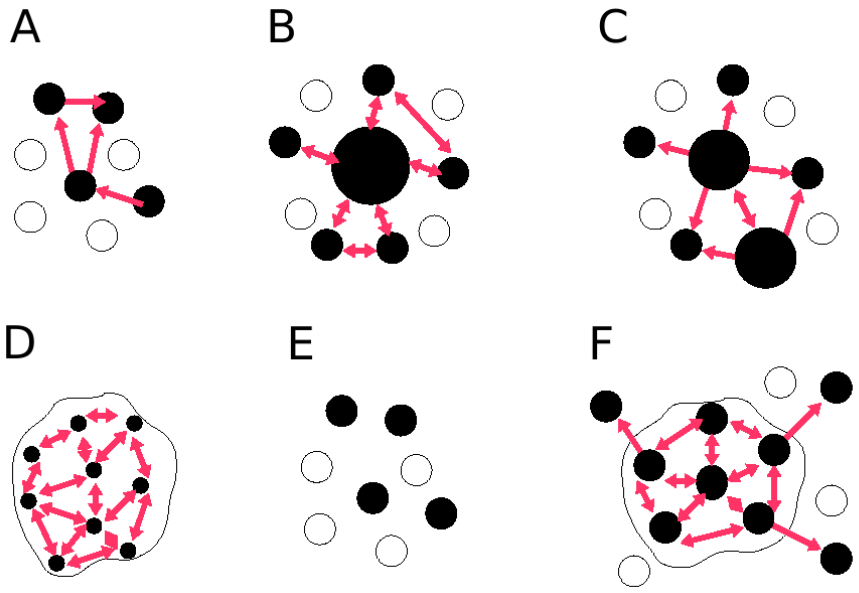


Figure I.13 – Exemples de métapopulations proposés par Harrison (1991) : (A) le modèle initial de Levins (1969), (B) le modèle continent-îles, (C) le modèle source-puits, (D) le modèle de population fragmentée, (E) le modèle de populations fragmentées en déséquilibre, et (F) un modèle intermédiaire. En noir sont représentés les habitats occupés et en blanc les habitats vides. Les flèches rouges symbolisent la dispersion.

À ces trois modèles théoriques majeurs de métapopulations qui mettent tous l'accent sur l'existence de phénomènes d'extinction-recolonisation et de flux de migrants faibles, il est possible d'ajouter d'autres formes d'organisation spatiale des populations :

- le modèle de population fragmentée (Figure I.13D), dans lequel les échanges entre populations locales discrètes sont intenses de sorte qu'il n'existe pas de phénomène d'extinction ; le système fonctionne alors comme une unique population structurée dans l'espace ;

- le modèle de populations fragmentées en déséquilibre (Figure I.13E), dans lequel les populations locales discrètes ne sont pas interconnectées et pour lequel il n'existe pas de recolonisation suite à des extinctions locales ;

- des modèles intermédiaires entre ces différentes formes d'organisation spatiale où des populations locales peuvent exister, tels que celui reporté sur la Figure I.13F qui allie un modèle source-puits avec un modèle de population fragmentée : dans de tels

modèles les échanges sont plus intenses au centre de l'aire de distribution de l'espèce et plus faibles en périphérie où des extinctions locales sont alors possibles.

### I.4.3 Comment caractériser les métapopulations marines ?

Bien que la majorité des premières études empiriques et théoriques sur l'écologie des métapopulations concernèrent les espèces terrestres (Hanski, 1999; Harrison, 1991), un nombre croissant d'études sur les métapopulations marines apparut dès la fin des années 80. Ainsi, Botsford *et al.* (1994) définirent les métapopulations d'espèces marines à cycle de vie bentho-pélagique comme des ensembles de sous-populations adultes reliées entre elles par la phase larvaire. Dans cette définition, c'est donc la dispersion larvaire qui régit la dynamique de la métapopulation. Celle-ci s'oppose ainsi au consensus qui se fit dans la lignée des travaux de Levins (1969), sur l'importance prépondérante des probabilités d'extinction des populations locales dans la définition des métapopulations (Grimm *et al.*, 2003; Smedbol *et al.*, 2002) : un fort risque d'extinction d'au moins une population locale est nécessaire pour définir une métapopulation. Or, le critère d'extinction locale est souvent difficilement applicable aux populations d'espèces marines à cycle bentho-pélagique. De plus, il est extrêmement difficile d'estimer la localisation et la taille des populations locales en milieu marin étant donné la difficulté d'en définir les contours et de les échantillonner correctement (Grimm *et al.*, 2003; Smedbol *et al.*, 2002).

Dans la définition d'une métapopulation proposée par Hanski en 1999, les extinctions locales ne sont plus le critère primordial : la métapopulation est plutôt définie comme un ensemble de populations locales occupant un habitat fragmenté et reliées par la dispersion, suggérant que la dynamique de l'une est influencée par la dynamique des autres et réciproquement. Il existe alors des échanges entre populations, sans qu'il y ait nécessairement d'extinction. L'accent est mis sur l'absence de synchronisme entre les dynamiques locales puisque les populations locales sont partiellement fermées (*i.e.* autorecrutement possible), et donc sur l'absence d'homogénéisation de la dynamique régionale. Cependant, dans ce concept les dynamiques locales et régionales demeurent liées.

La récente définition formulée par Kritzer et Sale (2003) correspond à l'application en milieu marin de la définition proposée par Hanski (1999). Ainsi, une **métapopulation marine** est un système de populations locales discrètes dont chacune détermine en grande partie sa propre dynamique interne mais dont une partie de la dynamique est également influencée par les autres populations locales à travers la dispersion d'individus (Figure I.14). Cette définition de la métapopulation prend donc en compte en premier lieu l'organisation spatiale des populations locales et leurs relations via les échanges larvaires. Cependant, elle ne précise pas leur dynamique et donc n'impose pas de critère basé sur des évènements d'extinction-recolonisation.

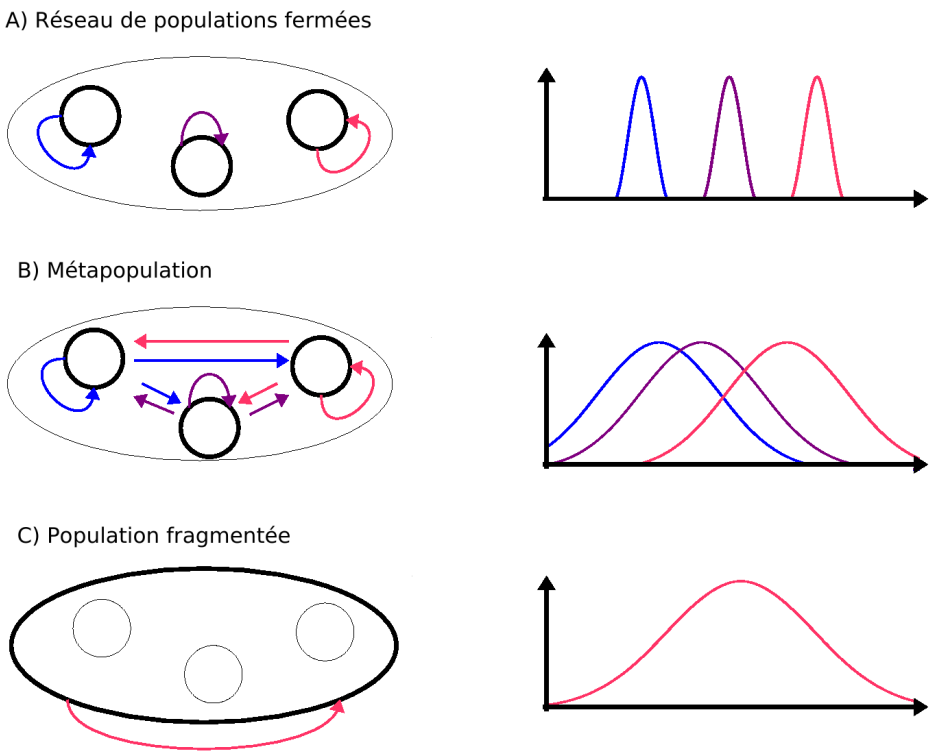


Figure I.14 – Trois types de populations spatialement structurées en fonction des échelles spatiales de la dispersion larvaire et les noyaux de dispersion associés, d'après Kritzer et Sale (2003). (A) Populations locales fermées : populations avec des dynamiques indépendantes et sans échange d'individus lors de la dispersion larvaire. (B) Métapopulation : réseaux de populations partiellement fermées, *i.e.* avec un certain degré d'autorecrutement (indépendance des dynamiques locales) mais une part non négligeable d'échanges entre populations via la dispersion larvaire. (C) Population fragmentée : ensemble de populations locales fonctionnant comme une seule population fermée au sein de laquelle les individus sont répartis en groupes discrets fortement connectés par la phase larvaire (dynamiques locales inter-connectées), l'ensemble fonctionnant comme une seule "grande" population. Les flèches symbolisent les échanges larvaires.

Dans ce contexte, deux **échelles spatiales** sont nécessaires pour entièrement appréhender la dynamique des métapopulations : l'échelle locale des sous-populations, et l'échelle régionale du réseau de populations locales. Dans la définition proposée par Kritzer et Sale (2003), le degré de connectivité démographique est le critère essentiel de la définition de la métapopulation, prenant en compte des processus locaux et régionaux. En plaçant la connectivité au centre de la définition des métapopulations marines, ces auteurs insistent sur le fait que la dynamique des populations locales, bien que fortement dépendantes des processus démographiques locaux, est aussi influencée par des processus d'apports

extérieurs. Le concept de la métapopulation, tout comme la théorie de la 'supply-side ecology' présentée en Section I.1.2, mettent donc en avant l'importance de la phase larvaire dans la dynamique des populations marines. La mesure de la connectivité en tant que taux d'échanges entre populations locales devient donc un élément central de l'étude des métapopulations marines.

### I.4.4 De la dispersion à la connectivité

La **connectivité** des populations est donc l'échange d'individus entre populations géographiquement séparées, celles-ci étant alors les sous-ensembles d'une métapopulation (Cowen et Sponaugle, 2009). Chez les organismes à cycle de vie bentho-pélagique, la connectivité entre populations inclue le plus souvent la dispersion larvaire et la survie des premiers stades de la vie benthique (Figure I.15A), c'est-à-dire les processus intervenant depuis la reproduction jusqu'au recrutement (Cowen *et al.*, 2007; Pineda *et al.*, 2007). S'il serait plus juste de définir la connectivité à l'issue de la phase dispersive lors de la sédentarisation, ceci est rarement possible dans la pratique où la connectivité est le plus souvent mesurée *in situ* à une date plus ou moins arbitraire. Une période de vie benthique plus ou moins longue au cours de laquelle une partie des individus nouvellement sédentarisés meurt est donc prise en compte. Enfin, la **connectivité reproductive** désigne la dispersion d'individus qui survivent et se reproduisent (Figure I.15B). Elle intègre ainsi les processus affectant les stades larvaires, juvéniles et adultes. La connectivité reproductive est parfois appelée **dispersion efficace** ou **dispersion réalisée**, telle que définie dans la Section I.2.1.

Par conséquence, il existe un lien direct entre la dispersion et la connectivité (Cowen *et al.*, 2007) : une dispersion sur de courtes échelles spatiales engendrera une faible connectivité entre populations distantes, tandis qu'une dispersion sur une plus grande distance augmentera la connectivité entre populations éloignées (Figure I.16). Selon l'importance des échanges larvaires entre les populations marines (Figure I.16), celles-ci peuvent être qualifiées de **'fermées'** en absence d'échanges (Figure I.14A) ou d'**'ouvertes'** lorsque les échanges sont intenses, libres, et sur de longues distances (Figure I.14C). La situa-

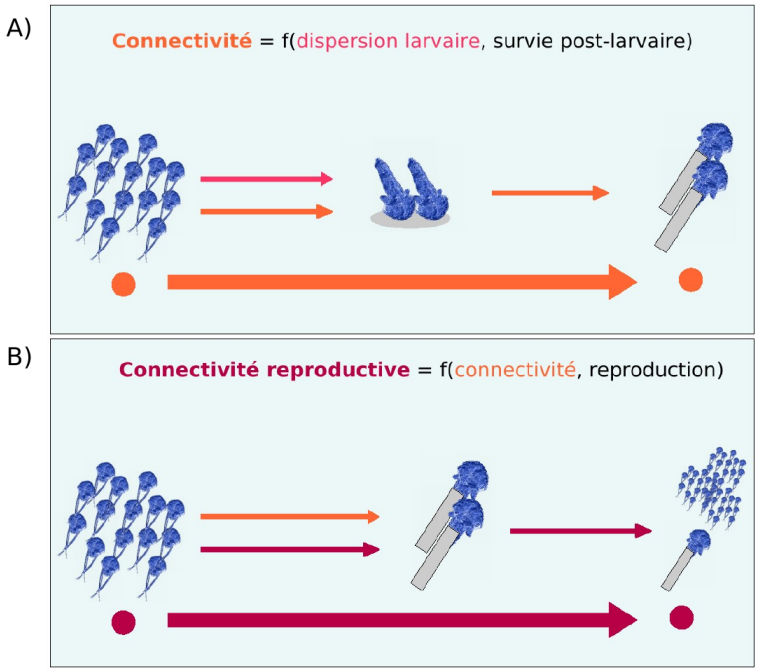


Figure I.15 – Définitions de (A) la connectivité et de (B) la connectivité reproductive, d'après Pineda *et al.* (2007). Les processus impliqués dans la connectivité sont indiqués par des flèches oranges, les processus impliqués dans la connectivité reproductive par des flèches pourpres.

tion intermédiaire correspond alors à la définition de métapopulation marine proposée par Kritzer et Sale (2003) (Figure I.14B).

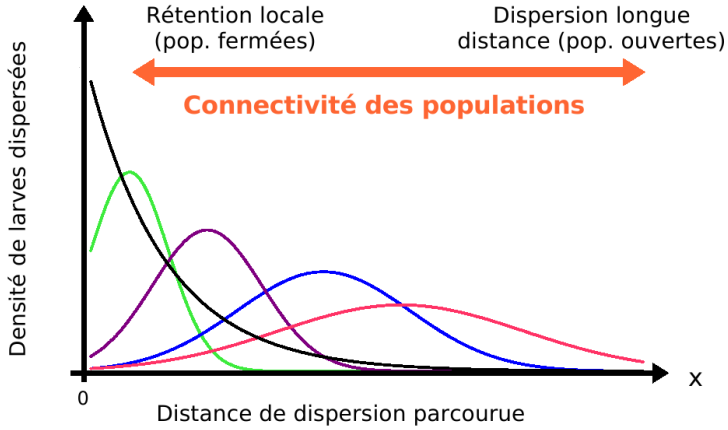


Figure I.16 – Lien entre dispersion et connectivité. L'intensité de la connectivité est fonction de l'allure des noyaux de dispersion. D'après Cowen *et al.* (2007).

### I.4.5 Les populations marines sont-elles ouvertes ou fermées ?

Historiquement, le milieu marin fut supposé être un milieu de libre échange, où les larves pouvaient se disperser sur de longues distances, rendant les populations marines ouvertes aux échelles de temps écologiques (Roughgarden *et al.*, 1988; Scheltema, 1986; Thorson, 1950). Cette supposition a été notamment appuyée par des études démontrant la faible structure génétique des populations marines sur de grandes échelles spatiales, et donc des échanges de gènes très intenses entre populations éloignées géographiquement (Hellberg *et al.*, 2002; Palumbi, 1994).

Cependant, depuis une dizaine d'années, la question de savoir si les populations marines étaient 'ouvertes' ou 'fermées' a été posée (Cowen *et al.*, 2000; Mora et Sale, 2002; Todd, 1998). En effet, des travaux issus d'échantillonnage *in situ* (Paris et Cowen, 2004), de modèles (Cowen *et al.*, 2000; James *et al.*, 2002), d'analyses biogéochimiques (Swearer *et al.*, 1999; Thorrold *et al.*, 2001) et/ou d'analyses génétiques (Jones *et al.*, 2005) ont montré que les taux d'échanges larvaires étaient fréquemment sur-estimés. Ainsi, la **rétention lavaire** et l'**autorecrutement** peuvent jouer un rôle important dans le maintien des populations marines (Warner et Cowen, 2002).

Sponaugle *et al.* (2002) ont en particulier identifié certains des mécanismes biologiques et physiques favorisant la rétention larvaire, tels que le comportement natatoire ou les structures hydrodynamiques complexes. La survie des populations locales et donc de la métapopulation dépendrait donc très fortement du succès de la rétention larvaire (Hastings et Botsford, 2006). Dans ce contexte, plusieurs études ont depuis cherché à mesurer le degré de connectivité des populations marines (Barnay *et al.*, 2003; Becker *et al.*, 2007; Xue *et al.*, 2008) ou à identifier des populations sources et des populations puits au sein de ces métapopulations (Bode *et al.*, 2006; Chiswell et Booth, 2008).

Dans le contexte de l'étude des métapopulations marines, Kinlan *et al.* (2005) préconisent cependant d'utiliser les termes 'ouvert' et 'fermé' avec précaution puisque ceux-ci sont relatifs ('plus ouvert que...', 'plus fermé que...'), et que la dispersion et la connectivité s'effectuent sur une vaste gamme d'échelles spatiales. Par ailleurs, une classification simpliste des distances de dispersion et donc des échelles spatiales de la connectivité (courtes *vs.* longues) n'est pas recevable, dans la mesure où des processus écologiques différents (maintien des populations locales *vs.* extension de l'aire de distribution) interviennent sur différents aspects de la dispersion (dispersion moyenne *vs.* phénomènes rares de dispersion extrême) (Kinlan *et al.*, 2005). Les notions relatives telles que court, long, ouvert, fermé, retenu, ou exporté ne doivent donc être utilisées que lorsqu'est précisée l'échelle à laquelle les processus biologiques observés sont pertinents.

### I.4.6 Comment décrire la connectivité ?

Les **matrices de connectivité** permettent de décrire les échanges larvaires entre les sous-populations d'une métapopulation. Ainsi, dans le cas d'une métapopulation comprenant $n$ populations, une matrice de dimension $n \times n$ permet de représenter les probabilités $p_{ij}$ qu'une population $i$ reçoivent des larves émises depuis la population $j$ (Figure I.17).

Les **matrices de distance temporelle** permettent, quant à elles, de décrire le temps nécessaire pour qu'une larve se disperse d'une population à une autre.

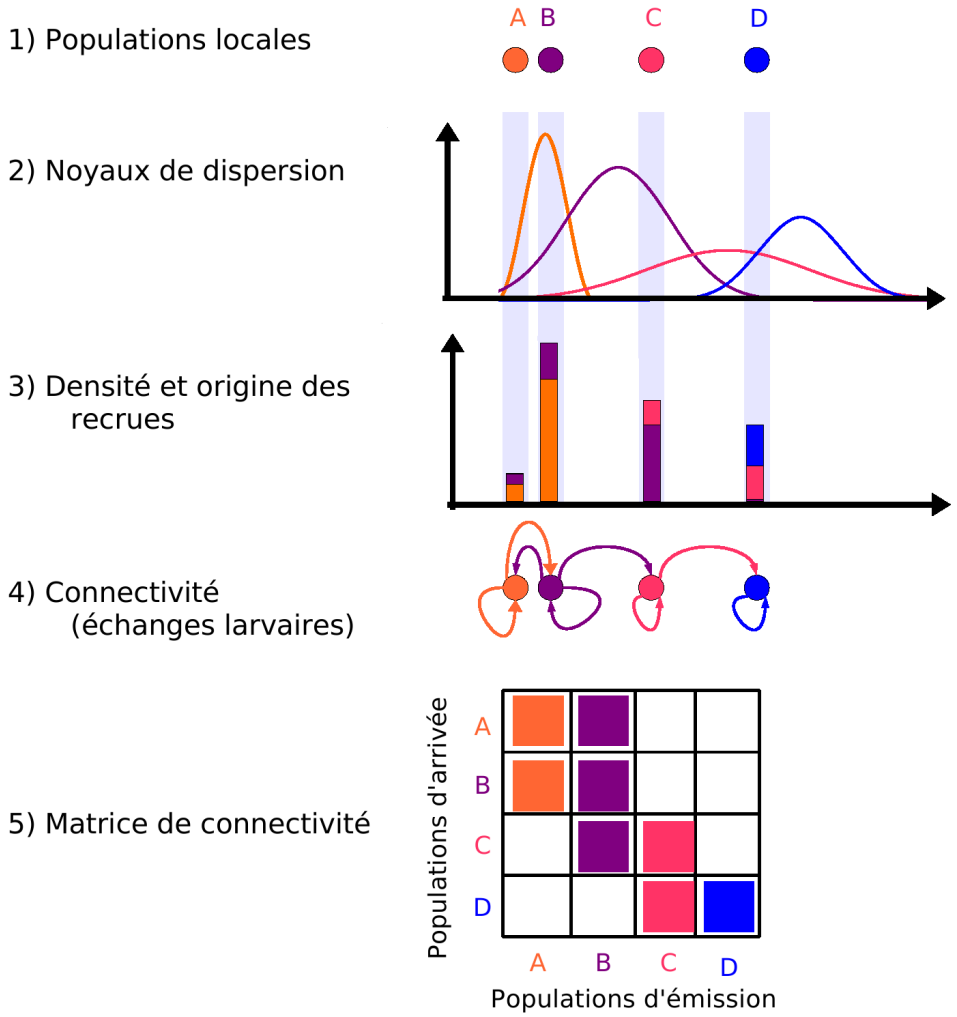


Figure I.17 – Un exemple simple de matrice de connectivité dans le cas d'une métapopulation théorique contenant 4 populations, d'après Botsford *et al.* (2009). Cette matrice (5) intègre successivement : (1) les 4 populations locales, (2) les probabilités de dispersion des larves telles que définies théoriquement par les noyaux de dispersion, (3) les densités et les origines des recrues, leur origine étant symbolisée par la couleur respective des populations A, B, C et D, et (4) les échanges entre sous-populations.

À partir des matrices de connectivité ou de distance temporelle, un **graphe de connectivité** représentant la connectivité de la métapopulation peut être construit (Treml *et al.*, 2008). Dans ce graphe, les populations sont représentées par des nœuds, reliées par des flèches orientées représentant la dispersion d'individus d'une population vers une autre et dont l'épaisseur est proportionnelle à l'intensité des échanges larvaires (Figure I.18). Selon la théorie des graphes, le nombre de populations (nœuds) est appelé ordre du graphe, tandis que le nombre total de flèches est appelé taille du graphe. Des analyses de graphe peuvent ensuite permettre de décrire les patrons spatio-temporels de la connectivité, d'identifier pour chaque population ses populations voisines (receveuses et émettrices), et de prédire d'éventuels chemins de dispersion (Newman, 2003).

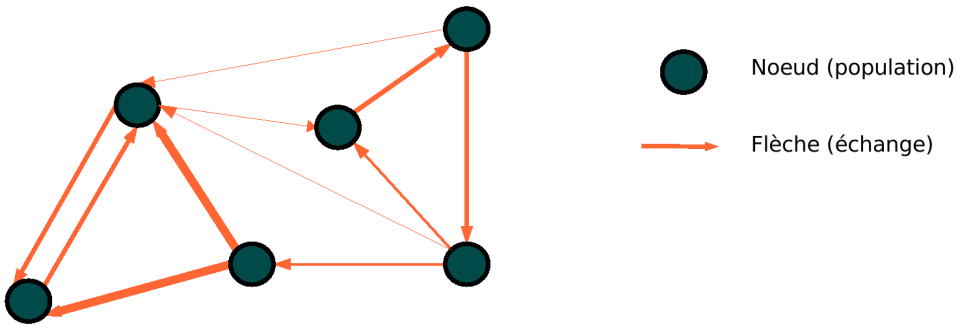


Figure I.18 – Graphe de connectivité, d'après Treml *et al.* (2008). Les nœuds du graphe représentent les différentes populations locales d'une métapopulation. Les flèches orientées indiquent la dispersion d'individus d'une population vers une autre et l'épaisseur des flèches est proportionnelle à l'intensité des échanges larvaires. Dans cet exemple, le graphe est d'ordre 6 et de taille 11 (6 nœuds, 11 flèches).

### I.4.7 Quelles sont les échelles spatio-temporelles de la connectivité ?

Les **échelles spatiales et temporelles** auxquelles la dispersion et la connectivité s'effectuent sont au centre de l'étude des métapopulations marines (Cowen et Sponaugle, 2009; Pineda *et al.*, 2007).

Des **échelles temporelles** croissantes, associées à des degrés de complexité croissants, peuvent ainsi être définies en fonction de l'objet d'étude (Figure I.19) :

- l'échelle temporelle du comportement individuel, incluant le comportement de ponte des adultes, les comportements de nage des larves, le comportement de sédentarisation des larves, et les migrations post-larvaires,
- l'échelle temporelle du transport larvaire résultant de l'interaction entre le comportement larvaire et les processus physiques de transport,
- l'échelle temporelle de la dispersion intégrant les processus de ponte, de transport, de survie larvaire et de sédentarisation,
- l'échelle temporelle de la connectivité non reproductive intégrant les processus de dispersion et de survie post-larvaire jusqu'au stade d'adultes matures,
- l'échelle temporelle de la connectivité reproductive, *i.e.* dispersion efficace, intégrant les processus de connectivité et de reproduction des jeunes recrues.

Définir les **échelles spatiales** de ces différents processus demeure plus difficile. L'échelle spatiale du comportement individuel est de l'ordre du milimètre au centimètre, par exemple avec des vitesses verticales de nage de quelques $mm.s^{-1}$ pour les larves d'invertébrés (Chia *et al.*, 1984). Les processus de transport, de dispersion larvaire et de connectivité se déroulent sur des échelles spatiales similaires, du mètre à la centaine de kilomètres. En effet, Cowen *et al.* (2006) ont démontré que la dispersion larvaire chez les poissons récifaux des Caraïbes pouvait être observée à des échelles allant de la dizaine à la centaine de kilomètres. En s'appuyant sur une étude comparative des distances de dispersion estimées sur la base de données génétiques pour de nombreux taxons marins, Kinlan et Gaines (2003) puis

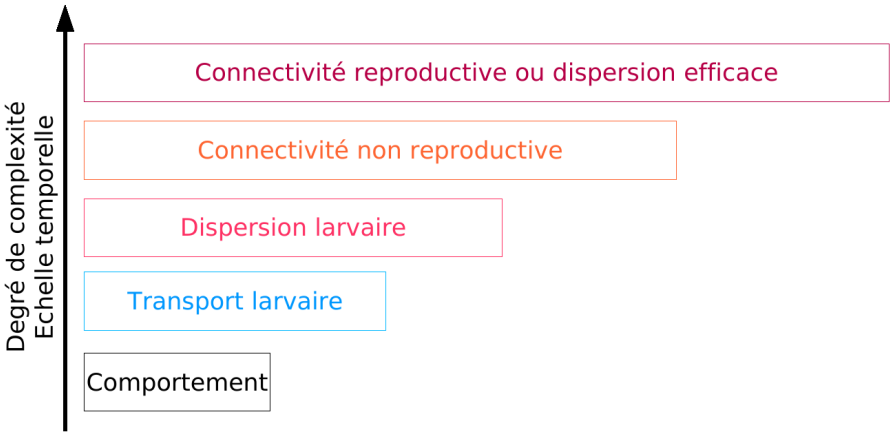


Figure I.19 – Les différentes échelles temporelles de la dispersion et de la connectivité, associées à des degrés de complexité croissants.

Gaines *et al.* (2007) ont estimé des distances de dispersion réalisée s'échelonnant du mètre au millier de kilomètres chez les invertébrés marins. Une distance modale plus grande est observée pour les poissons alors qu'elle est plus restreinte pour les algues (Figure I.20). En revanche, l'échelle spatiale de la connectivité reproductive peut être inférieure à l'échelle spatiale de la connectivité non reproductive, en particulier en limite d'aire de distribution des espèces.

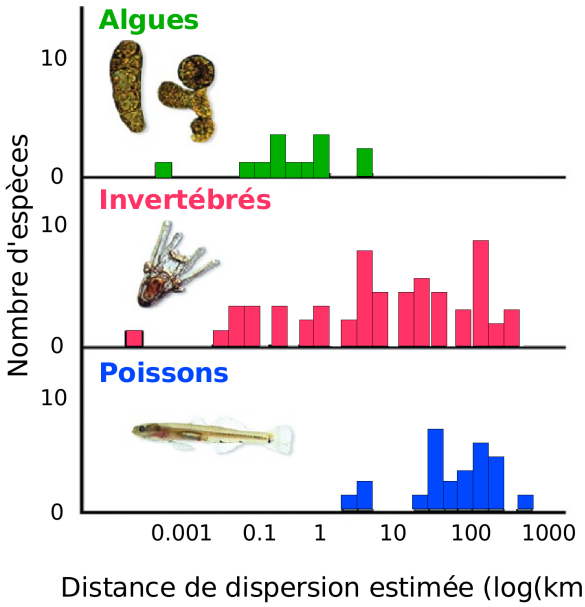


Figure I.20 – Distances moyennes de dispersion des propagules (*i.e.* spores ou larves) estimées pour plus de 100 espèces d'oganismes marins à partir de données de distance génétique. D'après Gaines *et al.* (2007) et Kinlan et Gaines (2003).

Étant donné la complexité de ces différentes échelles spatio-temporelles, l'étude de la dispersion et de la connectivité regroupe plusieurs disciplines opérant à différentes échelles spatio-temporelles (Figure I.21). À des échelles spatio-temporelles croissantes d'étude, on peut ainsi distinguer :

- l'étude de la physiologie larvaire, à l'échelle de l'individu,
- les études comportementales, à l'échelle d'un ou plusieurs individus,
- la dynamique des populations, à l'échelle des populations locales,
- la biologie et l'écologie des métapopulations, à l'échelle des métapopulations,
- la biologie de la conservation, de l'échelle locale à l'échelle régionale,
- les questionnements liés à l'évolution et la biogéographie, aux échelles de l'évolution et de la distribution des espèces,
- l'étude des conséquences des changements climatiques sur la dispersion et la connectivité des métapopulations marines, à l'échelle globale de l'écosystème marin.

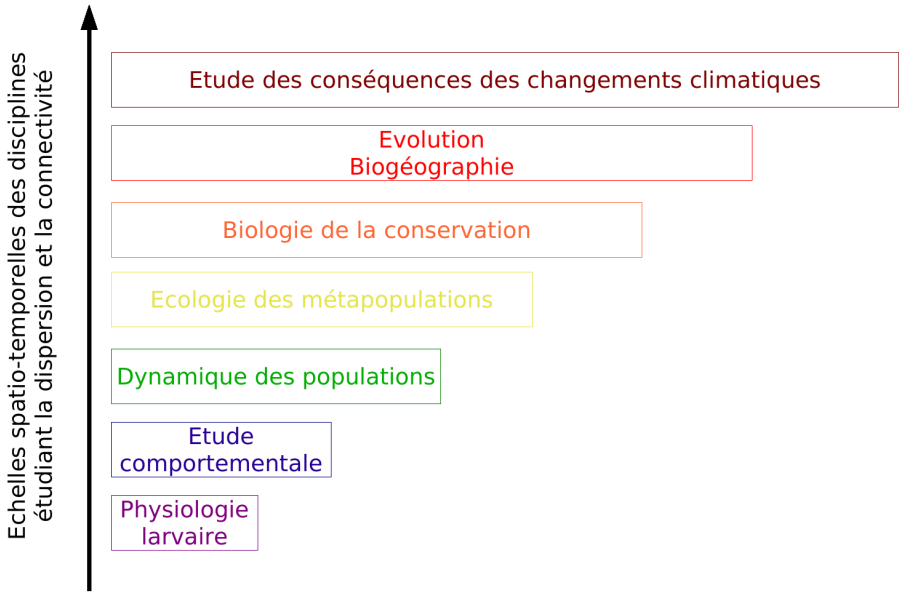


Figure I.21 – Échelles spatio-temporelles des disciplines et des questionnements scientifiques liés à l'étude de la dispersion et de la connectivité en milieu marin.

## I.5 Quelles sont les conséquences écologiques de la connectivité ?

Selon les échelles temporelle et spatiale auxquelles la dispersion et la connectivité sont appréhendées et étudiées, il sera possible de traiter plusieurs conséquences écologiques et évolutives de la connectivité.

### I.5.1 Connectivité et persistence des métapopulations marines

La persistence des populations marines dépend de la dynamique de la métapopulation à laquelle elles appartiennent (Hastings et Botsford, 2006). Ainsi, la persistence d'une population locale au sein d'une métapopulation est déterminée par la somme des apports larvaires totaux issus des populations de la métapopulation. Si, au contraire, la dynamique de la métapopulation ne permet à la population locale de recevoir des apports larvaires suffisants issus des populations distantes, alors la population locale disparaîtra. Le degré de connectivité étant inhérent à la définition et au fonctionnement des métapopulations, c'est donc la connectivité au sein de la métapopulation qui va déterminer sa dynamique

et les dynamiques des populations locales. Sur une échelle arbitraire de zéro à un, un degré nul de connectivité correspond au cas de populations isolées dont la survie dépend uniquement de leur propre apport larvaire, tandis qu'un degré égal à un correspond au cas d'une population fragmentée, dont la survie des patchs locaux dépend uniquement des apports larvaires globaux (Figure I.14).

D'autre part, l'intensité des interactions biotiques entre espèces (*e.g.* compétition, prédation, facilitation) qui gouvernent la structure et la dynamique spatio-temporelle des communautés benthiques sera influencée par le degré de connectivité des populations des différentes espèces (Guichard *et al.*, 2004). La notion de **métacommunauté** découle ainsi de la compréhension de la dynamique de populations en interactions et couplées à travers les mécanismes de dispersion larvaire (Mouquet et Loreau, 2002). A titre d'exemple, la connectivité entre populations peut entraîner une propagation à l'échelle régionale de processus écologiques agissant à l'échelle locale.

### I.5.2 Conséquences de la connectivité sur la conservation et la gestion de la biodiversité

La biodiversité marine doit actuellement faire face à de nombreux problèmes tels que la surpêche, l'eutrophisation, les invasions biologiques, et la dégradation et/ou la destruction des habitats (Fogarty et Botsford, 2007; Gray, 1997; Jones *et al.*, 2007). Pour proposer des mesures adaptées de **protection**, de **conservation** et de **gestion** de la **biodiversité marine**, la connaissance des modalités de dispersion et des patrons de connectivité est un pré-requis indispensable (Almany *et al.*, 2009; Botsford *et al.*, 2009; Roberts, 1997). J'en donnerai à titre d'illustration deux exemples ici : (i) la mise en place d'**aires marines protégées** (Jones *et al.*, 2007) et (ii) la gestion des invasions biologiques.

Ainsi, la taille, la localisation et le nombre de réserves marines à mettre en place pour assurer une conservation optimale de la diversité seront largement déterminés par les échelles spatiales de la dispersion des larves des espèces ciblées et le degré de connectivité des habitats (Jones *et al.*, 2007; Palumbi, 2004; Palumbi *et al.*, 2003). Par exemple, pour des

espèces à faible potentiel dispersif, les réserves marines pourront être de petite taille mais devront être proches les unes des autres alors que pour des espèces à fort potentiel dispersif, la distance séparant des réserves voisines tout comme la taille des réserves individuelles seront accrues (Figure I.22).

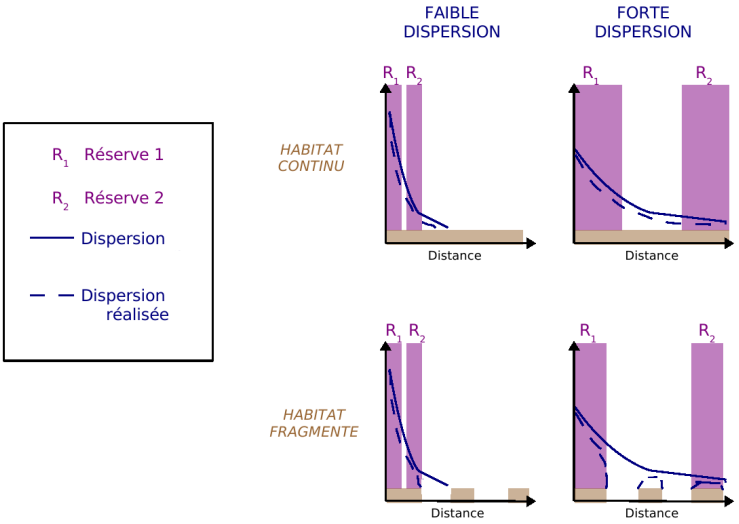


Figure I.22 – Dispersion et aires marines protégées : représentation schématique de la taille et de la localisation optimales des réserves marines, déterminées en fonction de la capacité de dispersion des organismes et du degré de fragmentation de l'habitat, d'après Jones *et al.* (2007). La dispersion, représentée par des noyaux de dispersion (en bleu), peut être faible (à gauche) ou forte (à droite) et l'habitat favorable (rectangle marron horizontal) peut être continu (en haut) ou fragmenté (en bas). En fonction des caractéristiques de la dispersion, de l'habitat, et de la dispersion réalisée, deux réserves marines optimales sont représentées (rectangles violets verticaux).

D'autre part, l'étude de la dispersion naturelle, ou assistée par l'homme, et de la connectivité est devenue un point central pour la compréhension des processus d'**invasions biologiques**, aujourd'hui considérées comme la deuxième cause de diminution de la biodiversité après la fragmentation et la destruction des habitats (Leppäkoski et Olenin, 2000).

Les invasions biologiques résultent de la dispersion d'une espèce au-delà des limites de son aire de distribution et assitée par l'homme, le plus souvent à l'occasion de multiples évènements d'introduction depuis de multiples sources et vers de multiples destinations (Figure I.23). Ainsi, en analysant les processus de dispersion en milieu côtier, Byers et Pringle (2006) ont mis en avant l'importance de certains traits d'histoire de vie liés au potentiel de dispersion d'une espèce (*i.e.* la fréquence et le nombre de pontes, le nombre de larves produites, et la durée de vie larvaire) dans le succès des invasions biologiques. Par ailleurs, dans le cas d'une espèce invasive nouvellement introduite et aux premiers stades de son expansion, Dunstan et Bax (2007) ont démontré l'importance des apports larvaires,

en lien avec l'hydrodynamisme local, dans l'établissement de nouvelles populations et de la rétention locale dans le maintien des populations nouvellement établies.

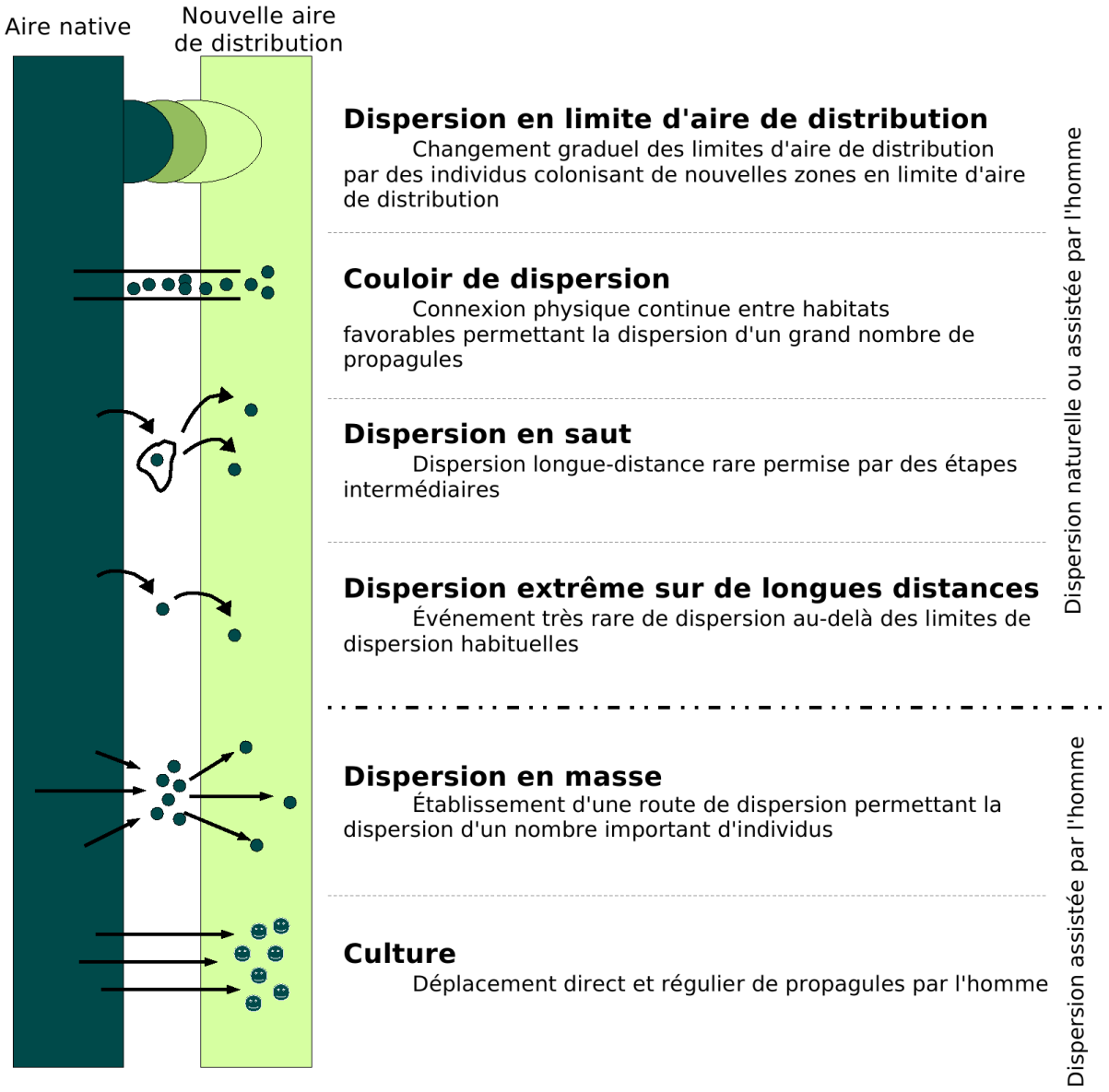


Figure I.23 – Dispersion au-delà des limites d'aire de distribution des espèces, d'après Wilson *et al.* (2009). Les différentes catégories présentées sont artificiellement délimitées ; le plus souvent, la dispersion d'une espèce au-delà des limites de son aire de distribution est une combinaison de plusieurs de ces catégories.

### I.5.3 Biogéographie et limites d'aire de distribution des espèces

Une récente méta-analyse de Lester *et al.* (2007) suggère l'absence de relation positive entre la distance moyenne de dispersion efficace des espèces marines et leurs aires de distribution (Figure I.24). L'existence de différences entre les échelles spatio-temporelles auxquelles la dispersion larvaire et l'établissement des aires de distribution des espèces se déroulent pourrait en être la cause. Cette méta-analyse ne permet cependant pas d'exclure le rôle des capacités de dispersion des organismes sur les **patrons de distribution biogéographique** des espèces.

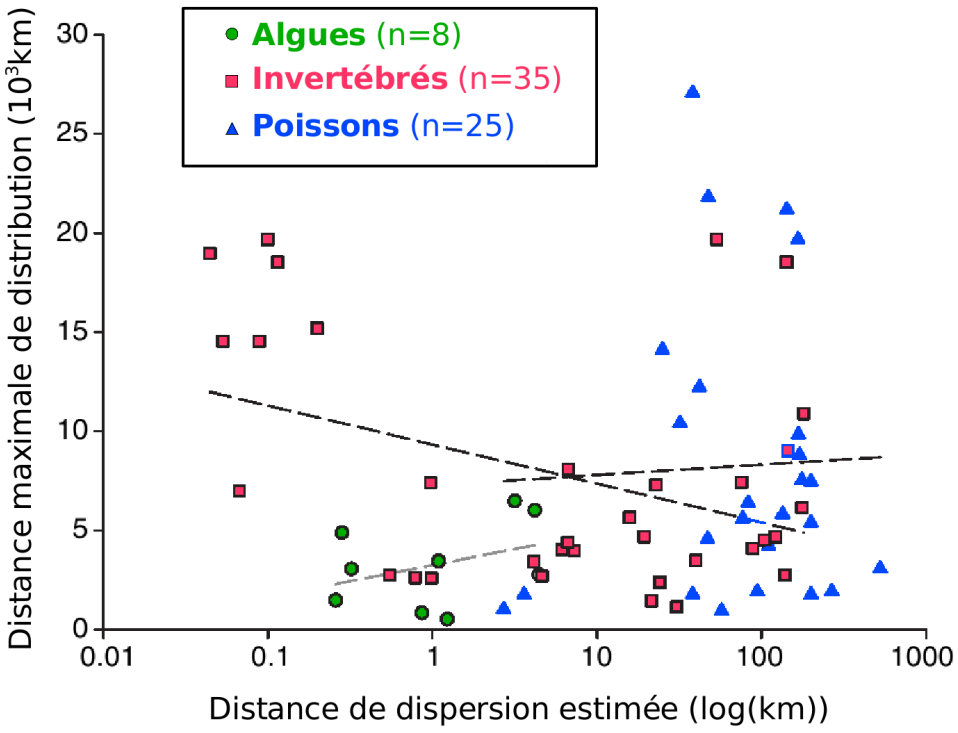


Figure I.24 – Relation entre l'aire de distribution des espèces marines (*i.e.* distance linéaire maximale entre les limites d'aire de distribution de l'espèce) et la distance de dispersion efficace estimée à partir de données génétiques, d'après Lester *et al.* (2007). Pour chaque groupe taxonomique (*i.e.* algues, invertébrés, poissons), la relation représentée par une ligne pointillée est non significative.

Ainsi, si les limites d'aire de distribution d'une espèce correspondent le plus souvent à des zones de fortes discontinuités hydrologiques, par exemple à cause de forts gradients thermiques, au-delà desquelles l'espèce ne peut survivre (Suchanek *et al.*, 1997; Zacherl *et al.*, 2003), elles sont également associées à des zones où l'hydrodynamisme complexe pourrait empêcher des apports larvaires suffisants au maintien des populations (Gaylord et Gaines, 2000; Zacherl *et al.*, 2003). Ainsi, selon Gaylord et Gaines (2000), les échelles spatiales auxquelles les espèces se dispersent et les barrières physiques à la dispersion que constituent les zones de convergence ou de divergence des grands courants océaniques pourraient jouer un rôle non négligeable dans l'établissement des limites d'aires de distribution comme illustré dans le cas des côtes américaines (Figure I.25).

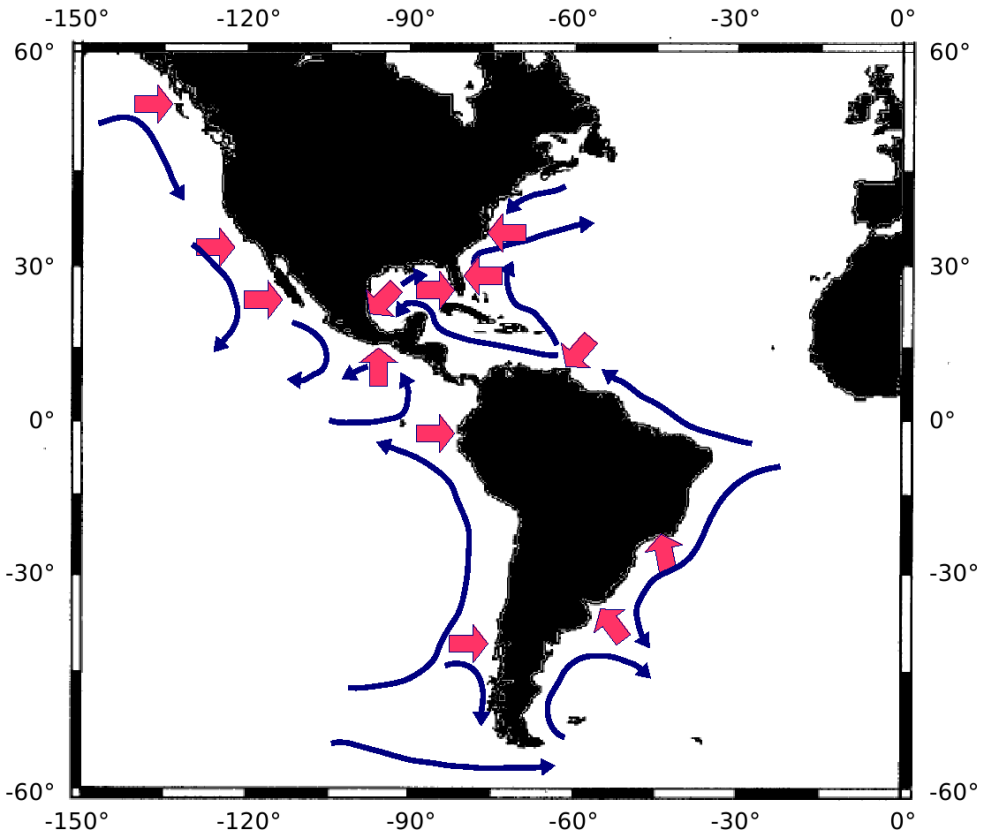


Figure I.25 – Frontières biogéographiques marines le long des côtes américaines d'après Gaylord et Gaines (2000). Les courants majeurs le long de ces côtes sont représentés par des flèches bleues, et les frontières biogéographiques marines sont représentées par des flèches roses. On constate que ces frontières ont tendance à se situer là où les courants majeurs se rencontrent (divergence, convergence).

### I.5.4 La connectivité dans le contexte du changement climatique

Les conséquences du **changement climatique** global sur les écosystèmes marins sont nombreuses et se répercutent en particulier sur la connectivité des métapopulations marines (FIelds *et al.*, 1993; Harley *et al.*, 2006; Munday *et al.*, 2009). Ces effets du changement climatique sur la connectivité en milieu marin sont résumés dans le Tableau I.1.

Ainsi, l'augmentation de la température de l'eau due au changement global pourrait modifier la phénologie de la reproduction des invertébrés côtiers (Lawrence et Soame, 2004), ce qui induirait entre autre des modifications des interactions trophiques (Edwards et Richardson, 2004; Kirby *et al.*, 2007) et donc diminuerait la survie larvaire et le succès de la dispersion. L'augmentation de la température pourrait aussi accélérer le développement larvaire et donc conduire à des durées de vie larvaire plus courtes (Duarte, 2007; O'Connor *et al.*, 2007), ou bien, à cause d'un effet combiné avec la modification des périodes de ponte, à des durées de vie larvaire plus longues (Rigal, 2009 ; Rigal *et al.*, *soumis*). Des modifications de la circulation des courants pourraient induire des changements dans les schémas de dispersion et donc modifier la connectivité. Enfin, la fragmentation et/ou la perte d'habitat entraînées par le changement global pourraient fortement diminuer la connectivité au sein des métapopulations marines.

Tableau I.1 – Conséquences possibles du changement climatique sur la connectivité d'après Munday *et al.* (2009). Entre parenthèses sont indiqués les niveaux de certitude des conséquences du changement climatique sur les populations marines (basse : BC, moyenne : MC, élevée : EC) et de leurs impacts sur la connectivité (bas : BI, moyen : MI, élevé : EI).

| Variables | Conséquences | Impact potentiel sur la connectivité |
|---|---|---|
| Réchauffement des eaux | •Changement dans la phénologie de la reproduction (EC)<br>•Diminution de la durée de vie larvaire (EC)<br>•Diminution de la fécondité (MC)<br>•Augmentation de la capacité natatoire des larves (MC)<br>•Augmentation de la variabilité de la survie larvaire (MC) | ⇒ Changement des patrons temporels de connectivité (MI)<br>⇒ Diminution de l'échelle spatiale de la connectivité, mais augmentation de l'intensité du recrutement (MI)<br>⇒ Diminution de la connectivité (EI)<br>⇒ Augmentation ou diminution de la connectivité (BI)<br>⇒ Augmentation de la variabilité du recrutement et la connectivité (EI) |
| Modification des courants | •Modification des schémas de transport larvaire par advection (MC)<br>•Changement de la disponibilité en nourriture planctonique (BC) | ⇒ Modification des échelles spatiales et des patrons de connectivité (EI)<br>⇒ Augmentation de la variabilité du recrutement et de la connectivité (EI) |
| Acidification des océans | •Effets possibles sur les capacités sensorielles des larves (MC)<br>•Problèmes pour la formation des structures calcaires des larves (BC) | ⇒ Diminution du recrutement et de la connectivité (EI)<br>⇒ Diminution de la survie larvaire et altération de l'orientation (EI) |
| Intensification des cyclones tropicaux | •Augmentation des perturbations physiques, de la fragmentation, et de la perte des habitats (EC)<br>•Changement à court terme des courants, du mélange vertical, et des conditions hydrologiques (salinité, température) (EC) | ⇒ Diminution locale de la connectivité au niveau des zones concernées (MI)<br>⇒ Changement localisé de la connectivité et effets positifs possibles sur le recrutement (BI) |
| Intensification des crues et sécheresses | •Changement temporel des communautés planctoniques induisant une plus grande variabilité de la survie larvaire (MC) | ⇒ Augmentation de la variabilité de la connectivité (MI) |
| Augmentation du niveau des océans | •Changement des courants dans certaines zones lagunaires entraînant une modification des schémas de dispersion larvaire (EC) | ⇒ Possible modification de la connectivité locale (BI) |

# I.6 Avec quelles méthodes peut-on étudier la dispersion larvaire et la connectivité en milieu marin ?

Étant donné l'extrême petite taille des stades larvaires (le plus souvent de quelques dizaines à quelques centaines de microns) en comparaison avec l'immensité de l'océan, l'étude de la dispersion et de la connectivité s'avère difficile. Cependant, de récents progrès méthodologiques ont permis d'étendre notre connaissance des mécanismes de dispersion de la phase larvaire et de la connectivité au sein des métapopulations marines (Botsford *et al.*, 2009; Cowen et Sponaugle, 2009; Levin, 2006).

## I.6.1 Méthodes directes

Les méthodes directes d'étude de la dispersion larvaire incluent l'analyse des distributions larvaires et de nouvelles recrues, des techniques de capture-marquage-recapture, ainsi que l'observation directe de la phase larvaire *in situ*. Ainsi, les larves suffisamment grosses pour être visible à l'oeil nu, telles que les larves d'ascidies peuvent être suivies individuellement par des plongeurs (Davis et Butler, 1989; Olson, 1985). En revanche, pour la majorité des larves de plus petite taille, seul le suivi à haute fréquence de la distribution des nuages larvaires de la ponte jusqu'à la sédentarisation renseigne sur la dispersion d'une population de larves (Lagadeuc, 1992b; Natunewicz et Epifanio, 2001; Paris et Cowen, 2004; Thiébaut *et al.*, 1994). Cette démarche nécessite d'avoir une ponte discrète et fortement localisée dans l'espace. Elle repose par ailleurs sur l'hypothèse que le nuage larvaire demeure suffisamment individualisé lors de sa dispersion. Combinées à l'échantillonnage *in situ* des larves, des bouées dérivantes surveillées par satellite peuvent être déployées, fournissant ainsi les schémas de transport attendus sous l'hypothèse que les larves se comportent passivement et sont localisées dans les eaux de surface (Arnold *et al.*, 2005; Natunewicz *et al.*, 2001).

Aux problèmes liés à l'échantillonnage des larves d'invertébrés, s'ajoute le problème de leur identification en routine en raison de grandes similarités morphologiques entre espèces (Le Goff-Vitry *et al.*, 2007a) et de la forte plasticité phénotypique des larves

d'une espèce en réponse aux conditions environnementales (Strathmann *et al.*, 1992). Le développement récent de différentes techniques de biologie moléculaire (*e.g.* analyse de séquence, polymorphisme de longueur des fragments de restriction, amplification aléatoire d'ADN polymorphe, hybridation *in situ*) tend néanmoins à pallier ce handicap technique (Hansen et Larsen, 2005; Larsen *et al.*, 2007; Le Goff-Vitry *et al.*, 2007a; Medeiros-Bergen *et al.*, 1995) (*cf.* Annexe A.2).

D'autres outils ont par ailleurs été développés pour étudier la dispersion larvaire et la connectivité par des méthodes d'étude indirectes.

### I.6.2 Méthodes indirectes par approches génétiques

Le premier type de méthode indirecte pour l'étude de la dispersion concerne les méthodes se basant sur des **approches génétiques**. En effet, les **flux géniques** et les migrations peuvent être déduits de l'étude des variations spatiales des fréquences alléliques et génotypiques (Hedgecock *et al.*, 2007). Différentes méthodes génétiques permettent d'évaluer la dispersion efficace, *i.e.* réalisée (connectivité reproductive, Figure I.15).

Premièrement, l'étude de la structure génétique des populations permet d'évaluer le degré de connectivité reproductive au sein d'une métapopulation en comparant les fréquences alléliques entre sous-populations spatialement distantes (Manel *et al.*, 2003). Selon les caractéristiques biologiques de l'espèce étudiée (durée de vie, type de reproduction) et les marqueurs génétiques choisis, l'estimation des flux géniques peut ainsi permettre d'estimer la connectivité génétique contemporaine ou historique. Cette méthode se base sur les statistiques traditionnellement utilisées en génétique des populations pour décrire les **structures génétiques**, c'est-à-dire les statistiques $F$ dont le $F_{ST}$ de Wright (*i.e.* variance standardisée des fréquences alléliques entre populations). De fortes similarités génétiques entre populations (*i.e.* $F_{ST}$ proche de zéro) suggèrent l'existence de flux géniques importants entre populations au cours des générations successives, résultant en particulier de forts échanges d'individus à travers la dispersion larvaire. À l'inverse, des différences génétiques significatives entre populations (*i.e.* $F_{ST}$ significativement différent de zéro) signalent des barrières importantes et pérennes aux échanges larvaires (Palumbi *et al.*, 2003).

Ces méthodes ont été fréquemment utilisées comme **'proxy' de la dispersion à l'échelle des temps évolutifs**. Cependant, elles ne sont pas toujours adaptées à l'étude des flux géniques récents dans la mesure où elles intègrent l'ensemble des évènements historiques de dispersion, *i.e.* sur plusieurs dizaines voire centaines de générations (Jolly *et al.*, 2009). De plus, Shanks (2009) a souligné que, bien que les distances de dispersion estimées par des méthodes génétiques étaient similaires aux distances de dispersion observées lorsque les durées de vie larvaire étaient courtes, elles sont très souvent surestimées lorsque la durée de vie larvaire est longue ($>$ 100 h) (Figure I.26). En effet, des durées de vie très longues peuvent permettre à de très rares individus d'être transportés sur de longues distances ce qui a tendance à minimiser les différences génétiques entre populations et donc à réduire les distances génétiques entre populations.

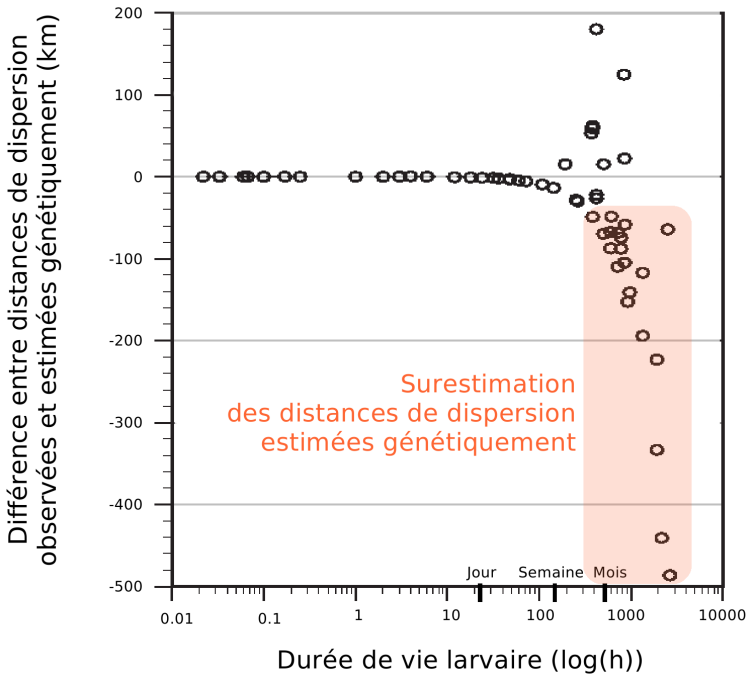


Figure I.26 – Biais dans les estimations génétiques de la distance de dispersion lorsque la durée de vie larvaire est longue, d'après Shanks (2009). La différence entre la distance de dispersion observée et la distance de dispersion estimée génétiquement est représentée en fonction d'une échelle logarithmique de la durée de vie larvaire.

En résumé, les distances génétiques s'avèrent de mauvais 'proxy' du transport larvaire mais rendent bien compte de la dispersion réalisée (connectivité reproductive) sur un grand nombre de générations. Ces distances ont notamment été utilisées dans de nombreuses

méta-analyses, telles que celles réalisées par Kinlan et Gaines (2003), Shanks (2009) ou Shanks *et al.* (2003a), pour décrire les grandes tendances de la relation entre la durée de vie larvaire et la connectivité globale. Dans ces méta-analyses, un modèle théorique particulier est utilisé, le modèle d'isolement par la distance (*isolation by distance* ou IBD en anglais) (Rousset, 1997; Slatkin, 1993) qui repose sur l'hypothèse d'une association entre la distance génétique et la distance géographique.

Deuxièmement, pour pallier les fortes hypothèses sous-jacentes aux modèles d'isolement par la distance, ainsi qu'à l'utilisation de l'indice $F_{ST}$ pour inférer les distances de dispersion, un nouveau corpus théorique et méthodologique a été développé en génétique des populations à travers l'utilisation de techniques dites d'**assignation statistique**. Ces techniques permettent l'assignation d'individus à des populations supposées parentales en se basant sur les fréquences de génotypes multi-locus observées dans ces populations (Manel *et al.*, 2005). Ces méthodes reposent généralement sur des méthodes de maximum de vraisemblance ou des analyses bayesiennes. Elles permettent d'évaluer la connectivité contemporaine, c'est-à-dire les migrations récentes, survenues il y a quelques générations voire une seule, sans faire l'hypothèse, irréaliste le plus souvent, d'équilibre démographique des populations.

Dans le cas où les recrues et les populations parentales sont suffisamment bien échantillonnées, les méthodes d'assignation peuvent donc permettre de décrire la forme, la largeur et le déplacement des noyaux de dispersion efficace. Si, en plus, des données sur la production larvaire de chaque population sont disponibles, l'amplitude des noyaux de dispersion pourra être déterminée et des matrices de connectivité pourront être calculées. Ces approches permettent une meilleure comparaison des distances de dispersion génétiques avec les prédictions de modèles hydrodynamiques (Dupont *et al.*, 2007; Jolly *et al.*, 2009). Cependant, la génétique des populations peut s'avérer limitée pour étudier la rétention locale ou pour estimer la connectivité de populations échangeant un nombre important de larve à chaque génération, par manque de finesse dans la caractérisation de la structure génétique des populations.

Tandis que les méthodes d'assignation permettent d'identifier la population d'origine d'une nouvelle recrue, les **analyses de parenté** ou de paternité permettent d'identi-

fier précisément ses parents. Ces analyses peuvent être réalisées avec différents types de marqueurs génétiques, à condition qu'ils soient suffisamment polymorphes, tels que les microsatellites (Jones *et al.*, 2005). L'analyse de parenté offre la possibilité de décrire la largeur, le déplacement, la forme et les variations temporelles des noyaux de dispersion dès lors que les recrues et les parents sont échantillonnés sur toute leur aire de distribution possible. La limite principale de cette méthode n'est pas liée aux marqueurs qui ne représentent plus un obstacle technique, mais à la qualité de l'échantillonnage qui se doit d'être le plus rigoureux possible. En effet, il faut impérativement échantillonner les recrues sur toute l'étendue potentielle de la dispersion et une proportion significative d'individus de la population source afin de disposer de la signature génétique de la plupart des parents.

### I.6.3 Méthodes indirectes par marquages biogéochimiques

Un second type de méthode indirecte pour l'étude de la dispersion regroupe des méthodes s'appuyant sur des **marquages biogéochimiques**. L'utilisation de marqueurs biogéochimiques **naturels et artificiels** contenus dans les tissus ou les structures calcifiées des organismes marins peut permettre d'obtenir des informations sur la dispersion larvaire (Thorrold *et al.*, 2002). Dans le cas de marqueurs naturels, cette technique repose sur la variabilité des propriétés physico-chimiques de l'environnement qui permet de générer des signatures biogéochimiques ou isotopiques qui s'enregistrent dans les tissus ou les structures calcifiées des organismes, telles que les otolithes des poissons ou les coquilles d'invertébrés. Ces structures peuvent aussi contenir un enregistrement chronologique des conditions environnementales grâce à des marques de croissance journalières. La reconstitution des conditions environnementales rencontrées par un organisme peut alors être obtenue en mesurant les compositions isotopiques ou en éléments traces de ces structures. Cependant, la précision spatiale de ces méthodes repose sur l'échelle spatio-temporelle de variabilité des propriétés physico-chimiques du milieu. Les structures calcifiées ont aussi été utilisées pour marquer artificiellement les individus : puisque celles-ci sont inertes d'un point de vue métabolique, un marqueur chimique artificiel sera conservé dans la structure calcifiée tout au long de la vie de l'individu.

Les marqueurs artificiels les plus couramment utilisés sont des colorants fluorescents tels que la tétracycline ou la calcéine, des éléments traces tels que le chlorure de strontium ($SrCl_2$), ou encore des marqueurs isotopiques radioactifs tels que le $^{85}Sr$ (Thorrold *et al.*, 2002). Les marqueurs naturels les plus fréquemment utilisés sont des métaux traces tels que le strontium, le barium ou le manganèse dont les taux d'assimilation dans les structures calcifiées varient en fonction des caractéristiques hydrologiques des masses d'eau (Zacherl *et al.*, 2003). De plus, les signatures en isotopes stables du carbone et de l'azote ($\delta^{13}C$, $\delta^{15}N$) contenues dans les tissus peuvent aussi fournir des informations sur les régimes alimentaires et donc sur les modalités du transport des différents stades du cycle de vie si ceux-ci occupent des niches trophiques différentes au cours de leur ontogénie (Riera *et al.*, 2000). Le rapport isotopique de l'oxygène ($\delta^{18}O$) renseigne quant à lui sur la température de l'eau rencontrée par une larve au cours de son développement.

Les signatures biogéochimiques ont ainsi été utilisées pour suivre la dispersion de larves de poissons (Thorrold *et al.*, 2001) et d'invertébrés tels que les crabes et les gastéropodes (DiBacco et Levin, 2000; Zacherl *et al.*, 2003) ou pour déterminer les populations d'origine des nouvelles recrues de deux espèces du genre *Mytilus* (Becker *et al.*, 2007). Ces signatures peuvent aussi été utilisées en combinaison avec des méthodes d'étude directes à des fins de capture-marquage-recapture (Jones *et al.*, 2005). Une nouvelle technique permettant le marquage transgénérationnel par des isotopes stables enrichis a récemment été développée avec succès (Thorrold *et al.*, 2006). Cette méthode repose sur la transmission maternelle de la composition en isotopes stables aux structures calcifiées des embryons. Cette signature isotopique est ensuite détectée par spectrométrie de masse après ablation au laser.

Dans le cas de marqueurs naturels, où tous les individus d'une population donnée sont naturellement marqués, ces méthodes s'avèrent particulièrement utiles, sous l'hypothèse que les signatures géochimiques naturelles varient à une échelle spatiale inférieure à l'échelle spatiale de la zone d'étude. En revanche, ce problème n'existe pas dans le cas de marqueurs artificiels, où les échelles spatiales sont définies par l'expérimentateur. Cependant, ces techniques se révèlent inefficaces pour étudier la dispersion chez les espèces dont la phase larvaire ne possède pas de structures calcifiées, comme par exemple chez les polychètes.

### I.6.4 Méthodes indirectes par modélisation couplée biologie-physique

Enfin, un dernier type de méthode indirecte pour l'étude de la dispersion et de la connectivité concerne la **modélisation couplée biologie-physique** (Werner *et al.*, 2007). Ces modèles couplés allient un modèle de circulation physique à un modèle de transport larvaire, voire de dispersion larvaire. Les modèles biophysiques permettent ainsi de simuler numériquement la dispersion et de calculer la connectivité (non reproductive), en prenant en compte un nombre plus ou moins important de paramètres biologiques et environnementaux ainsi que leurs interactions : date et lieu de ponte, quantité de larves émises, transport par des courants réalistes et propres à la zone d'étude, survie/mortalité et développement larvaire, comportement natatoire, comportement de sédentarisation. Lorsque le maillage spatial et le pas de temps du modèle sont adaptés aux échelles spatio-temporelles de la dispersion larvaire étudiée (zone d'étude et espèce), et lorsque les paramètres biologiques et écologiques des espèces sont bien connus, la modélisation est un outil puissant pour évaluer de manière quantitative la variabilité spatio-temporelle de la dispersion larvaire et de la connectivité marine.

Deux approches méthodologiques ont été développées, qui diffèrent radicalement dans l'objet d'étude (nuage larvaire *vs.* larve individuelle) : l'approche eulérienne et l'approche lagrangienne.

Premièrement, les **modèles eulériens** permettent le suivi de la **concentration en larves**, considérée comme un traceur, dans chaque maille du modèle en résolvant l'équation d'advection-diffusion-mortalité suivante dans un espace à trois dimensions ($x$,$y$,$z$) :

$$\frac{\partial C}{\partial t} + u\frac{\partial C}{\partial x} + v\frac{\partial C}{\partial y} + w\frac{\partial C}{\partial z} - K_x\frac{\partial^2 C}{\partial x^2} - K_y\frac{\partial^2 C}{\partial y^2} - K_z\frac{\partial^2 C}{\partial z^2} - \mu C = 0 \qquad \text{(Eq. I.6)}$$

où $C$ est la concentration en larves dans la maille de coordonnées ($x$,$y$,$z$), $u$, $v$ et $w$, les vitesses des courants en trois dimensions dans la maille ($x$,$y$,$z$) issues d'un modèle hydrodynamique, $K_x$, $K_y$, et $K_z$, les coefficients de diffusion horizontale et verticale, et $\mu$, le taux de mortalité. Dans les cas les plus simples, en l'absence de structure verticale des courants prononcée, les modèles eulériens pourront être simplifiés à un espace à deux dimensions ($x$,$y$). Les vitesses des courants $u$ et $v$ sont alors des vitesses de courant moyennées sur

la verticale. A l'inverse, dans des modèles sophistiqués, il sera possible d'adjoindre à la composante verticale du courant $w$ une vitesse de nage des larves. Le principal intérêt des modèles eulériens réside dans le fait que leur utilisation nécessite relativement peu de ressources informatiques en temps et en mémoire, en particulier lorsque la dispersion doit être simulée sur une longue période et/ou lorsque les spécificités individuelles des larves ne sont pas prises en compte. Cette méthode est donc préférée lorsque nos connaissances de la biologie larvaire sont limitées, par exemple lorsque l'on ne dispose pas d'information spécifique sur la croissance ou le comportement larvaire en réponse à l'environnement.

Des modèles eulériens théoriques ont ainsi permis de simuler l'influence d'une circulation côtière idéalisée sur la dynamique des populations de balanes (Roughgarden *et al.*, 1988) ou de tester plusieurs hypothèses sur les conséquences de différents courants océaniques simples et communs sur la dispersion larvaire et la dynamique des populations marines d'espèces à cycle bentho-pélagique (Gaylord et Gaines, 2000). Des modèles de dispersion eulériens ont aussi été utilisés avec succès pour simuler la dispersion larvaire de plusieurs invertébrés à cycle bentho-pélagique dans un environnement hydrodynamique réaliste, comme le polychète *Pectinaria koreni* en Manche (Ellien *et al.*, 2004; Jolly *et al.*, 2009), les bivalves *Mytilus galloprovincialis* et *Mytilus edulis* dans le sud-ouest de l'Angleterre (Gilg et Hilbish, 2003a), l'étoile de mer invasive *Asterias amurensis* dans le sud de l'Australie (Dunstan et Bax, 2007), ou encore les coraux de l'océan Pacifique Tropical (Treml *et al.*, 2008).

Deuxièmement, les **modèles lagrangiens** permettent le suivi de **trajectoires individuelles** de particules larvaires (**modèles individu-centrés**) (Miller, 2007; Werner *et al.*, 2001b), selon l'équation suivante :

$$\frac{d\vec{X}_i}{dt} = \vec{U}(\vec{X}_i, t) + \vec{U}'(\vec{X}_i, t) + \vec{u}_{sp}(\vec{X}_i, t) \qquad \text{(Eq. I.7)}$$

où $X_i$ est la position de la particule larvaire $i$ (en une, deux, ou trois dimensions), $\vec{U}$, le courant à la position $X$, $\vec{U}'$, la dérivée du courant par rapport au temps, et $\vec{u}_{sp}$, le déplacement propre de la particule larvaire (comportement natatoire ou de sédentarisation). Les modèles lagrangiens ont été largement utilisés ces dernières années pour suivre *in silico* les trajec-

toires potentielles d'un grand nombre de particules larvaires afin de simuler la dispersion des larves de poissons et d'invertébrés (Cowen *et al.*, 2000; Miller, 2007; Werner *et al.*, 2001b).

Les particules larvaires peuvent être caractérisées par des paramètres biologiques très simples ou bien par des paramètres biologiques spécifiques, en particulier de croissance ou de comportement natatoire, en fonction des connaissances biologiques des espèces étudiées (Metaxas et Saunders, 2009). En première approximation, les particules larvaires peuvent être modélisées simplement sans prendre en compte de caractéristiques propres à une espèce, les différentes études variant alors selon les caractéristiques hydrodynamiques de la zone étudiée. Ainsi la dispersion de particules passives a récemment été modélisée le long des côtes chiliennes (Aiken *et al.*, 2007) et dans le nord du Golfe de Californie au Mexique (Marinone *et al.*, 2008). Ce type d'étude est alors appelé étude d'ordre zéro de la connectivité. La distribution verticale des particules larvaires peut aussi être imposée, par exemple comme l'ont fait Edwards *et al.* (2007) en modélisant la dispersion de particules larvaires le long des côtes sud-est des États-Unis d'Amérique. D'autres travaux récents ont modélisé la dispersion de particules larvaires en se basant sur des paramètres biologiques spécifiques, tels que le comportement natatoire des larves de deux espèces d'huîtres, *Crassostrea virginica* et *Crassostrea ariakensis*, dans la baie de Chesapeake (North *et al.*, 2008), ou les paramètres de croissance et de comportement des larves de la morue *Gadus morhua* dans l'Atlantique Nord-Est (Vikebø *et al.*, 2007, 2005).

Ces outils de modélisation fournissent un cadre théorique et formel à l'étude de la dispersion larvaire puisqu'ils permettent de tester plusieurs hypothèses sur les facteurs influençant la dispersion et la connectivité. Ainsi, ces modèles ont été utilisés pour simuler la dispersion dans des environnements physiques simples, le plus souvent le long d'une côte rectiligne, pour tester l'importance relative de l'advection et de la diffusion (Byers et Pringle, 2006; Gaylord et Gaines, 2000) ou de la stochasticité de l'hydrodynamisme (Siegel *et al.*, 2008) sur la dispersion. Les modèles couplés biophysiques peuvent aussi permettre de simuler l'environnement physique de manière très réaliste, en prenant en compte tous les forçages qui gouvernent la circulation et le transport physique : topographie, conditions de marée, conditions météorologiques (régime de vent et pression atmosphérique), débits

fluviaux, turbulence à micro-échelle, mais aussi conditions aux limites ouvertes du modèle. Ils permettent aussi de tester le rôle relatif de différents paramètres biologiques tels que la date de ponte (Baums *et al.*, 2006; Edwards *et al.*, 2007; Mitarai *et al.*, 2008), la mortalité larvaire (Ellien *et al.*, 2004), la croissance et/ou la durée de vie larvaire (Aiken *et al.*, 2007; Edwards *et al.*, 2007; Siegel *et al.*, 2003; Vikebø *et al.*, 2005), ou encore le comportement natatoire des larves (Fiksen *et al.*, 2007; North *et al.*, 2008; Paris *et al.*, 2007; Vikebø *et al.*, 2007). En revanche, la prise en compte fine et réaliste de tous les paramètres biologiques qui influencent la dispersion larvaire, ainsi que de leurs interactions avec les conditions environnementales, demeure encore un défi (Hannah, 2007; Leis, 2007; Metaxas et Saunders, 2009).

Les résultats issus de la modélisation biophysique permettent de tracer des cartes de concentrations ou de positions simulées des larves, de suivre des trajectoires potentielles de transport, et de calculer des noyaux de dispersion et des matrices de connectivité. Il s'agit donc d'un outil très puissant qui permet d'identifier de manière quantitative l'importance relative des processus biologiques et physiques sur la dispersion, d'étudier la variabilité intra- et inter-annuelle de la dispersion et de la connectivité en réponse à la variabilité des conditions hydroclimatiques, de définir les échelles spatiales du transport et de la connectivité, ou d'évaluer le degré de connectivité entre populations. Cependant, la **connaissance fine des processus biologiques spécifiques** influençant la dispersion constitue souvent une limitation majeure à l'utilisation de tels modèles (Metaxas et Saunders, 2009). De plus, une validation hydrodynamique des modèles physiques de circulation est un pré-requis à l'application des modèles couplés pour simuler la dispersion larvaire au sein d'une zone d'étude donnée.

### I.6.5 Comparaison des méthodes d'étude

Ces différentes méthodes d'étude permettent d'obtenir des informations sur la dispersion et la connectivité à différentes **échelles spatio-temporelles** (Figure I.27). La combinaison de ces différentes approches permet donc une vision intégrée de la dispersion larvaire et de la connectivité, c'est-à-dire à toutes les échelles spatio-temporelles concernées.

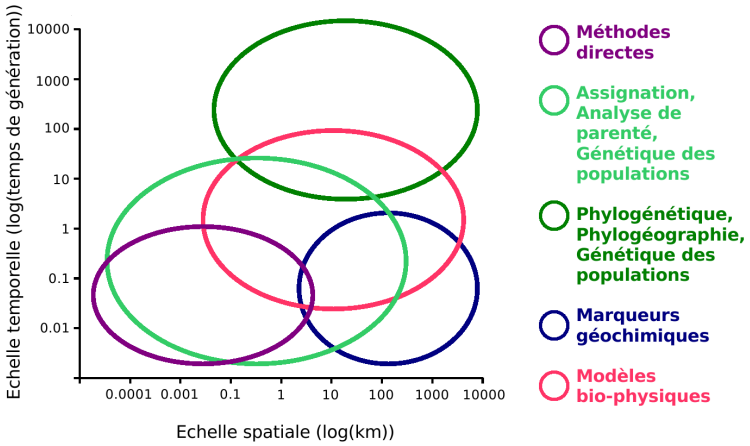


Figure I.27 – Comparaison des différentes méthodes d'étude de la dispersion et de la connectivité. Figure modifiée d'après Jones *et al.* (2009a). Les différentes méthodes d'études sont classées selon les échelles spatio-temporelles auxquelles elles s'appliquent et fournissent des informations sur la dispersion larvaire et la connectivité : méthodes directes (en violet), méthodes génétiques (en vert), méthodes biogéochimiques (en bleu), et modèles biophysiques (en rose).

Dans une récente analyse croisée réalisée par Shanks (2009), les relations entre la durée de vie larvaire et la distance de dispersion des larves ont été comparées à la suite de la mise en œuvre de différentes méthodes d'estimation de ces distances : observations *in situ*, formalisme théorique simple (distance = durée × vitesse), simulations issues d'un modèle biophysique lagrangien, et méthodes génétiques basées sur le modèle d'isolement par la distance à partir du calcul de l'indice $F_{ST}$ (Figure I.28).

L'analyse de ces différentes données met ainsi en avant :

- une distribution bimodale des distances de dispersion observées, soit inférieures à 1 km, soit supérieures à 20 km ;

- les limites de l'utilisation des méthodes génétiques pour estimer la distance de dispersion lorsque les durées de vie larvaire sont longues ;
- l'importance du comportement natatoire des larves, souvent négligé, sur les distances de dispersion, ce qui explique pourquoi les données issues des modèles tendent à surestimer la distance de dispersion ;
- qu'aucune des méthodes indirectes d'étude de la dispersion ne semble refléter correctement la variabilité observée, en particulier pour de longues durées de vie larvaire et de faibles distances de dispersion.

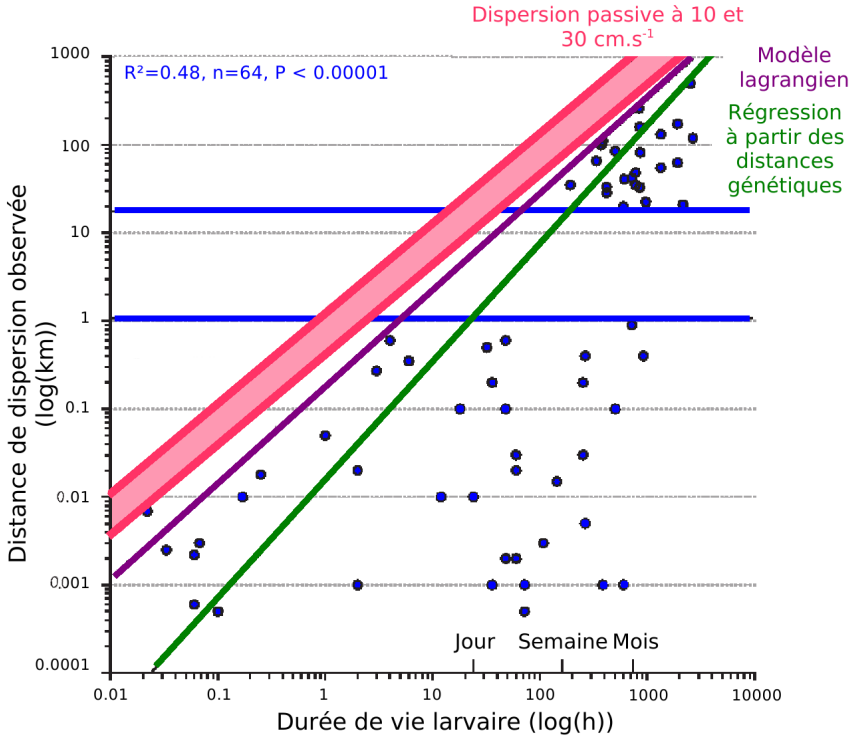


Figure I.28 – Analyse comparée des relations entre la durée de vie larvaire et la distance de dispersion déterminées suivant différentes méthodes : observations *in situ*, formalisme théorique simple (durée × vitesse), simulation à l'aide d'un modèle biophysique lagrangien, et méthodes génétiques, d'après Shanks (2009). Les données observées de distance de dispersion sont représentées par des points bleus. Les traits bleus horizontaux soulignent la distribution bimodale des distances de dispersion observées. Les résultats statistiques de la corrélation entre les données logarithmiques de la durée de vie larvaire et de la distance de dispersion observée sont indiqués. Les relations entre la durée de vie larvaire et la distance de dispersion calculée à partir d'un formalisme simple (distances parcourues par des larves passives dans un flux stationnaire de 10 et 30 $cm.s^{-1}$), à partir d'un modèle lagrangien, et à partir des distances génétiques sont figurées respectivement en rose, en violet, et en vert.

Ces résultats suggèrent ainsi qu'il est préférable d'utiliser différentes approches de manière croisée au sein d'études intégrées et interdisciplinaires combinant des méthodes génétiques, l'emploi de marqueurs biogéochimiques, et la modélisation conjointement avec des mesures *in situ* (Selkoe *et al.*, 2008). Ainsi, plusieurs études ont démontré l'utilité de combiner ces différentes approches. Nous en citerons dans le cas présent quelques exemples.

Jones *et al.* (2005) ont étudié la connectivité et la connectivité reproductive du poisson clown *Amphiprion polymnus* en Papouasie Nouvelle Guinée en combinant des analyses

géochimiques de marquage artificiel à la tétracycline des otolithes de tous les embryons produits au sein d'une population et des analyses de parenté par génotypage de toutes les nouvelles recrues et de l'ensemble des adultes de la population à l'aide de marqueurs microsatellites. Ces auteurs ont ainsi démontré l'importance de l'autorecrutement chez cette espèce.

Allain *et al.* (2007) ont prédit le recrutement des larves de l'anchois *Engraulis encrasicolus* dans le Golfe de Gascogne en combinant des analyses biogéochimiques et des simulations biophysiques, à partir de (1) la mesure de la croissance de larves d'anchois basée sur l'analyse des otolithes des larves échantillonnées dans le Golfe de Gascogne, (2) la reconstitution de la dérive individuelle de ces larves grâce à un modèle biophysique lagrangien, (3) la description de la relation entre la croissance mesurée et les conditions environnementales inférées à partir du modèle, (4) la construction d'un modèle individu-centré de croissance et de survie des larves d'anchois dans le Golfe de Gascogne, et enfin (5) l'utilisation de ce modèle pour prédire le recrutement à l'échelle de la zone d'étude.

Dans de nombreuses études récentes, des simulations biophysiques de transport larvaire ont aussi été couplées à des analyses génétiques estimant les flux géniques chez deux espèces du genre *Mytilus* dans le sud-ouest de l'Angleterre (Gilg et Hilbish, 2003a,b), chez le corail *Acropora palmata* dans l'est des Caraïbes (Baums *et al.*, 2006), chez le gastéropode invasif *Crepidula fornicata* en Manche (Dupont *et al.*, 2007), ou encore chez le polychète *Pectinaria koreni* en Manche (Jolly *et al.*, 2009).

## I.7 Problèmatique de la thèse

En assurant la dispersion, la **phase larvaire** joue un rôle fondamental dans la dynamique des populations d'organismes marins à cycle bentho-pélagique. Pour autant, son étude s'avère particulièrement complexe dans la mesure où de nombreux facteurs biologiques et physiques ainsi que leurs interactions interviennent. La **dispersion**, via les échanges larvaires entre sous-populations, détermine la **connectivité** (non reproductive et reproductive) au sein des **métapopulations marines**. En fonction des échelles spatio-temporelles considérées, la connectivité en milieu marin influencera directement la dynamique des métapopulations et la persistance des populations locales, les potentialités d'expansion des espèces en réponse à des changements des conditions environnementales, les limites d'aire de distribution des espèces, et la biogéographie. Les changements climatiques sont alors à même de modifier la dynamique des métapopulations marines à travers leurs conséquences directes et indirectes sur les facteurs de contrôle de la dispersion et de la connectivité. Par ailleurs, la mise en place de mesures efficaces de conservation et/ou de gestion des ressources marines et de la biodiversité se doit de prendre en considération la dynamique spatiale des populations. Face à l'**importance écologique et évolutive de la dispersion**, et à la difficulté d'étudier de manière directe la phase larvaire des organismes à cycle bentho-pélagique, de nombreuses méthodes indirectes d'étude de la dispersion larvaire et de la connectivité en milieu marin ont été développées, en particulier via l'utilisation de marqueurs génétiques ou biogéochimiques et la modélisation couplée biologie-physique.

Dans ce contexte, le but du présent travail est de mieux comprendre **l'influence relative des caractéristiques biologiques et des conditions hydrodynamiques et hydroclimatiques sur la dispersion et la connectivité** des invertébrés à cycle bentho-pélagique en zone côtière. En se focalisant sur deux échelles spatiales – l'échelle régionale du Golfe de Gascogne et de la Manche et l'échelle locale du Golfe Normand-Breton – il s'appuiera sur une approche couplée d'étude de la dispersion à partir d'observations *in situ* et de modélisation biologie-physique (Figure I.29).

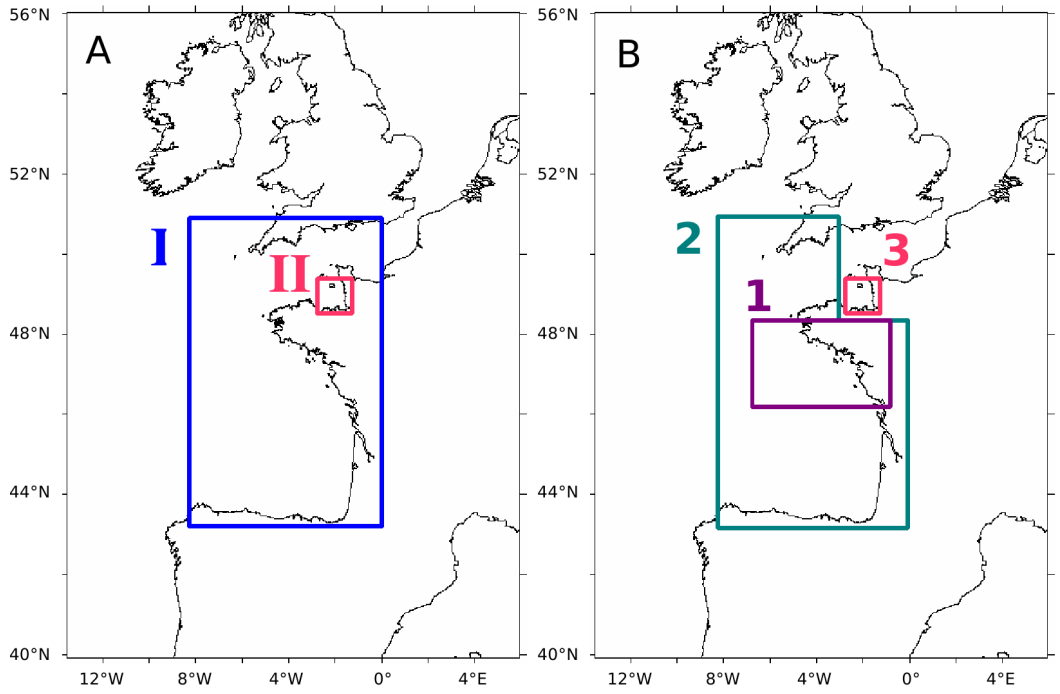


Figure I.29 – Échelles spatiales et méthodes d'étude. (A) Échelles spatiales des études sur le plateau continental du nord-ouest de l'Europe : I) Échelle régionale du Golfe de Gascogne et de la Manche occidentale, et II) Échelle locale du Golfe Normand-Breton. (B) Méthodes d'étude mises en œuvre aux différentes échelles : 1) Échantillonnage *in situ*, 2) Modélisation lagrangienne générique à l'échelle régionale, et 3) Modélisation eulérienne spécifique à l'échelle locale.

### I.7.1 Zone d'étude et problématiques associées

Dans le Nord-Est Atlantique, la **Mer d'Iroise** qui sépare le Golfe de Gascogne de la Mer d'Irlande et de la Manche est considérée comme une zone de transition biogéographique majeure entre les assemblages d'espèces marines tempérées chaudes, définissant la province biogéographique Lusitanienne au sud, et les assemblages d'espèces marines tempérées froides, définissant la province biogéographique Boréale au nord (Figure I.30) (Cox et Moore, 2000; Dinter, 2001).

D'autre part, des études phylogéographiques récentes ont mis en évidence un point de rupture phylogéographique le long des côtes bretonnes pour différentes espèces d'invertébrés à cycle de vie bentho-pélagique (Jolly *et al.*, 2005, 2006; Muths *et al.*, 2009; Rigal, 2005). Ces travaux révèlent d'importantes divergences génétiques de part et d'autre de la Mer d'Iroise, suggérant l'existence de sous-espèces, voire d'espèces cryptiques. Ainsi,

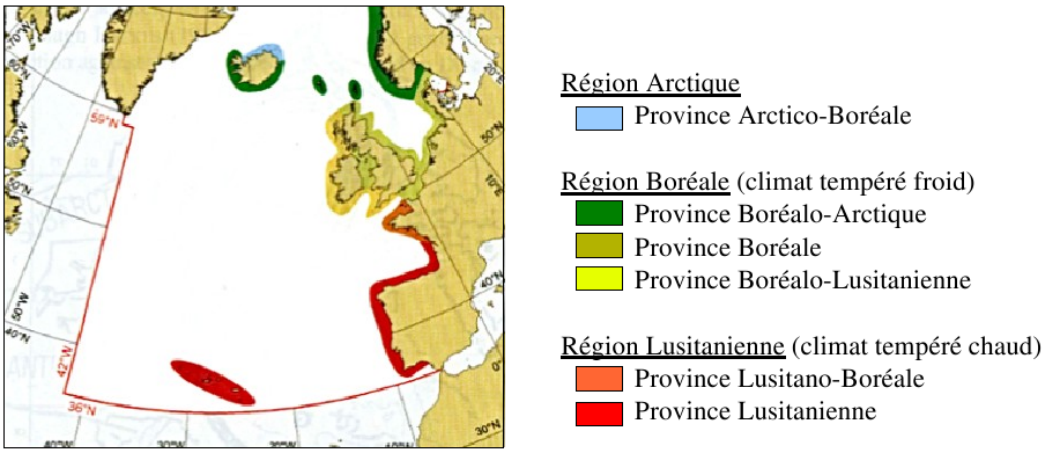


Figure I.30 – Biogéographie dans l'Atlantique Nord-Est, d'après Dinter (2001).

chez le polychète *Pectinaria koreni*, deux clades ont été identifiés : un clade nord regroupant les populations de la Manche, de la Mer d'Irlande, et de la Mer du Nord, et un clade sud incluant les populations du Golfe de Gascogne, ces deux clades ayant été observés en mélange à la frontière de leur distribution à la pointe de la Bretagne, *i.e.* en Mer d'Iroise. De même, chez le polychète *Sabellaria alveolata*, un important contraste phylogéographique est observé entre le Golfe de Gascogne et la région Manche-Mer d'Irlande, même si dans le cas de cette espèce, la présence d'espèces cryptiques n'est pas envisagée. Ce schéma opposant deux régions distinctes peut néanmoins être plus complexe comme cela a été rapporté pour le polychète *Owenia fusiformis* chez lequel trois clades principaux ont été différenciés. Le clade 1 est principalement présent en Mer du Nord et le long des côtes françaises de la Manche et de l'Atlantique alors que le clade 2 est cantonné à la mer d'Irlande et aux côtes sud de l'Angleterre. Le clade 3, trouvé à de plus faibles fréquences, est quant à lui présent des deux côtés de la Manche, exclusivement en zone intertidale.

La Mer d'Iroise se caractérise par un fort hydrodynamisme, avec en particulier la présence de fronts halins et thermiques (Le Boyer *et al.*, 2009; Pingree *et al.*, 1982, 1975) qui pourraient contraindre le transport larvaire et donc la connectivité entre le Golfe de Gascogne et la Manche, conformément aux hypothèses avancées par Gaylord et Gaines (2000) le long des côtes californiennes. Cependant, la présence transitoire à l'entrée de la Manche occidentale d'eaux dessalées en provenance du Golfe de Gascogne (*i.e.* extension des plumes de la Loire et de la Gironde) au début du printemps suggère des échanges

larvaires potentiels entre le nord du Golfe de Gascogne et la Manche occidentale sous certaines conditions hydroclimatiques (Kelly-Gerreyn *et al.*, 2006).

D'autre part, il existe dans le **Golfe de Gascogne** de nombreuses structures hydrodynamiques complexes à méso-échelle, telles que les plumes d'estuaires, des lentilles d'eau dessalées ou des phénomènes d'upwelling et de downwelling (Figure I.31), qui sont susceptibles d'influencer les schémas de dispersion larvaire (Koutsikopoulos et Le Cann, 1996; Puillat *et al.*, 2006, 2004). De telles structures peuvent favoriser tantôt la rétention locale, tantôt le transport vers le sud ou l'export vers le nord (Puillat *et al.*, 2006, 2004). L'impact de ces structures caractérisées par une forte variabilité intra- et inter-annuelle devrait toutefois être fonction de leur présence ou non lors de la période de reproduction des invertébrés côtiers, et de leur pérennité à l'échelle de la durée de vie des larves.

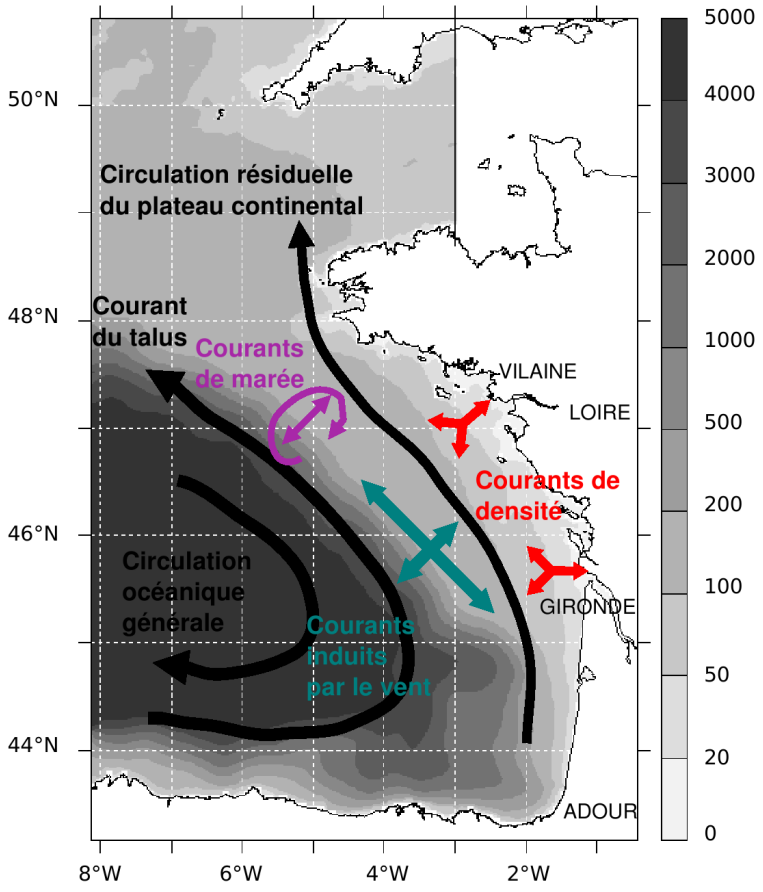


Figure I.31 – Bathymétrie et circulation dans le Golfe de Gascogne, d'après Koutsikopoulos et Le Cann (1996).

L'hydrodynamisme en **Manche occidentale** se distingue très fortement de celui du Golfe de Gascogne par le rôle primordial que tient la marée et par les faibles apports d'eau douce (Pingree *et al.*, 1985). Ainsi, les eaux de la Manche occidentale se caractérisent par un fort brassage sur la verticale et l'absence de stratification saisonnière à l'exception de la limite sud-ouest des côtes anglaises. La marée est également responsable d'une circulation résiduelle orientée schématiquement du sud-ouest vers le nord-est avec des vitesses de courants résiduels comprises en général entre 1 et 5 $cm.s^{-1}$ (Figure I.32) (Salomon et Breton, 1993). En modifiant l'écoulement des masses d'eau, la présence d'accidents topographiques, de caps ou d'îles est à l'origine de la formation de nombreuses structures tourbillonnaires pérennes ou non le long des côtes (Salomon et Breton, 1993). Ces structures sont particulièrement bien développées dans le **Golfe Normand-Breton** où leur rôle sur le transport du matériel dissous ou particulaire est important. Alors que les tourbillons induits par les caps se comportent comme des structures de rétention, les tourbillons qui se développent autour des îles agissent comme des zones de mélange intense (Ménesguen et Gohin, 2006). Il convient néanmoins de souligner que si la marée est responsable de l'essentiel du transport des masses d'eau à long terme, la circulation induite par le vent peut tenir un rôle non négligeable à des échelles de temps plus courtes (Pingree *et al.*, 1975).

### I.7.2 Modèles biologiques

Trois espèces cibles de polychètes occupant un habitat côtier fragmenté ont été sélectionnées dans la présente étude : *Pectinaria koreni*, *Owenia fusiformis*, et *Sabellaria alveolata* (Figure I.33). Ces trois espèces possèdent des caractéristiques biologiques contrastées en matière d'habitat, de durée de vie larvaire, et de comportement natatoire (Table I.2). Leur étude comparative permettra ainsi de vérifier l'importance des traits d'histoire de vie des espèces sur la dispersion et la connectivité dans différents contextes hydrodynamiques. Par ailleurs, leurs larves étant aisément identifiables sur de simples critères morphologiques, elles se prêtent à la réalisation d'observations *in situ* (Figure I.34).

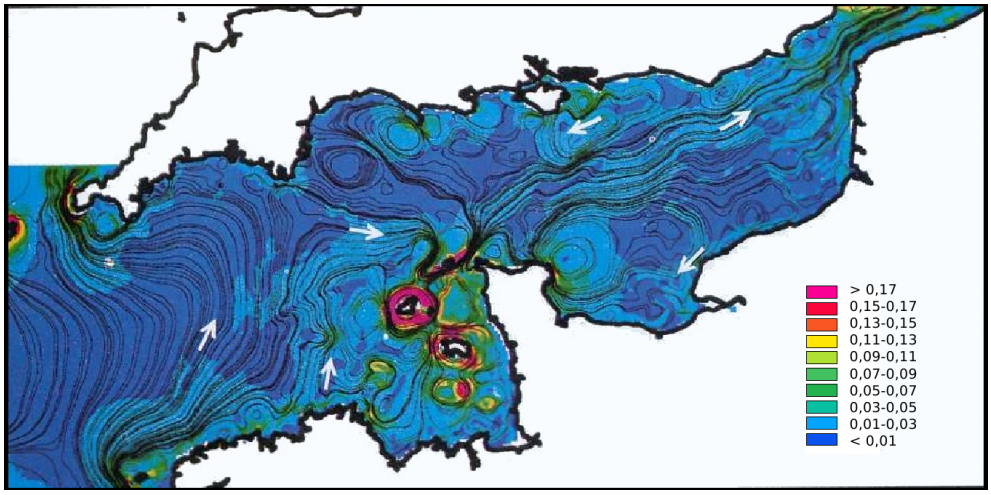


Figure I.32 – Circulation résiduelle en Manche. Les lignes de courant lagrangien sont représentées en condition de marée moyenne et sans vent. L'orientation du courant est indiqué par des flèches blanches. Les vitesses de courants résiduels sont indiquées en $m.s^{-1}$. Figure issue de Salomon et Breton (1993).

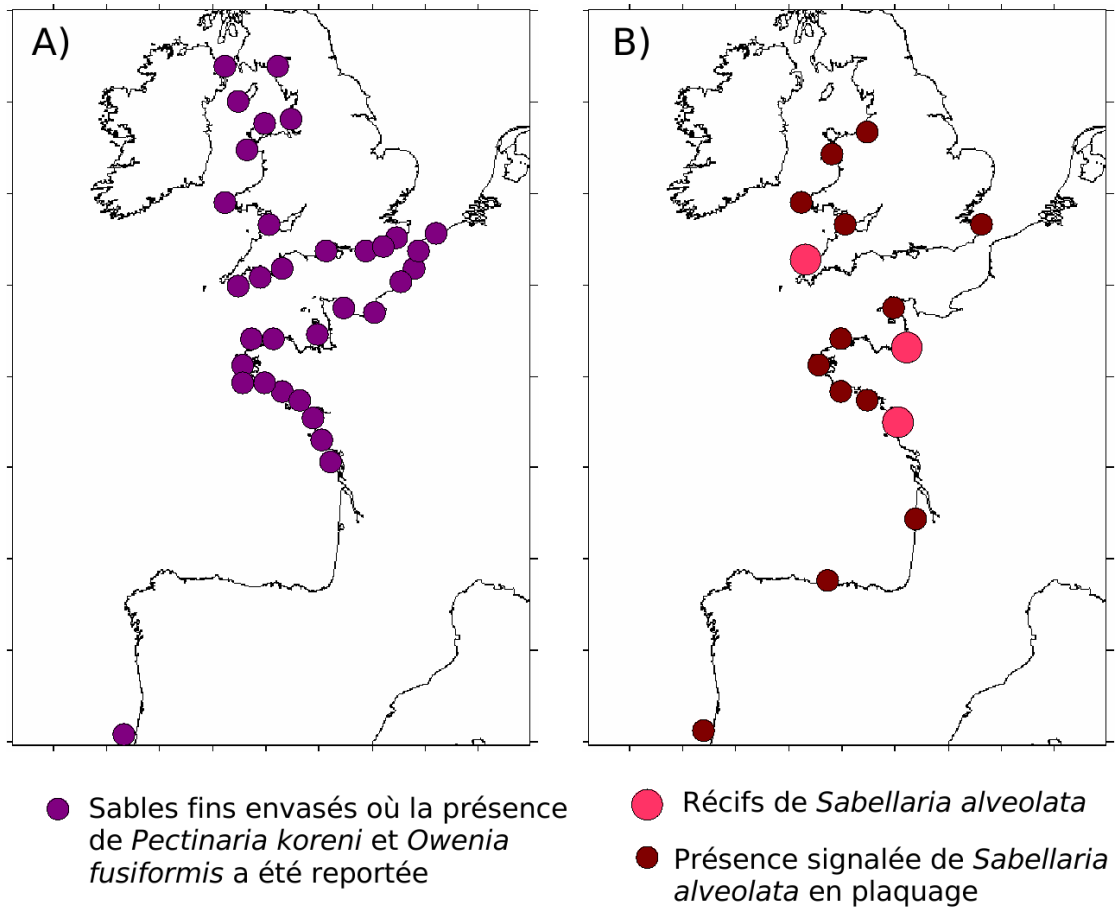


Figure I.33 – Distribution des trois espèces cibles en Atlantique Nord-Est : (A) sédiments fins envasés où la présence de *Pectinaria koreni* et de *Owenia fusiformis* a été reportée, d'après Jolly (2005), et (B) récifs ou plaquage de *Sabellaria alveolata*, d'après Rigal (2005).

Tableau I.2 – Caractéristiques biologiques des trois espèces cibles étudiées, d'après des données d'observation *in situ* (i) en Manche : [1a]Irlinger *et al.* (1991), [1b]Lagadeuc et Retière (1993), [1c]Lagadeuc (1992b), [1d]Thiébaut *et al.* (1996), [2a]Ménard *et al.* (1989), [2b]Gentil *et al.* (1990), [2c]Thiébaut *et al.* (1992), [2d]Dauvin (1992), [3c]Dubois *et al.* (2007) ; et (ii) dans le Golfe de Gascogne : [3a]Gruet (1982), et [3b]Gruet et Lassus (1983).

| | *Pectinaria koreni* | *Owenia fusiformis* | *Sabellaria alveolata* |
|---|---|---|---|
| Habitat fragmenté | Sables fins envasés | Sables fins envasés | Récifs biogéniques |
| Durée de vie | De 12 à 18 mois[1a] | De 3 à 4 ans[2a] | De 4 à 5 ans[3a] |
| Mode de reproduction | Univoltine[1a] | Multivoltine[2a] | Multivoltine[3a] |
| Période de ponte | Mars-Avril et Mai-Juin[1a] | Avril-Juin[2b] | Mars-Avril et Juin-Septembre[3b] |
| Durée de vie larvaire | 2 semaines[1b] | 4 semaines[2b] | de 4 à 10 semaines[3c] |
| Comportement de nage des larves | Migration ontogénique[1c] | Migration ontogénique[2c] | Possible migration tidale[3c] |
| Comportement de sélection de l'habitat | Non | Non[2d] | Oui : grégaire |
| Comportement post-larvaire | Oui : dérive[1d] juvénile | Non | Non |

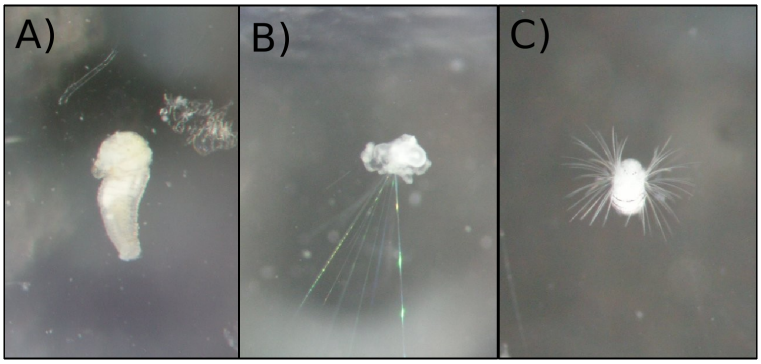


Figure I.34 – Larves des trois espèces cibles de polychètes occupant un habitat côtier fragmenté retenues dans la présente étude : (A) *Pectinaria koreni*, (B) *Owenia fusiformis*, et (C) *Sabellaria alveolata*.

### I.7.3 Méthodes d'étude mises en œuvre

Plusieurs approches complémentaires ont été mises en œuvre (Figure I.29B) : (i) d'une part, l'**observation *in situ*** des abondances larvaires de ces trois espèces dans le Nord du Golfe de Gascogne en relation avec la présence de structures hydrologiques à méso-échelle, (ii) d'autre part, la **modélisation couplée biologie-physique** de la dispersion et de la connectivité, **à l'échelle régionale** du Golfe de Gascogne et de la Manche occidentale en utilisant un modèle lagrangien générique et **à l'échelle locale** du Golfe Normand-Breton en utilisant un modèle eulérien spécifique. À l'échelle régionale du Golfe de Gascogne et de la Manche occidentale, l'utilisation d'un modèle lagrangien générique permettra de suivre individuellement les trajectoires des particules larvaires, et en particulier d'étudier si des larves peuvent être dispersées depuis des populations du Golfe de Gascogne vers des populations de la Manche et dans quelles circonstances (*i.e.* date de ponte, durée de vie larvaire, nature du comportement migratoire). À l'échelle locale du Golfe Normand-Breton, l'utilisation d'un modèle eulérien spécifique permettra de simuler la dispersion d'un nombre élevé de larves de *Sabellaria alveolata* avec une fine résolution spatiale et temporelle. À cette seconde échelle, l'élaboration du modèle et l'analyse des résultats simulés a pu s'appuyer sur de précédentes observations *in situ*.

### I.7.4 Plan de la thèse

L'objectif majeur de ce travail de thèse a été d'évaluer les rôles relatifs joués par les processus hydrodynamiques et hydroclimatiques, et les traits d'histoire de vie d'invertébrés à cycle bentho-pélagique sur la dispersion larvaire et la connectivité en milieu côtier dans le Golfe de Gascogne et la Manche occidentale. Le présent manuscrit s'articule ainsi autour de deux parties, correspondant respectivement à l'échelle régionale du Golfe de Gascogne et de la Manche occidentale et à l'échelle locale du Golfe Normand-Breton, et de quatre chapitres traitant les questions suivantes :

**(1) Comment les structures hydrodynamiques à méso-échelle du nord du Golfe de Gascogne influencent la distribution *in situ* du méroplancton ?**

À partir de l'**échantillonnage *in situ*** du méroplancton dans le Nord du Golfe de Gascogne, ce premier chapitre décrit les **distributions** horizontale et verticale des larves des trois espèces cibles d'invertébrés côtiers en fonction des **structures hydrologiques** à **méso-échelle** observées au cours du printemps lors de la mise en place de la stratification saisonnière de la colonne d'eau. Les résultats obtenus permettent de discuter de l'importance relative des facteurs hydrologiques et de la structuration spatiale de cet environnement sur les distributions larvaires et la dispersion.

**(2) De quels paramètres dépendent la dispersion et la connectivité le long des côtes Atlantiques françaises ? Existe-il une barrière physique à la dispersion et à la connectivité entre le Golfe de Gascogne et la Manche ?**

Dans ce second chapitre, un **modèle lagrangien** générique de dispersion larvaire est utilisé pour simuler en conditions hydroclimatiques réalistes la dispersion larvaire d'invertébrés à cycle bentho-pélagique et la connectivité entre populaions dans le Golfe de Gascogne et de la Manche occidentale. Les principaux facteurs hydrodynamiques et biologiques influençant la dispersion larvaire sont décrits en mettant plus particulièrement l'accent sur le lieu de ponte, la date de ponte, la durée de vie larvaire et les comportements migratoires. Les résultats issus des simulations sont analysés afin d'identifier les

facteurs qui favorisent ou limitent les flux larvaires à travers la **zone de transition biogéographique** entre le Golfe de Gascogne et la Manche.

**(3) Comment le changement climatique est-il susceptible de modifier la dispersion larvaire et la connectivité dans le Golfe de Gascogne et en Manche ?**

Dans ce troisième chapitre, plus court que les précédents, le modèle biophysique générique précédemment développé à l'échelle régionale est utilisé pour tester plusieurs hypothèses sur les conséquences possibles du **changement climatique** sur la dispersion et la connectivité des invertébrés marins. Nous testerons en particulier les conséquences d'une période de ponte précoce et de durées de vie larvaire raccourcies.

**(4) Quelle est l'importance relative des processus hydroclimatiques et des caractéristiques biologiques sur la connectivité des récifs biogéniques construits par le polychète *Sabellaria alveolata* en Baie du Mont-Saint-Michel (Golfe Normand-Breton) ?**

Dans ce dernier chapitre, un **modèle eulérien** spécifique de la dispersion larvaire de l'espèce *Sabellaria alveolata* à l'échelle locale du Golfe Normand-Breton est utilisé pour estimer la connectivité entre les récifs biogéniques construits par cette espèce en baie du Mont-Saint-Michel. Si *Sabellaria alveolata* est une espèce largement répandue sur le littoral européen, elle constitue des récifs de grande ampleur uniquement dans un nombre réduit de sites tels que la baie de Bourgneuf sur le littoral Atlantique, la baie du Mont-Saint-Michel en Manche ou Duckpool en Mer d'Irlande. Les résultats obtenus, qui décrivent l'influence relative de la variabilité intra- et inter-annuelle des conditions hydroclimatiques sur la dispersion et la connectivité de cette espèce, permettent d'évaluer le rôle de la dispersion dans un contexte **conservation d'un patrimoine naturel**.

## Première partie

# Impact des facteurs hydroclimatiques sur la dispersion larvaire à l'échelle régionale du Golfe de Gascogne et de la Manche occidentale

# Dispersion et connectivité dans le Golfe de Gascogne et en Manche occidentale

Tandis que l'hydrodynamisme en Manche occidentale dépend principalement des conditions de marée, l'hydrodynamisme du Golfe de Gascogne se caractérise par de nombreuses structures hydrodynamiques à méso-échelle (de l'ordre de la centaine de mètres à la dizaine de kilomètres), incluant en particulier des fronts thermiques ou halins, des plumes d'eau dessalées issues des principaux fleuves (*i.e.* Gironde, Loire, Vilaine), des lentilles d'eau dessalées détachées de ces plumes, ou encore des upwellings côtiers (*i.e.* remontée en surface d'eaux profondes, froides et riches en nutriments). Ces structures à méso-échelle sont susceptibles de fortement contrôler le transport et la dispersion larvaire, et donc la connectivité des populations marines. Sachant que la Mer d'Iroise qui sépare le Golfe de Gascogne de la Manche occidentale correspond à une zone de transition entre les provinces biogéographiques boréale et lusitanienne, la première partie de cette thèse vise à identifier les principaux facteurs qui influencent la dispersion et la connectivité des populations d'invertébrés à cycle bentho-pélagique à une echelle régionale, à travers une zone de transition biogéographique. À la suite de l'analyse de résultats issus d'observations *in situ* et du développement d'un modèle lagrangien générique de transport larvaire, les attendus de cette première partie sont de déterminer dans quelle mesure les mécanismes de transport contemporains peuvent favoriser ou non le maintien d'une barrière biogéographique et dans quelle mesure des modifications des schémas de dispersion pourraient modifier les aires de distribution des espèces.

Le premier chapitre est basé sur des mesures hydrologiques *in situ* et un échantillonnage du méroplancton réalisés dans le Nord du Golfe de Gascogne, de l'estuaire de la Loire à la baie de Douarnenez. Il décrit la distribution des différents stades larvaires des trois espèces cibles de polychètes retenues dans le cadre de cette étude en relation avec la variabilité des structures hydrologiques observées à méso-échelle. Les trois espèces cibles choisies (*i.e. Pectinaria koreni*, *Owenia fusiformis* et *Sabellaria alveolata*) possèdent des traits d'histoire de vie contrastés (habitat des populations adultes, durée de vie larvaire,

comportement larvaire) ainsi que des structures génétiques différentes au regard des zones biogéographiques identifiées.

Dans le second chapitre, la dispersion larvaire d'invertébrés marins côtiers est modélisée à l'échelle du Golfe de Gascogne et de la Manche occidentale grâce à l'utilisation d'un modèle couplé biologie-physique. La dispersion larvaire est simulée de manière lagrangienne (suivi des trajectoires individuelles des particules larvaires) en conditions hydroclimatiques réalistes afin de décrire la connectivité à l'échelle de la zone d'étude et les probabilités d'échanges. Il s'agit avant tout d'un modèle générique visant à comprendre le rôle de différents paramètres biologiques en interactions avec les propriétés hydrodynamiques de la zone d'étude sur les schémas de transport des larves d'un invertébré côtier occupant un habitat fragmenté. Il convient néanmoins de préciser que certains paramètres pris en compte dans le modèle correspondent à ce qui était connu chez les polychètes *Pectinaria koreni* et *Owenia fusiformis* en ce qui concerne la localisation des populations adultes ou la durée de vie larvaire.

Enfin, dans un troisième chapitre, plus court que les précédents, les conséquences potentielles du changement climatique sur la dispersion larvaire et la connectivité des populations marines à l'échelle du Golfe de Gascogne et de la Manche occidentale sont explorées. Deux conséquences potentielles sont en particulier développées sous l'hypothèse qu'une augmentation des températures entrainera, d'une part, des pontes précoces et, d'autre part, des durées de vie larvaire raccourcies.

Ces deux premiers chapitres font l'objet d'un article en préparation et d'un article soumis, tandis que le troisième chapitre est inclu dans un article de synthèse regroupant plusieurs cas d'étude. Cet article de synthèse est présenté en Annexe E.

# Chapter 1

# Meroplankton distribution in relation with coastal mesoscale hydrodynamic structures in the northern Bay of Biscay

## The role of frontal structures and river plumes in the distribution of coastal invertebrate larvae

Sakina-Dorothée AYATA, Robin STOLBA, Thierry COMTET, and Éric THIÉBAUT

Manuscript in preparation[a]

[a]This chapter corresponds to a draft that will be submitted for publication in *Journal of Plankton Research*. It benefited from the valuable work of Robin Stolba for the larval sorting of the cruise of June 2008, and from the help of Thierry Comtet and Robin Stolba for the molecular biology analyses.

## 1.1 Abstract

The numerous and complex mesoscale hydrodynamic structures observed in the northern Bay of Biscay (e.g., fronts, river plumes, low salinity lenses, upwellings) may strongly constrain larval transport of marine benthic organisms with a complex life cycle and may impact connectivity among discrete marine populations. In this context, the present work aimed to describe the larval horizontal and vertical distribution of three target species of polychaetes with contrasted life history traits (i.e., *Pectinaria koreni*, *Owenia fusiformis* and *Sabellaria alveolata*) in the northern Bay of Biscay in relation with the seasonal variability of the mesoscale structures. During two consecutive cruises in May and June 2008, hydrographic variables were recorded and mesozooplankton samples were collected along seven inshore-offshore transects of eight stations. The analysis of the hydrological typology of the sampled water masses highlighted the presence of river plume waters extending along the Southern Brittany coast and characterised by low surface salinities. In addition, strong latitudinal thermal gradients were observed in relation with the seasonal stratification of the water masses. For the three species, the highest larval abundances were generally observed at the coastal stations characterised by the lowest surface salinity, i. e., within the low salinity water plumes from the Vilaine and Loire. Combined with multiple regressions and redundancy analyses, variance partitioning demonstrated the preponderant importance of the spatial structure of the hydrological environment in the variability of larval abundances. Geographical space alone also explained a significant part of the spatial variations of larval abundances, probably in relation with the spatial variations of adult distribution, whereas hydrological properties alone were insignificant. The variability of larval abundances between the two cruises could be related to the strong spring variability of the hydrodynamic conditions in the Bay of Biscay, due to the variability of the river run-offs and to the meteorological conditions, and to spawning events from adult populations. For two of the three target species, *P. koreni* and *O. fusiformis*, the analysis of larval vertical distribution at seven stations showed higher larval concentrations in surface mixed layer waters or in the thermocline.

## 1.2 Introduction

For benthic invertebrates with a complex life cycle, pelagic larval transport is a key process in dispersal and population connectivity, playing a major role in population establishment and persistence, biodiversity conservation, invasion of alien species, and species distribution (Cowen & Sponaugle, 2009; Levin, 2006). Larval transport results from the interactions of both biological traits (e.g., larval vertical behaviour, larval life span, spawning location and date) and hydrodynamic processes (i.e., advection, eddy-diffusion) (Pineda , 2007). In coastal environment, numerous and complex mesoscale hydrodynamic features, such as eddies, fronts, river plumes, or upwellings, which are highly variable in space and time, can strongly constrain the transport of planktonic organisms (Largier, 2003). Eddies increase the residence time of water masses and can trap pelagic larvae, favouring larval retention in the vicinity of either parental populations or unsuitable habitat (Ayata , 2009; Dubois , 2007). Hydrological fronts, due to sharp gradients in physical properties between two water masses in contact, have important implications in plankton ecology (Largier, 1993; Le Fèvre, 1986). They are often characterised by high abundances and biomasses of phyto- and zooplankton, due to high primary production favoured by high nutrient inputs and/or organism accumulation caused by convergent currents (Frontier, 1986; Pingree , 1974). Since passive larvae are advected by the ocean currents, their distribution can be tied to the distribution of water masses such as estuarine plumes (Shanks , 2002). Thus, river plume frontal systems and tidally-generated fronts can influence the distribution of passive larvae, by restraining them among different water masses, and by acting as physical barriers to offshore transport of coastal invertebrate larvae (Shanks , 2003c; Thiébaut, 1996). However, invertebrate larvae do not always behave passively and can be able to migrate vertically (Garland , 2002). During upwelling events, when surface currents can induce offshore transport, coastal invertebrate larvae are not necessarily flushed offshore because of their swimming behaviour (Shanks , 2003b). Similarly, in estuaries characterised by a two-layer circulation, the interaction of vertical swimming behaviour of coastal invertebrate larvae with horizontal currents differing from the surface

to the bottom can influence the direction of their transport and favour their retention in the vicinity of suitable habitat (Thiébaut , 1992).

In the Bay of Biscay (North-East Atlantic) numerous and complex mesoscale features, including frontal systems, river plumes, upwellings, or low salinity lenses, have been reported (Koutsikopoulos & Le Cann, 1996; Puillat , 2006). In the north of the Bay, seasonal thermal fronts occur in the Ushant Sea and in the Bay of Douarnenez (Mariette & Le Cann, 1985; Morin , 1991). In spring, wind-induced coastal upwellings have been described in the north and in the east of the Bay of Biscay. When low salinity waters of river plumes are pushed offshore, low salinity lenses of 50-80 km width and about 30 m thickness can be formed (Puillat , 2006). Those mesoscale structures, mainly governed by short term meteorological variability, are highly variable in space and time (Puillat , 2006). In the south-eastern part of the Bay of Biscay, previous zooplankton surveys have underlined the role of a few hydrological variables, including surface salinity and stratification, in explaining the zooplankton distribution and demonstrated the importance of low salinity river plume waters in structuring zooplanktonic communities (Albaina & Irigoien, 2007; Cabal , 2008; Zarauz , 2007). However, in the northern part of the Bay, previous plankton surveys have only focused on phytoplankton communities (Maguer , 2009; Morin , 1991). Those studies highlighted the seasonal evolution of nutrient and chlorophyll *a* distributions in relation with seasonal hydrological variability of river plume waters from the Vilaine and the Loire rivers.

Several statistical methods that model spatial and temporal relationships in ecological data have been recently developed and used to describe the distribution of zooplankton in relation with hydrological environment. For example, generalized linear models (GLM) aim at modelling the variations of a given variable (e.g., larval densities) as an additive linear function of several explanatory variables (e.g., hydrological parameters). Generalized additive models (GAM) are the non-parametric extension of the GLM, by making the assumption that the components of the additive function are spline smooth functions of the explanatory variables (see Albaina & Irigoien, 2007, or Zarauz , 2007, for examples of the use of those methods to analyse zooplankton distribution). However, a limitation of those methods is that they neglect the spatial structure of the environmental variables.

Likewise, most multivariate analysis technics, such as clustering and ordination which are commonly used to describe the structure of zooplankton communities, do not separate the spatial component of the community structure from the environment component. Yet, the spatial patterns of the response variable (e.g., larval distributions) depend on (1) the environment alone, (2) the geographic space alone, (3) the interaction of the space with the environment, i.e., the spatial structure of the environment, and (4) other undetermined factors (Borcard , 1992). Hence, the spatial structure of the hydrological environment should be taken into account when describing spatial patterns of zooplankton. For example, using variance partitioning based on canonical correspondence ordination (CCA), Belgrano (1995a,b) demonstrated the importance of the spatial structure of the hydrological environment in structuring meroplankton distribution in the North Sea. Here, we used variance partitioning based on multiple regressions and redundancy analyses (RDA), which are the direct extension of multiple regressions for multivariate response variables, in order to describe the meroplankton distribution in the northern Bay of Biscay.

In the present study, we focused on the larval distribution of three target species of coastal polychaetes with contrasted life history traits, mainly in terms of adult habitat and larval life span: *Pectinaria koreni*, *Owenia fusiformis* and *Sabellaria alveolata*. *P. koreni* and *O. fusiformis* inhabit patches of muddy fine sand sediments in shallow coastal waters. *P. koreni* is a univoltine species living 15-18 months with two main spawning periods, in March-April and May-June in the Bay of Seine, English Channel, (Irlinger , 1991) and from May to July and in automn in the northern Bay of Biscay (Le Bris, 1988). From *in situ* observations of *P. koreni* larvae in the Bay of Seine, a 2-week planktonic larval duration has been estimated (Lagadeuc & Retière, 1993). *O. fusiformis* is a multivoltine species living about three to four years with a main spawning period in April-June in the Bay of Seine (Gentil , 1990; Ménard , 1989) and a planktonic larval duration reaching one month (Thiébaut , 1992; Wilson, 1932). *Sabellaria alveolata* is a gregarious polychaete building intertidal biogenic reefs. It is a multivoltine species that lives four to five years in the Bay of Biscay (Gruet, 1982). From *in situ* survey in the Bay of Biscay, its reproductive period was estimated to last all the year, with two main reproductive peaks in March-April and June-July (Gruet & Lassus, 1983). From *in situ* survey in the Bay of Mont-Saint-

Michel, English Channel, a planktonic larval duration lasting from four to ten weeks was calculated (Dubois , 2007).

Focusing on these three target species of coastal polychaetes, the aim of the present study was to describe the horizontal and vertical distribution of larvae in relation with seasonal mesoscale hydrological structures observed in spring in the northern Bay of Biscay. Through the use of variance partitioning, we tested if larval distribution patterns were explained by (1) the hydrological environment alone, i.e., if the larvae were constrained within typical water masses under the assumption that they behave passively, (2) the geographical space alone, i.e., if spawning location influenced larval distribution, and/or (3) the interaction of the hydrological environment with the geographical space, i.e., if the spatial structure of the hydrological environment was the most important factor in structuring meroplankton distribution in the Bay of Biscay. Main processes involved in the control of larval transport in coastal zones of the Bay of Biscay are then discussed.

## 1.3 Material and methods

### 1.3.1 Study area

The Bay of Biscay (43°N-48°30'N, 12°W-1°W) is an open oceanic bay of the NE Atlantic, delimited by the French coasts in the north and east and by the Spanish coasts in the south. In the north, the Bay of Biscay is connected to the English Channel at the tip of Brittany through the Ushant Sea. Whereas the continental shelf is very narrow in the south of the Bay of Biscay along the Spanish coasts (maximum width of 30 km), it enlarges itself northwards along the French coasts (maximum width of 180 km). The hydrodynamics of the bay has been extensively studied and is relatively well known (Koutsikopoulos & Le Cann, 1996). Since the circulation over the continental shelf mainly depends on winds and horizontal density gradients, with weak tidal influence at the south of 48°30'N, strong interannual and seasonal variations in hydrodynamics and hydrology have been reported. Over the abyssal plain the general circulation is weak, with a clockwise circulation along the continental slope and mesoscale eddies. The Bay of Biscay receives strong freshwater run-offs from the Vilaine, the Loire, the Gironde, and the Adour. The Loire and the Gironde are the two main rivers of the bay, with annual mean freshwater outflows of 900 $m^3.s^{-1}$ each, minimum discharges of 200 $m^3.s^{-1}$ in summer and maximum outflows reaching on average 3,000 $m^3.s^{-1}$ in winter and spring. From January to the beginning of April, the water column is homogeneous in the Bay of Biscay, except in the vicinity of estuaries and coastal areas where strong freshwater inputs, combined with relatively low vertical mixing, can cause strong haline stratification. Thermal stratification appears in spring, in April in the western coastal part of the Bay or in May over the continental shelf, and occurs until mid-September. This seasonal thermocline results from the increase in sea surface temperature and the decrease in mean wind speed and mean freshwater run-offs. Strong vertical temperature gradients, with temperature differences between surface and bottom layers of 9-10°C, are observed in summer and early autumn. Thermal stratification reveals a homogeneous cold pool of water extending from the Southern Brittany down to the Gironde estuary between approximately the 70 and 130 m isobaths, with nearly constant temperature of 11°C all along the year. In the vicinity of the Loire and Gironde estuaries,

the presence of low salinity surface waters (LSSW) in spring induces significant density gradients responsible for strong density currents over the shelf (2-20 $cm.s^{-1}$), generally oriented northwards because of the Coriolis force. Over the continental shelf of the Bay of Biscay, wind-induced currents are highly variable in direction and speed at temporal scales from day to season, although a general wind-induced circulation parallel to the isobaths can be observed. In the north of the bay wind-induced currents usually reach 10 $cm.s^{-1}$ to 20-30 $cm.s^{-1}$ locally. From spring to summer, wind mainly blows from NW (Le Cann & Pingree, 1995). During thermal stratification, local transitory upwellings are induced by NW to N winds in the south of the Loire (coastline oriented N-S), and by W to NW winds in the north of the Loire (coastline oriented NW-SE) (Puillat , 2006). On the contrary, a persistent upwelling occurs in the south of the bay along the Cantabrian coasts. Lenses of low salinity surface waters of 50-80 km wide and about 30 m thick, have been reported over the shelf during W to N wind events and can be transported offshore at least 100 km from the coastline (Puillat , 2006). At the western tip of Brittany, the Ushant Sea is described as a transitional area between the well mixed waters of the English Channel and the stratified waters of the Bay of Biscay in the south and the Celtic Sea in the west (Pingree , 1982). Moreover, strong thermal fronts are caused in spring and summer in the Ushant Sea and in the Douarnenez Bay by tidal mixing (Morin , 1991; Pingree , 1975). Low salinity (<35) waters from the Loire and Gironde have been reported from March to April in the Ushant Sea and at the entrance of the English Channel under NE winds and strong river run-offs (Kelly-Gerreyn , 2006).

### 1.3.2 Sampling strategy

Data were collected in the northern Bay of Biscay (48°30'N-46°30'N, 2°W-5°W) aboard the RV *Côtes de la Manche* during the LARVASUD cruises which were carried out from 10 to 18 May and from 9 to 13 June 2008. Along seven inshore-offshore transects, eight stations were sampled and numbered from the 20 m-isobath to the open sea (Figure 1.1). The three first stations were separated by 3 nautical miles, whereas the other ones were separated by 6 nautical miles; the total transect length was about 67 km. A total of 54 stations were

sampled during each cruise. The two cruises occurred in average and neap tide conditions and sampling was performed only during daytime, since no diel vertical migration was previously observed for the larvae of the three target species.

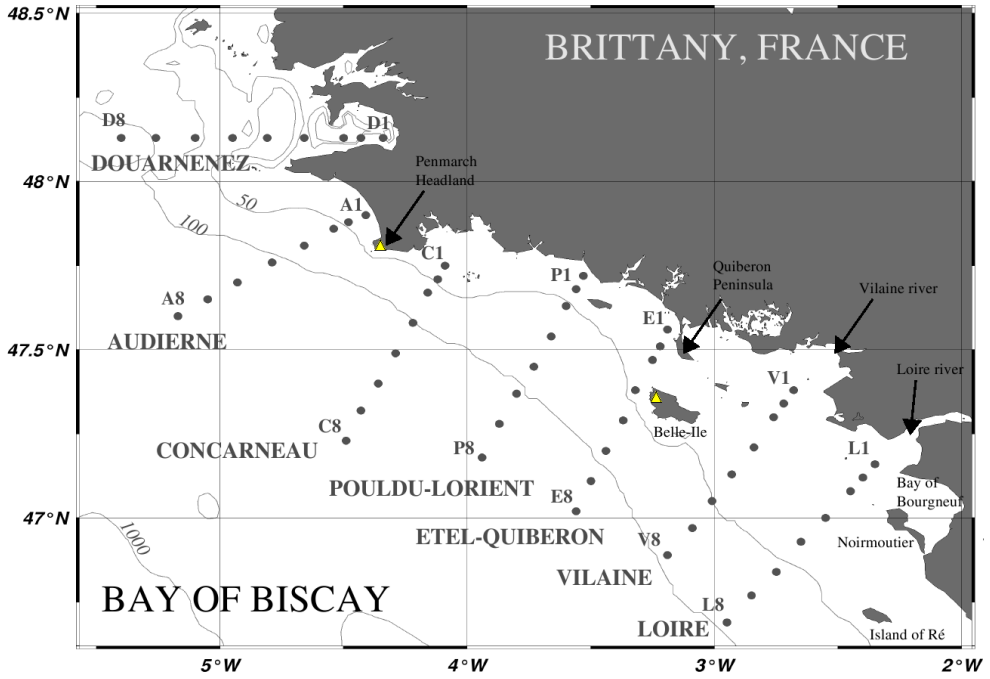


Figure 1.1: Study area and locations of the sampled stations. The name of the seven inshore-offshore transects and the name of the first and last stations of each transect are indicated. Yellow triangles indicate the locations of the semaphores of Penmarch and Belle-Ile.

Transects were localized in front of the main coastal bays and estuaries of the study area where coastal invertebrates confined to fine sediments form isolated populations: Douarnenez Bay, Audierne Bay, Concarneau Bay, Lorient Harbour, Quiberon Peninsula, Vilaine estuary, and Loire estuary (Figure 1.1). Hence, the transect localization was chosen to coincide with the main adult populations of *Pectinaria koreni* and *Owenia fusiformis* that occupy patchy habitats of muddy fine sand sediments at about 10-20 m depth (Glémarec, 1969; Guillou, 1980; Jolly , 2005, 2006) (Figure 1.2). Concerning *Sabellaria alveolata* that builds intertidal reefs, large reefs have been reported on sandflats in the lower intertidal zone in the Bay of Bourgneuf in the southern vicinity of the Loire Estuary (Gruet, 1982), while veneers adhering to rocks in the mid-level of the intertidal zone have also been reported all along the southern Brittany coasts (Rigal, 2005).

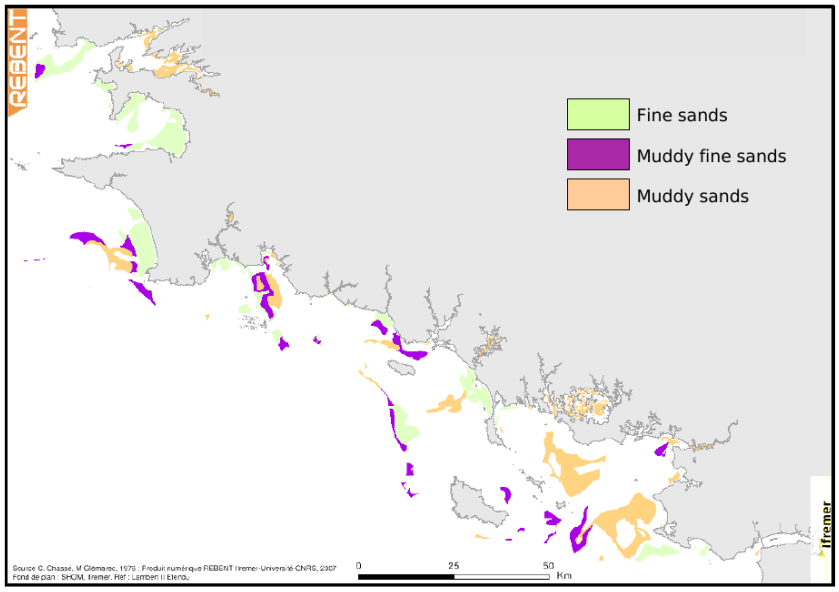


Figure 1.2: Distribution of coastal and infralittoral fine sediments in the northern Bay of Biscay, from Chassé & Glémarec (1976), numeric product of REBENT Ifremer-Université-CNRS, 2009. *Pectinaria koreni* and *Owenia fusiformis* populations occupy patchy habitats of muddy fine sand coastal sediments, but have also been reported in fine sand and muddy sand sediments.

### 1.3.3 Environmental data

At each station, hydrological data were recorded along the water column using a Conductivity-Temperature-Depth (CTD) probe SeaBird SBE 19+ with pumping system in May and a CTD probe SeaBird SBE 19 in June (Figure 1.3A). Vertical profiles from the surface to the bottom or to a maximum of 50m-depth were obtained. CTD data recorded during the down cast were averaged every meter. Data on water density were expressed as values of $\sigma_t$ (sigma-t) (UNESCO, 1983). Thermocline, halocline, and pycnocline depths, that can differ from each other in the Bay of Biscay, were calculated using a theoretical two-layer model of the water column (Figure 1.4). In such a model and for a given hydrological variable $X$, the water column is assumed to be composed of two distinct and homogeneous layers, a surface layer of width $z_x$, and a bottom layer of width $z_b - z_x$. Thus, the mix layer depth $z_x$ is given by the formula:

$$z_x = z_b \frac{|X_m - X_b|}{|X_s - X_b|} \qquad \text{(Eq. 1.1)}$$

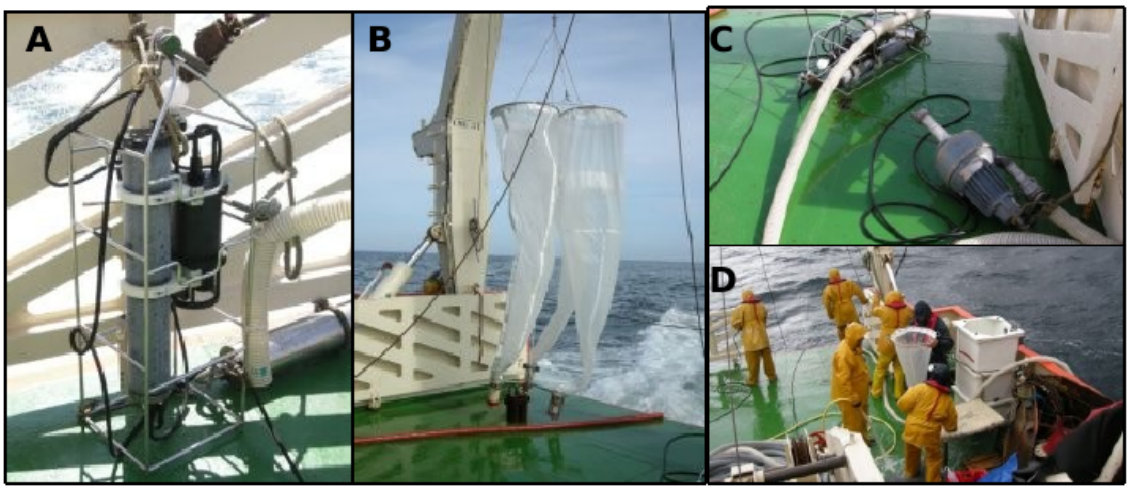


Figure 1.3: Sampling material: (A) CTD probe, (B) triple WP2 net, (C) pumping system including pump and pipes, and (D) net and tub used to filter the pumped water.

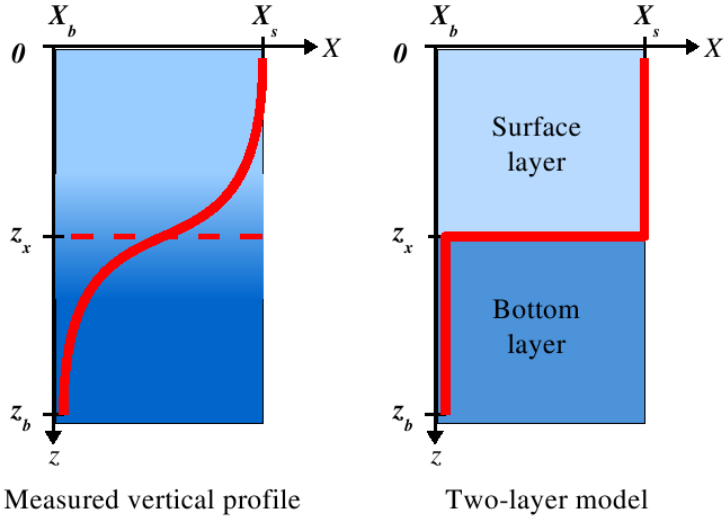


Figure 1.4: Two-layer model of the water column used to calculate the mix layer depth $z_x$ of a hydrological variable $X$.

with $z_b$ the water column height, $X_m$ the mean value of the variable $X$ from surface to bottom, $X_b$ the value of the variable $X$ in the bottom layer, and $X_s$ the value of the variable $X$ in the surface layer. The variable $X$ stands for the temperature $T$, the salinity $S$, or the density $\sigma_t$ to calculate the thermocline, the halocline, and the pycnocline depth respectively.

At each station, a stratification index $\hat{S}$ of the water column was defined by integrating and averaging the vertical density profile, i.e., as the mean of the density differences along the water column (Fortier & Leggett, 1982; Thiébaut , 1992):

$$\hat{S} = \frac{1}{n}\sum_{i=1}^{i=n}\Delta\sigma_{ti}.\Delta z_i \qquad \text{(Eq. 1.2)}$$

with $n$ the number of pairs of adjacent measurements, $\Delta\sigma_{ti}$ the difference in water density between the i$^{\text{th}}$ pair of measurements, and $\Delta z_i$ the depth interval between the i$^{\text{th}}$ pair of measurements. In the present case, the depth interval $\Delta z_i$ was fixed at 1 m.

To complement *in situ* data, satellite images of chlorophyll *a* surface concentrations during the two cruises were obtained from IFREMER[b]. Here 4-day merged images will be presented to minimize cloud coverage.

Wind data recorded in spring 2008 at two semaphores located in the north and in the centre of the study area, one at the Penmarch headland between Audierne and Concarneau (47°47'N, 04°22'W), the other one at Belle-Ile Island offshore Quiberon Peninsula (47°18N, 3°13'W), were provided by Météo France (see Figure 1.1). The wind data recorded at the two semaphores were very close, indicating that wind conditions were homogeneous all over the study area. Only the data collected at Penmarch will be presented (see Annex A.1 for the wind conditions recorded in Belle-Ile). Daily-averaged zonal and meridional wind components were calculated from hourly raw data.

River flows from the Vilaine and the Loire recorded daily in 2008 were provided by the French freshwater office database[c].

### 1.3.4 Mesozooplankton sampling

To describe the horizontal larval distribution, zooplankton samples were collected at each station using a vertical haul from the bottom (or from a maximum depth of 50 m) to the surface with a triple WP2 plankton net (3 replicates) of 80 µm mesh-size and 0.125 m$^2$ of mouth area (Figure 1.3B). A TSK flow meter (Tsurumi Seiki Co., Ltd., Yokohama,

[b] http://cersat.ifremer.fr/data/view/nausicaa
[c] http://www.hydro.eaufrance.fr

Japan) was fixed at one of the net mouth to determine the filtered water volume. Filtered volumes varied from 2.6 to 19.9 $m^3$ per station, with a mean value of about 10 $m^3$. Immediately after collection, the samples from the first net were preserved with 3 % formaldehyde buffered with sodium tetraborate, whereas the samples from the second net were preserved in 96 % ethanol for molecular identification of larvae (see Annex A.2). Finally, the zooplancton sampled from the third net was observed alive on board to verify the presence of the target species larvae.

To determine the larval vertical distribution in relation with the water column stratification, zooplankton samples were also collected at fixed depths using a pumping system. A 5 cm diameter collection pipe was attached to the CTD armature and to an immerged pump (Figure 1.3C). CTD records provided informations on the depth and on the water properties from which samples were collected. Three to four depths were selected to collect plankton samples within the surface layer (about 3-5 m), within the halocline and/or thermocline layer (about 10-15 m), and within the bottom layer (about 20-40 m). Water from the pump was filtered through a 80 µm mesh net suspended in a large tub of water (Figure 1.3D). With a pumping rate of 300 $l.min^{-1}$, a volume of 1.5 $m^3$ of water was filtered at each sampled depth (pumping time of 5 min). Like the WP2 vertical haul samples, those samples were preserved immediately after collection in 3 % buffered formaldehyde.

Owing to the time required to sort the zooplankton samples, larval vertical distributions were described only for a few typical stations when the larval abundances obtained from the WP2 vertical haul sampling were important enough given the small volume pumped (i.e., at least a few hundreds of $ind.m^{-3}$).

### 1.3.5 Larval identification and counting

In the laboratory, each sample was washed free of formaldehyde with filtered sea water on a 80 µm sieve, transferred to a 250 ml beaker and made up to 200 ml with filtered sea water. It was then homogenized by vigorous random stirring and a sub-sample of 5 ml was pipetted into a reticulate Dolfuss receptacle of 200 distinct cells where larvae were randomly distributed. The larvae of the three target species were enumerated in

3 to 5 sub-samples, in order to count at least a hundred of larvae per sample and per species (Frontier, 1972). When total zooplankton concentration was low (mainly in vertical or offshore station samples), the sample was made up to 100 ml only. Conversely, when concentration was high, the sub-sample volume was reduced to 3 ml. Between 3 and 20 % of the total sample was totally sorted. Larval abundances were expressed as number of larvae per $m^3$.

Larvae were identified and counted under a dissecting stereomicroscope. Larval developmental stages were morphologically identified for *Pectinaria koreni*, *Owenia fusiformis* and *Sabellaria alveolata* larvae.

For *P. koreni*, four larval stages were identified from the larval development description given by Lagadeuc & Retière (1993):

- Stage 1: 2-5 day old trochophore larva, between 150 and 230 µm long, with apparition of oral lobes;
- Stage 2: 4-10 day old metatrochophore larva, between 230 and 580 µm, with clearly visible oral lobes and segmentation;
- Stage 3: 8-12 day old metatrochophore larva, between 580 and 750 µm, with internal palea visible by transparency and the progressive appearance of setae;
- Stage 4: aulophore larva, longer than 750 µm, with external palea and the apparition of a mucus tube.

For *O. fusiformis*, four development stages for the mitraria larvae were identified according to Wilson (1932):

- Stage 1: 1-6 day old mitraria larva, between 150 and 200 µm long, with strait prototroch and two to eight bristles;
- Stage 2: 6-17 day old mitraria larva, between 200 and 550 µm, with the prototroch arched in front, behind and at sides; the overall number of bristles increases;
- Stage 3: 17-24 day old mitraria larva, between 550 and 600 µm, with an arched prototroch and a trunk rudiment visible dorsally;

- Stage 4: 25-30 day old mitraria larva, between 600 and 710 µm, with a clearly visible segmented trunk.

For *S. alveolata*, four larval stages were identified according to Cazaux (1964), Wilson (1968b) and Dubois (2007):

- Stage 1: trochophore larva, between 90 and 120 µm long, without any segmentation;
- Stage 2: young metatrochophore larva, between 120 and 350 µm, with apparition of the first abdominal segment;
- Stage 3: old metatrochophore larva, between 350 and 500 µm, with a darker pigmentation, an increase in abdominal segmentation and the formation of two tentacular buds;
- Stage 4: erpochete larva, ready for settlement, longer than 500 µm, with larger abdominal segments, lengthening of tentacular palps and formation of the future palea of the worm.

Those morphological identifications were confirmed by molecular analyses (see Annex A.2 ).

### 1.3.6 Statistical analysis

All the statistical analyses were performed using the R software version 2.7 (R Development Core Team, 2005)[d]. The typology of the water masses based on their hydrological properties was described using ten variables: the surface temperature ($T_s$, °C), the temperature gradient from surface to bottom or a 50m-depth ($\Delta T$, °C), the thermocline depth ($z_T$, m), the surface salinity ($S_s$), the salinity gradient from surface to bottom or a 50m-depth ($\Delta S$), the halocline depth ($z_S$, m), the surface density ($\sigma_s$, kg.m$^{-3}$), the density gradient from surface to bottom or a 50m-depth ($\Delta\sigma_t$, kg.m$^{-3}$), the pycnocline depth ($z_{\sigma_t}$, m), and the stratification index ($\hat{S}$). Two complementary analyses were performed on the matrix of the hydrological variables. First, a cluster analysis was realised using the Ward's method on the Euclidean distance matrix calculated between stations (*Hclust* function of the R software). Second, a principal component analysis (PCA) was made on the correlation matrix of the hydrological data through the *rda* function of the vegan library version 1.5 of the R software. The clustering method was used to group stations according to their physico-chemical properties and identify hydrological regions while the PCA was used to determine which variables account for most of the hydrological variability between stations.

For each cruise, the horizontal distribution of each species was analysed as a function of (1) the environment alone, (2) the geography alone, and (3) the interaction of environment and space (spatial component of the environment) using a variance partitioning method based on partial multiple regressions (Borcard , 1992; Legendre & Legendre, 1998). For these analyses, three matrices were used following Borcard (1992) (Figure 1.5): (1) the response vector $Y$ of the $\log_{10}$-transformed horizontal larval abundances ($log_{10}$(larval abundance+1)), (2) the explanatory matrix $X$ of the environmental variables, i.e., the hydrological variables, and (3) the explanatory matrix $W$ of the spatial variables. To ensure the extraction of the more complex structures, spatial variables were described as the different terms of a cubic polynomial function of the centred geographic coordinates ($x$,$y$) of the stations, such as:

$$W = f(x, y, x^2, xy, y^2, x^3, xy^2, x^2y, y^3). \quad \text{(Eq. 1.3)}$$

[d] http://www.r-project.org

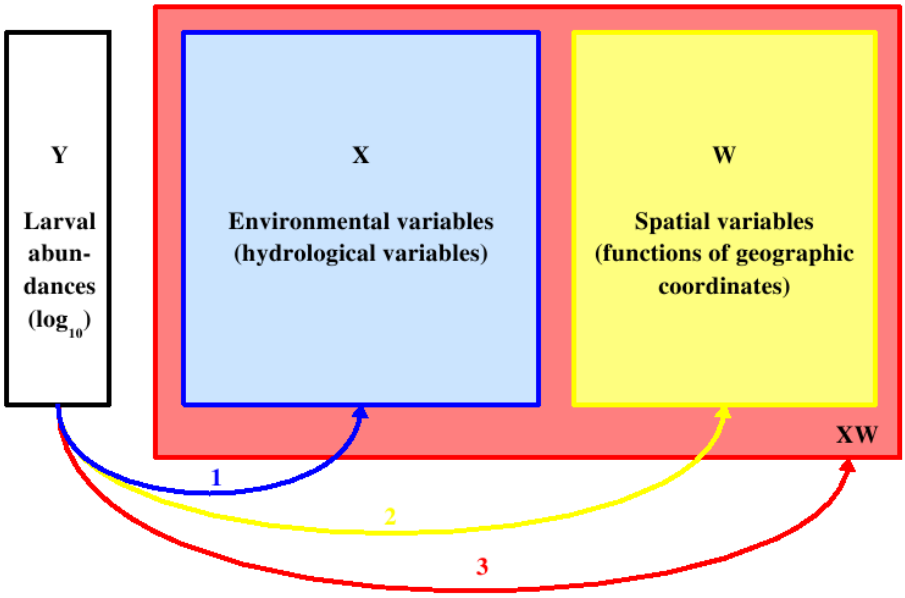


Figure 1.5: Response variable and explanatory variables used for the statistical analyses. Response variable is in white ($Y$) and response variables are in colour ($X$, $W$, and $XW$). Colored arrows indicate the three successive partial multiple regressions.

Multiple regression models the relationships between a response variable $Y$ and a set of explanatory variables $X$ by the linear function $Y = X.b$ such as:

$$Y_i = b_0 + \sum_{j=1}^{j=k} b_j X_{ij} \qquad \text{(Eq. 1.4)}$$

with $k$ the number of explanatory variables, $b_0$ the intercept, and $b_j$ the regression coefficients.

Variance partitioning was then performed through three successive multiple regressions. In a first step, larval abundances were analysed as a function of the hydrological environment, through multiple regressions between the response variable $Y$ and the environmental variables $X$ (Arrow 1 in Figure 1.5).

To avoid redundancy between the ten hydrological variables used to define the typology of the water masses, variables were selected prior to the multiple regressions: the matrix of Pearson's product-moment correlation coefficients was calculated between each pair of hydrological variables (*cor* function of the R software), and only the variables with a correlation coefficient lower than 0.75 were arbitrarily chosen. For the cruise of May,

the selected explanatory variables were: the surface temperature $T_s$, the surface salinity $S_s$, the halocline depth $z_S$, and the pycnocline depth $z_{\sigma_t}$. For the cruise of June, the selected explanatory variables were: the surface temperature $T_s$, the surface salinity $S_s$, the pycnocline depth $z_{\sigma_t}$, and the stratification index $\hat{S}$. In a second step, multiple regressions were performed between the larval abundances $Y$ and the spatial variables $W$ (Arrow 2 in Figure 1.5). Finaly, in a third step, multiple regressions were performed between the larval abundances $Y$ and both the environmental and spatial variables $XW$ (Arrow 3 in Figure 1.5).

From these three successive steps, variance of the larval abundances can be partitionned (Table 1.1, Figure 1.6). The first multiple regression provided the proportion of variance explained by the environment ($a+b$: environment alone and interaction of the environment and space), while the second multiple regression indicated the proportion of variance explained by the geographical space ($b+c$: geographical space alone and interaction of the environment and space). The proportion of variance explained by the environment and the geographical space ($a+b+c$) was given by the third multiple regression.

Table 1.1: Variance partitioning based on three partial multiple regressions between a response vector $Y$ and two explanatory matrices $X$ and $W$ (Borcard , 1992), with $a$ the part of variance explained by the environment alone, $b$ the part of variance explained by the geographical space alone, $c$ the part of variance explained by the interaction of the space with the environment (spatial structure of the environment), and $d$ the undetermined part of variance.

| | Tested factors | Response vector | Explanatory matrix | Explained variance | Residual |
|---|---|---|---|---|---|
| Step 1 | Hydrological environment | $Y$ | $X$ | $a+b$ | $c+d$ |
| Step 2 | Geographical space | $Y$ | $W$ | $c+b$ | $a+d$ |
| Step 3 | Spatial structure of the environment | $Y$ | $XW$ | $a+b+c$ | $d$ |

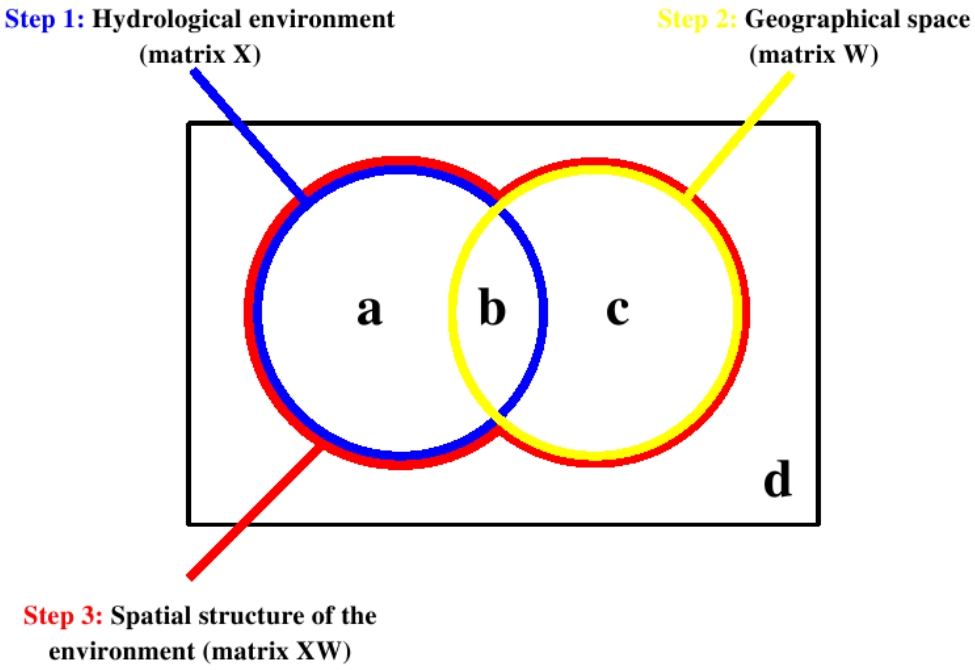


Figure 1.6: Variance partitioning based on three partial multiple regressions between the two explanatory matrices $X$ and $W$ representing the hydrological data (environment) and the geographical data (space). The variance explained by each of the three partial multiple regressions is represented by one colour. The signification of the variances $a$, $b$, $c$, and $d$ are given in Table 1.1.

Variance partitioning was also conducted on the horizontal distributions of each larval stages of each species using redundancy analyses (RDA) instead of multiple regressions (Legendre & Legendre, 1998). RDA are the direct extension of multiple regressions to multivariate response data, i.e., when the response variable is represented by a matrix instead of a vector (here $Y_j$ instead of $Y$ to represent the abundances of the different larval stages $j$). To perform the RDA and to calculate the variance partitioning the *rda* function and the *varpart* function of the *vegan* library were used (R software).

## 1.4 Results

### 1.4.1 Meteorological and run-offs conditions in spring 2008

In the northern Bay of Biscay, wind conditions were mainly from W-NW during spring 2008, with decreasing average speed over time, from 8.5 $m.s^{-1}$ in March to 5.6 $m.s^{-1}$ in April and 3.3 $m.s^{-1}$ in May (Figure 1.7A). In June, average wind speed slightly increased to reach 4.8 $m.s^{-1}$. The two cruises of May and June occurred under low to moderate wind speed of 2.6 and 6.0 $m.s^{-1}$ respectively. After the cruise of May, slow winds of various directions (average speed of 3.9 $m.s^{-1}$; NE, SE and SW directions) were recorded during ten days. The week before the second cruise was characterized by stronger NW winds (average speed of 6.4 $m.s^{-1}$), with maximal speed of 8 to 9 $m.s^{-1}$.

Two peaks in river run-offs were measured in March and April 2008, with run-offs higher than 1,800 $m^3.s^{-1}$ for the Loire (Figure 1.7B). During the cruise of May, river run-offs were low. Just before the cruise of June, a peak in the river outputs of the Vilaine and the Loire was recorded ($> 2,000$ $m^3.s^{-1}$ for the Loire).

### 1.4.2 Environmental variables during the cruise of May

During the cruise of May 2008, an important low salinity plume (i.e., surface salinity lower than 32) was observed along the southern Brittany coasts from the Loire estuary to the entrance of Concarneau bay (Figure 1.8A). Minimal surface salinities were measured at the most inshore stations, with a minimum value of 26.5 for the first station of the Loire transect (station L1). Along the two transects of Douarnenez and Audierne, as for the more offshore stations of the other transects, surface salinity was higher than 34. A haline front was observed from the Loire estuary to the north of Lorient at 25 to 10 nautical miles from the coastline.

Surface temperatures followed a latitudinal gradient, with the lowest temperatures in the north (i.e., lower than 13.5 °C at the stations D8 and D7) and the highest temperatures in the south (i.e., higher than 16.7 °C at the stations L2 and L3) (Figure 1.8B). Cross-shore thermal gradients were small, except along the Douarnenez transect, characterised

by a strong thermal front of more than 1.5 °C at the entrance of the bay, between the stations D3 and D4, and along the Loire transect.

The highest chlorophyll *a* concentrations were localized only in the vicinity of the Vilaine and the Loire estuaries in the river plume waters (Figure 1.9A).

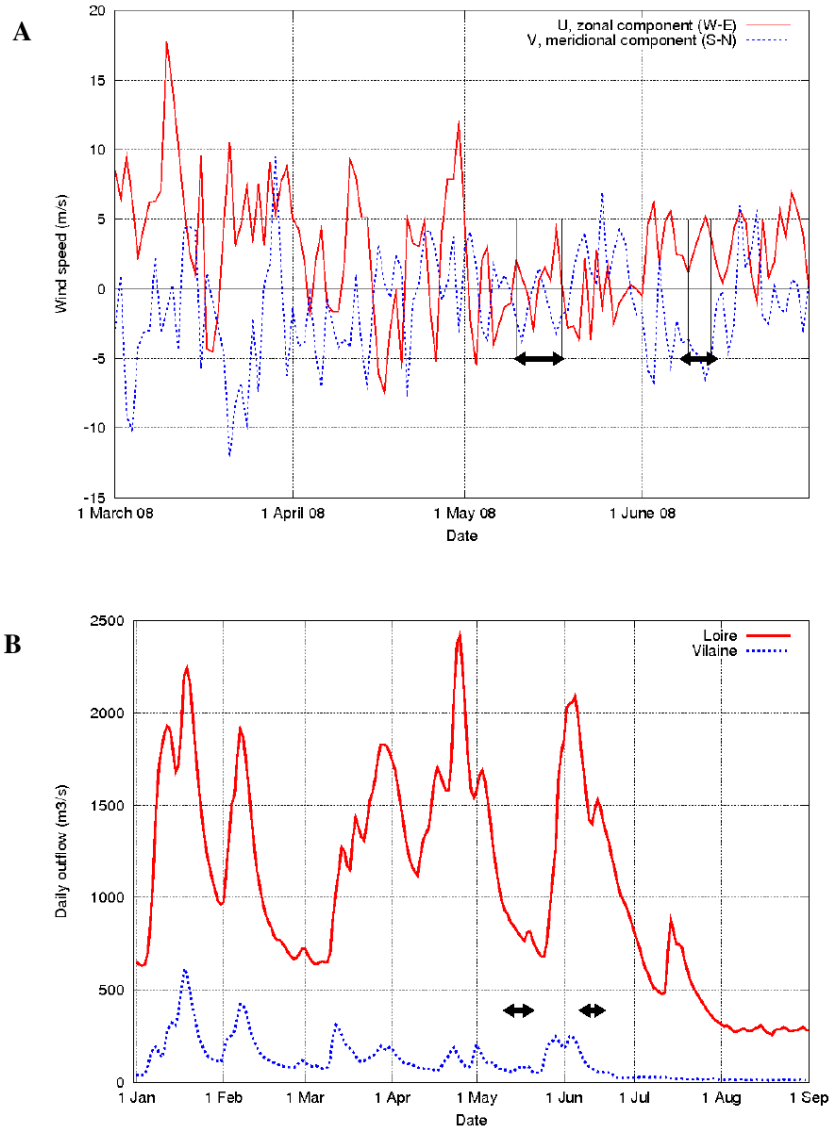


Figure 1.7: Hydroclimatic conditions during the spring 2008 in the northern Bay of Biscay. (A) Wind conditions at Penmarch headland in spring 2008 (Météo France data). (B) Cumulative daily run-offs of the two main rivers of the northern Bay of Biscay in 2008: the Vilaine (blue dashed line) and the Loire (red solid line). The cruises of May and June are indicated by black arrows.

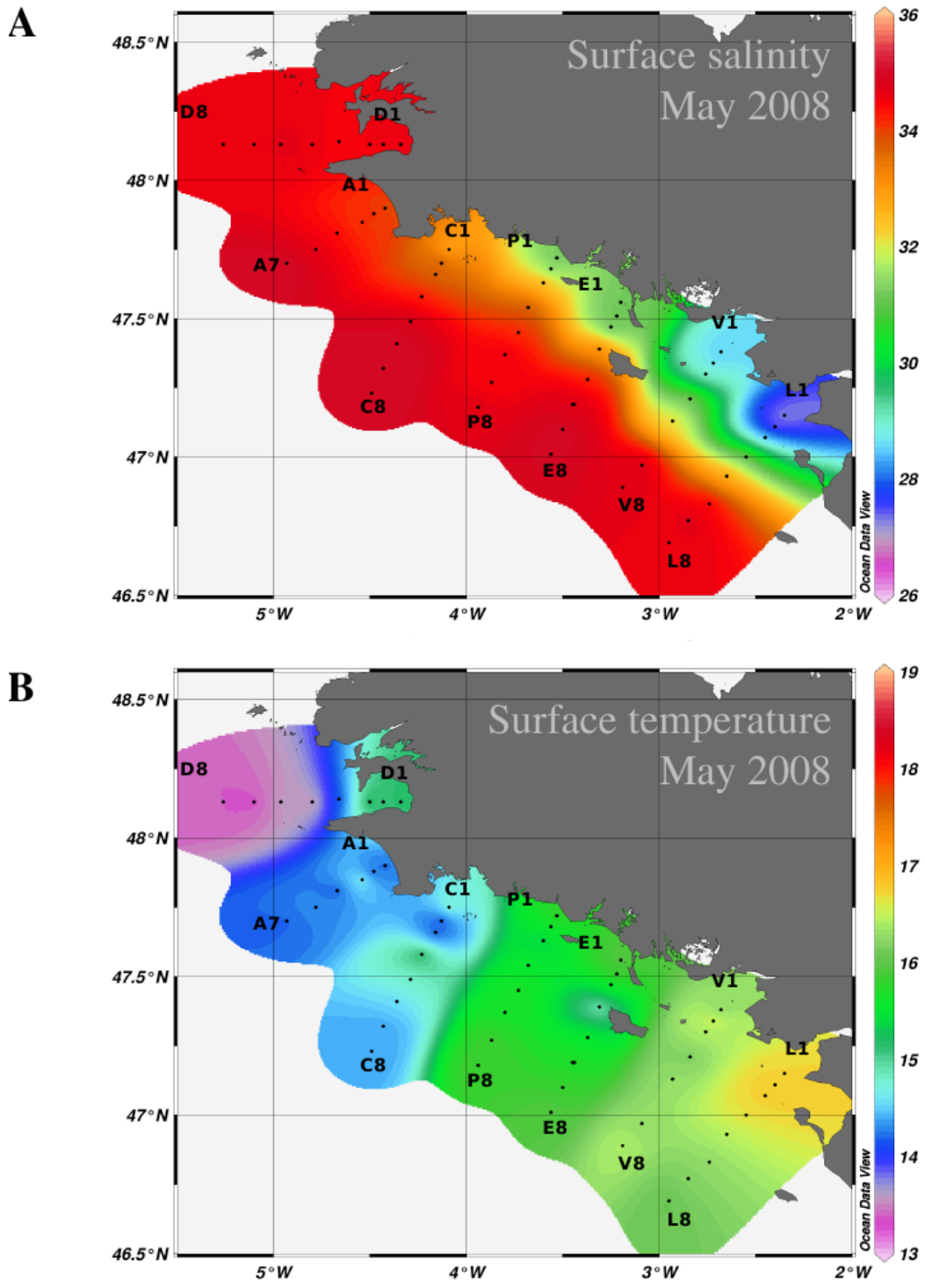


Figure 1.8: Horizontal distribution of (A) surface salinity and (B) surface temperature (°C) recorded in the northern Bay of Biscay during the cruise of May 2008.

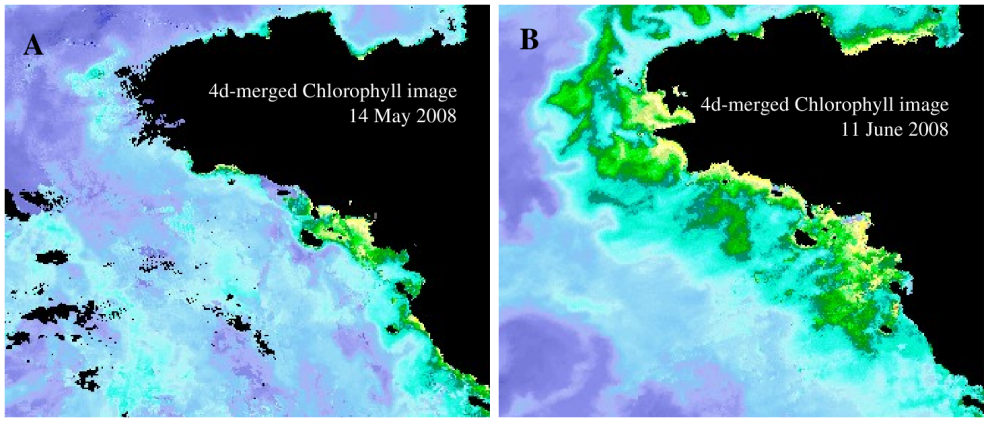


Figure 1.9: Satellite images of surface Chlorophyll $a$ concentrations in (A) May and (B) June 2008 (Ifremer data, MORIS/MODIS images).

Vertical stratification was low (stratification index $\hat{S}$ lower than 0.1), except for the coastal stations located in the river plumes. When observed, the vertical depths of thermocline and halocline differed (Figure 1.10A-B). They varied between 5 m and 10 m and between 10 and 15 m, respectively. Water density distribution was mainly governed by salinity variations.

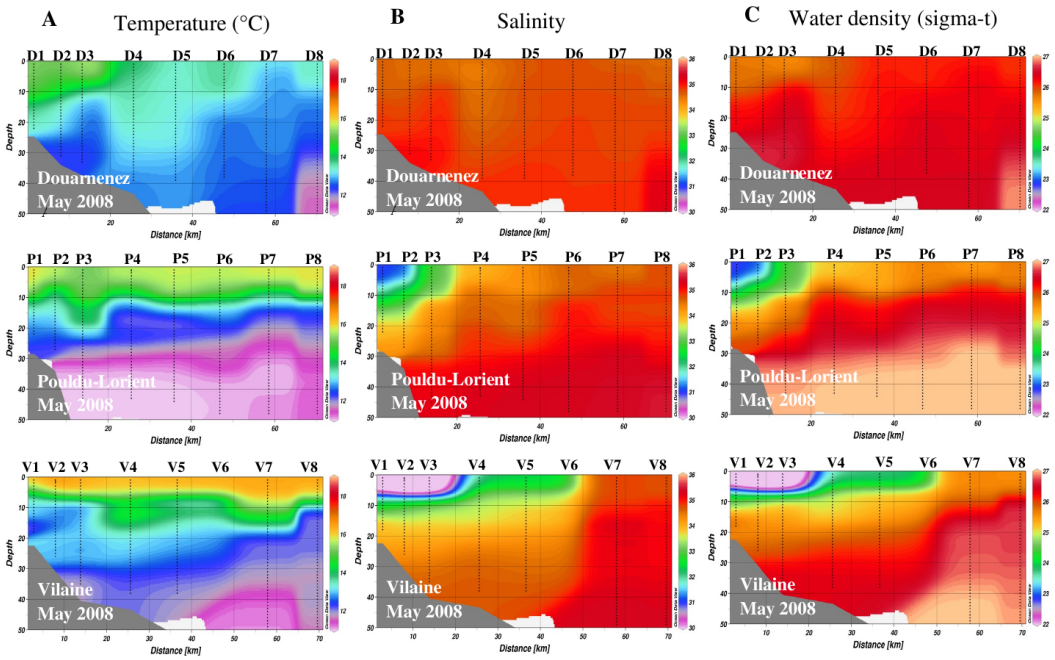


Figure 1.10: Variations of the vertical hydrological structures along the transects of Douarnenez, Pouldu-Lorient, and Vilaine: (A) temperature $T$, (B) salinity $S$, and (C) water density $\sigma_t$ profiles during the cruise of May 2008. Note that the colour scales differ from the Figure 1.8.

From the hydrological properties of the stations sampled during the cruise of May, the cluster analysis distinguished two main hydrological regions (Figure 1.11A).

The first cluster grouped the more inshore stations of the southern transects (Figure 1.11B). It was characterised by stronger vertical stratification ($\hat{S} = 0.16 \pm 0.09$), higher surface temperature ($T_s = 16.20 \pm 0.45$ °C), lower surface salinity ($S_s = 30.54 \pm 1.92$), lower surface density ($\sigma_t = 22.37 \pm 1.52$), and shallow thermocline, halocline, and pycnocline (depths of 12.22 ± 3.99 m, 10.58 ± 4.32 m, and 10.80 ± 4.19 m respectively). This cluster corresponded to coastal stations located in the Loire and Vilaine river plumes.

The second cluster was composed by the stations of the northern transects and by the offshore stations of the southern transects (Figure 1.11B). This group was characterised by oceanic waters with a weaker vertical stratification ($\hat{S} = 0.03 \pm 0.01$), lower surface temperature ($T_s = 15.10 \pm 1.05$ °C), higher surface salinity ($S_s = 34.39 \pm 1.07$), higher surface density ($\sigma_t = 25.58 \pm 0.88$), and deeper thermocline, halocline, and pycnocline (depths of 15.19 ± 4.83 m, 19.94 ± 7.49 m, and 17.64 ± 6.85 m, respectively).

The stations of this second cluster could be separated in two sub-groups by their surface temperature (Figure 1.11B): one southern sub-group with higher surface temperatures ($T_s = 16.20 \pm 0.45$ °C), and one northern sub-group with lower surface temperatures ($T_s = 14.34 \pm 0.71$ °C).

The principal component analysis applied to the same data set showed that the two first factorial axes explained 64.4 % and 16.8 % of the total variance respectively (Figure 1.11C). The first factorial axis separated the stations of the two hydrological regions distinguished by the cluster analysis. It was negatively scored by the surface salinity, the surface density, and the depths of the halocline, pycnocline, and thermocline, separating river plumes stations with lower surface salinity and shallower halocline from marine water stations.

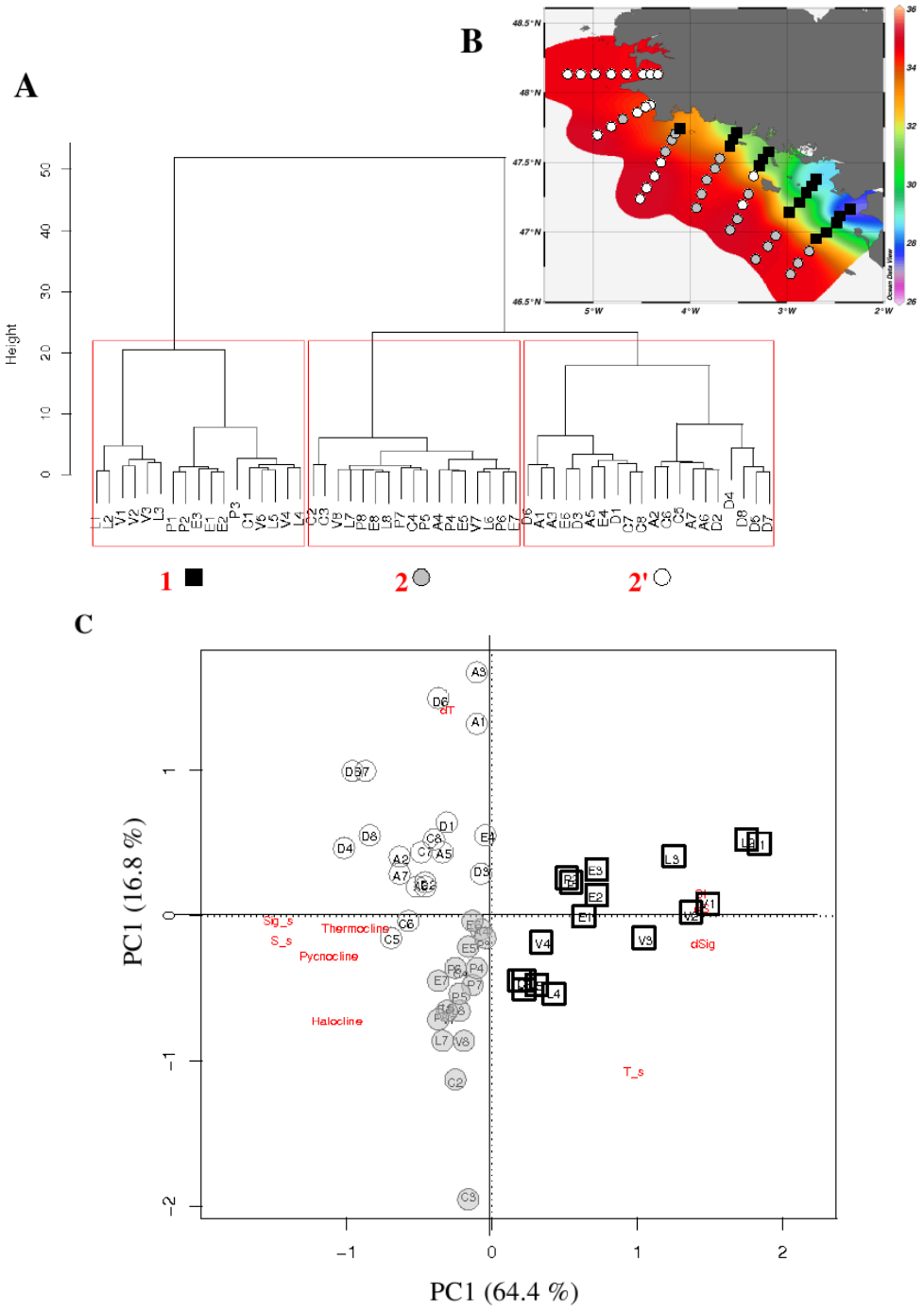


Figure 1.11: Hydrological typology in the northern Bay of Biscay in May 2008. (A) Cluster analysis performed on the hydrological data, (B) spatial distribution of the three clusters according to the surface salinity distribution, and (C) PCA performed on the hydrological data. Black squares indicate the stations belonging to the cluster 1, grey circles the stations of the cluster 2, and white circles the stations of the cluster 2'.

### 1.4.3 Larval horizontal distribution during the cruise of May

In May 2008, *P. koreni* larvae were present in 63.8 % of the stations, *O. fusiformis* larvae in 53.4 % and *S. alveolata* in 34.5 %, with average larval abundances of 101 ± 289 ind.m$^{-3}$, 67 ± 188 ind.m$^{-3}$, and 54 ± 201 ind.m$^{-3}$ respectively. For all the species, highest concentrations were reported in the three more coastal stations of the Vilaine transect (V1, V2 and V3), with maximum values of 1,587 ind.m$^{-3}$ for *P. koreni* larvae, 1,100 ind.m$^{-3}$ for *O. fusiformis* larvae, and 1,459 ind.m$^{-3}$ for *S. alveolata* larvae. An inshore-offshore gradient and a latitudinal gradient were observed with higher abundances close to the shore and in the south of the study area (Figure 1.12). For *P. koreni* and *O. fusiformis*, larvae were sampled in the coastal stations of each transect. On the contrary, *S. alveolata* larvae where only observed in the coastal stations of the southern transects, from the Bay of Concarneau to the Loire estuary.

*P. koreni* larval population was mainly composed of the first three larval development stages in similar proportions. The trochophore stage (i.e., stage 1) and the two metatrochophore stages (i.e., stages 2 and 3) formed 29, 38 and 33 % of the larval population respectively (Figure 1.13A). These larval stages were homogeneously distributed in the space (see Annex A.3) with maximal abundances reaching about 386 ind.m$^{-3}$ for the stage 1 at the station V1, 692 ind.m$^{-3}$ for the stage 2 at the station V2, and 532 ind.m$^{-3}$ for the stage 3 at the station V2. By contrast, the aulophore stage (i.e., stage 4), was only reported in a few stations (i.e., E4, V1, V2, and V3) with a maximal abundance of 31 ind.m$^{-3}$ at the station V1.

Larval population of *O. fusiformis* was largely dominated by the development stage 3 (i.e., 78 % of the larval population) and in a lesser extent by the development stage 4 (i.e., 17 % of the larval population) (Figure 1.13B). While these two larval stages were evenly distributed (see Annex A.3), the youngest stages (i.e., stages 1 and 2) were confined to the more coastal stations. In the Douarnenez Bay, only the larval stage 3 was reported.

For *S. alveolata*, the larval population was also dominated at 80 % by the development stage 2, with a few younger and older larvae (stage 1: 9 %; stage 3: 9 %; stage 4: 2 %) (Figure 1.13C).

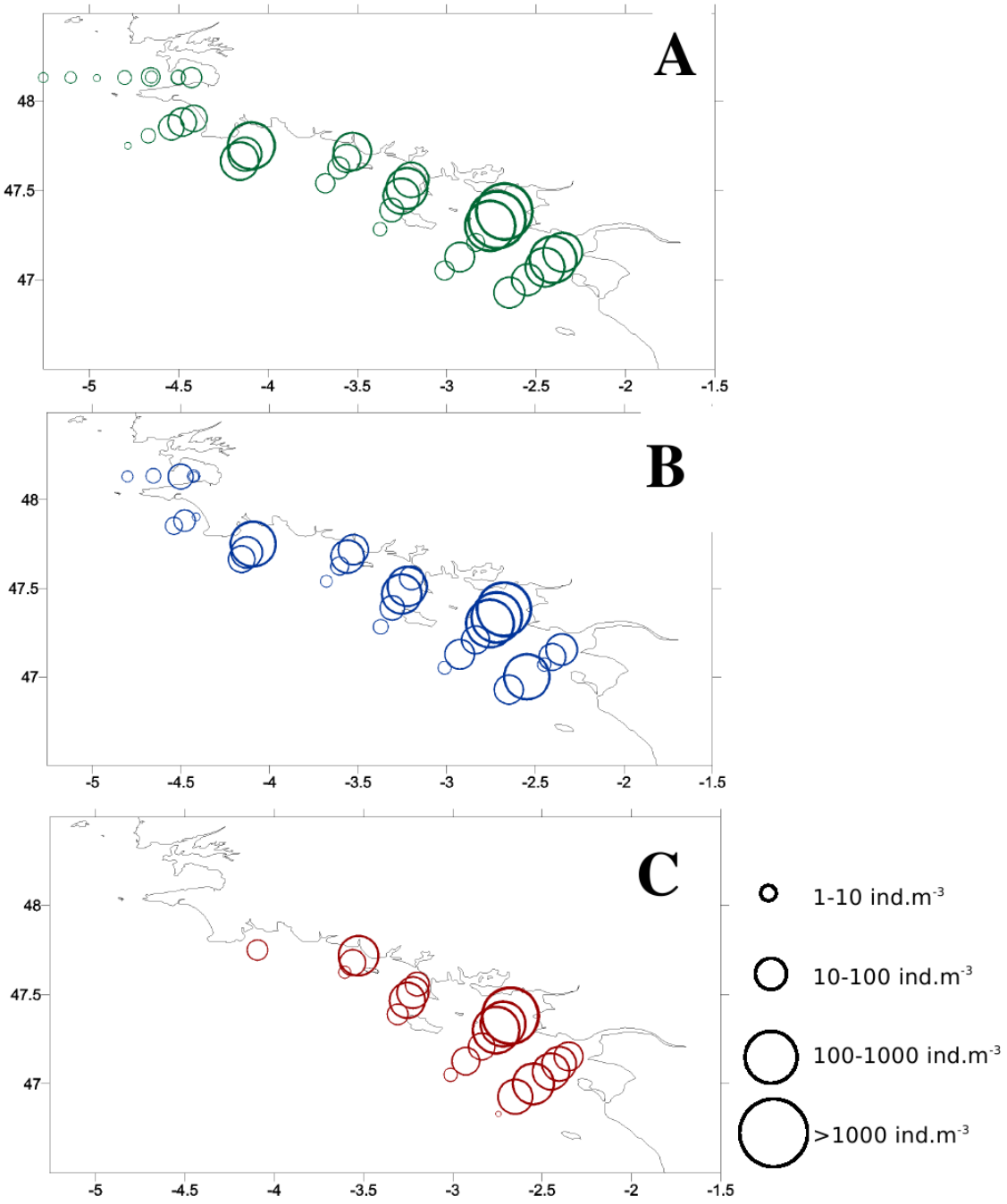


Figure 1.12: Horizontal distribution of (A) *Pectinaria koreni*, (B) *Owenia fusiformis*, and (C) *Sabellaria alveolata* larvae in May 2008 in the northern Bay of Biscay.

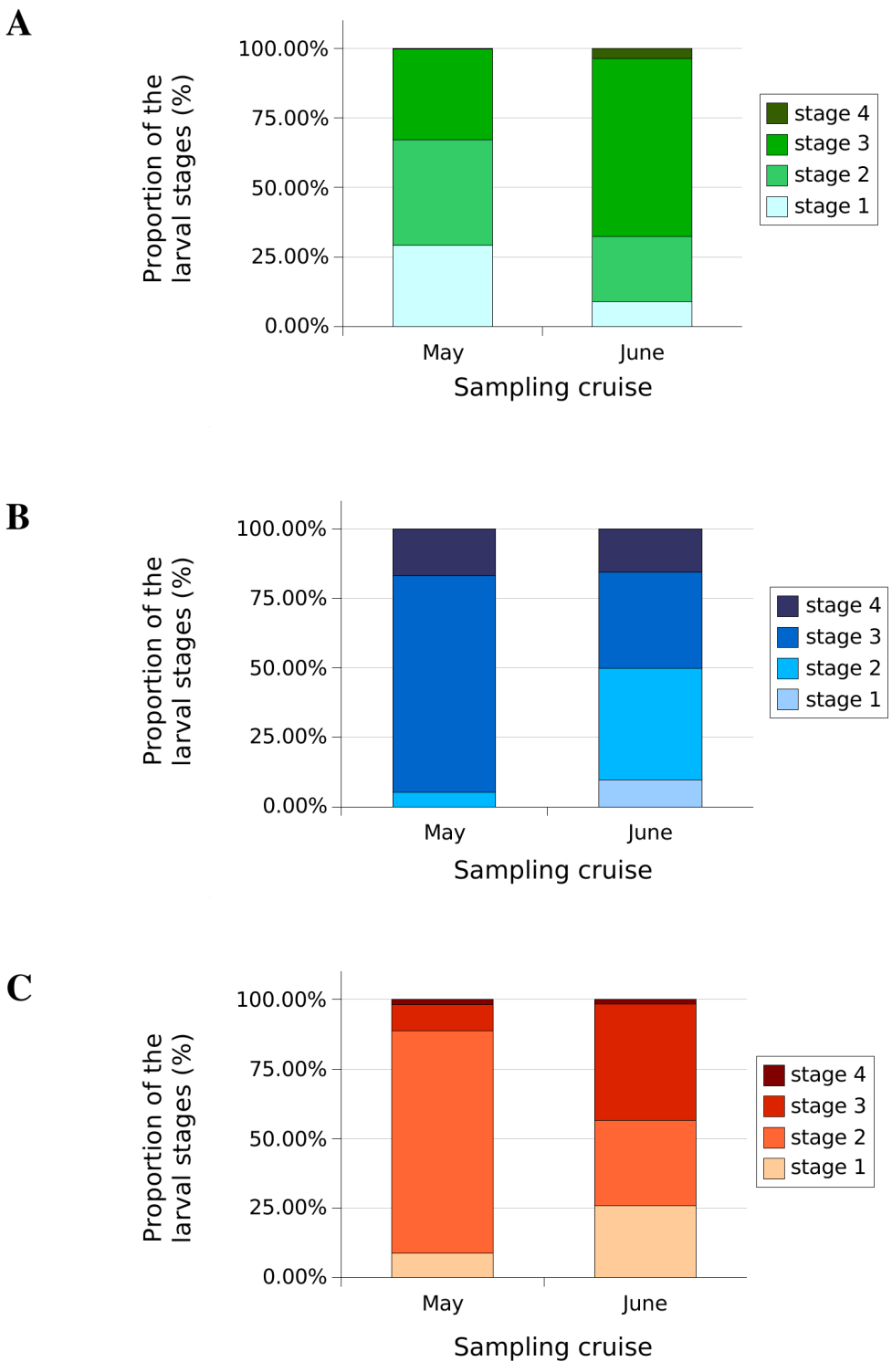


Figure 1.13: Relative proportions of the different larval stages of (A) *Pectinaria koreni*, (B) *Owenia fusiformis*, and (C) *Sabellaria alveolata* in May and in June 2008 in the northern Bay of Biscay.

For the three species, the multiple regressions showed significant relationships between total larval abundances and the selected hydrological variables (*P. koreni*: $R^2 = 0.5669$, $p = 1.863.10^{-8}$; *O. fusiformis*: $R^2 = 0.4486$, $p = 5.548.10^{-6}$; *S. alveolata*: $R^2 = 0.696$, $p = 3.868.10^{-12}$). Significant negative correlations were observed between larval abundances and surface salinity and significant positive correlations were observed between larval abundances and stratification index (Table 1.2), indicating that the larvae were mainly located in the river plume stations.

Table 1.2: Multiple regressions between the larval abundances and the hydrological environment in May 2008. Significance codes of the p-value are indicated by stars, with '***' for $p < 0.0001$, '**' for $p < 0.001$, and '*' for $p < 0.01$.

| Species | Tested factors | Regression coefficients $b$ | p-value | |
|---|---|---|---|---|
| *P. koreni* | Intercept | 14.717 | $1.03.10^{-5}$ | *** |
| | $T_s$ | -0.244 | 0.0361 | * |
| | $S_s$ | -0.283 | $5.19.10^{-6}$ | *** |
| | $z_S$ | -0.040 | 0.0689 | . |
| | $z_{\sigma_t}$ | 0.009 | 0.7058 | |
| *O. fusiformis* | Intercept | 9.279 | 0.006 | ** |
| | $T_s$ | -0.061 | 0.619 | |
| | $S_s$ | -0.211 | $8.8.10^{-4}$ | *** |
| | $z_S$ | -0.049 | 0.040 | * |
| | $z_{\sigma_t}$ | 0.023 | 0.387 | |
| *S. alveolata* | Intercept | 7.598 | $2.35.10^{-3}$ | ** |
| | $T_s$ | 0.122 | 0.177 | |
| | $S_s$ | -0.255 | $4.16.10^{-7}$ | *** |
| | $z_S$ | -0.044 | 0.012 | * |
| | $z_{\sigma_t}$ | 0.023 | 0.242 | |

Variance partitioning from the multiple regressions highlighted that the variations of larval abundances were mainly explained by the spatial structure of the hydrological environment (interaction between environment and geography), at 56 % for *P. koreni*, 44 % for *O. fusiformis*, and 68 % for *S. alveolata* (Figure 1.14A). For these three species, the geographical space alone accounted for 26, 27 and 16 % of the total abundances variance

respectively, whereas hydrological environment alone explained less than 1 % of the total variance.

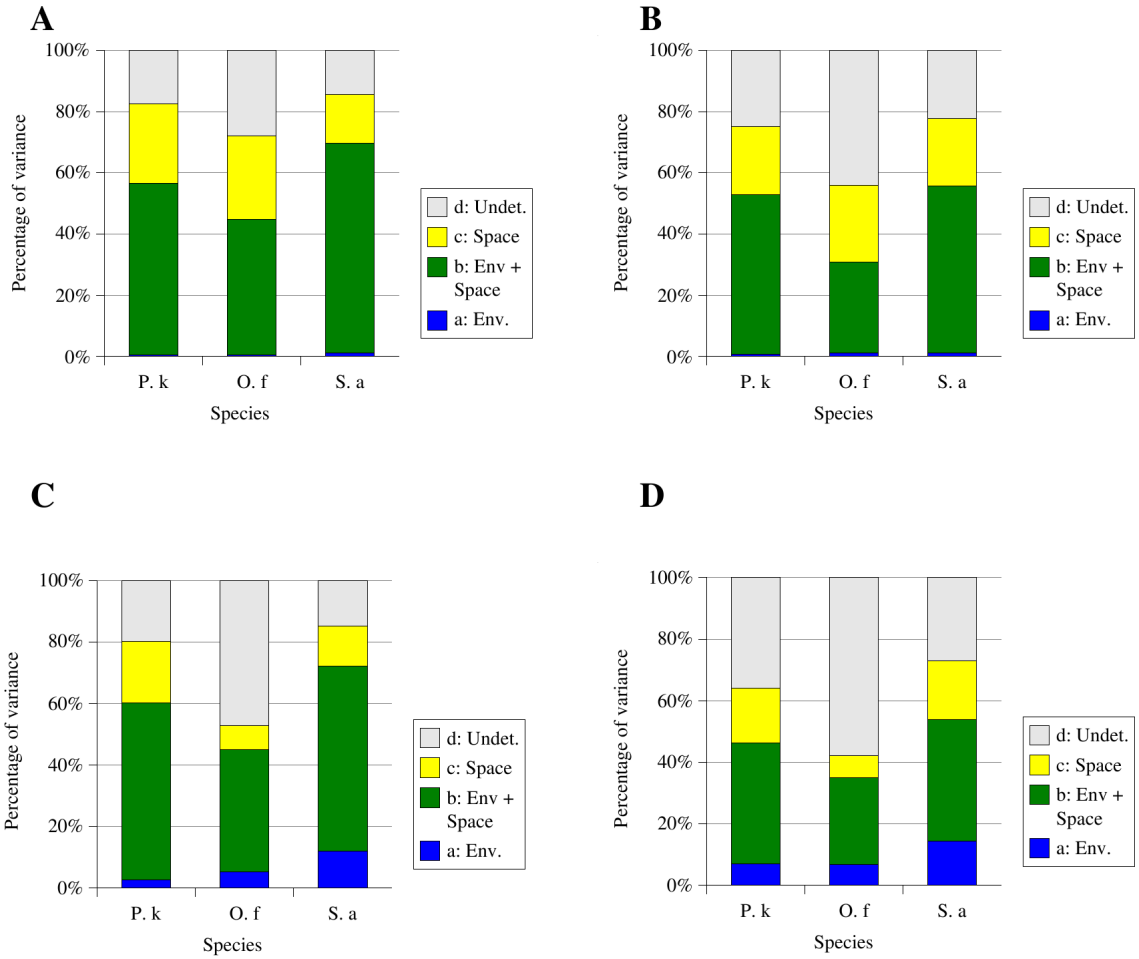


Figure 1.14: Variance partitioning of (A) total larval abundances in May, (B) larval stage abundances in May, (C) total larval abundances in June, and (D) larval stage abundances in June. The whole variance of the response matrix was partitioned into four fractions $a$, $b$, $c$, and $d$ due to the environment alone, the spatial structure of the environment, the geographical space alone, and the undetermined variations respectively. Variance partitioning on total larval abundances was performed through partial multiple regressions. Variance partitioning on larval stage abundances was performed through redundancy analyses.

The redundancy analysis computed on the abundances of *P. koreni* larval stages and the hydrological variables explained 52.8 % of the total variance and indicated only one significant canonical axis that explained 94.2 % of the constrained variance ($p < 0.001$). The RDA biplot diagram showed that the first axis was mainly related to the surface salinity, the pycnocline depth, and the halocline depth, the first three larval development stages being more abundant in the less saline waters (Figure 1.15). The scores of the first three development stages were close together suggesting a similar horizontal distribution according to the hydrological properties of the water masses. Only the score of the auloplore larvae (i.e., stage 4) differed. This result may be partly explained by the very low occurrence of this later stage, only reported in two coastal stations (A1 and V1). Similar results were also reported for *O. fusiformis* and *S. alveolata*, confirming similar horizontal distribution of the different larval stages according to the hydrology (see Annex A.3).

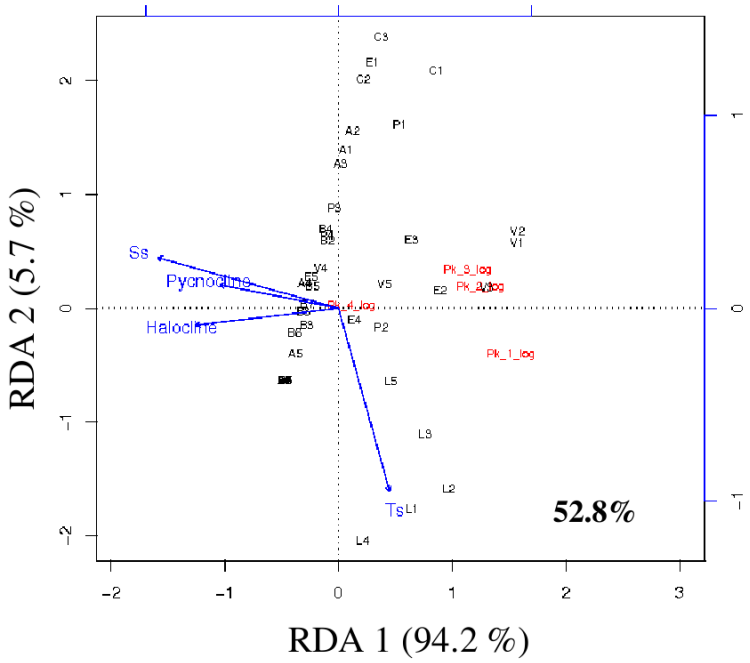


Figure 1.15: RDA biplot diagrams of the abundances of the different larval stages of *Pectinaria koreni* in May 2008 in the northern Bay of Biscay. Blue arrows represent the biplot scores of hydrological variables. Sampling sites are in black and larval stages in red. The percentage of the total variance explained by the RDA is indicated.

Variance partitioning from the successive redundancy analyses showed that the variations in abundances of the different larval stages were mainly explained by the spatial structure of the hydrological environment. This fraction accounted for 52, 30, and 55 % of the variations of stage abundances for *P. koreni*, *O. fusiformis*, and *S. alveolata* respectively (Figure 1.14B). The geographical space alone explained respectively 22, 25 and 22 % of the variations in stage abundances, whereas the hydrological environment alone explained less than 1 % of the variance.

### 1.4.4 Environmental variables during the cruise of June

During the cruise performed in June 2008, low salinity surface waters were observed in the vicinity of the Vilaine and the Loire estuaries, but the river plume was more diluted than during the cruise of May, i.e., it was more extended and less salty (Figure 1.16A). A minimal salinity of 29.75 was recorded at the station L2. For all the stations of the six transects from Audierne Bay to the Loire estuary (excluding the station E8) surface salinity was lower than 34, indicating both a northern and an offshore extension of the diluted river plume. In the stations of the Vilaine and Loire transects, surface salinity was lower than 32, except for the most offshore stations V8, L7 and L8, as indicated by a slight haline front along the Loire and Vilaine transects at 30-35 nautical miles from the coastline.

A general warming of the surface waters was observed, with sea surface temperature above 14.5 °C in most stations, except for the stations D7 and D8, which were separated from the other stations of the Douarnenez transect by the Ushant thermal front (Figure 1.16B). Maximal surface temperatures exceeding 17.9 °C were reported in the offshore stations from the Bay of Concarneau to the Loire estuary.

During this cruise, chlorophyll *a* concentrations were high all over the continental shelf of the study area with maximal values in inshore waters in response to the spring phytoplankton bloom (Figure 1.9B).

Vertical profiles indicated a strong thermal stratification (with $\hat{S}$ ranging from 0.02 to 0.19) except for the stations D6, D7 and D8 (Figure 1.17). Along the Vilaine and Loire transects, spatial variations of water density mainly depended on salinity variations, while they were mainly related to temperature variations along the other transects.

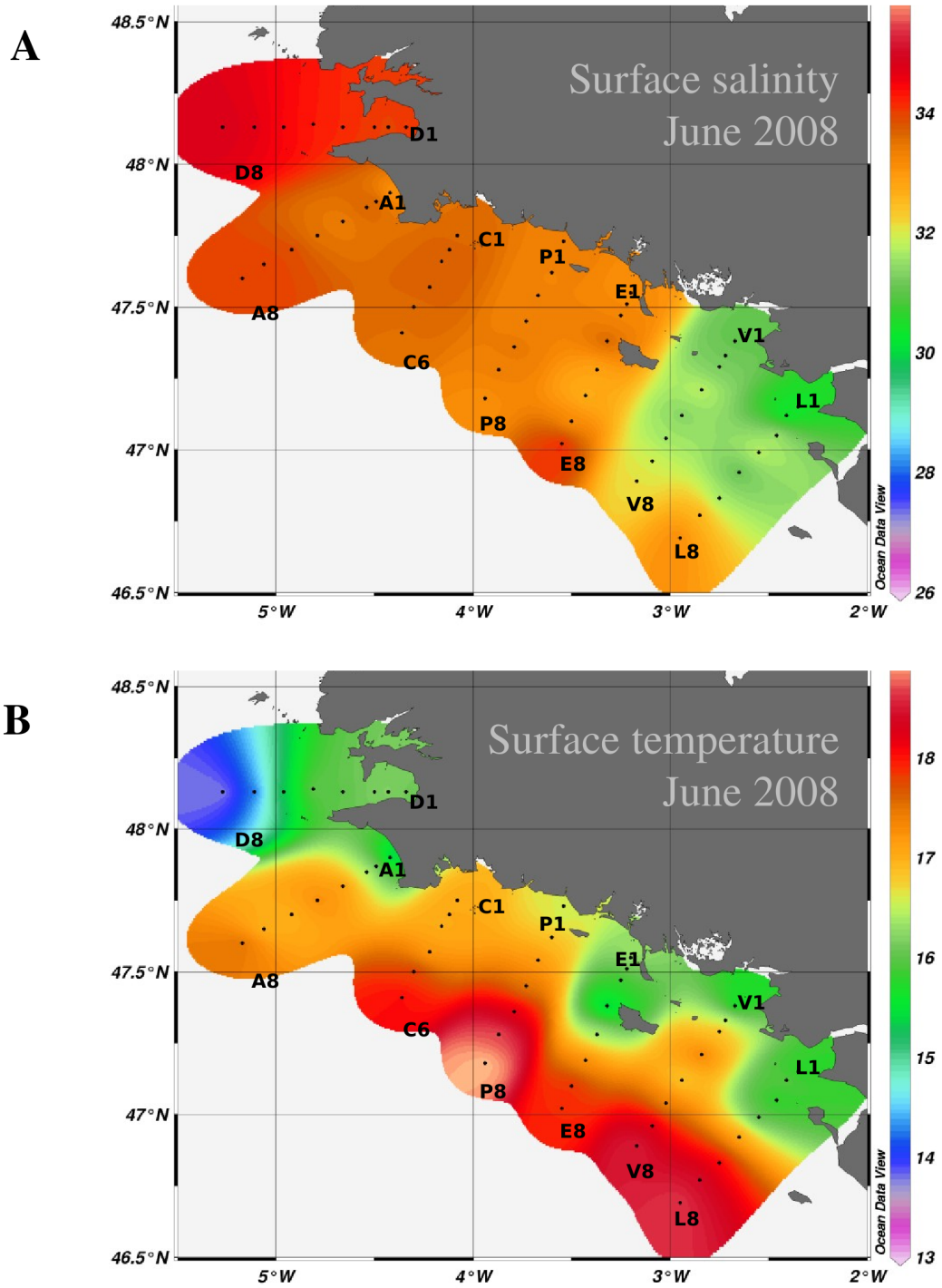


Figure 1.16: Horizontal distribution of (A) surface salinity and (B) surface temperature (°C) recorded in the northern Bay of Biscay during the cruise of June 2008.

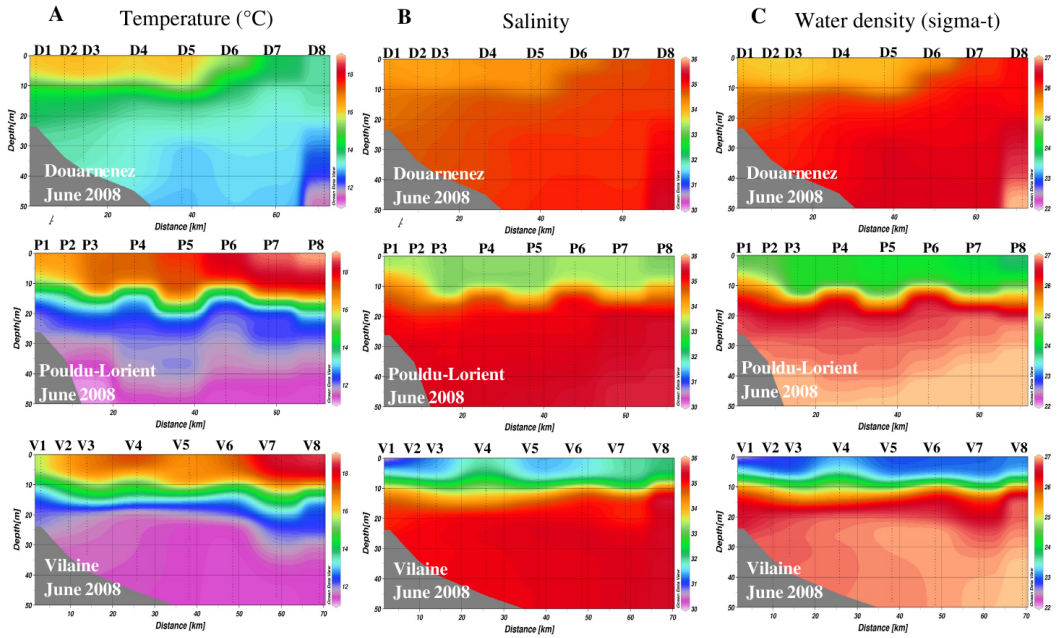


Figure 1.17: Variations of the vertical hydrological structures along the transects of Douarnenez, Pouldu-Lorient, and Vilaine: (A) temperature $T$, (B) salinity $S$, and (C) water density $\sigma_t$ profiles during the cruise of June 2008. Note that the colour scales differ from the Figure 1.16.

The cluster analysis based on the hydrological properties of the sampled stations separated again two main hydrological regions (Figure 1.18A). The stations of the first cluster were localized in front of the Vilaine and Loire estuaries (Figure 1.18B). They were characterised by stronger vertical stratification ($\hat{S} = 0.12 \pm 0.04$), lower surface salinity ($S_s = 31.24 \pm 0.67$), lower surface density ($\sigma_t = 22.74 \pm 0.38$), and shallower thermocline, halocline, and pycnocline (depths of 11.64 ± 3.04 m, 8.07 ± 2.10 m, and 9.01 ± 2.37 m respectively). The second cluster included all the other stations (Figure 1.18B) which were characterised by lower stratification ($\hat{S} = 0.05 \pm 0.03$), higher surface salinity ($S_s = 33.53 \pm 0.65$), higher surface density ($\sigma_t = 24.56 \pm 0.61$), and deeper thermocline, halocline, and pycnocline (depths of 14.58 ± 5.57 m, 11.73 ± 5.35 m, and 12.89 ± 5.23 m respectively). This second cluster also included the stations L3 and L4, because of their low surface temperature (15.60 and 15.83°C respectively).

Within the second cluster, the stations can be divided in two sub-clusters in function of the surface temperature (Figure 1.18A-B). The first sub-cluster is characterised by higher surface temperatures ($T_s = 17.02 \pm 1.06$ °C) and deeper thermocline (15.25 ± 3.26 m)

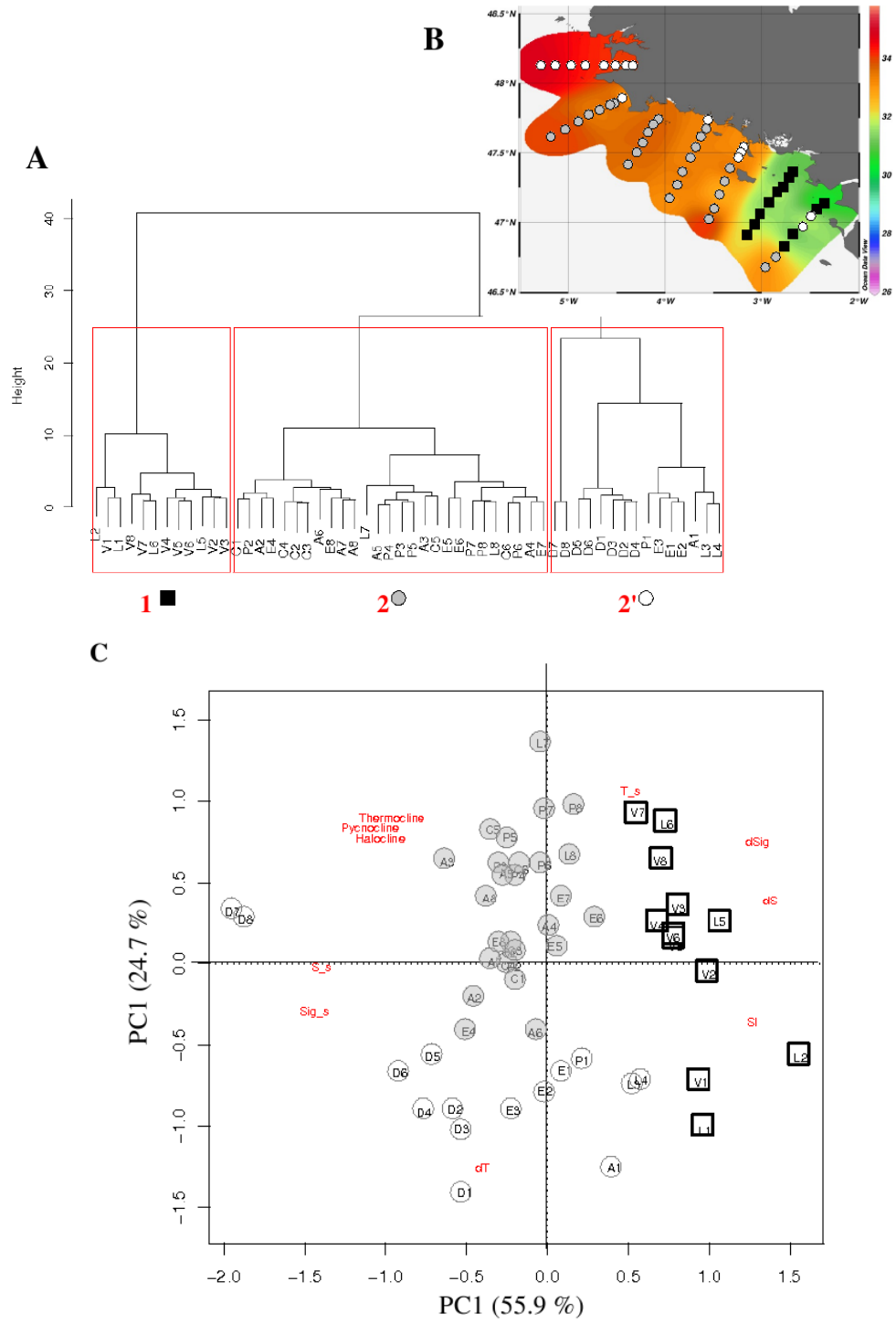


Figure 1.18: Hydrological typology in the northern Bay of Biscay in June 2008. (A) Cluster analysis performed on the hydrological data, (B) spatial distribution of the three clusters according to the surface salinity distribution, and (C) PCA performed on the hydrological data. Black squares indicate the stations belonging to the cluster 1, grey circles the stations of the cluster 2, and white circles the stations of the cluster 2'.

and included most of the stations of the Audierne, Concarneau, Pouldu-Lorient and Etel-Quiberon transects. Conversely, the second sub-cluster was characterised by lower surface temperatures ($T_s$ = 15.59 ± 0.92 °C) and shallower thermocline (13.33 ± 8.60 m) and included the stations of the Douarnenez transect and some coastal stations of the Audierne, Pouldu-Lorient and Etel-Quiberon transects.

The principal component analysis showed that the first two axes accounted for 80.6 % of the variability between stations with 55.9 % explained by the first axis and 24.7 % by the second axis (Figure 1.18C). The first axis was mainly scored negatively by the depths of the halocline, thermocline and pycnocline while the second axis discriminated the stations positively according to the vertical temperature gradient and negatively according to the surface temperature, the thermocline depth, and the vertical gradients of salinity and density. This analysis clearly isolated the stations D7 and D8 from the other stations, because of their deeper thermocline, halocline, and pycnocline. In this factorial plane, the stations of the first cluster (Figure 1.18B) had positive coordinates along the first axis. The second factorial axis separated the stations of the two sub-clusters according to their thermal properties (surface temperature, vertical temperature gradient, and thermocline depth) (Figure 1.18A).

### 1.4.5 Larval horizontal distribution during the cruise of June

During the cruise of June, the percentage of larval occurrence was similar as the one observed during the cruise of May, with occurrence frequencies of 70.4 % for *P. koreni* larvae, 48.1 % for *O. fusiformis* larvae, and 31.5 % for *S. alveolata* larvae. However, average larval abundances were 1.4 to 8 times lower, with values of 72 ± 127 ind.m$^{-3}$, 11 ± 25 ind.m$^{-3}$, and 7 ± 19 ind.m$^{-3}$ respectively. Maximal larval abundances were about 10 times lower. Horizontal distribution slightly differed from the distribution observed in May and higher larval abundances were recorded in coastal and/or southern stations (Figure 1.19).

*P. koreni* larvae were observed in the coastal stations of each transect, with maximum densities at stations E2, E3, V1, and L2 (maximum of 558 ind.m$^{-3}$). Along the southern

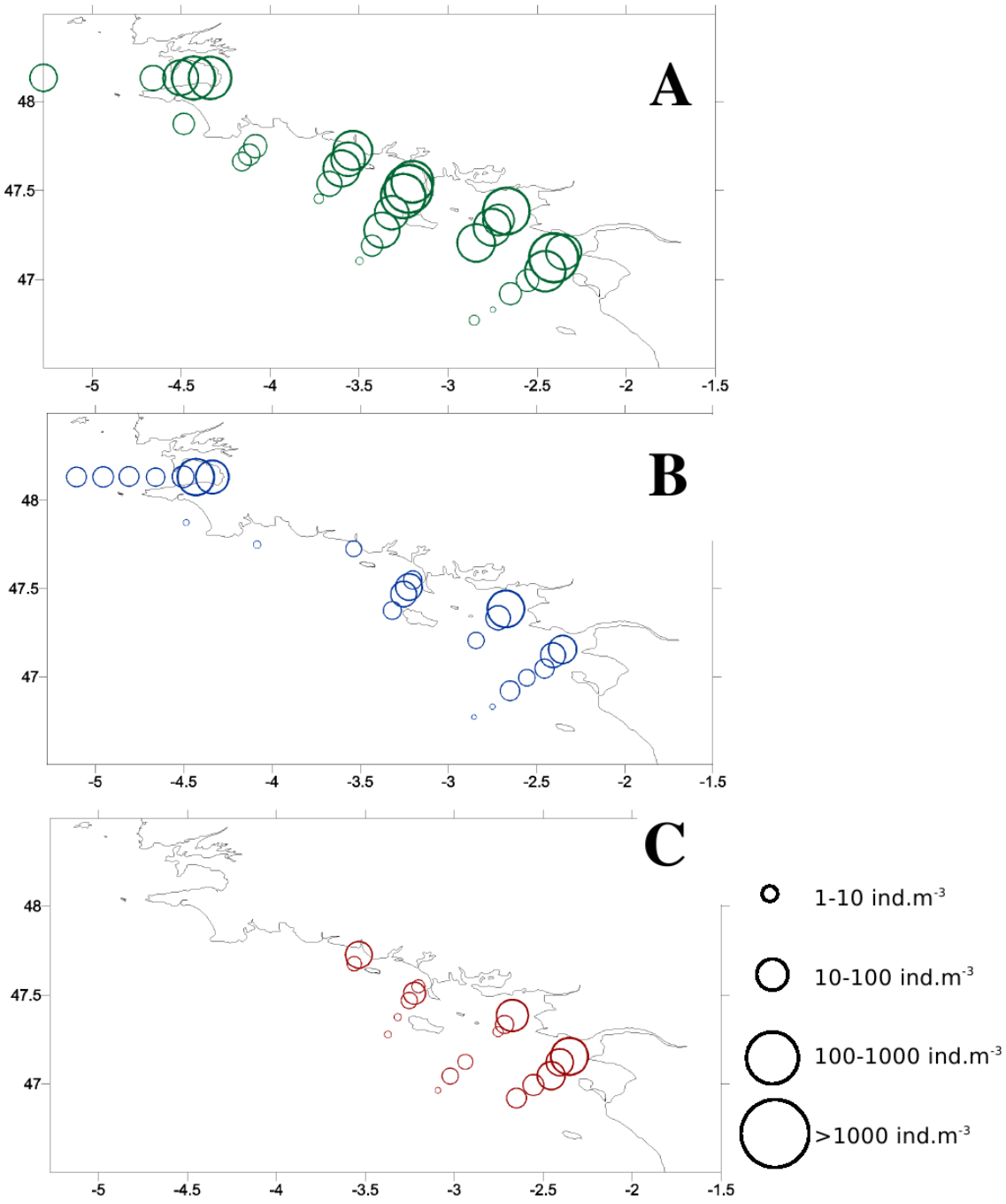


Figure 1.19: Horizontal distribution of (A) *Pectinaria koreni*, (B) *Owenia fusiformis*, and (C) *Sabellaria alveolata* larvae in June 2008 in the northern Bay of Biscay.

transects of Etel-Quiberon, Vilaine, and Loire, *P. koreni* larvae were recorded in all the stations, except in E8 and L8. Hence, *P. koreni* larvae were observed in more offshore stations than during the cruise of May. In June, the distribution of *O. fusiformis* larvae was more contrasted between the different transects than during the cruise of May. *O. fusi-*

*formis* larvae were mainly sampled along the northern transects of Douarnenez (D1-D7), and the southern transects of Etel-Quiberon (E1-E4), Vilaine (V1-V4) and Loire (L1-L7), with a maximal abundance in the station V1 (121 ind.m$^{-3}$). Compared to the distribution observed in May, *O. fusiformis* larvae were almost absent along the central transects of Audierne, Concarneau, and Pouldu-Lorient, but at relatively higher concentrations in the Bay of Douarnenez (> 100 ind.m$^{-3}$ in D2). The larval distribution of *S. alveolata* in June was close to the distribution observed in May. *S. alveolata* larvae were reported only in the coastal stations of the four southern transects of Pouldu-Lorient (P1-P2), Etel-Quiberon (E1-E5), Vilaine (V1-V7), and Loire (L1-L5), with maximal abundances in the stations V1 and L1 (i.e., 122 ind.m$^{-3}$).

*P. koreni* larval population was older in June than in May, and was mainly composed of old metatrochophore larvae (i.e., stage 3: 70 %) (Figure 1.13). Trochophore larvae (i.e., stage 1) and young metatrochophore larvae (i.e., stage 2) formed 10 and 26 % of the larval population respectively. The aulophore larvae (i.e., stage 4) represented 4 % of the larval population, and were reported all along the Vilaine transect with a maximal abundance of 93 ind.m$^{-3}$ at the station V5.

The larval populations of *O. fusiformis* and *S. alveolata* were younger than in May, with 10 % of stage 1, 41 % of stage 2, 35 % of stage 3 and 16 % of stage 4 for *O. fusiformis*, and 25, 30 and 41 % of the larval stages 1, 2, and 3 respectively for *S. alveolata*.

Multiple regressions on $\log_{10}$-transformed larval concentrations and hydrological variables recorded during the cruise of June indicated significant relationships for the three species (*P. koreni*: $R^2 = 0.6031$, $p = 2.325.10^{-9}$; *O. fusiformis*: $R^2 = 0.4513$, $p = 4.945.10^{-6}$; *S. alveolata*: $R^2 = 0.7212$, $p = 4.791.10^{-13}$). For the three species, significant negative correlations were observed between larval abundances and surface temperature (Table 1.3). Significant positive correlations were also observed between larval abundances and stratification index for *P. koreni* and *S. alveolata*, and a significant positive correlations was also demonstrated between larval abundances of *P. koreni* and surface salinity.

Table 1.3: Multiple regressions between the larval abundances and the hydrological environment in June 2008. Significance codes of the p-value are indicated by stars, with '***' for $p < 0.0001$, '**' for $p < 0.001$, and '*' for $p < 0.01$.

| Species | Tested factors | Regression coefficients $b$ | p-value | |
|---|---|---|---|---|
| *P. koreni* | Intercept | -14.287 | 0.048 | * |
| | $T_s$ | -0.250 | $4.89.10^{-3}$ | ** |
| | $S_s$ | 0.560 | $3.32.10^{-3}$ | ** |
| | $z_{\sigma_t}$ | -0.047 | 0.034 | * |
| | $\hat{S}$ | 23.626 | $4.88.10^{-5}$ | *** |
| *O. fusiformis* | Intercept | 0.092 | 0.986 | |
| | $T_s$ | -0.276 | $1.24.10^{-4}$ | *** |
| | $S_s$ | 0.152 | 0.287 | |
| | $z_{\sigma_t}$ | -0.034 | 0.049 | * |
| | $\hat{S}$ | 6.618 | 0.116 | |
| *S. alveolata* | Intercept | 4.432 | 0.200 | |
| | $T_s$ | -0.150 | $5.93.10^{-4}$ | *** |
| | $S_s$ | -0.058 | 0.506 | |
| | $z_{\sigma_t}$ | -0.012 | 0.261 | |
| | $\hat{S}$ | 8.311 | $2.18.10^{-3}$ | ** |

As observed for the cruise of May, the variance partitioning indicated that the larval horizontal distributions were mainly explained by the spatial structure of the hydrological environment (interaction between environment and space) which accounted for 52 % of the total abundances variability for *P. koreni*, 45 % for *O. fusiformis*, and 54 % for *S. alveolata* (Figure 1.14C). For these species, geographical structure alone explained respectively 34, 30 and 24 % of the variations of the total abundances, whereas hydrological environment alone only explained between 2 and 6 % of their variations.

For *P. koreni*, the redundancy analysis between the abundances of the larval stages and the hydrological variables explained 46.2 % of the total variance. The analysis indicated only one significant canonical axis explaining 94.7 % of the constrained variance ($p < 0.001$). On the RDA biplot diagram, surface salinity, surface temperature, and pycnocline depth were scored positively along this axis, whereas the stratification index was scored negatively (Figure 1.20A). The different larval stages had negative coordinates, indicating that they were all located preferentially in stations with higher stratification, and lower surface salinity and temperature. Similar results were also found for *O. fusiformis* and

*S. alveolata* suggesting that the different larval stages of these two species were located in the same water mass (see Annex A.3).

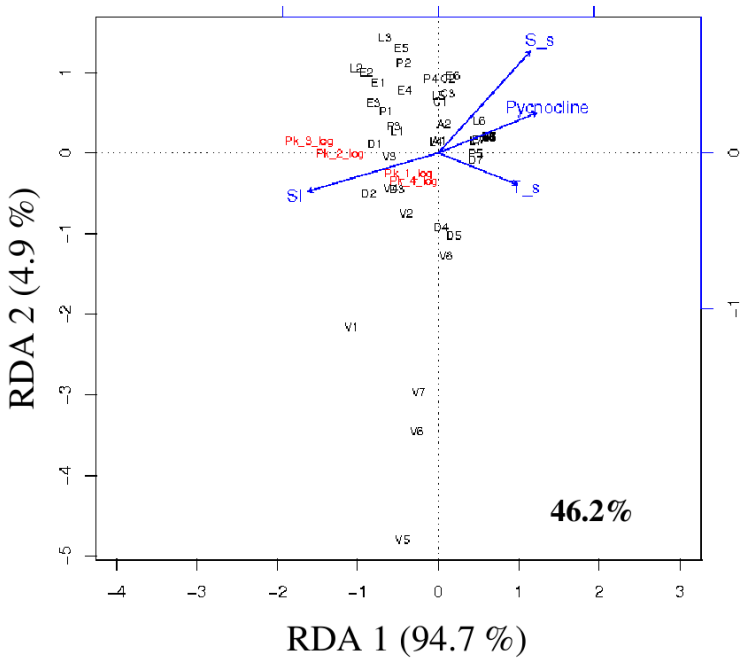


Figure 1.20: RDA biplot diagrams of the abundances of the different larval stages of *Pectinaria koreni* in June 2008 in the northern Bay of Biscay. Blue arrows represent the biplot scores of hydrological variables. Sampling sites are in black and larval stages in red. The percentage of the total variance explained by the RDA is indicated.

Variance partitioning from the successive redundancy analyses confirmed that the variations of larval stage abundances were mainly due to the spatial structure of the hydrological environment which accounted for 39 % for *P. koreni*, 28 % for *O. fusiformis*, and 39 % for *S. alveolata* (Figure 1.14D). For these three species, the geographical space alone explained 18, 7 and 19 % of the variations in larval stage abundances respectively. The fraction of the variance explained by the hydrological environment reached 7, 7 and 14 % of the variance respectively. Hence, the importance of the spatial structure of the hydrological environment in explaining the variations in the distribution of the different larval stages decreased in June, whereas the environment alone played a more important role than in May and the part of unexplained variance increased.

### 1.4.6 Larval vertical distribution

During each cruise, the larval vertical distributions was described for a few coastal stations which were characterised by high larval abundances and contrasted vertical hydrological profiles in terms of haline and thermal stratification: the stations D2, C1, P2, and V2 for the cruise of May 2008 (see vertical profiles of the stations D2, P2 and V2 on Figure 1.10, station C1 having a similar profile as P2), and the stations D2, P1, and V1 for the cruise of June 2008 (see vertical profiles of the stations D2, P1, and V1 on Figure 1.17). The detailed vertical larval distributions of these stations are presented in Annex A.4. In this section, only the average vertical distributions are described for each species.

The younger larval development stages of *P. koreni* (i.e., stages 1 to 3) were mainly located in the surface layer waters (5 m) and at lower concentrations in the transition layers (halocline and/or thermocline, 10 m-15 m) in May (Figure 1.21A). In June, they were mainly sampled in surface and thermocline layers except at the station P1 where larvae were homogeneously distributed along the water column. *P. koreni* aulophores (i.e., stage 4) were only observed in bottom layer waters.

In May and in June, stages 1 to 3 of *O. fusiformis* larvae were mainly located in surface waters and in transition layers. Conversely, larvae of stage 4 were observed in transition and bottom layers (Figure 1.21B), especially when at high concentrations, such as at 28 m depth at the P2 station in May (338 ind.m$^{-3}$).

The different larval stages of *S. alveolata* were evenly distributed along the water column (Figure 1.21B), with higher concentrations of young larvae (i.e., stage 1) in bottom and transition layers.

These results indicated that the *P. koreni* and *O. fusiformis* larvae were mainly restricted to surface and halocline and/or thermocline layers, confirming their distribution in river plume waters. For these two species, an ontogenic vertical migration was also observed, with a deeper distribution of the oldest stages. On the contrary, *S. alveolata* larvae were not restricted to surface river plume waters but tended to be distributed over the whole water column.

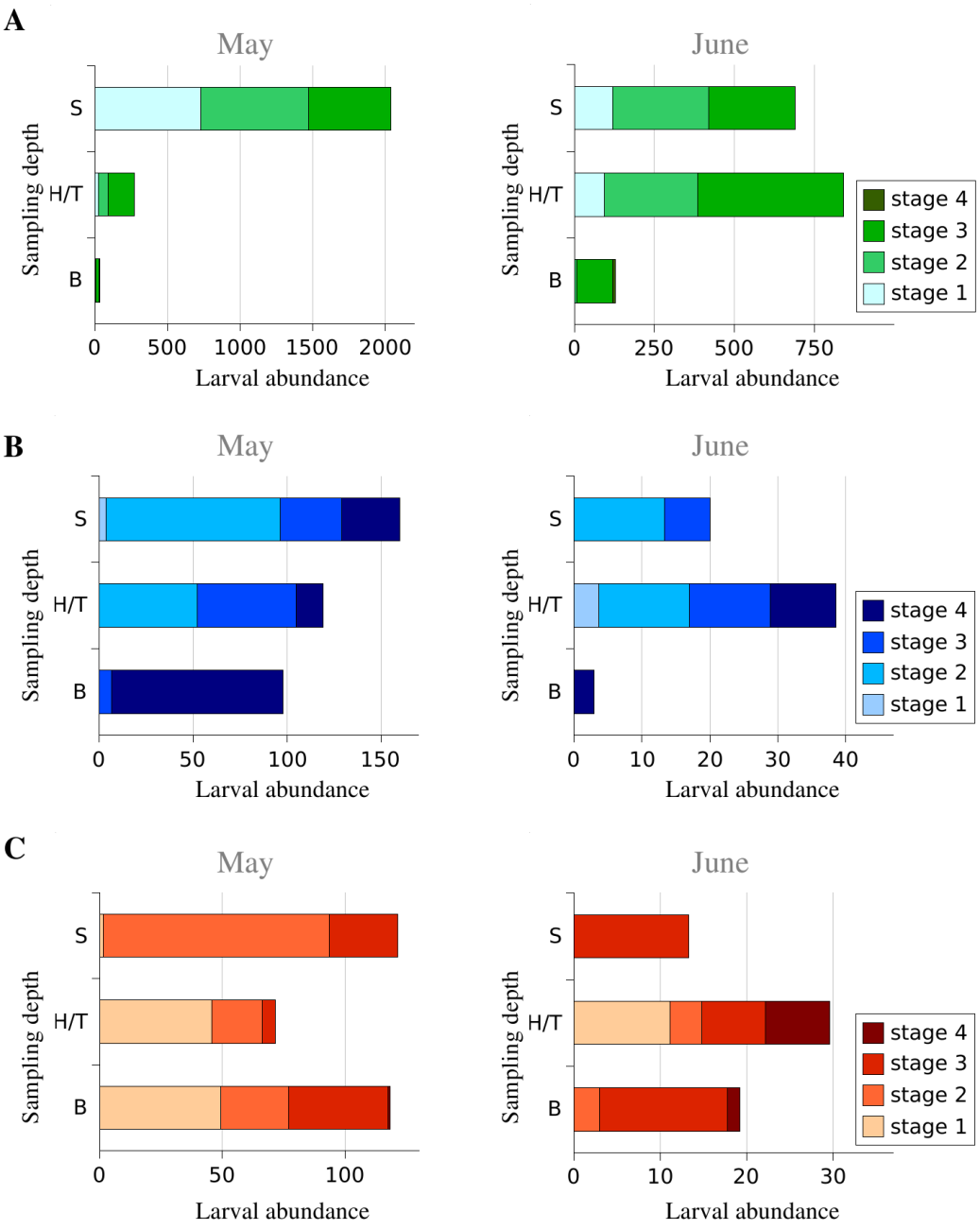


Figure 1.21: Vertical distribution of the different larval stages of (A) *Pectinaria koreni*, (B) *Owenia fusiformis*, and (C) *Sabellaria alveolata* in the northern Bay of Biscay. Larval abundances per sampling depth are given in larvae.m$^{-3}$. S: surface layer, H/T: halocline and/or thermocline, B: bottom layer. The results are the averages obtained for the stations D2, C1, P2, and V2 for the cruise of May, and for the stations D2, P1, and V1 for the cruise of June.

## 1.5 Discussion

To our knowledge, this study is the first to focus on the meroplankton distribution in the northern Bay of Biscay, a highly complex and variable environment. The results presented here highlighted the role of the mesoscale hydrological structures on coastal invertebrate larval distributions. They confirmed the importance of taking into account spatial structures of the environmental variables when describing the distribution of meroplankton organisms as the spatial pattern of larvae are strongly linked to the spatial pattern of the hydrological variables (Belgrano , 1995a,b).

Although temporal variations in hydrological conditions and hydrodynamical structures occur at interannual and seasonal scales in the Bay of Biscay (Koutsikopoulos & Le Cann, 1996; Planque , 2003; Puillat , 2004), the description of mesoscale features have underlined the importance of shorter temporal variations at the scales of a few days to a week (Puillat , 2006). Hydrological variability results from the combined action of environmental factors, such as tide, wind, river run-offs, or solar heat fluxes. Above the Armorican continental shelf, located along the southern coasts of Brittany, instantaneous tidal currents can locally reach 50 $cm.s^{-1}$ but are frequently lower than 10 $cm.s^{-1}$ alongshore between Concarneau and the the Loire estuary. In the northern Bay of Biscay, residual tidal currents are weak and play only a minor role on the long-term transport of water masses and its variability. By contrast, this transport mainly relies on wind-induced currents and density currents which are sensitive to short-term variations of environmental conditions (Puillat , 2006). The currents induced by the dominant NW winds in spring and summer generally reach 10 $cm.s^{-1}$ with maximum values of 20 to 30 $cm.s^{-1}$ locally. The density currents caused by peaks in the Loire run-offs in winter and spring usually reach 10 $cm.s^{-1}$ (Lazure & Jégou, 1998). Given the highly variable environment of the Bay, sampling periods shorter than two weeks are required to allow a synoptic view of the hydrological conditions of the area (Planque , 2006). In the present study, for which sampling was performed during five to nine consecutive days, satellite data indicated similar conditions in sea surface temperature at the beginning and at the end of each cruise

(Figure 1.22), validating the synoptic view given by each cruise. Furthermore, during each cruise, no abrupt change in wind direction or intensity has been reported. The first cruise occurred during a period of low wind speed despite frequent changes in direction while the second cruise occurred during a period of rising NW wind. Both cruises were performed after a peak in the freshwater discharge from the Loire River.

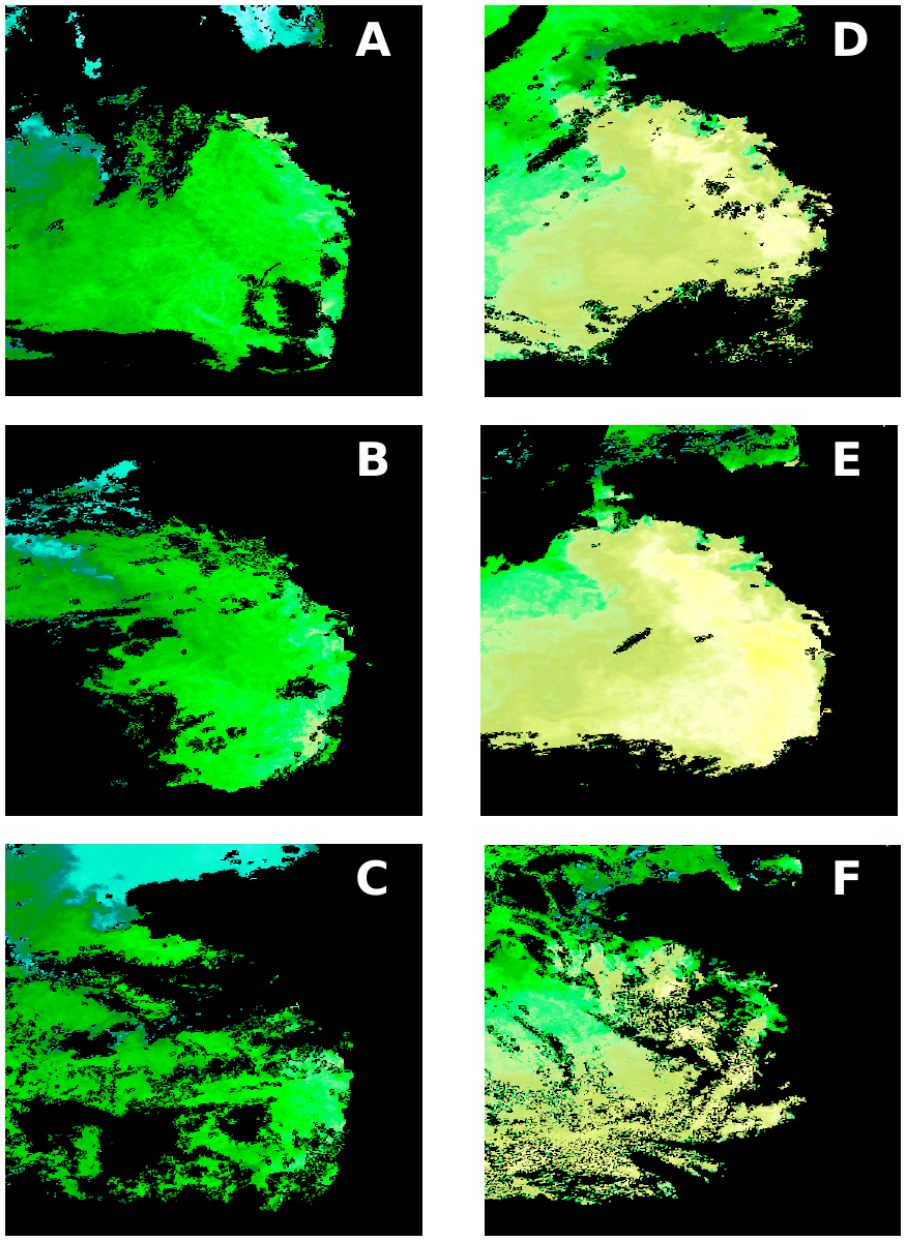


Figure 1.22: Satellite images of the sea surface temperatures in the Bay of Biscay recorded by the NOAA-17 satellite during the two sampling cruises: A) May 11 20:00 UTC, B) May 14 20:00 UTC, C) May 18 20:00 UTC, D) June 09 20:00 UTC, E) June 11 20:00 UTC, F) June 18 20:00 UTC. Data provided by Ifremer.

In the Bay of Biscay, water masses can be distinguished by their hydrological vertical structures and their temporal changes in hydrography (Planque , 2006). In spring 2000, from mid-April to mid-May, Planque (2006) identified six principal hydrological regions: (1) one large region in the central area of the northern part of the shelf that appears to be stable over time and strongly structured vertically (i.e., a deep mixed layer and a high stratification index), (2) one coastal region with a very low surface salinity, a rapid increase in surface temperature and a shallow mixed layer, (3) four regions surrounding the central area and which are highly dynamic and displayed rapid changes in their hydrological properties over time. During the cruises of May and June 2008, oceanic waters and river plume waters were identified by their hydrological properties. However, their location and hydrological properties changed sharply between the two cruises. River plumes water induced by freshwater outputs were sampled in the south of the study area, in the vicinity of the Vilaine and the Loire estuaries, with strong stratification, low surface salinity and density, and shallow mixed layers. During the cruise of May, waters with surface salinities lower than 34 were confined alongshore from Penmarch Headland (between the Audierne and Concarneau transects) in the north to the Ile de Ré in the south of the study area, with a maximum offshore extension of about 50 km. Waters with surface salinities below 32 were located alongshore from the firsts coastal stations of the Pouldu-Lorient transect in the north, till the Noirmoutier Peninsula in the south of the Loire estuary, with a maximal offshore extension of 35 km. Oceanic waters which were characterized by weak stratification, high surface salinity and density, and deep mixed layers were observed in the north of the study area and also in offshore stations in May. A large latitudinal gradient in surface temperature was reported from the Loire estuary to the Bay of Douarnenez.

During the cruise of June, weak haline stratification was observed all over the study area, except in the stations D7 and D8 at the extreme north-west of the area. This extended haline stratification was due to the transport and the dilution of the river plume waters. Surface salinities lower than 34, were more extended both cross-shore and alongshore than in May. They were recorded more than 70 km offshore, and all along the southern Brittany coast, from the Audierne Bay in the north to the south of the study area. Surface salinities lower than 32 were observed along the southern transects of the

Vilaine and the Loire, till 50 km offshore. Moreover, the halocline depth was reduced. Those observations suggest that (i) the river plume waters sampled during the cruise of May were transported both offshore (south-westward) and alongshore (north-westward) along the Brittany coasts, and (ii) the surface waters with salinities lower than 32 sampled in June were caused by the strong freshwater outflows of the Loire that were recorded in the beginning of June. Indeed, salinity distributions could not be related to the freshwaters outflow alone, since the cruise of May occurred two weeks after a peak of the river run-offs ($> 2,000$ $m^3.s^{-1}$), whereas the cruise of June occurred just after a peak of the Loire outputs. The observed dilution and north-westwards and south-westwards transport of river plume waters (salinity $< 34$) during the second cruise may have resulted from strong N to NW winds the week before the sampling. Concomitantly with a peak in freshwater output from the Loire in the beginning of June, those NW winds could have favoured the southwards to south-westwards transport of the plume waters (salinity $< 32$) (Puillat , 2006). Spatial discontinuities in the diluted river plume of June could suggest the presence of lenses of low salinity surface waters (LSSW), as previously reported under N to W winds events (Puillat , 2006, 2004), concordantly with the record of NW wind conditions between the two cruises and during the second cruise. According to Ekman theory, W to NW winds can induce local coastal upwellings in the north of the Loire estuary (coastline oriented NW-SE), whereas N to NW winds can induce upwellings in the south of the Loire estuary (coastline oriented N-S) (Lazure & Jégou, 1998).

From May to June, thermal stratification of the water column became more intense, especially in offshore waters, and was concomitant with the development of the phytoplankton bloom observed by remote sensing. The seasonal thermocline which is stronger in the south of the study area will reach a maximum during the summer period (Puillat , 2004). Below 30-40 m, the temperature was inferior to 12°C. This cold water mass, isolated from the warmer surface water, is called the 'Bourrelet Froid' and is present throughout the year, except in winter when the water column is well-mixed. This water mass elongates along the shelf break from southern Brittany to 45°N and corresponds to a zone of weak tidal stirring. In June, an inversion in the distribution of the surface temperature was observed, with warmer waters offshore than inshore. The presence of colder waters in

the coastal zone could confirm the hypothesis of a coastal upwelling. On the other hand, this inversion in temperature distribution might also result from a quicker warming of the surface waters located offshore than in the inshore less saline and cold waters from the Loire. Thermal inversion with colder waters in the surface layer is commonly reported near the estuaries during the winter (Puillat , 2004) but seems unlikely in June. Along the Douarnenez transect, thermal fronts were observed during the two cruises, at the entrance of the Bay of Douarnenez in May and in the Ushant Sea in June (Le Fèvre , 1983; Mariette & Le Cann, 1985; Morin , 1991).

The typology of the Bay of Biscay water masses has been previously linked to biological properties, such as phytoplankton primary production (Maguer , 2009; Morin , 1991) or zooplankton communities (Albaina & Irigoien, 2007; Zarauz , 2007). In spring 2002, Maguer (2009) reported a highly variable phytoplankton biomass across the continental shelf of the Bay of Biscay. The highest biomasses were observed in the river plumes and were dominated by large phytoplankton cells ($> 10$ µm) which used preferentially nitrate from the river inputs. In the central area of the shelf, the phytoplankton biomass and the contribution of large phytoplankton cells to the total chlorophyll *a* biomass were lower than in the inshore area. Most of the nitrogen used by the small phytoplankton cells was in the form of ammonium. In the south west of the Bay of Biscay, off the Gironde estuary, zooplankton communities were determined by the presence of river plumes and internal wave generation over the slope during the onset of spring stratification (Albaina & Irigoien, 2007; Zarauz , 2007).

In the present study, the horizontal distributions of the larvae of three coastal polychaetes (i.e., *Pectinaria koreni*, *Owenia fusiformis*, and *Sabellaria alveolata*) could be related to the hydrological mesoscale structures. For these three species inhabiting various patchy habitats (subtidal muddy fine sediment or intertidal biogenic reefs) and with a planktonic larval duration ranging from 2 to 10 weeks, maximal larval abundances were generally sampled in coastal waters, more or less extended offshore. For each species, the same hydrological variables explained the observed patterns in larval horizontal dis-

tributions despite different spawning locations and larval life span. Larvae were mainly located in stations of low surface salinity and density, shallow mixed layer, and strong vertical stratification, i.e., the river plumes. Furthermore, while a spatial gradient in the larval abundances as a function of the developmental stage is expected in a homogeneous environment, with older larvae located offshore, and younger larvae in the vicinity of their spawning location, no clear difference in the spatial distribution of the different larval development stages was observed in the present study, suggesting a mixing of larvae of various ages within the river plume waters.

These results confirmed the important role of river plume waters in concentrating and transporting coastal invertebrate larvae (Shanks , 2002; Thiébaut, 1996). River plumes and associated fronts may act as physical barriers for the dispersal of pelagic larvae, by restraining them in the vicinity of their spawning location and favouring retention, or by driving their alongshore transport, limiting offshore export and allowing connectivity between neighbouring populations (Largier, 2003). For example, in the Bay of Seine (English Channel), Thiébaut (1996) has demonstrated the role of the Seine river plume waters in limiting the offshore export of *Pectinaria koreni* larvae by concentrating them in a coastal belt close to the adult populations. River plume could also provide a competitive advantage for planktotrophic larvae, since chlorophyll *a* concentrations are higher in plume waters than in offshore oceanic waters. Given alongshore density currents of about 10 $cm.s^{-1}$ along the southern coasts of Brittany (Lazure & Jégou, 1998), an average advective transport of 6.84 $km.d^{-1}$ is likely although this crude estimation of larval transport can be largely influenced by the spatial variability in alongshore currents and the effects of wind-induced currents.

The importance of the river plume fronts as physical boundaries will also depend on their temporal variability at the temporal scales of the planktonic larval duration. As an example, transitory wind events are likely to disrupt the plume frontal systems and induce large-scale dispersal in response to upwelling events (Shanks , 2003b; Thiébaut, 1996). In the present study, larvae were constrained close to the shoreline in May, because of the limited spatial extension of the river plume, whereas they were observed more offshore in June, because of the offshore transport of the diluted river plume. Although

larvae remained mainly confined within the plume waters, larval retention close to adult populations was lower in June than in May and may greatly affect larval settlement rate.

The existence of spatial structures in the variations of the hydrological environmental variables could overestimate their role because of their high spatial autocorrelation (Legendre & Trousselier, 1988). The use of variance partitioning from multiple regressions or redundancy analyses allows to avoid this problem by isolating the non spatial environmental variation, the spatially structured environmental variation and the spatial variation on the total variance of species distribution or community structure (Borcard , 1992). Our results indicated that the variations in the hydrological properties of water masses alone explained only a few percentages of the variance of larval abundances, although these properties, as salinity or temperature, are known to directly influence larval mortality or development (Anger , 1998; O'Connor , 2007). On the contrary, the interaction between hydrological variables and geographical space explained most of the variation in the larval distribution of coastal invertebrates in the northern Bay of Biscay (from 45 to 74 % of the variations in total abundance), highlighting the importance of the spatial organisation of the hydrological environment in larval distributions. Moreover, the role played by the interaction between hydrological environment and space was higher in May, i.e., when the river plume signature was stronger than in June. Thus, a common spatial structure in the plankton distribution and the environment may lead to an overestimation of the role played by the set of measured environmental variables on the biological variables (Legendre & Trousselier, 1988). Similar results were observed by Belgrano (1995a,b) in the description of the meroplankton distribution along the French-Belgian-Dutch coasts in the North Sea, a region which is also characterised by the presence of a front separated coastal waters from offshore waters. In their study, the spatial structure of the hydrological environment was also the main factor responsible for the spatial structure of the meroplankton community structure, accounting for 42.6 to 50.3 % of the variations of the larval distributions of various coastal invertebrates during different successive cruises.

Geographical space alone also accounted for a non-negligible part of the variations in the observed larval distributions, from 13 to 34 % of the variations of the total abundances. The variability expressed by this fraction can be partly explained by spatial variations in

environmental variables which were not considered or by ecological processes (Legendre & Fortin, 1989). An important spatial parameter to consider when describing larval distribution is the location and the size of adult populations, which determine the possible spawning locations and the quantity of released larvae. In the case of *S. alveolata*, the main adult population was limited to the large intertidal reefs of the Bay of Bourgneuf, in the south of the Loire estuary, which would explain that the highest larval concentrations of this species were observed in the south of the study area (Gruet, 1982). On the contrary, for *P. koreni* and *O. fusiformis*, inhabiting subtidal patchy muddy fine sand sediments, the extensive locations of adult populations remained poorly known and was mainly based on historical data on the distribution of benthic communities (Glémarec, 1969; Guillou, 1980; Hily, 1976). However, recent surveys of the benthic macrofauna in the main patches of fine sand sediments have been performed since 2004 in the main coastal embayments along the coasts of Southern Brittany by the benthic observation network REBENT[e] (Tables 1.4 and 1.5). Densities of both species were highly variable in space at the scale of the surveyed area despite large year-to-year fluctuations and spatial heterogeneity within a bay. Densities of *O. fusiformis* were then higher in the southern part of the study area, in the Vilaine estuary and off Quiberon. *P. koreni* was more common than *O. fusiformis* although it was more abundant in the Vilaine estuary and in the bay of Douarnenez, and in a lesser extent off Quiberon and in the Bay of Concarneau.

Another important parameter which can influence the observed larval distributions of the three target species was the characteristics of the different larval releases (e.g., date, intensity, synchrony at the scale of the study area) for species with an extended reproductive period and several successive spawning events (Dubois , 2007, for *S. alveolata*; Thiébaut , 1998, for *P. koreni*). For each species, averaged larval concentrations were higher in May than in June and a decrease in larval densities of about one order of magnitude was even reported for *O. fusiformis* and *S. alveolata*. Given the planktonic larval durations of the three target species (i.e., 2 weeks for *P. koreni*, 4 weeks for *O. fusiformis* and 4-10 weeks for *S. alveolata*) and the temporal variations in the relative proportions of the different development stages, it seems unlikely that the sampled larvae originated from the same

[e]http://www.rebent.org

Table 1.4: Average densities (ind.m$^{-2}$) of *Pectinaria koreni* in different bays along the coasts of Southern Brittany. At each site, three stations a few hundred meters away from one another were sampled. At each station, three replicates of 0.1 m$^2$ were collected (REBENT data, F. Gentil and C. Broudin, comm. pers.). na: not available.

| | 2004 | 2005 | 2006 | 2007 | 2008 | mean |
|---|---|---|---|---|---|---|
| Vilaine estuary | 13.3 | 25.6 | 12.2 | 4.4 | 4.4 | 12 |
| Vilaine Bay 1 | na | na | na | 1.1 | 1.1 | 1.1 |
| Vilaine Bay 2 | na | na | na | 1.1 | 0 | 0.6 |
| Quiberon | 11.1 | 3.3 | 3.3 | 0 | 2.2 | 4 |
| Etel | 1.1 | 2.2 | 1.1 | 0 | 4.4 | 1.8 |
| Concarneau | 1.1 | 7.8 | 11.1 | 1.1 | 2.2 | 4.7 |
| Audierne | 0 | 0 | 0 | 0 | 0 | 0 |
| Douarnenez North | 3.3 | 1.1 | 0 | 2.2 | 0 | 1.3 |
| Douarnenez South | na | na | na | 20 | 2.2 | 11.1 |

Table 1.5: Average densities (ind.m$^{-2}$) of *Owenia fusiformis* in different bays along the coasts of Southern Brittany. At each site, three stations a few hundred meters away from one another were sampled. At each station, three replicates of 0.1 m$^2$ were collected (REBENT data, F. Gentil and C. Broudin, comm. pers.). na: not available.

| | 2004 | 2005 | 2006 | 2007 | 2008 | mean |
|---|---|---|---|---|---|---|
| Vilaine estuary | 57.8 | 41.1 | 40 | 2.2 | 1100 | 248.2 |
| Vilaine Bay 1 | na | na | na | 1.1 | 3.3 | 2.2 |
| Vilaine Bay 2 | na | na | na | 106.7 | 0 | 53.4 |
| Quiberon | 214.4 | 61.1 | 64.4 | 75.6 | 78.9 | 98.9 |
| Etel | 3.3 | 12.2 | 1.1 | 0 | 0 | 3.3 |
| Concarneau | 17.8 | 16.7 | 15.6 | 12.2 | 4.4 | 11.3 |
| Audierne | 1.1 | 0 | 0 | 0 | 0 | 0.2 |
| Douarnenez North | 17.8 | 4.4 | 3.3 | 4.4 | 3.3 | 6.6 |
| Douarnenez South | na | na | na | 24.4 | 23.3 | 23.9 |

larval cohorts between the first and the second cruises. For *O. fusiformis* and *S. alveolata*, younger larvae were collected in June, indicating that spawning events occurred between the two cruises. For *P. koreni*, although an older larval population was observed in June, these larvae would have originated from a spawning event occurring at the end of May, since the planktonic larval duration of this species is about two weeks, whereas 24 days separated the two cruises. A spawning event just before the second cruise may also explain the higher densities of *P. koreni* larvae reported in the Bay of Douarnenez in June than in May.

If larvae behave as passive particles, one can expect that their distribution remain tied to a water mass as reported for some polychaete and echinoderm larvae in Kiel Bay (Banse, 1986) or for some mollusc and polychaete larvae in the Chesapeake Bay estuarine plume (Shanks , 2002). The analysis of the vertical distributions of *P. koreni* and *O. fusiformis* larvae indicated that they were mainly located within the river plume waters, i.e., near the surface and/or at the thermocline, suggesting that their transport could be mainly determined by surface currents and the displacement of this water mass. Previous studies in the Seine estuary and in the Seine river plume have already indicated that *P. koreni* and *O. fusiformis* larvae were preferentially located above or near the halocline when the water column is stratified, whereas homogeneous distributions along the water column were observed when the stratification was low ($\hat{S} < 0.1$) and the water column well-mixed (Lagadeuc, 1992a; Thiébaut , 1992). As previously reported, the oldest larval stages of these two species were preferentially sampled in bottom layer waters in response to ontogenic vertical migrations (Lagadeuc, 1992a; Thiébaut , 1992, 1998). Although the distribution of *P. koreni* and *O. fusiformis* larvae, except the oldest stages, seemed to be tied to the distribution of the plume waters, their concentrations at some depths and the differences in the larval distribution of the two species suggested that larvae may not have been acting as passive particles. On the contrary, *S. alveolata* larvae were evenly distributed over the whole water column, although the different larval development stages exhibited a patchy vertical distribution. In the vicinity of the Vilaine and the Loire estuaries, the larvae of *S. alveolata* located in the bottom layers may benefit from the 2-layer estuarine circulation to favour their retention near the adult reefs (Koutsikopoulos & Le Cann, 1996). Furthermore, for this species, tidal migrations have also been suggested in the Bay of Mont-Saint Michel, that may promote the inshore transport of larvae by tidal stream transport (Dubois , 2007). Planktonic larvae are then complex organisms able to partly regulate their vertical position to feed or to avoid predators with some effects on their horizontal dispersal (Woodson & McManus, 2007).

## 1.6 Conclusion

In conclusion, the horizontal and vertical distributions of the larvae of three coastal polychaetes, with contrasted life history traits, were described in relation with the spatial and temporal variability of the hydrological features recorded in spring in the northern Bay of Biscay. A description of the typology of the water masses in May and in June over the continental shelf discriminated between high salinity oceanic waters and low salinity river plume waters. The spatial distribution of the low salinity river plumes, that were identified along the southern Brittany coasts, was responsible for the spatial variations observed in the larval abundances of the three species. Indeed, larvae were principally reported within the plume waters, suggesting that the river plume front may act as a physical barrier to offshore larval dispersal of coastal invertebrates and favour alongshore transport in the complex and highly variable environment of the northern Bay of Biscay. Cross-shore transport of larvae was mainly governed by wind-induced currents which influence the location of the river plumes. The distribution of adult populations, the distribution of spawning events and larval vertical behaviours can also alter the observed distribution of larvae.

## 1.7 Acknowledgements

We thank the captains and the crews of the R/V *Côtes de la Manche* (INSU-CNRS), as well as R. Michel, V. Ouisse, K. Robert, and J. Trigui (Station Biologique de Roscoff) and C. Ellien (University Pierre & Marie Curie) for their valuable help in sampling. We also thank C. Broudin, M. Matabos, F. Rigal and G. Schaal for their help in the logistic of the cruises. Some of the equipments (CTD probes, sampling pumping system, TSK flow meter) were generously lent by M. Blanchard, P. Gentien, and M. Lunven (IFREMER-Brest), J.-C. Brun-Cottan (University of Caen), F. Jalabert (Station Biologique de Roscoff), and É. Grossteffan (IUEM, Brest). This work was financed by the French EC2CO program (Ecosphére continentale et côtière). S.-D. Ayata was supported by a PhD grant from the French Ministry of National Education and Research.

# De l'échantillonnage *in situ* à la modélisation couplée biologie-physique

Dans ce chapitre, les distributions horizontale et verticale des différents stades larvaires de trois espèces cibles de polychètes (*Pectinaria koreni*, *Owenia fusiformis* et *Sabellaria alveolata*) ont été décrites en relation avec les structures hydrologiques à méso-échelles rencontrées dans le Nord du Golfe de Gascogne au printemps 2008. Différentes **régions hydrologiques** ont été mises en évidence, en particulier les eaux des plumes dessalées de la Vilaine et de la Loire s'étendant le long des côtes sud bretonnes et des eaux sous influence océanique sur la partie centrale du plateau continental. Dans cet environnement fortement structuré hydrologiquement, les larves des trois espèces cibles ont été préférentiellement échantillonnées dans les stations localisées dans les eaux des **plumes estuariennes** qui se caractérisaient par leur faible salinité de surface et leur forte stratification haline. Des analyses statistiques de partition de la variance, basées sur des régressions multiples et des analyses de redondance, ont ainsi souligné le rôle prépondérant de l'**organisation spatiale de l'environnement hydrologique** sur les abondances larvaires, et un rôle non négligeable de l'**espace géographique** seul. Ce dernier terme inclut l'influence de variables environnementales non prises en compte dans nos observations ou de processus écologiques structurés dans l'espace. Par ailleurs, une variabilité des abondances larvaires entre les deux campagnes d'échantillonnage a pu être mise en relation avec (i) la forte **variabilité printanière** des conditions hydrodynamiques dans le Golfe de Gascogne en raison de la variabilité des débits des principaux fleuves et des conditions météorologiques, et (ii) une variabilité spatio-temporelle des **événements de ponte** au niveau des populations adultes.

L'échantillonnage *in situ* ne peut nous donner qu'une vision à un instant donné des caractéristiques hydrologiques et des abondances larvaires. En effet, les campagnes d'observation sur le terrain demeurent côuteuses en moyens (humains, financiers, matériels), tandis que le tri et l'analyse des échantillons planctoniques en laboratoire restent très fastideux et chronophage. Pour ces raisons, il est difficilement envisageable, et même quasiment impossible, de réaliser des échantillonnages réguliers et à haute fréquence du zooplancton

à l'échelle de la zone d'étude. En outre, l'analyse des distributions larvaires ne permet pas d'inférer les trajectoires des larves et les patrons de dispersion dans le cas de populations vraisemblablement connectées, même si elle demeure un prérequis nécessaire à l'identification des processus biophysiques susceptibles de réguler la dispersion.

En revanche, la modélisation couplée biologie-physique peut permettre de réaliser un grand nombre de simulations en conditions hydrologiques réalistes afin de modéliser la dispersion larvaire. La modélisation lagrangienne permet en particulier de suivre les trajectoires potentielles d'un très grand nombre de particules larvaires émises au sein des différentes populations adultes. Dans ce contexte, le prochain chapitre présentera des expériences réalisées *in silico* afin de quantifier l'influence relative des conditions hydroclimatiques et des traits d'histoire de vie sur le transport larvaire, et d'estimer la connectivité des populations d'invertébrés marins le longs des côtes atlantiques françaises, en particulier entre le Golfe de Gascogne et la Manche occidentale, c'est-à-dire à travers une zone de transition biogéographique.

# Chapter 2

# How does the connectivity between populations mediate range limits of marine invertebrates?

## A case study of larval dispersal in the North-East Atlantic: connectivity between the Bay of Biscay and the English Channel

Sakina-Dorothée AYATA, Pascal LAZURE, and Éric THIÉBAUT

Manuscript submitted to *Progress in Oceanography*[a]

[a]Submission for a special issue on contributions in the GLOBEC project.

## 2.1 Abstract

For many marine species, larval dispersal plays a crucial role in population persistence, re-colonization of disturbed areas, and distribution of species range limits through the control of population connectivity. Along the French Atlantic coast (NE Atlantic), a **biogeographic transition zone** has been reported between temperate and cold-temperate marine faunal assemblages. Hydrodynamics in this area are highly complex and variable including numerous **mesoscale features** (e.g., river plumes, fronts, upwellings, low salinity lenses), which could constrain larval transport and connectivity. In this context, the aim of this study is to assess how hydrodynamic conditions and biological traits influence larval transport and contribute to population connectivity along the French Atlantic coast, between the Bay of Biscay and the English Channel, i.e., along the biogeographic transition zone. A **coupled biophysical individual based model** was used at a regional scale to track larval trajectories under realistic hydroclimatic conditions (tides, river run-offs, and meteorological conditions) and for some common life history traits. Larval particles were released monthly from February to August for the years 2001 to 2005, from 16 spawning populations corresponding to the main bays and estuaries of the study area. Two planktonic larval durations (2 vs. 4 weeks) and 3 vertical distributions (no swimming behaviour, diel vertical migration, ontogenic vertical migration) were considered. **Dispersal kernels** are described by 17 parameters and analysed in a multivariate approach to calculate **connectivity matrices and indices**. The main factors responsible for the variability of the dispersal kernels were the spawning month in relation to the seasonal variations in river run-off and wind conditions, the planktonic larval duration, the spawning population location, and the larval behaviour. No significant inter-annual variability is observed. Self-retention rates are high and larval exchanges occur mainly within the main hydrodynamical areas: the Western English Channel, the Southern Brittany, and the Central Bay of Biscay. Connectivity between the English Channel and the Bay of Biscay populations is low and occurs only under peculiar hydroclimatic conditions (i.e., high river run-off and strong SW winds) and for some biological traits (i.e., long planktonic larval duration and spring spawning).

## 2.2 Introduction

Connectivity, defined by Cowen (2007) as the "exchange of individuals among geographically separated subpopulations that comprise a metapopulation", is a crucial process for the dynamics of marine populations and metapopulations. For most benthic organisms with complex life cycles, connectivity is assured through the release of pelagic larvae, the transport of those larvae by ocean currents in interaction with larval behaviour, and the settlement and the metamorphosis of competent larvae into benthic juveniles (Pineda , 2007). Thus, larval dispersal plays a crucial role in connectivity and its success has tremendous ecological consequences in local population persistence, re-colonization of disturbed areas, spreading of invasive species and range limits of species distributions (Cowen & Sponaugle, 2009; Levin, 2006).

Range limits of marine species often co-localize with hydrological discontinuities, where water masses with different physical properties, such as temperature, come into contact. It has been traditionally assumed that the physiological constraints imposed by those sudden changes in environmental parameters were responsible for the localization of range limits of marine species at oceanographic discontinuities (Suchanek , 1997). However, Gaylord & Gaines (2000) have demonstrated that discontinuities in ocean flow fields could be sufficient to restrict larval dispersal and determine the distribution of marine species. Based on a coupled population dynamics-dispersal model, their results suggested that the common hydrodynamical features usually observed at biogeographic boundaries (e.g., convergent circulation, divergent circulation) could function as one- or two-way barriers to dispersal and could be more or less permeable, depending on life-history traits and hydrodynamic variability (Figure 2.1).

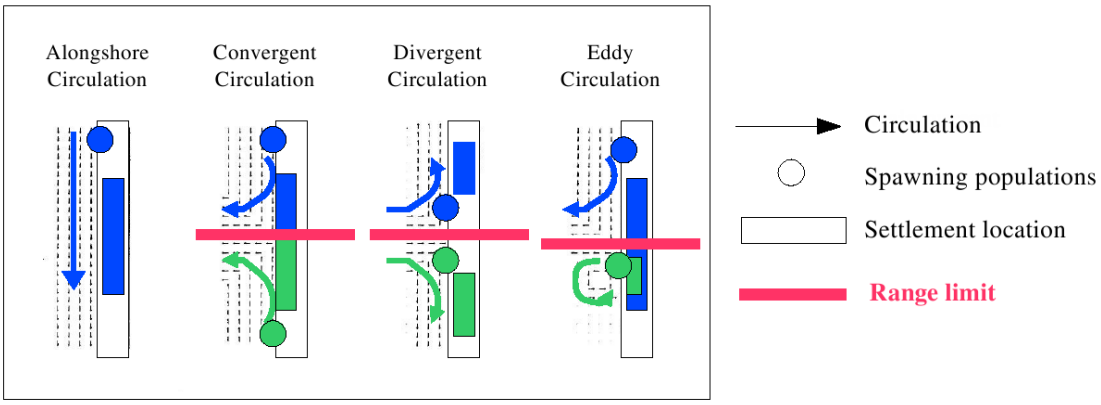


Figure 2.1: Oceanic circulation and range limits of marine species. Four types of common circulation usually observed at biogeographic boundaries are presented: alongshore circulation, convergent circulation, divergent circulation, and eddy circulation. In each type of circulation, one or two upstream spawning populations are considered. From the settlement locations inferred from the circulation patterns, range limits are deduced. From Gaylord & Gaines (2000).

As an example, the recent extension of the northern range limit of the marine gastropod *Kelletia kelletii* in the North-East Pacific beyond Point Conception, California, a major biogeographical boundary coincident with the range limits for many marine taxa, was partly imputed to modifications in coastal circulation (Zacherl , 2003).

In the North-East Atlantic Ocean, the Ushant Sea ("Mer d'Iroise") has been described as a biogeographic transition zone between the temperate and cold-temperate marine assemblages (Lusitanean province in the south and Boreal province in the north) (Cox & Moore, 2000; Dinter, 2001). Furthermore, phylogeographic discontinuities have been recently reported between the Bay of Biscay and the English Channel populations of different benthic invertebrates (Figure 2.2), including the polychaetes *Pectinaria koreni* and *Owenia fusiformis* (Jolly , 2005, 2006).

A complex frontal system has been described in the Ushant Sea (Le Boyer , 2009; Mariette & Le Cann, 1985; Pingree , 1975) that could constrain larval transport and connectivity between the Bay of Biscay and the English Channel (Le Fèvre, 1986). However, intrusions of low salinity waters from the Bay of Biscay have been reported at the entrance of the English Channel (Kelly-Gerreyn , 2006), suggesting a possible transport of water from the Bay of Biscay to the Western English Channel under peculiar hydroclimatic con-

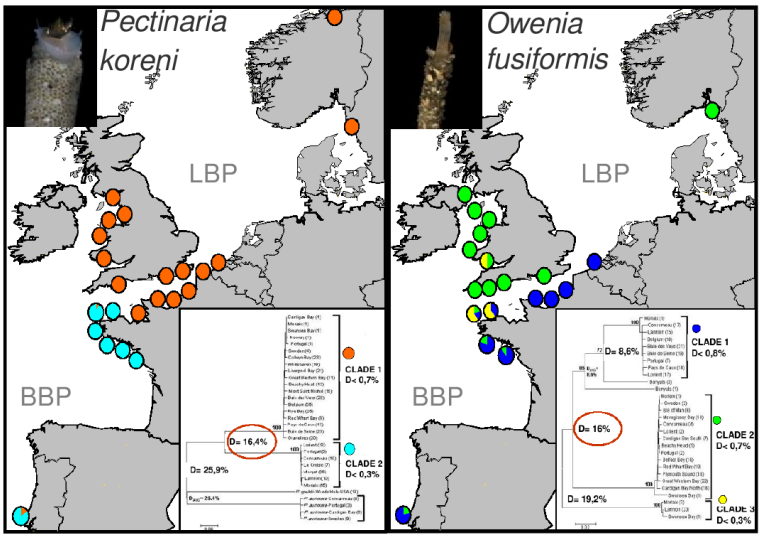


Figure 2.2: Geographic distributions of divergent lineages within the species complexes of two polychaetes in the North-East Atlantic: *Pectinaria koreni* and *Owenia fusiformis* (from Jolly, 2005). Results were obtained from the study of the polymorphism of the mitochondrial gene of the cytochrome oxidase I (COI). The Lusitanean and Boreal biogeographic provinces are indicated (LBP and BBP respectively). Genetic divergences from 16 to 20 % between the divergent clades correspond to the Miocene-Pliocene transition (4-5 My), a period of strong changes in sea elevation, suggesting vicariant effects (Jolly , 2006).

ditions. Low salinity intrusions resulted from (1) a north-westwards transport of plume waters from the Loire and Gironde rivers, favoured by high run-off and NE winds, and (2) an eastwards transport into the Western English Channel under SW/SE winds. On the other hand, the hydrodynamics of the Bay of Biscay are highly complex and variable (Koutsikopoulos & Le Cann, 1996) with numerous mesoscale structures, such as river plumes, low salinity lenses, fronts and upwellings (Puillat , 2006, 2004). All these mesoscale structures are known to greatly affect larval dispersal or retention (Shanks , 2002, 2003b,c) and consequently connectivity.

The study of larval dispersal and connectivity in marine environments is challenging because pelagic larvae are numerous and small, from a few hundreds of microns for invertebrate larvae to a few centimetres for fish larvae, making them difficult to track *in situ*. Recently, progress has been made in the study of larval dispersal and connectivity (Cowen & Sponaugle, 2009; Levin, 2006), including genetic approaches, chemical tracking such as trace elemental fingerprinting and coupled bio-physical modelling (Metaxas & Saunders,

2009). Using individual-based models (IBM), the trajectories of a large number of particles can be tracked in theoretical or realistic hydrodynamical fields. Particles can be described in a first approximation with very simple biological parameters to relate their larval life span or their vertical distribution (Aiken , 2007; Edwards , 2007; Marinone , 2008) or, when known, with species-specific biological traits (North , 2008). Here, a 3-dimensional bio-physical model was used to describe larval dispersal and connectivity of benthic invertebrates inhabiting fragmented habitats in the Western English Channel and in the Bay of Biscay. The hydrodynamic model was forced by realistic hydroclimatic conditions while invertebrate larval biology was kept as simple as possible in the biological model, using common life history traits of benthic invertebrates in temperate regions (spawnings from February to August, common larval swimming behaviours, planktonic larval durations of 2 or 4 weeks). Our goal was then to build a generic model of larval dispersal of benthic invertebrates with common life history characteristics inhabiting fragmented habitats of the study area.

In this context, the present study focused on the larval dispersal and connectivity of benthic invertebrates in the North-East Atlantic, in order to (1) assess the relative roles played by hydroclimatic variability and biological traits in larval transport and connectivity patterns in the Bay of Biscay and in the Western English Channel, and (2) determine if and when connectivity could be possible from the Bay of Biscay to the English Channel populations, i.e., through the Ushant frontal system. Eventually, the aim of the present work was to answer the following question: how does the connectivity between populations mediate range limits of marine invertebrates in the North-East Atlantic?

## 2.3 Material and methods

### 2.3.1 Study area: hydrodynamic and hydrological characteristics

The Bay of Biscay (43°N - 48.5°N, 12°W - 1°W) is an open oceanic bay of the North-East Atlantic Ocean delimited by the Spanish coast in the south and by the French coast in the east. The English Channel is the arm of the North-East Atlantic Ocean located between the north coasts of France and the south coasts of the United Kingdom, and connecting the Atlantic Ocean to the North Sea. The Ushant Sea separates the Bay of Biscay from the English Channel at the western tip of Brittany. Whereas the English Channel is relatively shallow (average depth from 120 m to 45 m from west to east), the Bay of Biscay depth can exceed 4 000 m in its abyssal plain (south-western part of the bay). In the Bay of Biscay, the continental shelf is very narrow in the south along the Spanish coast (maximum width of 30 km) and enlarges itself northwards along the French coast (maximum width of 180 km in front of Brittany).

In the English Channel, tides dominate the transport regime eastwards and are responsible for 60 % of the long-term residual flow (Pingree & Maddock, 1977), although, this long-term flow can be reversed from east to west by strong northern winds (Salomon & Breton, 1993). At the western entrance of the English Channel, the shelf residual circulation is weak (about 3 $cm.s^{-1}$) and oriented north-westwards (Pingree & Le Cann, 1989). Over the continental shelf of the Bay of Biscay, the circulation mainly depends on winds and horizontal density gradients, with weak tidal influence south of 48°30'N, so that strong seasonal variations in hydrodynamics and hydrology have been reported (Koutsikopoulos & Le Cann, 1996; Lazure , 2009; Planque , 2003; Puillat , 2004). Over the abyssal plain the general circulation is weak, with a clockwise circulation along the continental slope and mesoscale eddies.

The Bay of Biscay receives strong freshwater run-off from the Vilaine, the Loire, the Gironde, and the Adour. The Loire and the Gironde are the two main rivers of the Bay, with annual mean freshwater outflows of 900 $m^3.s^{-1}$ each, minimum discharges of 200 $m^3.s^{-1}$ in summer and maximum ones reaching on average 3 000 $m^3.s^{-1}$ in winter and spring. From January to the beginning of April, the water column is homogeneous in the Bay of

Biscay, except in the vicinity of estuaries and coastal areas where strong run-off, combined with relatively low vertical mixing, can cause strong haline stratification. Moreover, in winter and early spring, the presence of low salinity cold water from the main estuaries is responsible for inversions in temperature vertical profiles causing strong vertical thermal gradients. Thermal stratification appears in spring, in April in the western coastal part of the Bay or in May over the continental shelf, and occurs until mid-September. This seasonal thermocline results from the increase in sea surface temperature and the decreases in mean wind speed and mean freshwater run-off. Strong vertical temperature gradients, with temperature differences between surface and bottom layers of 9-10°C, are observed in summer and early autumn. Thermal stratification reveals a homogeneous cold pool of water extending from the Southern Brittany down to the Gironde estuary between approximately the 70 and 130 m isobaths, with nearly constant temperature of 11°C all along the year.

In the vicinity of the Loire and Gironde estuaries, the presence of low salinity surface waters (LSSW) in spring induces significant density gradients responsible for strong density currents over the shelf (2-20 $cm.s^{-1}$), generally oriented northwards because of the Coriolis force. Over the continental shelf of the Bay of Biscay, wind-induced currents are highly variable in direction and speed at the temporal scale of the day to the season, although a general wind-induced circulation parallel to the isobaths can be observed. Near the coast, wind-induced circulation is complex and results from topography marked by vertical shear and vertical water movements. In the north of the bay wind-induced currents usually reach 10 $cm.s^{-1}$ to 20-30 $cm.s^{-1}$ locally (Koutsikopoulos & Le Cann, 1996). The response of shelf water to steady wind stress is relatively rapid (Pingree & Le Cann, 1989). From spring to late summer, NW winds are dominant, whereas from autumn to early spring SW winds are prevailing. During thermal stratification, local upwellings are induced by N and NW winds in the south of the Loire (coastline oriented N-S), and by W to NW winds in the north of the Loire (coastline oriented NW-SE in the South-Brittany) (Puillat , 2006). On the contrary, a persistent upwelling occurs in the south along the Cantabrian coasts. LSSW lenses, mesoscale structures of lower salinity of 50-80 km wide and about 30 m thick, have

been reported over the shelf during W to N wind events and can be transported offshore at least 100 km from the coast (Puillat , 2006).

In the English Channel, the water column is well mixed all year because of strong tidal mixing and low river run-off, except at its western entrance where a seasonal stratification is observed (Salomon & Breton, 1993). In this context, the Ushant Sea is described as a transitional area between the well-mixed waters of the English Channel and the stratified waters of the Bay of Biscay in the south and the Celtic Sea in the west (Pingree , 1982). Moreover, strong thermal fronts are caused in the Ushant Sea by tidal mixing, respectively in spring and in summer (Le Boyer , 2009; Morin , 1991; Pingree , 1975). Low salinity waters from the Loire and the Gironde have been reported in the Ushant Sea in early spring (March-April) in 2002, 2003, and 2004, with fastest travel under NE winds (Kelly-Gerreyn , 2006), suggesting that the northwards transport of plume waters from the Bay of Biscay to the Ushant Sea may be a common phenomenon. More rarely, low salinity waters can penetrate into the Western English Channel in spring tide and under SW to SE winds (Kelly-Gerreyn , 2006).

### 2.3.2 Hydrodynamic model

The three-dimensional (3D) hydrodynamic model MARS (Model for Applications at Regional Scale, Lazure & Dumas, 2008) was used to simulate the circulation in the study area. It is a finite difference, mode splitting model in a sigma-coordinate framework (see Annex B.1 for the detailed equations of the hydrodynamic model). The MARS-3D model has been validated in the Bay of Biscay from survey data and satellite observations of currents, salinity, and temperature (Lazure & Dumas, 2008; Lazure , 2009; Lazure & Jégou, 1998). It has already been successfully applied to study the transport of fish larvae (Allain , 2007; Huret , *submitted*) and toxic phytoplankton (Xie , 2007). In the present study, the model version 6.16 was used with the configuration 'extended Bay of Biscay', whose domain extends from the Spanish coast to 50°30'N in latitude and from 08°W to the French coast in longitude, with an open eastern boundary in the English Channel fixed at 03°05'W. The horizontal grid is regular with a mesh size of 4 km. Thirty sigma

levels (i.e., terrain-following coordinates) are used, with thinner layers near the surface, such as for a 100 m water column the vertical grid spacing corresponds to a resolution of 0.1 m at the surface and 4.5 m in the middle of the column and below. The coastline and bathymetry were provided by the SHOM (Hydrological and Oceanographic Service of the French Navy) with a resolution of 1/25000. The time step was adaptive and varied from 200 to 400 s.

The open boundary conditions (i.e., free surface elevations) were obtained from a larger barotropic two-dimensional (2D) model of the NW European continental shelf extending from Portugal to Iceland (40°N - 65°N, 20°W - 15°E), with a horizontal resolution of 5.6 km. This 2D model is forced by the FES2004 solution (Lyard , 2006) which provides 14 tidal components (i.e., M2, S2, K2, N2, 2N2, O1, K1, P1, Q1, Mf, Mtm, Mm, Msqm, and M4). For the two nested models, surface wind stress and pressure, air temperature, nebulosity, and relative humidity were provided by the meteorological ARPEGE model from Météo France. This regional model is centred above France with a spatial resolution of 0.5° in longitude and latitude. It gives 4 analysed wind and pressure fields per day assimilating recorded data. Temperature and salinity conditions at the open boundaries were obtained from Reynaud's monthly climatology (Reynaud , 1998). Initial conditions in temperature, salinity, and velocity fields were given after a 1-year spin-up simulation. Discharges of the four main rivers, the Vilaine, the Loire, the Gironde, and the Adour, were obtained from historical time series at daily frequency provided by the French freshwater office database (http://www.hydro.eaufrance.fr/).

### 2.3.3 Particle tracking algorithm

Particle trajectories were calculated in three dimensions for each time step from the velocity fields calculated on-line by the hydrodynamic model and using the diffusion scheme described by Visser (1997). The Lagrangian trajectories are obtained from (1) the Eulerian velocity fields and classical Runge-Kutta advection scheme, (2) a random walk process based on the vertical turbulent eddy diffusivity field (Hunter , 1993; Visser, 1997), and (3) vertical swimming velocities.

Hence, the particle positions are computed at each time step of the hydrodynamic model using by the following equations adapted in a sigma coordinate system:

$$\begin{cases} x_{t+\Delta t} = x_t + u(x,y,\sigma,t)\Delta t \\ y_{t+\Delta t} = y_t + v(x,y,\sigma,t)\Delta t \\ \sigma_{t+\Delta t} = \sigma_t + w(x,y,\sigma,t)\Delta t + R_w(\sigma_t, \Delta t, K_\sigma) + w_p \Delta t \end{cases} \quad \text{(Eq. 2.1)}$$

with ($x_t$,$y_t$,$\sigma_t$) the particle coordinates in the sigma framework at the time $t$, ($u$,$v$,$w$) the velocity field linearly interpolated at the position ($x_t$,$y_t$,$\sigma_t$) and obtained from the 3D hydrodynamic model, $\Delta t$ the model time step, $R_w$ a non-naive random walk function (Visser, 1997), $K_\sigma$ the vertical eddy diffusivity (also obtained from the 3D model), and $w_p$ the particle swimming velocity (see Section 2.3.4). In the sigma framework, the particle sigma depth is equal to zero at the bottom ($\sigma_t = 0$) and to one at the surface ($\sigma_t = 1$). $R_w$ is given by the sum of random displacements $d_{\delta t}(\sigma_t, K_\sigma)$ obtained on $n_{dtz}$ sub-loops with a smaller time step $\delta_t = \frac{\Delta t}{n_{dtz}}$ (North , 2006; Ross & Sharples, 2004), such as:

$$\begin{cases} R_w(\sigma_t, \Delta t, K_\sigma) = \sum_{i=1}^{i=n_{dtz}=\frac{\Delta t}{\delta_t}} d_{\delta t}(\sigma_t, K_\sigma) \\ d_{\delta t}(\sigma_t, K_\sigma) = \frac{\partial K_\sigma}{\partial \sigma}\delta t + R\sqrt{2K_\sigma(z_t + 0.5K'_\sigma(z_t)\delta t)r^{-1}} \end{cases} \quad \text{(Eq. 2.2)}$$

with $R$ a random process with a mean equal to zero and a variance $r$ equal to one, here a uniform deviate given by the Fortran 90 random number generator. The number of sub-loops of the random walk process has been fixed at $n_{dtz} = 200$, leading to a random walk time step $\delta_t$ ranging from 1 to 2 s. Ross & Sharples (2004) underlined the need that both $K'_\sigma$ and $K''_\sigma$ are continuous and differentiable, to avoid artificial particle accumulation. This criterion is ensured when for a sufficiently small time-step:

$$\delta t << min \frac{1}{\|K''_\sigma\|} \quad \text{(Eq. 2.3)}$$

which is verified for a random walk time step $\delta_t$ ranging from 1 to 2 s.

As usually fixed for larval dispersal models, the top and bottom boundaries as well as coastal boundaries are reflecting boundaries.

### 2.3.4 Generic individual-based model of invertebrate larvae

To simulate the transport of planktonic larvae of near shore invertebrates inhabiting fragmented habitats, a generic Lagrangian model was designed for typical benthic invertebrates of muddy fine sand sediments.

Larval particles were released from 16 spawning populations (Figure 2.3) along the French Atlantic coast corresponding to the main bays and estuaries of the study area where coastal invertebrates confined to muddy fine sand sediments were reported (Cabioch, 1968; Glémarec, 1969; Guillou, 1980; Hily, 1976).

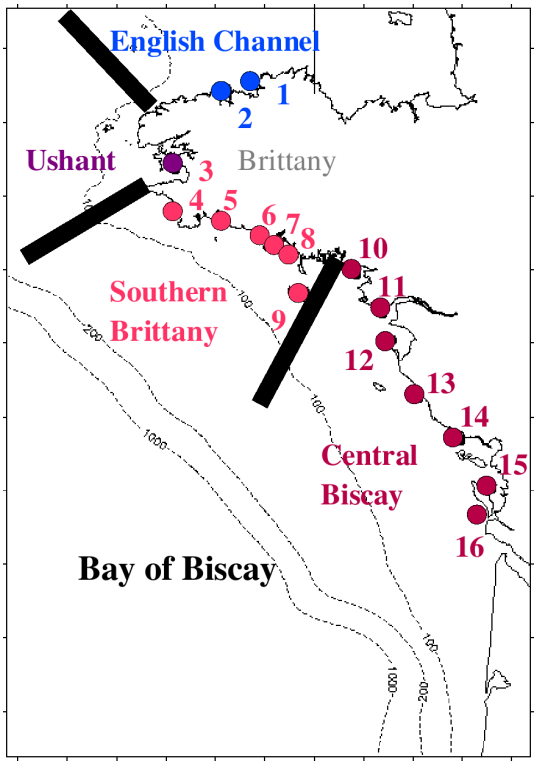


Figure 2.3: Locations of the 16 spawning populations along the French coast grouped by main hydrological areas: English Channel (1-Lannion, 2-Morlaix,), Ushant Sea (3-Douarnenez), Southern Brittany (4-Audierne, 5-Concarneau, 6-Pouldu, 7-Lorient, 8-Etel, 9-Belle-Ile), and Central Biscay (10-Vilaine, 11-Loire, 12-Bourgneuf, 13-Saint-Gilles, 14-Ile de Ré, 15-Antioche, 16-Oléron).

Those 16 spawning populations can be grouped in four main hydrological areas (Figure 2.3):

- two populations in Northern Brittany / Western English Channel (Lannion, Morlaix),
- one population in the Ushant Sea (Douarnenez),
- six populations in Southern Brittany, i.e., where the coastline is oriented WNW-ESE (Audierne, Concarneau, Pouldu, Lorient, Etel, Belle-Ile),
- seven populations in Central Bay of Biscay, i.e., where the coastline is oriented NNW-SSE and where the estuaries of the main rivers are located (Vilaine, Loire, Bourgneuf, Saint-Gilles, Ile de Ré, Antioche, Oléron).

Since initial particle depth did not alter dispersal patterns (see Annex D.1) and since eggs are usually positively buoyant, particles were arbitrarily released at 5 m depth, centered above the grid cell of the spawning population. Spawnings are simulated monthly, from February to August, in average tide conditions for the years 2001 to 2005 to cover a wide range of hydrodynamic conditions that can be encountered by larvae released from late winter to summer. These seasons correspond to usual spawning periods of most benthic invertebrates in temperate regions (Olive, 1995). For each spawning date, 1,000 larval particles are released from each spawning population to obtain statistically reliable dispersal patterns.

Simple biological traits were used in this study: a constant planktonic larval duration, a schematic larval behaviour, and no larval mortality. Two values of planktonic larval duration (PLD) were considered: a relatively short PLD of 2 weeks and a relatively long PLD of 4 weeks, which are typical values for marine invertebrates (Kinlan & Gaines, 2003). Particle positions at the end of the PLD are used to calculate the dispersal kernels and connectivity matrices (see sections 2.3.6 and 2.3.8). Since larval vertical swimming behaviour can alter dispersal patterns, even for weak-swimming larvae (North , 2008), simple larval behaviours were tested to assess their potential role in dispersal patterns and connectivity in the Bay of Biscay. Three simple vertical larval distributions, commonly reported for

marine invertebrate larvae, were considered: no behaviour (i.e., passive particles) used as a reference case, an ontogenic migration, and a diel migration (Figure 2.4).

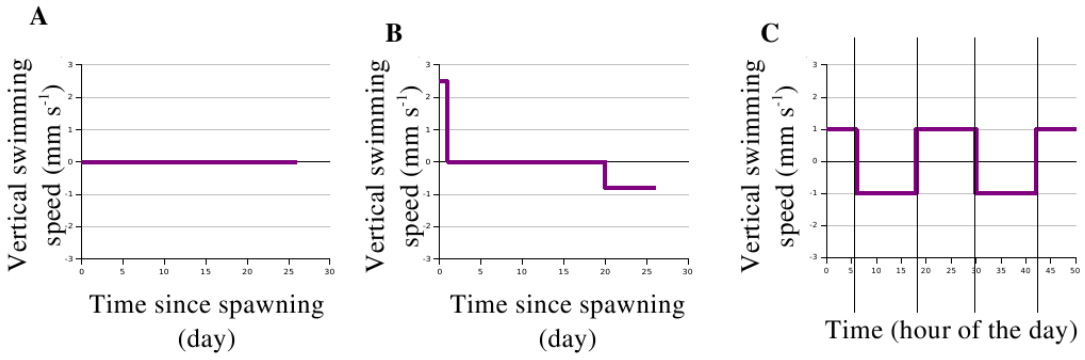


Figure 2.4: Vertical swimming velocities. (A) passive particles, (B) ontogenic migration, (C) diel migration.

The vertical migrations were computed only for a PLD of 4 weeks. For passive larval particles, the vertical swimming velocity $w_p$ was set to 0. Ontogenic swimming behaviour was inspired from the ontogenic swimming velocity scheme proposed by Guizien (2006) for the larvae of the polychaete *Owenia fusiformis* such as:

$$\begin{cases} w_p = 2.5 \text{ mm.s}^{-1} & \text{when } t < 1 \text{ d} \\ w_p = 0 \text{ mm.s}^{-1} & \text{when } 1 \text{ d} \leq t < 20 \text{ d} \\ w_p = -0.8 \text{ mm.s}^{-1} & \text{when } 20 \text{ d} \leq t < 28 \text{ d} \end{cases} \quad \text{(Eq. 2.4)}$$

Diel vertical migration, which has been observed for a wide range of invertebrate phyla, was computed such as larvae swim downward during the day and upward during the night. Common swimming velocities reported for invertebrate larvae such as polychaetes or bivalves (Chia , 1984; Woodson & McManus, 2007) were used:

$$\begin{cases} w_p = -1 \text{ mm.s}^{-1} & \text{when 6 am} \leq t < 6 \text{ pm (day)} \\ w_p = 1 \text{ mm.s}^{-1} & \text{when 6 pm} \leq t < 6 \text{ am (night)} \end{cases} \quad \text{(Eq. 2.5)}$$

### 2.3.5 Numerical experiments

A first set of simulations was conducted in the absence of larval behaviour (passive dispersal) to test the role played by the hydrodynamic variability on the larval dispersal and connectivity in the Western English Channel and in the Bay of Biscay. For this first set of simulations, the passive dispersal was simulated from the 16 spawning populations for 35 spawning dates (7 months, 5 years) with 2 values of PLD: 1120 dispersal kernels of passive dispersal were obtained. A second set of simulations was realized to test the role played by simple swimming behaviours on dispersal patterns. For those simulations, larval particles with vertical behaviour (ontogenic migration and diel migration) were released from the 16 spawning populations for 7 spawning dates during the year 2003 and the PLD was fixed at 4 weeks; 224 additional dispersal kernels were obtained. These results were compared with the passive dispersal kernels obtained for the same spawning dates and populations. For this second set of simulations, a total of 336 dispersal kernels were thus analysed.

### 2.3.6 Dispersal kernel descriptors

To statistically analyze the dispersal patterns, 17 descriptors were defined to describe the 3D dispersal kernels, i.e., the density of larval particles at a given position normalized by the number of particles released. These 17 dispersal kernel descriptors were modified from the definition of the 2D dispersal kernel given by Edwards (2007) and included:

- mean 3D positions in degree (longitude, latitude) and in sigma coordinate (vertical position), and associated variances and 2D-covariance: $x_m$, $y_m$, $\sigma_m$, $s_x$, $s_y$, $s_\sigma$, $s_{xy}$,
- mean longitudinal and latitudinal orthodromic dispersal distances calculated from the initial position ($x_0$, $y_0$) in km, with $R_e = 6371$ km as the Earth radius, and associated variances: $dx_m$, $dy_m$, $s_{dx}$, $s_{dy}$ (Figure 2.5A), with:

$$\begin{cases} dx_m = R_e \left( x_m \frac{\pi}{180} - x_0 \frac{\pi}{180} \right) \\ dy_m = R_e \left( y_m \frac{\pi}{180} - y_0 \frac{\pi}{180} \right) \end{cases} \quad \text{(Eq. 2.6)}$$

- orthodromic distance $d$ and direction from East $\theta$ (in degree) of the mean 2D position ($x_m$,$y_m$) (Figure 2.5A):

$$\begin{cases} d = R_e acos\left[sin\left(x_m\frac{\pi}{180}\right)sin\left(x_0\frac{\pi}{180}\right) + cos\left(x_m\frac{\pi}{180}\right)cos\left(x_0\frac{\pi}{180}\right)cos\left(y_m\frac{\pi}{180} - y_0\frac{\pi}{180}\right)\right] \\ \theta = \frac{180}{\pi}atan\frac{y_m - y_0}{x_m - x_0} - 180(y_m < y_0) \end{cases} \quad \text{(Eq. 2.7)}$$

- variance ellipse major axis $amaj$, minor axis $amin$, direction from East $\theta_m$ (in degree), and isotropy $iso$ (Figure 2.5B):

$$\begin{cases} amaj = \sqrt{\left|\frac{1}{2}\left(s_x + s_y + \sqrt{(s_x - s_y)^2 + 4s_{xy}^2}\right)\right|} \\ amin = \sqrt{\left|\frac{1}{2}\left(s_x + s_y - \sqrt{(s_x - s_y)^2 + 4s_{xy}^2}\right)\right|} \\ \theta_m = \frac{180}{\pi}atan\frac{amaj^2 - s_x}{s_{xy}} \text{ with } \theta_m = 90° \text{ if } s_{xy} = 0 \\ iso = \frac{amin}{amaj} \end{cases} \quad \text{(Eq. 2.8)}$$

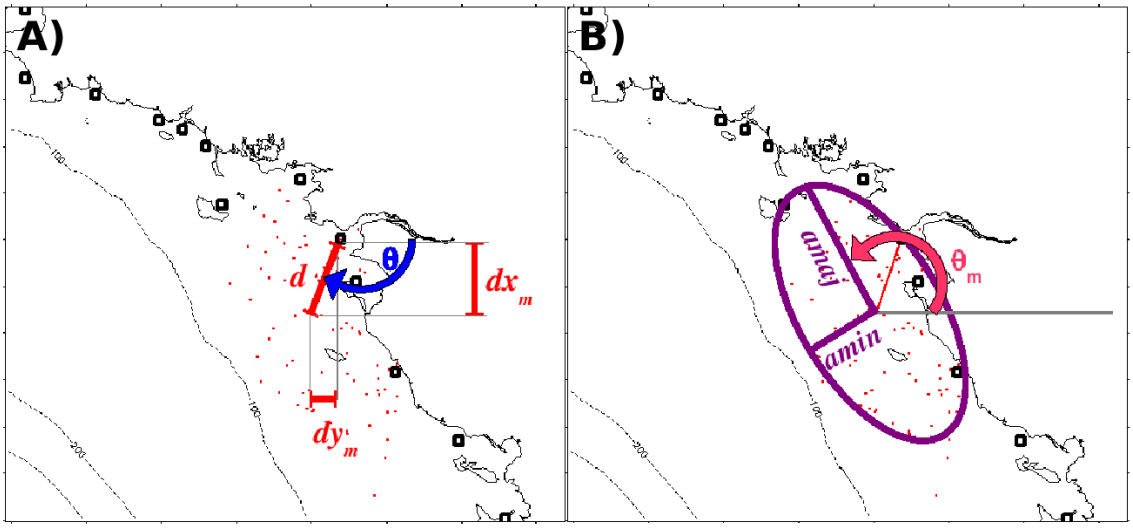


Figure 2.5: (A) Definition of the mean 2D dispersal descriptors: mean longitudinal and latitudinal orthodromic distances $dx_m$ and $dy_m$, mean orthodromic distance $d$ and mean dispersal direction from East $\theta$. (B) Definition of the descriptors of the 2D dispersal variability: variance ellipse major axis $amaj$, minor axis $amin$ and direction from East $\theta_m$.

Among those descriptors, Edwards (2007) argued that 5 are necessary to precisely describe the 2D-dispersal kernels: the dispersal distance and direction ($d$, $\theta$), the major and minor axes ($amaj$, $amin$) and the direction ($\theta_m$) of the variance ellipse. However, using all the 17 descriptors described above allowed us to include descriptors on the vertical distribution of the larval particles ($\sigma_m$, $s_\sigma$) and to take into account their absolute 2D-positions ($x_m$, $y_m$). In our case, they correspond to useful descriptors to describe the alongshore / cross-shore transport and the meridional transport between the Bay of Biscay and the English Channel.

### 2.3.7 Redundancy analysis of the dispersal kernel

For the two sets of simulations, canonical redundancy analyses (RDA) have been conducted on the 17 dispersal kernel descriptors described above. RDA are the direct extension of multiple regression analysis applied to multivariate response data (Legendre & Legendre, 1998). For a given simulation set, we used the matrix of the 17 dispersal kernel descriptors as the table of response variables and the characteristics of the simulations as the table of explanatory variables. For the first set of simulations, the explanatory variables were then: the spawning year, the spawning month, the spawning population, and the PLD. For the second set of simulations, the explanatory variables were: the spawning month, the spawning population, and the swimming behaviour (no behaviour, ontogenic migration, diel migration). The tables of explanatory and response variables were centered and reduced prior to the analysis. To perform the RDA, the *rda* function of the *vegan* package Version 1.16-8 (Oksanen , 2008)[b] was used in the R software Version 2.6.2 (R Development Core Team, 2005)[c]. The significance of the RDA results was tested by permutation tests. One-way and two-way analyses of variance (ANOVA) were also performed to test for the significant effects of larval behaviour and the spawning month on each dispersal kernel descriptor (*aov* function of the R software) and on the connectivity size. For each ANOVA, the normality of the data was verified prior to the analysis and the homogeneity of variances was tested by an analysis of variance on the residuals (*aov* function of the R software).

[b] http://vegan.r-forge.r-project.org
[c] http://www.r-project.org

When ANOVA indicated significant differences, *a posteriori* tests were conducted using Tukey Honest Significant Differences test (*TukeyHSD* function of the R software).

### 2.3.8 Connectivity matrices, transport success, and connectivity size

Connectivity matrices describe the exchange rate between distant populations as the percentage $p_{ij}$ of particles released from one spawning population $j$ (i.e., source population) that settle to an other population $i$ (i.e., sink population) at the end of the PLD (Figure 2.6). Connectivity matrices are square matrices of rank $n$, with $n$ the number of populations.

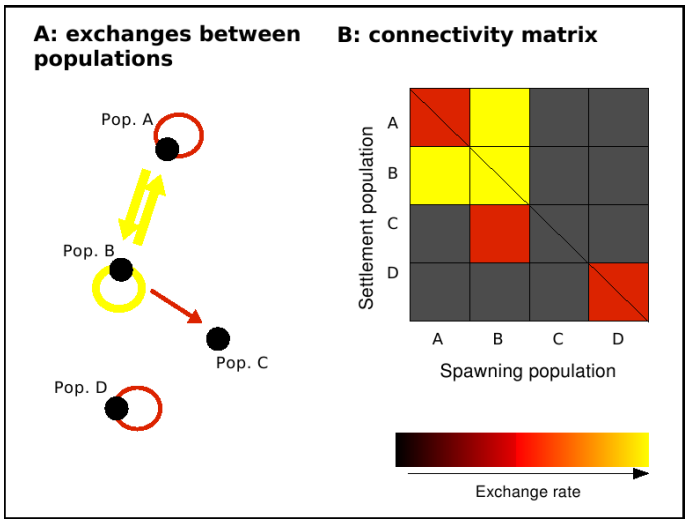


Figure 2.6: Connectivity and connectivity matrix. (A) Example of connectivity patterns for a metapopulation of 4 local populations (Pop. A to Pop. D). Arrows indicate larval exchanges between populations. The arrow width and color are proportional to the intensity of larval exchanges. (B) Corresponding connectivity matrix between the 4 populations. Lighter colors indicate stronger exchanges.

In the present work, particles were considered to have successfully settled if their final position was located in one of the settlement areas. Settlement areas, representing the patches of the fragmented habitat of fine sand sediments, were defined as the rectangles of 0.20° in longitude (about 22 km) and 0.25° in latitude (about 17 km) centred above the 16 spawning populations. Settlement areas were non-overlapping, so that they could be slightly smaller where spawning populations were close to each other. The connectivity matrices between the 16 spawning populations were calculated for each spawning date,

PLD value, and larval behaviour. For a given PLD and behaviour, monthly-mean connectivity matrices were calculated from the five matrices obtained for the same month for the years 2001 to 2005.

The transport success (or settlement success) was defined as the percentage of released particles per spawning population that successfully settle. The transport success $T_j$ from a spawning population $j$ was given by the sum along columns $j$ of the exchange rates $p_{ij}$ of the connectivity matrix: $T_j = \sum_{i=1}^{i=n} p_{ij}$. The diagonal of a connectivity matrix gives the self-retention success ($p_{ii}$). Since the 16 spawning populations considered here were ordered along a latitudinal gradient along the French Atlantic coast, the exchange rates above the diagonal ($p_{ij}$ with $i < j$) corresponded to northward larval transport, whereas the exchange rates below ($p_{ij}$ with $i > j$) corresponded to southward larval transport. Hence the northwards transport success was given by the sum along columns of the exchange rates above the diagonal ($\sum_{i=1}^{i<j} p_{ij}$) whereas the southwards transport success was the sum along columns of the exchanges rates bellow the diagonal ($\sum_{i>j}^{i=n} p_{ij}$). Transport success, self-retention rate, northwards exchange rate and southwards exchange rate were also calculated for each spawning date, i.e., for each connectivity matrix, as the averages of the rates obtained for the 16 spawning populations.

In graph theory, connectivity corresponds to a weighted oriented graph, whose vertices (or nodes) represent populations and directed edges (or arrows) directional exchange rates between populations (Treml , 2008). In this context, the total number of connexion within a graph, equal to the sums of the adjacency matrix, is the graph's size and is called hereafter the "connectivity size". Connectivity size was then the total number of oriented connexions between populations. For example, in the metapopulation presented Figure 2.6, the connectivity size is equal to 6.

## 2.4 Results

### 2.4.1 Variability of the passive dispersal patterns

The redundancy analysis conducted on the passive dispersal kernel descriptors against the four explanatory variables (i.e., spawning year, spawning month, spawning populations, PLD), showed that only the first two canonical axes were significant (Figure 2.7).

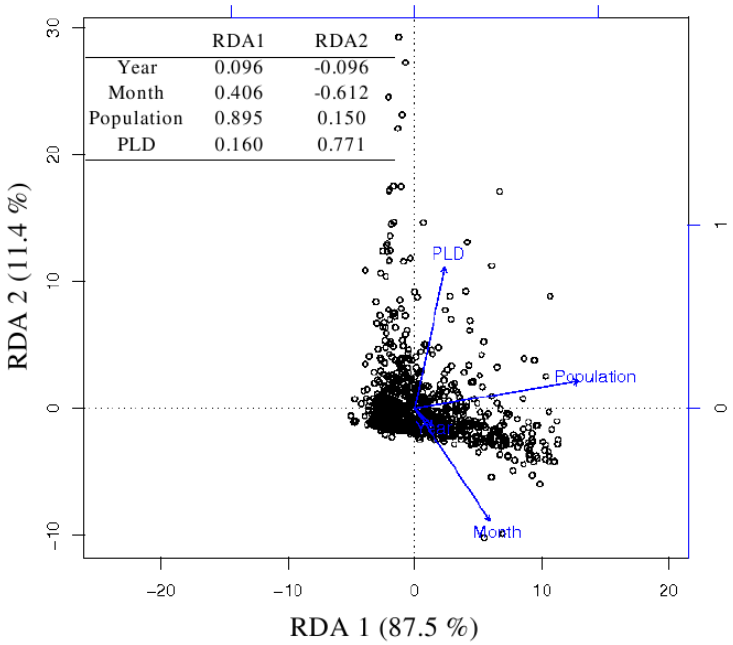


Figure 2.7: Graphical representation of the redundancy analysis (RDA) of the passive dispersal kernels. Dots represent the spawning events and arrows the explanatory variables. The first axis RDA1 explained 87.5 % of the variance ($p < 0.001$), and the second axis RDA2 explained 11.4 % ($p < 0.001$). The biplot scores of each constraining variables are indicated for both axes.

The first axis RDA1 explained 87.5 % of the variance ($p < 0.001$) and was mainly scored by the spawning population and the spawning month (biplot scores, Figure 2.7). The second axis RDA2 explained only 11.4 % of the variance ($p < 0.001$) and was scored by the PLD and the spawning month. The relative contributions of the explanatory variables to these two axes indicated that the variability of the passive dispersal kernels was mainly due to the spawning population location, and in a lesser extent the spawning month and the PLD. The spawning year had no significant effect on the dispersal. A RDA was also conducted on the five descriptors of the 2D-dispersal kernels proposed by Edwards

(2007). Although it showed only one significant axis, similar results were obtained but with a higher contribution of the PLD in the variability of the kernel descriptors (see Annex D.2).

Since no significant inter-annual variation of the dispersal kernels was observed, only the mean trajectories and the average longitudinal and latitudinal distances obtained for the year 2003 are presented to illustrate the influence of the other explanatory variables (Figure 2.8, Figure 2.9).

As indicated by the RDA, mean particle trajectories and distances varied with the spawning location and the spawning month. In the Western English Channel, particles released from the two spawning populations of Northern Brittany were always transported north-eastwards following the English Channel residual circulation (Figure 2.8, positive longitudinal and latitudinal distances in Figure 2.9A). For these two populations, mean orthodromic distance reached 55 ± 18 km (n = 70) for a PLD of 4 weeks. In the Ushant Sea, the majority of the particles released from the Bay of Douarnenez (spawning population #3) were not transported out of the bay whatever the spawning month so that the mean orthodromic distance did not exceed 13 ± 7 km (n = 35) for a PLD of 4 weeks.

Conversely, seasonal patterns were observed for the dispersal of the particles released in Southern Brittany and in Central Bay of Biscay, in relation to the seasonality of river run-off and wind conditions. From February to April 2003 larval trajectories were oriented north-westwards following the coastline (Figure 2.8, positive latitudinal and negative longitudinal distances in Figure 2.9B-C). From May to August 2003, larval trajectories were mainly oriented southwards (Figure 2.8, negative latitudinal distances in Figure 2.9B-C), except for the particles released from Audierne population (spawning population #4) for which transport was still north-westwards in May and June 2003 (Figure 2.8). Among the spawning populations of the Bay of Biscay, dispersal patterns slightly differed depending on local topography and circulation. As an example, for the spawning populations #15-16 (i.e., Antioche and Oléron), larval transport in February, March and April was first oriented southwards and then north-westwards. From the Southern Brittany populations, transport occurred on shorter distances (mean orthodromic distance of 66 ± 46 km, n = 210, PLD = 4 weeks) than from Central Bay of Biscay populations (mean orthodromic

distance of 83 ± 59 km, n = 245, PLD = 4 weeks). These differences were mainly due to very short transport distances for Southern Brittany populations from May to August (mean orthodromic distances of 103 km in February-April vs. 19 km in May-August).

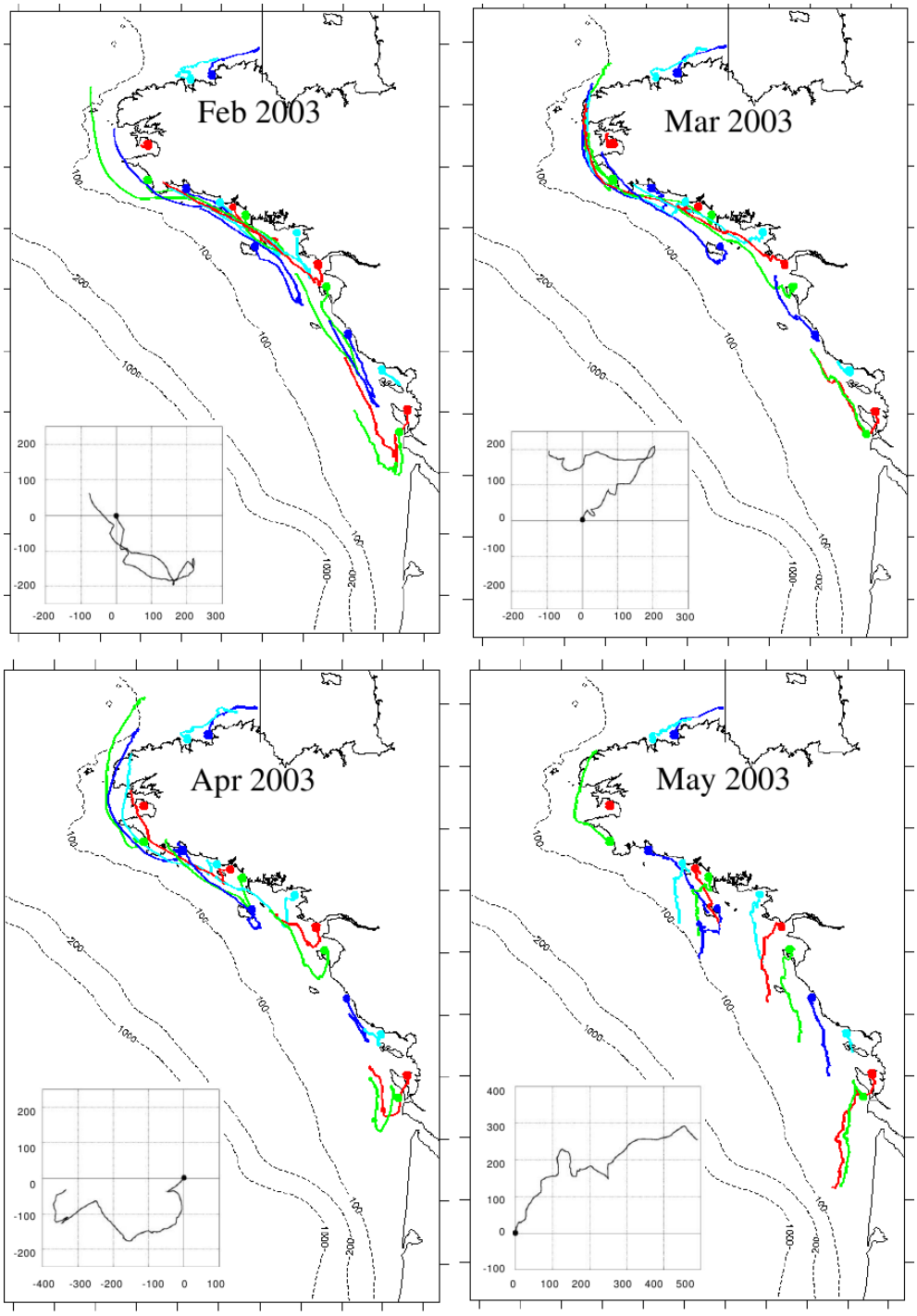

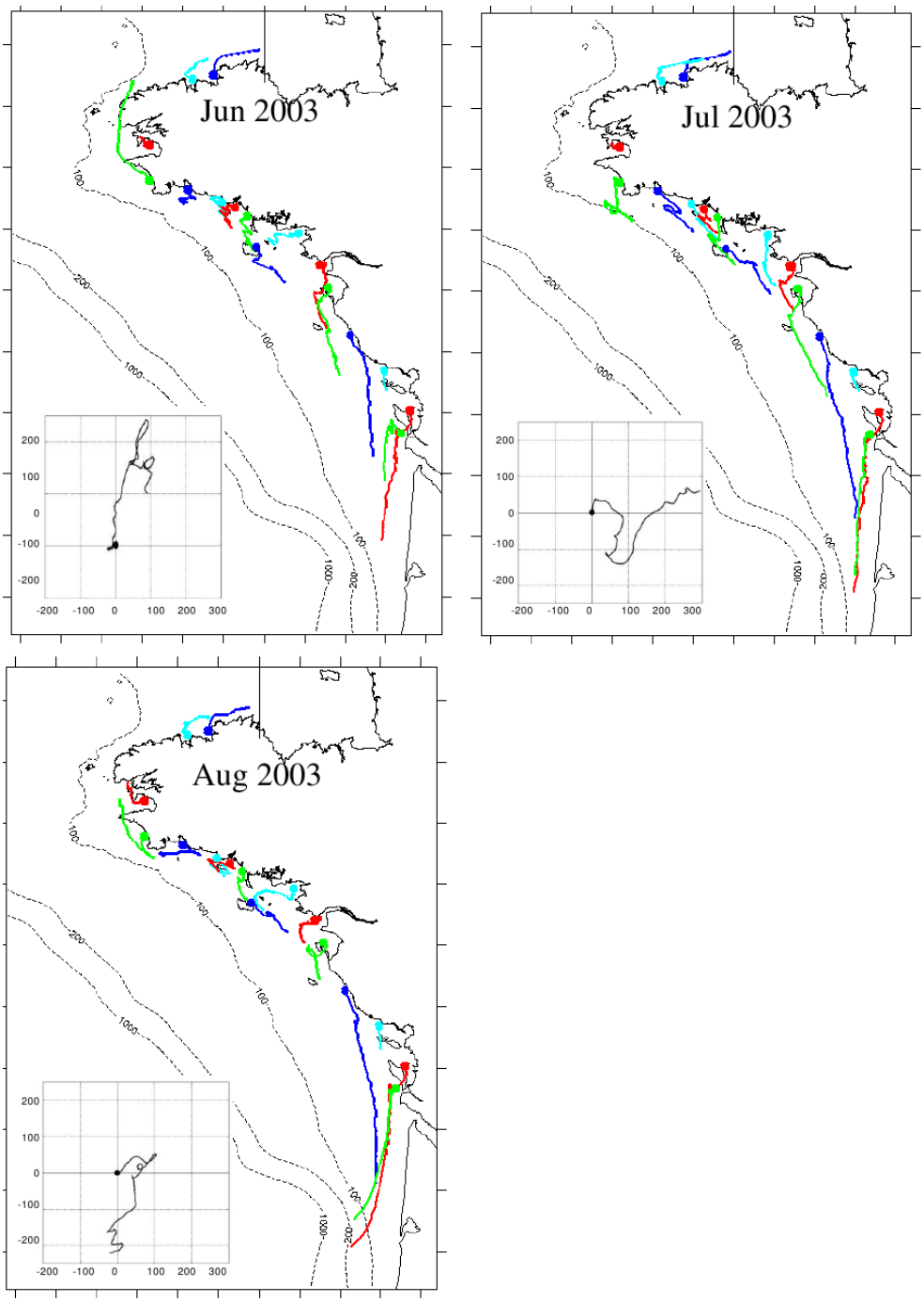


Figure 2.8: Mean particle trajectories obtained in 2003 for particle releases in February, March, April, May, June, July, and August. Mean trajectories are represented for a PLD of 4 weeks and are calculated as the average 2D-positions of 1000 particles released from each spawning location. The progressive vector diagrams of wind conditions in Ushant during the dispersals are indicated. Black circles on the progressive vector diagrams indicate the spawning day.

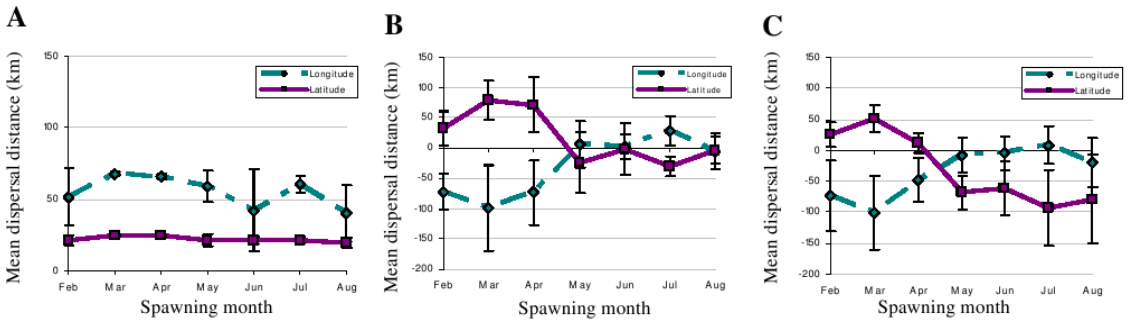


Figure 2.9: Monthly longitudinal and latitudinal transport distances from the spawning populations of (A) the English Channel (populations #1-2), (B) the Southern Brittany (populations #4-9), and (C) the Central Bay of Biscay (populations #10-16). The mean distances are the averages obtained in 2003 after 4 weeks of passive dispersal. Positive longitudinal distance indicates northwards transport. Positive latitudinal distances indicates eastwards transport.

To illustrate the variability induced by the PLD in the dispersal patterns, the five main descriptors of the dispersal kernels (i.e., mean dispersal distance and direction, major axis, minor axis and direction of the variance ellipse) obtained with a PLD of 2 and 4 weeks are given in Table 2.1 for three spawning dates and five spawning populations. The three spawning dates corresponded to a release in early spring, in late spring or in summer (i.e., March, May, July 2003). The five spawning populations were representative of the different spawning areas: Northern Brittany (#2: Morlaix), Southern Brittany (#4: Audierne, #7: Lorient), and Central Bay of Biscay (#11: Loire, #16: Oléron). In general, shorter PLD did not alter the dispersal direction but induced shorter dispersal distance and reduced dispersal variability (Table 2.1). Indeed, smaller axes of the ellipses of variance indicated denser clouds of particles. After 2 weeks of dispersal, mean dispersal distance reached 40 $\pm$ 29 km (n = 560), whereas it is almost doubled after 4 weeks of dispersal, reaching 73 $\pm$ 51 km (n = 560). The orientation $\theta_m$ of the ellipse and the variance of the sigma depth of the particles $s_\sigma$ were independent with the PLD.

Table 2.1: Main dispersal kernel descriptors obtained after 2 and 4 weeks of passive dispersal for releases in March, May and July 2003 from 5 spawning locations (Morlaix, Audierne, Lorient, Loire, Oléron).

| Month | Spawning | $d$ | | $\theta$ | | $amaj$ | | $amin$ | | $\theta_m$ | | $s_\sigma$ (%) | |
|---|---|---|---|---|---|---|---|---|---|---|---|---|---|
| | | 2 w | 4 w | 2 w | 4 w | 2 w | 4 w | 2 w | 4 w | 2 w | 4 w | 2 w | 4 weeks |
| March | Morlaix | 45 | 74 | 22 | 20 | 37 | 36 | 5 | 9 | 13 | 12 | 8 | 8 |
| | Audierne | 35 | 105 | -31 | -89 | 30 | 37 | 11 | 24 | -49 | 42 | 8 | 8 |
| | Lorient | 67 | 178 | -6 | -31 | 25 | 37 | 6 | 29 | -2 | 78 | 9 | 9 |
| | Loire | 45 | 155 | -22 | -20 | 42 | 81 | 8 | 9 | -24 | -19 | 9 | 9 |
| | Oléron | 51 | 108 | -50 | -45 | 22 | 33 | 7 | 8 | -30 | -35 | 8 | 8 |
| May | Morlaix | 20 | 54 | 24 | 20 | 30 | 46 | 5 | 5 | 13 | 13 | 8 | 8 |
| | Audierne | 59 | 83 | -40 | -77 | 24 | 48 | 19 | 29 | -80 | 81 | 9 | 9 |
| | Lorient | 18 | 62 | 126 | 124 | 12 | 30 | 6 | 18 | -7 | 19 | 7 | 7 |
| | Loire | 32 | 69 | -137 | -106 | 33 | 52 | 16 | 32 | -2 | 4 | 5 | 5 |
| | Oléron | 30 | 86 | -131 | -112 | 18 | 43 | 12 | 23 | 60 | 79 | 3 | 3 |
| July | Morlaix | 13 | 60 | -77 | 19 | 16 | 41 | 8 | 6 | 3 | 12 | 9 | 9 |
| | Audierne | 25 | 39 | -123 | 119 | 16 | 56 | 7 | 17 | -58 | -54 | 4 | 4 |
| | Lorient | 8 | 29 | -116 | 128 | 15 | 28 | 5 | 11 | -13 | -33 | 9 | 9 |
| | Loire | 17 | 40 | -129 | 97 | 25 | 50 | 11 | 11 | -43 | -53 | 7 | 7 |
| | Oléron | 26 | 129 | -110 | -100 | 32 | 92 | 9 | 15 | 90 | 80 | 6 | 6 |
| Mean (35 dates, 16 populations) | | 40 | 73 | | | 21 | 39 | 8 | 15 | | | 7 | 7 |

### 2.4.2 Role of larval behaviour on dispersal patterns

To assess the relative role played by larval behaviour in dispersal, 3 larval vertical distributions commonly reported in marine invertebrates were tested (no behaviour, ontogenic migration, diel migration). For passive dispersal, mean sigma depth $\sigma_m$ of the particles varied with spawning populations and time since spawning (Figure 2.10A).

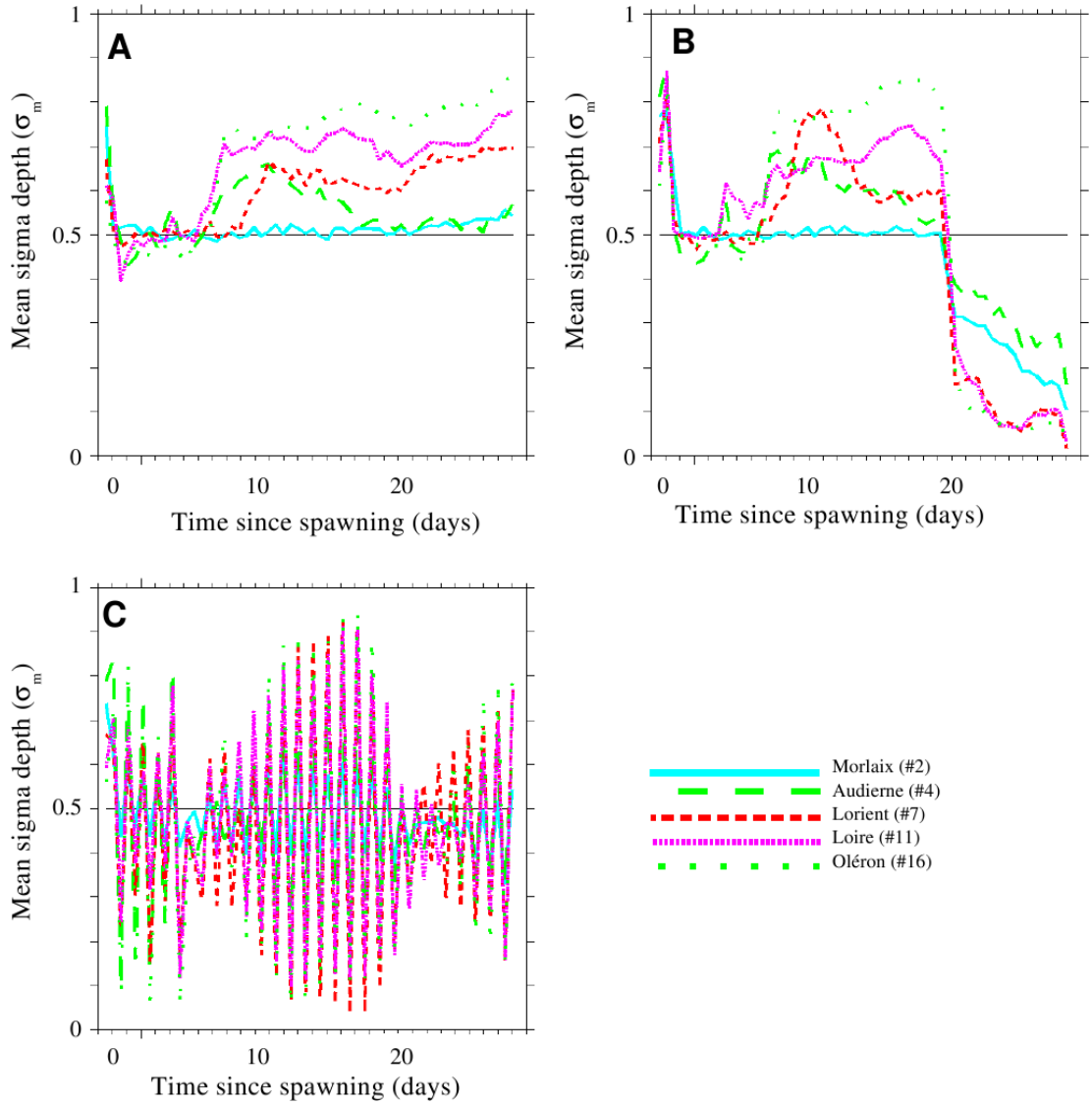


Figure 2.10: Mean sigma depth of 1000 particles released from Morlaix, Audierne, Lorient, Loire, and Oléron in May 2003, (A) without swimming behaviour, (B) with an ontogenic vertical migration, (C) with a diel vertical migration.

The first day of dispersal, mean sigma depth reached 0.5, i.e., the centre of the water column. As expected, the mean sigma depth of the passive particles released from the English Channel population remained close to 0.5 during all the dispersal (see population #2 - Morlaix in Figure 2.10A), indicating that passive particles were evenly distributed over the vertically-homogeneous water column of the English Channel. On the contrary, quick increases in mean sigma depths of passive particles from other spawning populations were observed. Indeed, since larval release occurred in coastal waters, passive particles were likely to encounter low salinity waters, especially in the vicinity of estuaries. Passive particles would then be trapped within the upper-layer lower-density plume waters when transported offshore, i.e., at constant mean vertical depth but with increasing water column height, resulting in an increase in the mean sigma depth. Large increases in sigma depth could also be linked to coastal upwelling events. Mean vertical position of larvae could also change with spawning month in relation to the relative position of the river plumes at spawning (see Annex D.3).

As expected, vertical swimming behaviours modified mean sigma depths (Figure 2.10B-C). With an ontogenic migration, vertical depth patterns observed at the beginning of the dispersal were close to those observed with no behaviour because of null vertical swimming speed (Figure 2.10B). Then, after 20 days, particles moved with a negative swimming velocity so that they were mainly located close to the bottom at the end of the dispersal phase (Figure 2.10B). A diel vertical migration imposed bi-daily variation of the mean vertical positions of the particles (Figure 2.10C). Variations in the amplitude of the mean depth $\sigma_m$ were related to the variations of the vertical eddy diffusivity following the spring/neap tide cycles.

The redundancy analysis conducted on the dispersal kernels descriptors of the second set of simulations (7 months, 16 populations, 3 behaviours, 1 PLD, 1 year) used three explanatory variables: spawning month, spawning population, and larval behaviour (Figure 2.11).

This analysis showed 2 significant canonical axes: the first axis RDA1 explained the major part of the variance (94.3 %, $p < 0.001$) and was scored by larval behaviour and the spawning month, whereas the second axis RDA2 explained only a small part of the variance

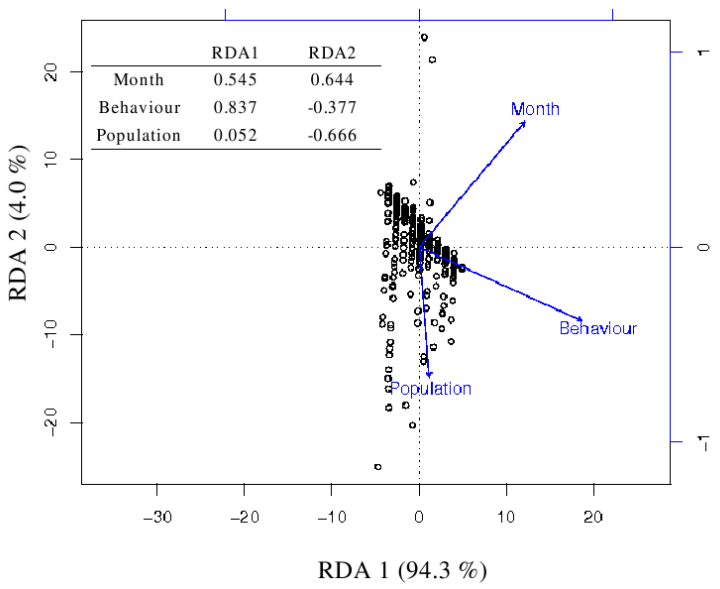


Figure 2.11: Graphical representation of the RDA analysis of the dispersal kernels obtained with vertical swimming behaviours. The first axis RDA1 explained 94.3 % of the variance ($p < 0.001$), and the second axis RDA2 explained 4.0 % ($p < 0.001$). The biplot scores of each constraining variables are indicated for both axes.

(4.0 %, $p < 0.001$) and was scored by the spawning population and the spawning month. This analysis confirmed the role of the spawning month and the spawning population location in the variability of the dispersal kernels and indicated that the particle vertical behaviour significantly contributed to dispersal variability.

The values of the main dispersal kernel descriptors obtained with ontogenic and diel vertical migrations are given in Tables 2.2 and 2.3. One-way ANOVAs were conducted on each of the 17 dispersal kernel descriptors to test the role played by the larval behaviour (passive particles, ontogenic migrations, diel migrations) on those descriptors. Results indicated a significant effect ($p < 0.05$) of the swimming behaviour on the mean dispersal distance $d$. Tukey HSD a posteriori tests showed that mean dispersal distance $d$ varied only between the passive dispersal and the dispersal with an ontogenic migration ($p < 0.05$). ANOVA results also indicated that vertical swimming behaviour had a significant effect ($p < 0.001$) on the mean sigma depth $\sigma_m$ and on the variances of the 3-D positions, including the variance ellipse axes ($s_x$, $s_y$, $s_{dx}$, $s_{dy}$, $s_\sigma$, $amaj$, $amin$). Tukey HSD a posteriori tests showed that mean sigma depth $\sigma_m$ and variance ellipse minor axis $amin$ varied between each pair of behaviour types ($p < 0.05$), whereas variance ellipse major

Table 2.2: Main dispersal kernel descriptors obtained after 4 weeks of dispersal with ontogenic migrations and for releases in March, May and July 2003 from five spawning locations (Morlaix, Audierne, Lorient, Loire, Oléron).

| Month | Spawning | $d$ | $\theta$ | $amaj$ | $amin$ | $\theta_m$ | $s_\sigma$ (%) |
|---|---|---|---|---|---|---|---|
| March | Morlaix | 68 | 20 | 39 | 7 | 14 | 7 |
| | Audierne | 94 | -84 | 38 | 26 | 45 | 5 |
| | Lorient | 156 | -20 | 41 | 25 | -54 | 4 |
| | Loire | 161 | -20 | 79 | 9 | -18 | 9 |
| | Oléron | 108 | -45 | 33 | 8 | -36 | 8 |
| May | Morlaix | 67 | 19 | 44 | 4 | 12 | 6 |
| | Audierne | 72 | -69 | 45 | 26 | -86 | 5 |
| | Lorient | 62 | -214 | 18 | 10 | -26 | 2 |
| | Loire | 54 | -268 | 44 | 21 | -4 | 1 |
| | Oléron | 67 | -106 | 27 | 17 | 44 | 1 |
| July | Morlaix | 58 | 21 | 41 | 6 | 10 | 6 |
| | Audierne | 12 | -122 | 47 | 17 | -46 | 4 |
| | Lorient | 35 | -214 | 23 | 8 | -31 | 5 |
| | Loire | 49 | -255 | 31 | 9 | -59 | 4 |
| | Oléron | 31 | -265 | 32 | 9 | -82 | 4 |

axis $amaj$ differed between the dispersal with a diel vertical migration and the two other types of migrations ($p < 0.05$).

More specifically, the mean dispersal and the variance ellipse axes obtained with vertical migrations were lower than those obtained with passive dispersal (Tables 2.1, 2.2 and 2.3; Figure 2.12), indicating denser clouds of particles. Mean dispersal distance reached 74 km with no vertical behavior, 59 km with an ontogenic migration, and 63 km with a diel migration. For example in May 2003, although vertical behaviour did not significantly affected the mean particle trajectories, it decreased the spatial extension of particle clouds, such as for the particles released from spawning populations of Lorient (#7), Loire (#11) and Oléron (#16) (Figure 2.12). On the other hand, with a diel vertical migration, larval particles released from the Bay of Biscay populations remained closer to the shore (Figure 2.12C).

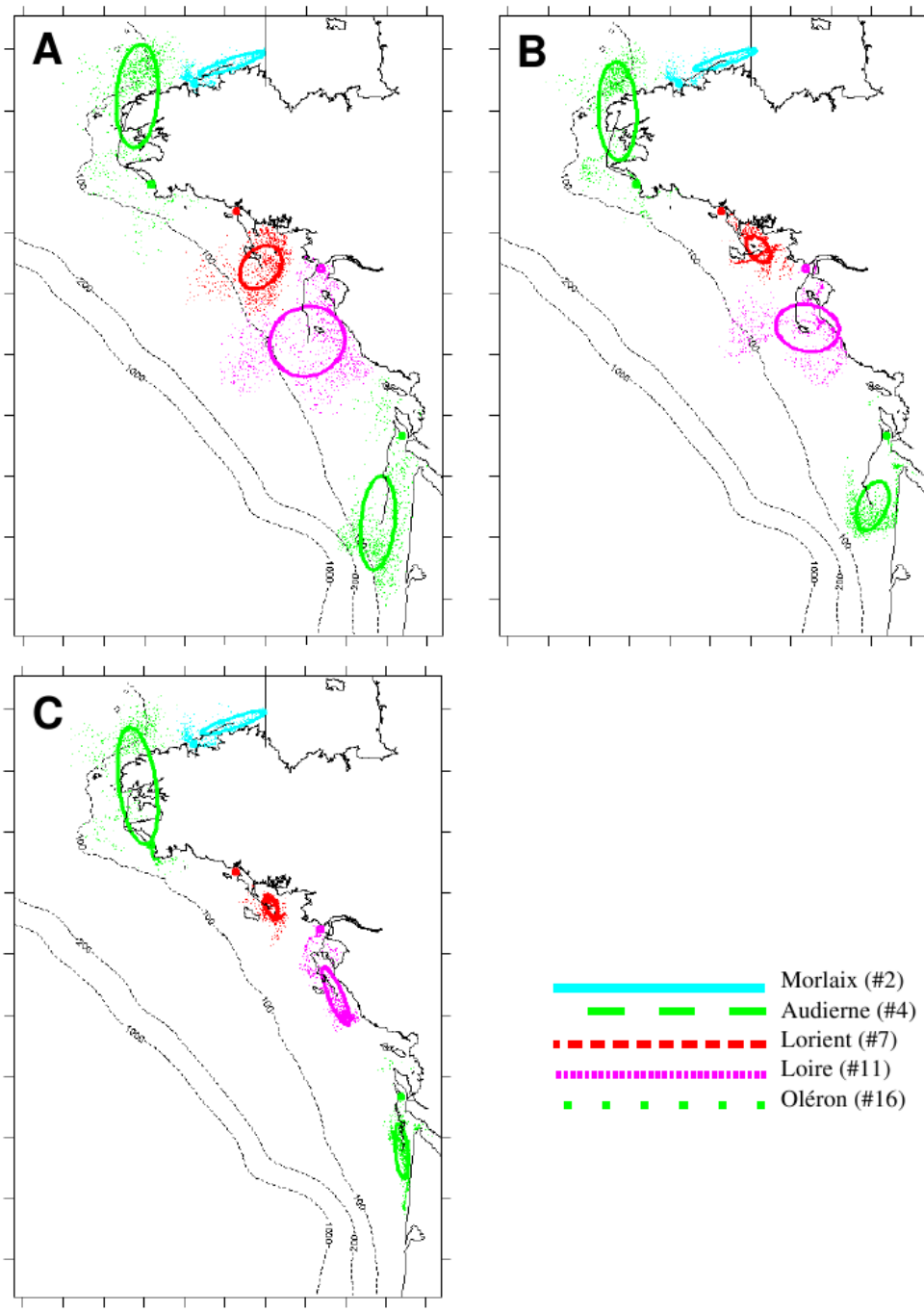


Figure 2.12: Dispersal of larval particles (A) without behaviour, (B) with an ontogenic migration, and (C) with a diel migration for a release in May 2003 and a PLD of 4 weeks. Final positions of 1000 particles released from Morlaix, Audierne, Lorient, Loire, and Oléron (the five spawning locations are indicated) and ellipses of variances are represented. The main descriptors of those dispersal kernels are presented in Tables 2.1, 2.2 and 2.3.

Table 2.3: Main dispersal kernel descriptors obtained after 4 weeks of dispersal with diel migrations and for releases in March, May and July 2003 from five spawning locations (Morlaix, Audierne, Lorient, Loire, Oléron).

| Month | Spawning | $d$ | $\theta$ | $amaj$ | $amin$ | $\theta_m$ | $s_\sigma$ (%) |
|---|---|---|---|---|---|---|---|
| March | Morlaix | 77 | 21 | 33 | 10 | 7 | 6 |
| | Audierne | 102 | -84 | 32 | 22 | 24 | 8 |
| | Lorient | 102 | -84 | 32 | 22 | 24 | 8 |
| | Loire | 131 | -19 | 47 | 7 | -19 | 5 |
| | Oléron | 94 | -47 | 35 | 5 | -29 | 5 |
| May | Morlaix | 58 | 19 | 46 | 5 | 12 | 4 |
| | Audierne | 57 | -71 | 54 | 25 | -76 | 6 |
| | Lorient | 58 | -213 | 11 | 6 | -42 | 3 |
| | Loire | 65 | -251 | 31 | 9 | -56 | 2 |
| | Oléron | 50 | -269 | 25 | 9 | -81 | 2 |
| July | Morlaix | 58 | 21 | 41 | 6 | 10 | 6 |
| | Audierne | 15 | -211 | 28 | 9 | -23 | 6 |
| | Lorient | 10 | -262 | 6 | 3 | -12 | 2 |
| | Loire | 30 | -269 | 55 | 6 | -49 | 3 |
| | Oléron | 14 | -98 | 38 | 9 | -86 | 5 |

### 2.4.3 Connectivity patterns

#### *2.4.3.1 Connectivity patterns of passive dispersal*

For each spawning date, connectivity matrices and exchange rates were calculated, distinguishing northwards exchanges, southwards exchanges, and self-retention. Figure 2.13 represents the monthly-averaged connectivity matrices obtained after 4 weeks of passive dispersal. Whatever the month, higher exchange rates were observed between neighbouring populations, usually with maximum exchange rates located along the matrix diagonal, i.e., corresponding to self-retention. Whatever the spawning date, the percentage of self-retention was constant, with a mean value of 8.19 ± 1.93 % (n = 35, PLD = 4 weeks). Between spawning populations, highest self-retention rates were observed for populations #3 (Douarnenez, 61.83 %) and #14 (Ile de Ré, 27.70 %). From February to April, northwards exchanges were higher than southwards exchanges (6.10 ± 4.73 % and 2.48 ± 2.03 % respectively, n = 15, PLD = 4 weeks). In contrast, northwards exchanges were lower than southwards exchanges (1.35 ± 1.21 % and 4.49 ± 1.36 % respectively, n = 20, PLD = 4 weeks) from May to August.

As suggested by the analysis of the dispersal kernels, connectivity patterns from the three northerner populations did not vary with the spawning month. Particles from Northern Brittany populations (#1-2) never supplied the southern populations and the Douarnenez population (#3) was relatively isolated from the other populations, with high self-retention rates (61.83 ± 16.49 %, n = 35, PLD = 4 weeks).

Seasonal variations of connectivity were observed for the populations of the Bay of Biscay. From February to April, exchanges occurred preferentially northwards. Highest northwards exchanges occurred in March, in particular from the Central Bay of Biscay populations to the Southern Brittany populations with a mean value of 10.67 ± 2.70 %, whereas southwards exchanges reached only 1.05 ± 1.17 % (n = 5 , PLD = 4 weeks). Southwards exchanges were also observed in February and April, indicating bidirectional exchanges between the Southern Brittany and the Central Bay of Biscay populations (northwards and southwards exchange rates of 4.99 ± 4.77 % and 3.98 ± 2.58 % in February and of 2.63 ± 2.37 % and 2.40 ± 0.99 % in April, n = 5, PLD = 4 weeks). From May to

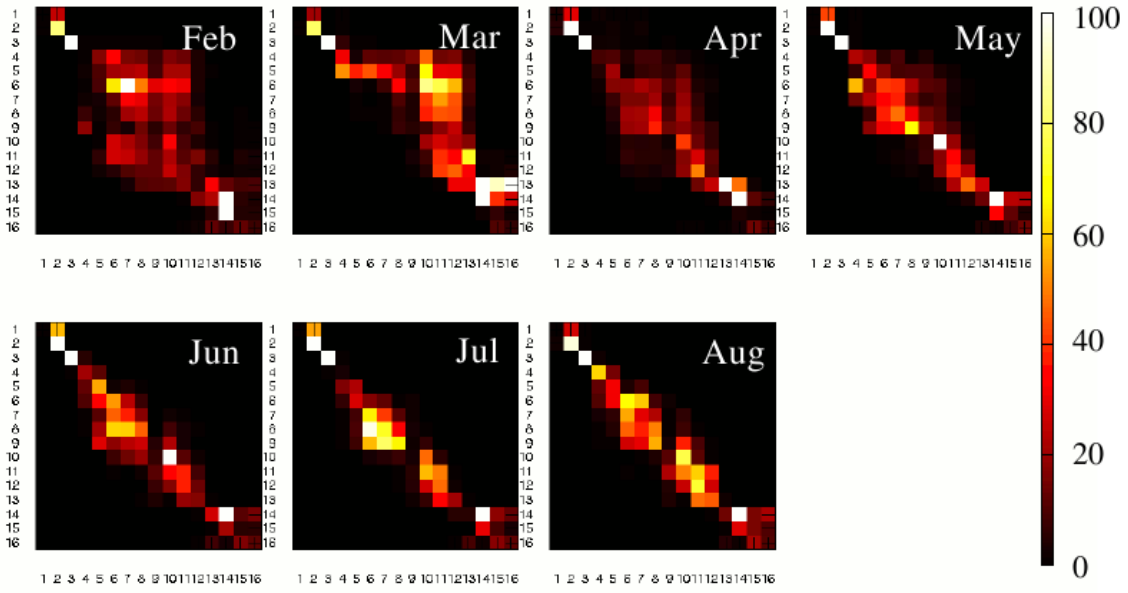


Figure 2.13: Monthly-averaged connectivity matrices obtained after 4 weeks of passive dispersal between the 16 spawning populations. Connectivity is given in per mil (number of exchanged individual per 1,000 released larvae from a source population on the x-axis to a sink population on the y-axis). Each monthly-averaged matrix results from the average of the 5 matrices obtained for the same month for the years 2001 to 2005. The names and locations of the spawning populations are indicated Figure 2.3.

August, exchanges occurred preferentially southwards, but only between relatively close populations, indicating that the particles transported southwards during those months were not able to encounter suitable settlement areas in coastal zones.

As expected, shorter PLD induced higher self-retention rates and higher exchange rates between neighbouring populations (Figure 2.14). Larval exchanges were 1.82 times higher for a PLD of 2 weeks than 4 weeks. Conversely, exchanges from the Central Bay of Biscay populations to the Southern Brittany populations were favoured with longer PLD. More specifically, populations #10 (Vilaine) to #13 (Saint-Gilles) were able to supply populations #4 (Audierne) to #12 (Bourgneuf) for a PLD of 4 weeks. On the contrary, exchanges from populations #13 (Saint-Gilles) to populations further north than population #10 (Vilaine) were never observed for a PLD of 2 weeks.

One-way ANOVA on the connectivity size from the 70 connectivity matrices obtained without behaviour (2 PLD, 5 years, 7 months) confirmed that spawning year had no influence on connectivity, contrary to PLD and spawning month (Table 2.4).

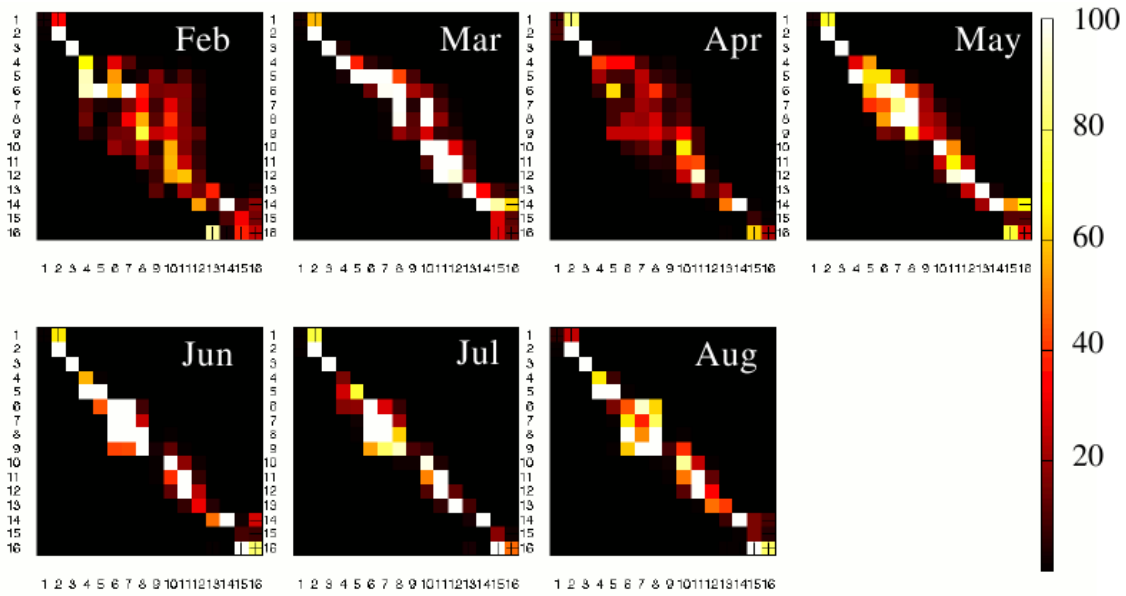


Figure 2.14: Monthly-averaged connectivity matrices obtained after 2 weeks of passive dispersal between the 16 spawning populations. Connectivity is given in per mil (number of exchanged individual per 1,000 released larvae from a source population on the x-axis to a sink population on the y-axis). Each monthly-averaged matrix results from the average of the five matrices obtained for the same month for the years 2001 to 2005. The names and locations of the spawning populations are indicated Figure 2.3.

Connectivity size increased with the PLD and the spawning month (Figure 2.15). Tukey HSD a posteriori tests showed a significantly different connectivity size between February and July or August spawnings ($p < 0.05$). For a PLD of 2 weeks, mean connectivity size varied from 24 to 60 connections, with a mean of 37 $\pm$ 8 connections, whereas it varied from 32 to 89 connections, with a mean of 55 $\pm$ 13 connections, for a PLD of 4 weeks. For a 4-week PLD, mean connectivity size reached 65 $\pm$ 12 connections from February to April, then only 48 $\pm$ 9 connections from May to August.

#### *2.4.3.2 Influence of larval vertical behaviours on connectivity patterns*

The mean connectivity matrices obtained in 2003 for 3 simple larval behaviours and a PLD of 4 weeks are presented in Figure 2.16 (7-month averaged matrices). A diel vertical migration did not significantly alter the mean connectivity matrix obtained in 2003 (Figure 2.16C), whereas self-retention was strongly increased by an ontogenic migration (see diagonal Figure 2.16B) and reached 10%, whereas self-retention reached only 7% for

passive particles and diel migration. Consequently, the transport success is higher with an ontogenic migration (21%) than without behaviour or with a diel migration (17 %).

Table 2.4: One-way ANOVA on passive connectivity, with 2 PLD values, 5 spawning years, and 7 spawning months (passive dispersal). The significance of the analysis are indicated

| Factor | Freedom Degree | Sum Square | Mean Square | F Value | Pr(>F) | Significance |
|---|---|---|---|---|---|---|
| PLD | 1 | 5906.4 | 5906.4 | 48.82 | $1.495.10^{-9}$ | *** |
| Residuals | 68 | 8226.5 | 121 | | | |
| Year | 4 | 1339.8 | 334.9 | 1.7 | 0.1603 | |
| Residuals | 65 | 12793.1 | 196.8 | | | |
| Month | 6 | 3533 | 588.8 | 3.5 | 0.004743 | ** |
| Residuals | 63 | 10599.9 | 168.3 | | | |

Significance codes: 0 '***' 0.001 '**' 0.01 '*'.

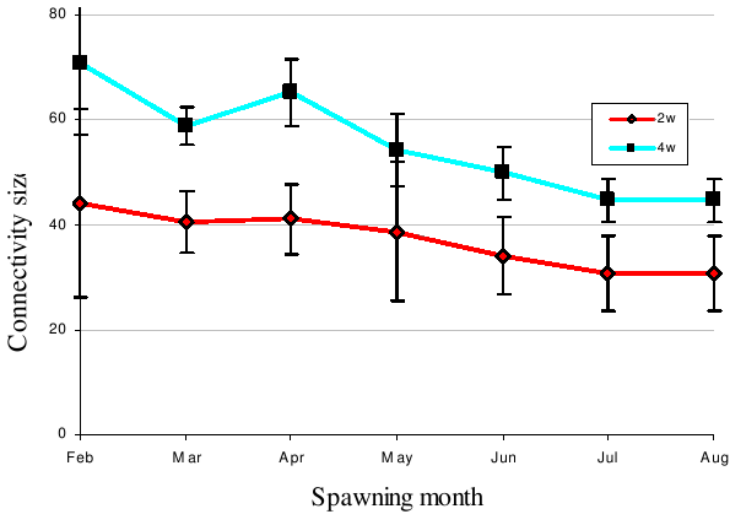


Figure 2.15: Mean connectivity sizes obtained per spawning month for a PLD of 2 weeks (in red) and 4 weeks (in light blue). The mean connectivity sizes are calculated for the years 2001 to 2005 from the 7 monthly-mean connectivity matrices obtained for each PLD value without behaviour.

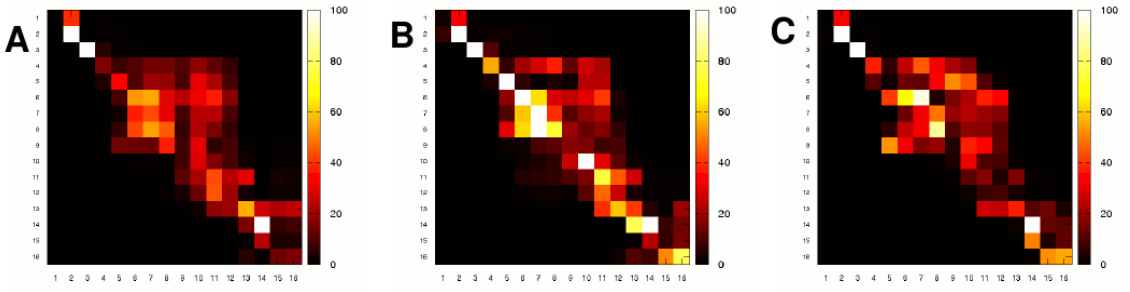


Figure 2.16: Consequences of larval behaviour on the averaged connectivity matrices obtained in 2003 after 4 weeks of dispersal (A) without behaviour, (B) with an ontogenic migration, (C) with a diel migration.

Table 2.5: Two-way ANOVA on connectivity sizes obtained with larval behaviour (no behaviour, ontogenic migration, diel migration) and 7 spawning months in 2003 for a PLD of 4 weeks. The significance of the analysis are indicated

| Factor | Freedom Degree | Sum Square | Mean Square | F Value | Pr(>F) | Significance |
|---|---|---|---|---|---|---|
| Behaviour | 2 | 1492.3 | 746.1 | 28.42 | $2.81.10^{-5}$ | *** |
| Month | 6 | 4895.8 | 816 | 31.08 | $1.23.10^{-6}$ | *** |
| Residuals | 12 | 315 | 26.3 | | | |

Significance codes: 0 '***' 0.001 '**' 0.01 '*'.

Within the second set of simulations, connectivity size varied significantly with the spawning month and the larval behaviour ($p < 0.001$) (Table 2.5, Figure 2.17). Whatever the larval behaviour, connectivity size decreased from February to May 2003, then was constant from May to August 2003 (Figure 2.17). Without behaviour, the mean connectivity size reached $58 \pm 19$ connections, with a maximal value of 89 connections in February and a minimum value of 39 connections in May. Connectivity size was lightly lower with an ontogenic migration (mean connectivity size of $55 \pm 19$ connections, max = 90 in February, min = 40 in July) and much lower with a diel migrations (mean connectivity size of $39 \pm 12$ connections, max = 61 in February, min = 27 in May). To conclude, an ontogenic migration increased the self-retention and hence the total transport success whereas a diel migration did not modify the mean transport success but decreased the connectivity size.

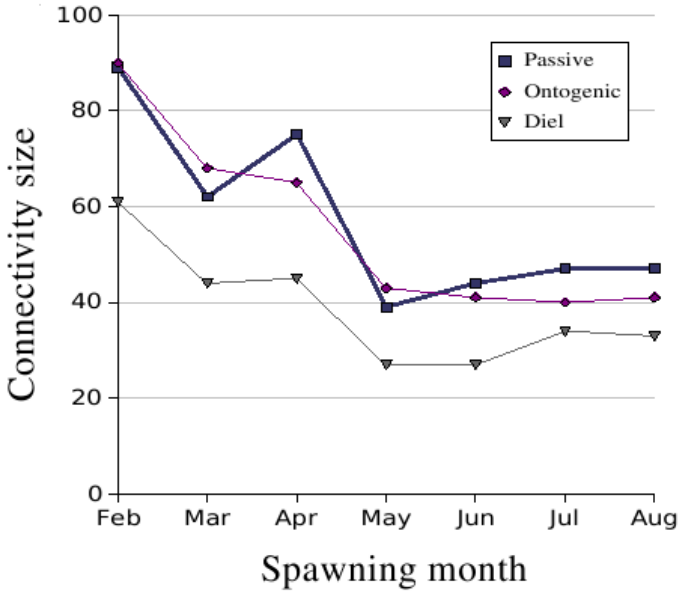


Figure 2.17: Consequences of larval behaviour on the connectivity sizes per spawning month. Results were obtained in 2003 after 4 weeks of dispersal.

### *2.4.3.3 Connectivity between the Bay of Biscay and the English Channel*

For passive dispersal, connectivity from the Southern Brittany populations to the English Channel population was observed for only 5 spawning dates among 35 (i.e., March 2003 and 2004, April 2002 and 2003, and May 2001), and only for a PLD of 4 weeks. When existing, larval exchanges from the Bay of Biscay to the English Channel populations were very low, from 0.1 % (the minimal value for 1,000 particles released) to 0.7 %. The connectivity matrices obtained for 4 of those 5 spawning dates are presented in Figure 2.18.

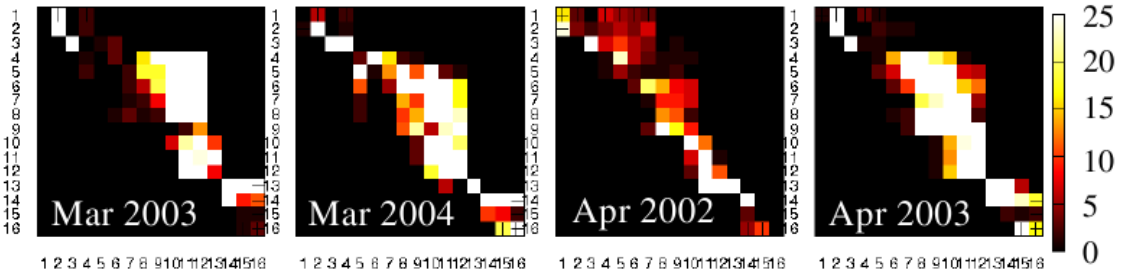


Figure 2.18: Exceptional connectivity patterns obtained in March 2003 and 2004 and April 2002 and 2003 after 4 weeks of passive dispersal. The names and locations of the spawning populations are indicated in Figure 2.3.

In March 2003 and 2004, and in May 2001, only a total of 3 to 4 particles from Audierne (population #4) reached the English Channel populations (populations #1-2) while a high connectivity existed from the Central Bay of Biscay populations to the Southern Brittany populations. In April 2003, a total of 8 particles from populations #4-7 (Audierne, Concarneau, Pouldu, Lorient) reached the English Channel populations (#1-2). High connectivity between the Central Bay of Biscay and Southern Brittany was also observed. In April 2002, a total of 40 particles from populations #4-7 (Audierne, Concarneau, Pouldu, Lorient) reached the English Channel populations. All those exceptional connectivity patterns resulted from extremely strong northwards followed by eastwards larval transport. In particular for the year 2002, S-SE winds in March 2002 favoured the density-driven northward transport of plume waters, and were followed by SW winds in April 2002, favouring intrusion of plume waters into the English Channel.

In March and April 2003, connectivity from the Bay of Biscay to the Western English Channel was also observed when vertical larval behaviour was considered (ontogenic and diel migrations). With a diel vertical migration, only 2 particles from Southern Brittany were able to settle in the western Channel in March and April instead of 3 and 8 with no behaviour. An ontogenic migration permitted a larger number of larval particles from Southern Brittany to successfully settle in the English Channel populations, with a total of 9 particles in March 2003 (mainly from Audierne, population #4) and of 25 particles in April 2003 (mainly from Concarneau, population #5, with a connectivity of 1 % to Morlaix, population #2). A higher connectivity between Southern Brittany and English Channel was then observed in April 2003 for a PLD of 4 weeks and with an ontogenic migration than without behaviour.

## 2.5 Discussion

A generic bio-physical model of invertebrate larval dispersal was developed in the Bay of Biscay and the Western English Channel. The 3D hydrodynamic model was forced with realistic hydroclimatic forcing to reproduce the highly complex and variable hydrodynamics fields of the area. It was coupled with an individual based model (IBM) of Lagrangian larval transport using common life history traits of benthic invertebrates inhabiting a fragmented habitat. The aim of this work was to assess the relative role of hydrodynamics and biological traits in the larval dispersal in the North-East Atlantic, and to investigate the connectivity of marine invertebrate populations between the Bay of Biscay and the English Channel through a biogeographical transition zone.

The MARS-3D hydrodynamic model has been previously validated in the study area by the comparison with observed hydrodynamic and hydrological structures, through neutrally buoyant floats, remote sensing sea surface temperature, CTD casts and coastal salinity measurements (Lazure & Dumas, 2008; Lazure , 2009). It has been applied to a wide range of study in the Bay of Biscay, such as the retention of toxic phytoplankton in a coastal embayment (Xie , 2007) or the transport of fish larvae on the continental shelf (Allain , 2007; Huret , *submitted*).

In a first assumption, to describe dispersal and connectivity patterns in a fragmented habitats, simple biological traits of invertebrate larvae were chosen. First, no temporal and spatial variation of the reproductive outputs was considered and a constant number (1,000) of larval particles was released per spawning event for each population. Second, no larval mortality was taken into account because the variability of this parameter remains poorly known for marine invertebrate larvae (Levin, 2006). Those two joint assumptions allowed us to explore statistically relevant larval transport pathways and to determine the likelier connectivity patterns between the main bays and estuaries of the study area. The present work, based on simple biological traits (i.e., spawning date, 2 PLD, simple larval vertical migrations), corresponds to an 'order zero' connectivity study in the Bay of Biscay, such as previously done in the south-eastern US continental shelf (Edwards ,

2007) or in the northern Gulf of California (Marinone , 2008) and focused mainly on the interactions between larval dispersal and hydrodynamics variability.

### 2.5.1 Relative role of hydrodynamics and biological traits in dispersal

In a first set of simulations, passive dispersal was simulated for 35 monthly spawning dates from February to August for the years 2001 to 2005, from 16 coastal populations located in the main bays and estuaries of the study area, and for two common values of PLD. Our results indicated that no significant inter-annual variability of the dispersal kernels was observed whereas strong variability of the dispersal kernels was due to spawning month, spawning population location, and PLD. In a second set of simulations which consider common larval swimming behaviours, results underlined the importance of larval behaviour on dispersal and connectivity patterns.

#### *2.5.1.1 Spawning date, spawning population, and seasonality of the circulation*

The absence of year-to-year variations in dispersal patterns may be surprising as inter-annual variations of the hydrology of the Bay of Biscay have been reported by Planque (2003) from the comparison of hydroclimatic data measured in the 1990s and multi-decadal historical records. Their analysis revealed that hydroclimatic factors, such as sea surface temperature, wind speed and river run-off, were highly variable at the temporal scale of a several decades. This strong inter-annual hydroclimatic variability induces high inter-annual variability of hydrological structures, as shown by Puillat (2004) from a synthesis of 9 years of hydrographic measurements in the bay during the 1990s. Variability is caused by long-term variations in river run-off from the Loire and Gironde, responsible for the presence of low salinity waters, and in wind conditions, responsible for the transport of those low salinity waters (Kelly-Gerreyn , 2006; Puillat , 2004). The hydrographic variability on the French continental shelf of the Bay of Biscay results also from high seasonal and short-term meteorological variability. Indeed, the circulation in the Bay of Biscay is well known for its strong seasonal patterns (Koutsikopoulos & Le Cann, 1996; Puillat , 2004), because of the seasonal variations in river run-off and in wind speed and

direction (SW winds from September to March, NW winds from March to September). Moreover, short-term meteorological variability plays an important role in hydrodynamic variability by inducing mesoscale structures, such as transient upwellings or fresh water lenses (Kelly-Gerreyn , 2006; Puillat , 2006).

In the present work, the MARS 3-D hydrodynamic model was forced by realistic climatic forcing from recorded data of river run-off and wind conditions in order to reproduce realistic hydrodynamic variability. In our simulations, larval dispersal was simulated monthly over five years with a PLD of two or four weeks, which means that the temporal scale of larval life (PLD) was equal or shorter than the temporal scale of spawning (time interval between two consecutive spawning events). Hence, at the spatial and temporal scales of larval dispersal that were considered in our study, the year-to-year variations in dispersal kernels were negligible compared to the variations due to the spawning month (seasonal variations) and the spawning location (mesoscale variations). Depending on the spawning month and population, larval particles encountered different mesoscale structures, such as river plumes, that, combined with wind conditions, alter their transport by density-driven and wind-induced currents (Kelly-Gerreyn , 2006).

Mean transport direction differed from the three main spawning areas: the English Channel, the Southern Brittany, and the Central Bay of Biscay. In the English Channel, larval particles were transported northeastwards, whatever the spawning month, because of the strong northeastwards tidal residual circulation (Salomon & Breton, 1993). Although wind-induced currents can greatly affect larval transport over short-term periods of a few days, their influence is reduced over 2 or 4 weeks. In Southern Brittany and in the Central Bay of Biscay spawning areas, seasonal shifts in transport direction were observed. In late-winter and early spring, northwestwards transport was observed because of the geostrophic northwestwards transport of plume waters along the Brittany coasts, favoured by NE winds consistently with Ekman theory (Kelly-Gerreyn , 2006). In late spring and summer, transport from the Bay of Biscay populations occurred generally southwestwards to southeastwards, because of W to N winds, also known to favour cross-shore transport and transient upwellings in the area (Puillat , 2006, 2004).

Previous modelling has underlined the influence of the spawning date in larval transport suggesting that a favourable temporal window of spawning may exist to maximize the success of dispersal (e.g. Ayata , 2009; Edwards , 2007). Here, the simulated spawning dates extended from February to August, which correspond to common spawning dates of benthic invertebrates in temperate zones (Olive, 1995). As mentioned above dispersal kernels varied throughout the season with the spawning month. For a given species able to spawn from early spring to summer, connectivity patterns could be very complex and variable in relation with the hydrodynamic variability of the Bay of Biscay. The larvae of such species with an extended spawning period will likely undergo very different transport pathways depending on their release date, since early and late spawnings will induce different dispersal and connectivity patterns. The larvae released in early spring from the Bay of Biscay populations would mainly be transported to the north and contribute to northward exchanges, whereas larvae released in late spring or early summer would preferentially be transported to the south and contribute to southwards exchanges. Since the larvae of a given species inhabiting fragmented habitat will have different fates depending on their spawning date, larvae released early or late will contribute differently to the metapopulation dynamics. Strong variability of larval transport and connectivity patterns could then represent an advantage for the perennity of invertebrate local populations in fragmented habitats by increasing the likelihood of successful larval transport (Byers & Pringle, 2006). In the Bay of Biscay, connectivity patterns will also vary between early-spawning and late-spawning species. For invertebrate species spawning from February to April, larval transport and connectivity would mainly be northwards, whereas they would be southwards for species spawning from May to August. Metapopulation dynamics would then differ between early-spawning and late-spawning species and species phenology could be partly responsible for the species distribution.

#### *2.5.1.2 Planktonic larval duration, larval behaviour, and environment*

In the present study, simple common biological traits of the larval life were considered. First, planktonic larval duration (PLD) was supposed to last 2 or 4 weeks as commonly

reported for many marine invertebrates (Kinlan & Gaines, 2003). PLD value played a significant role in the simulated dispersal kernels, mainly affecting the mean dispersal distances. As observed before, longer PLD increased the mean dispersal distances (Edwards , 2007; Marinone , 2008; Mitarai , 2008) but decreased the mean connectivity (Treml , 2008). More specifically, a decrease of 50 % of the PLD from 4 to 2 weeks induced (1) a decrease of 44.62 % of mean dispersal distance, (2) an increase in self-retention and larval exchanges between neighbour populations, (3) a decrease of the connectivity (exchange rates) between more distant populations, and (4) a decrease in the connectivity size (number of connexions) of the metapopulation.

In the study area, temperature fields are highly variable in time and space, and should then induce large temporal and spatial variations of the PLD. For species able to spawn during all of the spring season, spawning date will affect larval development rate because of the temporal gradient of water temperature encountered during the spawning season (Reitzel , 2004). From published experimental laboratory studies on 72 marine taxa, O'Connor (2007) proposed a general relationship between water temperature $T$ (in°C) and $PLD$ (in days) as follows:

$$ln(PLD_T) = ln(PLD_{T_c}) - 1.34 \times ln\left(\frac{T}{T_c}\right) - 0.28 \times \left(ln\left(\frac{T}{T_c}\right)\right)^2 \text{ with } T_c = 15^\circ \text{ C.} \quad \text{(Eq. 2.9)}$$

From February to August, monthly-mean temperatures of coastal waters along the Bay of Biscay French coasts vary from 10°C to 19°C (Gómez-Gesteira , 2008), so that the PLD would decrease by 3 weeks, i.e. from 39 to 17 days from the beginning to the end of the spawning period. Hence larvae released in late spring or in summer could exhibit shorter PLD, because of warmer water temperature, than for the larvae released in early spring, i.e., when water temperature is colder (Rigal, 2009; Rigal , *submitted*). For larvae released in early spring in the Bay of Biscay, longer PLD would favour northwards transport along longer distances, hence northwards exchanges with distant populations. In contrast, for larvae released in late spring or in summer, shorter PLD would favour southwards transport along shorter distances, favouring southwards exchanges with neighbouring populations and self-retention. Variations of the PLD could also be induced by spatial variations in

the temperature field. For a given spawning date, water temperatures encountered by the larvae can vary in space depending on the larval trajectory. In particular, temperature gradients occur horizontally between coastal and offshore waters and/or vertically between surface and bottom waters of the continental shelf of the Bay of Biscay. As an example, a surface water temperature gradient is commonly reported cross-shore in summer in the Bay of Biscay and can reach 4°C between coastal and offshore waters, with temperatures of 15°C and 19°C respectively (Lazure , 2009). From the equation proposed by O'Connor (2007), such an increase in water temperature from 15°C to 19°C could decrease the PLD od one week, from 24 to 17 days. PLD reduction due to temperature increases in time or space could then induce significantly shorter dispersal distance and lower long-distance connectivity.

The general relationship described by O'Connor (2007) may however vary between species. Species-specific environment-dependent larval growth and development are frequently taken into account in individual based models of fish larval dispersal (e.g. Allain , 2007) because growth parameters of fish larvae are relatively well known. On the contrary, individual-based models of invertebrate larval dispersal taking into account larval growth are scarce (e.g. Pedersen , 2003) because of the lack of sufficient knowledge on invertebrate larval biology, especially for non-commercial species. Since temperature fields are calculated by the MARS-3D model, future modelling work in the context of climatic change will require considering individual PLD as a function of the temperatures encountered by the larval particle throughout its life time following laboratory experiments (O'Connor , 2007).

Second, three simple vertical larval behaviours were considered in this study: no behaviour as a reference case, an ontogenic vertical migration, and a diel vertical migration. In our simulations, vertical distribution of passive larvae varied depending on the hydrodynamic conditions encountered by the larval particles. In the English Channel, where the water column is vertically homogeneous because of intense tidal mixing (Salomon & Breton, 1993), mean depth of passive particles corresponded to mean water column depth ($\sigma_m = 0.5$). On the contrary, in the vicinity of estuaries, where strong vertical stratification existed, passive particles were mainly located in the top layers of the water column

($\sigma_m > 0.5$), i.e., trapped in the low salinity water plume. Thus, even passive particles are not evenly distributed throughout the whole water column but remain mainly confined in a typical water mass (Shanks , 2002). Furthermore, invertebrate larvae do not always behave passively and vertical swimming behaviour may affect larval dispersal according to the vertical shear stress (Woodson & McManus, 2007). In stratified environments, such as the Bay of Biscay in spring, ontogenic and diel vertical migrations have been proven to affect larval transport by favouring retention (Queiroga , 2007; Thiébaut , 1992). As recently suggested by North (2008), vertical behaviour of weakly swimming larvae significantly altered dispersal kernels, transport success, and connectivity. During the major part of the larval life (i.e., the first 20 days), the mean depths of larvae subject to an ontogenic migration were close to the mean depths of passive particles because of their null vertical velocity. At the end of larval life, when particles had a negative swimming velocity, those particles are located closer to the bottom, inducing shorter dispersal distances. Even if swimming behaviour occurred during the last days of larval life, and even for small swimming velocities ($< 1$ m.s$^{-1}$), such an ontogenic migration significantly favoured self-retention and increased the total transport success. With diel vertical migration, particle mean depth varied with the hour of the day and with variations in depth amplitude caused by the variations of the vertical eddy diffusivity related to spring/neap tide cycles. Indeed, highest amplitudes were observed in neap tide (low vertical eddy diffusivity) because diel migrations prevailed over vertical mixing; on the contrary, lowest amplitudes were observed in spring tide (high vertical eddy diffusivity), because vertical mixing prevailed. In our study, diel vertical migration did not modify the direction of the larval transport, although such migration has been reported to affect transport direction when interacting with semi-diurnal tidal currents in the NW European continental shelf (Hill, 1994). Also, this behaviour did not alter the total transport success nor the self-retention, contrary to what has been observed in the case of upwelling systems (Queiroga , 2007) when diel vertical migration interacts with the upwelling/downwelling circulation. However, Garland (2002) suggested that diel vertical migrations could permit competent larvae to test the bottom for settlement during the day, which could favour settlement success. Besides its effect on the dispersal distance, vertical larval behaviour mainly decreased the size of

the variance ellipses by reducing inter-individual variability in the larval trajectories. In the future, species-specific applications of this Lagrangian model will need to take into account species-specific larval mortality, growth, and behaviour.

### 2.5.2 Connectivity between the Bay of Biscay and the English Channel

In relation with the transport patterns previously described, connectivity patterns indicated that larval exchanges mainly occurred within the main spawning areas (i.e., Western English Channel, Southern Brittany and Central Bay of Biscay) and that self retention was high. The northern populations of the English Channel and of the Ushant Sea were relatively isolated from the other populations whereas Southern Brittany and Central Bay of Biscay populations freely exchanged larvae. Nevertheless, larval transport and connectivity were observed between the Bay of Biscay and the English Channel populations for peculiar hydroclimatic conditions and biological traits. Connectivity occurred for a PLD of 4 weeks, and for spawning that occurred in March 2003 and 2004, April 2002 and 2003, and May 2001. This result is partly consistent with the observations of low salinity surface water (LSSW) intrusions from the Bay of Biscay in the Western English Channel for three consecutive years (2002 to 2004), suggesting frequent northwards transport of plume waters in late winter (March-April) (Kelly-Gerreyn , 2006). LSSW intrusions in the English Channel were reported as a consequence of high river discharges and wind conditions, with faster travel of LSSW under NE winds and better intrusion under spring tide (Kelly-Gerreyn , 2006). Afterwards, from early spring to summer, frontal structures are established in the Ushant Sea between mixed and stratified waters (Pingree , 1975). In early spring, two haline fronts have been reported in the Ushant Sea and at the entrance of the Douarnenez Bay (Morin , 1991), i.e., at the location of the two thermal fronts established later in summer (Mariette & Le Cann, 1985). These two frontal structures may act as barriers to dispersal (Le Fèvre, 1986), especially (1) from the Bay of Biscay to the Western English Channel populations and (2) from the Douarnenez Bay population (population #3) to the open sea. The high self-retention observed for the population of Douarnenez might also partly result from a bias due to the horizontal resolution of the

model (4 km) given the narrow width of the entrance of the bay (less than 12 km, represented by three grid cells in the model). In future work, models using a smaller horizontal resolution should be developed to test the role of the spatial gridding on dispersal and connectivity patterns (Guizien , 2006). In the Ushant Sea, Le Boyer (2009) have reported northwards jet like structures and cyclonic frontal eddies that could either favour northwards larval transport or locally trap the larvae.

The transport of larval particles and connectivity from Southern Brittany to the English Channel require the concordance of several hydrodynamic and biological processes: (1) a larval release in the plume waters, which is likely for coastal invertebrates that spawn in late winter and early spring, (2) a northward transport of the plume waters, likely for spring meteorological conditions, (3) a cross-frontal transport through the Ushant Sea under the influence of transitory wind events, (4) an eastward reorientation of the plume waters to enter the English Channel under the influence of tidal residual currents, and (5) a planktonic larval duration long enough to ensure the transport by plume waters from the Southern Brittany to the English Channel populations.

Connectivity of marine invertebrate populations between the Bay of Biscay and the Western English Channel is coherent with the phylogeographic patterns along the Brittany coasts described by Jolly (2005) for the polychaete *Pectinaria koreni*. However, connectivity from the Western English Channel to the Bay of Biscay population was never observed, indicating that the Ushant Sea acts as a partly-permeable one-way barrier for connectivity: northwards larval exchanges are scare, whereas southwards larval exchanges are unlikely. Moreover, the general lack of suitable habitats along the French coasts of the Western English Channel for some species inhabiting muddy fine sand sediments, could limit the connectivity of such species between the western and the eastern English Channel (Barnay , 2003). These findings are coherent with the description of the Western English Channel as a transition zone between the temperate and cold-temperate biogeographic provinces (Cox & Moore, 2000; Dinter, 2001).

## 2.6 Conclusions

Invertebrate larval dispersal and connectivity was modeled between the Bay of Biscay and the Western English Channel. Common life history characteristics of benthic invertebrates inhabiting fragmented habitats were used to simulate Lagrangian larval transport under realistic meteorological forcings. Our results highlighted the role played by the mesoscale seasonal variability of hydrodynamics on transport patterns and connectivity. At the temporal and spatial scale of larval life considered here, no significant year-to-year variations were observed in dispersal kernels. On the contrary, spawning month, spawning population, PLD, and larval vertical behaviour played major roles in dispersal kernel variability. Connectivity between Southern Brittany and Western English Channel populations has been reported but only under peculiar hydrodynamic conditions and for specific biological traits. As proposed by Gaylord & Gaines (2000) and Zacherl (2003), biogeographical distributions of marine species depend not only on individual physiological tolerances but may partly rely on population processes including larval transport and recruitment success. The present study confirms that connectivity could mediate range limits of marine invertebrates in the North-East Atlantic according to the interactions between hydrodynamics and larval PLD, spawning period or suitable habitat availability.

In future work, models using a smaller horizontal resolution should be developed to test the role of the spatial gridding on dispersal and connectivity patterns (Guizien , 2006). The next step of this work would then be to apply this model to specific invertebrate species, using species-specific biological traits (reproductive outputs of adult populations, larval mortality, larval growth and PLD variations, larval behaviour). Model results would then be confronted with *in situ* observations of larval distributions.

Such modelling work also provides a useful tool to test several hypotheses on changes in connectivity and range limits in response to climate changes (Lett , *submitted*). Indeed, since water temperature increases are likely to induce earlier spawning and shorter PLD, such a bio-physical model can be used to asses the consequences of those two hypotheses on larval dispersal and connectivity patterns. Those consequences will be presented in the next chapter of this thesis (Chapter 3).

## 2.7 Acknowledgements

The present study was financed by the French National Program EC2CO (Ecosphère Continentale et Côtière). S.-D. Ayata is supported by a PhD grant from the French Ministry of National Education and Research. The authors are grateful to Laure Noël for the English proofreading.

# De l'utilisation de modèles couplés biologie-physique à l'exploration des impacts potentiels des changements climatiques sur les populations marines

Dans ce chapitre, la **dispersion larvaire lagrangienne** a été simulée à l'échelle du Golfe de Gascogne et de la Manche occidentale en conditions hydroclimatiques réalistes (marées, débits des principaux fleuves, conditions météorologiques). Les simulations ont été réalisées à la suite de l'émission de larves dans les principales baies de la zone d'étude en prenant en considération des traits d'histoire de vie caractéristiques des populations d'invertébrés à cycle bentho-pélagique en milieu côtier tempéré (période de ponte, durée de vie larvaire, comportement natatoire des larves). L'analyse des noyaux de dispersion a mis en évidence l'importance du **mois de ponte**, en relation avec les variations saisonnières des débits des principaux fleuves et des conditions de vents, de la **durée de vie larvaire**, de la **localisation des populations parentales**, et du **comportement natatoire des larves** dans la variabilité des patrons de dispersion larvaire. En revanche, aucun effet significatif de la variabilité interannuelle des conditions hydroclimatiques sur la dispersion n'a été observé à l'échelle de la vie larvaire (2 ou 4 semaines) entre 2001 et 2005.

Par ailleurs, le suivi des particules larvaires nous a permis de décrire la connectivité entre les principaux estuaires et baies le long des côtes Atlantiques françaises. De forts taux de rétention au sein des populations parentales ont été observés, suggérant un **important auto-recrutement**. Les échanges larvaires s'effectuent principalement au sein des principales zones hydrologiques et hydrodynamiques que sont la Manche occidentale, la Mer d'Iroise, le nord du Golfe de Gascogne (sud de la Bretagne), et le centre du Golfe de Gascogne. Entre le Golfe de Gascogne et la Manche, c'est-à-dire à travers la **zone de transition biogéographique** séparant les provinces lusitanienne et boréale, la **connectivité est très faible, unidirectionnelle** (du Golfe de Gascogne vers la Manche) et n'a lieu que dans des conditions hydroclimatiques particulières (forts débits et vents de NE ou E) et pour certains traits d'histoire de vie (ponte au début du printemps et durée de vie larvaire longue de 4 semaines).

# Chapitre 3

# Dispersion et connectivité dans un environnement changeant

## Pistes de réflexions sur l'impact potentiel du changement climatique

## 3.1 Les impacts potentiels du changement climatique sur la dispersion et la connectivité

Les schémas de dispersion potentielle et les patrons de connectivité précédemment décrits dans le Golfe de Gascogne et en Manche (*cf.* Chapitre 2) sont fortement susceptibles de changer au cours des prochaines décennies, voire des prochaines années, puisque le changement climatique global devrait fortement impacter les populations côtières en modifiant les caractéristiques hydrodynamiques de l'océan, les traits d'histoire de vie des espèces à travers une action sur la physiologie et le comportement des individus ou les interactions biologiques (Harley *et al.*, 2006).

### 3.1.1 Un constat : l'augmentation de la température des océans

Le groupe d'experts intergouvernemental sur l'évolution du climat ou GIEC a en effet conclu à une hausse globale des températures depuis le début du vingtième siècle de 0,74°C et à des projections probables pour la fin du 21$^{ème}$ siècle comprises entre 1,1 et 6,4°C (Intergovernmental Panel on Climate Change, 2007).

Une telle hausse des températures depuis le milieu des années 80 a ainsi été observée en différents points du plateau continental du nord-ouest de l'Europe. Au large de Plymouth, la température a augmenté d'environ 1°C au cours de la décennie 1990-2000 (Hawkins *et al.*, 2003). Dans les eaux océaniques du Golfe de Gascogne, le réchauffement rapporté de 1985 à 2006 était de 0,45°C par décennie au sud de la Bretagne (deCastro *et al.*, 2009). En mer du Nord et en mer Baltique, l'augmentation de la température moyenne de l'eau de surface était d'environ 0,6°C entre 1985 et le début des années 2000 (MacKenzie et Schiedek, 2007).

En accord avec ces observations globales et régionales, une augmentation de 0,7°C de la moyenne annuelle des températures des eaux de surface a été observée au cours des trente dernières années (de 1970 à 2005) au large de l'île de Batz en Manche occidentale (48°46'50"N-04°03'40"W) (Figure 3.1). Alors que la température annuelle moyenne était

de 12,3°C de 1970 à 2005, elle n'était que de 12,0°C pendant la période 1970-1987 mais a atteint à 12,7°C pendant la période 1988-2005.

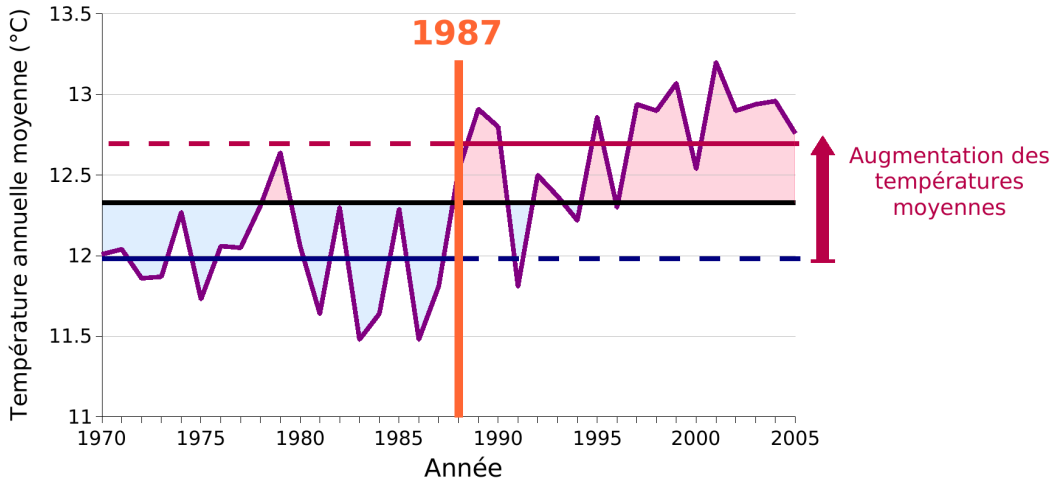


FIGURE 3.1 – Évolution des températures annuelles de surface au large de Roscoff de 1970 à 2005 (température moyenne de 12,3°C, ligne noire). La moyenne des températures annuelles atteint 12,0°C pendant la période 1970-1987 (ligne bleu), et 12,7°C pendant la période 1988-2005 (ligne rose). Les données de température proviennent du suivi mensuel d'un site au large de l'île de Batz, Manche occidentale (48°46'50"N-04°03'40"W, *cf.* carte Figure 3.2). Données mises à disposition par P. Morin, Station Biologique de Roscoff.

### 3.1.2 Hypothèses de travail

#### *3.1.2.1 Hypothèse 1 : une phénologie avancée*

Pour cette même période, *i.e.* de 1970 à 2005, la distribution du méroplancton en Manche occidentale et en Mer d'Iroise a pu être suivie grâce aux données issues de l'échantillonneur de plancton en continu (*Continuous Plankton Recorder* ou CPR) et gérées par la 'Sir Alister Hardy Foundation for Ocean Science' (SAHFOS) (Batten *et al.*, 2003; Beaugrand, 2004; Richardson *et al.*, 2006). Le CPR est un échantillonneur en continu du zooplancton déployé sur leurs routes de navigation par les navires marchands et récoltant le zooplancton filtré sur une maille de 270 µm à une profondeur d'environ 10 m. Chaque échantillon correspond à une distance parcourue de 10 milles nautiques, soit un volume d'eau filtrée d'environ 3 $m^3$. Concernant le méroplancton, les différents taxons pris en compte sont : les larves de polychètes, les larves cyphonautes de bryozoaires, les larves cirripèdes de balanes,

les larves de crustacés décapodes, les larves de bivalves et les larves d'échinodermes. Les procédures standardisées de récolte et de traitement des échantillons sont présentées de manière détaillée par Richardson *et al.* (2006). Dans le cadre de ma thèse, l'analyse des données a porté exclusivement sur les larves d'échinodermes pour deux raisons : (1) leur présence en nombre suffisant dans les échantillons, (2) la forte dominance possible d'une espèce dans ces données (Kirby et Lindley, 2005).

Les abondances mensuelles moyennes de larves d'échinodermes observées par le CPR en Manche occidentale et en Mer d'Iroise (47°N-51°N ; 7°W-1°W) indiquent que les larves sont présentes plus tôt dans l'année au cours de la période 1988-2005 qu'au cours de la période 1970-1987 (Figure 3.2). Entre ces deux périodes, le décalage temporel des abondances maximales est ainsi d'environ 2 mois, avec un décalage de plus de 10 jours entre les pics saisonniers (calculés comme la différence entre les centres de gravité des abondances mensuelles, selon la formule proposée par Edwards et Richardson, 2004). Ce changement de phénologie en Manche occidentale et en Mer d'Iroise a déjà été observé pour de nombreux taxons planctoniques en Mer du Nord (Edwards et Richardson, 2004; Kirby *et al.*, 2007), et est probablement à mettre en parallèle avec l'augmentation de température enregistrée au cours des dernières décennies.

Étant donné un tel changement dans la phénologie du méroplancton, on peut formuler comme première hypothèse de travail que le changement climatique entraîne des pontes plus précoces chez les invertébrés à cycle de vie bentho-pélagique le long des côtes Atlantiques françaises.

#### *3.1.2.2 Hypothèse 2 : des durées de vie larvaire raccourcies*

Le changement climatique est aussi succeptible d'induire une diminution de la durée de vie larvaire en réponse à l'augmentation de température de surface des eaux marines (Duarte, 2007; O'Connor *et al.*, 2007). De plus, des interactions sont possibles entre une phénologie précoce et un développement larvaire accéléré en réponse à des variations de la température. À ce sujet, de récents travaux combinant des observations *in situ* et des cultures expérimentales de larves du gastéropode invasif *Crepidula fornicata* en

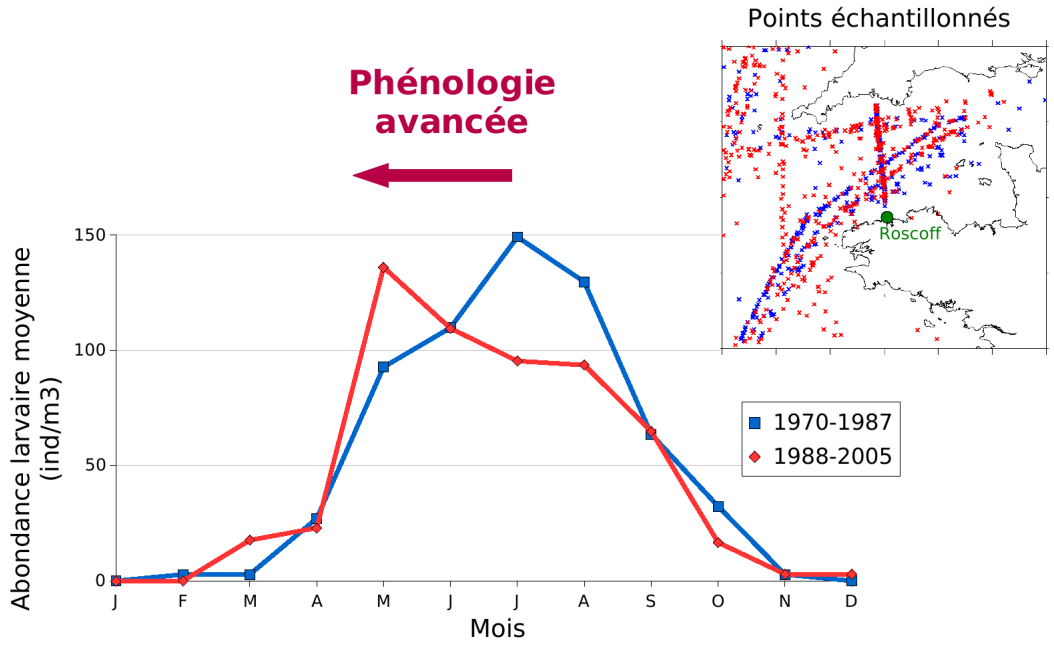


FIGURE 3.2 – Abondances mensuelles des larves d'échinodermes dans les échantillons récoltés par le CPR en Manche occidentale et en Mer d'Iroise entre 1970 et 2005. La carte indique les points d'échantillonnage pour la période 1970-1987 en bleu et pour la période 1988-2005 en rouge. Données mises à disposition par la SAHFOS.

baie de Morlaix (Manche occidentale), suggèrent que des pontes précoces induites par un réchauffement des eaux pourraient conduire à des durées de vie larvaire ralongées étant données les températures rencontrées plus froides (Rigal, 2009 ; Rigal *et al.*, *soumis*).

## 3.2 La modélisation couplée biologie-physique comme outil exploratoire

Pour estimer l'impact du changement climatique sur la dispersion et la connectivité des populations marines, l'idéal serait de disposer de modèles hydrodynamiques en accord avec les différents scénarios climatiques envisagés, de manière à simuler la dispersion en conditions hydrodynamiques prédites, et avec des paramètres biologiques estimés spécifiquement *in situ* et en laboratoire. Bien que des modèles climatiques régionaux aient été développés sous certains de ces scénarios, leur couplage avec des modèles de circulation et *a fortiori* de dispersion larvaire en est à ses balbutiements. Dans l'attente de tels modèles biophysiques, les conséquences potentielles du changement global sur la dispersion potentielle et

la connectivité peuvent cependant être explorées. L'article présenté en Annexe E présente ainsi une revue basée sur plusieurs cas d'étude où la modélisation couplée biologie-physique de la dispersion et de la connectivité permet d'apporter plusieurs éléments de réflexion sur les conséquences potentielles du changement climatique sur les populations marines.

A l'échelle du Golfe de Gascogne, on testera plus spécifiquement les conséquences d'un changement dans la phénologie de la reproduction (pontes précoces) et d'une accélération du développement larvaire (durées de vie larvaires raccourcies) sur la dynamique des populations d'invertébrés marins en zone côtière.

## 3.3 Conséquence d'une accélération du développement larvaire sur la dispersion et la connectivité

Au chapitre précédent, nous avons comparé les noyaux de dispersion et les matrices de connectivité moyennes obtenus pour des durées de vie larvaire de 2 et 4 semaines. Ces résultat ont montré que la durée de vie larvaire avait un impact significatif sur les noyaux de dispersion et qu'une durée de vie larvaire courte (2 semaines) avait pour conséquence des distances moyennes de dispersion plus courtes, et ce indépendamment le mois de ponte et la population d'émission des larves.

En Europe, une augmentation maximale de la température de 5.3°C est attendue (Christensen *et al.*, 2007). Conformément à ces prédiction, un température de 9°C augmenterait pour atteindre un maximum de 14.3°C. Une telle variation de température aurait alors pour conséquence une diminution de 50 % de la durée de vie larvaire de 4 à 2 semaines selon l'équation proposée par O'Connor *et al.* (2007). Or, nous avons vu qu'une telle variation de la durée de vie larvaire induit une diminution de 45 % de la distance moyenne de dispersion de 73 $\pm$ 51 km à 40 $\pm$ 29 km (Figure 3.3).

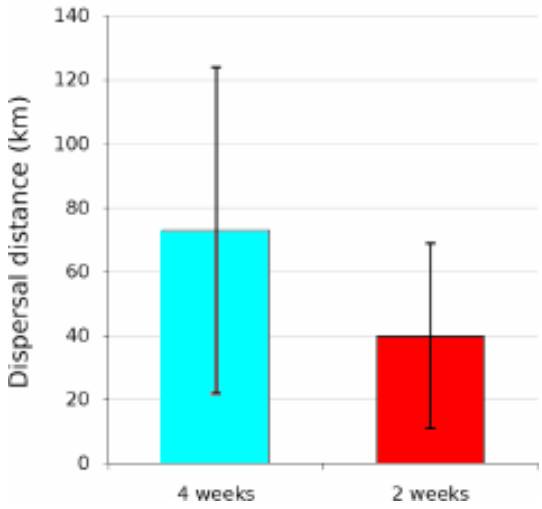


FIGURE 3.3 – Conséquence d'une diminution de la durée de vie larvaire de 4 à 2 semaines sur la distance de dispersion orthodromique moyenne. Les moyennes sont calculées pour 35 dates de ponte et 16 populations.

Une diminution de la durée de vie larvaire de 4 à 2 semaines modifierait aussi la connectivité des populations puisqu'elle augmenterait l'auto-recrutement et les échanges larvaires entre populations proches. Cependant, elle aurait aussi pour conséquence une diminution de la connectivité entre des populations plus éloignées. La taille de la connectivité, définie comme le nombre total de connections entre les populations, diminuerait alors de $55 \pm 13$ à $37 \pm 8$ (Figure 3.4) : une partie de la connectivité serait ainsi perdue. À l'échelle spatiale du Golfe de Gascogne et de la Manche, une diminution de la durée de vie larvaire pourrait donc avoir pour conséquences des distances de dispersion plus courtes, une rétention plus forte, une connectivité locale plus intense, une connectivité régionale plus faible, et enfin une taille de connectivité plus petite des populations d'invertébrés.

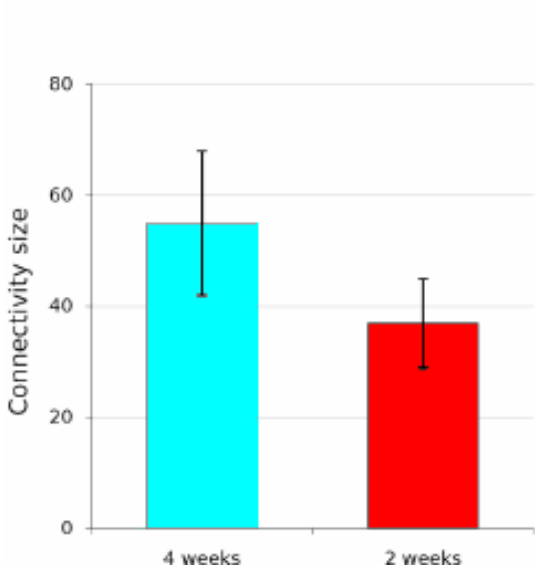


FIGURE 3.4 – Conséquence d'une diminution de la durée de vie larvaire de 4 à 2 semaines sur la taille de connectivité. Les moyennes sont calculées pour 35 dates de ponte et 16 populations. La taille de connectivité est définie comme le nombre de connections obtenues dans les matrices de connectivité entre les 16 populations.

## 3.4 Conséquence d'un avancement de la période de reproduction sur la dispersion et la connectivité

Des pontes mensuelles ont été simulées de Février à Août pour les années 2001 à 2005, soit pour un total de 35 dates. Alors qu'aucune variabilité interannuelle des noyaux de dispersion n'a été mise en évidence, le mois de ponte joue un rôle crucial sur la variabilité des noyaux de dispersion, à cause de la forte variabilité saisonnière des conditions hydrodynamiques dans le Golfe de Gascogne. Ainsi, pour l'année 2003, pour les populations situées le long des côtes sud-bretonnes, le transport larvaire était principalement orienté vers le nord-ouest en Avril (Figure 3.5A), tandis qu'il était principalement orienté vers le sud-est en Mai (Figure 3.5B).

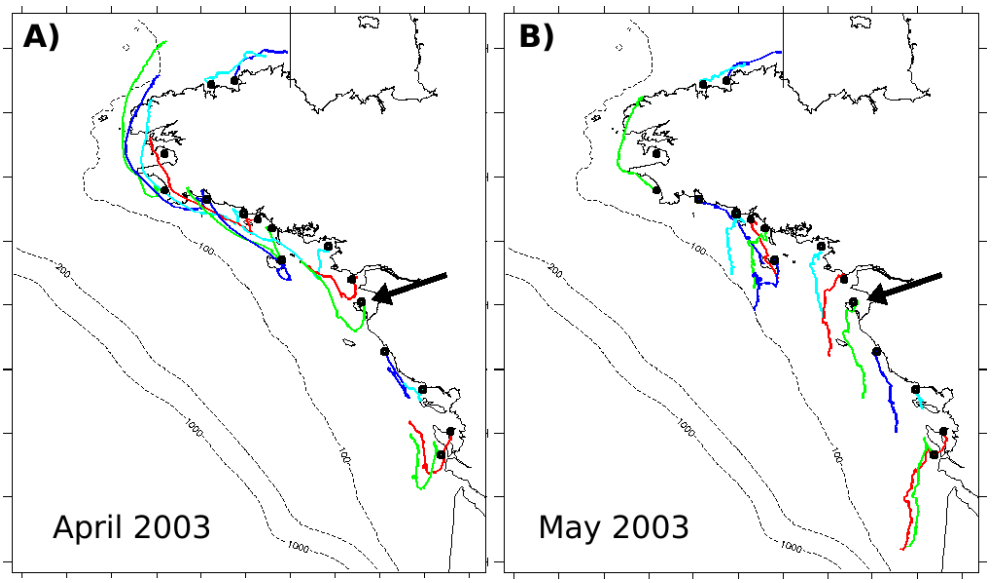


FIGURE 3.5 – Comparaison de la dispersion larvaire simulée à un mois d'intervalle : (A) ponte simulée en Avril 2003, (B) ponte simulée en Mai 2003. Résultats obtenus sans comportement natatoire (dispersion passive) et pour une durée de vie larvaire de 4 semaines. Les flèches noires indiquent la position de la population # 12.

Pour les populations situées le long des côtes sud-bretonnées, un transport larvaire vers le nord-ouest a été observé de Février à Avril 2003, tandis qu'un transport larvaire vers le sud-est a été observé de Mai à Août 2003 (Figure 3.6). Ce résultat général obtenu pour les autres années simulées suggère que la direction du transport larvaire pourraît être inversé du SE vers le NO si la ponte a lieu plus tôt dans la saison, ici en Avril à la place de Mai. Cette inversion de la direction de la dispersion a des conséquences sur les taux d'échanges larvaires puisqu'elle favorise la connectivité vers des populations plus septentrionales. Des pontes précoces pourrait aussi augmenter la taille de la connectivité, définie comme le nombre de connections entre populations, de 48 $\pm$ 9 connections pour une ponte de Mai à Août à un total de 65 $\pm$ 12 connections pour une ponte de Février à Avril (pour une durée de vie larvaire de 4 semaines). Pour les populations d'invertébrés du Golfe de Gascogne, une phénologie avancée pourrait ainsi induire une inversion du sens de la dispersion, une connectivité vers les populations septentrionales plus élevée, et une plus grande taille de connectivité.

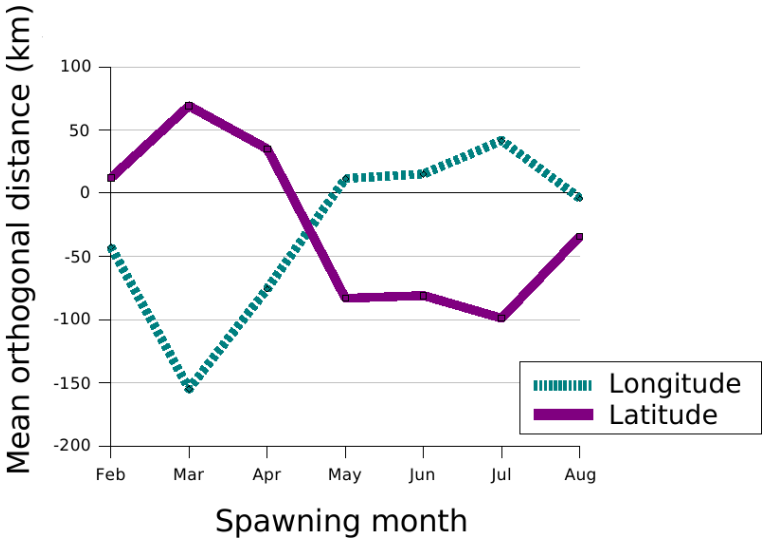


FIGURE 3.6 – Évolution saisonnière du sens et de la direction du transport larvaire : distances moyennes de transport latitudinal et longitudinal pour la population # 12 (indiquée par une flèche noire sur la Figure 3.5). Une distances de transport latitudinale positive et une distance de transport longitudinal négatif indiquent un transport vers le NO. Inversement, une distances de transport latitudinale négative et une distance de transport longitudinal positif indiquent un transport vers le SE. Résultats obtenus sans comportement natatoire (dispersion passive) et pour une durée de vie larvaire de 4 semaines.

Les résultas obtenus ici à l'échelle du Golfe de Gascogne et de la Manche seront plus généralement discutés dans l'article présenté en Annexe E.

## Conclusion de la partie I

Dans cette partie, plusieurs approches ont été mises en œuvre afin de décrire la dispersion larvaire et la connectivité des populations d'invertébrés à cycle bentho-pélagique à l'échelle régionale du Golfe de Gascogne et de la Manche occidentale : d'une part l'observation *in situ*, d'autre part la modélisation couplée biologie-physique.

Comme nous l'avons vu, le Golfe de Gascogne se caractérise par une forte variabilité saisonnière des conditions hydroclimatiques et de nombreuses structures hydrologiques à méso-echelles (fronts, plumes et lentilles dessalées, upwelling côtier) susceptibles d'affecter le transport larvaire. L'étude *in situ* de la distribution larvaire de trois espèces côtières de polychètes a mis en évidence le rôle prépondérant de l'organisation spatiale de ces structures à méso-échelles dans la variabilité de la distribution des abondances larvaires.

Par ailleurs, les résultats issus de la simulation lagrangienne de la dispersion larvaire, *via* l'utilisation d'un modèle couplé biologie-physique en conditions hydroclimatiques réalistes, ont souligné l'importance de la variabilité saisonnière des conditions hydroclimatiques et des traits d'histoire de vie dans le transport larvaire et la connectivité entre populations, en particulier le rôle du mois de ponte, du lieu de ponte, de la durée de vie larvaire et du comportement natatoire des larves. Ces résultats suggèrent que des échanges entre les populations d'invertébrés de sédiments fins côtiers du Golfe de Gascogne et celles de la Manche occidentale, *i.e.* à travers la zone de transition biogéographique entre les provinces lusitanienne et boréale, sont possibles mais faibles, unidirectionnels (du Golfe de Gascogne vers la Manche) et rares (seulement sous certaines conditions hydroclimatiques et pour certains traits d'histoire de vie).

Enfin, le modèle biophysique générique développé pour l'étude de la dispersion larvaire d'invertébrés côtiers à cycle de vie bentho-pélagique a permis de tester plusieurs hypothèses sur les conséquences possibles du changement climatique sur la dispersion et la connectivité entre populations.

Dans une seconde partie traitant de l'étude de la dispersion larvaire et de la connectivité à l'échelle locale du Golfe Normand-Breton en Manche occidentale, nous verrons un autre exemple de l'utilisation de modèle couplé biologie-physique : l'utilisation d'un modèle

eulérien spécifique de dispersion dans un contexte de conservation d'une espèce à forte valeur patrimoniale et de la biodiversité marine.

## Deuxième partie

# Impact des facteurs hydroclimatiques sur la dispersion larvaire à l'échelle locale du Golfe Normand-Breton

## Dispersion et connectivité dans le Golfe Normand-Breton

Dans la première partie de cette thèse, la dispersion larvaire et la connectivité des populations d'invertébrés à cycle bentho-pélagique ont été décrites le long des côtes Atlantiques françaises, à l'échelle régionale du Golfe de Gascogne et de la Manche occidentale. Dans cette seconde partie, nous nous intéresserons à la dispersion et à la connectivité à l'échelle locale du Golfe Normand-Breton en Manche occidentale. Ce golfe se caractérise par un fort mélange vertical, dû aux conditions de marée, et par l'existence de structures tourbillonnaires pérennes qui pourraient favoriser la rétention larvaire à l'échelle du golfe, et plus particulièrement de la Baie du Mont-Saint-Michel.

Le polychète *Sabellaria alveolata* est responsable de la formation de vastes récifs biogéniques, les récifs d'Hermelles, qui constituent d'importants îlots de biodiversité en Baie du Mont-Saint-Michel. Or ceux-ci sont soumis à des pressions anthropiques croissantes. Se pose alors la question de leur survie, de leur pérennité, et de leur restauration. Dans ce contexte de conservation de la biodiversité marine, un modèle biophysique eulérien spécifique de la dispersion larvaire de *Sabellaria alveolata* a été développé à petite échelle dans le Golfe Normand-Breton. Les paramètres biologiques spécifiques utilisés ont été estimés à partir de données d'observation *in situ* de la fécondité, la durée de vie larvaire et la mortalité larvaire. De plus, le modèle permet de simuler le comportement grégaire de sédentarisation des larves compétentes et le délai à la métamorphose. Le but de cette étude est d'estimer le rôle des facteurs hydroclimatiques dans la dispersion larvaire de cette espèce et de quantifier le degré de connectivité entre les deux principaux récifs de la Baie du Mont-Saint-Michel.

# Chapter 4

# Role of hydroclimatic processes on the sustainability of biogenic reefs

## Modelling larval dispersal and settlement of the reef-building polychaete *Sabellaria alveolata*

Sakina-Dorothée AYATA, Céline ELLIEN, Franck DUMAS,
Stanislas DUBOIS, and Éric THIÉBAUT

*Continental Shelf Research* **29**: 1605-1623 (2009)

## 4.1 Abstract

The honeycomb worm *Sabellaria alveolata* forms **biogenic reefs** which constitute biodiversity hotspots on tidal flats. The largest known reefs in Europe, located in the Bay of Mont-Saint-Michel (English Channel), are suffering **increasing anthropogenic disturbances** which raise the question of their sustainability. As the ability to recover depends partly on the recolonization of damaged reefs by larval supply, **evaluating larval dispersal and the connectivity** between distant reefs is a major challenge for their conservation. In the present study, we used a **3D biophysical model** to simulate larval dispersal under realistic hydroclimatic conditions and estimate larval retention and exchanges among the two reefs of different sizes within the bay. The model takes into account fine-scale hydrodynamic circulation (800 m $\times$ 800 m ), advection-diffusion larval transport, and gregarious settlement behaviour. According to the field data, larval dispersal was simulated for a minimal planktonic larval duration ranging from 4 to 8 weeks and the larval mortality was set to 0.09 $d^{-1}$. The results highlighted the role played by a **coastal eddy** on larval retention within the bay, as suggested by previous *in situ* observations. Very different dispersal patterns were revealed **depending on the spawning reef location**, although the two reefs were located only 15 km apart. The settlement success of the larvae released from the smallest reef was mainly related to tidal conditions at spawning, with the highest settlement success for releases at neap tide. The settlement success of the larvae from the biggest reef was more dependent on meteorological conditions: favourable W and SW winds may promote a ten-fold increase in settlement success. **Strong year-to-year variability** was observed in settlers' numbers, with favourable environmental windows not always coinciding with the main reproductive periods of *Sabellaria*. Settlement kinetics indicated that the ability to delay metamorphosis could significantly improve the settlement success. Although bidirectional exchanges occurred between the two reefs, the highest settlers' numbers originated **from the biggest reef** because of its stronger reproductive output. Because of the recent decline of this reef due to increasing anthropogenic disturbances larval supply in the bay may not be suffi-

cient enough to ensure the sustainability of the remarkable habitat formed by *Sabellaria alveolata* reefs.

## 4.2 Introduction

In coastal temperate regions, reef-building organisms including polychaetes (e.g., sabellariids, serpulids) and bivalves (e.g., mytilids, ostreids) act as ecosystem engineers by physically creating, modifying and maintaining habitats (Jones , 1997). By adding micro-scale topographic complexity to the environment, biogenic reefs offer shelters for a large number of marine species and form local hotspots of biodiversity. Although the direct positive effects of the structures built by ecosystem engineers can last longer than the lifetime of the engineer itself, sheltered species diversity tends to decline with the degradation of the reef (Hastings , 2007). Thus, the protection of such habitats constitute a major challenge for the biodiversity conservation as they are increasingly threatened by both climate changes and anthropogenic disturbances, such as pollution, overfishing of reef-associated species, or physical degradation of the reefs (Dubois , 2006, 2002; Vorberg, 1995). To inventory, preserve and restore the biogenic reefs, action plans have been recently proposed like the European Habitats Directive ("Council Directive 92/43/EEC on the Conservation of Natural Habitats and of Wild Fauna and Flora") whose Annexure I lists the biogenic reefs of open seas and tidal areas among the "natural habitat types of community interest whose conservation requires the designation of special areas of conservation" (Holt , 1998). Nevertheless, more research is generally needed to evaluate the extinction risk of those reefs and to propose specific protection management.

Like most marine benthic invertebrates, reef-building organisms exhibit a benthopelagic life cycle including a planktonic larval stage of development and two sedentary benthic juvenile and adult stages. For those organisms, successful settlement requires that larvae reach a suitable habitat within a competence period at the end of larval development. It depends on numerous factors involved in larval dispersal and results either from the local retention of larvae or from the connectivity among spatially isolated populations (Caley , 1996). Since they drive planktonic larvae, oceanographic processes (e.g., tidal residual currents, wind-induced currents, upwellings, river plumes or gyres) and their variability on time and space scales relevant to the life history of the organism greatly control larval dispersal. On the other hand, dispersal abilities also depend on the in-

teractions between hydrodynamics and biological properties, like spawning period, larval stage duration or larval behaviour. Larval dispersal and connectivity (i.e., the exchange of individuals among geographically isolated marine populations) play then a major role in marine population and metapopulation dynamics in the face of habitat fragmentation (Hastings & Botsford, 2006; Kinlan , 2005). A marine metapopulation is defined as a system of discrete local populations which are strongly dependent upon local demographic processes but are also influenced by external supply for population replenishment (Kritzer & Sale, 2003). The metapopulation concept, which has been dramatically developed in marine ecology during the last decade, has become crucial for the maintenance of local adult populations, their ability to recover from natural and anthropogenic disturbances or the implementation of marine conservation and management strategies (Botsford , 2001; Hastings & Botsford, 2006). Spatially explicit models highlight the importance of the size and location of discrete local populations and of the spatial scales of dispersal and connectivity in the metapopulation dynamics (Botsford , 1994; Gaines , 2003; Gerber , 2003).

The honeycomb worm *Sabellaria alveolata* is the most common reef-building polychaete along the NE Atlantic coasts, living in the intertidal fringe from the Solway Firth (west Scotland) to the south of the Moroccan coasts (Cunningham , 1984). Along the European coasts, the largest reef structures are located in the Bay of Mont-Saint-Michel (English Channel) where they form irregularly shaped, patchy banks that may exceed 1 m high and cover a surface of several hundreds of hectares (Figure 4.1).

The two main formations reported within the bay (i.e., Sainte-Anne reef and Champeaux reef) provide a complex habitat for macrofauna and exhibit high levels of biodiversity that contrast with the surrounding soft-bottom environments (Dubois , 2002). If these biodiversity hotspots are a highly dynamic habitat subject to numerous natural perturbations (e.g., storms), they are also increasingly threatened by direct and indirect anthropogenic disturbances including the colonization by mussels and oysters from local aquaculture, the development of ephemeral green algae in response to eutrophication or the physical degradation of the reef through trampling and shellfish farming (Dubois , 2006, 2002).

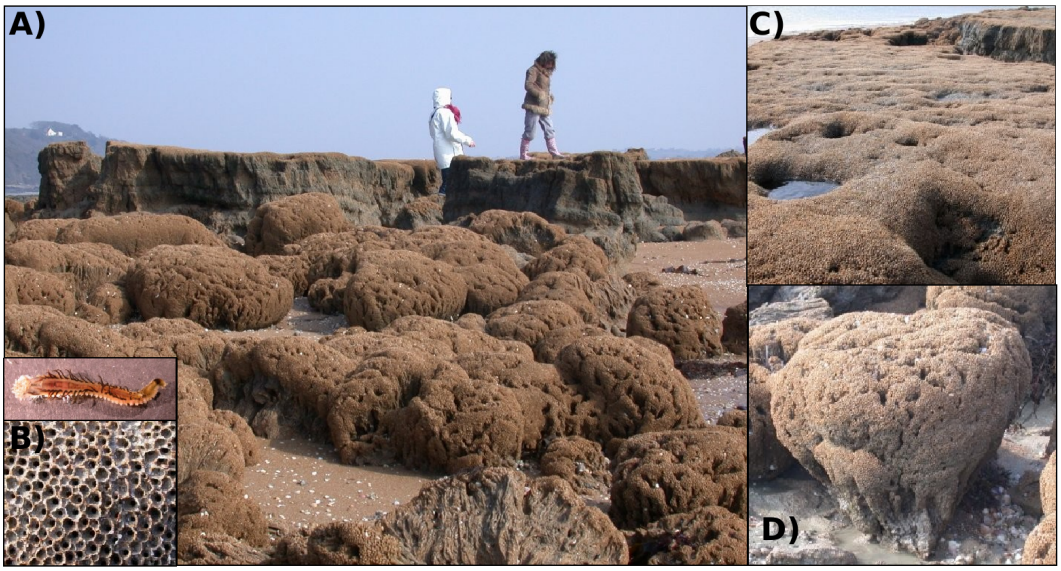


Figure 4.1: *Sabellaria alveolata* reefs. (A) Reefs in the Bay of Mont-Saint-Michel, with zoom-in pictures of (B) an adult worm out of its tube and the surface of the reef, (C) platforms structures, and (D) ball-shaped structures.

These disturbances may cause significant damages to the reef structure and a reduction in density of new recruits has already been reported (Dubois , 2006).

According to these damages, the long-term persistence of *Sabellaria alveolata* reefs in the Bay of Mont-Saint-Michel is questionable and would partly depend on sufficient larval supply during the worm life span, which varies between 4 and 5 years and can rarely reach 8-10 years (Wilson, 1971). Larval supply may be all the more important since large year-to-year variations in the recruitment of *Sabellaria alveolata* were commonly reported (Gruet, 1986; Wilson, 1971). Indeed, as a species with a long larval life span (Cazaux, 1970; Dubois , 2007; Wilson, 1968b), one speculative possibility to explain recruitment failure would be the lack of larval supply due to circulation conditions flushing larvae away from the reefs (Holt , 1998). Conversely, several processes have been proposed to explain local successful settlement and reduced larval losses in this species. First, competent *Sabellaria alveolata* larvae, i.e., larvae that have acquired the ability to settle, exhibit an active habitat selection and are able to delay metamorphosis (Pawlick, 1988; Wilson, 1968a). Second, in the Bay of Mont-Saint-Michel, *Sabellaria alveolata* presents an extended reproductive period with a semi-continuous spawning from April to October (Dubois, 2003; Dubois , 2007). This long period of larval occurrence in the water column

increases the probability that some larvae match favourable environmental conditions and successfully settle. Third, preliminary field observations on larval distribution carried out within the bay in July 2002 suggested that the tidal residual circulation, especially the occurrence of eddy structures could limit larval horizontal transport and contribute to larval retention for few weeks (Dubois , 2007).

While understanding factors that control larval dispersal and larval supply to benthic populations is a fundamental issue in conservation biology, quantifying empirically these parameters and their spatio-temporal variations remains extremely difficult. Nevertheless, recent methodological developments including molecular ecology, geochemical fingerprinting and hydrodynamic modelling provide new powerful tools to study larval dispersal (see the review by Levin, 2006). Numerical simulations constitute a quantitative approach to better understand the role of highly changeable hydrodynamics and biological factors on larval dispersal, and estimate dispersal distance and potential origin of larval supply. Although biophysical models vary a lot in terms of spatial scales and complexity, two main types of model are commonly used to simulate larval dispersal in marine organisms: (1) Eulerian models that solve an advection-diffusion equation and provide the spatial and temporal evolution of larval concentrations at each mesh point and (2) Lagrangian models (also called individual-based models or IBM) that compute individual particle pathways (see Section I.6.4). The latter have been widely used during the last years to follow the trajectories of a large number of larval particles with specific parameters (e.g., larval growth, larval behaviour) in order to simulate the dispersal of different marine invertebrates and fishes (see review by Miller, 2007, and references therein). Conversely, advection-diffusion models allow to save computing time when larval transport is simulated for a long period of time and when no individual specificities are considered, usually because of limited knowledge of biological parameters such as growth conditions or behaviour response to the environment. Although a comprehensive larval dispersal model should account for 3-dimensional (3D) flow regimes, individual larval locomotion and some demographic parameters, dispersal has been successfully modelled as an advection-diffusion process for several invertebrates like polychaetes (Jolly , 2009), bivalves (Gilg & Hilbish, 2003a), echinoderms (Dunstan & Bax, 2007), and corals (Treml , 2008). Here, we

propose to explore realistic potential dispersal of *Sabellaria alveolata* larvae in an Eulerian framework using a 3D hydrodynamic model of the Bay of Mont-Saint-Michel which predicts tidally and wind-induced currents, and drives an advection-diffusion larval transport model accounting also for larval mortality and settlement. In this context, the aims of our study are (1) to assess the role of hydrodynamic variations on the variability of larval dispersal and larval settlement within the bay, (2) to estimate larval exchanges between the two isolated reefs of the bay (Figure 4.2) and (3) to evaluate the influence of spawning date and delayed metamorphosis on settlement kinetics. These results will be discussed in terms of *Sabellaria alveolata* reefs sustainability in the Bay of Mont-Saint-Michel and the designation of conservation strategies. Is the self-replenishment sufficient to ensure the long-term persistence of the reefs within the bay? What is the relative importance of both reefs on regional larval supply? Should protection measures privilege one reef?

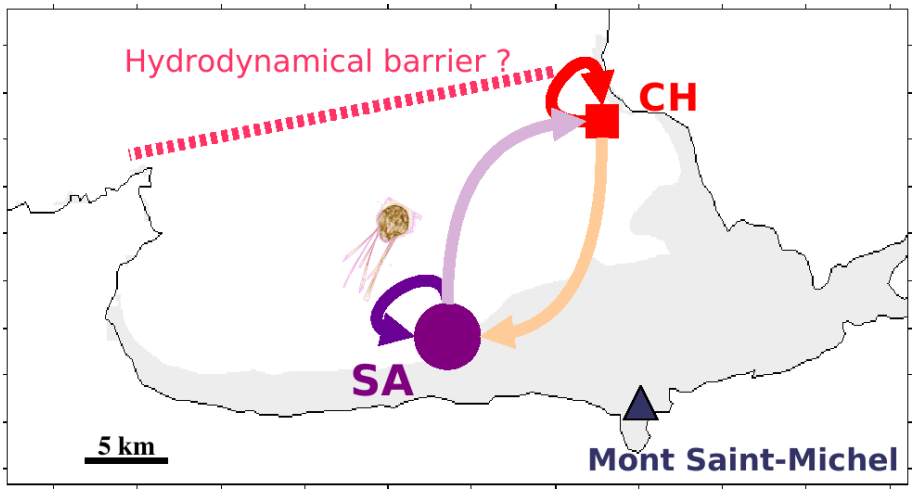


Figure 4.2: Larval exchanges' hypotheses between the two *Sabellaria alveolata* reefs of the Bay of Mont-Saint-Michel, Sainte-Anne (SA, in purple) and Champeaux (CH, in red). Arrows indicate larval exchanges' hypotheses, with local retention in Sainte-Anne in purple, and colonisation from Sainte-Anne to Champeaux in light purple, local retention in Champeaux in red, and colonisation from Champeaux to Sainte-Anne in light orange.

## 4.3 Material and methods

### 4.3.1 Study area

The Bay of Mont-Saint-Michel forms a coastal embayment in the southeast of the Gulf of Saint-Malo (western English Channel) and covers an area of about 500 $km^2$ between the Pointe du Grouin and Granville, including 240 $km^2$ of tidal flats (Figure 4.3). It is a macrotidal system with a tidal range reaching 16 m during spring tide and maximal instantaneous tidal currents varying between 0.5 and 0.8 $m.s^{-1}$ (Orbi & Salomon, 1988). Freshwater inputs coming from three small rivers (i.e., the See, the Selune and the Couesnon) do not exceed 25 $m^3.s^{-1}$ and have insignificant effect on the circulation. The water column is well-mixed in most of the bay all along the year because the strong tidal currents cause intense vertical mixing (Pingree , 1985).

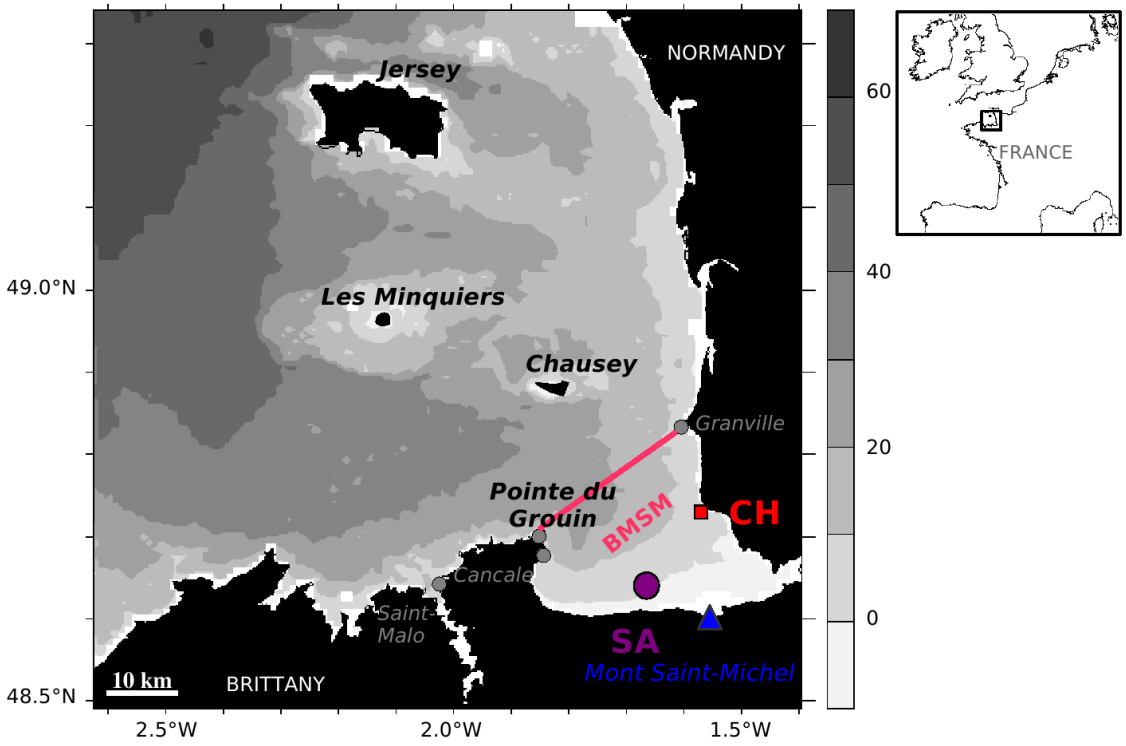


Figure 4.3: Location of the Bay of Mont-Saint-Michel (BMSM) in the Gulf of Saint-Malo. The two *Sabellaria alveolata* reefs are indicated: Sainte-Anne (SA) in purple, and Champeaux (CH) in orange.

In the Gulf of Saint-Malo, residual circulation depends mainly on the tides and is characterized by the occurrence of several cyclonic and anticyclonic gyres (Salomon & Breton, 1993; Salomon , 1996). They result either of the tidal motion rotating around islands as around the Channel Islands (e.g., Jersey and Chausey Islands) or of cape-effects as off Cancale. Those gyres are perennial, although the gyre off Cancale can be sporadically altered under particular wind conditions (i.e., constant southern wind exceeding 8 $m.s^1$) (Salomon & Breton, 1993).

Two main *Sabellaria alveolata* reefs of different sizes are present in the intertidal zone of the Bay of Mont-Saint-Michel: (1) the largest one in the central part of the bay (i.e., Sainte-Anne reef, 48°13'50 N-01°14'00 W) with a projected 3D-surface area of 2.23 $km^2$ and (2) the smallest one in the East of the bay (i.e., Champeaux reef, 48° 14'40 N-01°13'30 W) with a projected 3D-surface area of 0.29 $km^2$. Sainte-Anne reef is located adjacent to extensive culture structures for mussels and oysters. The reefs form a mosaic of three morphological stages representative of the reef dynamics (Figure 4.1): ball-shaped structures, platforms, and degraded reef (Gruet, 1982). Each stage corresponds to different infaunal species assemblages and to different demographic structures of the *Sabellaria alveolata* population (Dubois , 2002).

### 4.3.2 The hydrodynamical model

The circulation in the Gulf of Saint-Malo is simulated using a 3D hydrodynamic model, i.e., the Model for Applications at Regional Scale (MARS) (Lazure & Dumas, 2008), which is a primitive equation, finite-difference model in sigma coordinates. It solves the Navier-Stokes equations under the conventional Boussinesq and hydrostatic assumptions (see Annex B.1 for the detailed equations of the hydrodynamic model). One original aspect of the model is that the barotropic mode (free surface wave propagation) is semi-implicitly solved using an Alternate Direction Implicit scheme; it allows a coupling with the baroclinic mode (internal motion) using identical time discretization. Grid cells emerging at low tide have the ability to dry and wet in a mass-conservative way (Plus , 2009). This model has been shown to reproduce accurately both hydrodynamic and hydrological

structures, such as instantaneous tidal currents or tidal elevation on the Bay of Biscay continental shelf (Lazure & Dumas, 2008) or in a very shallow coastal embayment, the Arcachon Bay (Plus , 2009). It has been qualitatively evaluated in the Bay of Mont-Saint-Michel by the comparison with the observed hydrodynamic structures, such as the gyre off Cancale, evidenced by neutrally buoyant floats (Orbi & Salomon, 1988), measurements of radioactive tracers (Bailly du Bois & Dumas, 2005), or direct current measurements (Sentchev , 2009). The MARS 3D model was extensively used to study the transport of dissolved and particulate matter on the NW European continental shelves (Allain , 2007; Delhez , 2004; Lazure & Dumas, 2008; Lazure & Jégou, 1998; Xie , 2007).

In the present study, the model domain extends from 48°14'90' N to 49°13'40' N in latitude and from 02°27'34' W to 01°23'42' W in longitude according to the well-known limits of hydrodynamic residual structures in the English Channel (Salomon & Breton, 1993). Those model boundaries are also sufficient for the potential maximal distance reached by the larvae during their dispersal. The horizontal grid is regular with a mesh size of 800 m. Ten sigma levels (i.e., terrain-following curvilinear coordinates) are used with relative heights from the bottom to the surface of: 15 %, 15 %, 15 %, 15 %, 12.5 %, 10 %, 7.5 %, 4.5 %, 3.5 %, and 2 %; spacing is much closer near the surface to better resolve the surface layers. The coastline was provided by the 'Service Hydrographique et Oceanographique de la Marine' (SHOM) (map resolution of 25/1000). The model bathymetry was estimated from: (1) LIDAR data with a 5 m resolution for the intertidal flat of the bay (Populus , 2004), (2) IFREMER hydrographic data from mono-beam sounder with one measurement every 4 m along transects located every 200 m in the subtidal area of the bay, and (3) SHOM numerical bathymetry maps for the rest of the gulf. The open boundary conditions (i.e., free surface elevation) were obtained from two larger nested barotropic models (one for the NW European continental shelf extending from Portugal to Iceland, with a horizontal resolution of 5.6 km, and one for the English Channel, with a horizontal resolution of 3 km) which took into account the 8 main tidal waves ($M_2$, $S_2$, $N_2$, $K_2$, $O_1$, $K_1$, $P_1$ and $Q_1$). Tidal constituents along the open boundaries of the largest model were extracted from the Schwiderski atlas (Schwiderski, 1983). Here, for the three models, surface wind stress and pressure were provided by the meteorological

ARPEGE model from MeteoFrance. This regional model has a spatial resolution of 0.51° in longitude and latitude and gives four analysed wind and pressure fields per day. Given the flat surrounding topography, orographic channelling potentially caused by local winds are considered negligible and the role played by local winds on the circulation of the bay is not taken into account. Simulated wind stress was highly correlated to wind data observed at different weather stations along the coasts of the Gulf of Saint-Malo. River discharges in the Bay of Mont-Saint-Michel are considered negligible (mean outflow of 7 $m^3.s^{-1}$) and are thus not taken into account in the model.

### 4.3.3 The larval transport model

To simulate the transport of *Sabellaria alveolata* larvae, an Eulerian approach was chosen instead of a Lagrangian approach because of the lack of enough data to parametrize individual larval behaviour and development in response to environmental parameters. The larval transport is calculated by solving the following advection-diffusion-mortality equation in a mass-conservative form using the 3D current velocity fields calculated by the hydrodynamic model:

$$\frac{\partial DC}{\partial t} + \frac{\partial D\left(uC - k_x \frac{\partial C}{\partial x}\right)}{\partial x} + \frac{\partial D\left(vC - k_y \frac{\partial C}{\partial y}\right)}{\partial y} + \frac{\partial D\left(w^*C - \frac{k_z}{D^2}\frac{\partial C}{\partial \sigma}\right)}{\partial \sigma} = \frac{\partial r}{\partial t} - \mu DC - \frac{\partial s}{\partial t} \quad \text{(Eq. 4.1)}$$

where $C$ is the larval concentration per grid cell, $D$ is the water column height, $t$ is the time, $x$ and $y$ are the horizontal coordinates, $\sigma$ is the vertical sigma coordinate, $u$ is the zonal velocity, $v$ is the meridional velocity, $w^*$ is the vertical velocity in the sigma coordinate framework, $k_x$ and $k_y$ are the horizontal eddy diffusivity coefficients, $k_z$ is the vertical eddy diffusivity, $r$ is the larval release term (see Section 4.3.4), $\mu$ is the constant mortality rate, and $s$ is the larval settlement term (see Section 4.3.5).

Coastal boundaries are perfectly reflecting while the open sea boundaries are absorbing: a larva that is transported outside these boundaries is lost and can not return in the model domain. Even if preliminary observations suggested that the vertical distribution

of *Sabellaria alveolata* larvae in the Bay of Mont-Saint-Michel may vary over short-term periods (Dubois, 2003; Dubois , 2007), field observations are still lacking to describe analytically the vertical distribution of the larvae and to parametrize it in the present model in a realistic manner. Larvae are thus considered in a first approximation as passive, i.e., not able to control their vertical position. As no falling or swimming velocity is taken into account in the transport equation, simulated larval densities are homogeneous along the vertical axis.

Although larval mortality is an important demographic parameter in the understanding of the role of the larval phase on benthic populations' dynamics (i.e., fate of larval supply, connectivity between distant populations) (Cowen , 2000; Ellien , 2004), accurate estimations of larval mortality and its variability are generally lacking for most invertebrates. Here, the mortality rate was fixed at 0.09 $d^{-1}$ following an 8-month temporal survey of *Sabellaria* larvae abundances in the bay (Dubois , 2007). It was supposed constant in time and space. A preliminary sensitivity study to this parameter with rates ranging from 0 to 0.36 $d^{-1}$ indicated that the final number of settlers was inversely proportional to the mortality rate but that its variation did not alter larval dispersal patterns and settlement dynamics.

### 4.3.4 Larval release

*Sabellaria alveolata* is a gonochoric species with a sex ratio of 1:1 (Dubois, 2003). It is an iteroparous breeder whose individuals become mature after one year. Within the bay, the spawning occurs throughout most of the year (from April to October) with two main periods in May-June and in September (Dubois , 2007). Ovigerous females are reported throughout the year and represent up to 65 % of the female populations (15 % on average) (Dubois, 2003). If the fecundity is highly variable among females and seasons, a mean value of 100,000 ovocytes per female has been calculated (Dubois, 2003). Despite an external fertilization, the aggregative distribution of adults suggests a high fertilization success, so a fertilization success of 80 % was assumed (Eckman, 1996).

Spawning was simulated within the bay at the locations of the two reefs that correspond to four grid cells for the Sainte-Anne reef and to one grid cell for the Champeaux reef. According to field observations (Dubois, 2003; Dubois , 2002), the size of the adult population for both reefs was estimated from (1) the surface of each reef, (2) the proportions of the different reef structures, and (3) the mean density of adult worms for each type of reef structure (Table 4.1). The number of larvae released by each reef during a spawning event was calculated from (1) the adult population size, (2) a 1:1 sex ratio, (3) the mean proportion of ovigerous females within the population, (4) the mean fecundity and (5) a fertilization rate of 80 % (Table 4.1). For each spawning event, a total of $2.52 \times 10^{14}$ and $4.8 \times 10^{13}$ larvae were then released from the Sainte-Anne and Champeaux reefs, respectively.

Table 4.1: Properties of *Sabellaria alveolata* populations used to calculate the number of released larvae for each spawning event.

| | Sainte-Anne reef | Champeaux reef |
|---|---|---|
| Reef area ($m^2$)[a] | $2.23 \times 10^6$ | $0.29 \times 10^6$ |
| Ball-shaped structures | | |
| Proportion (%)[a] | 20 | 20 |
| Worm density (ind $m^2$)[b] | 25,000 | 25,000 |
| Platform structures | | |
| Proportion (%)[a] | 30 | 60 |
| Worm density (ind $m^2$)[b] | 35,000 | 35,000 |
| Degraded reef | | |
| Proportion (%)[a] | 50 | 20 |
| Worm density (ind $m^2$)[b] | 6500 | 6500 |
| Adult stock | $4.2 \times 10^{10}$ | $0.8 \times 10^{10}$ |
| Sex-ratio[a] | 1:1 | 1:1 |
| Mean proportion of mature females (%)[a] | 15 | 15 |
| Mean fecundity[a] | 100,000 | 100,000 |
| Fertilization rate | 0.8 | 0.8 |
| Number of released larvae | $2.52 \times 10^{14}$ | $4.8 \times 10^{13}$ |

[a] Dubois (2003)
[b] Dubois *et al.* (2002)

Dubois *et al.* (2007) suggested that the seasonal reproduction of *Sabellaria alveolata* may be related to spring temperature increase and to spring and autumn phytoplanktonic blooms. By contrast, the numerous exogenous and endogenous cues that may control the short-term rhythmicity of spawning events at the population level remain unknown while it has been reported that spawning of intertidal polychaetes may occur at the incoming tide and during a few successive days (Bentley & Pacey, 1992; Olive, 1992). On the other hand, for different marine invertebrates like mussels or sea urchins, the occurrence in the water column of specific chemical signals (e.g., phytoplankton blooms, sperm from conspecifics) may enhance the synchrony of spawning and trigger mass spawning (Starr , 1990). In most simulations, larvae were then released instantaneously at high tide in the lowest grid cells located above the reefs as follows in the sigma coordinate framework:

$$\begin{cases} \dfrac{\partial r(x,y,\sigma,t)}{\partial t} = \dfrac{N_0}{V_{xy\sigma(1)}} \quad when \begin{cases} t = t_0 \\ \{x,y\} \in \{\text{reef coordinates}\} \\ \sigma = \sigma(1) \\ D(x,y) > 0.5 \end{cases} \\ \dfrac{\partial r(x,y,\sigma,t)}{\partial t} = 0 \qquad otherwise \end{cases} \qquad \text{(Eq. 4.2)}$$

where $r(x, y, \sigma, t)$ is the larval release function in the grid of coordinates ($x$,$y$,$\sigma$,$t$), $N_0$ is the total number of released larvae, $t_0$ is the time at high tide and $V_{xy\sigma(1)}$ is the volume of the lower cell of coordinates ($x$, $y$, $\sigma(1)$).

The volume of the lower cell of coordinates ($x$, $y$, $\sigma(1)$) is given by

$$V_{xy\sigma(1)} = S(x,y) h_{\sigma(1)} D(x,y) \qquad \text{(Eq. 4.3)}$$

where $S(x, y)$ is the surface of a cell equal to 0.16 km$^2$, $h_{\sigma(1)}$ is the relative height of the lowest sigma layer equal to 0.15 and $D(x, y)$ is the total water column height.

To evaluate the impact of this simple formulation of spawning, three other formulations of larval release are considered: a uniform continuous spawning of 4 h over one tidal cycle, a symmetric semi-continuous spawning over three tidal cycles and a symmetric semi-

continuous spawning over five tidal cycles. The detailed equations for these larval release formulations are given in Annex **??**.

### 4.3.5 Larval settlement

From laboratory cultures, Wilson (1968b, 1970) reported large variations in *Sabellaria alveolata* larval life span, from 6 weeks to 11 months, partly in relation tonatural variability amongindividuals and culture conditions (food, temperature). Conversely, Dubois (2007) estimated from *in situ* larval sampling inthe Bay of Mont-Saint-Michel that planktonic lifetime rangedbetween 4 and 10 weeks. On the other hand, competent larvaepositively respond to chemical cues produced by thecongenericadult and juvenile tubes and could delay metamorphosis if proper environment for settlement is not encountered (Pawlick, 1988; Wilson, 1968a). In the present study, we considered that when the larvae become competent, they can delay their settlement during four more weeks. The age at competence, i.e., the minimal planktonic larval duration (PLD), was set at 6 weeks, leading to a maximal PLD of 10 weeks. To assess the consequences on settlement of PLD variations related to seasonal variations in environmental conditions (e.g., temperature, food availability), nine values of minimal PLD ranging from 4 to 8 weeks were also tested.

Chemosensory responses of larvae to specific cues associated with the bottom are likely (1) to modify larval behaviour in the water column and favour larval concentration near the bottom, and (2) to increase the probability of substratum acceptance (Eckman, 1996). As the behaviour of *Sabellaria* competent larvae and the maximal perception distance of the chemical cues remain unknown, larval settlement was simulated according to the following criteria: (1) larvae can settle from the beginning of the competence period (i.e., minimal PLD) and delay their metamorphosis during 4 weeks (i.e., maximal PLD = minimal PLD + 4 weeks); (2) larval settlement was restricted to the grid cells above the adult reefs and within the last 3 m above the bottom; (3) 50 % of the competent larvae present within the last 3 m above an adult reef settled. The detailed equation of the larval

settlement term is given below:

$$\begin{cases} \dfrac{\partial s(x,y,\sigma,t)}{\partial t} = r_s p_\sigma C(x,y,\sigma) \quad when \begin{cases} t_{minPLD} <= t < t_{minPLD} + t_{delay} \\ \{x,y\} \in \{\text{reef coordinates}\} \\ \sigma < \sigma_{perception} = \dfrac{z_{perception} + H}{\zeta + H} \end{cases} \\ \dfrac{\partial s(x,y,\sigma,t)}{\partial t} = 0 \qquad otherwise \end{cases} \quad \text{(Eq. 4.4)}$$

where $s$ is the larval settlement function, $r_s$ is the settlement rate fixed at 50 %, $p_\sigma$ is the proportion of the sigma layer in which larvae can detect adult habitat, $t_{minPLD}$ is the age at competence, $t_{delay}$ is the maximal metamorphosis delay fixed at 4 weeks, $z_{perception}$ is the maximal perception distance fixed at 3 m, $H$ is the absolute value of bottom position, $z$ is the sea surface elevation.

For any sigma layer, the proportion of the sigma layer in which larvae can detect adult habitat is defined as:

$$\begin{cases} p_\sigma = 1 & when\ \sigma < \sigma_{inf} \\ p_\sigma = \sigma_{perception} - \sigma_{inf} & when\ \sigma = \sigma_{inf} \\ p_\sigma = 0 & when\ \sigma > \sigma_{inf} \end{cases} \quad \text{(Eq. 4.5)}$$

where $\sigma_{inf}$ is the higher sigma level above the maximal perception distance $z_{perception}$ defined by $\sigma_{inf} <= \sigma_{perception} < \sigma_{inf+1}$.

### 4.3.6 Simulations

For both reefs, several sets of larval dispersal simulations were performed to investigate the influences of tides and winds at different temporal scales over the whole *Sabellaria alveolata* spawning period (Table 4.2). First, four types of larval release (instantaneous spawning, uniform continuous spawning during one tidal cycle, symmetric semi-continuous spawning during three tidal cycles, and symmetric semi-continuous spawning during five tidal cycles) were tested during average tide conditions in June 2002 and with no wind forcing. Second, the influence of the lunar tidal cycle was determined following instantaneous spawning

events in different tidal conditions and with no wind forcing between March and October 2002: 16 spawning events in average tide, seven spawning events in neap tide, and seven spawning events in spring tide. Third, to assess the role of wind stress, the 16 previous simulations performed for a spawning in average tide were realised again under a real wind forcing. Finally, to estimate the influence of inter-annual variability in the meteorological conditions, larval dispersal was simulated between 2000 and 2004, for seven spawning events in average tide each year, under a real wind forcing. A sensitivity analysis on the age at competence was also performed with minimal PLD ranging from 4 to 8 weeks for an instantaneous spawning release in average tide condition and with no wind forcing.

Table 4.2: Conditions of the different simulations of *Sabellaria alveolata* larval dispersal in the Bay of Mont-Saint-Michel.

| Conditions | Simulations | | | | | | |
|---|---|---|---|---|---|---|---|
| Year | 2002 | 2002 | 2002 | 2002 | 2002 | 2000-2004 | 2002 |
| Spawning period | June | March-October | April-October | April-October | March-October | April-October | June |
| Lunar tidal conditions at larval release | Average tide | Average tide | Neap tide | Spring tide | Average tide | Average tide | Average tide |
| Larval release type | Instantaneous or continuous during 1, 3, or 5 tidal cycles | Instantaneous at high tide | Instantaneous at high tide | Instantaneous at high tide | Instantaneous at high tide | Instantaneous at high tide | Instantaneous at high tide |
| Wind forcing | No | No | No | No | Real wind | Real wind | No |
| Minimal PLD | 6 weeks | 6 weeks | 6 weeks | 6 weeks | 6 weeks | 6 weeks | From 4 to 8 weeks |
| Simulation frequency | 1 per release type | 2 per month | 1 per month | 1 per month | 2 per month | 1 per month | 1 per minimal PLD |
| Number of simulations | 4 | 16 | 7 | 7 | 16 | 28 | 9 |

For each simulation, the following parameters were calculated at the end of the dispersal phase:

1. the density of autochthonous and allochthonous settlers for each reef;
2. the retention rate within each reef (i.e., ratio between the number of autochthonous settlers in a reef and the total number of larvae released from this reef);
3. the colonization rate of each reef (i.e., ratio between the number of allochthonous settlers in the colonized reef and the total number of larvae emitted from the colonizing reef);
4. the total settlement rate from each reef (i.e., ratio between the total number settlers from a reef and the total number of larvae emitted from this reef);

5. the allochthonous settlement ratio for each reef (i.e., ratio between the number of allochthonous and autochthonous settlers within a reef).

## 4.4 Results

### 4.4.1 Residual circulation in the Gulf of Saint-Malo

Without wind forcing, the tidal residual circulation of the Gulf of Saint-Malo was characterized by large spatial variations in current velocity, from less than 2 cm.s$^1$ to more than 20 cm.s$^1$. It exhibited also remarkable meso-scale features including an alongshore current (eastwards off the Brittany then northwards off the Normandy, velocity from 5 to 10 cm.s$^1$) and several cyclonic (anticlockwise) and anticyclonic (clockwise) gyres (Figure 4.4A). Cyclonic gyres were formed around the Jersey Island and Les Minquiers Archipelago while an anticyclonic cape gyre of about 15 km in diameter occurred off Cancale. The areas with the slowest currents ($<$ 2.5 cm.s$^1$) were located in the South of Granville and in the North of Chausey Island. Maximal currents (420 cm.s$^1$) were locally reported off different capes and around Les Minquiers.

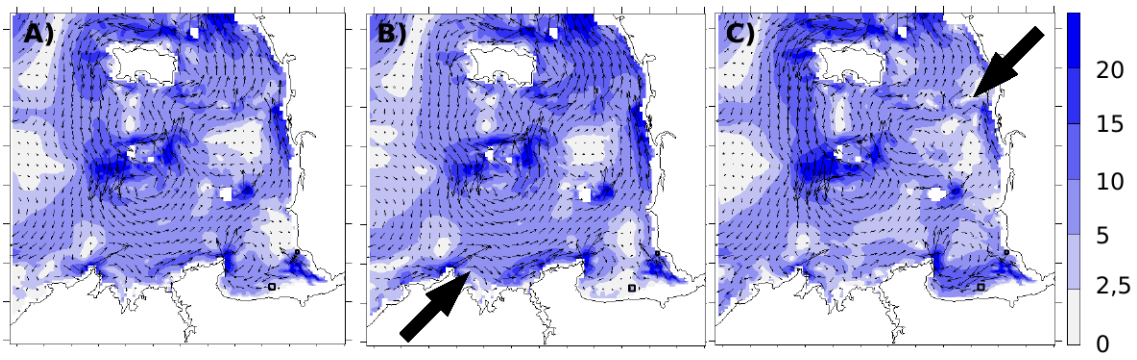


Figure 4.4: Simulated depth-averaged residual Lagrangian velocity fields in the Gulf of Saint-Malo for average tide conditions and no wind forcing (A), a constant SW-wind forcing of 11 m.s$^1$ (B), and a constant NE-wind forcing of 11 m.s$^1$ (C). Empty arrows indicate the wind orientation. Residual velocities are given in cm.s$^1$.

Wind forcing could partly alter this circulation scheme according to its direction and velocity. As an example, Figures 4.4B and C illustrate the effect of a uniform moderate wind stress (velocity of 11 m.s$^1$) from SW and NE on the residual circulation, these compass directions corresponding to dominant winds in the bay. Under a SW wind forcing,

the spatial extent of the gyre off Cancale was then reduced to the western half of the Bay of Mont-Saint-Michel (Figure 4.4B). The alongshore currents off Saint Malo and the Normandy coasts were accelerated and low currents ($< 2.5$ cm.s$^1$) were reported in the South of the bay. Under a NE wind forcing, the gyre off Cancale was extended to the entire Bay of Mont-Saint-Michel (30 km of diametre) (Figure 4.4C). Residual currents within the gyre were strengthened (410 cm.s$^1$ in the south) while the northwards current along the Normandy coasts was slightly decreased.

### 4.4.2 Influence of tides on larval dispersal and settlement

#### *4.4.2.1 General pattern of larval dispersal*

Without wind forcing, dispersal simulations of larvae released instantaneously at high tide and in average tide conditions showed that most larvae were progressively retained in the gyre off Cancale (Figure 4.5). The larval cohort never extended further than 20 km westward from the Pointe du Grouin but could spread northwards along the Cotentin coast.

However, dispersal patterns differed according to the emission reef (Figure 4.5). Following a spawning event from Sainte-Anne, larvae were first transported westwards (Figure 4.5A) and were then trapped in the gyre off Cancale (Figure 4.5B). When the larvae become competent, i.e., after 6 weeks, the highest larval concentrations (i.e., 412,000 ind.m$^2$) were located outside the bay in the north of Cancale and a significant northward export of the larval cohort was reported along the Cotentin coast on a distance of 60 km from Granville (42,000 ind.m$^2$) (Figure 4.5C). Larval densities reached only 2,900 and 2,000 ind.m$^2$ above the adult reefs of Champeaux and Sainte-Anne respectively after 6 weeks of dispersal. After 10 weeks, the settlement rate within the bay is equal to $3.19\times10^4$ %.

On the contrary, following a larval release from Champeaux, a larger proportion of larvae remained confined in the innermost part of the bay (Figure 4.5E). After 6 weeks of dispersal, highest larval concentrations were observed in the gyre off Cancale (43,000 ind.m$^2$) and within the bay (42,000 ind.m$^2$) (Figure 4.5F). Larval concentrations above the adult reefs of Champeaux and Sainte-Anne were of 800 and 1,000 ind.m$^2$, respectively. The

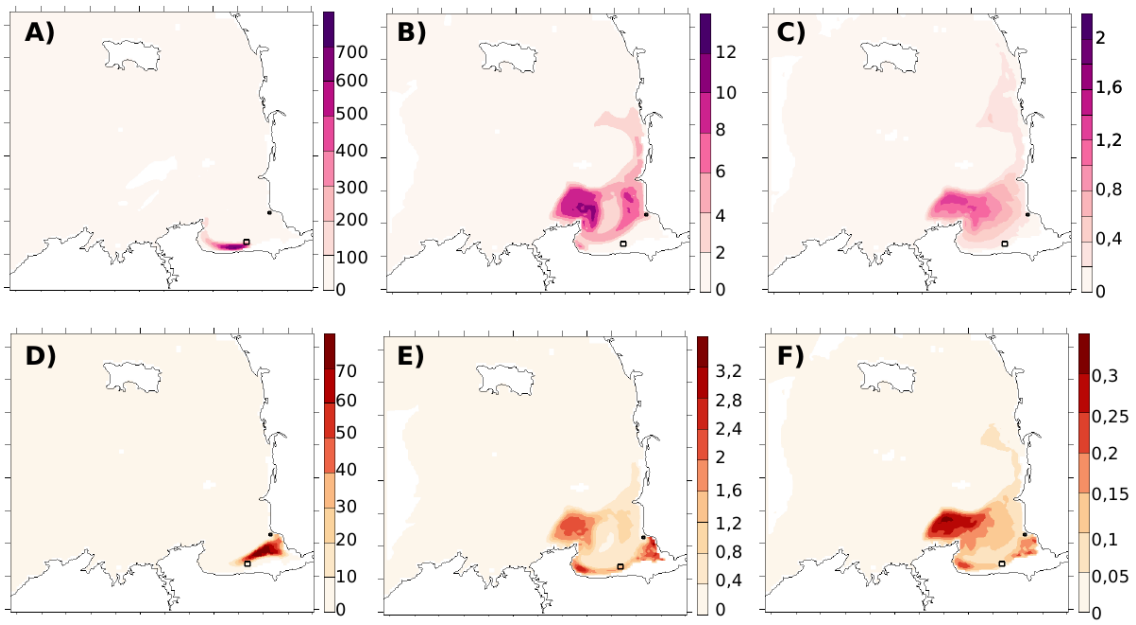


Figure 4.5: Predicted larval distributions following a spawning event from Sainte-Anne (A-C) and from Champeaux (D-F) at high tide and in average tide conditions after 3 days (A and D), 3 weeks (B and E), and 6 weeks (C and F). The two black squares represent the reefs of Sainte-Anne and Champeaux. No wind forcing is considered. Larval concentrations are given in $10^4$ ind.m$^2$. Note that the scales of the larval concentrations differ between the maps.

northward extension of the larval patch along the Normandy coast did not exceed 30 km from Granville. The settlement rate after 10 weeks reached $2.39\times10^3$ %.

These patterns will be used afterwards as reference conditions to assess the influence of tides and winds on larval dispersal.

#### *4.4.2.2 Influence of larval release duration*

The dispersal patterns were not modified if larval release occurred uniformly and continuously during one tidal cycle or semi-continuously and symmetrically during three or five tidal cycles (data not shown). Likewise, the total settlement rates from Sainte-Anne and Champeaux did not significantly vary with the larval release duration (Figure 4.6). The settlement rate from Sainte-Anne ranged from $8.87\times10^4$ % to $9.03\times10^4$ % while the settlement rate from Champeaux varied from $2.39\times10^3$ % to $2.63\times10^3$ % with a lightly lower settlement rate when the larval release was instantaneous.

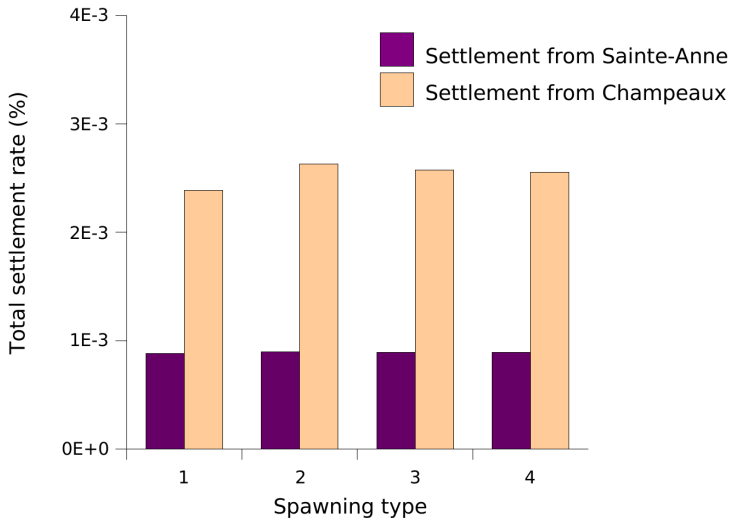


Figure 4.6: Variations in the settlement rates of larvae released from the reefs of Sainte-Anne and Champeaux in relation to the larval release duration: (1) instantaneous spawning, (2) continuous and uniform spawning during 1 tidal cycle, (3) semi-continuous and symmetric spawning during 3 tidal cycles, and (4) semi-continuous and symmetric spawning during 5 tidal cycles. Larval dispersal is simulated without wind forcing during 10 weeks.

#### *4.4.2.3 Influence of the lunar tidal cycle at spawning time*

Without wind forcing, the stages of the spring-neap tidal cycle at larval release had different consequences on the settlement success of larvae according to the emission reef (Figure 4.7). For larvae released from Sainte-Anne, the settlement success did not depend on the tidal range at spawning date: the retention rate varied slightly between $2.17\times10^4$ % and $3.47\times10^4$ % (Figure 4.7A) while the colonization rate fluctuated between $3.79\times10^4$ % and $5.67\times10^4$ % (Figure 4.7B). On the contrary, the settlement rates of larvae released from Champeaux significantly decreased with the tidal range (Spearman rank correlation coefficient $r_s$ = - 0.834 with p-value $< 0.001$ for the retention rate and $r_s$ = - 0.883 with p-value $< 0.001$ for the colonization rate). At this site, the retention rate decreased from $2.11\times10^3$ % to $7.13\times10^4$ % when the tidal range increased from 3.3 to 12.2 m (Figure 4.7A). In average, it was about twice smaller for a release in spring tide ($8.68\times10^4$ % $\pm$ $0.82\times10^4$ %, n = 7) than in neap tide ($15.9\times10^4$ % $\pm$ $3.5\times10^4$ %, n = 7). Likewise, the colonization rate from Champeaux to Sainte-Anne decreased from $19.3\times10^4$ % to $5.34\times10^4$ % for a rise in the tidal range from 3.3 to 12.2 m (Figure 4.7B). The mean per-

centage of larvae released at Champeaux and successfully settling at Sainte-Anne showed a two-fold decrease between a spring tide spawning ($6.78\times10^4$ % $\pm$ $0.95\times10^4$ %, n = 7) and a neap tide one ($14.5\times10^4$ % $\pm$ $2.5\times10^4$ %, n = 7). Even if retention and colonization rates were always higher for larvae released at Champeaux rather than at Sainte-Anne whatever the tidal range, maximal differences between both reefs were observed for a spawning at neap tide. In these conditions, the retention rate in Champeaux may be seven times higher than the retention rate in Sainte-Anne while the colonization rate from Champeaux may be five times higher than the colonization rate from Sainte-Anne. For a release in average tide from Champeaux, the variability of the settlement rates was due to tidal conditions the days following the larval release (neap or spring tide).

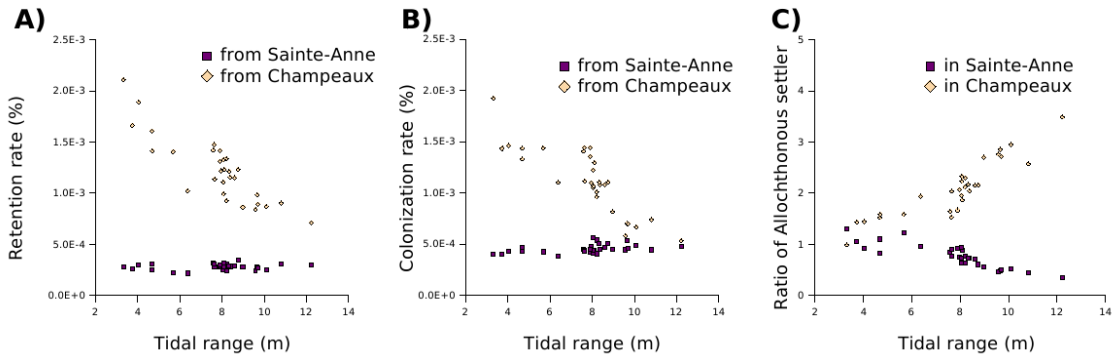


Figure 4.7: Variations in retention rates (A), colonization rates (B) and allochthonous settlers' ratio (C) according to the tidal range at spawning for larvae released from the two reefs. Larval releases occur at high tide and dispersal is simulated without wind forcing during 10 weeks.

The ratio of allochthonous settlers vs. autochthonous settlers varied according to the reefs and the tidal range (Figure 4.7C). Since the settlement of the larvae released from the Sainte-Anne reef was mostly independent of the tidal range during the spawning, the variation of this ratio was directly due to the variation of the number of settlers from Champeaux. At Sainte-Anne, the ratio decreased from 1.31 to 0.34 when the tidal range increased (Figure 4.7C). While the settlement at this reef depended rather on allochthonous settlers for a release in neap tide, settlers were mainly autochthonous for a release in average or spring tide. At Champeaux, the ratio increased from 0.99 to 3.49 when the tidal range increased indicating that the proportion of allochthonous settlers became

increasingly important (Figure 4.7C). For a release at spring tide, allochthonous settlers at Champeaux could be three times more abundant than autochthonous settlers.

The effect of the lunar tidal cycle at spawning time on the settlement success of larvae released at Champeaux was related to the role of this environmental parameter on the dispersal patterns (Figure 4.8). Only a few days after spawning, differences in larval dispersal were already reported according to the tidal range so that the transport to the south was amplified for a release in spring tide (Figure 4.8D) in comparison with a release in neap tide (Figure 4.8A). After 3 weeks of dispersal, most larvae were located in the innermost part of the bay for a release in neap tide (larval concentration 470,000 ind.m$^2$) (Figure 4.8B) whereas larvae were mainly trapped in the gyre off Cancale for a release in spring tide (larval concentration 430,000 ind.m$^2$) (Figure 4.8E). At larval competency, after 6 weeks of dispersal, even if the extent of the larval cohort was similar whatever the tidal range at spawning time, large spatial variations in larval distribution were still apparent: larval concentrations within the bay were higher for a release in neap tide (43000 ind.m$^2$) (Figure 4.8C) than for a release in spring tide (41,000 ind.m$^2$) (Figure 4.8F).

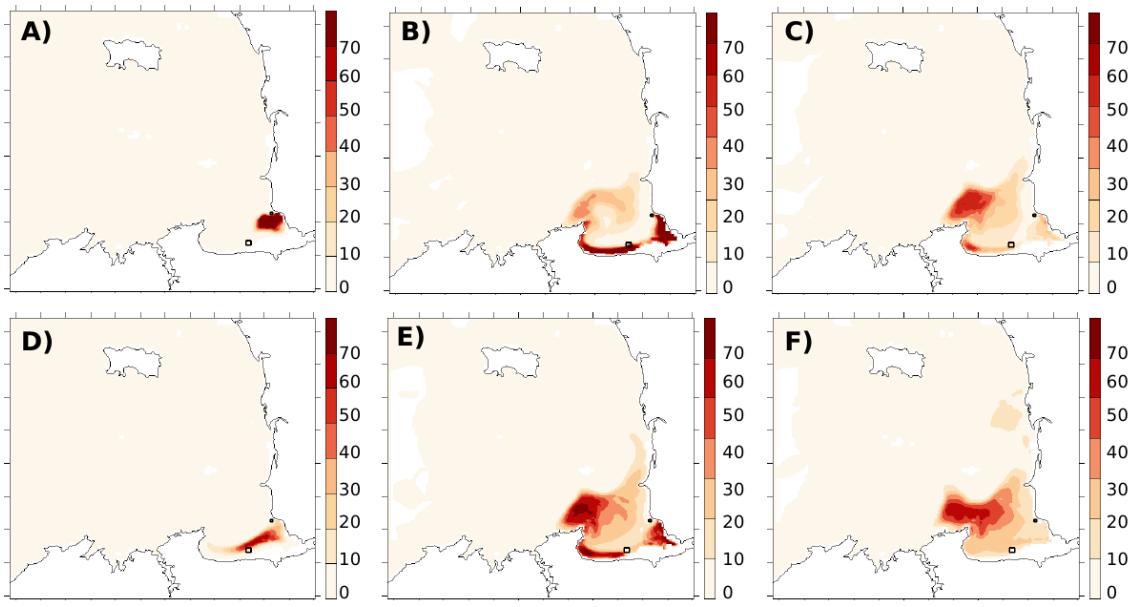


Figure 4.8: Predicted distributions of larvae released from Champeaux in conditions of neap tide (A-C) and spring tide (D-F) after 3 days (A and D), 3 weeks (B and E) and 6 weeks (C and F) of dispersal without wind forcing. The two black squares represent the reefs of Sainte-Anne and Champeaux. The larval concentrations are given in $10^4$ ind.m$^2$. Note that the scales of the larval concentrations differ between the maps.

### 4.4.3 Influence of wind conditions on larval dispersal and settlement

#### *4.4.3.1 Seasonal variability of settlement under realistic meteorological conditions*

Results for bimonthly larval releases from March to October 2002 under real wind conditions (releases at high tide during average tide conditions) indicated that a realistic wind forcing influenced larval settlement within the bay and could induce a seasonal variability in the success of the larval cohorts (Figure 4.9). However, the effect of this forcing showed some variations according to the release reef.

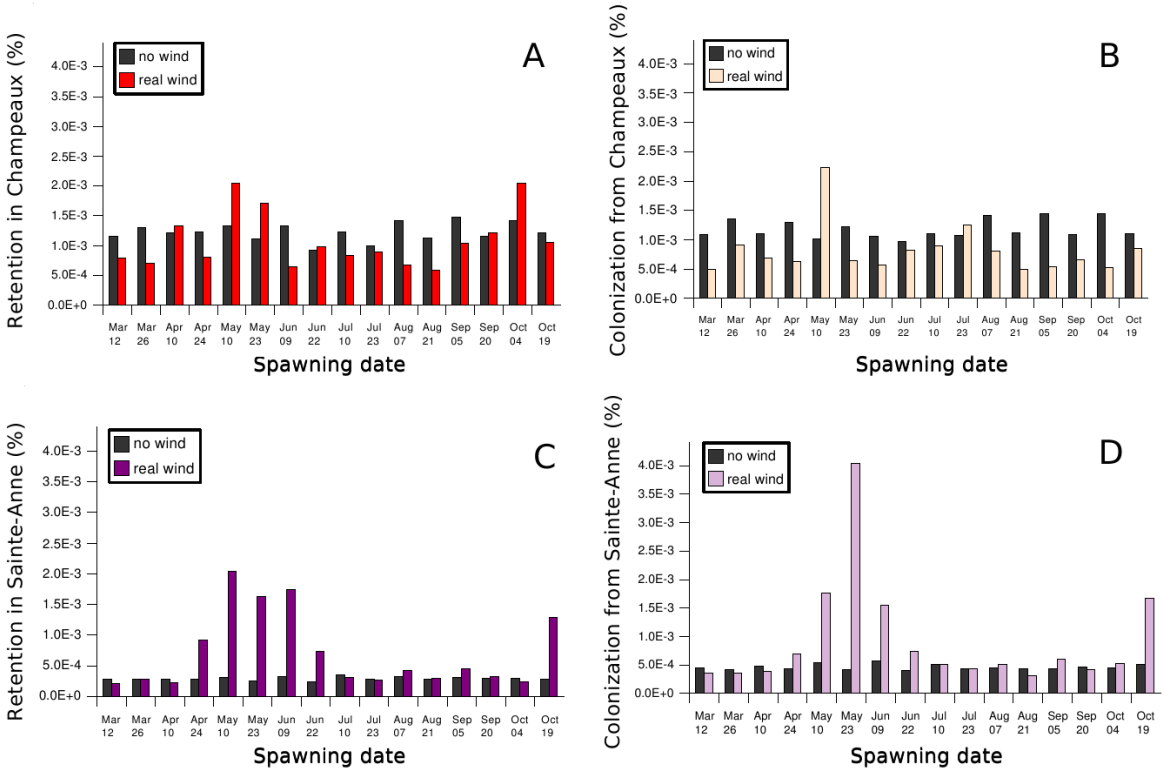


Figure 4.9: Seasonal variations in retention and colonization rates for 16 spawning events, from March to October 2002, with and without real wind forcing: retention rate in Champeaux (A); colonization rate from Champeaux to Sainte-Anne (B); retention rate in Sainte-Anne (C); colonization rate from Sainte-Anne to Champeaux (D). Larval releases occur at high tide in average tide conditions and dispersal is simulated during 10 weeks.

For a release at Champeaux, the wind forcing in 2002 tended to have no effect or to slightly decrease the retention rate (average retention rate of $1.09\times10^3$ % $\pm$ $0.47\times10^3$ % with wind forcing vs. $1.23\times10^3$ % $\pm$ $0.15\times10^3$ % without wind forcing) except for three spawning events (Figure 4.9A). Thus, the retention rate in Champeaux was increased

about 1.5 folds for the larvae released on 10 May, 23 May and 4 October. Likewise, the colonization rate from Champeaux to Sainte-Anne was generally smaller than those obtained without wind forcing (average colonization rate of 0.81 $\times 10^3$ % $\pm$ 0.43$\times 10^3$ % with wind forcing vs. 1.18$\times 10^3$ % $\pm$ 0.16$\times 10^3$ % without wind forcing) (Figure 4.9B). Only larvae released on 10 May exhibited a two-fold increase in the colonization rate of Sainte-Anne reef in the presence of wind forcing.

By contrast, the retention and colonization rates of larvae released from Sainte-Anne could be strongly modified by the meteorological conditions in 2002. The wind forcing strongly enhanced the retention rates for six spawning events out of 16, from the end of April to the end of June and in mid-October (Figure 4.9C). In comparison with no wind forcing, the retention was multiplied by about 3 for a larval release on 24 April and 22 June, by 4.5 for a release on 19 October, by 5.4 for a release on 9 June and by about 6.5 for a release on 10 and 23 May. For the other 10 spawning events, the retention rates obtained under real wind forcing were close to those obtained without wind forcing. Because of wind forcing, the colonization rate from Sainte-Anne to Champeaux was also strongly increased at the same dates, from a factor 1.6 for a larval release on 24 April to a factor 9.8 for a larval release on 23 May (Figure 4.9D).

The maximum increase in the retention and colonization rates from Sainte-Anne was achieved with a nearly constant westerly or south-westerly wind as shown for larval releases on 10 May, 23 May and 19 October 2002 (Figure 4.10). Other wind conditions generated dispersal patterns comparable to those obtained with tidal forcing only. If the maximal extent of the larval cohort after 6 weeks of dispersal was slightly modified by wind forcing (compare with Figures 4.5 and 4.8), the location of the highest larval concentrations was highly dependent on meteorological conditions.

For a release on 10 May 2002, larvae were subjected to a SW wind for the first 3 weeks and then alternatively to NW and W winds (mean velocity of 5.3 m.s$^1$) (Figure 4.10C). After 3 and 6 weeks of dispersal, larvae were mainly located within the bay and in the gyre off Cancale (Figure 4.10A-B). At both periods, the highest larval concentrations (4,120,000 and 15,000 ind.m$^2$, respectively) were confined in the south-eastern part of the bay. For a release on 19 October 2002, the wind was mainly from W-SW and then

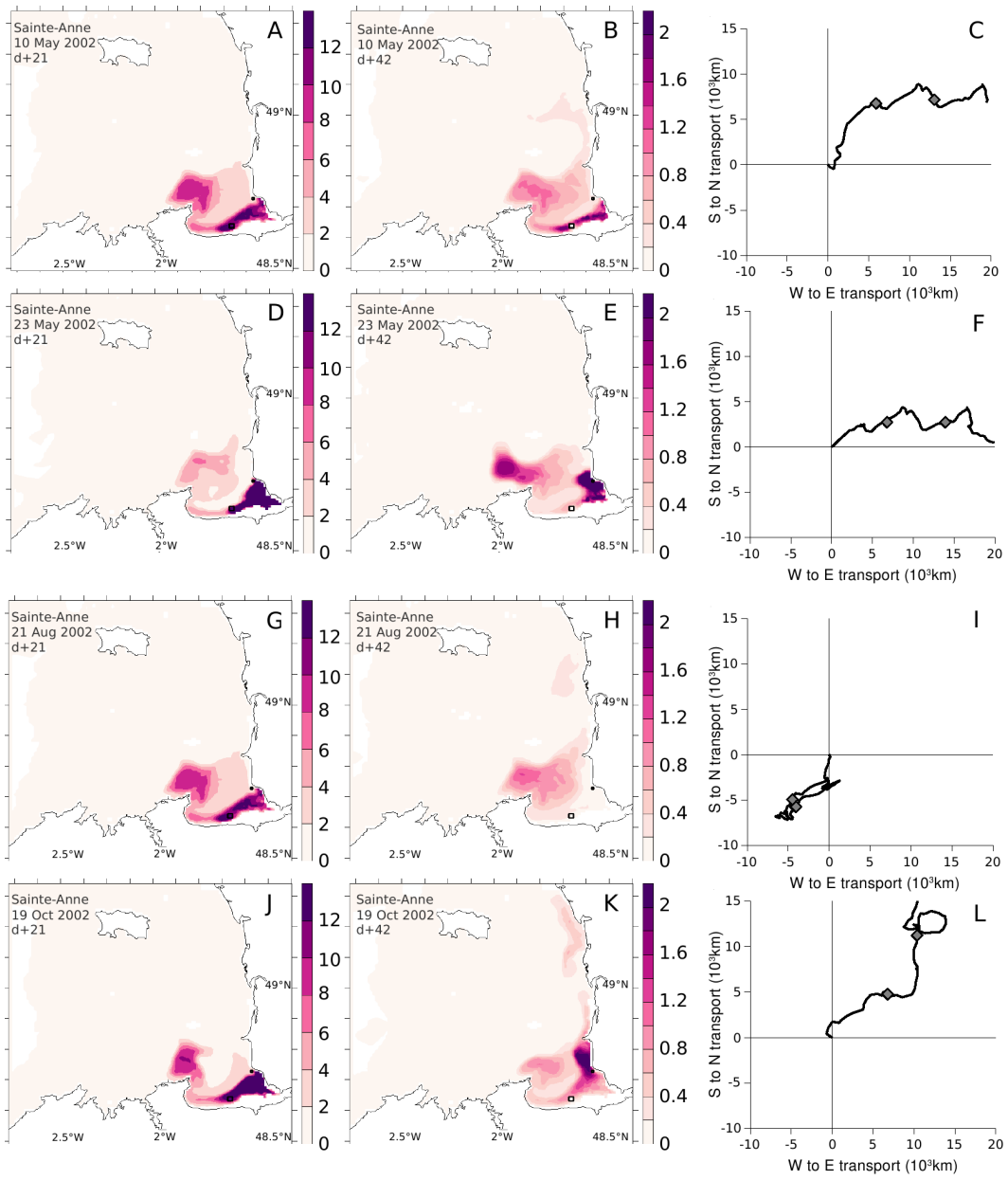


Figure 4.10: Examples of predicted distributions of larvae released from Sainte-Anne on 10 May (A-C), 23 May (D-F), 21 August (G-I), and 19 October 2002 (J-L) after 3 weeks (A, D, G, J) and 6 weeks (B, E, H, K) of dispersal with real wind forcing. Larval releases occur at high tide in average tide conditions. The two black squares represent the adult reefs of Sainte-Anne and Champeaux. The larval concentrations are given in $10^4$ ind.m$^2$. Note that the scales of the larval concentrations differ between the maps. Progressive vector diagrams (PDV) of the wind forcing in the Gulf of Saint-Malo during larval dispersal are indicated for each spawning event (C,F,I,L), with West-East transport ($10^3$ km) as abscissa and South-North transport ($10^3$ km) as ordinate. The gray diamonds indicate the 3$^{rd}$ and the 6$^{th}$ weeks of dispersal. Wind data were provided by Meteo France (Arpege model).

S (average velocity of 6.9 m.s$^1$) except for a 2 week period characterized by an E wind (5.9 m.s$^1$) (Figure 4.10L). After 3 weeks of dispersal, larval distribution was close to the one obtained for a release on 10 May with maximal concentrations (4,150,000 ind.m$^2$) reported in the south-eastern part of the bay (Figure 4.10J). After 6 weeks, the S wind forcing resulted in a larval transport to the north along the Normandy coasts with maximal larval concentrations (415,000 ind.m$^2$) between Champeaux and Granville (Figure 4.10K). For both release dates, the different wind conditions induced very similar enhance of colonization rate while the increase in the retention rate was stronger for a release on 10 May.

For a release on 23 May 2002, larvae were subjected to a fairly constant W wind with some short NW wind events (mean velocity of 4.8 m.s$^1$) (Figure 4.10F). In response to this forcing, the quantity of larvae trapped in the gyre off Cancale remained low. After 3 and 6 weeks of dispersal, maximal larval concentrations (4,200,000 and 24,000 ind.m$^2$) were confined in the eastern part of the bay (Figure 4.10D-E), explaining the large increase of the colonization rate from Sainte-Anne to Champeaux. During the dispersal of the larvae released on 21 August 2002, wind blew from NE during the first 7 weeks (mean velocity of 4.3 m.s$^1$) and then from SW during the last 3 weeks (mean velocity of 6.8 m.s$^1$) (Figure 4.10I). These wind conditions leaded to larval dispersal patterns similar to those observed without wind forcing so that larvae were mainly located outside the bay, either trapped in the gyre off Cancale or transported northwards along the Cotentin coast (Figure 4.5B-C and 4.10G-H).

#### *4.4.3.2 Year-to-year variability of larval settlement under realistic wind conditions*

Variations in meteorological conditions induced high intraand inter-annual variability of the larval settlement (i.e., origin and number of settlers) as shown from the simulations of monthly spawning events under real wind forcing from April to October between 2000 and 2004 (Figure 4.11). The number of settlers varied by a factor 3 to 4 within a year while the most favourable period for settlement varied among years. The highest settlements were obtained in October in 2000, in July, August and October in 2001, in May and June in

2002, in May in 2003 or in April in 2004. As already mentioned, variations in settlement were mainly related to the meteorological conditions encountered by larvae through their life span. For instance, for the spawning events simulated in May, only the wind conditions observed in 2002 and 2003 were favourable to high settlements. For both years, the wind blew from SW for the first 3 weeks and then mainly from W with an average velocity of 5.3 and 4.4 $m.s^1$, respectively. By contrast, larvae released in May 2000, 2001, and 2004 were subject to changing wind conditions (NE then W and SW in 2000; NE, NW and W in 2001; W, N and W in 2004) that induced lower settlements.

At the scale of the bay, the highest settlements were mainly due to the high retention and colonization rates of larvae released from the Sainte-Anne reef. Indeed, for those spawning events, the abundance of both autochthonous settlers in Sainte-Anne and allochthonous settlers in Champeaux were strongly increased, except for the spawning of October 2000 for which only the allochthonous settlers in Champeaux was enhanced (Figure 4.11). Settlers from Sainte-Anne represented between 42.1 % and 95.3 % of the total number of settlers in the bay whereas larvae released at Sainte-Anne represented 84 % of the reproductive output during one spawning event. Settlement at the Sainte-Anne reef was mainly due to local larval supply (mean allochthonous settlement ratio of $0.59 \pm 0.47$) while settlement at the Champeaux reef resulted from distant larval supply (mean allochthonous settlement ratio of $3.83 \pm 4.03$).

### 4.4.4 Settlement kinetics and metamorphosis delay

To evaluate the influence of the capacity of competent larvae to delay metamorphosis, the settlement kinetics was analyzed for all the simulations. As an example, Figure 4.12 provides the cumulative number of settlers following a larval release at Sainte-Anne, from the beginning to the end of the settlement period; four distinct spawning events for which larval dispersal has been already described have been selected (see Figure 4.10).

Although the final settlers' abundance was highly variable depending on the spawning date, the settlement kinetics for larvae retained locally or colonizing the Champeaux reef was similar for most spawning events. Thus, for a larval release on 10 May, 21 August and

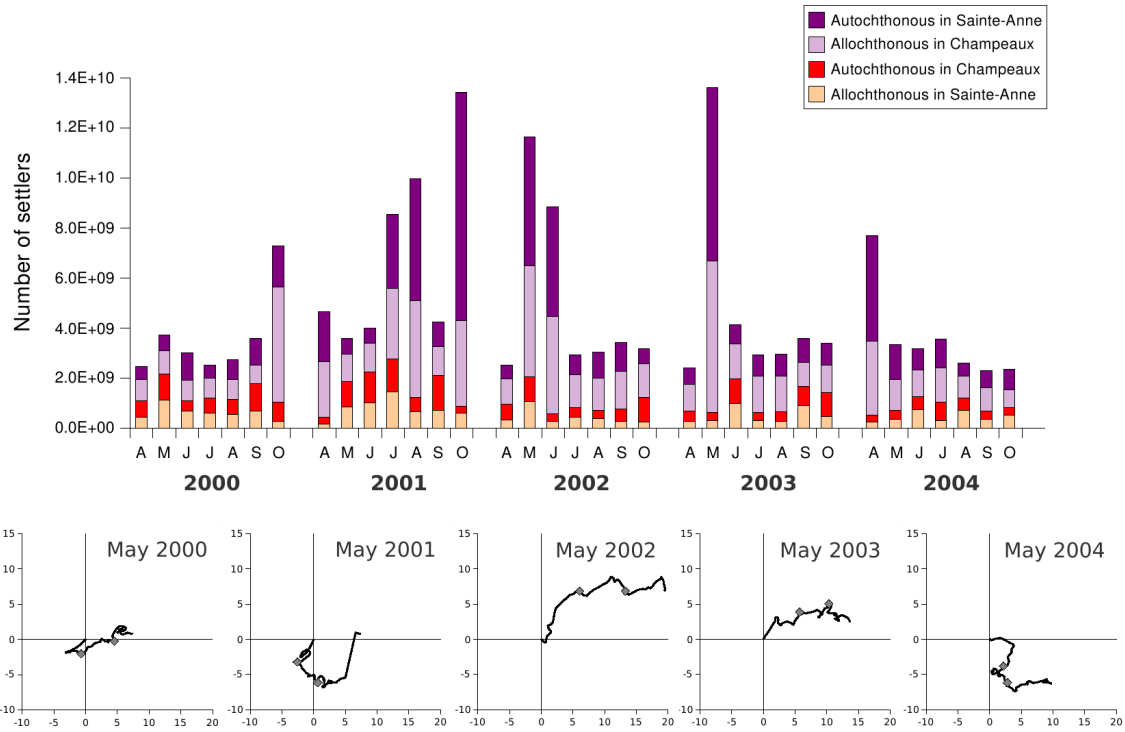


Figure 4.11: Intra- and inter-annual variability of the origin and number of settlers for different larval releases between 2000 and 2004. For each year, 7 spawning events are simulated from April to October with a larval release at high tide during average tide conditions. Larval dispersal is simulated under real wind forcing during 10 weeks. Progressive vector diagrams (PVD) of wind forcing in the Gulf of Saint-Malo corresponding to the dispersal following a release in May are given for each year, with West-East transport ($10^3$ km) as abscissa and South-North transport ($10^3$ km) as ordinate. The gray diamonds indicate the 3$^{rd}$ and the 6$^{th}$ weeks of dispersal. Wind data were provided by Meteo France (Arpege model).

19 October 2002, the cumulated number of settlers increased sharply during the first week of the settlement and reached an asymptote after 10-15 days. Conversely, for some spawning events the settlement kinetics was more complex. For a larval release in Sainte-Anne on 23 May 2002, the temporal evolution of the number of colonizers increased regularly over the first 15 days while the evolution of the number of local settlers occurred in two steps: one between 0 and 5 days and an other one between 8 and 15 days (Figure 4.12B). The hydroclimatic conditions encountered by larvae after this spawning (i.e., mainly western wind) ensured the transport of competent larvae to the eastern part of the bay that favoured a strong and regular colonization rate of the Champeaux reef over 2 weeks and a low initial settlement rate of the Sainte-Anne reef over 5 days (see Figure 4.9B). However,

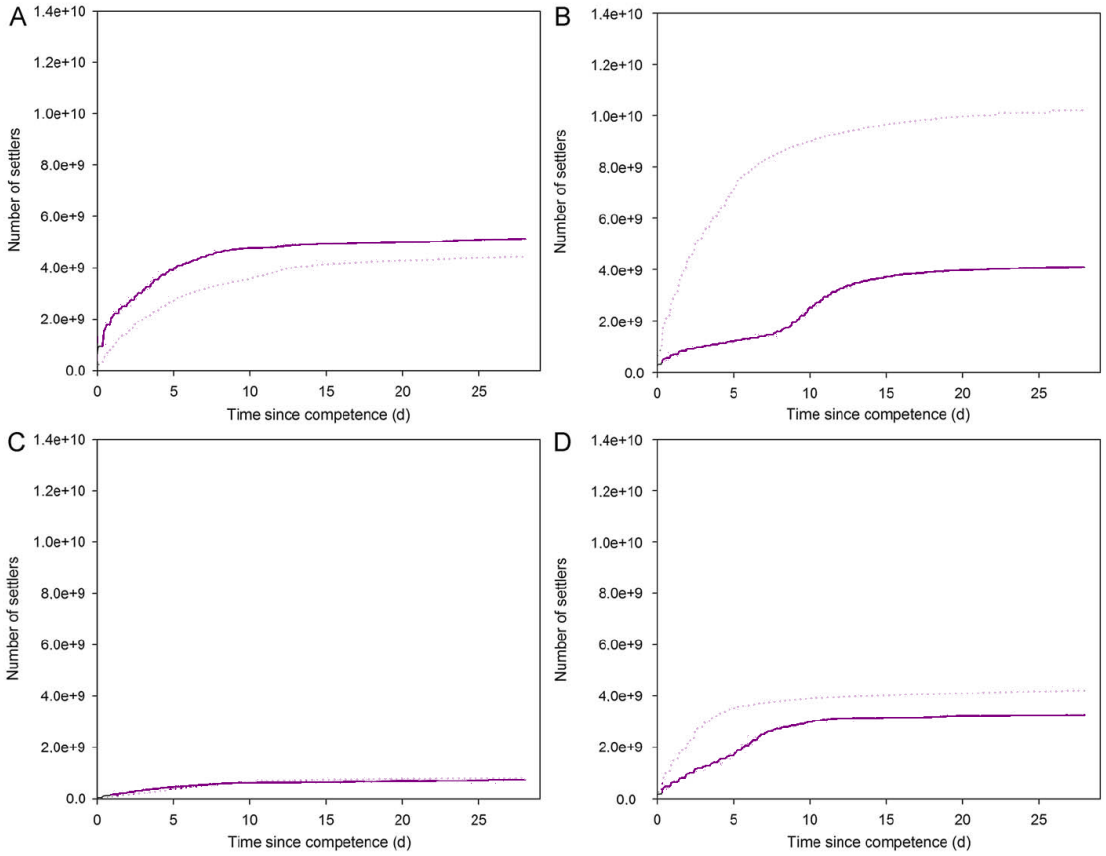


Figure 4.12: Temporal evolution of the cumulative numbers of settlers for 4 spawning events from Sainte-Anne on 10 May (A), 23 May (B), 21 August (C) and 19 October 2002 (D), from the beginning of the settlement (t = 0 d after 6 weeks of dispersal) to the end of dispersal (t = 28 d after 10 weeks of dispersal). Larvae are released at high tide in average tide conditions and dispersal occurred under real wind forcing. Dark purple continuous line: autochthonous settlers in Sainte-Anne, light purple dashed line: allochthonous settlers in Champeaux.

a short event of northern wind between 50 and 55 days after the spawning promoted a slight westwards transport of larvae above the SainteAnne reef that induced a second local settlement phase 9 days after the settlement beginning. Such a result suggests that the delay of the metamorphosis could significantly improve the settlement success within the bay in response to short-term variations in larval transport.

The total number of settlers varied according to the minimal PLD, i.e., the age at competence (Figure 4.13). For an instantaneous larval release and a without wind forcing dispersal, the total number of settlers decreased exponentially from $1.43\times10^{10}$ to $7.04\times10^{8}$ when the age at competence increased from 4 to 8 weeks. This exponential decrease in

settlers' number obtained for a longer minimal PLD was mainly related to larval losses through natural mortality and in a lesser extent to an increase in larval export. However, such quantitative variations in the PLD did not alter larval dispersal patterns or the relative influence of the two reefs to the replenishment of adult populations.

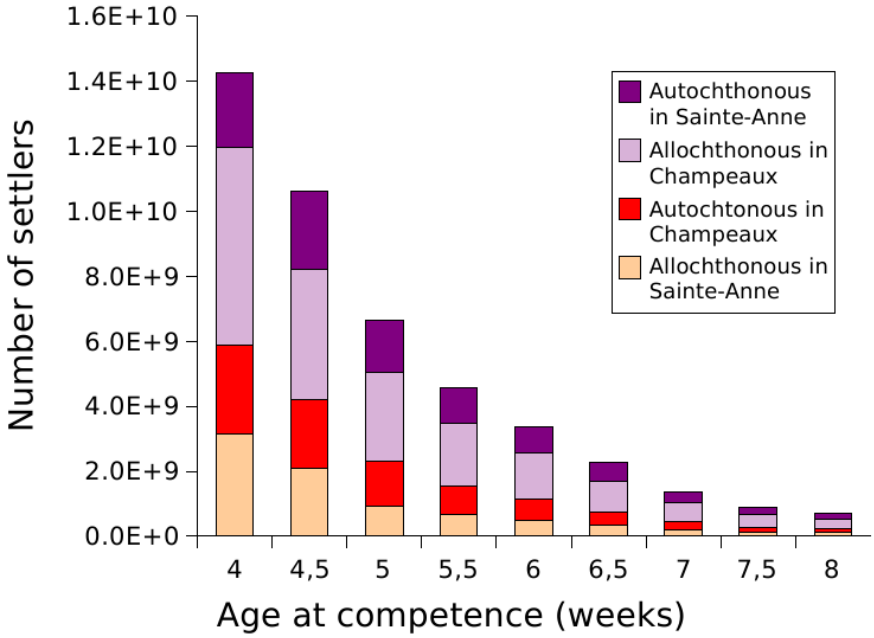


Figure 4.13: Variability of the origin and number of settlers for different ages at competence (minimal PDL). Age at competence is given in weeks. The maximum delay to metamorphosis is fixed at 4 weeks. Larval release is instantaneous at high tide during average tide conditions. Larval dispersal is simulated without wind forcing.

## 4.5 Discussion

Field observations performed in 2002 have shown that large-scale spatial distribution of *Sabellaria alveolata* larvae was patchy and was mainly controlled by residual currents (Dubois , 2007). Highest densities (up to 28,000 larvae $m^2$) were generally located in nearshore waters close to the adult reefs or were trapped within the gyre off Cancale (Figure 4.14). A northward extension of the larval patch was also reported along the western coast of Normandy with larval densities reaching about 100 larvae $m^2$.

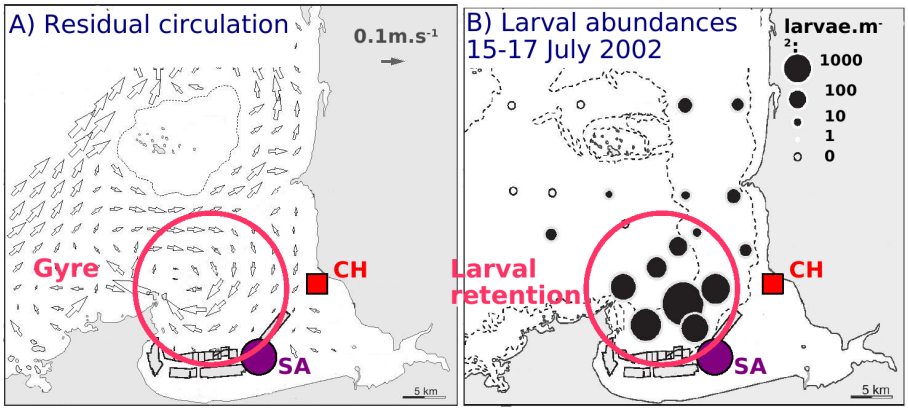


Figure 4.14: Hypothesis of larval retention in the Bay of Mont-Saint-Michel due to the perennial gyre, from Dubois (2007). (A) Residual circulation and (B) *In situ* distribution of *Sabellaria alveolata* larvae on 15 to 17 July 2002 in the Bay of Mont-Saint-Michel. Diameters of the circles are proportional to the log-transformed abundance data.

Although these observations highlighted a potential larval retention within the bay, the lack of long-term observations hampered evaluating the consequences of larval supply variability on the large year-to-year variations in recruitment reported in the Bay of Mont-Saint-Michel (Gruet, 1986). Furthermore, the role of the connectivity between the two *Sabellaria* reefs on settlement dynamics within the bay remained unknown. As an alternative, we used in the present study a 3D hydrodynamic model with a numerical code already evaluated on the NW European continental shelf (Lazure & Dumas, 2008) or in a coastal shallow embayment (Plus , 2009). It provided simulated results which were qualitatively in good agreement with spatial and temporal larval field surveys (Dubois , 2007). Even if absolute values of settlement might be uncertain due to biological simplifications (e.g., no seasonal variations in larval release, constant larval mortality rate, passive

behaviour), the variations of these values in response to spatial and temporal variations of physical forcing remained meaningful and could be studied in a sensitivity analysis.

### 4.5.1 Relative importance of hydrodynamic processes

Simulated larval dispersal patterns and settlement success were highly variable between the two reefs although they were located only 15 km apart. Settlement success was generally lower for the larvae released from the Sainte-Anne reef than for the larvae from the Champeaux reef, especially without wind forcing. On the other hand, settlement success of larvae from Champeaux varied mainly in response to variations in tidal conditions at spawning date while settlement success of larvae from SainteAnne was more dependent on meteorological conditions during dispersal. These discrepancies between the two parental reefs due to their spatial location indicate that small-scale and nearshore physical processes play an important role in larval transport and could vary at the scale of a few kilometers (Largier, 2003). As previously pointed out by several studies investigating the importance of scale griding in larval dispersal modelling (Baums , 2006; Guizien , 2006), our work underlines the necessity of developing models whose spatial resolution is adapted to the scale of the predominant hydrodynamical features of the study area.

#### *4.5.1.1 Tidal residual transport of larvae*

Without wind forcing, larvae released from Sainte-Anne were quickly transported to the West of the bay and then exported northwards through the gyre off Cancale. Afterwards, they either remained trapped within the gyre or were transported along the western coasts of Normandy. Since most larvae were already located outside the Bay of Mont-Saint-Michel within a few weeks after the spawning event, settlement success was low and was not affected by the tidal conditions during larval release. Conversely, larvae released from Champeaux were slowly transported to the West. A significant part of the larval patch was maintained in the inner part of the bay during the whole larval life span while some larvae were flushed outside the bay, within the gyre off Cancale or along the Normandy coasts. Therefore, such retention within the bay promoted the settlement success of larvae

released from Champeaux but varied with tidal conditions at spawning. Settlement rates decreased when the tidal range, and consequently tidal currents, increased. Hence, for a larval release at Champeaux during a neap tide, slower currents advected larvae that remained close to the shore on shorter distances alongshore in comparison with a larval release during a spring tide: larval retention in the innermost part of the bay was increased while the larval 'flushing' outside the bay was decreased.

#### *4.5.1.2 Tidal conditions at spawning*

The transport of the larval cohort at the very beginning of the dispersal appeared to be primordial for the rest of the larval dispersal and the settlement success, suggesting that larval fate could be determined very early in the larval life span (Verdier-Bonnet , 1997).

Although no information occurs on spawning trigger mechanisms for *Sabellaria alveolata*, mechanical action of the flood currents on mature females has been reported to induce larval release for some intertidal polychaetes (Bentley & Pacey, 1992) and wave activity has been shown as tightly linked with spawning events in the sabellariid reef-building polychaete *Phragmatopoma lapidosa* (McCarthy , 2003). Chemical cues related to phytoplankton blooms and/or sperm from conspecifics have also been reported to promote massive spawning in widely separated invertebrate phyla (Starr , 1990). On the other hand, the influence of the lunar or the tidal cycle upon spawning has been demonstrated in many marine polychaetes which spawn coincidentally either with spring tides or neap tides (Bentley & Pacey, 1992). In the present model, the mathematical formulation of larval release (i.e., instantaneous, continuous and uniform over a tidal cycle, semi-continuous and symmetric over three or five tidal cycles) had no significant effect on the settlement rates, suggesting that the simplistic formulation of this biological mechanism retained for most simulations (i.e., instantaneous release) did not alter our conclusions on the relative role of hydrodynamic processes. Conversely, if *Sabellaria alveolata* spawning occurs in relation to lunar cycle, this mechanism might significantly influence settlement success of larvae released from Champeaux, by preventing their export out of the bay for a release in neap tide.

#### 4.5.1.3 Influence of wind forcing on dispersal

Although tidal residual currents are the main cause of the longterm water mass transport in the English Channel, wind-induced currents can play a significant role at shorter time scales and have been described to prevail in the variability of larval dispersal (Ellien , 2004; Lagadeuc, 1992a). Wind conditions can greatly modify the larval dispersal patterns and ultimately increase or decrease the settlement success by altering the local circulation. Such effect was particularly observed for larvae released from Sainte-Anne with a settlement success varying by one order of magnitude according to realistic meteorological forcing. As already reported for the tide effects on larval dispersal, settlement success was high when wind-induced hydrodynamic conditions constrained the larvae within the bay since larval release. Thus, the occurrence of SW and NW winds decreased the spatial extension of the gyre off Cancale, slowed down residual currents in the inner part of the bay, and increased the residence time of larvae within the bay. Over the reproductive period of *Sabellaria alveolata*, the variations in the meteorological conditions should induce a very high seasonal and inter-annual variability of larval dispersal patterns (Ellien , 2004; Pedersen , 2006) and settlement success (Botsford , 2001). The co-occurrence of particular wind conditions and high recruitment events have been commonly reported for several species with a pelagic dispersive stage in different coastal environments like the blue crab *Callinectes sapidus* in the Middle Atlantic Bight (Jones & Epifanio, 1995) or several species of crabs, sea urchins and sea stars in the Northern California (Wing , 1995).

#### 4.5.1.4 Temporal variations of dispersal patterns

The consequences of this variability on population sustainability would vary according to the temporal scales of observation. Within a year, high settlements would occur only if larvae are released in a temporal window favourable to larval retention. If such a window seemed to be present each year, the period at which it has been simulated was highly variable from one year to another (e.g., October in 2000, May in 2003, April in 2004), suggesting that the date of massive settlements could vary among years. Furthermore, while the *Sabellaria alveolata* reproductive period has been estimated to extend from March to

October, larval release is not continuous and two main periods of spawning have been identified in May-June and in September (Dubois, 2003; Dubois , 2007). From our simulations under realistic meteorological conditions for the years 2000-2004, a larval release in May-June or September could lead to very high settlements only for some particular years like 2002 or 2003. The presence or the absence of an optimal environmental window during the two main spawning periods may explain the large year-to-year variations in recruitment success although other causes could be proposed including post-settlement mortality (Wilson, 1971). Moreover a spatio-temporal field survey carried out in 2001 has revealed a very low concentration of *Sabellaria alveolata* larvae compared to the same 2002 field survey (Dubois, 2003; Dubois , 2007), hence supporting the idea of large yearto-year variability in optimal environmental windows. On the other hand, at temporal scales relevant to the life history of the organism, an extended spawning period from spring to autumn could increase the likelihood that larval cohorts benefit some years of favourable hydroclimatic conditions. For an iteroparous species, Byers & Pringle (2006) showed that multiple spawning events over multiple years increase the variability of hydrodynamics encountered by the larvae produced by an individual and enhance larval retention. Although numerous larvae may be transported away from local populations, an extended reproductive period can be described as an efficient strategy to maximize retention and long-term sustainability of adult populations.

#### *4.5.1.5 Role of eddy structures on larval dispersal and retention*

The complex role of eddy structures on larval dispersal and retention has been recently pointed out (Baums , 2006; Largier, 2003). Thus, eddies are commonly reported to cause trapping of particles and act as a crossing barrier to larval dispersal, enhancing local retention and settlement. On the other hand, coastal eddies can concentrate larvae from different source populations and promote the connectivity among populations. In the English Channel, two types of eddies were distinguished in a recent work based on a steady state modelling analysis: gyres around islands that form strong dissemination areas, and

head-land eddies that constitute tracer accumulation area (Ménesguen & Gohin, 2006) (Figure 4.15).

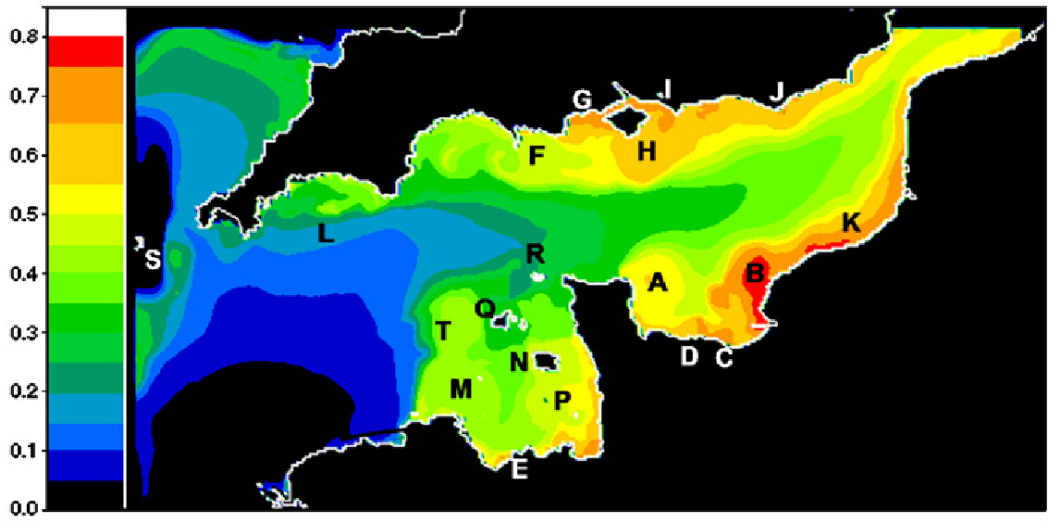


Figure 4.15: Localization and type of the eddies of the English Channel, revealed by steady state analysis, from Ménesguen & Gohin (2006). The map representes the distribution of a pure conservative tracer injected homogeneously all over the model grid. Warm colors indicate high tracer concentrations, i.e., retention areas, whereas cold colors indicate low tracer concentrations, i.e., diffusive areas. See the original publication to a detailed description of each of the eddy structure labelled by a capital letter.

Our results are coherent with this description which classifies the gyre off Cancale as a retention structure and confirm field observations on meroplankton distribution suggesting that this gyre may act as a physical trap for *Sabellaria alveolata* larvae (Dubois , 2007). Nevertheless, as eddies occur on many spatial and temporal scales, their efficiency to promote larval retention and enhance local settlement depends on their life time relative to larval life span and on their size relative to the spatial extent of the benthic population (Largier, 2003). In our case, simulated depth-averaged residual currents highlighted the longterm persistence of the gyre off Cancale for different wind directions and a wind velocity of 11 $m.s^1$. Such a velocity is rarely exceeded during the *Sabellaria alveolata* reproductive period from April to October between 2000 and 2004 (i.e., less than 0.75 % of daily wind measurements) and one can assume that the gyre off Cancale acts as a retention area during the whole *Sabellaria* larval life span. By contrast, the extent of the gyre largely exceeded the restricted habitat occupied by *Sabellaria* reefs. Thus, depending

on the variability of meteorological conditions, the geographical location and the spatial extent of the gyre off Cancale were highly variable with either positive or negative effects on the settlement of *Sabellaria alveolata* larvae. Settlement success was promoted only if competent *Sabellaria* larvae were transported above the reefs by the currents. The lowest settlement rates were then simulated when most larvae were advected outside the bay and were then trapped in the gyre in the North of Cancale. Conversely, the highest settlement rates were reported when larvae were early constrained in the inner part of the bay and were maintained there close to adult reefs. This situation occurred when western winds constrained the location and the extent of the gyre within the bay.

### 4.5.2 Relative role of biological parameters

Larval dispersal results from interactions between hydrodynamic features and biological factors including spawning location and date, as already discussed above, but also PLD, capacity to delay metamorphosis, larval mortality, and larval behaviour. Compared to an individual-based model, individual variability has not been taken into account in our Eulerian approach of larval dispersal. However, an individual-based model of larval dispersal including individual variability of vertical behaviour and some population dynamics parameters cannot be parametrize currently as deeper knowledge of the *Sabellaria alveolata* larval biology in response to environmental variability is still lacking. In this context, our results yet allow to discuss the limitation of setting simple biological traits in dispersal models.

#### *4.5.2.1 Larval mortality and planktonic larval duration*

Larval mortality is a parameter of the larval biology that remains poorly known for most marine benthic invertebrates because of the difficulties to obtain accurate estimates from field studies and of its large variability among species and environments (Rumrill, 1990). Usually, in larval dispersal model, the mortality term is either neglected or arbitrary fixed while a misrepresentation of the larval mortality can alter the simulated larval distribution (Dekshenieks , 1997) or biased the estimations of local larval supply and connectivity

between distant populations (Cowen , 2000; Ellien , 2004). As an example, retention is more likely than expected when model incorporates mortality (Cowen , 2000). Here, to be as realistic as possible, we used a mortality rate obtained from bimonthly field observations of *Sabellaria* larval densities at four stations in the Bay of Mont-Saint-Michel ($\mu = 0.09$ d$^1$). This value was in good agreement with the range of mortality rate reported for 23 species of marine invertebrates by Rumrill (1990) (mean = 0.229 d$^1$; SD = 0.228; range = 0.016-0.820 d$^1$). However, we assumed that there was no spatial and temporal variation in mortality rate. Larval mortality can result from unfavourable environmental parameters such as temperature and food availability, predation, and intrinsic individual variability (Rumrill, 1990). The unfavourable environmental conditions rarely induce a direct mortality, but rather an indirect one, by prolonging the PLD and consequently enhancing the exposition to predation and larval transport (O'Connor , 2007). In the Bay of Mont-Saint-Michel, the lack of strong hydrological gradients may justify the assumption of no spatial variation in the mortality rate due to environmental conditions (Dubois , 2007). By contrast, the seasonal variations of temperature and chlorophyll a concentrations over the extended reproductive period of *Sabellaria* from April to October may induce a seasonal variation in the PLD and the mortality rate. This variation would not affect the relative differences between reefs in the numbers and origins of larvae for each spawning event. But it should strongly influence the prediction of the absolute values of settlers' density and strengthen the seasonal variation in the settlement rate already described in relation to seasonal changes in meteorological conditions. Indeed, *Sabellaria alveolata* has a long PLD which can generate high larval losses because of larval mortality and larval export away from the adult reefs which form a very restrictive habitat. The sensitivity analysis performed on the PLD indicated that a longer PLD induced lower settlers' density because of higher larval losses through mortality. On the other hand, numerous shellfish farming structures are located in the south-western part of the bay which could induce spatially heterogeneous mortality due to predation by cultivated oysters and mussels (Lehane & Davenport, 2006; Troost , 2008). This stronger mortality above oyster and mussel beds may preferentially affect young larvae released from the Sainte-Anne reef or competent larvae able to settle on this reef, suggesting that the role attributed to the

Sainte-Anne reef on the dynamics of *Sabellaria* recruitment at the scale of the bay may be overvalued.

#### *4.5.2.2 Larval swimming behaviour*

In the present model, precompetent larvae were considered as completely passive, while competent larvae were able to actively select the settlement habitat. This assumption of passive dispersal in our case can be justified by several reasons in a first approximation. First, because of very low freshwater inputs and rapid vertical mixing of the entire water column due to intense tidal currents, the transport in the Bay of Mont-Saint-Michel is mainly governed by barotropic processes with limited vertical current shear stress. Second, from a 24 h time series on *Sabellaria alveolata* vertical larval distribution at one station in the bay, Dubois (2007) indicated the absence of diel or ontogenic migration but mentioned a variation in the centre of mass of the larval vertical distribution according to the tidal cycle: higher larval concentrations were close to the surface during flood and close to the middle of the water column during ebb. If such larval migration known as selective tidal stream transport is commonly reported to enhance larval retention by favouring landward transport, its effect in the bay would be reduced due to the low variations in current velocities between the top and the middle of the water column. Third, in a recent review on larval transport, Bradbury & Snelgrove (2001) argued that passive mechanisms are probably predominant at broad scales for most marine invertebrates because of their poor swimming abilities but that active habitat selection and the capacity to delay metamorphosis can be prevalent at local scales. In fact, invertebrate larvae are complex organisms able to control their distribution over a wide range of spatial and temporal scales and to develop specific behaviour to feed, avoid predation or move within the pelagic environment (Levin, 2006; Woodson & McManus, 2007). Field studies have already reported vertical migrations for marine invertebrate larvae, including polychaetes, with a significant effect on larval transport, promoting either larval retention or larval export (Dubois , 2007; Levin, 2006). Recent modelling approach have highlighted that the explicit consideration of larval behaviour is essential to simulate larval dispersal, even

with restricted larval swimming abilities (e.g., Cowen & Sponaugle, 2009; North , 2008). However, if behaviour can be easily implemented in individual-based models, numerous field and laboratory experiments are necessary to properly describe the specific behavioural responses of organisms to environmental cues and avoid the use of simple and likely unrealistic behaviours. By neglecting the tidal variations in the vertical distributions of *Sabellaria* larvae, one can just expect that our model has tended to underestimate larval retention.

#### *4.5.2.3 Larval settling behaviour and metamorphosis delay*

Conversely, the 3D modelling in our study allowed us to take into account an active settling behaviour. It is nevertheless crudely parametrized because of the lack of information on the maximal distance from which competent larvae are able to perceive the chemical cues produced by the adult worms (Wilson, 1968a, 1970) or on the optimal range of hydrodynamic conditions for settlement (Pawlick & Butman, 1993). Furthermore, the complex topography of *Sabellaria* reefs and its influence on flow conditions in the benthic boundary layers could not be properly described in our model with a horizontal grid of 800 m and 10 sigma levels.

In our simulations the larvae became competent after 6 weeks of dispersal but were able to delay their metamorphosis 4 more weeks. The settlement kinetics indicated that the majority of the larvae actually settled during only the first 10 days following the beginning of the settlement period and that the number of larvae that settled later decreased sharply. Although the number of settling larvae was very low during the last days of the dispersal, the ability to delay metamorphosis may give to the competent larvae a "second chance" to settle, as observed for the autochthonous settlers in Sainte-Anne for the release of the 23 May 2002. As commonly reported, such results tend to confirm that delaying metamorphosis could be a benefit for a larva by enhancing its likelihood of locating a suitable site for metamorphosis, at least for a short period. This benefit should be important all the more as the PLD will be short and larval densities near natal sources will be still

high. Conversely, for some species this property could affect the post-metamorphic success of individuals in terms of survival or growth rate (Pechenik , 1993).

### 4.5.3 Sustainability of biogenic reefs

The largest biogenic reefs of the European coasts are the *Sabellaria alveolata* reefs of the Bay of Mont-Saint-Michel. A previous study on the *in situ* distribution of the *Sabellaria alveolata* larvae in the Bay of Mont-Saint-Michel (Dubois , 2007) highlighted the role of the tidal residual currents, especially of the gyre off Cancale, on the larval retention in the bay, but the connectivity between the two reefs of the bay remained unknown. The present work brings answers about the intensity and the variability of the potential larval exchanges between the two *Sabellaria alveolata* reefs of the Bay of Mont-Saint-Michel. Our results indicated that despite very low settlement rates (i.e, <0.004 %), the hydrodynamic specificities of the bay could allow larval retention at the bay scale and favour the larval exchanges between the two reefs. At the bay scale, and as long as the larval supply remains high, existing reefs (and potentially newly formed reefs) could benefit of favourable hydroclimatic conditions all along the long reproductive period, especially if the spawning occurs in neap tide conditions, or under retention-favourable meteorological conditions as SW and NW winds. Previous studies have highlighted the importance of local scale retention and self-recruitment in the population dynamics of bentho-pelagic organisms (Cowen & Sponaugle, 2009). Considering the spatial scale of the larval dispersal of *Sabellaria alveolata* in the Gulf of Saint-Malo, larvae from the reefs of the Bay of Mont-Saint-Michel could supply some small veneers (thin honeycomb reefs adhering to rocks) along the Normandy coasts, but larval supplies from distant populations are unlikely. Contrary to a source-sink hypothesis of one-way exchanges from the biggest reef of Sainte-Anne to the smaller reef of Champeaux, the present work indicated that the two reefs freely exchange individuals through the larval dispersive stage, as supported by a microsatellite genetic analysis (Farcy, 2003) (Figure 4.16).

Although the simulated settlers' density could be quite sensitive to the mortality term (Cowen , 2000; Ellien , 2004), the highest numbers of settlers calculated from our simu-

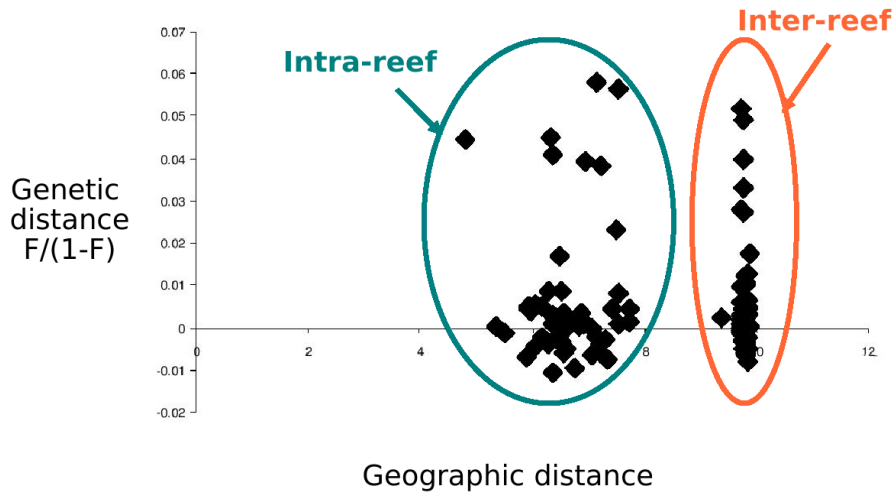


Figure 4.16: Relationship between the genetic distance and the geographic distance (log) between pairs of individuals of *Sabellaria alveolata* reefs in the Bay of Mont-Saint-Michel. Comparison within and between reefs are indicated. Although light but significant genetic differences between the two reefs ($F_{ST} = 0.006$, $p < 10^{-5}$), genetic analyses indicated no isolation by the distance suggesting important larval exchanges (Farcy, 2003).

lations were in the same order of magnitude as the adult stocks within the bay. If those high larval supplies occur often enough compared to the life span of adult individuals, this might be sufficient to sustain the reefs in the bay. In our simulations the Sainte-Anne reef is responsible for the main larval supply in the bay because of its high reproductive outputs. However the adult stocks in the Sainte-Anne reef dramatically decreased since 2002, because of both the fragmentation (Figure 4.17) and the colonization of the reef by the cultivated oyster Crassostrea gigas (Dubois, Desroy, and Le Mao, pers. obs.). Moreover the development of shellfish farming, which is responsible for high abundances of cultivated oysters and mussels in the bay, could also induce high larval mortality and contribute to a strong decrease of the larval supply, especially in Sainte-Anne (Dubois , 2007). In this context, the huge decrease in the reproductive outputs of the Sainte-Anne reef could adversely affect the sustainability of the two reefs of the Bay of Mont-Saint-Michel. If the Sainte-Anne reef disappears our results suggest that, even if larval retention occurs, the larval supply from Champeaux might not be sufficient enough to sustain itself and recolonize the Sainte-Anne reef. Since bidirectional larval exchanges exist between the two reefs, conservation policies should focus on the protection of both reefs, with special

interest for the protection of the declining Sainte-Anne reef which is responsible under favourable conditions for the highest larval supply.

Figure 4.17: Degradation and fragmentation of the Sainte-Anne reef.

## 4.6 Conclusion

This modelling study underlined the crucial role played by hydroclimatic conditions in larval dispersal and connectivity of the *Sabellaria alveolata* reefs in the Bay of Mont-Saint-Michel, but also pointed out the lack of precise knowledge of the *Sabellaria* larval biology. Significant efforts should be made in future experimental and *in situ* works in order to precisely evaluate the parameters of the larval biology, in particular the larval swimming behaviour, the larval mortality rate, and the PLD, as a function of individual and environmental parameters such as ontogeny, temperature, food availability, or predation pressure. In this context, a more precise knowledge of the larval biology will be a central issue for the development of future dispersal models and for a more accurate evaluation of the role of the larval phase on the reefs' sustainability.

## 4.7 Acknowledgements

The present study was financed by the French National Programme on Coastal Environment (PNEC) - Site Atelier 'Baie du Mont-Saint-Michel'. S.-D. Ayata is supported by a PhD grant from the French Ministry of National Education and Research. The authors are grateful to Dr. J.E. Eckman and two anonymous reviewers for their helpful comments on the first version of the manuscript.

## Conclusion de la partie II

Dans cette partie, un modèle biophysique eulérien spécifique de la dispersion et de la sédentarisation des larves du polychète constructeur de récif *Sabellaria alveolata* a été mis en œuvre à l'échelle du Golfe Normand-Breton, en se basant sur des données *in situ* de taux de reproduction, de durée de vie larvaire et de mortalité larvaire. Ainsi, la connectivité entre les deux principaux récifs de la Baie du Mont-Saint-Michel ainsi que sa variabilité ont été estimées en conditions hydroclimatiques réalistes.

Les résultats issus de simulation ont confirmé le rôle important joué par un tourbillon côtier dans la rétention larvaire à l'échelle de la baie. En comparant les résultats obtenus pour les deux principaux récifs de la baie, seulement distants d'une quinzaine de kilomètres, des schémas de dispersion larvaire très différents ont été mis en évidence selon le récif d'émission. De fortes variabilités interannuelles du nombre de larves sédentarisées ont été observées *in silico*. Bien que des échanges bidirectionnels semblent exister entre les deux principaux récifs de la baie, le plus grand nombre de larves sédentarisées pourrait provenir du plus grand des deux récifs, en raison de son fort potentiel reproducteur. Cependant, étant donné l'important déclin de ce récif observé ces dernières années, cette étude suggère que le nombre de larves émises à l'échelle de la baie pourrait ne plus suffire pour permettre la pérennité de ce remarquable habitat formé par les récifs de *Sabellaria alveolata*. A l'échelle locale, la modélisation couplée biologie-physique de la dispersion larvaire se révèle donc un outil puissant pour l'étude de la connectivité entre populations géographiquement proches et pour la protection de la biodiversité marine.

## Chapitre C

# Conclusion générale

La question qui a guidé ce travail de thèse a été de comprendre dans quelles mesures les processus hydrodynamiques et hydroclimatiques ainsi que les traits d'histoire de vie des espèces influencent la dispersion larvaire et la connectivité des invertébrés côtiers à cycle bentho-pélagique dans le Golfe de Gascogne et la Manche occidentale. En particulier, nous avons tenté de comprendre comment ces processus biophysiques pouvaient expliquer la séparation entre les provinces biogéographiques lusitanienne et boréale en Atlantique Nord-Est, et comment la connectivité contribuait à la pérennité de populations locales dans un contexte de conservation de la biodiversité. Pour répondre à ces questions, le présent travail de thèse s'est articulé autour de deux parties, correspondant respectivement à l'échelle régionale du Golfe de Gascogne et de la Manche occidentale et à l'échelle locale du Golfe Normand-Breton, en se basant sur deux approches conjointes et complémentaires : l'observation *in situ* du méroplancton et la modélisation couplée biologie-physique de la dispersion larvaire.

Dans ce chapitre de conclusion générale, nous rappellerons les principaux résultats obtenus au cours de cette thèse, avant de discuter de l'intérêt et des limites des méthodes d'étude employées. Puis nous discuterons de l'importance relative des facteurs biologiques et hydroclimatiques sur la dispersion et la connectivité, avant de décrire les patrons historiques et contemporains de connectivité dans le Golfe de Gascogne et en Manche occidentale. Enfin, nous dégagerons des perspectives à ce présent travail de thèse.

## C.1 Rappel des principaux résultats

### C.1.1 Influence des structures hydrodynamiques à méso-échelle sur la distribution *in situ* du méroplancton

Nous avons décrit, pour la première fois, la distribution du méroplancton dans le nord du Golfe de Gascogne ainsi que ses relations avec les structures hydrologiques à méso-échelle (Chapitre 1). La description de la typologie des masses d'eau échantillonnées au printemps 2008 dans le nord du Golfe de Gascogne met en évidence des structures hydrologiques observées à méso-échelle, et en particulier l'existence le long des côtes sud-bretonnes de plumes d'eaux dessalées issues de la Loire et de la Vilaine, se distinguant des eaux océaniques plus salées du large. C'est la structure spatiale de cet environnement hydrologique, et non l'environnement lui-même, qui est le principal facteur responsable des variations spatiales de la distribution du méroplancton dans le nord du Golfe de Gascogne. Les larves de trois espèces cibles de polychètes côtiers aux traits d'histoire de vie contrastés (*Pectinaria koreni*, *Owenia fusiformis*, et *Sabellaria alveolata*) ont principalement été observées au sein des plumes dessalées. Ces résultats suggèrent que les plumes d'eaux dessalées de la Loire et de la Vilaine jouent probablement un rôle de barrière physique à la dispersion vers le large des larves d'invertébrés côtiers dans le nord du Golfe de Gascogne. La dispersion des larves, qui conditionne le taux d'autorecrutement, le degré de connectivité entre populations ou l'ampleur des pertes démographiques au cours de la vie larvaire, est ainsi principalement régulée par les facteurs climatiques (débit des fleuves, vent) qui déterminent le déplacement des plumes estuariennes. L'examen de la distribution verticale des larves souligne néanmoins le fait que les larves ne peuvent être assimilées à des particules passives.

### C.1.2 Influence relative des paramètres hydroclimatiques et biologiques sur la dispersion et la connectivité dans le Golfe de Gascogne et en Manche occidentale

Les résultats issus de simulations lagrangiennes de la dispersion larvaire dans le Golfe de Gascogne et la Manche occidentale (Chapitre 2) soulignent l'importance de la variabilité saisonnière à méso-échelle des conditions hydrodynamiques sur la dispersion larvaire et la connectivité entre populations le long des côtes atlantiques françaises. Aux échelles temporelles et spatiales de la vie larvaire, aucun effet de la variabilité interannuelle des conditions hydroclimatiques n'est observé sur les schémas de dispersion. En revanche, la description des noyaux de dispersion met en évidence l'importance du mois de ponte, en relation avec les variations saisonnières des débits des fleuves et des conditions de vent, de la localisation de la population d'émission, de la durée de vie larvaire, et du comportement larvaire sur les schémas de dispersion.

L'analyse des matrices de connectivité entre populations souligne que la rétention locale est prépondérante et que les échanges larvaires ont principalement lieu au sein des principales régions hydrodynamiques et hydrologiques que sont la Manche occidentale, la Mer d'Iroise, le nord du Golfe de Gascogne et le centre du Golfe de Gascogne. La connectivité entre les populations du Golfe de Gascogne et de la Manche occidentale, c'est à dire à travers la zone de transition biogéographique lusitano-boréale, semble très faible, unidirectionnelle et rare. Une telle connectivité est en particulier observable pour des durées de vie larvaire longues (quatre semaines) et lorsque de forts vents de nord-est accompagnent de forts débits des principaux fleuves. Ces travaux tendent à confirmer que la délimitation des aires de distribution des espèces côtières à cycle bentho-pélagique pourrait en partie reposer sur le succès de la dispersion. Les contraintes imposées par les facteurs biologiques et hydrodynamiques sur la connectivité pourraient donc contribuer à la définition des limites d'aires de distribution des espèces en Atlantique Nord-Est.

### C.1.3 Conséquences potentielles du changement climatique sur la dispersion larvaire et la connectivité

Le modèle précédemment développé nous a permis de tester deux hypothèses sur les conséquences possibles du changement global sur la dispersion larvaire et la connectivité le long des côtes atlantiques françaises au sein des métapopulations d'invertébrés côtiers à cycle bentho-pélagique (Chapitre 3). Les résultats obtenus indiquent que des durées de vie larvaire raccourcies, dues à un développement larvaire accéléré causé par une élévation des températures, pourraient réduire les distances de dispersion, augmenter la rétention locale, favoriser la connectivité entre populations voisines, diminuer la connectivité entre populations plus éloignées, mais aussi diminuer la taille de la connectivité (nombre d'échanges) au sein des métapopulations. Des pontes précoces, en réponse à un changement de phénologie induit par une élévation des températures, pourraient quant à elles provoquer une inversion des schémas de dispersion en favorisant le transport vers le nord, conduisant à une plus forte connectivité vers les populations situées plus au nord, à une plus faible connectivité vers les populations situées plus au sud. La taille de la connectivité pourrait également être plus importante.

### C.1.4 Importance des processus hydroclimatiques sur la dispersion larvaire en baie du Mont-Saint-Michel et conséquences sur la pérennité des récifs biogéniques de *Sabellaria alveolata*

Les résultats issus de simulations eulériennes de la dispersion larvaire de l'espèce patrimoniale *Sabellaria alveolata* dans le Golfe Normand-Breton ont confirmé le rôle joué par un tourbillon côtier dans la rétention larvaire à l'échelle de la baie du Mont-Saint-Michel (Chapitre 4). Des schémas de dispersion larvaire très différents ont été observés selon le récif parental considéré, bien que les deux récifs de la baie ne soient distants que d'une quinzaine de kilomètres. Le succès de la sédentarisation des larves émises du plus petit des deux récifs semble principalement dépendre des conditions de marée lors de la ponte, avec des taux de sédentarisation plus élevés lorsque les larves sont émises en conditions de morte eau. Le succès de la sédentarisation des larves émises du plus grand des deux récifs

apparaît comme plutôt dépendant des conditions météorologiques, avec des vents d'ouest ou de sud-ouest favorisant la rétention de ces larves à l'échelle de la baie, augmentant jusqu'à dix fois le succès de la sédentarisation.

Une forte variabilité interannuelle de la quantité de larves qui se sédentarisent a été observée, avec un fenêtre environnementale favorable qui ne coïncide pas toujours avec les principales périodes de reproduction de *Sabellaria alveolata* en baie du Mont-Saint-Michel. L'étude des cinétiques de sédentarisation indique que le délai à la métamorphose peut permettre une augmentation du succès de la dispersion. Des échanges larvaires bidirectionnels entre les deux récifs semblent possibles, bien que la plupart des recrues proviennent du plus grand des deux récifs étant donné son fort potentiel reproducteur. Cependant, l'accélération de la fragmentation et la destruction de ce grand récif, provoquée par des pressions anthropiques croissantes, pourraient diminuer les apports larvaires de ce grand récif : ceux-ci pourraient donc ne plus suffire pour assurer la pérennité des récifs de *Sabellaria alveolata* en baie du Mont-Saint-Michel.

## C.2 Comparaison, intérêts et limites des méthodes utilisées

Le premier chapitre de cette thèse repose sur l'**échantillonnage *in situ*** du méroplancton, afin de décrire la distribution spatio-temporelle de larves d'invertébrés à cycle benthopélagique en relation avec les structures hydrologiques. Ce type de méthodologie fournit une vision à un instant donné des caractéristiques hydrologiques et des abondances larvaires. À partir de ces données, le rôle des structures hydrologiques côtières à méso-échelle sur le transport et la dispersion larvaire peut être décrit. D'éventuels chemins de dispersion peuvent être inférés sous réserve (i) de pouvoir identifier les larves au niveau spécifique, et (ii) de connaître les caractéristiques biologiques des espèces étudiées (localisation et taille des populations adultes, période de reproduction, durée de vie larvaire). Étant donné les coûts humains, financiers et matériels des campagnes océanographiques et le temps nécessaire au tri et à l'analyse des échantillons planctoniques en laboratoire, un échantillonnage extensif de la zone d'étude à l'échelle de la période de reproduction des

organismes étudiés n'est pas envisageable afin d'estimer la variabilité spatio-temporelle des distributions larvaires.

En revanche, la **modélisation** est un outil très puissant permettant de simuler la dispersion larvaire pour un très grand nombre de conditions environnementales réalistes, *i.e.* circulation océanique en conditions hydroclimatiques réalistes, en considérant un certain nombre de processus biologiques, tels que les taux de fécondité des populations génitrices, la période de reproduction des espèces, les durées de vie larvaires spécifiques, les taux de mortalité larvaire estimés *in situ*, ou les comportements larvaires spécifiques de nage et/ou de sédentarisation.

Une grande partie de ce travail de thèse a donc reposé sur l'utilisation de modèles couplés biologie-physique permettant de simuler la dispersion larvaire et la connectivité des populations d'invertébrés côtiers à cycle bentho-pélagique. Miller (2007) a identifié trois types de modèles couplés biophysiques couramment utilisés pour étudier la dispersion larvaire et le recrutement des populations de poissons : (1) les modèles explicatifs, les plus courants, supposés fournir une explication à un phénomène observé empiriquement, (2) les modèles déductifs, dont l'objectif est de quantifier les importances relatives de différents processus responsables de phénomènes observés, et (3) les modèles générateurs d'hypothèses, les plus rares, qui fournissent des hypothèses testables par les modèles eux-mêmes ou par des observations empiriques indépendantes. Dans le cadre du présent travail de thèse, des modèles explicatifs et déductifs ont été utilisés, d'une part pour simuler la dispersion larvaire en conditions hydroclimatiques réalistes, d'autre part pour estimer l'importance relative de différents paramètres biophysiques sur la dispersion et la connectivité.

Cependant, il existe plusieurs **limitations** à l'utilisation de ces modèles pour l'étude de la dispersion larvaire. En effet, la **validité des résultats** issus des modèles biophysiques repose en partie sur la validation du modèle physique de circulation et sur l'adéquation de la résolution spatio-temporelle du modèle pour correctement simuler le transport larvaire (Miller, 2007). Les algorithmes utilisés pour simuler la circulation océanique se basent sur les lois physiques de la dynamique des fluides. Ces lois étant déterministes, des paramètres de variabilité sont souvent ajoutés pour rendre compte des phénomènes de turbulence (Visser, 1997). Ces modèles hydrodynamiques sont ainsi à même de simuler finement la circu-

lation et les champs de température et de salinité. Le code de calcul du modèle MARS-3D (Lazure et Dumas, 2008) utilisé au cours de cette thèse a été **évalué quantitativement** en comparant les résultats produits par le modèle avec les structures hydrodynamiques et hydrologiques observées à l'échelle du Golfe du Gascogne (Lazure et Dumas, 2008; Lazure *et al.*, 2009; Lazure et Jégou, 1998) ou à l'échelle du Golfe Normand-Breton (Bailly du Bois et Dumas, 2005; Orbi et Salomon, 1988; Sentchev *et al.*, 2009). La configuration du modèle MARS-3D à l'échelle du Golfe de Gascogne et de la Manche occidentale a aussi été précédemment utilisée avec succès pour simuler le transport de particules ou de matière dissoute (Allain *et al.*, 2007; Delhez *et al.*, 2004; Lazure et Dumas, 2008; Lazure et Jégou, 1998; Xie *et al.*, 2007). Par ailleurs, la **résolution spatio-temporelle** des modèles couplés biophysiques influe fortement sur les schémas de dispersion larvaire, en particulier lorsque les phénomènes de turbulence intra-maille sont mal reproduits à cause d'échelles spatio-temporelles trop grandes, c'est-à-dire quand la résolution est trop faible (Guizien *et al.*, 2006). Il serait intéressant de tester l'impact de la résolution spatiale sur la dispersion simulée pour les larves d'invertébrés côtiers le long des côtes bretonnes. Pour celà, il faudrait disposer d'une configuration de même ou de plus petite emprise spatiale (par exemple, à l'échelle du nord du Golfe de Gascogne) avec une résolution spatiale plus fine (*i.e.* inférieure à 4 km), afin de comparer les résultats obtenus par un tel modèle avec ceux issus du modèle utilisé au cours de cette thèse. Un tel modèle permettrait par ailleurs de préciser le rôle des populations de la baie de Douarnenez dans les échanges entre le Golfe de Gascogne et la Manche.

En outre, la **paramétrisation des processus biologiques** dans les modèles couplés biophysiques s'avère très souvent difficile (Metaxas et Saunders, 2009). En effet, tandis que la partie physique des modèles repose sur des lois physiques connues, il n'existe pas de loi régissant les processus biologiques. Le nombre et le type de paramètres biologiques pris en compte par les modèles relèvent alors du choix du modélisateur. Il existe cependant un consensus sur les processus à prendre en compte : la ponte (date, lieu, quantité de larves émises), la mortalité larvaire, la durée de vie larvaire, et les comportements larvaires de nage et de sédentarisation. En revanche, la paramétrisation de ces processus est délicate, en partie en raison de notre manque de connaissance empirique sur les processus biologiques

impliqués, sur leurs valeurs moyennes et sur leurs variabilités. Les paramètres biologiques utilisés dans les modèles biophysiques de dispersion sont donc parfois fixés arbitrairement, à moins qu'ils ne proviennent d'observations *in situ* ou d'études expérimentales. Dans tous les cas, il est préférable d'effectuer des analyses de sensibilité afin d'estimer l'importance de tel ou tel paramètre sur les schémas simulés de transport et de dispersion. De plus, les processus biologiques peuvent être décrits de manière plus ou moins complexe. Pour illustrer ceci, prenons comme exemples le taux de mortalité larvaire et la durée de vie larvaire.

Le taux de mortalité larvaire utilisé dans les modèles biophysiques de dispersion est le plus souvent constant. Il est parfois fixé arbitrairement comme étant égal à zéro (*cf. Chapitre 2, e.g.* Aiken *et al.*, 2007; Marinone *et al.*, 2008; Marta-Almeida *et al.*, 2006; Mitarai *et al.*, 2008; North *et al.*, 2008; Treml *et al.*, 2008; Viard *et al.*, 2006). Il peut aussi être fixé égal à une valeur issue de la littérature, comme par exemple des travaux de Rumrill (1990) ou de Pedersen *et al.* (2008) chez les larves d'invertébrés ou bien de Houde (1988) chez les larves de poissons (Barnay *et al.*, 2003; Ellien *et al.*, 2004; Guizien *et al.*, 2006; Huret *et al.*, 2007; Lefebvre *et al.*, 2003). Enfin, un taux de mortalité spécifique peut être calculé à partir d'observations expérimentales ou *in situ* (*cf.* Chapitre 4), cette dernière méthode de paramétrisation étant préférable. Cependant, étant donné que la mortalité larvaire dépend à la fois de la prédation, de la nutrition, et des conditions hydrologiques environnementales (stress dû à la température ou à la salinité), il est possible dans des modèles plus complexes de considérer que ce paramètre est fonction d'autres paramètres calculés par le modèle, comme par exemple des champs de prédateurs, de température, et/ou de salinité (Fiksen *et al.*, 2007; Lett *et al.*, 2008). La relation entre le taux de mortalité et ces autres paramètres doit alors être issue d'études expérimentales. Cette dernière approche permet ainsi de prendre en compte la variabilité spatio-temporelle de la mortalité.

De manière similaire, la durée de vie des larves est fréquemment fixée de manière arbitraire à une valeur constante, dans l'ordre de grandeur des durées de vie larvaire estimées ou observées (Shanks, 2009; Siegel *et al.*, 2003) ou déduites d'observations *in situ* spécifiques. Or la croissance, et donc la durée de vie larvaire, varie d'une part entre indivi-

dus (Rigal, 2009), d'autre part en fonction des conditions environnementales rencontrées par la larve telles que la température (O'Connor *et al.*, 2007; Reitzel *et al.*, 2004) ou la disponibilité en nourriture. Quelques modèles couplés biophysiques ont ainsi pris en compte des durées de vie larvaire variables et fonction de l'environnement rencontré par les larves afin de simuler la dispersion larvaire d'huître (Dekshenieks *et al.*, 1996, 1997), de homard (Incze et Naimie, 2000), ou de balane (Pfeiffer-Herbert *et al.*, 2007).

Ces exemples de paramétrisation de la mortalité larvaire et de la durée de vie larvaire soulignent la **nécessité de l'observation *in situ* et de l'étude expérimentale des processus biologiques** afin de correctement et spécifiquement paramétrer ces processus dans les modèles biophysiques de dispersion. D'autre part, des observations *in situ* sont indispensables pour permettre la comparaison des résultats issus de simulations *in silico* avec des données de terrain. Un **aller-retour** est donc nécessaire entre l'observation et l'expérimentation, d'une part, et la modélisation, d'autre part, afin de faire avancer notre connaissance de la dispersion larvaire des organismes à cycle bentho-pélagique.

Par ailleurs, l'étude de la dispersion par des outils de modélisation ne prend généralement pas en compte la survie des premiers stades de vie benthique, d'éventuelles migrations post-larvaires comme observées chez *Pectinaria koreni* (Olivier *et al.*, 1996; Thiébaut, 1996), ni la survie des recrues jusqu'à l'obtention de leur maturité sexuelle (dispersion efficace ou connectivité reproductive). La dispersion simulée par de tels modèles est donc vraisemblablement très supérieure à la dispersion efficace.

## C.3 Importances relatives et interactions des facteurs biophysiques sur la dispersion

Le transport et la dispersion larvaires dépendent de l'interaction de facteurs hydrodynamiques et biologiques (Cowen et Sponaugle, 2009; Sponaugle *et al.*, 2002). Les travaux réalisés au cours de cette thèse fournissent des informations à la fois qualitatives et quantitatives sur les importances relatives des facteurs hydrodynamiques et biologiques sur la dispersion et la connectivité au sein des métapopulations d'invertébrés à cycle bentho-pélagique le long des côtes françaises de la Manche et de l'Atlantique.

Dans le Golfe de Gascogne, plusieurs facteurs hydroclimatiques influençant le transport et la dispersion ont été mis en évidence. D'une part la **structuration spatiale** de l'environnement hydrologique à **méso-échelle** est le principal facteur responsable de la variabilité de la distribution du méroplancton dans le nord du Golfe de Gascogne (Chapitre 1). L'échantillonnage *in situ* a en particulier souligné l'importance des **plumes d'eaux dessalées** dans la rétention larvaire au sein de masses d'eau particulières, jouant le rôle de **barrière** à la dispersion vers le large des larves (Shanks *et al.*, 2002; Thiébaut, 1996). Le transport des larves piégées dans les plumes dessalées sera donc gouverné par la circulation thermo-haline le long de la façade atlantique (Figure C.1). Ainsi, en fonction des structures hydrologiques à méso-échelle, la dispersion larvaire variera selon la localisation des populations génitrices.

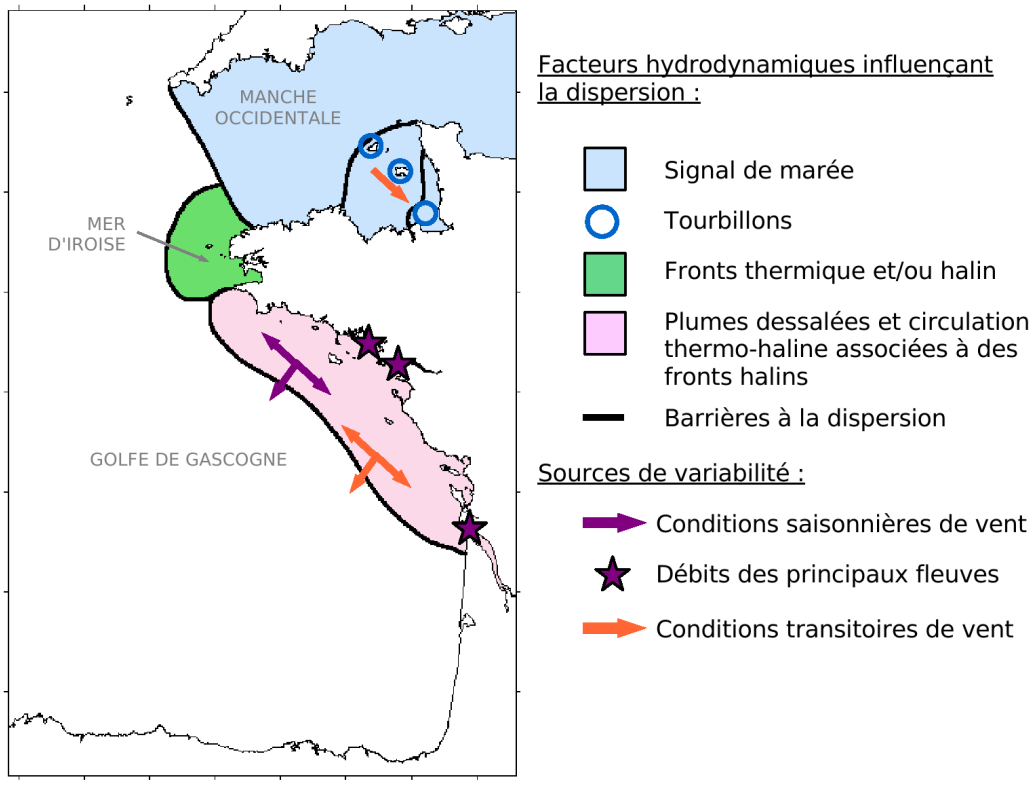


Figure C.1 – Schéma récapitulatif des principaux facteurs hydroclimatiques influençant la dispersion larvaire le long des côtes françaises de la Manche et de l'Atlantique. Les principales sources de variabilité saisonnière (en violet) et transitoire (en orange) sont indiquées.

D'autre part, la **forte variabilité saisonnière** de l'hydrodynamisme du Golfe de Gascogne impacte significativement les schémas de dispersion et les patrons de connectivité selon la période de reproduction (Chapitre 2). En effet, la circulation thermohaline dépend de la variabilité saisonnière des débits fluviaux et est modulée par les conditions saisonnières de vent (Figure C.1). Ainsi, les conditions hydroclimatiques dans le Golfe de Gascogne favorisent le transport larvaire vers le nord au printemps et vers le sud en été, selon la saisonnalité des conditions de vent. En fonction de la période de reproduction, les schémas de dispersion seront donc radicalement différents. De plus, des conditions transitoires de vents d'ouest à nord-ouest pendant la période de stratification saisonnière peuvent aussi induire des upwellings côtiers le long des côtes sud-bretonnes (Lazure et Jégou, 1998; Puillat *et al.*, 2006, 2004), favorisant ainsi la dilution des nuages larvaires et l'export des larves vers le large (Chapitre 1). À l'échelle du Golfe de Gascogne, les schémas de dispersion sont donc très variables en fonction de la variabilité spatio-temporelle et de la complexité des structures hydrologiques à méso-échelle (Koutsikopoulos et Le Cann, 1996; Puillat *et al.*, 2006, 2004), en particulier en fonction du lieu et de la date de ponte. Les résultats de simulation ont par ailleurs indiqué que pour des comportements natatoires simples, les schémas de transport et de connectivité peuvent être modifiés et leur variabilité peut diminuer.

Nos résultats suggèrent qu'à l'interface entre le Golfe de Gascogne et la Manche occidentale, les **structures frontales** de la Mer d'Iroise, d'origine thermique et/ou haline (Le Boyer *et al.*, 2009; Pingree *et al.*, 1982, 1975), constituent des **barrières** à la dispersion larvaire (Figure C.1). Ces barrières sont fonctions de la variabilité hydroclimatique et des traits d'histoire de vie des espèces.

En Manche occidentale, les simulations lagrangiennes et eulériennes de la dispersion larvaire soulignent que le **signal de marée** constitue le facteur prépondérant régulant le transport et la dispersion dans cette zone (Figure C.1). À l'échelle locale du Golfe Normand-Breton, un autre type de barrière physique à la dispersion larvaire a été mis en évidence : les **structures tourbillonnaires** (Figure C.1). Ces tourbillons peuvent être rétentifs lorsqu'ils sont générés par des caps, comme le tourbillon de Cancale à l'entrée de la Baie du Mont-Saint-Michel, ou diffusifs lorsqu'ils sont provoqués par des îles, comme au-

tour de l'île de Jersey ou de l'archipel des Minquiers (Ménesguen et Gohin, 2006). Au sein de la Baie du Mont-Saint-Michel, la présence d'un tourbillon rétentif a des conséquences importantes sur la rétention et le succès de la sédentarisation des larves de l'espèce patrimoniale *Sabellaria alveolata* (Dubois *et al.*, 2007). Une précédente étude alliant analyses génétiques et modèle de dispersion chez le gastéropode invasif *Crepidula fornicata* avait également suggéré un rôle important des structures tourbillonnaires dans la dispersion larvaire (Dupont *et al.*, 2007). L'utilisation d'un modèle couplé biologie-physique à fine échelle spatiale a confirmé ainsi le rôle des structures tourbillonnaires dans les schémas de dispersion (Baums *et al.*, 2006; Limouzy-Paris et al, 1997). En particulier, des schémas de dispersion larvaire très différents ont été décrits selon le récif parental depuis lequel les larves sont émises. Ainsi, le succès des larves émises depuis le petit récif situé en fond de baie varie peu et dépend principalement des conditions de marée au moment de la ponte. En revanche les larves issues du grand récif situé au sud de la baie sont rapidement piégées par le tourbillon de Cancale. Leur succès de sédentarisation est relativement faible et dépend en grande partie de la localisation de la structure tourbillonnaire au regard de celle des récifs. Ainsi, de très forts succès de sédentarisation peuvent être observés lors d'événements transitoires de vent (Figure C.1), capables de temporairement modifier l'emprise spatiale du tourbillon de Cancale vers le sud-est, favorisant ainsi un recrutement au sein des deux récifs de la baie. De plus, le comportement grégaire des larves compétentes et leur capacité à retarder leur métamorphose favorisent le succès de la dispersion larvaire de *Sabellaria alveolata*.

En conclusion, l'étude des interactions entre les facteurs hydroclimatiques et biologiques sur la dispersion, explorés dans le Golfe de Gascogne et la Manche occidentale, met en avant deux aspects distincts : (i) d'une part l'impact de la forte variabilité saisonnière de l'hydrodynamisme dans le Golfe de Gascogne en lien avec les caractéristiques biologiques des espèces (date de ponte, durée de vie larvaire, comportement natatoire), et (ii) d'autre part l'existence d'un fort signal régulier de marée et de structures hydrodynamiques pérennes dans le Golfe Normand-Breton, qui peuvent être transitoirement modifiés par des conditions météorologiques, en lien avec les caractéristiques biologiques

d'une espèce récifale (sédentarisation grégaire, délai à la métamorphose, longue durée de vie larvaire).

## C.4 Patrons historiques et contemporains de dispersion et de connectivité dans le Golfe de Gascogne et en Manche

Jolly *et al.* (2009) ont récemment décrit les patrons de connectivité historiques et contemporains chez le polychète *Pectinaria koreni* en Manche. Ces travaux, combinant des analyses génétiques basées sur différents marqueurs (ADN mitochondrial, microsatellites) à un modèle biophysique de dispersion à méso-échelle, ont permis de dissocier les évènements anciens d'expansion des populations des patrons de connectivité contemporains. Ces résultats ont ainsi mis en évidence l'existence de deux lignées ancestrales au sein des populations de *Pectinaria koreni* en Manche orientale, en Mer du Nord et en Mer d'Irlande. Les migrations de ces deux lignées de part et d'autres des îles britanniques ont ensuite permis un contact secondaire en Manche. L'étude de la connectivité contemporaine a révélé d'intenses échanges larvaires le long des côtes françaises de la Manche, de la Normandie à la Mer du nord, avec de possibles échanges trans-Manche entre les populations des côtes françaises et anglaises. De manière similaire, les patrons de connectivité historiques et contemporains à l'échelle du Golfe de Gascogne et de la Manche occidentale peuvent maintenant être décrits en combinant les résultats obtenus au cours de cette thèse aux résultats issus de précédentes analyses phylogénétiques.

### C.4.1 Dispersion ancienne et existence d'une zone de transition phylogéographique

En effet, des analyses phylogénétiques, basées sur la description de la distribution des haplotypes du gène mitochondrial de la COI (cytochrome oxidase I), ont révélé l'existence, chez plusieurs espèces d'invertébrés côtiers à cycle bentho-pélagique, de plusieurs lignées évolutives distinctes dans le Golfe de Gascogne et en Manche (Jolly *et al.*, 2005, 2006; Jolly, 2005; Rigal, 2005).

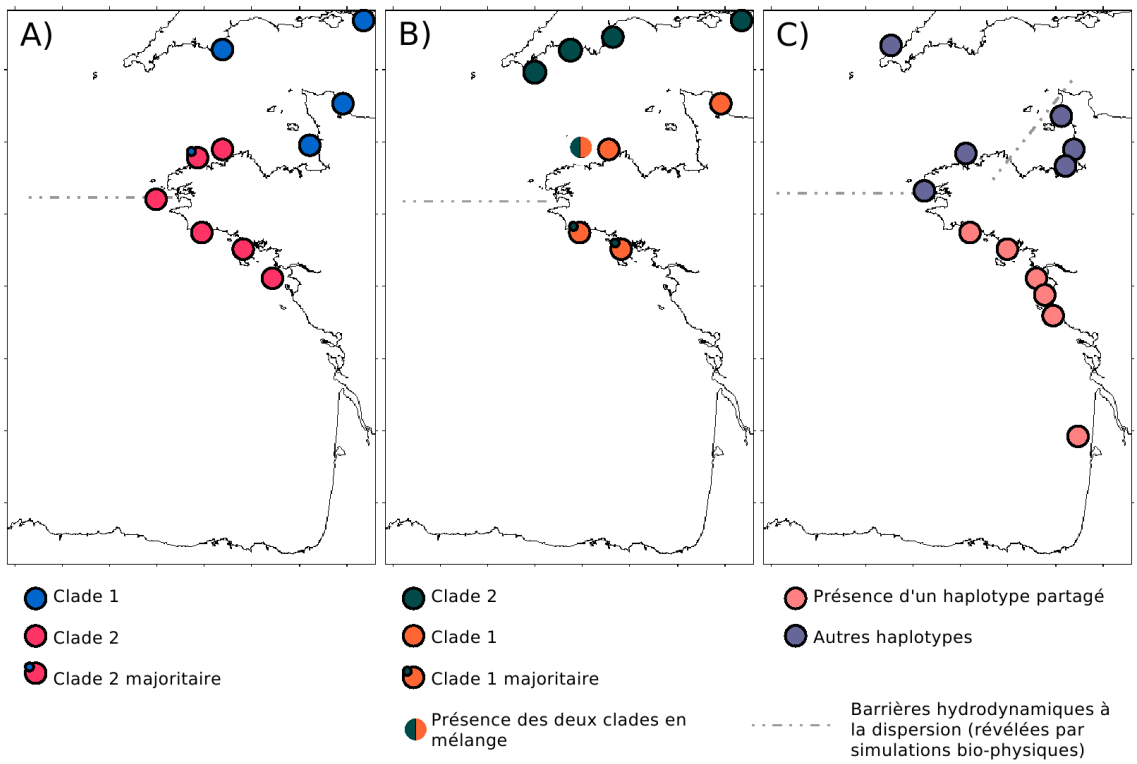


Figure C.2 – Distribution des haplotypes du gène mitochondrial codant pour la COI chez les trois espèces cibles de polychètes côtières : (A) *Pectinaria koreni*, (B) *Owenia fusiformis*, et (C) *Sabellaria alveolata*, d'après Jolly (2005), Jolly *et al.* (2006) et Rigal (2005). Les barrières hydrodynamiques à la dispersion révélées au cours du présent travail de thèse sont indiquées.

Chez *Pectinaria koreni*, ces analyses révèlent l'existence de deux lignées évolutives distinctes (Figure C.2A) : (i) une lignée comprenant l'essentiel des populations de la Manche (clade 1), et (ii) une lignée comprenant les populations situées le long des côtes bretonnes et du Golfe de Gascogne (clade 2) (Jolly *et al.*, 2005, 2006; Jolly, 2005). De plus, une zone de coexistence de ces deux lignées a été identifiée le long des côtes nord de la Bretagne, incluant en particulier la baie de Morlaix. Étant donné leur fort taux de divergence (environ 16 %), ces deux lignées évolutives pourraient même correspondre à deux espèces cryptiques (Jolly *et al.*, 2005). Chez *Owenia fusiformis*, ces analyses identifient là encore deux lignées évolutives distinctes au sein des populations subtidales dans le Golfe de Gascogne et en Manche occidentale (Figure C.2B) : (i) une lignée comprenant les populations situées le long des côtes françaises de l'Atlantique et de la Manche (clade 1), et (ii) une lignée comprenant les populations situées le long des côtes anglaises de la Manche (clade

2) (Jolly *et al.*, 2006; Jolly, 2005). Chez cette espèce, la coexistence de ces deux clades a été signalée le long des côtes bretonnes, en particulier au sein des baies de Morlaix, Concarneau et Lorient. Enfin, chez *Sabellaria alveolata*, un haplotype propre aux populations du Golfe de Gascogne (Figure C.2C) ainsi qu'un déficit en diversité haplotypique de ces dernières a été mis en évidence (Rigal, 2005).

Ces patrons de distribution résultent principalement de phénomènes historiques (*i.e.* divergence ancienne entre lignées évolutives) et de mises en contacts secondaires entre lignées évolutives distinctes à la suite d'évènements de recolonisation. Cependant, le maintien actuel de ces patrons de distribution pourrait dépendre d'évènements contemporains, en particulier de l'existence d'une barrière contemporaine à la dispersion larvaire (et donc aux flux de gènes) entre le Golfe de Gascogne et la Manche.

### C.4.2 Dispersion contemporaine et barrières actuelles à la dispersion et à la connectivité

Nos résultats confirment l'existence d'une barrière actuelle à la dispersion pouvant limiter les flux de gènes contemporains entre les populations d'invertébrés côtiers à cycle bentho-pélagique du Golfe de Gascogne et de la Manche, et ainsi maintenir les patrons phylogénétiques précédemment décrits.

De précédentes observations hydrologiques avaient signalé (i) le transport en mars-avril d'eaux dessalées issues de Loire et de la Gironde vers le nord le long des côtes sud-bretonnes lorsque de forts débits étaient accompagnés de vent de nord-est (observations confirmées en 2008 lors des campagnes LARVASUD, *cf.* Chapitre 1), et (ii) l'entrée de ces eaux en Manche occidentale, favorisée par des conditions tidales de vive-eau et par des vents de sud-ouest à sud-est (Kelly-Gerreyn *et al.*, 2006). Ces observations suggèrent donc un éventuel transport larvaire du Golfe de Gascogne vers la Manche occidentale par ces eaux dessalées. La simulation de la dispersion larvaire le long des côtes atlantiques françaises (Chapitre 2) a confirmé que des échanges larvaires étaient potentiellement importants au sein des deux grandes régions hydrologiques que forment la Manche occidentale (côtes nord-bretonnes) et le Golfe de Gascogne (côtes sud-bretonnes et centre du Golfe de Gascogne), décrivant

une barrière hydrodynamique à la dispersion en Mer d'Iroise (Figure C.2). Ainsi, nos travaux mettent en avant le rôle de la Mer d'Iroise dans le maintien de la zone de transition biogéographique entre les provinces lusitanienne et boréale. Conformément aux hypothèses de Gaylord et Gaines (2000), cette zone de fort hydrodynamisme agit comme une barrière physique à la dispersion larvaire. Selon les descriptions de ces auteurs, la Mer d'Iroise peut être qualifiée de barrière unidirectionnelle semi-perméable, puisque des échanges larvaires ne sont possibles que depuis le Golfe de Gascogne vers la Manche, et qu'ils sont rares. En effet, ils nécessitent une conjonction de facteurs hydroclimatiques et biologiques : forts débits printaniers de la Loire et de la Gironde, période et ponte en présence de ces eaux dessalées, transport vers le nord des eaux dessalées, traversée du front de la Mer d'Iroise permise par des conditions transitoires de vent, entrée des eaux dessalées en Manche permise par les conditions de marée et de vent, et enfin durée de vie larvaire suffisamment longue et rencontre d'habitat favorable par des larves compétentes.

Pour des durées de vie larvaire de l'ordre 4 semaines, *i.e.* correspondant aux durées de vie larvaire rapportées pour *Owenia fusiformis*, des échanges larvaires sont donc possibles entre les populations du Golfe de Gascogne et de la Manche occidentale (Morlaix, Lannion). Chez *Pectinaria koreni*, des durées de vie larvaire d'environ 2 semaines ont été estimées *in situ* dans l'environnement trophique très riche de la baie de Seine (Lagadeuc et Retière, 1993). Si on envisage pour cette espèce des durées de vie larvaires plus longues pour des pontes précoces, des échanges larvaires depuis le Golfe de Gascogne vers la Manche occidentale seraient possibles. D'autre part, les données acquises au cours de cette thèse (*cf.* Chapitre 1) suggèrent une présence continue de larves de *Pectinaria koreni* de l'estuaire de la Loire à la Mer d'Iroise pendant la période de ponte, confortant la possibilité de tels échanges. De précédents travaux de modélisation larvaire ont par ailleurs suggéré que les populations d'*Owenia fusiformis* situées dans les baies de Morlaix et Lannion constituaient des populations puits pour les populations du Golfe de Gascogne (Barnay *et al.*, 2003). Étant donné les très faibles effectifs actuels des populations de *Pectinaria koreni* et *Owenia fusiformis* en baie de Lannion et en baie de Morlaix (moins de 20 ind.m$^{-2}$, F. Gentil. et É. Thiébaut, comm. pers.), des extinctions seraient possibles en l'absence d'apport larvaire allochtone, suivies d'éventuelles recolonisation à partir de larves émises depuis les

populations du nord du Golfe de Gascogne. La distribution phylogéographique de *Pectinaria koreni* (Figure C.2A) pourrait donc être aujourd'hui fortement associée aux patrons actuels de connectivité décrits dans cette thèse : des échanges larvaires sont possibles entre les populations du clade 2, mais aucun échange n'est possible entre ces populations et les populations du clade 1 situées plus à l'est, étant donné la faible production de larves et l'absence d'habitat favorable entre la baie de Lannion et la Baie du Mont-Saint-Michel. Chez *Owenia fusiformis*, la distribution phylogéographique précédemment décrite (Figure C.2B) est elle aussi en accord avec l'existence contemporaine d'échanges larvaires entre le Golfe de Gascogne et la Manche, mais pourrait d'avantage résulter d'évènements anciens pour expliquer l'opposition entre les côtes françaises et les côtes anglaises en Manche. Enfin, chez *Sabellaria alveolata*, dont la durée de vie larvaire est beaucoup plus longue (de 4 à 10 semaines) (Dubois *et al.*, 2007), et donc pour qui les distances de dispersion parcourues seraient plus élevées, une rupture phylogénétique demeure au niveau de la Mer d'Iroise (Figure C.2C), en particulier entre les populations du sud-Bretagne et les populations de Crozon et de Lannion. Or, les populations de *Sabellaria alveolata* situées le long des côtes sud-bretonnes ne comprennent que quelques centaines d'individus. Ces populations pourraient vraissemblablement se comporter comme des puits recevant des larves émises depuis les importants récifs situés en baie de Bourgneuf, à l'embouchure de la Loire. Ces derniers fonctionneraient comme des populations sources pour les populations des côtes sud-bretonnes, mais les larves émises depuis ces récifs ne pourraient pas atteindre la Mer d'Iroise. Ainsi, comme l'a confirmé la description des abondances larvaies de cette espèce dans le nord du Golfe de Gascogne, la distribution des populations adultes pourraient jouer un rôle majeur dans le maintien de cette rupture phylogéographique.

À l'échelle locale du Golfe Normand-breton, des analyses génétiques au sein des récifs de *Sabellaria alveolata* à partir de marqueurs microsatellites ont montré une forte diversité génétique intra- et inter-recif, indiquant une importante taille efficace des populations (nombre d'individus participant à la reproduction) (Farcy, 2003). Ces analyses ont souligné l'absence de structure génétique entre les deux récifs de la Baie du Mont-Saint-Michel, suggérant un libre échange de gènes entre les deux récifs, *i.e.* une connectivité reproductive contemporaine forte. Nos simulations eulériennes de la dispersion larvaire et de la connec-

tivité non reproductrice chez *Sabellaria alveolata* sont en accord avec ces analyses, et permettent d'expliquer les raisons biophysiques de ces échanges (rétention exceptionnelle due au vent, rétention régulière due à la marée).

Pour conclure, les patrons contemporains de dispersion permettent de révéler des barrières hydrodynamiques actuelles à la dispersion (plume dessalée du Golfe de Gascogne, front de la Mer d'Iroise, structures tourbillonnaires du Golfe Normand-Breton), expliquant ainsi, chez plusieurs espèces d'invertébrés côtiers à cycle bentho-pélagique, le maintien de patrons de connectivité historique (phylogéographie) observés à l'échelle du Golfe de Gascogne et de la Manche occidentale et les patrons de connectivité contemporains observés en baie du Mont-Saint-Michel.

## C.5 Perspectives de ce travail de thèse

À l'issu de ce travail de thèse, plusieurs perspectives de recherche se dégagent, d'une part pour approfondir nos connaissances sur la dispersion et la connectivité contemporaines, d'autre part, pour étudier leurs possibles évolutions futures.

### C.5.1 Approfondir nos connaissances sur la dispersion contemporaine

Dans le but d'approfondir nos connaissances sur la dispersion et la connectivité contemporaines en Atlantique Nord-Est, plusieurs pistes de travail sont envisageables. D'une part, par l'étude de la phase larvaire *in situ*, et, d'autre part, par le développement et le perfectionnement des modèles biophysiques de dispersion larvaire.

#### *C.5.1.1 Distribution spatio-temporelle des larves des différentes lignées évolutives*

Nous avons vu que l'étude de la dispersion larvaire permettait de proposer des hypothèses quant au maintien de barrières hydrodynamiques entre des populations issues de lignées évolutives distinctes. Cependant, nos travaux ne nous permettent pas d'expliquer le maintien d'une barrière phylogénétique lorsque les populations de lignées divergentes sont présentes en sympatrie, *i.e.* au même endroit au même moment. Une explication pos-

sible à ce phénomène, serait une différence phénologique entre les individus issus des différentes lignées évolutives. Tester cette hypothèse revient ainsi à décrire la distribution spatio-temporelle des larves de ces différentes lignées.

Pour cela, il est nécessaire de développer des outils moléculaires afin d'identifier au niveau infra-spécifique les larves issues de ces différentes lignées. Des analyses préliminaires ont été réalisées pendant cette thèse sur le typage moléculaire des larves de *Pectinaria koreni* et d'*Owenia fusiformis*, à partir du séquençage d'un fragment du gène mitochondrial de la COI (*cf.* Annexe A.2). Ces premiers résultats ont ainsi suggéré la présence en mai 2008 en baie de Vilaine de larves de *Pectinaria koreni* du clade 2 et de larves d'*Owenia fusiformis* du clade 1. L'amélioration des protocoles testés et leur application en routine devraient donc permettre de décrire la distribution spatio-temporelle de ces différents clades le long des côtes sud-bretonnes en mai et juin 2008.

### *C.5.1.2 Application spécifique des modèles génériques de dispersion*

Une prochaine étape de ce travail de thèse pourrait être l'application du modèle générique de dispersion larvaire lagrangienne développé dans le Chapitre 2 à des espèces particulières dont les paramètres biologiques sont suffisamment bien connus, en matière de localisation et de taille des populations adultes, de mortalité larvaire, de croissance et de durée de vie larvaire, et de comportement larvaire. Ainsi, les résultats d'un tel modèle spécifique pourront être confrontés à des observations *in situ* des distributions et des abondances larvaires d'espèces cibles. Dans cette optique, plusieurs pistes de recherche sont envisageables, d'une part concernant les espèces cibles étudiées au cours de cette thèse, d'autre part concernant une autre espèce cible potentielle, le gastéropode invasif *Crepidula fornicata*.

Mis en place en Bretagne en 2003, le Réseau d'Observation Benthique (REBENT, http ://www.rebent.org) a pour objectif de recueillir et de mettre en forme les données relatives aux habitats benthiques et aux biocénoses associées dans la zone côtière afin de décrire ces habitats et de détecter leurs évolutions spatio-temporelles. Il s'appuie à la fois sur un suivi stationnel (voir données présentées à la fin du Chapitre 1) et sur une approche sectorielle de cartographie des habitats qui est actuellement en cours. Concernant

les polychètes *Pectinaria koreni* et *Owenia fusiformis*, la prise en considération future de ces données permettrait de définir précisément les contours actuels des habitats favorables au développement de leurs populations et d'estimer les stocks adultes. Par ailleurs, un modèle de comportement larvaire spécifique des larves de *Pectinaria koreni* et *Owenia fusiformis* pourrait être développé en s'appuyant sur une analyse de la variabilité de la distribution verticale des larves en fonction des paramètres environnementaux. Si certaines informations sont actuellement disponibles (*cf.* Chapitre 1), ce jeu de données pourrait être complété par le dépouillement additionnel d'échantillons obtenus lors des missions LARVASUD.

D'autre part, un autre modèle biologique envisageable serait le gastéropode invasif *Crepidula fornicata* (Figure C.3A). En effet, des travaux récents sur la phase larvaire de cette espèce, basés sur des observations *in situ* et des études expérimentales, ont permis de décrire le développement et la durée de vie larvaire de cette espèce en fonction des températures rencontrées (Figure C.3B) (Rigal *et al.*, *soumis*). Un tel formalisme pourrait ainsi être utilisé dans un modèle couplé biophysique de dispersion larvaire afin de prendre en compte la variabilité saisonnière des durées de vie larvaire (Reitzel *et al.*, 2004; Rigal, 2009).

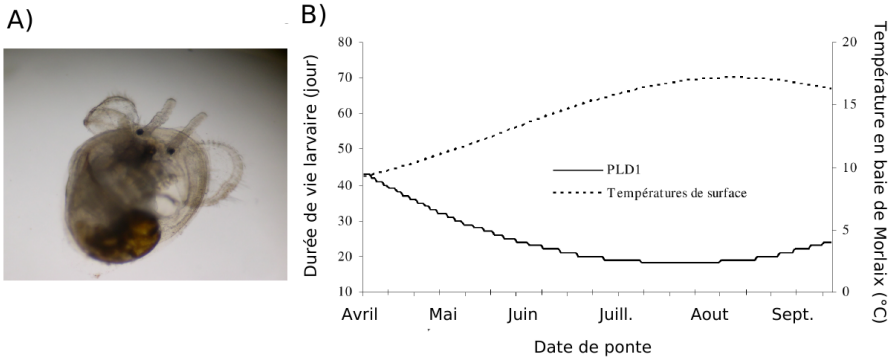


Figure C.3 – (A) Larve véligère de *Crepidula fornicata* et (B) durée de vie larvaire (PLD) de cette espèce en fonction des températures de surface rencontrées en baie de Morlaix. Photographie et données fournies par F. Rigal. La formule précise de la durée de vie larvaire calculée en fonction des températures rencontrées est issue de Rigal (2009) et Rigal *et al.* (*soumis*).

#### *C.5.1.3 Emprise spatiale des modèles de dispersion*

Au cours de cette thèse, des modèles de dispersion ont été utilisés à deux échelles spatiales : d'une part à l'échelle régionale du Golfe de Gascogne et de la Manche occidentale, d'autre part à l'échelle locale du Golfe Normand-Breton. L'importance de la résolution spatiale des modèles de dispersion a été discuté dans la Section C.2 de ce chapitre. Il serait maintenant intéressant de mettre au point des modèles biophysiques de dispersion à d'autres échelles spatiales, en particulier :

- un modèle à plus grande emprise spatiale couvrant le Golfe de Gascogne, la Manche, la Mer d'Irlande et la Mer du Nord afin d'intégrer les populations d'invertébrés côtiers de ces différentes zones au modèle de métapopulation étudié au Chapitre 2 ; un tel modèle permettrait ainsi de décrire la dispersion et la connectivité entre les populations de *Pectinaria koreni* et d'*Owenia fusiformis* du Golfe de Gascogne, de la Manche, de la Mer d'Irlande et la Mer du Nord, pour lesquelles la connectivité passée a été décrite (Jolly *et al.*, 2005, 2006; Jolly, 2005) ;

- un modèle à emprise spatiale intermédiaire à l'échelle des côtes bretonnes, permettant une résolution spatiale fine des différentes baies de ces côtes (comme Douarnenez et Morlaix), dans le but d'étudier plus finement la dispersion et la connectivité le long des côtes bretonnes ;

- un modèle à petite emprise spatiale à l'échelle locale de la baie de Morlaix, pour laquelle aucun modèle hydrodynamique fin n'a encore été développé ; si un modèle analytique simple de dispersion larvaire du gastéropode invasif *Crepidula fornicata* a été développé dans cette baie (*cf.* Annexe E), la mise au point d'un modèle couplé biophysique à fine résolution spatiale pourrait ainsi permettre de confirmer les résultats issus du modèle analytique et de mieux appréhender le rôle de la phase larvaire dans la dynamique de population de cette espèce.

### C.5.2 Explorer les évolutions futures de la dispersion larvaire et leurs impacts sur la distribution des espèces

Un nouveau challenge se profile pour l'étude de la distribution de la biodiversité marine et de la dispersion larvaire dans le contexte actuel du changement climatique. En effet, les espèces marines sont maintenant confrontées à un monde changeant, où la fragmentation et la destruction des habitats augmentent, où les invasions biologiques sont de plus en plus fréquentes, et où l'environnement hydrologique et climatique est modifié. De récents travaux de Engler et Guisan (2009) ont mis en avant l'importance des processus de dispersion, même décrits de manière simple, dans la prédiction des évolutions futures de la distribution des espèces végétales terrestres (Figure C.4). L'étude prospective des évolutions futures de la distribution des espèces dépend donc de la présence d'habitats favorables et de la capacité des espèces à coloniser ces habitats par dispersion.

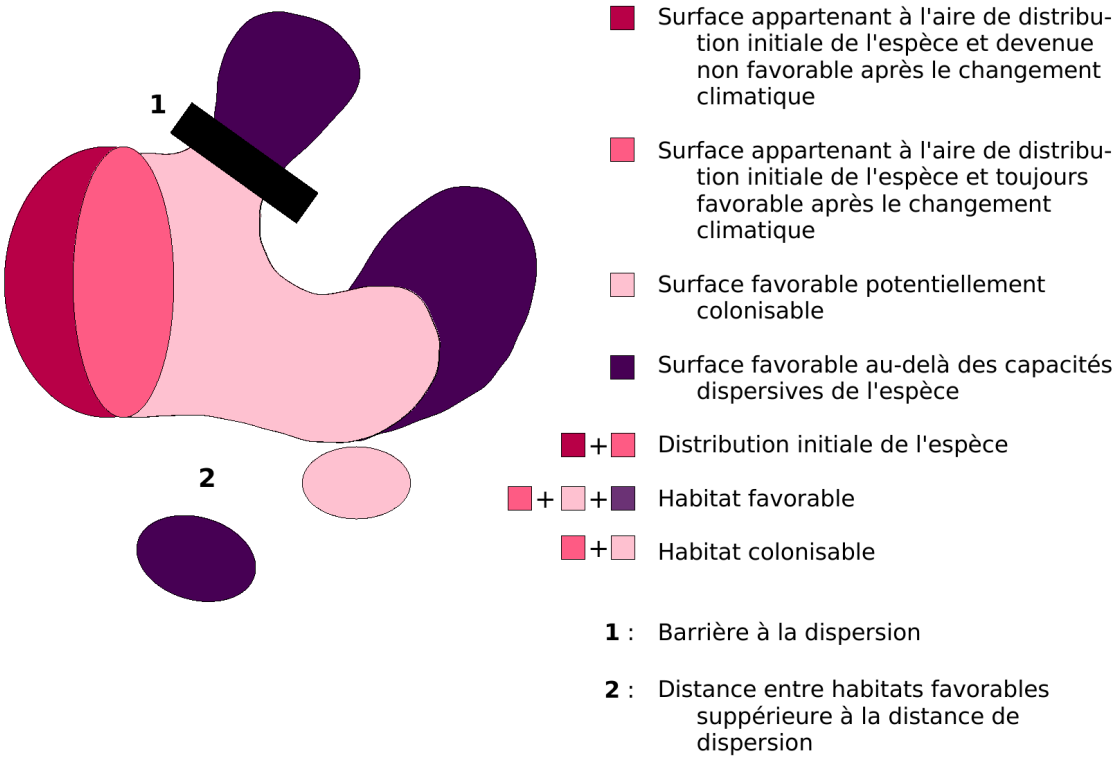


Figure C.4 – Représentation schématique de la distribution d'une espèce en réponse au changement climatique, d'après Engler et Guisan (2009).

La description des assemblages faunistiques en Manche a montré qu'il existait du sud-ouest vers le nord-est des limites successives d'aire de distribution chez de nombreuses espèces d'invertébrés benthiques en relation avec les gradients de température (Cabioch *et al.*, 1977). Étant donné les augmentations de températures observées en Manche depuis la seconde moitié du vingtième siècle, un possible déplacement des espèces vers le nord-est serait envisageable sous l'hypothèse que le changement climatique serait favorable aux extensions des limites d'aire de distribution. Pour tester cette hypothèse, il faudrait donc prendre en compte les capacités dispersives des espèces à l'échelle du Golfe de Gascogne, de la Manche, de la Mer du Nord et de la Mer d'Irlande, en incluant conjointement dans un modèle bio-hydroclimatique :

- la distribution des habitats favorables, fonction de la distribution des sédiments et des tolérances thermiques des espèces,
- l'évolution de la phénologie de la reproduction,
- les variations de durée de vie larvaire en fonction des températures rencontrées au cours de la dispersion,
- d'éventuels changements de circulation sous l'impact des conditions climatiques.

# Annexes

# Annexe A

# Les missions LARVASUD

**Sommaire**

# A.1 Conditions de vent enregistrées à Belle-Ile

## Sommaire



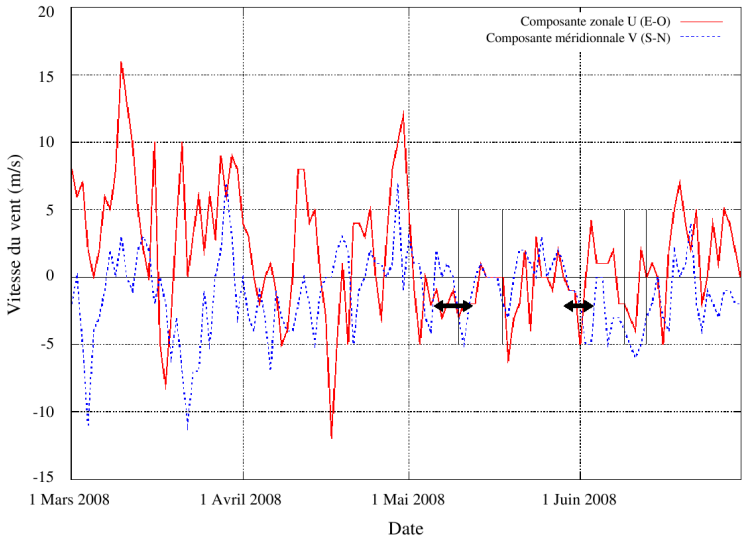


Figure A.1 – Conditions de vent enregistrées à Belle-Ile au printemps 2008 (données Météo France). Les missions de mai et de juin sont indiquées par des flèches noires. Les vitesses des composantes zonale et méridionale du vent (U en trait plein rouge et V en trait pointillé bleu) sont données en $m.s^{-1}$.

## A.2 Identification des larves de polychètes par typage moléculaire

### A.2.1 Introduction

L'identification au niveau spécifique des larves d'invertébrés marins peut se révèler difficile sur la base de simples critères morphologiques étant donné (i) la petite taille de ces larves (quelques centaines de $\mu$m), (ii) les grandes similarités morphologiques entre espèces proches (Le Goff-Vitry *et al.*, 2007a), et (iii) la forte plasticité phénotypique des larves en réponse aux conditions environnementales (Strathmann *et al.*, 1992). De plus, plusieurs stades de développement larvaire morphologiquement distincts sont souvent décrits pour une seule espèce, rendant l'identification au niveau spécifique encore plus ardue (Miller *et al.*, 1991). L'identification morphologique des organismes méroplanctoniques nécessite donc expertise et temps, ce qui peut être incompatible avec un comptage en routine d'un grand nombre d'échantillons.

Plusieurs approches moléculaires ont cependant été récemment proposées pour faciliter l'identification des larves d'invertébrés (Garland et Zimmer, 2002; Rogers, 2001). Ces techniques regroupent des méthodes immunologiques (c'est-à-dire basées sur la spécificité de la reconnaissance par des anticorps) et génétiques (c'est-à-dire basées sur la spécificité des séquences d'ADN) (Tableau A.1). Cependant, l'utilisation de ces techniques pour décrire la distribution *in situ* du méroplancton reste rare (par exemple Hansen et Larsen, 2005; Larsen *et al.*, 2007; Medeiros-Bergen *et al.*, 1995).

Dans le but de décrire la distribution des différents stades larvaires des polychètes *Pectinaria koreni* et *Owenia fusiformis* dans le Nord du Golfe de Gascogne, nous avons tenté de mettre au point une technique d'identification moléculaire de ces larves à partir du séquençage d'un fragment du gène mitochondrial codant pour la cytochrome oxydase I (COI). Cette séquence diagnostique a été choisie chez *Pectinaria koreni* et *Owenia fusiformis* pour plusieurs raisons : (i) des protocoles pour l'amplification de ce gène ont été mis au point chez des organismes adultes (Jolly *et al.*, 2005, 2006; Thiercelin, 2007), (ii) les séquences de ce gène ont été décrites (Jolly *et al.*, 2005, 2006), et (iii) l'analyse de ces séquences a mis en évidence l'existence de plusieurs lignées évolutives distinctes le long des côtes atlantiques françaises, suggérant en particulier l'existence de plusieurs espèces

cryptiques (Jolly *et al.*, 2005, 2006). Par ailleurs, le gène mitochondrial 16S a déjà été séquencé avec succès chez des individus adultes des deux espèces cibles (Jolly *et al.*, 2006). L'amplification et le séquençage de ce gène ont donc aussi été testées.

Ainsi, le séquençage du gène de la COI et/ou 16S chez les larves de *Pectinaria koreni* et *Owenia fusiformis* échantillonnées au printemps 2008 dans le Nord du Golfe de Gascogne devrait permettre (i) de confirmer les identifications au niveau spécifique et basées sur des critères morphologiques, et (ii) de décrire la distribution spatio-temporelle de larves issues de différentes lignées évolutives. En effet, les larves de ces deux espèces sont morphologiquement proches de larves d'espèces voisines et présentes dans la zone d'étude (*i.e. Pectinaria auricoma*, *Myriochele heeri*).

Tableau A.1 – Méthodes moléculaires d'identification des larves d'invertébrés à cycle bentho-pélagique. PCR (*polymerase chain reaction*) : réaction en chaîne de polymérisation.

| Technique | Principe | Utilisation pour l'identification au niveau spécifique |
|---|---|---|
| Anticorps spécifiques | Reconnaissance et marquage des cellules des larves par des anticorps monoclonaux ou polyclonaux | Larves des moules du genre *Mytilus* le long des côtes de Galice (Lorenzo-Abalde *et al.*, 2005; Pérez *et al.*, 2009) |
| Hybridation *in situ* couplée à de la détection par fluorescence (*fluorescent in situ hybridization* ou FISH) | Sondes spécifiques oligonucléotidiques d'ADN capables de s'hydrider *in situ* et d'émettre un signal fluorescent détectable (identification et visualisation directes des larves contenues dans un échantillon de méroplancton) | Larves de bivalves dans la baie de Morlaix (Le Goff-Vitry *et al.*, 2007a,b) |
| Polymorphisme de longueur de fragments de restriction (*restriction fragment length polymorphism* ou RFLP) | Polymorphisme de longueur des fragments de restrictions obtenus à la suite de la digestion d'une séquence d'ADN diagnostique par des enzymes de restriction particuliers | Larves de bivalves dans la baie de Maizuru au Japon (Hosoi *et al.*, 2004) ; larves de moules hydrothermales récoltées le long de la dorsale médio-Atlantique (Comtet *et al.*, 2000) |
| Amplification aléatoire d'ADN polymorphe (*random amplified polymorphic DNA* ou RAPD) | Amplification par PCR de régions redondantes du génome en utilisant une unique amorce choisie aléatoirement, et identification des organismes selon le polymorphisme des fragments amplifiés | Larves de bivalves intertidaux et en particulier des coques du genre *Cerastoderma* (André *et al.*, 1999) |
| Amplification par PCR de *loci* microsatellites | Polymorphisme des *loci* microsatellites hypervariables et spécifiques | Larves d'huître (Morgan et Rogers, 2001) |
| Amplification puis hybridation | Amplification d'une séquence cible du génome par PCR suivie d'une hybridation à une sonde luminescente ou radioactive | Larves d'holoturie et description des distributions horizontale et verticale de ces larves dans le Golfe du Maine (Medeiros-Bergen *et al.*, 1995, marqueur : $ADN_{mt}$ 16S) |
| PCR multiples et imbriquées (*single step nested multiplex PCR* ou SSNM-PCR) | Amplification en une étape de PCR de plusieurs gènes diagnostiques en utilisant plusieurs amorces et identification de larves selon la taille des amplificats obtenus par PCR multiples | Larves de bivalves (Hare *et al.*, 2000; Larsen *et al.*, 2005, marqueurs respectifs : $ADN_{mt}$ COI, $ADN_n$ 18S), et description de la composition des assemblages de larves de bivalves et la distribution spatiale de ces larves dans plusieurs estuaires danois (Hansen et Larsen, 2005; Larsen *et al.*, 2007) |
| Amplification par PCR et séquençage des séquences d'ADN diagnostiques | Comparaison des séquences obtenues | Larves d'échinoderme récoltées en Mer du Nord (Kirby et Lindley, 2005, marqueur : $ADN_{mt}$ 16S) |

### A.2.2 Matériels et méthodes

#### *A.2.2.1 Préparation des échantillons et extraction de l'ADN larvaire*

À partir des échantillons de zooplancton récoltés au filet WP2 au printemps 2008 dans le Nord du Golfe de Gascogne lors des missions LARVASUD et conservés dans l'éthanol à 96 %, des larves identifiées morphologiquement comme des larves de *Pectinaria koreni* et *Owenia fusiformis* ont été prélevées individuellement, sous loupe binoculaire, dans 5 µl d'éthanol. Chaque larve a été rincée dans un bain de 500 µl de PBS (solution saline de phosphate tamponné contenant 0.1% de Tween 20), puis prélevée dans un volume de 0,5 µl de PBS et transférée dans un tube Eppendorf de 1,5 ml.

Deux protocoles d'extraction de l'ADN larvaire ont alors été testés. La première méthode, dite méthode d'Hygushi, repose sur la digestion des larves par la protéinase K dans un tampon particulier (tampon d'Hygushi). Pour chaque larve isolée dans un tube Eppendorf de 1,5 ml, 30 µl de tampon d'Hygushi puis 3 µl de protéinase K ont été ajoutés, avant incubation à 56°C pendant 1h. L'échantillon a ensuite été placé à 95°C pendant 15 minutes pour désactiver la protéinase K, et enfin disposé sur glace pour refroidir. L'échantillon d'ADN larvaire a ensuite été stocké au réfrigérateur ou au congélateur.

Le seconde méthode d'extraction de l'ADN larvaire repose sur l'utilisation du kit d'extraction NucleoSpin Tissue XS (Macherey-Nagel GmbH & Co. KG, Allemagne), conçu pour permettre l'extraction d'ADN d'un petit échantillon biologique (de quelques milligrammes). Cette méthode repose sur la digestion complète de la larve, puis le passage de l'échantillon digéré sur colonne de filtration pour obtenir de l'ADN purifié. Suivant les consignes du fabricant, le protocole se divise en huit étapes présentées dans le Tableau A.2.

Au vue des résultats d'amplification et de séquençage obtenus par la suite, cette dernière méthode semble fournir de meilleurs résultats.

Tableau A.2 – Protocole d'extraction de l'ADN larvaire en utilisant le kit d'extraction NucleoSpin Tissue XS.

| Étape | Protocole détaillé |
|---|---|
| 1. Préparation de l'échantillon | |
| 2.Pré-lyse | Ajout de 80 µl de tampon T1<br>Centrifugation rapide<br>Ajout de 8 µl de protéinase K<br>Léger vortex et centrifugation rapide<br>Incubation à 56°C dans un bain à sec pendant 3 h<br>Vérification à la loupe binoculaire du succès de la digestion |
| 3. Lyse | Ajout de 80 µl de solution B7<br>Passage au vortex, 2 fois 5 secondes<br>Incubation à 70°C pendant 5 minutes |
| 4. Ajustement du milieu de réaction | Ajout de 80 µl d'éthanol absolu<br>Passage au vortex, 2 fois 5 secondes<br>Centrifugation rapide |
| 5. Liaison de l'ADN | Disposer les colonnes dans les puits<br>Placer 240 µl de chaque échantillon sur une colonne<br>Centrifugation à 11000g pendant 1 minute<br>Vérification que la colonne est vide |
| 6. Lavage de la membrane | Ajout de 50 µl de tampon de rinçage B5 (premier rinçage)<br>Centrifugation à 11000g pendant 1 minute<br>Ajout de 50 µl de tampon de rinçage B5 (second rinçage)<br>Centrifugation à 11000g pendant 2 minutes |
| 7. Élution de l'ADN | Placer la colonne dans un tube Eppendorf de 1,5 ml<br>Ajouter 20 µl de tampon d'élution BE<br>Centrifugation à 11000g pendant 1 minute |
| 8. Élimination du surplus l'alcool | Laisser les tubes ouverts pendant une dizaine de minutes<br>Stockage au réfrigérateur |

#### *A.2.2.2 Amplification des séquences d'ADN cibles*

L'amplification par réaction de polymérisation en chaîne (PCR) permet d'obtenir une grande quantité de fragments d'un segment d'ADN cible, sélectionné grâce à des amorces spécifiques. En plus de l'amplification des deux séquences d'$ADN_{mt}$ cibles (COI et 16S), un fragment du gène nucléaire 18S a été amplifié afin de vérifier la qualité des extractions d'ADN.

Pour amplifier le gène de la COI, trois jeux d'amorces ont été utilisés : les amorces extérieures M1 et M2 de Nelson et Fisher (2000), les amorces universelles LCO et HCO telles que définies par Folmer *et al.* (1994), et les amorces OwCOIF et OwCOIR conçues spécifiquement pour *Owenia fusiformis* par Thiercelin (2007). Pour amplifier le gène mitochondrial 16S, les amorces universelles 16Sar-L et 16Sbr-L de Palumbi *et al.* (1991) ont été utilisées. Enfin, pour amplifier le gène nucléaire 18S, les amorces universelles Uni1304F et Uni1670R (MWG Biotech) ont été utilisées.

Chaque amplification s'est déroulée dans un milieu réactif de 15 µl contenant 1,5 µl de tampon 10X (Euroclone), 1,2 µl de solution de $MgCl_2$ à 25 mM (Euroclone), 0,3 µl de dNTPs à 10 mM (soit à une concentration de 2,5 mM par dNTP) (ABgene), 0,6 µl de chacune des amorces directe et indirecte à 10µM, 0,1 µl de Taq polymerase Thermoprime Hi Fidelity (ABgene), 8,7 µl d'eau MiliQ stérile, et 2 µl de la solution d'ADN extrait.

Les réactions de PCR ont été réalisées dans un thermocycleur GeneAmp PCR System 2700 (Applied Biosystems). Différents programmes ont été utilisés en fonction des amorces utilisées (Tableau A.3).

Les produits de PCR ont ensuite été visualisés sous lumière UV après électrophorèse sur gel d'agarose à 1 % (Ultra-pure DNA-Grade agarose, Eurogenetec) contenant du bromure d'éthidium (BET) avec 3µl de BET pour un gel de 100 ml de triborate EDTA (TBE).

Tableau A.3 – Cycles d'amplification (T. Comtet, com.pers. ; Jolly *et al.*, 2005, 2006; Thiercelin, 2007).

| Amorces | Conditions |
|---|---|
| Amorces COI<br>extérieures M1 M2<br>(Nelson et Fisher, 2000) | (1) une dénaturation initiale à 94°C de 4 minutes<br>(2) 40 cycles avec :<br>- 1 minute de dénaturation à 94°C<br>- 1 minute d'hybridation avec l'amorce à 50°C<br>- 1 minute 30 secondes d'élongation à 72°C<br>(3) une élongation finale à 72°C de 10 minutes |
| Amorces COI<br>universelles Folmer<br>(Folmer *et al.*, 1994) | (1) une dénaturation initiale à 94°C de 4 minutes<br>(2) 5 cycles avec :<br>- 35 secondes de dénaturation à 94°C<br>- 35 secondes d'hybridation avec l'amorce à 45°C<br>- 1 minute 10 secondes d'élongation à 72°C<br>(3) 35 cycles avec :<br>- 35 secondes de dénaturation à 94°C<br>- 35 secondes d'hybridation avec l'amorce à 50°C<br>- 1 minute 10 secondes d'élongation à 72°C<br>(4) une élongation finale à 72°C de 7 minutes |
| Amorces COI<br>spécifiques OwCOIF et OwCOIR<br>(Thiercelin, 2007) | (1) une dénaturation initiale à 94°C de 4 minutes<br>(2) 40 cycles avec :<br>- 35 secondes de dénaturation à 94°C<br>- 35 secondes d'hybridation avec l'amorce à 56°C<br>- 1 minute 20 secondes d'élongation à 72°C<br>(3) une élongation finale à 72°C de 10 minutes |
| Amorces 16S<br>universelles 16Sar-L et 16Sbr-L<br>(Palumbi *et al.*, 1991) | (1) une dénaturation initiale à 94°C de 2 minutes<br>(2) 35 cycles avec :<br>- 35 secondes de dénaturation à 94°C<br>- 35 secondes d'hybridation avec l'amorce à 50°C<br>- 35 secondes d'élongation à 72°C<br>(3) une élongation finale à 72°C de 7 minutes |
| Amorces 18S<br>universelles Uni1304F et Uni1670R<br>(MWG Biotech) | (1) une dénaturation initiale à 94°C de 4 minutes<br>(2) 35 cycles avec :<br>- 1 minute de dénaturation à 94°C<br>- 1 minute d'hybridation avec l'amorce à 57°C<br>- 1 minute d'élongation à 72°C<br>(3) une élongation finale à 72°C de 7 minutes |

Plusieurs protocoles d'amplification ont été testés, en particulier :

- Amplification de la COI avec les amorces universelles Folmer, chez *Pectinaria koreni* et *Owenia fusiformis* ;
- Amplification de la COI avec les amorces spécifiques OwCOIF et OwCOIR chez *Owenia fusiformis* ;
- Amplification de la COI avec les amorces extérieures M1 et M2, puis seconde amplification avec les amorces universelles Folmer des amplificats obtenus chez *Pectinaria koreni* et *Owenia fusiformis* ;
- Amplification de la COI avec les amorces universelles Folmer, puis seconde amplification avec les amorces spécifiques OwCOIF et OwCOIR des amplificats obtenus chez *Owenia fusiformis* ;
- Amplification du 16S avec les amorces universelles 16Sar-L et 16Sbr-L chez *Pectinaria koreni* ;
- Amplification du 18S avec les amorces universelles Uni1304F et Uni1670R chez *Pectinaria koreni* et *Owenia fusiformis*.

#### *A.2.2.3 Séquencage des produits d'amplification et alignement des séquences*

Le séquençage des produits des amplifications a été réalisé au sein de la Plateforme Genomer de la Station Biologique de Roscoff. Les produits de PCR ont été purifiés selon le protocole ExoSAP-IT et séquencés grâce à un séquenceur ABI 3100 en utilisant la chimie de séquençage BigDye terminator (Perkin Elmer) selon le protocole du fabriquant. Le séquençage a été réalisé dans un sens uniquement, à partir de l'amorce universelle LCOI de Folmer *et al.* (1994), de l'amorce spécifique OwCOIF de Thiercelin (2007), ou de l'amorce 16Sbr-L de Palumbi *et al.* (1991).

Les premières séquences ainsi obtenues ont été lues grâce au logiciel BioEdit Sequence Alignment 7.0.1 (Hall, 1999). Seules les séquences dont le chromatogramme était de bonne

qualité seront présentées ici, l'étape de correction des séquences n'ayant pas encore été réalisée. Les résultats de séquençage sont donc préliminaires.

### A.2.3 Premiers résultats obtenus

#### *A.2.3.1 Résultats des amplifications*

Le succès des amplifications d'ADN nucléaire 18S confirme que les protocoles d'extraction d'ADN larvaire ont correctement fonctionné (Tableau A.4). Cependant, à la lecture des gels de migration des produits de ces PCR, de meilleurs résultats ont été obtenus sur l'ADN larvaire extrait selon le protocole de kits d'extraction NucleoSpin Tissue XS (taux de succès de 4/8 contre 1/8, *cf.* Figure A.3D). Cette technique d'extraction semble donc préférable à la méthode d'Hygushi.

Des amplifications réalisées sur des solutions diluées d'ADN larvaire semblent indiquer que la quantité d'ADN extrait est suffisante pour permettre des PCR et ne peut aussi être mise en cause dans les échecs des réactions d'amplification.

Tableau A.4 – Succés des réactions d'amplification. Le succès d'une amplification est ici défini comme le rapport entre le nombre d'individus pour lesquels une bande lumineuse individualisée est identifiée, à la lecture des gels de migration des amplificats, sur le nombre total d'individus dont l'ADN a été amplifié. Le succès du séquençage est défini comme le nombre de séquences exploitables sur le nombre total d'individus dont l'ADN a été séquencé.

| Organisme | Protocole de PCR | Succès de la PCR | Figure | Succès du séquençage |
|---|---|---|---|---|
| *P. koreni* | 18S | 11/16 | A.2A | |
| | 18S sur ADN dilué | 13/16 | A.2B | |
| | COI Folmer sans pré-cycles | 0/16 (smear) | A.2C | |
| | COI Folmer | 0/34 | | |
| | COI M1 M2 | 0/34 | | |
| | COI M1 M2 puis Folmer | 1/21 | A.2D | 1/2 |
| | 16S | 4/16 | A.2E | 2/4 |
| *O.fusiformis* | 18S | 16/16 | A.3A | |
| | COI Folmer sans pré-cycle | 0/16 | A.3B | |
| | COI M1 M2 | 0/16 | A.3C | |
| | COI M1 M2 puis Folmer | 5/16 | A.3D | |
| | COI M1 M2 puis Folmer puis OwCOI | 8/16 | A.3E | 0/16 |
| | COI OwCOI | 8/16 | A.3F | 6/6 |

L'amplification du gène mitochondrial de la COI semble de meilleure qualité lorsque les protocoles suivants sont utilisés (Tableau A.4) :

- chez *Pectinaria koreni*, lorsque deux réactions d'amplification sont emboîtées, avec une première PCR utilisant les amorces COI externes M1 et M2 et une seconde PCR utilisant les amorces COI universelles Folmer (avec pré-cycles) ;
- chez *Owenia fusiformis*, lorsque la PCR utilise les amorces COI spécifiques Owenia, ou bien lorsque deux réactions d'amplification sont emboîtées, avec une première PCR utilisant les amorces COI externes M1 et M2 et une seconde PCR utilisant les amorces COI universelles Folmer (avec pré-cycles).

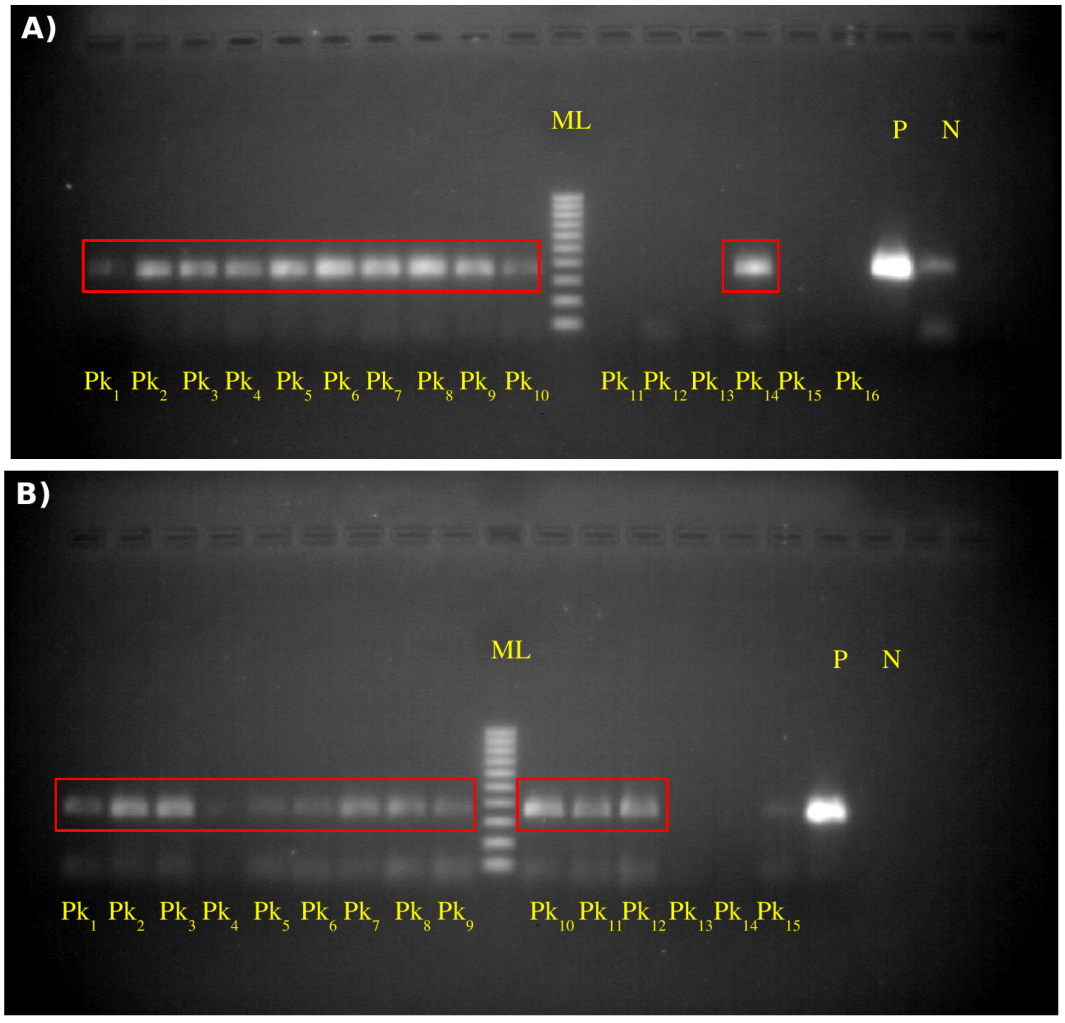
A)
ML
P
N
Pk1 Pk2 Pk3 Pk4 Pk5 Pk6 Pk7 Pk8 Pk9 Pk10
Pk11 Pk12 Pk13 Pk14 Pk15 Pk16
B)
ML
P
N
Pk1 Pk2 Pk3 Pk4 Pk5 Pk6 Pk7 Pk8 Pk9
Pk10 Pk11 Pk12 Pk13 Pk14 Pk15

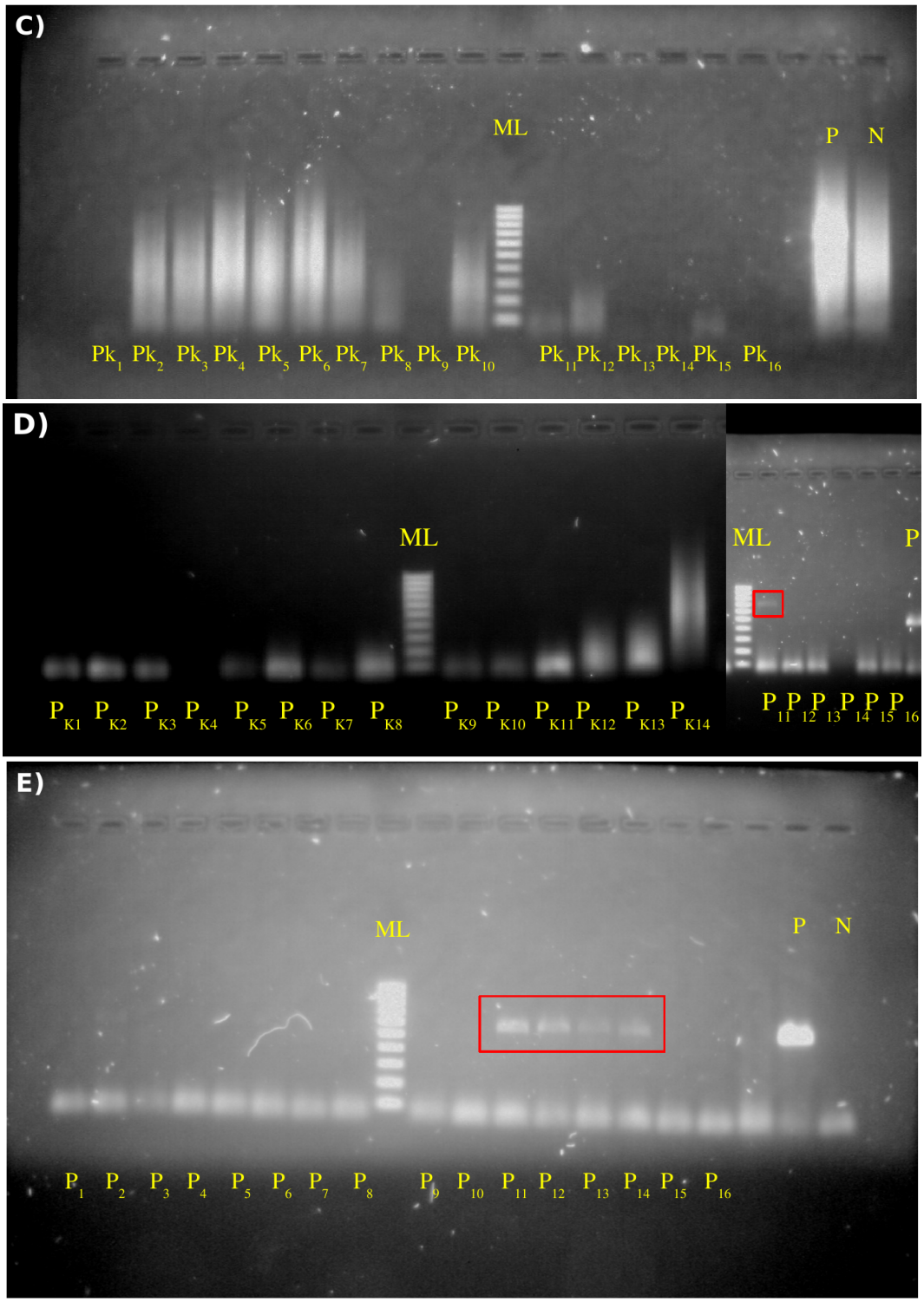


Figure A.2 – Migrations sur gel des produits de PCR chez *Pectinaria*, avec de haut en bas et de gauche à droite : A) PCR 18S, B) PCR 18S sur ADN larvaire dilué, C) PCR COI Folmer sans pré-cycle, D) PCR COI M1 M2 puis Folmer (avec pré-cycle), E) PCR 16 S. Pour chaque larve de *Pectinaria*, l'ADN a été extrait selon le protocole d'extraction par kit NucleoSpin Tissue XS. ML : marqueur de longueur, P : contrôle positif, N : contrôle négatif.

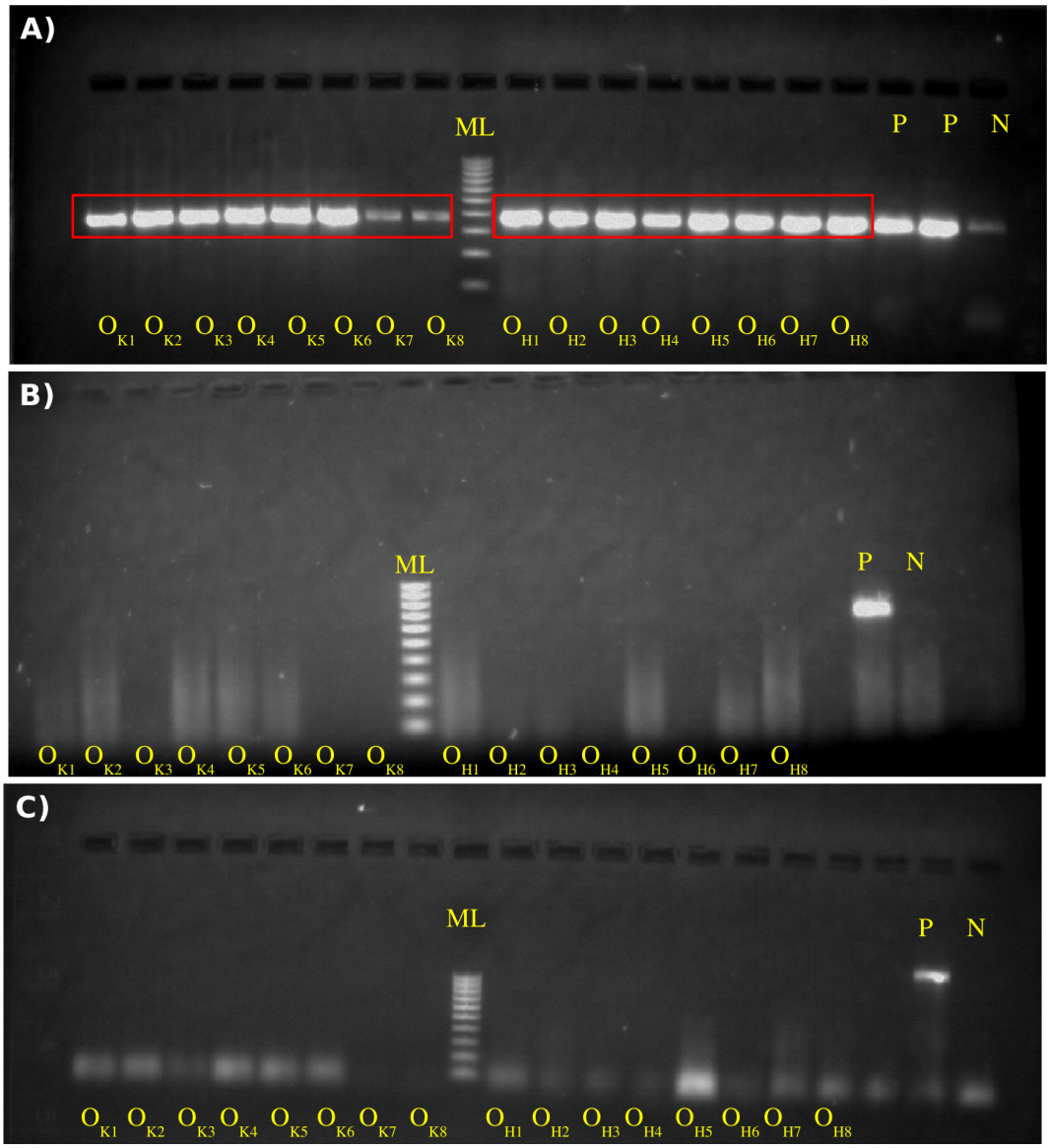
A)
ML
P P N
O K1 O K2 O K3 O K4 O K5 O K6 O K7 O K8 O H1 O H2 O H3 O H4 O H5 O H6 O H7 O H8
B)
ML
P N
O K1 O K2 O K3 O K4 O K5 O K6 O K7 O K8 O H1 O H2 O H3 O H4 O H5 O H6 O H7 O H8
C)
ML
P N
O K1 O K2 O K3 O K4 O K5 O K6 O K7 O K8 O H1 O H2 O H3 O H4 O H5 O H6 O H7 O H8

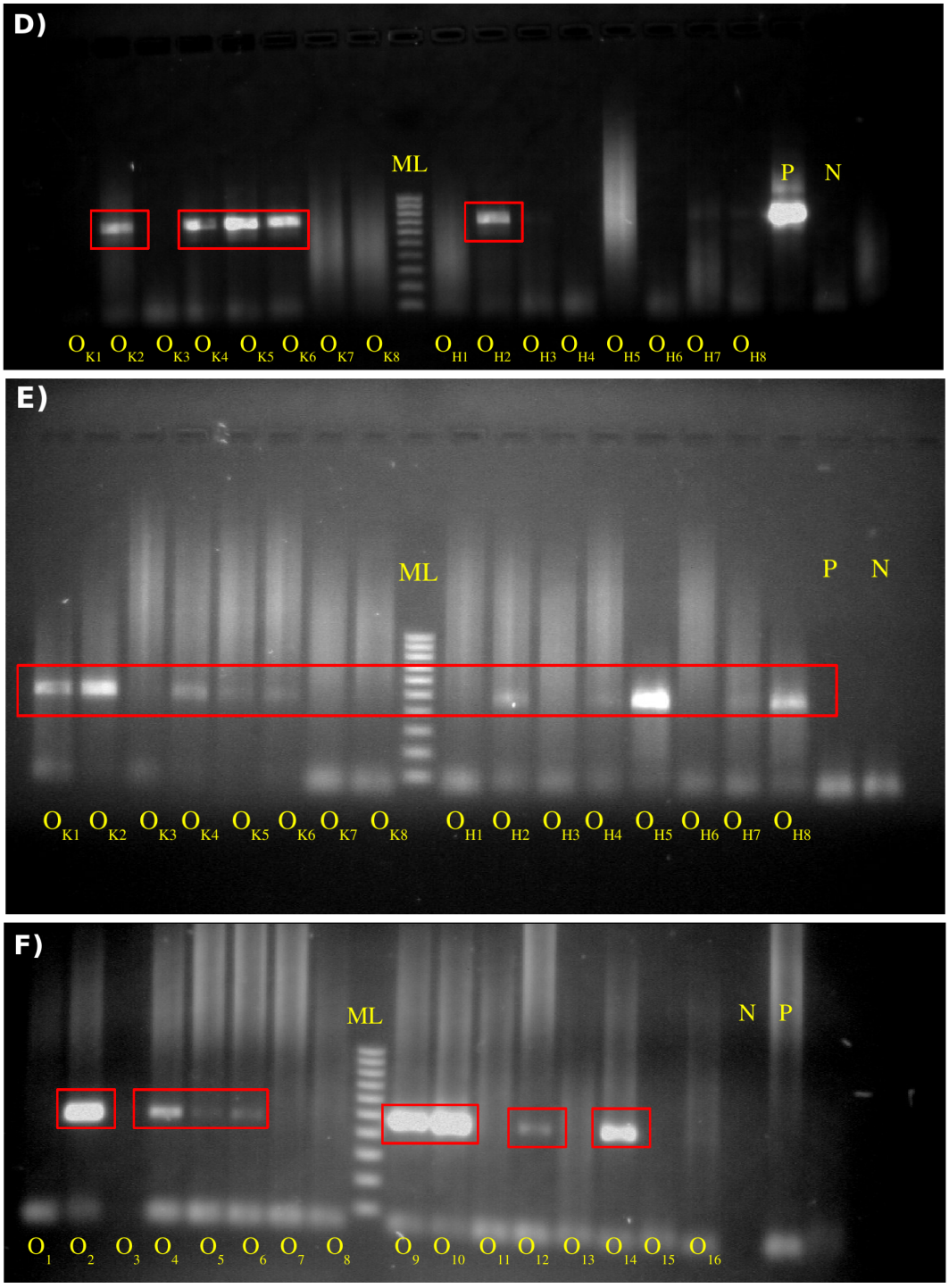


Figure A.3 – Migrations sur gel des produits de PCR chez *Owenia*, avec de haut en bas et de gauche à droite : A) PCR 18S, B) PCR COI Folmer sans pré-cycle, C) PCR COI M1 M2, D) PCR COI M1 M2 puis Folmer (avec pré-cycle), E) PCR COI M1 M2 puis Folmer (avec pré-cycle) puis spécifique, F) PCR COI spécifique. Pour chaque larve de *Owenia*, l'ADN a été extrait selon le protocole d'Hygushi (individus numérotés $O_{Hi}$) ou selon le protocole d'extraction par kit NucleoSpin Tissue XS (individus numérotés $O_{Ki}$ et $O_i$). ML : marqueur de longueur, P : contrôle positif, N : contrôle négatif.

### A.2.3.2 Résultats préliminaires de séquençage

Des résultats préliminaires de séquençage, c'est-à-dire des séquences brutes telles qu'obtenues à la sortie du séquenceur, ont été acquis pour trois protocoles d'amplification (*cf.* protocoles du Tableau A.4) :

- amplification du gène 16S chez *Pectinaria koreni* (séquence amplifiée d'environ 550 paires de base) (Figure A.4),
- amplification du gène COI chez *Pectinaria koreni* (séquence amplifiée d'environ 600 paires de base) (Figure A.5),
- amplification du gène COI chez *Owenia fusiformis* à partir d'une seule PCR spécifique (séquence amplifiée d'environ 450 paires de base) (Figure A.6).

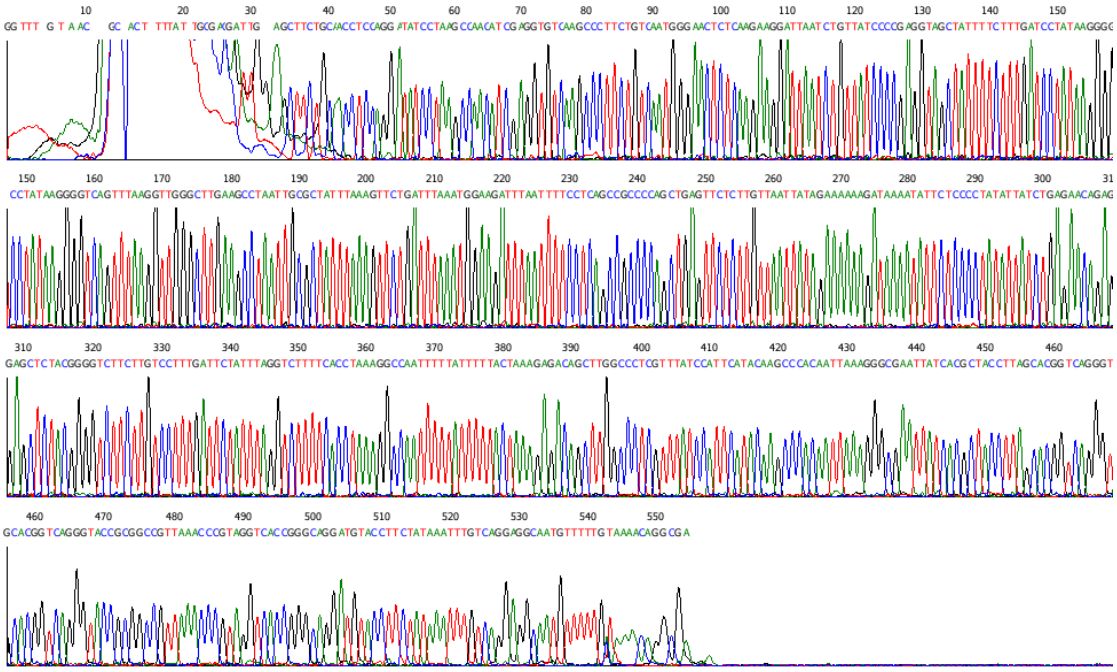

Figure A.4 – Chromatogramme d'une séquence brute obtenue après séquençage et amplification du gène 16S chez *Pectinaria*. Individus $P_{11}$ dont le produit de l'amplification est visible Figure A.2D. Larve échantillonnée en May 2008 en Bretagne Sud à proximité de l'embouchure de la Vilaine (station V1).

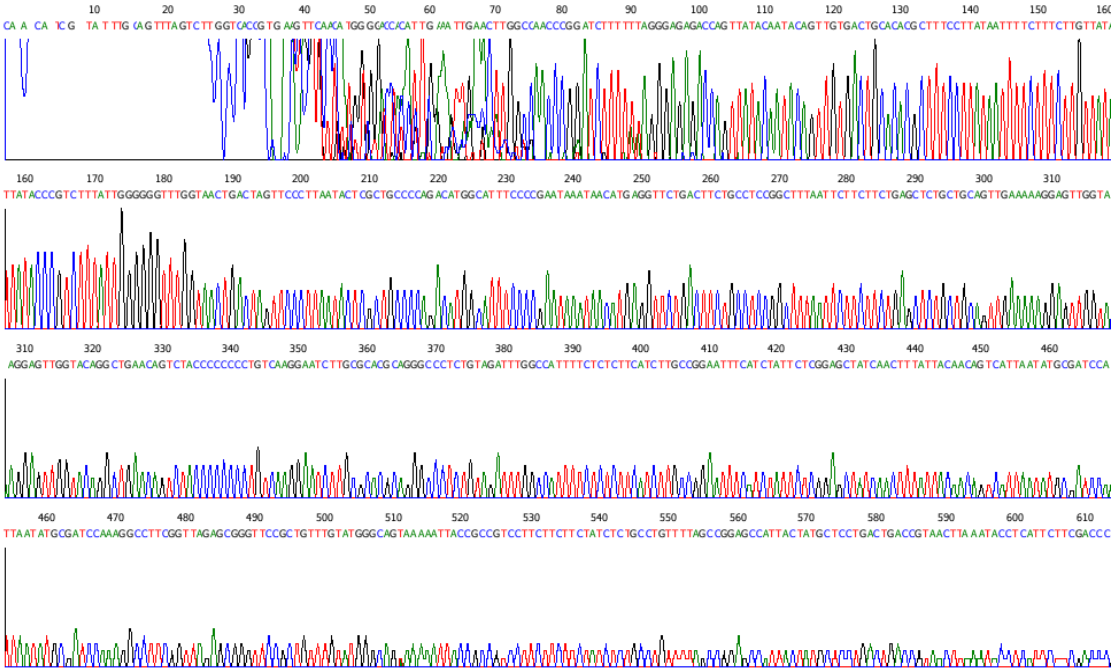

Figure A.5 – Chromatogramme d'une séquence brute obtenue après séquençage et amplification du gène COI chez *Pectinaria*. Individus $P_{11}$ dont le produit de l'amplification est visible Figure A.2E. Larve échantillonnée en May 2008 en Bretagne Sud à proximité de l'embouchure de la Vilaine (station V1).

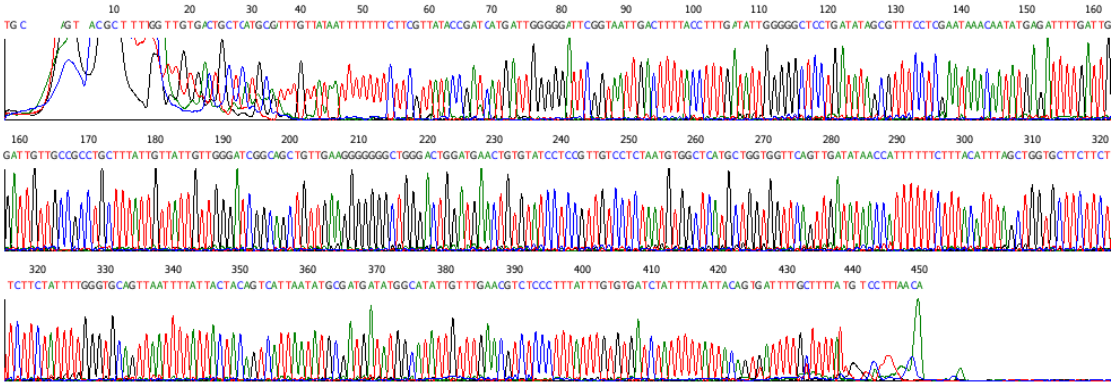

Figure A.6 – Chromatogramme d'une séquence brute obtenue après séquençage et amplification du gène COI chez *Owenia*. Individus $O_{10}$ dont le produit de l'amplification est visible Figure A.3F. Larve échantillonnée en May 2008 en Bretagne Sud à proximité de l'embouchure de la Vilaine (station V1).

Ces séquences brutes ont été comparées sous GenBank avec la fonction *blast*[a]. Ces résultats préliminaires confirment l'identification au niveau spécifique des larves de *Pectinaria koreni* et *Owenia fusiformis* à partir de critères morphologiques. De plus, ces résultats préliminaires semblent suggérer la présence dans les échantillons de méroplancton récoltés en Mai 2008 à l'embouchure de la Vilaine (station V1) du clade C2 de l'espèce *Pectinaria koreni* et du clade C1 de l'espèce *Owenia fusiformis* (pourcentage de couverture de 83 à 96 %, avec des identités maximales de 99 à 100 %).

Ces résultats préliminaires de séquençage devront être confirmés à l'issue de la correction de ces séquences à partir de la relecture des chromatogrammes obtenus puis de leur alignement avec des séquences références pour les deux espèces.

### A.2.4 Conclusions

En conclusion, ces résultats très préliminaires d'identification moléculaire des larves de *Pectinaria koreni* et *Owenia fusiformis* récoltées au printemps 2008 dans le Nord du Golfe de Gascogne ont confirmé les identifications au niveau spécifique basées sur des crièstres morphologiques. Cependant, l'utilisation en routine de l'identification moléculaire des larves de *Pectinaria koreni* et *Owenia fusiformis* demeure difficile étant donné son faible taux de succès.

Par ailleurs, les méthodes mises au point semblent être à même de permettre l'identification de larves issues de ces différentes lignées évolutives au sein de ces espèces. Le génotypage de larves échantillonnées devrait donc permettre de décrire la distribution spatio-temporelle des larves issues de différentes lignées évolutives. En effet, les lignées divergentes de *O. fusiformis* (clades 1 et 2) sont présentes en sympatrie dans le nord du Golfe de Gascogne (Jolly *et al.*, 2006). Ces lignées pourraient rester génétiquement distinctes s'il existe des différences phénologiques entre leurs périodes de reproduction, ce qui entrainerait une barrière reproductive entre ces lignées. L'identification de cohortes larvaires issues de lignées divergentes permettra ainsi de tester cette hypothèse.

[a]http ://blast.ncbi.nlm.nih.gov/Blast.cgi

## A.3 Distribution horizontale des différents stades larvaires

### A.3.1 Distribution horizontale des différents stades larvaires en Mai 2008

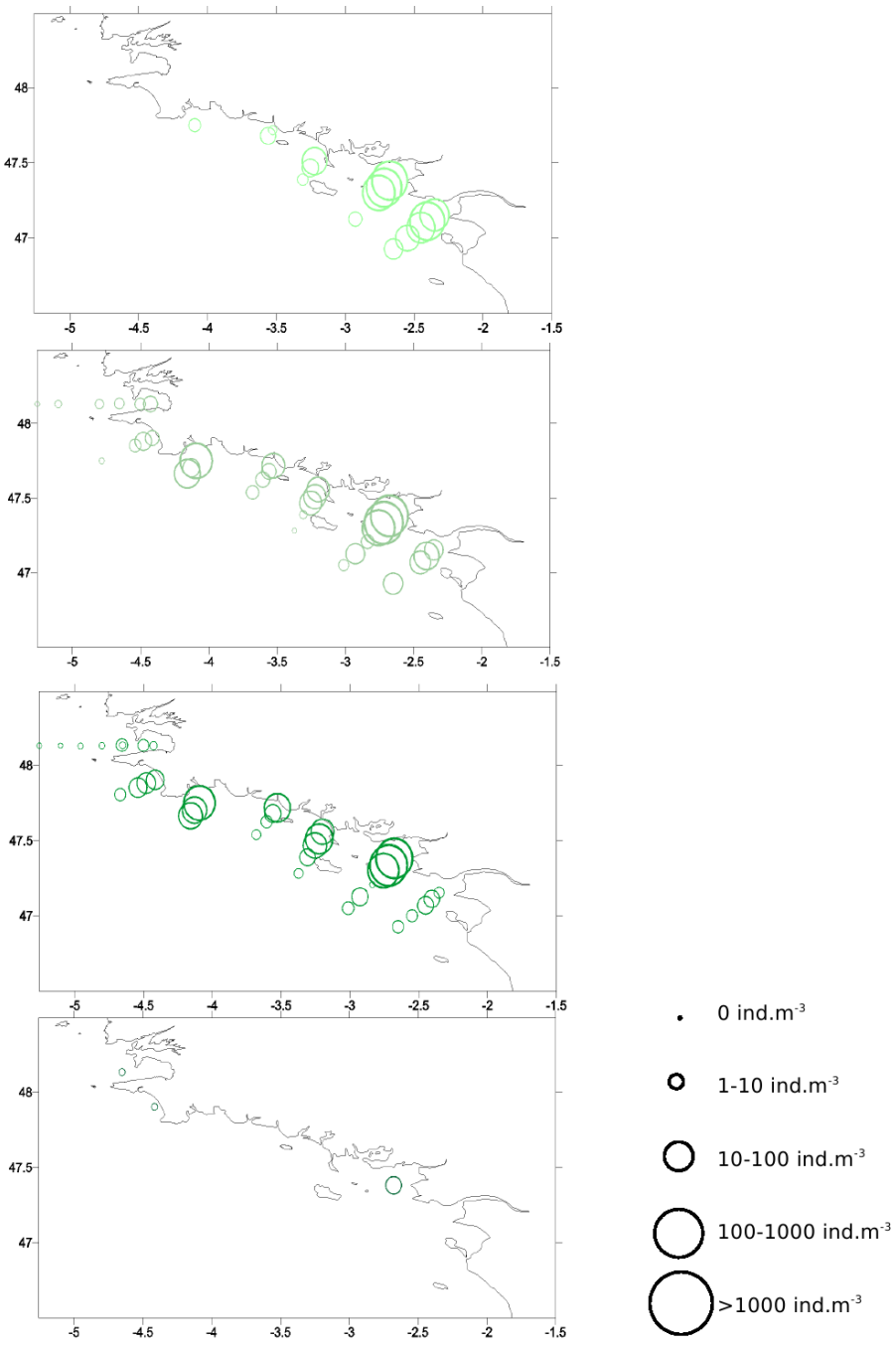


Figure A.7 – Distribution horizontale des différents stades larvaires de *Pectinaria koreni* en Mai 2008, avec de haut en bas : stade 1, stade 2, stade 3 et stade 4.

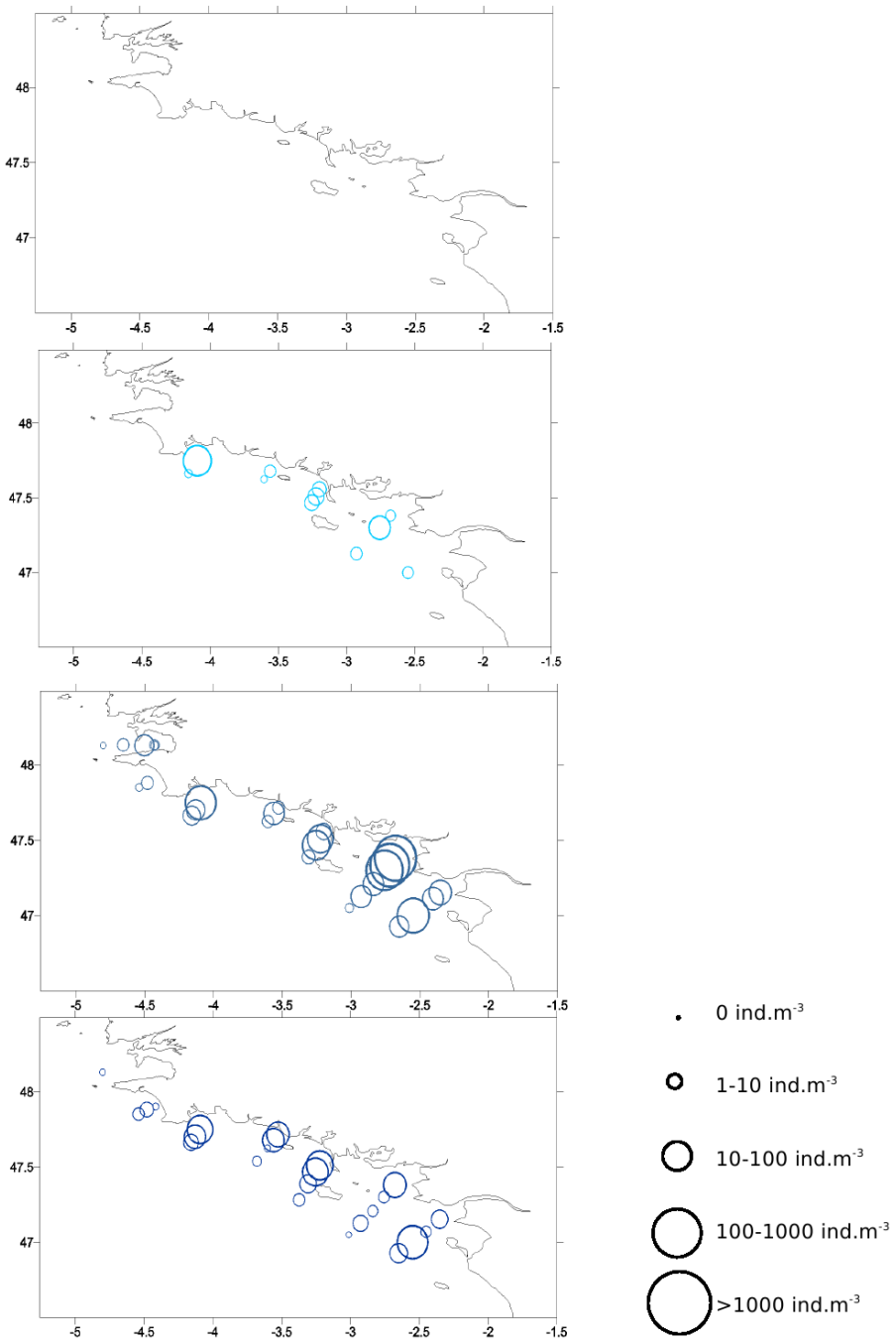


Figure A.8 – Distribution horizontale des différents stades larvaires de *Owenia fusiformis* en Mai 2008, avec de haut en bas : stade 1, stade 2, stade 3 et stade 4.

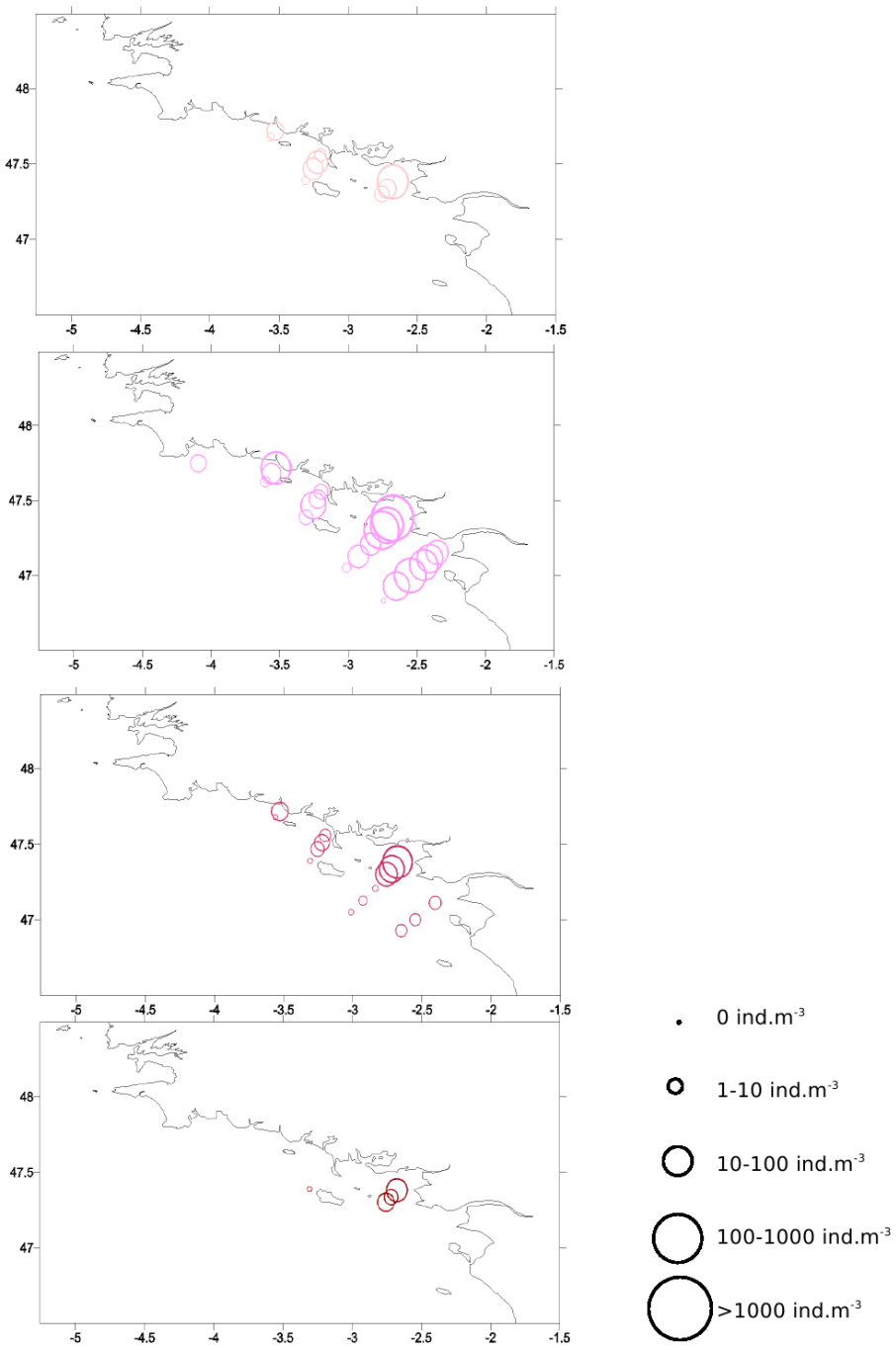


Figure A.9 – Distribution horizontale des différents stades larvaires de *Sabellaria alveolata* en Mai 2008, avec de haut en bas : stade 1, stade 2, stade 3 et stade 4.

### A.3.2 Distribution horizontale des différents stades larvaires en Juin 2008

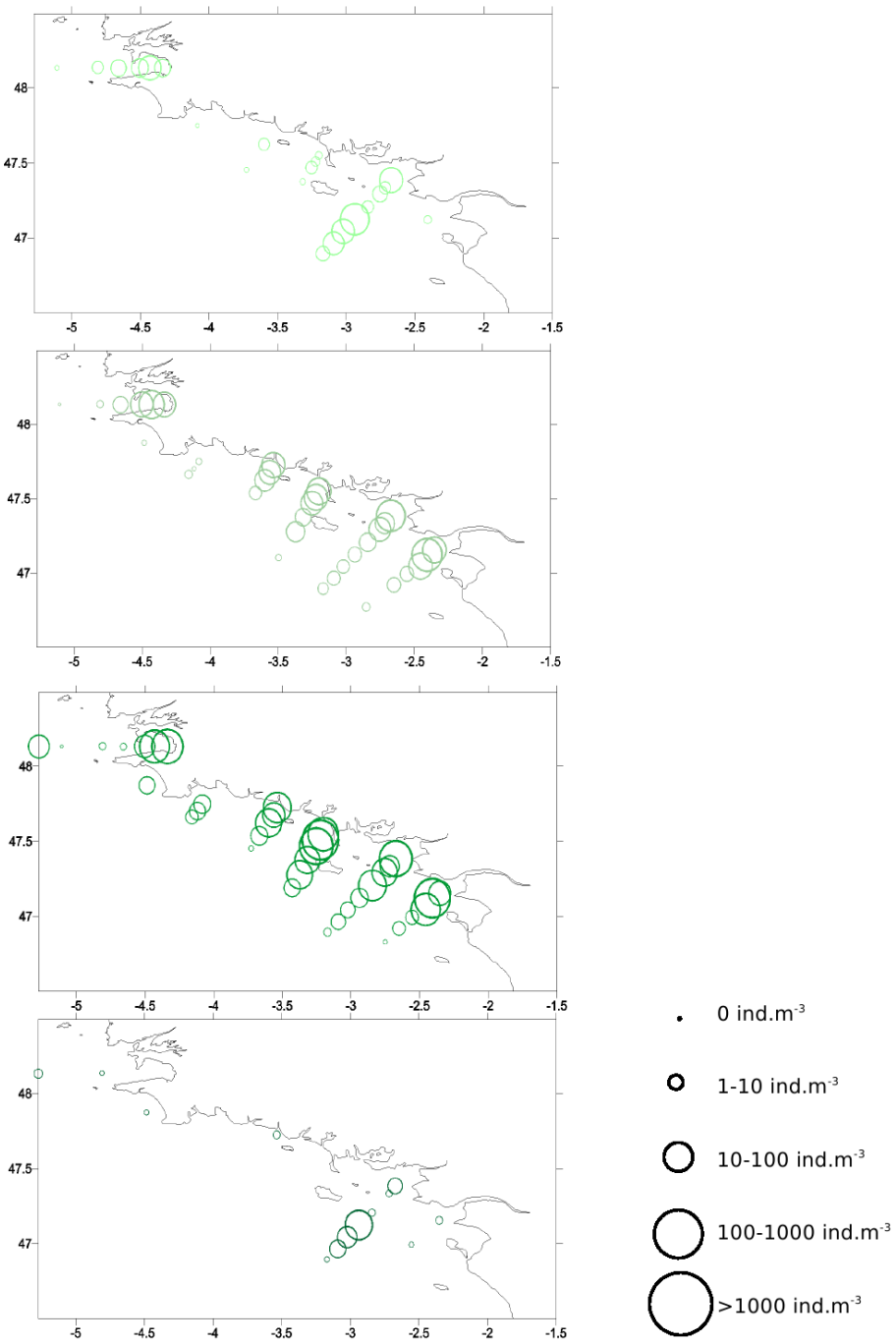


Figure A.10 – Distribution horizontale des différents stades larvaires de *Pectinaria koreni* en Juin 2008, avec de haut en bas : stade 1, stade 2, stade 3 et stade 4.

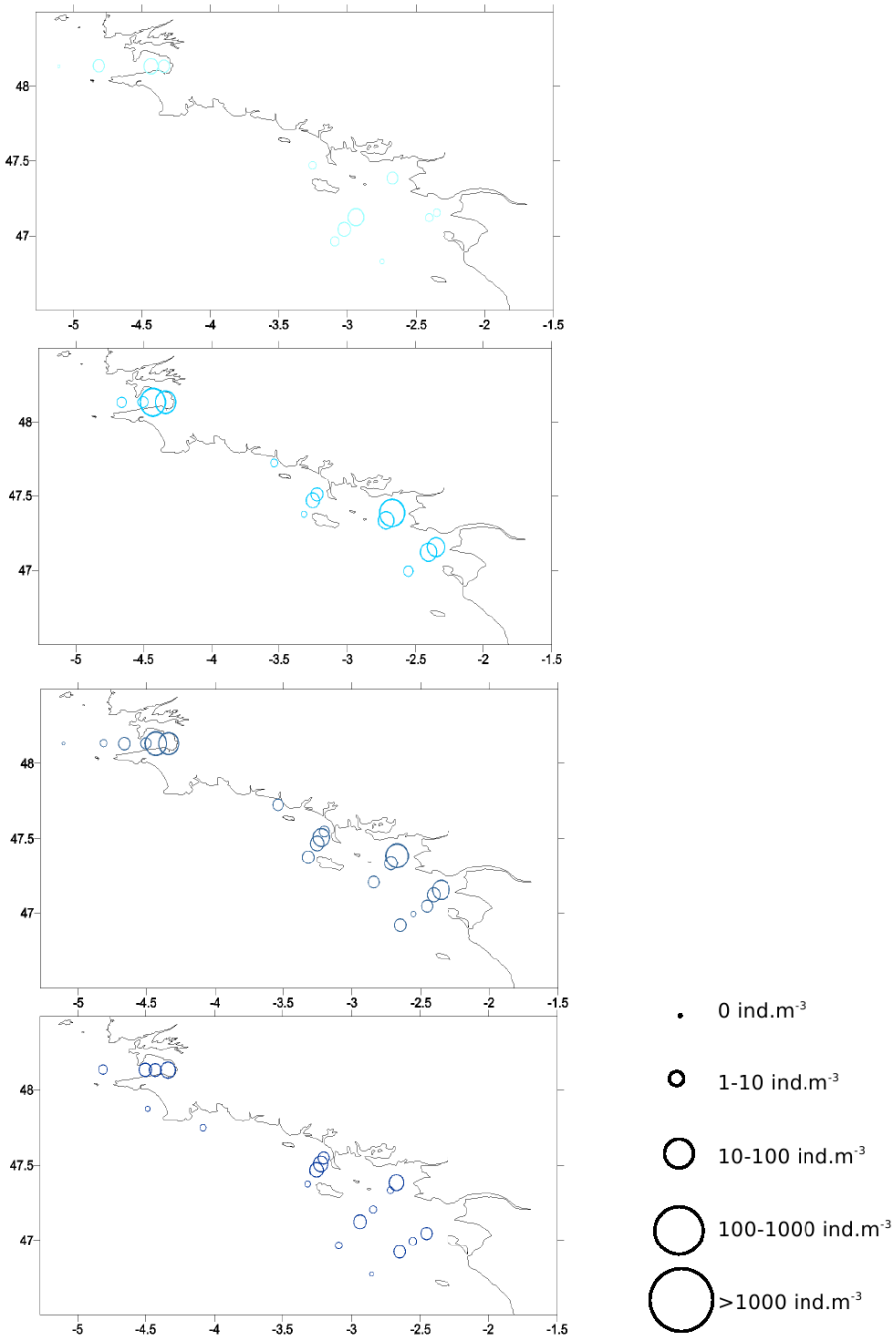


Figure A.11 – Distribution horizontale des différents stades larvaires de *Owenia fusiformis* en Juin 2008, avec de haut en bas : stade 1, stade 2, stade 3 et stade 4.

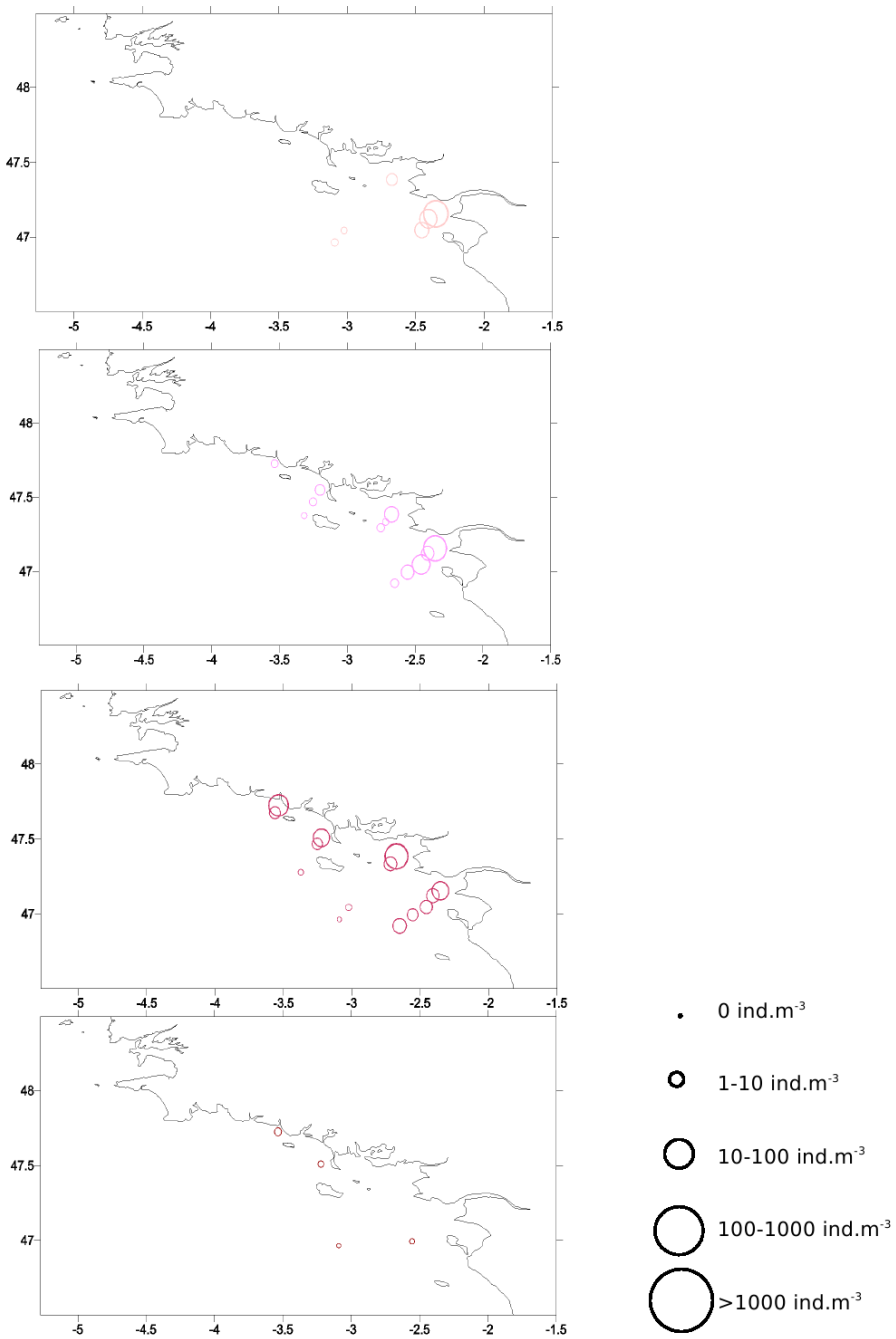


Figure A.12 – Distribution horizontale des différents stades larvaires de *Sabellaria alveolata* en Juin 2008, avec de haut en bas : stade 1, stade 2, stade 3 et stade 4.

### A.3.3 Analyse de redondance des distributions larvaires

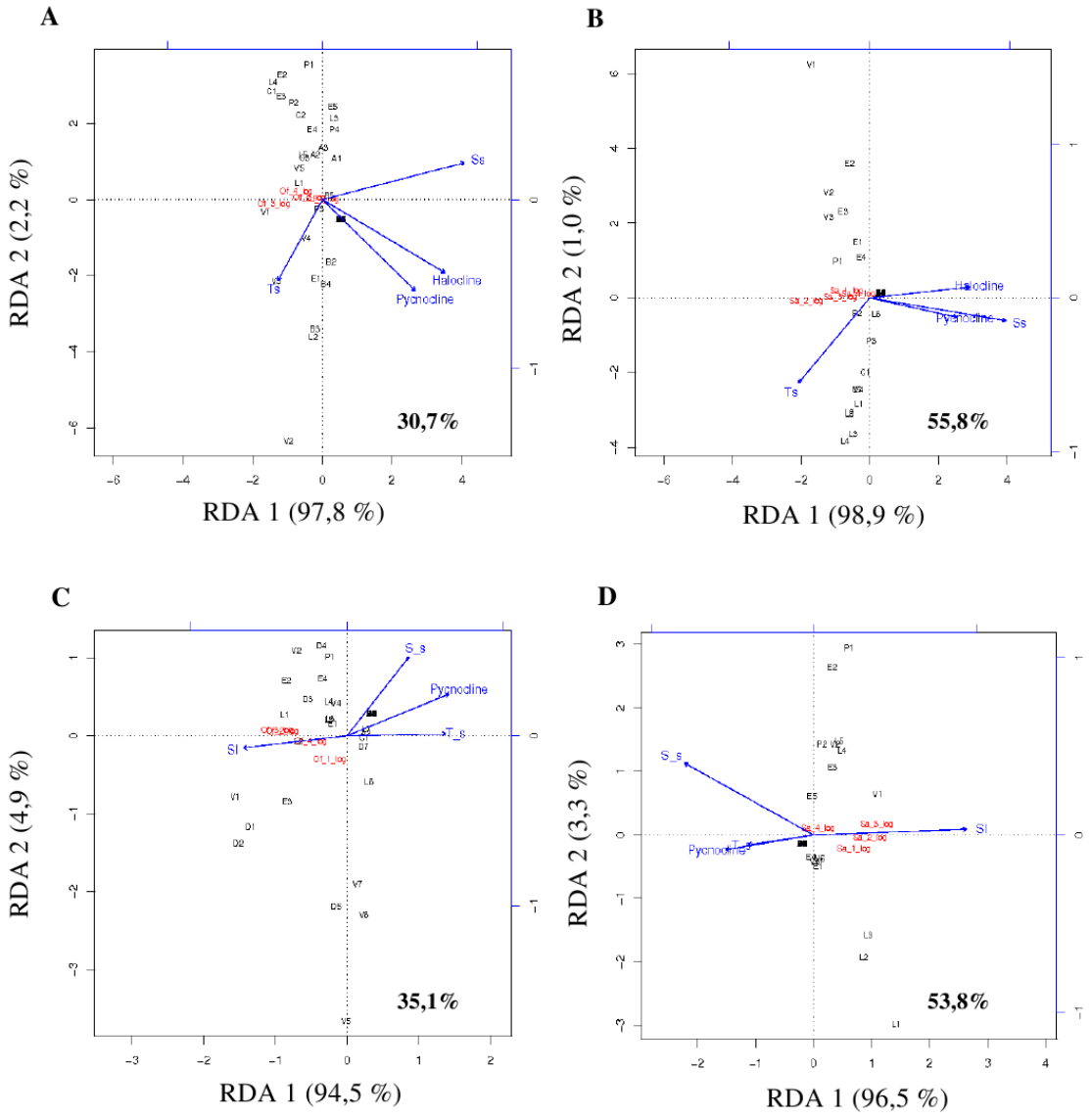


Figure A.13 – Analyses de redondance de la distribution des différents stades larvaires de (A) *Owenia fusiformis* en Mai 2008, (B) *Sabellaria alveolata* en Mai 2008, (C) *Owenia fusiformis* en Juin 2008, et (D) *Sabellaria alveolata* en Juin 2008. Le pourcentage de variance expliqué par chaque axe est indiqué, ainsi que le pourcentage de la variance totale expliqué par l'analyse.

## A.4 Distribution verticale des différents stades larvaires

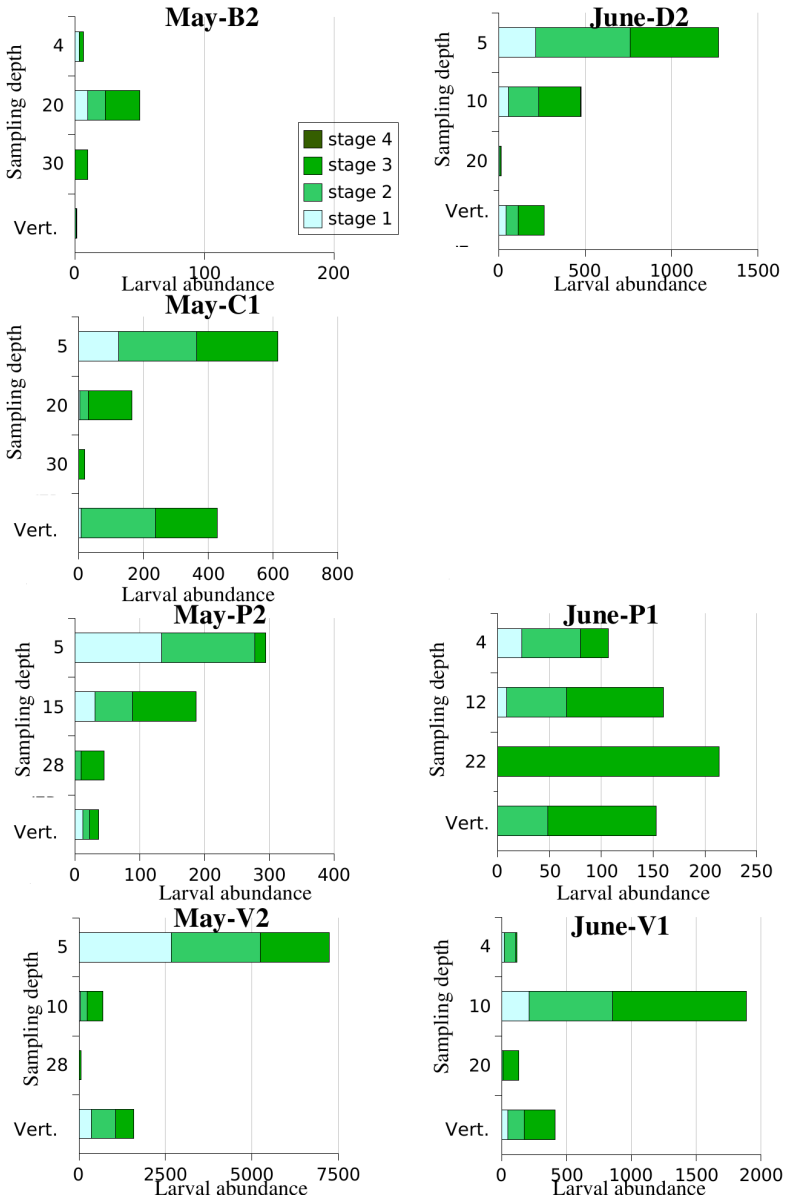


Figure A.14 – Vertical distribution of the larval stages of *P. koreni*. Larval abundances per sampling depth are given in larvae.m$^{-3}$. The sampling depth is indicated in m and correspond to the surface layer, the halocline and/or thermocline, and the bottom layer. The sampled station and the date of the cruise are indicated. The depth-averaged larval abundances obtained by vertical hauls of WP2 net are indicated (Vert.).

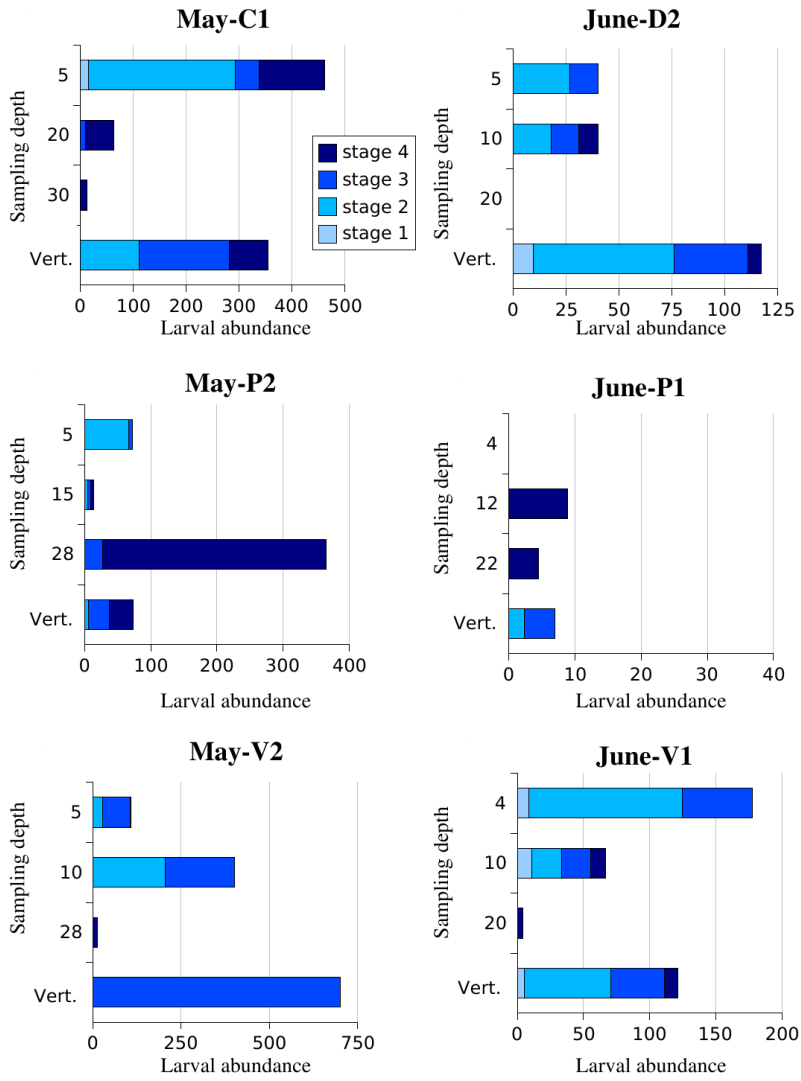


Figure A.15 – Vertical distribution of the larval stages of *O. fusiformis*. Larval abundances per sampling depth are given in larvae.m$^{-3}$. The sampling depth is indicated in m and correspond to the surface layer, the halocline and/or thermocline, and the bottom layer. The sampled station and the date of the cruise are indicated. The depth-averaged larval abundances obtained by vertical hauls of WP2 net are indicated (Vert.).

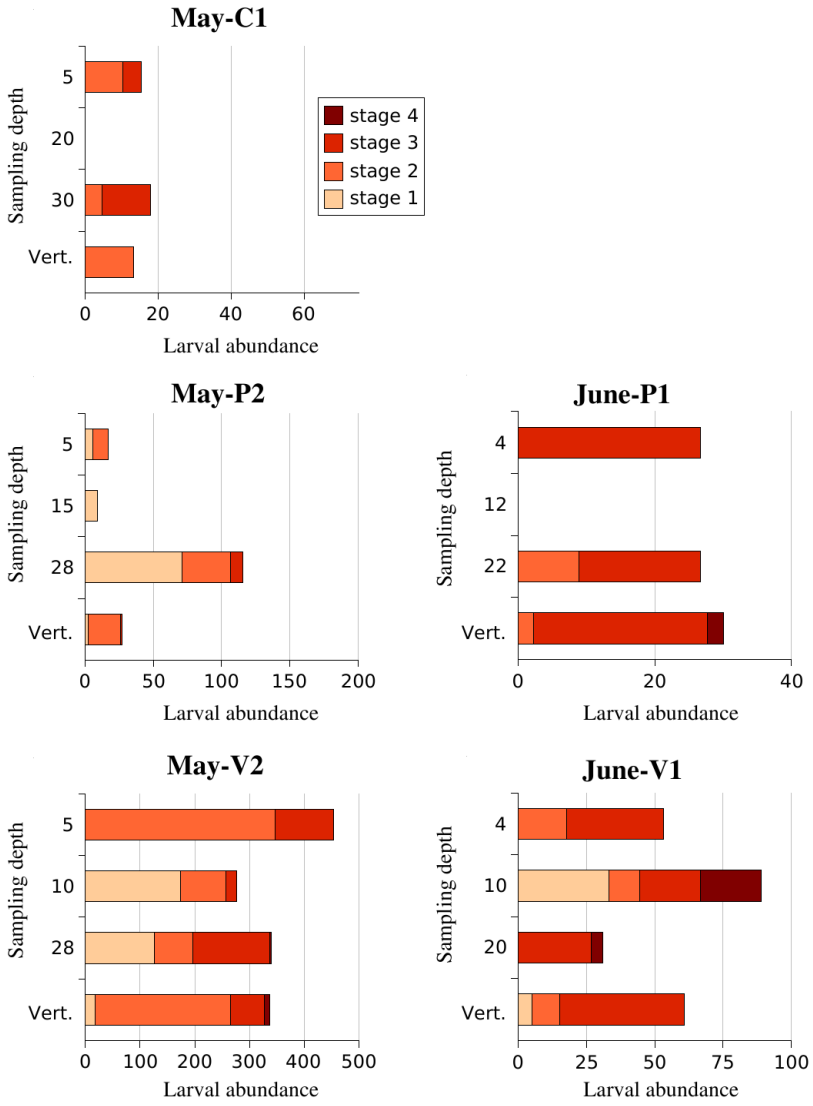


Figure A.16 – Vertical distribution of the larval stages of *S. alveolata*. Larval abundances per sampling depth are given in larvae.m$^{-3}$. The sampling depth is indicated in m and correspond to the surface layer, the halocline and/or thermocline, and the bottom layer. The sampled station and the date of the cruise are indicated. The depth-averaged larval abundances obtained by vertical hauls of WP2 net are indicated (Vert.).

# Annexe B

# The MARS-3D model

## B.1 Hydrodynamic model

The Model for Applications at Regional Scale (MARS) is a primitive equation, finite-difference model (Lazure et Dumas, 2008). It is solved in a sigma coordinate framework such as :

$$\sigma = \frac{z + H}{\zeta + H} \qquad \text{(Eq. B.1)}$$

where $\sigma$ is the vertical coordinate, $H(x, y)$ is the absolute value of bottom position, and $\zeta(x, y)$ is the sea surface elevation, with $z$ and $\sigma$ increasing upward. The water column height is then $D(x, y) = H(x, y) + \zeta(x, y)$.

To simplify the writing of any advection term of any variable $A$, the following notation $L(A)$ is used :

$$L(A) = u\frac{\partial A}{\partial x} + v\frac{\partial A}{\partial y} + w^*\frac{\partial A}{\partial \sigma} \qquad \text{(Eq. B.2)}$$

where $u$ is the zonal velocity, $v$ is the meridional velocity, and $w^*$ is the vertical velocity in the sigma coordinate framework $(x, y, \sigma)$ given by :

$$w^* = \frac{1}{D}\left(w - \sigma\frac{\partial \zeta}{\partial t} - u\left(\sigma\frac{\partial \zeta}{\partial x} + (\sigma - 1)\frac{\partial H}{\partial x}\right) - v\left(\sigma\frac{\partial \zeta}{\partial y} + (\sigma - 1)\frac{\partial H}{\partial y}\right)\right) \qquad \text{(Eq. B.3)}$$

where $w$ is the vertical velocity in the physical framework $(x, y, z)$.

The conventional Boussinesq and hydrostatic approximations are used to solve the Navier-Stokes equations in the Cartesian coordinates $(x, y, \sigma)$ :

$$\frac{1}{D}\frac{\partial \rho}{\partial \sigma} = -\rho g \qquad \text{(Eq. B.4)}$$

$$\frac{\partial \zeta}{\partial t} + L(D) = 0 \qquad \text{(Eq. B.5)}$$

$$\frac{\partial u}{\partial t} + L(u) - fv = -g\frac{\partial \zeta}{\partial x} - \frac{1}{\rho_0}\frac{\partial P_a}{\partial x} + \pi_x + \frac{1}{D}\frac{\partial(\frac{nz}{D}\frac{\partial u}{\partial \sigma})}{\delta \sigma} + F_x \qquad \text{(Eq. B.6)}$$

$$\frac{\partial v}{\partial t} + L(v) + fu = -g\frac{\partial \zeta}{\partial y} - \frac{1}{\rho_0}\frac{\partial P_a}{\partial y} + \pi_y + \frac{1}{D}\frac{\partial(\frac{nz}{D}\frac{\partial v}{\partial \sigma})}{\partial \sigma} + F_y \qquad \text{(Eq. B.7)}$$

where $D(x, y)$ is the water column height, $\zeta$ is the sea surface elevation, $\rho$ is the water density as a function of salinity, temperature and pressure, $g$ is the gravity, $f$ is the Coriolis parameter, $u$ is the zonal velocity, $v$ is the meridional velocity in the sigma framework $(x, y, \sigma)$, $\rho_0$ is the reference density of seawater, $P_a$ is the atmospheric pressure at sea level, $\pi_x$ and $\pi_y$ are the zonal and meridional components of the baroclinic pressure gradient, $nz$ is the vertical eddy viscosity, $F_x$ and $F_y$ are the horizontal friction terms. The detailed formulations of the Coriolis parameter $f$, the friction terms $F_x$ and $F_y$, the eddy coefficient $nz$, and the horizontal components of the baroclinic pressure gradient $\pi_x$ and $\pi_y$ are given in Lazure and Dumas (2008). Eddy coefficients are calculated from a 1-Equation closure model following a classical $k-l$ formulation well suited for coastal domain (Luyten *et al.*, 1996).

The mode splitting approach leads to build a specific barotropic model by integrating the Equations Eq. B.5 to Eq. B.7 over the vertical from bottom ($\sigma = 0$) to top ($\sigma = 1$) and considering kinematic boundary conditions :

$$B.10\frac{\partial \zeta}{\partial t} + \frac{\partial D\bar{u}}{\partial x} + \frac{\partial D\bar{v}}{\partial y} = 0 \qquad \text{(Eq. B.8)}$$

$$\frac{\partial \bar{u}}{\partial t} = -g\frac{\partial \zeta}{\partial x} - \frac{1}{\rho_0}\frac{\partial Pa}{\partial x} + \frac{1}{\rho_0 D}(\tau_{sx} - \tau_{bx}) + \int_{\sigma=0}^{\sigma=1}[fv - L(u) + \pi_x + F_x]d\sigma \qquad \text{(Eq. B.9)}$$

$$\frac{\partial \bar{v}}{\partial t} = -g\frac{\partial \zeta}{\partial y} - \frac{1}{\rho_0}\frac{\partial Pa}{\partial y} + \frac{1}{\rho_0 D}(\tau_{sy} - \tau_{by}) + \int_{\sigma=0}^{\sigma=1}[-fu - L(v) + \pi_y + F_y]d\sigma \qquad \text{(Eq. B.10)}$$

where $\tau_{sx}$ and $\tau_{sy}$ are the surface stress components, and $\tau_{bx}$ and $\tau_{by}$ are the bottom stress components, $\bar{u}$ and $\bar{v}$ are the mean zonal and meridional currents over depth given by :

$$(\bar{u}, \bar{v}) = \int_{\sigma=0}^{\sigma=1} (u, v) d\sigma. \qquad \text{(Eq. B.11)}$$

The barotropic model is solved using an Alternate Direction Implicit scheme which is a semi-implicit method. This method is only implicit concerning the direction of the computation. The free surface elevation $\zeta$ is computed every half time step, whereas the mean zonal and meridional currents over depth ($\bar{u}$ and $\bar{v}$) are computed alternatively (i.e., every time step). Computations of $\bar{u}$ and $\zeta$ are performed in a row-wise manner at a given time step by solving Equations Eq. B.6, Eq. B.8 and Eq. B.9, whereas computations of $\bar{v}$ and $\zeta$ are performed in a column-wise manner a half time step later by solving Equations Eq. B.7, Eq. B.8 and Eq. B.10. The use of a spatially centred subsecond order scheme and the staggered Arakawa C grid lead to a tridiagonal linear system being solved using lower-upper factorization.

# Annexe D

# Complementary informations on the Lagrangian bio-physical model of the larval dispersal at the regional scale of the Bay of Biscay

Sommaire

## D.1 Influence of particle initial depth on dispersal patterns

Particule initial depth has no influence on mean vertical position (Figure D.1) and on horizontal dispersal (Figure D.2).

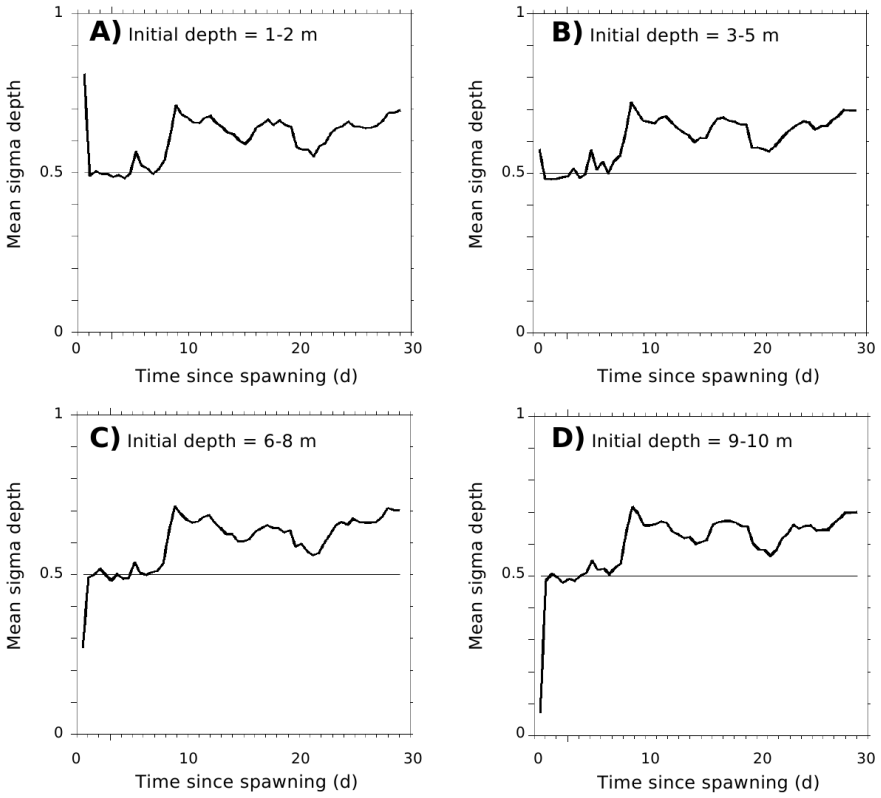


Figure D.1 – Mean sigma depth $\sigma_m$ of 1000 particules released at different initial depths : (A) in subsurface (1-2 m depth), (B) above the middle of the water column (3-5 m depth), (C) under the middle of the water column (6-8 m depth), and (D) close to the bottom (9-10 m depth). Particles are released in May 2002 in the Vilaine spawning location and are followed during 4 weeks. Mean sigma depth is represented as a function of the time since spawning. After one day of dispersal, particule initial depth has no influence on mean vertical position.

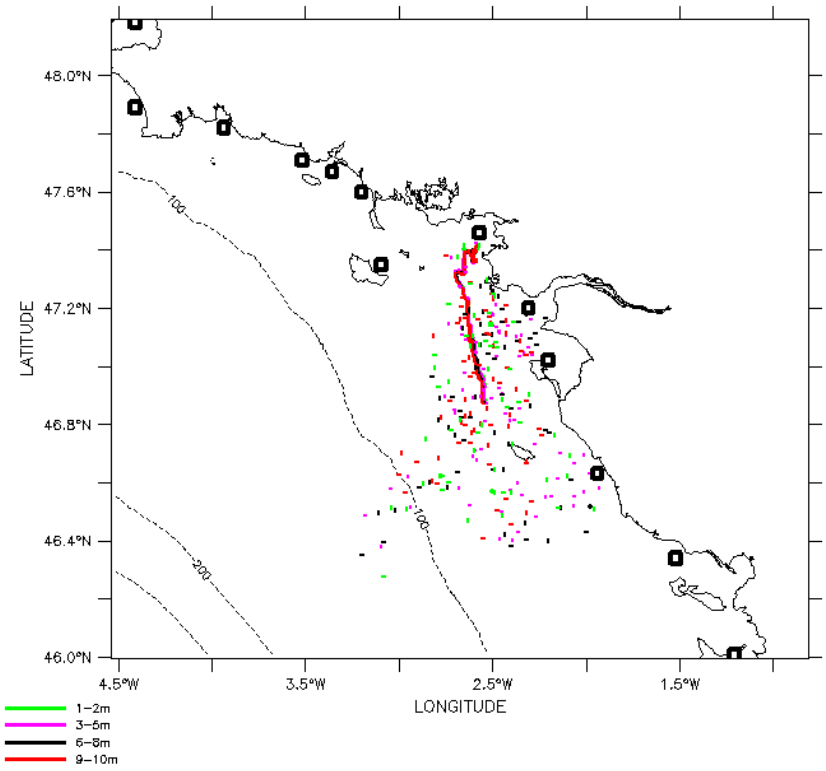


Figure D.2 – Horizontal dispersal of particules released at different initial depths. Particules are released every meter from 1 m depth to 10 m depth and each color represents an initial depth. Mean trajectories and final positions after 4 weeks of dispersal are indicated for each initial depth. Particles are released in May 2002 in the Vilaine spawning location. Particule initial depth has no influence on horizontal dispersal.

## D.2 Redundancy analyses based on five dispersal kernels

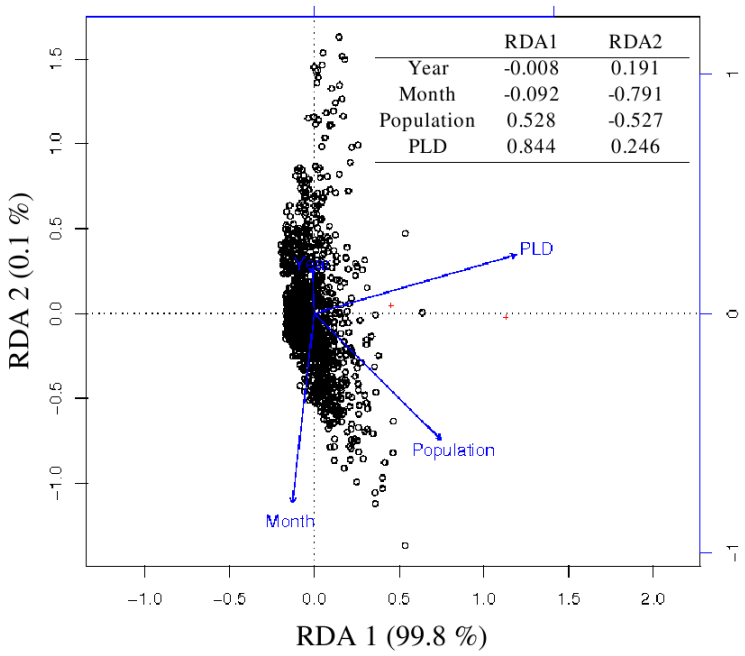


Figure D.3 – Graphical representation of the RDA analysis of the passive dispersal kernels using the five descriptors proposed by Edwards *et al.* (2007). The analysis only revealed one significant axis, RDA1, explaining 99.8 % of the variance ($p < 0.001$) and scored by the PLD, the spawning location, and the spawning month.

## D.3 Variability of the mean larval vertical position in relation with spawning month

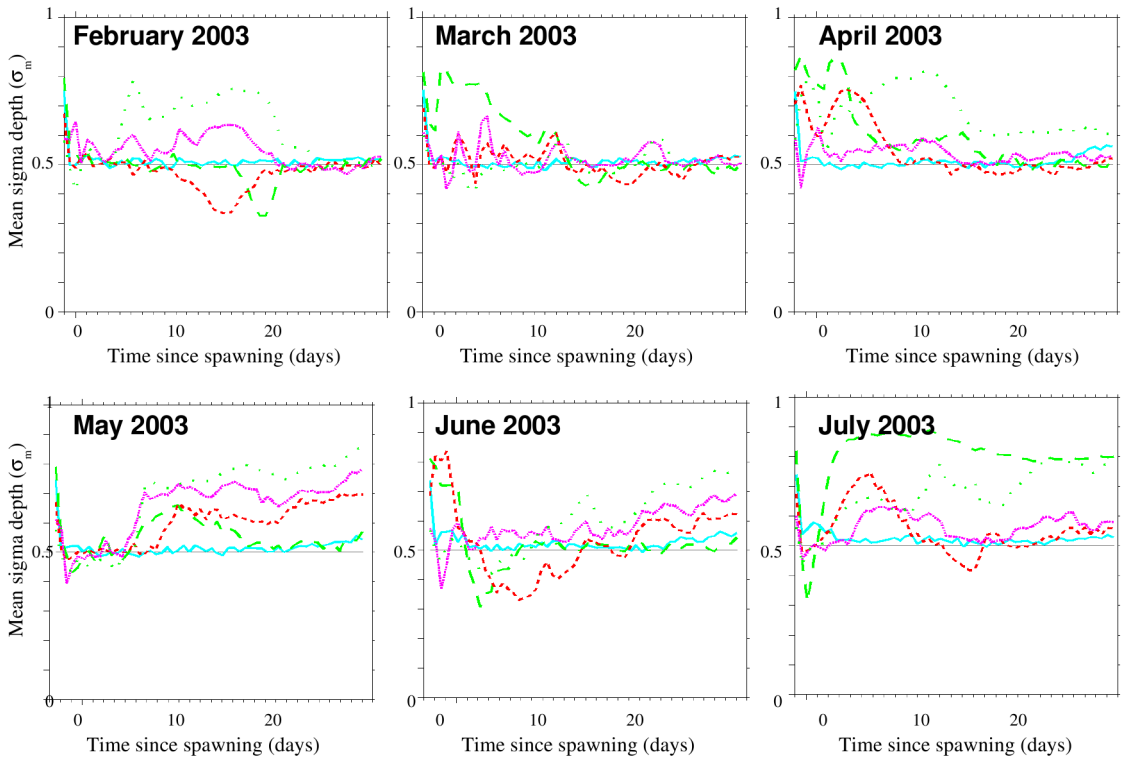


Figure D.4 – Mean sigma depth of 1000 passive particules released from Morlaix (light blue line), Audierne (light green long-dashed line), Lorient (red dashed line), Loire (pink dashed line), and Oléron (light green short-dashed line). Spawning dates are indicated.

# Appendix E

# Biophysical modelling to investigate the effects of climate change on marine population dispersal and connectivity

Christophe LETT, Sakina-Dorothée AYATA, Martin HURET, and Jean-Olivier IRISSON

Manuscript *submitted* to *Progress in Oceanography*[a]

[a]Submission for a special issue on contributions in the GLOBEC project.

## Abstract

Climate may act on the dispersal and connectivity of marine populations through changes in the oceanic circulation and temperature, and by modifying species' prey and predator distributions. As dispersal and connectivity remain difficult to assess in situ, a first step in studying the effects of climate change can be achieved using biophysical models. To date, only a few biophysical models have been used for this purpose. Here we review these studies and also include results from other recent modelling efforts. We show that increased sea temperature, a major change expected under climate warming, may impact dispersal and connectivity patterns via changes in reproductive phenology (e.g., shift in the spawning season), transport (e.g., reduced pelagic larval duration under faster development rates), mortality (e.g., changes in the exposure to lethal temperatures), and behaviour (e.g., increased larval swimming speed). Projected changes in circulation are also shown to have large effects on the simulated dispersal and connectivity patterns. Although these biophysical modelling studies are useful preliminary approaches to project the potential effects of climate change, we highlight their current limitations and discuss the way forward, in particular the need for adequate coupled hydrodynamic-biogeochemical simulations using atmospheric forcing from realistic climate change scenarios.

## E.1 Introduction

Pelagic dispersal of larvae is a crucial process in the life cycle of most marine populations as it enables exchange of individuals, or connectivity, between distant sites. Consequently, the interest in marine population dispersal and connectivity is broad and worldwide. A special issue on "Marine population connectivity" (Cowen , 2007) and a theme section on "Larval connectivity, resilience and the future of coral reefs" (Jones , 2009b) are among the recent signs of this interest. Despite recent progress (Jones , 2009a; Levin, 2006), larval dispersal and connectivity remain difficult to assess in situ. It is indeed challenging to observe directly the dispersion of a multitude of small individuals diluted in vast expanses of oceanic waters. Assessing the potential effects of climate change on dispersal and connectivity in these populations is even harder. Harley (2006) synthesized the potential effects of climate change on marine populations. They showed the life cycle of a generic marine organism with larval and adult stages (green in Figure E.1) and the effects of climate change acting directly on this population (yellow in Figure E.1), or indirectly via interactions with other species (blue in Figure E.1). Some of these effects are expected to affect larval dispersal.

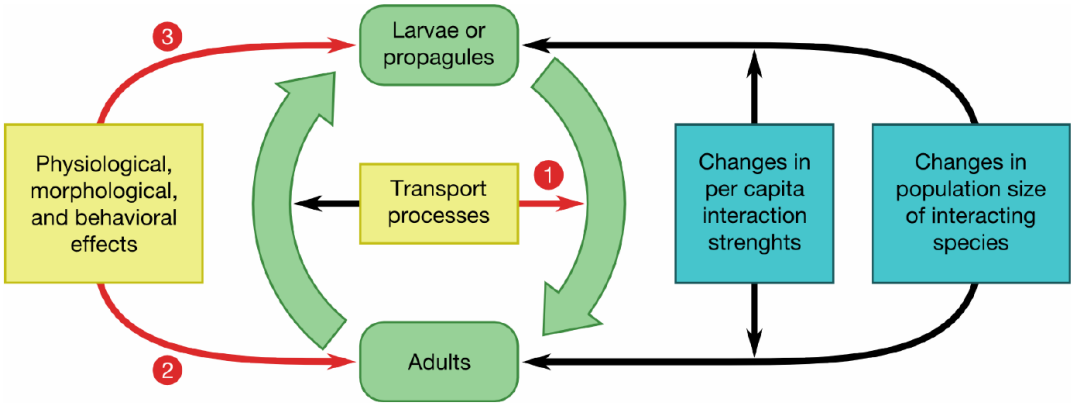


Figure E.1: Potential effects of climate change on a generic marine population (adapted from Harley (2006)). The life cycle of this generic organism is in green. The effects of climate change are in yellow (direct effects) and blue (indirect effects). The arrows in red highlight the effects more specifically investigated in this paper. Numbers are used in the text to refer to these arrows.

Potential effects of climate change on marine populations include changes in current circulation and water temperature (Harley , 2006). Modification in circulation could modify dispersal pathways. The importance of external atmospheric forcing (temperature but also wind, heat fluxes, or freshwater input) on turbulence, stratification, and thermohaline- and wind-induced circulation gives insights on how regional circulation and mesoscale features may be affected by climate change. Climate change may also downscale from global perturbations (e.g., the reduction of Atlantic Meridional Overturning Circulation, Stouffer (2006)) to regional scale. Thus, larval transport patterns may be directly and strongly influenced by climate change. Water temperature increase may also act on several key parameters of larval life. There is evidence of shifts in abundance and distribution of marine fish (Perry , 2005; Rijnsdorp , 2009) and larvae (Hsieh , 2009) that are believed to be largely driven by changes in temperature (Pörtner & Farrell, 2008). A direct effect of the increase of water temperature could be reduced exposure to lethal temperatures and, as a consequence, increased survival. A recent meta-analysis (O'Connor , 2007) demonstrated a negative relationship between temperature and pelagic larval durations (PLDs) for a wide range of marine species. Reduced PLDs induced by temperature increases could lead to substantial modifications of dispersal and connectivity patterns. The differences between the development and behavioural abilities of tropical fish larvae versus temperate ones also give a sense of what the consequences of a temperature increase could be for the ontogeny of larvae in temperate ecosystems; most tropical species develop faster and reach higher swimming speeds and endurance than temperate ones (Leis, 2006). Finally, warmer temperatures could also induce changes in reproductive phenology, especially by inducing earlier spawning (Edwards & Richardson, 2004; Olive , 1990).

To summarise, an increase in water temperature may impact marine population dispersal and connectivity patterns via changes in spawning phenology (earlier spawning of adults), larval transport (shorter pelagic larval durations), larval mortality (reduced exposure to lethal temperatures and shorter larval life) and behaviour (increased larval swimming speed). Changes in ocean circulation and in exposure to lethal temperatures are examples of factors acting at the population level (represented by the "transport processes" yellow box in Harley (2006); arrow number 1 in Figure E.1). Earlier spawning of

adults on the one hand, and shorter pelagic larval duration and increased larval swimming speed on the other, are examples of factors acting at the individual level (the "physiological, morphological, and behavioral effects" yellow box in Harley (2006); arrows number 2 and 3 respectively in Figure E.1).

A first step in the assessment of the effects of climate change on marine population dispersal and connectivity can be achieved using biophysical models. Biophysical models of marine population dispersal have been extensively developed in the last 20 years to simulate the fate of the pelagic life stages of marine organisms (reviews by Cowen & Sponaugle (2009); Lett (2009); Metaxas & Saunders (2009); Miller (2007); Runge (2005); Werner (2007, 2001a)). The processes represented in these biophysical models include transport, growth, behaviour, mortality, and settlement of eggs and larvae in a virtual marine environment. This environment usually consists of dynamic three-dimensional fields of physical (velocity, temperature, etc.) and biological (phytoplankton and zooplankton concentrations, etc.) variables provided by coupled hydrodynamic-biogeochemical models. A few biophysical models have been explicitly used to investigate the potential effects of climate change on connectivity. Here we review this information (Heath , 2008; Irisson, 2008; Lett , 2009; Munday , 2009; Vikebø , 2007) and other recent modelling efforts (Ayata , *submitted*; Huret , *submitted*). We then highlight the limitations of the current modelling approaches and suggest the best way forward.

## E.2 Biophysical models and climate change

Vikebø (2007) used a biophysical model to simulate transport and growth of larvae and pelagic juveniles of cod (*Gadus morhua*) in the Nordic Seas under normal and anomalous environmental conditions. Anomalous conditions were obtained by increasing the river runoff to the seas by a factor of three in their hydrodynamic model. This scenario led to dramatic changes in circulation and temperature in the hydrodynamic simulations, which had important consequences for the dispersal and growth of early life stages of cod in the biophysical model. In particular, transport patterns shifted significantly and individual growth was reduced. Although Vikebø (2007) recognized that they used an

extreme scenario, an increase in river runoff is consistent with the expected effects of climate change in the region.

Heath (2008) used a biophysical model for the same species (cod, *Gadus morhua*) in the North Sea. In their model, temperature along the drift trajectory was used to simulate growth of larvae and faster growing larvae experienced higher survival rates. Larvae were tracked until they attained a given length at which time they settled. Over the 1980-1999 period, Heath (2008) obtained significant increases of the probability of cod eggs spawned in two specific areas to be retained in their natal area, and attributed this trend to climate change. More precisely, this result is likely due to an increase in sea temperature in these areas over time, as warmer waters led to faster growth in the model and therefore to reduced mortality and earlier settlement. Both effects contributed to increased retention.

Munday (2009) used the biophysical model from Paris (2007) to investigate the effects of shorter PLDs on dispersal and connectivity patterns of a coral reef fish (*Thalassoma bifasciatum*). A 20 % reduction in PLD led to fewer larvae dispersing over long distances and changed the overall recruitment pattern, increasing self-recruitment dramatically. As a result, local connectivity increased, but only in areas of sufficiently high reef density whereas connections between reefs were weaker or lost in areas of low reef density. Therefore, Munday (2009) concluded that, in fragmented habitats like coral reef ecosystems, the precise effect of reduced PLD on connectivity patterns likely depends on the distribution of suitable habitats for settlement.

Lett (2009) used the evolutionary biophysical model developed by Mullon (2002) to explore how environmental constraints could affect the spatial and temporal spawning patterns of small pelagic fish in the southern Benguela upwelling system. They imposed simple constraints to drifting ichthyoplankton for multiple generations and assumed philopatry: successful individuals reproduce at the same time and place as their parents. This allowed the seasonal and spatial patterns of spawning to emerge from a selective process driven by environmental conditions. When they used the constraint of staying close to the shelf in waters warmer than 15°C throughout the drift period, the spawning patterns that emerged were in broad agreement with those observed for anchovy (*Engraulis encrasicolus*) and sardine (*Sardinops sagax*) in the southern Benguela. When they changed

the temperature-related mortality from 15°C to 14°C or 16°C, the selected spawning patterns changed significantly, both spatially and temporally. Lett (2009) interpreted these changes within the context of climate change, with a cooler (14°C) threshold mimicking warmer waters and a warmer (16°C) threshold mimicking cooler waters. Lett (2009) obtained contrasting results for these two assumptions; earlier westward spawning was predicted for the warming scenario, later eastward spawning was predicted for the cooling scenario. There has been a slight warming trend in sea surface water in the southern Benguela during the last decade (Demarcq, 2009). Regional climate projections currently available suggest an average increase of near-surface temperature by 2.5°C over the Benguela region between 1980–1999 and 2080–2099 (Christensen , 2007). However, Wang (2010) reported that climate projections showed a particularly high degree of uncertainty in coastal upwelling regions. In addition, the water that is upwelled at the coast comes from greater depths and might not display the warming trends predicted for surface waters. An intensification of upwelling-favourable winds is also expected under climate change (Bakun, 1990) and was observed in the southern Benguela for the last decade (Demarcq, 2009). Therefore, considering either warming or cooling of southern Benguela coastal waters as a result of climate change are two plausible assumptions.

Ayata (*submitted*) simulated larval dispersal and connectivity for a generic invertebrate species inhabiting a coastal, fragmented habitat in the Bay of Biscay and in the western English Channel. From their results, the consequences of two possible effects of an increase in sea surface temperature on dispersal and connectivity can be discussed: (1) shorter PLD and (2) earlier spawning. For a maximum temperature increase of 5.3°C over Europe (Christensen , 2007), such as from 9 to 14.3°C, the PLD would decrease from 4 to 2 weeks following the universal relationship proposed by O'Connor (2007) between PLD and water temperature. Ayata (*submitted*) compared dispersal kernels and connectivity matrices obtained for these two PLD values among 16 populations and demonstrated a significant impact of PLD on the dispersal kernels. Whatever the spawning month and the spawning population, shorter PLD resulted in shorter mean dispersal distances. On average, a decrease of 50 % in PLD (from 4 to 2 weeks) caused a decrease of 45 % in mean dispersal distance (Figure E.2A).

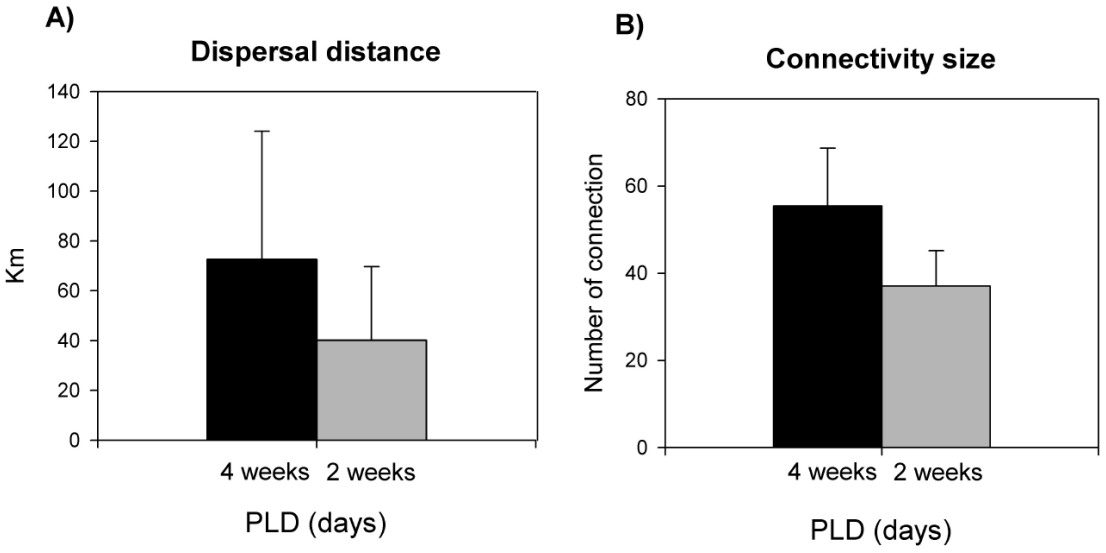


Figure E.2: Consequence of a decrease in PLD from 4 to 2 weeks in (A) mean dispersal distance and (B) connectivity size for a generic invertebrate species in the fragmented habitat of the Bay of Biscay. Connectivity size is defined as the number of connections between all 16 spawning populations. Averages and standard deviations (error bars) were calculated for 35 spawning dates from February to August 2001 to 2005 and for 16 spawning populations (see Ayata , *submitted*, for details). A decrease of 50% in the PLD from 4 to 2 weeks resulted in decreases of mean dispersal distance from 73 ± 51 km to 40 ± 29 km (mean ± SD) and of connectivity size from 55 ± 13 to 37 ± 8 connections.

Regarding connectivity, such a decrease in PLD increased retention and larval exchange between neighbouring populations (local connectivity) but decreased exchanges between more distant populations (regional connectivity). Moreover, the connectivity size, defined as the total number of connections between all spawning populations, decreased by 30 %, indicating an overall loss of connectivity (Figure E.2B). Ayata (*submitted*) also simulated monthly spawning from February to August for 2001 to 2005 (35 dates). Whereas no year-to-year variations in dispersal kernels were observed, the date of spawning within each year had a significant influence on the variability of dispersal kernels, likely because of the strong seasonal patterns in the circulation of the Bay of Biscay. Larval transport occurred north-westwards from February to April and south-eastwards from May to August. These results suggested that, for the invertebrate populations of the Bay of Biscay, earlier spawning, in April instead of May, could cause reversed dispersal directions from SE to NW, hence favouring the connectivity to more northern populations (Ayata , *submitted*). Earlier spawning would also increase the connectivity, from 48 ± 9 (mean ± SD) connections

for spawning occurring between May and August to 65 ± 12 connections for spawning occurring between February and April (for a PLD of 4 weeks).

Another modelling study in the Bay of Biscay (Huret , *submitted*) investigated the effects of spawning date and PLD on anchovy (*Engraulis encrasicolus*) dispersal. The simulation covered the period 1996-2007. As in Ayata (*submitted*) for the northern Bay of Biscay, Huret (*submitted*) showed that in the southeastern bay the peak spawning season (May-June) of anchovy occurs just after a shift in coastal circulation from northward to southward. Earlier spawning due to a likely temperature increase would then cause a significant change in the dispersal pattern of anchovy early life stages, in particular for those spawned near the coast. Huret (*submitted*) also evaluated the effect of the duration of the pelagic phase on several indices describing the dispersal kernel. A reduction of the PLD would have the average effect of linearly reducing the mean dispersal distance and the variance of the distribution around its mean position (inertia), as well as increasing the aggregation of larvae.

In addition to direct and indirect effects of temperature increase on development rates or phenology, we also evaluated the impact of other physical properties (stratification, turbulence and circulation) on anchovy larval dispersal in the Bay of Biscay. The modelling exercise consisted of separate perturbations of the atmospheric forcing of two contrasting years (2001 and 2002): (1) temperature, (2) wind, and (3) combined temperature and wind. We call these 'what if' climate change scenarios, in contrast to dynamic downscaling of projections from global circulation models. The perturbations are based on estimates from Christensen 's (2007) regional projections, under IPCC projections for the end of the $21^{\text{th}}$ century. The first scenario considers an increase in air temperature by 3°C, which is within the expected range of variation over Europe (2.2 to 5.3°C, Christensen (2007)). The second scenario considers a wind increase of 30 %, well within the range of climatic variability. Such an increase in average and extreme wind speeds is expected over northern Europe, although with a relatively low degree of confidence (Christensen , 2007). The third scenario is a combination of both the temperature and wind increase. TableE.1 shows that the air temperature increase (1) and combined (3) scenarios result in an average increase in sea surface temperature (SST) of about 2.2°C over the Bay of Biscay, whereas in the

wind increase scenario (2) SST decreases by 0.58°C. The stratification is strengthened in scenario 1 and weakened for scenarios 2 and 3 with the wind increase.

Table E.1: Annual mean (± SD) of the anomalies (scenarios 1, 2, or 3 relative to the reference run) of sea surface temperature and deficit of potential energy. The latter relates to the strength of the stratification.

| | 1. Air T | +3°C | 2. Wind | +30% | 3. Combined | (T+3°C, Wind+30%) |
|---|---|---|---|---|---|---|
| | 2001 | 2002 | 2001 | 2002 | 2001 | 2002 |
| Surface temperature (°C) | 2.18 (± 0.22) | 2.26 (± 0.21) | -0.57 (± 0.38) | -0.59 (± 0.34) | 2.15 (± 0.22) | 2.22 (± 0.20) |
| Deficit of potential energy ($kg.m^{-1}.s^{-2}$) | 3.23 (± 1.87) | 2.85 (± 1.81) | -11.3 (± 8.05) | -9.13 (± 6.81) | -6.37 (± 5.65) | -4.64 (± 4.77) |

| 'What if' scenarios | | Surface temperature (°C) | Deficit of potential energy ($kg.m^{-1}.s^{-2}$) |
|---|---|---|---|
| 1. Air T +3°C | 2001 | 2.18 (± 0.22) | 3.23 (± 1.87) |
| | 2002 | 2.26 (± 0.21) | 2.85 (± 1.81) |
| 2. Wind +30% | 2001 | -0.57 (± 0.38) | -11.3 (± 8.05) |
| | 2002 | -0.59 (± 0.34) | -9.13 (± 6.81) |
| 3. Combined (T+3°C, Wind+30%) | 2001 | 2.15 (± 0.22) | -6.37 (± 5.65) |
| | 2002 | 2.22 (± 0.20) | -4.64 (± 4.77) |

Under these modified oceanographic conditions, the average distance transported and the dispersion of the particle distribution (inertia and positive area) are the two most affected descriptors of the dispersal kernel, whereas the direction of drift is not significantly modified (Figure E.3, TableE.2). Note that, despite opposite effects of increased air temperature and wind on surface temperature and stratification (TableE.1), their effects on our descriptors are both positive (scenarios 1 and 2) and are cumulative when acting together (scenario 3). Comparing the variations of these descriptors between scenarios (TableE.2) highlights the greater impact of temperature (scenarios 1 and 3) on the mean distance transported, and of wind (scenarios 2 and 3) on dispersion. Stronger stratification caused by increased temperatures concentrates particles in the surface layers and they are thus more affected by surface wind or thermohaline circulation, whereas stronger winds

may increase turbulence and dispersal of particles in a deeper mixed layer, eventually increasing dispersal of particles in the horizontal dimension.

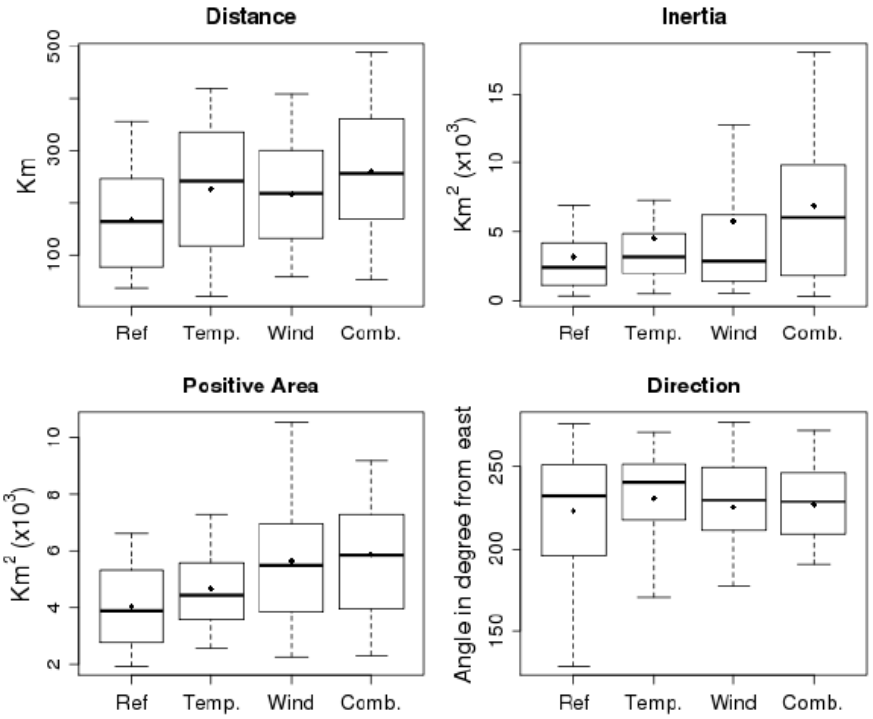


Figure E.3: Boxplots (medians are the thick lines, quartiles are the boxes, ranges are the dashed lines) of four dispersal kernel descriptors under the different climate change scenarios (Ref: reference, Temp: air temperature +3°C, Wind: wind +30%, Comb: combined temperature and wind increase). Mean values are plotted as black bullets. Within scenario variability is obtained from 14 different releases between the beginning of March and end of August in 2001 and 2002. Duration of the drift is 50 days. Distance is the distance between the centre of gravity of the particle distribution at their starting and final positions. Inertia and positive area both represent dispersion; inertia is the variance of the distribution at the end of the drift and positive area is the sum of model grid cells with positive concentrations of particles. It relates to dispersion at a smaller scale than inertia. Direction is the direction of the mean transport from east counterclockwise. See Huret (*submitted*) for further details on the spatial descriptors of the dispersal kernel.

Table E.2: Relative increases in four descriptors of the dispersal kernel under the three 'what if' scenarios.

| | 1. Air T +3°C | 2. Wind +30% | 3. Combined (T+3°C, Wind+30%) |
|---|---|---|---|
| Distance transported | 40% | 33% | 58% |
| Inertia | 24% | 63% | 70% |
| Positive area | 13% | 33% | 33% |
| Direction | 5% | 1% | 3% |

| 'What if' scenarios | Distance transported | Inertia | Positive area | Direction |
|---|---|---|---|---|
| 1. Air T +3°C | 40% | 24% | 13% | 5% |
| 2. Wind +30% | 33% | 63% | 33% | 1% |
| 3. Combined (T+3°C, Wind+30%) | 58% | 70% | 33% | 3% |

Irisson (2008) studied the effect of fast development of swimming abilities in warm waters on local retention of fish populations, using a modelling framework that allowed explicit simulations of larval behaviour throughout the larval phase (Irisson , 2004). In brief, larvae were advected by currents but could also swim, up to a maximum speed that increased as larvae grew. Larvae selected trajectories that allowed them to self-recruit while spending as little energy on swimming as possible. This left more energy allocatable to growth and indirectly affected survival, because large or fast-growing larvae usually survive better (Cowan & Houde, 1992; Sponaugle & Grorud-Colvert, 2006). Simulations were carried out for generic, weakly swimming, temperate fish larvae (PLD of 27 d, maximum swimming speed at settlement of 5 cm $s^{-1}$) in a stratified flow (averaging 20 cm $s^{-1}$ at the surface and 12 cm $s^{-1}$ at depth) around two idealized coastal environments (an island and a promontory). Although weak, the swimming abilities of larvae allowed them to dive down, towards slower currents, at the beginning of the larval phase and to stay within eddies in the lee of the feature later on, hence facilitating their retention (Figure E.4).

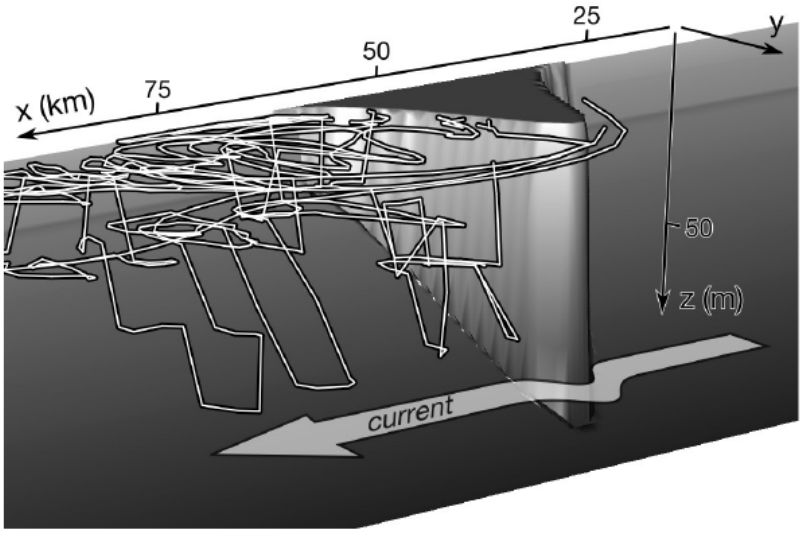


Figure E.4: Simulated 3D trajectories (white curves with black outline) of larvae between 0 and 110 m-depth around a promontory. The current flows from the right to the left of the plot, as depicted by the arrow near the bottom. Larvae start near the promontory, swim deeper initially and then actively stay in the lee of the promontory.

Provided food is sufficient, an increase in water temperature accelerates ontogeny, particularly of swimming abilities, and shortens the PLD (O'Connor , 2007), which both affect trajectories. The simulation of a 2°C increase in water temperature showed that larvae were able to swim downward earlier and to be retained in the lees of the topographic features in greater numbers (Irisson, 2008). The percentage of successfully recruiting larvae increased (TableE.3). The rate of self-recruitment was estimated as recruitment percentage $*$ PLD $*$ daily mortality rate (0.27, Houde & Zastrow (1993), adjusted upwards after the 2°C increase according to Houde (1974) and Houde (1989)). The combination of shorter PLD and higher recruitment percentage resulted in a threefold increase in self-recruitment rate in the climate change scenarios (TableE.3). These simulations highlighted the influence of oriented swimming on retention, even at slow speeds (2 cm $s^{-1}$ on average here), and suggested that the warming of oceanic waters could result in greater retention through faster development.

Table E.3: Effects of a 2°C increase in water temperature on the pelagic larval duration (PLD), percentage of self-recruiting trajectories, and recruitment rate in the island and promontory configurations. The reduction of PLD is computed after O'Connor (2007).

| Configuration | Parameter | Scenario | |
|---|---|---|---|
| | | Present | +2°C |
| | PLD (d) | 27 | 21.7 |
| Island | recruitment ( %) | 45 | 48 |
| | recruitment rate $\times 10^3$ | 0.092 | 0.28 |
| Promontory | recruitment ( %) | 72 | 75 |
| | recruitment rate $\times 10^3$ | 0.15 | 0.44 |

| Configuration | Scenario | PLD (d) | recruitment % | recruitment rate |
|---|---|---|---|---|
| Island | Reference | 27 | 45 | $0.092 \times 10^3$ |
| | +2°C | 21.7 | 48 | $0.28 \times 10^3$ |
| Promontory | Reference | 27 | 72 | $0.15 \times 10^3$ |
| | +2°C | 21.7 | 75 | $0.44 \times 10^3$ |

## E.3 Discussion

The hydrodynamic simulations reported here are the best available representations of the marine environments that populations presently face in the different systems under study. These environments were used in biophysical models depicting dispersal of early life stages to test the influence of a few variables that are expected to be particularly sensitive to climate change (spawning season, pelagic larval duration, exposure to hot and cold water temperatures, and swimming speed). Our results, combined with previous studies, show that a decrease in pelagic larval durations caused by an increase in water temperature (within the range currently expected under climate change; Christensen (2007); Meehl (2007)) would increase self-recruitment, suppress long distance dispersal and, overall, reduce average dispersal distance. However, these effects are not universal. Indeed, in the Bay of Biscay, the mean dispersal distance for a small pelagic fish would increase because of climate-induced changes in water circulation. Furthermore, the overall effect of reduced PLD on connectivity probably depends on the distribution of settlement habitats. We also showed that early spawning could completely reverse the direction of dispersal, as occurred in the model of the Bay of Biscay, for example. Similarly, changes in river runoff could dramatically affect circulation patterns and dispersal routes. Finally, a reduction

in PLD could combine with fast development of swimming abilities in warm waters and could lead to an increase in larval retention, and therefore self-recruitment.

These conclusions need to be taken with caution however, because when testing the effects of climate change on a particular variable we implicitly assumed that all others remained unchanged and that there were no interactions between these variables. However, such interactions could play an important role in altering dispersal and connectivity. As an example, if phenological changes, such as early spawning, occur in reponse to an increase in temperature, the new environment encountered by larvae (e.g. different prey and predator distributions) could have both a positive or a negative effect on larval mortality. The modification of spawning dates can also influence connectivity patterns in any number of ways depending on its interaction with circulation (more retention vs. enhanced long distance dispersal and anything in between). Observations of egg distributions over decades (e.g., Bellier (2007)) also suggest that spawning locations, the starting point of our dispersal models, could be modified by adult populations in response to a changing environment. To get better insights into the consequences of climate change, biophysical models should integrate the influence of various environmental variables (temperature, circulation, etc.) on the different processes occurring during the pelagic phase (larval transport, growth, behaviour, mortality, and settlement). There is also a need to better understand and consider the potential acclimation and adaptation of individuals to changing environmental conditions in biophysical models (Franklin & Seebacher, 2009).

The simulations we described did not include state-of-the-art regional climate change scenarios, such as those provided by the Intergovernmental Panel on Climate Change (Christensen , 2007). The parameterizations used to describe climate change (shortening of PLD, warming of water, increase of wind speed, etc.) were within the range of variations provided by these scenarios and they are a preliminary approach to assess the response of regional connectivity to climate variability. However they lack the spatial and temporal dimensions of this variability. For example, many of our examples rely on an homogeneous increase in sea water temperature, a simplifying assumption that is clearly wrong. Indeed, from satellite sea surface temperature (SST) data in the North Atlantic between 1985 and 2005, Gómez-Gesteira (2008) projected a mean annual increase in the coastal SST of

3.5°C per century at latitudes close to 48°N, but with a maximum increase, in spring, of 5.1°C along the French Atlantic coast and of 4.4°C along the Cantabrian coast.

Besides this type of 'experimental' use of models, where only one variable is changed at a time, another approach could be to use contrasted present conditions and compare connectivity between years, regions, etc. Such work was done in the Caribbean, to compare the response to climate change of regions differing in habitat fragmentation (Paris , 2008), in Australia (Munday , 2009) and in the Bay of Biscay (Ayata , *submitted*) to predict shifts in drift direction depending on currents observed during different periods of the year. Basing a model on observed past or present data and iterating those in time allows retention of the complex interactions among variables while still studying the long term effects of different conditions.

Our approach constitutes a first step in the investigation of the effects of climate change on marine population dispersal and connectivity, in the absence of adequate hydrodynamic simulations for climate change scenarios in the regions under study. Atmosphere-ocean general circulation models using climate change scenarios exist at the global scale (Meehl , 2007; Russell , 2006). Downscaling at regional scale is still rare (Auad , 2006; Christensen , 2007) and reveals many uncertainties (Ådlandsvik, 2008; Meier , 2006). Pierce (2009) pointed out the importance of downscaling from an ensemble of global models to reduce the internal variability and errors contained in individual models. Interest in such methodological developments is growing as they allow regional projections of the dynamics of marine populations (e.g., Hollowed (2009)) and because this is the scale at which biophysical models of dispersal operate. An even greater challenge would be the projection of the dynamics of the whole ecosystem, starting with its biogeochemistry (Denman , 2007), which would be needed if growth is included in larval biophysical models. Indeed, larvae that grow quickly in warm waters have a fast metabolism and need to eat more (Houde, 1974). Since a large part of the mortality in temperate waters is believed to be caused by the lack of food, accurate modelling of prey fields is necessary. Methods for the downscaling of global climate projections at the regional lower trophic level are developing (Solidoro , 2010) and coupled hydrodynamic-biogeochemical simulations forced by downscaled regional projections are becoming available (Neumann, 2010). They should

help investigations of the influence of climate change on plankton dynamics and therefore on feeding opportunities for the early life stages of other marine populations.

Finally, even for models operating in present-day conditions, there still is a significant gap between our abilities to simulate larval dispersal with biophysical models and to experimentally measure connectivity. Considerable progress has been achieved on both sides. The possibility of estimating connectivity patterns through parentage analysis (Jones , 2005; Planes , 2009) and mass marking Almany2007,Becker2007,Thorrold2007 is promising, although these methods may be difficult to apply for some systems or species. Comparing real (observed) and virtual (modelled) drifters is also a useful way to validate the physical transport predicted by biophysical models (Chérubin & Richardson, 2007; Edwards , 2006; Fach & Klinck, 2006). A challenge for the future is to integrate all these advances (Jones , 2009a; Levin, 2006; Metaxas & Saunders, 2009).

We have focused our study on the potential effects of climate change on marine population dispersal and connectivity. Biophysical models of marine population dispersal are expected to provide useful information, particularly if, as explained above, they are used within multidisciplinary studies integrating other complementary approaches. Of course, climate-related changes in dispersal and connectivity are not the only explanations for shifts currently observed in the distribution of marine fishes (Perry , 2005; Rijnsdorp , 2009) and larvae (Hsieh , 2009). Other processes, in particular trophic interactions (the blue part in Figure E.1), are also likely to play a crucial role. For example, we showed that changes in spawning phenology impacted dispersal and connectivity patterns of a given population, but these changes could also lead to trophic mismatches (Cury , 2008; Edwards & Richardson, 2004). We recommend using a suite of models, comprising larval dispersal models, models describing the spatial dynamics of both larval and adult stages (e.g., Andrews (2006)) and trophic models (e.g., Travers (2007)), in combination with experimental assessments, to investigate ecological responses of marine systems to climate change at the individual, population, and community levels.

## E.4 Acknowledgments

The authors thank the organisers of the GLOBEC-France symposium, and particularly F. Carlotti, for giving them the opportunity to meet, discuss, and propose the present contribution. S.- D. Ayata was supported by a PhD grant from the French Ministry of National Education and Research and by the French national project EC2CO (Ecosphère Continentale et Côtière). M. Huret received financial support for this work from european project RECLAIM (FP6 - Contract 044133). J.-O. Irisson work is part of a PhD grant from the French Ministry of National Education and Research. He thanks S. Planes and C. Paris, his advisor and co-advisor, for their help and support.

# Appendix F

# Complementary informations on the eulerian bio-physical model of the larval dispersal of *Sabellaria alveolata*

## F.1 Mathematical formulations of complex larval release

For a uniform continuous spawning over one tidal cycle, a symmetric semi-continuous spawning over 3 tidal cycles and a symmetric semi-continuous spawning over 5 tidal cycles, the larval release term is given by the general equation:

$$\begin{cases} \dfrac{\partial r(x,y,\sigma,t)}{\partial t} = p\dfrac{N_0}{V_{xy\sigma(1)}}\dfrac{1}{\Delta t} & when \begin{cases} t_b <= t < t_e = t_b + \Delta t \\ \{x,y\} \in \{reef\ coordinates\} \\ \sigma = \sigma(1) \\ D(x,y) > 0.5 \end{cases} \\ \dfrac{\partial r(x,y,\sigma,t)}{\partial t} = 0 & otherwise \end{cases} \qquad \text{(Eq. F.1)}$$

where $r$ is the larval release function, $N_0$ is the total number of larvae released during the spawning event, $V_{xy\sigma} = V_{xy\sigma(1)}$ is the volume of the lower cell of coordinates $(x, y, \sigma(1))$, $t_b$ is the beginning time of larval release, $t_e$ is the ending time of larval release, $\Delta t$ is the continuous spawning time duration, and $p$ is the percentage of released larvae during $\Delta t$. The values of $t_b$, $t_e$, and $p$ for each spawning type are given in Table F.1A1 assuming a tidal cycle lasting 12 h 20 min. In each case, larval release is centred on one high tide.

Table F.1: Values of the parameters used in the mathematical formulation of complex larval release

| Spawning type | $\Delta t$ | $t_b$ | $t_e$ | $p$ (%) |
|---|---|---|---|---|
| Uniform continuous spawning over one tidal cycle | 4h | HT-2h | HT+2h | 100 |
| Symmetric semi-continuous spawning over three tidal cycles | 4h | HT-14 h 20 min | HT+10h 20 min | 25 |
| | | HT-2 h | HT+2 h | 50 |
| | | HT+10 h 20 min | HT+14 h 20 min | 25 |
| Symmetric semi-continuous spawning over five tidal cycles | 4h | HT-26 h 40 min | HT-22 h 40 min | 10 |
| | | HT-14 h 20 min | HT-10 h 20 min | 20 |
| | | HT-2 h | HT+2 h | 40 |
| | | HT+10 h 20 min | HT+14 h 20 min | 20 |
| | | HT+22 h 40 min | HT+26 h 40 min | 10 |

HT = High tide.

# Appendix G

# Does larval supply explain the low proliferation of the invasive gastropod *Crepidula fornicata* in a tidal estuary?

François RIGAL, Frédérique VIARD, Sakina-Dorothée AYATA and Thierry COMTET

Manuscript submitted to *Biological invasion*

## G.1 Abstract

Human-mediated transport and aquaculture have promoted the establishment of non-indigenous species in many estuaries around the world over the last century. This phenomenon has been demonstrated as a major cause of biodiversity alterations, which prompted scientists to provide explanations for the success or failure of biological invasions. *Crepidula fornicata*, a gastropod native from the East coast of North America, has successfully invaded many European bays and estuaries since the $19^{\text{th}}$ century, with some noticeable exceptions. We investigated whether larval supply may explain the failure in the proliferation of this species within a particular bay, the Bay of Morlaix (France), by analysing patterns of larval distribution and size structure over ten sites sampled three times. Our results evidenced a strong spatial structure in both larval abundance and size at the bay scale, even if larval abundances were low. The location of spawning adults played a critical role, with high numbers of early larvae above the main spawning location. The larval size structure further showed that settlement-stage larvae were absent, which suggested that released larvae might have been exported out of the bay. The use of an analytical model considering tidal effects confirmed that larval retention might be low. The limitation in larval supply resulting from the interactions between spawning location and local hydrodynamics may thus impede the proliferation of this species which has been well established since more than 50 years. This study provided an example of factors which may explain the failure of the transition between two major steps of biological invasions, i.e. sustainable establishment and proliferation.

**Keywords:** *Crepidula fornicata*, spatial distribution, propagule supply, larval dispersal, bentho-pelagic cycle

## G.2 Introduction

In marine ecosystems, invasions by non-indigenous species (NIS) are a major component of biodiversity changes (Carlton & Geller, 1993; Leppäkoski & Olenin, 2000; Reise , 2006). Among marine ecosystems, bays and estuaries are particularly prone to invasions (Cohen & Carlton, 1998; Nehring, 2006) mostly due to human-mediated activities which largely contribute to the worldwide transportation and subsequent introduction of aquatic organisms (Carlton & Geller, 1993; Naylor , 2001; Voisin , 2005). The success of biological introductions not only depends on the introduced species but also on the environmental conditions prevailing in the invaded bays and estuaries citepNehring2006. Therefore, in the context of biological conservation and NIS management, it is crucial to analyse not only the factors which explain the success of introductions and invasions, but also the factors responsible for their potential failure.

In benthic marine invertebrates with a pelagic developmental stage, larvae are known to play a major role at all steps of the invasion process. Larvae may first be the primary introduction stage of a NIS, being transported within ballast waters for long periods (Carlton & Geller, 1993). Due to their microscopic size, they may be transported in huge numbers and then may ensure propagule pressure. Once a species has been introduced, its larvae may facilitate its long-term establishment by promoting the demographic reinforcement of its local benthic populations through recruitment (Dunstan & Bax, 2007). Finally, larvae may in part allow the regional spread of the NIS through natural dispersal, and once several populations have been established larvae may ensure connectivity (Dupont , 2007, 2003; Kinlan , 2005). Larval supply may thus play a major role in the failure or success of invasions.

Larval supply results from the balance between the arrival of larvae (either from the parental population, when retention occurs, or from distant populations) and the loss of locally-produced larvae through dispersal and mortality. In this scheme, the adult populations obviously play a central role by supplying larvae, but also by determining the place where larvae will recruit (Bhaud, 2000; Roughgarden , 1988), which is even more constraining in species with a gregarious behaviour. Therefore, local hydrodynamics will also control larval supply through either larval retention which will enhance larval

settlement in the vicinity of adults or larval exportation. Understanding the processes responsible for the successful establishment of introduced species thus requires to jointly examine the larval pool distribution and the adult locations and characteristics.

In this context, this study aimed to investigate the spatial distribution of larvae of an emblematic marine invader of the North East Atlantic, the slipper limpet *Crepidula fornicata*, at a local scale (i.e. within a bay). This gastropod, native from the East coast of the USA, was first accidentally introduced into the UK at the end of the 19 th century. This species was then introduced repeatedly along the European coasts during the 20th century mostly because of aquaculture and trade of the Japanese oyster Crassostrea gigas (Blanchard, 1997). *C. fornicata* has successfully invaded many European bays and estuaries where it has major ecological and economical impacts (Reise , 2006). However, its success over Europe is not uniform, and in some places, this species failed to invade the introduced area. For instance, de Montaudouin de Montaudouin (2001) highlighted the role of several features, i.e. the presence of *Zostera sp.* beds and the absence of bottom trawl fishing, to explain why *C. fornicata* failed to invade the bay of Arcachon (France).

In the bay of Morlaix (France) *C. fornicata* was first recorded more than fifty years ago (Blanchard, 1995). Although its population is now well established it displays a moderate proliferation. Factors involved in such a low proliferation of *C. fornicata* in this bay are still unknown.

In this paper, we addressed the question of the role played by the larvae in the sustainable settlement of *C. fornicata* in the bay of Morlaix. We focussed on the spatial distribution of the larvae (both in terms of abundance and size structure) at ten sites of the bay sampled three times during the main breeding season, and analysed these data regarding both adult distribution (abundance and reproductive status) and environmental characteristics. We addressed more specifically the following questions: (1) do the abundance and mean larval size differ among sites within the bay? (2) how much the larval pool distribution is controlled by the adults distribution or the variation in environmental variables (i.e. temperature, depth, salinity, chlorophyll a)? By addressing these questions, we aimed to examine the importance of the larval-adult coupling in the dynamics of marine invader populations and how local hydrodynamic processes affect the larval supply.

## G.3 Materials and methods

### G.3.1 Sampling

The sampling was conducted in the bay of Morlaix (48°05'-48°09'N; 3°49'-3°59'W) which is located in northern Brittany along the English Channel (Figure G.1).

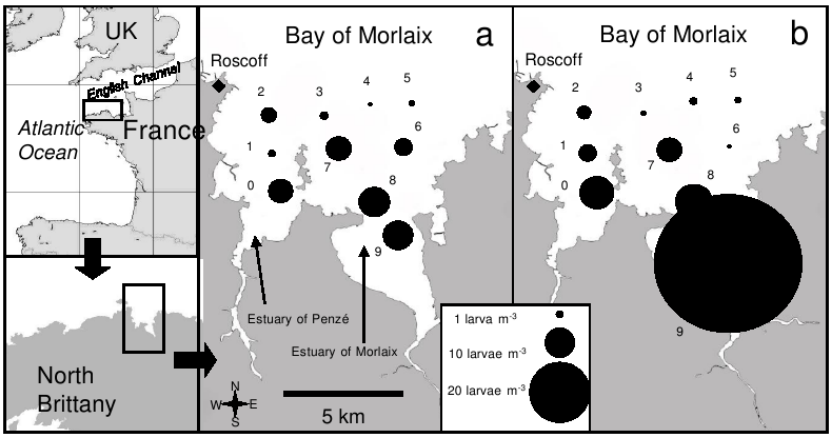


Figure G.1: Location of the ten sampling sites in the Bay of Morlaix and spatial distribution of the abundance (larvae.m$^{-3}$) of *Crepidula fornicata* larvae for the 1$^{st}$ (A) and 2$^{nd}$ (B) sampling dates

*Crepidula fornicata* larvae were sampled at three dates over a period of one month, during the main breeding period, in summer 2006. Sampling was conducted at ten sites (numbered 0 to 9, Table G.3), chosen to cover the inner and outer parts of the bay within a about 6 × 6 km grid. For each date, samples were collected over 4 to 5 hours around the neap high tide using a WP2 plankton net with a 200$\mu m$ mesh size (UNESCO, 1968). For the first (20$^{th}$ July 2006) and second (04$^{th}$ August 2006) dates, vertical tows from the bottom to the surface were used in order to get measures of larval concentrations. For the third one (21$^{st}$ August 2006 ), oblique 5-min tows, corresponding to ca. 70 m$^3$ of water filtered, were carried out to increase the amount of larvae collected in order to analyse the size structure of the larval pool. Each plankton sample was placed in a 2-liter bottle and preserved in the laboratory in 96 % ethanol within 5 hours after collection. Larvae of *C. fornicata* were sorted, counted and their shell length measured using a dissecting microscope with an ocular micrometer. For the first and second sampling

dates, concentration of larvae.m$^{-3}$ was calculated using the abundance and the filtered volume, measured by means of a flowmeter (TSK model) mounted on the net aperture.

Environmental parameters were measured with a CTD probe (SBE 19+, Seabird) at each sampling site. Because of no or very low stratification, we calculated the mean water temperature and salinity. Depth was also recorded at each site. The chlorophyll a concentration was measured only for the first and second dates from surface water with a Turner Design fluorometer, following the method of Lorenzen (1966).

At each of the ten sites, stacks (i.e. perennial groupings of individuals, a typical feature of this species) of benthic adult *C. fornicata* were sampled one week before the first larval sampling by scuba diving following a semi-quantitative approach: all the stacks or isolated individuals found by two divers during a 13-minute dive were collected. *C. fornicata* is a sequential protandrous hermaphrodite (i.e. it changes sex from male to female) and females breed their embryos during several weeks. The sex and the presence of brooded embryos or larvae were thus recorded to examine the reproductive status of individuals from each site.

### G.3.2 Data analyses

Two main larval features were studied: abundance and size structure. To investigate the spatial structure of larval abundances, data from the first and second sampling dates were used. First, multiple regression analyses with abundance (larvae.m$^{-3}$) and geographical coordinates as explanatory variables were performed to test for the homogeneity of the larval abundances across the bay. Then, to investigate the relationships between larval abundance, benthic population characteristics (adult abundance and reproductive status) and environmental variables, a normalized principal component analysis (PCA) was carried out using the software StatBox v. 6.40 pro.

To analyze the larval size structure, the mean size at each site was compared by using a multiple comparison Kruskal-Wallis test for each of the three sampling dates. When significant differences were detected, an a posteriori test was used to determine which sites contributed to the observed differences. To further analyze the size structure, data

from the third sampling date (i.e. for which large samples were obtained) were used to generate larval size-frequency histograms using 40 $\mu m$ size-class intervals, first for each site then by pooling data over the ten sites. The size-class interval fits three criteria: (1) size classes have at least 5 individuals; (2) the number of adjacent empty classes is minimized and (3) the interval is larger than the error on measurements (Jollivet , 2000). Size-frequency histograms were smoothed using a weighted moving average at the $3^{rd}$ order to rule out spurious peaks (Frontier & Pichod-Viale, 1991). The number of age groups was estimated using the Normsep software (Gros & Cochard, 1978) which assumes that the sizes within each age-group follow a Gaussian distribution. Based on maximum likelihood criteria, it then allows to split the overall size-frequency histogram into several age-groups.

Finally, to determine if the spatial pattern in size structure was related to the distribution of benthic adults and environmental variables, a canonical redundancy analysis (RDA) (Legendre & Legendre, 1998), was performed using the table of size classes across sites as response variables and the table of adult abundances and environmental descriptors, including geographical coordinates, across sites as explanatory variables. The RDA is a direct extension of the multiple regression analysis for the modelling of multivariate response data (here the size-class distributions). For the RDA analyses, the R software version 2.7.0 was used (R Development Core Team, 2005)[a]. Before the RDA computation, the numbers of larvae per size class were transformed using the Hellinger transformation (Legendre & Gallagher, 2001) in order to lower the weight of the small size classes (which are very abundant). We then used the automatic forward selection procedure, based on the Monte Carlo permutation test computed in the R library Packfor, to select a subset of the explanatory variables, with a cut-off point of 0.20 (P. Legendre, pers. comm.). RDA was then performed with this subset. The contribution of each explanatory variable and the significance of the RDA axes were tested by analyses of variance and permutation tests using the R tool rdaTest in the R package Vegan 1.11-4[b].

[a] http://www.r-project.org
[b] http://vegan.r-forge.r-project.org/

### G.3.3 Analytical model

In the English Channel, currents are driven by tides, winds and density gradients (Barnay , 2003; Ellien , 2000; Salomon & Breton, 1991). In our study, since the wind showed a mean speed of less than 0.5 $m.s^{-1}$ in July and August 2006, its influence on the hydrodynamics was considered negligible. The temperature and salinity profiles obtained from CTD measurements showed a weak stratification in July and August in the inner part of the bay, while the water column was found to be homogeneous in the outer part. The stratification, which can lead to strong effects on dispersal patterns (Thiébaut , 1992) was thus also considered negligible. According to these observations, we expected a strong influence of the tidal regime in the hydrodynamics of the bay of Morlaix. Since no hydrodynamical model at a fine spatial scale exists to allow the study of larval transport in the bay of Morlaix, we developed a simple analytical model inspired from Black (1990). It allowed us to investigate the impact of the tide on the transport of larvae released at different sites in the bay, and in particular to test for larval retention processes (see complementary information in Section G.8).

The bay was schematically divided into two regions differing by their hydrodynamic characteristics (Section G.8, Figure G.2) : (i) the inner part of the bay (region $B$), only under the influence of a zonal tidal current u(t), and where the spawning adults are located, and (ii) the external part of the bay (region $E$), under the influence of both the zonal tidal current $u(t)$ and a meridional offshore residual current $U$, perpendicular to $u(t)$. The size of the region $E$ is determined by the maximum distance covered by a larva released in $B$ during the tidal movement (maximal tidal excursion $x_T$). Its width $L$ thus depends on the location of the release site within $B$. See Section G.8 for more details on the definition of each region.

The numbers of larvae in regions $B$ and $E$ at time $t$ are noticed $N_B(t)$ and $N_E(t)$, respectively. The volumes of regions $B$ and $E$ at time $t$ are noticed $V_B(t)$ and $V_E(t)$, respectively. The larval concentrations are assumed to be homogeneous within each region. In this model only the advection is taken into account (i.e. the number of larvae in each region only varies under the effects of the currents $u(t)$ and $U$). During each time step $\Delta t$,

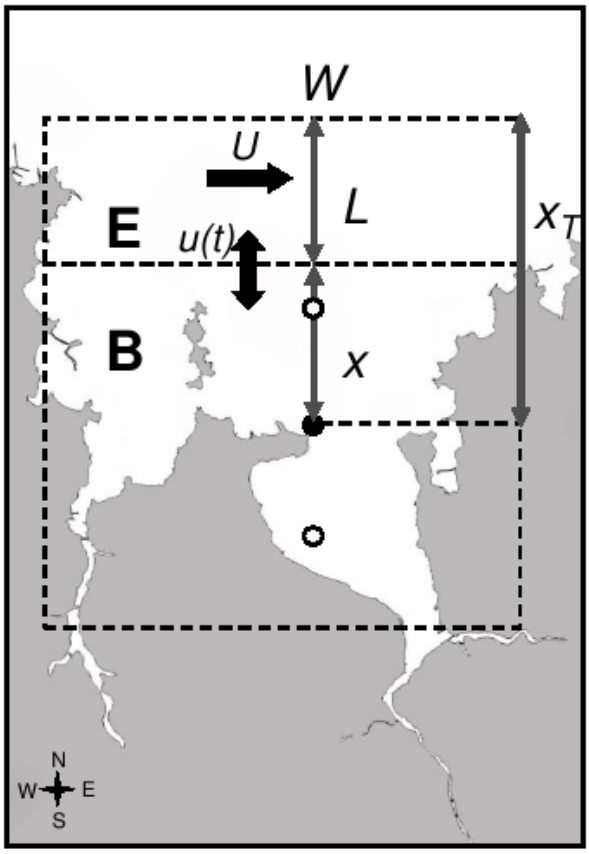


Figure G.2: Schematic view of the bay used to construct the analytical model. Meaning of the letters are presented in Table G.1. The two white dots indicate the innermost and outermost spawning locations which were used in the model, with a distance within the bay of 8 and 1 km, respectively.

the volume of water exchanged between the two regions by the tidal current $u(t)$ is noticed $V_1(t)$ and the volume of water removed from the region $E$ by the current $U$ is noticed $V_2(t)$. Detailed equations for $V_B(t)$, $V_E(t)$, $V_1(t)$ and $V_2(t)$ are given in the Section G.8.

At each time step $\Delta t$, a portion $\frac{V_2(t)}{V_E(t)}$ of the larvae of $E$ is removed by the current $U$. During the ebbing tide, a portion $\frac{V_1(t)}{V_B(t)}$ of the larvae of $B$ is transported to $E$. Hence the changes of $N_B(t)$ and $N_E(t)$ during ebb are given by the following equations:

$$\begin{cases} N_B(t+\Delta t) = N_B(t) - \dfrac{V_1(t)}{V_B(t)} N_B(t) \\ N_E(t+\Delta t) = N_E(t) + \dfrac{V_1(t)}{V_B(t)} N_B(t) - \dfrac{V_2(t)}{V_E(t)} N_E(t) \end{cases} \qquad \text{(Eq. G.1)}$$

During the rising tide, $B$ receives a portion $\frac{V_1(t)}{V_E(t)}$ of the larvae from $E$. The changes of $N_B(t)$ and $N_E(t)$ during flow then follow:

$$\begin{cases} N_B(t+\Delta t) = N_B(t) + \dfrac{V_1(t)}{V_E(t)} N_E(t) \\ N_E(t+\Delta t) = N_E(t) - \dfrac{V_1(t)}{V_E(t)} N_E(t) - \dfrac{V_2(t)}{V_E(t)} N_E(t) \end{cases} \quad \text{(Eq. G.2)}$$

According to these equations, we tested two scenarios, one at spring tide, one at neap tide. For each scenario, we used 9 spawning locations and 5 values of the offshore current $U$ (1, 2, 3, 4 and 5 cm.s$^{-1}$, corresponding to a range of values commonly reported in the literature; Salomon & Breton, 1991). This lead to 90 simulations. A time step $\Delta t$ of one hour was chosen, since the values of the tidal current $u(t)$ and of the free surface elevation $\epsilon(t)$ used in the volume calculations were obtained hourly from the SHOM (Service Hydrographique et Océanographique de la Marine, www.shom.fr). The simulations were performed for 15 days, which corresponds to the estimate of the larval life span at the temperatures prevailing in the bay in July and August 2006 (Rigal , *submitted*).

Table G.1: Parameters of the analytical model of *Crepidula fornicata* in the Bay of Morlaix

| Parameter | Description | Values | Source |
|---|---|---|---|
| $L$ | Width of the region $E$ | $x_T - x$ | |
| $x_T$ | Maximal tidal excursion | 10,000 m | Cabioch & Douvillé (1979) |
| $x$ | Distance between the release location and the boundary between regions $E$ and $B$ | from 1,000 m to 8,000 m | SHOM© |
| $W$ | Width of the region $E$ and $B$ | 10,813 m | SHOM© |
| $h$ | Mean depth of the regions B and E | 15 m | SHOM © |
| $\epsilon(t)$ | Free surface elevation | Hourly values range from 2.15 to 7.94 m | SHOM© |
| $S$ | Surface of the bay (under the hydrographic zero) | 38,421,300 m$^2$ | SHOM© |
| $\Delta t$ | Time step of the simulation | one hour | |
| $u(t)$ | Tidal current | Hourly values range from 5.14 to 51.39 cm.s$^{-1}$ | map of the bay (SHOM©) |
| $U$ | Tidal residual current | Hourly values range from 1 to 5 cm.s$^{-1}$ | Salomon & Breton (1991) |

## G.4 Results

### G.4.1 Spatial structure of larval abundance and mean larval size within the bay

Over the three sampling dates, 1,742 *C. fornicata* larvae were sampled and measured. Whatever the date and site, larval abundances ranged between less than 1 (site 5, 07/20/06) and 34 larvae.m$^{-3}$ (site 9, 08/04/06) (Figure G.1). These values were not randomly distributed: the multiple regression analysis showed a significant correlation between the larval abundances and the latitudinal axis (1$^{st}$ sampling: p=0.003 and 2$^{nd}$ sampling: p=0.007), thus evidencing a spatial structure from the inner to the outer part of the bay.

As observed for the abundance, the mean larval size (per date, per site) differed among sites ranging between 389±25 $\mu m$ (mean ± standard deviation) on 20 th July (site 0), and 572±54 $\mu m$ on 21$^{st}$ August (site 5). A multiple comparison Kruskal-Wallis test ($p < 0.0001$ for the three dates, Table G.2) followed by an a posteriori test revealed, for each sampling date, that the inner sites (in particular sites 8 and 9) displayed a significantly lower mean size. Interestingly, all the larvae had a size lower than the typical size at competence (i.e. 800- 1,000 $\mu m$, following Pechenik & Heyman, 1987). Only 3 larvae out of the 1,270 that were sorted during the last sampling date could have reached competence, based on this sole size criterion. Those 3 larvae were collected in the outer part of the bay, one at site 2 (800$\mu m$) and two at site 3 (800 and 900$\mu m$).

Table G.2: Comparison of the mean size of *C. fornicata* larvae between the sites for the 3 sampling dates. Results of the Kruskal-Wallis tests and of the a posteriori tests are indicated for each sampling date ($1^{st}$-$2^{nd}$-$3^{rd}$) by N (non significant) and **S** (significant, in bold).

| Kruskal-Wallis Tests | | | |
|---|---|---|---|
| | H | df | p |
| $1^{st}$ sampling (07/20/06) | 86.96 | 9 | <0.0001 |
| $2^{nd}$ sampling (08/04/06) | 69.82 | 9 | <0.0001 |
| $3^{rd}$ sampling (08/21/06) | 170.53 | 9 | <0.0001 |

*a posteriori* tests

| | Site 1 | Site 2 | Site 3 | Site 4 | Site 5 | Site 6 | Site 7 | Site 8 | Site 9 |
|---|---|---|---|---|---|---|---|---|---|
| Site 2 | N-N-N | | | | | | | | |
| Site 3 | N-N-N | N-N-N | | | | | | | |
| Site 4 | N-N-N | N-N-N | N-N-N | | | | | | |
| Site 5 | N-N-N | N-N-N | N-N-N | N-N-N | | | | | |
| Site 6 | N-N-**S** | N-N-**S** | N-N-**S** | N-N-**S** | N-N-N | | | | |
| Site 7 | N-N-N | N-N-N | N-N-N | N-N-N | N-N-N | N-N-S | | | |
| Site 8 | **S**-**S**-**S** | **S**-**S**-**S** | N-**S**-**S** | N-N-**S** | **S**-**S**-N | **S**-N-**S** | **S**-**S**-**S** | | |
| Site 9 | **S**-**S**-**S** | **S**-**S**-**S** | N-**S**-**S** | N-N-**S** | **S**-N-N | **S**-N-N | **S**-**S**-**S** | N-N-N | |
| Site 0 | N-N-**S** | N-N-**S** | N-N-**S** | N-N-**S** | N-N-N | N-N-N | N-N-**S** | **S**-N-N | **S**-N-N |

### G.4.2 Adult characteristics and environmental descriptors

The distribution of adults showed a strong heterogeneity among sites (Table G.3). Almost all adults were sampled in the inner sites with up to 304 individuals at site 8. Absence of adults was noticed only in the outer part of the bay at the four sites 2, 4, 5 and 6. The number of brooding females showed the same pattern with maximum values recorded in the inner part of the bay (Table G.3).

Mean temperatures and chlorophyll a concentrations also differed between sites. In particular, the Penzé estuary (site 0) displayed the highest temperatures with a maximum value of 18.4°C in July while the lowest mean temperature (15.6°C) was recorded at site 5 at the end of August. Chlorophyll a concentrations displayed higher values in the Penzé estuary (site 0, 2.33 $\mu g.l^{-1}$, $1^{st}$ and $2^{nd}$ sampling dates) and in the outer sites (e.g. site 5, 2.47 $\mu g.l^{-1}$, $1^{st}$ sampling). Conversely, the salinity was homogeneous at the bay scale with a weak decrease at site 0 for the third sampling (35.05). This absence of spatial structure for salinity evidenced an important oceanic influence within the bay.

Table G.3: Location (coordinates and depth) of the ten sampling sites. For each one, the number of mature individuals and number of brooding females are indicated.

| Sites | Coordinates (degree, min) | | Depth | Benthic adult characteristics | |
|---|---|---|---|---|---|
| | Latitude (°N) | longitude (°W) | (m) | Number of mature individuals | Number of brooding females (%) |
| 0 | 48° 40,579 | 3° 56,192 | 15 | 29 | 8 (27.6) |
| 1 | 48° 41,510 | 3° 56,473 | 27 | 9 | 4 (44.4) |
| 2 | 48° 42,454 | 3° 56,580 | 28 | 0 | 0 |
| 3 | 48° 42,440 | 3° 54,773 | 20 | 34 | 9 (26.5) |
| 4 | 48° 42,723 | 3° 53,255 | 28 | 0 | 0 |
| 5 | 48° 42,742 | 3° 51,895 | 26 | 0 | 0 |
| 6 | 48° 41,664 | 3° 52,161 | 25 | 0 | 0 |
| 7 | 48° 41,583 | 3° 53,980 | 18 | 7 | 3 (42.9) |
| 8 | 48° 40,185 | 3° 53,162 | 12 | 304 | 88 (28.9) |
| 9 | 48° 39,488 | 3° 52,343 | 19 | 115 | 29 (25.5) |

### G.4.3 Relationship between larval abundances, adult characteristics and environmental descriptors

This relationship was analysed with a PCA carried out on the first and second sampling dates. The first two PCA axes explained more than 75 % of the dataset variation (53 and 30 %, respectively, for the first sampling, Figure G.3; 52 and 24 %, respectively, on the second dataset, data not shown). Larval abundances were positively and significantly correlated with the number of mature individuals (i.e. males and females) for the first sampling date but not for the second one. At both dates, the number of mature individuals and the number of brooding females were positively and significantly correlated. Both were negatively and significantly correlated with chlorophyll a concentration and depth. Depth and salinity were also negatively correlated (Table G.4).

For the first (Figure G.3) and second (not shown) sampling dates, PCA allowed to discriminate 2 clusters according to the first axis, opposing the inner (sites 0, 8 and 9) and outer (sites 1 to 7) sites of the bay. According to the contribution of environmental variables along the first axis, the inner sites were characterized by a higher number of adults and brooding females (which contribute for 21.9 and 21.6 % to axis 1, respectively) and displayed higher larval abundances (which contribute for 19 % to axis 1) for the first sampling date. Outer sites were mainly characterized by higher depth (18 %) and higher

Table G.4: Pearson correlation coefficients matrix between variables for the 1st and the 2nd sampling dates. Numbers in bold indicate significant correlations ($p < 0.05$). La = larval abundance (larvae.m$^{-3}$), Nmi = number of mature individuals, Nbf = number of brooding females, Sa = salinity, MT = mean temperature (°C), Ch = chlorophyll a concentration ($\mu$g.l$^{-1}$), De = depth (m).

| First sampling date | La | Nmi | Nbf | Sa | MT | Ch |
|---|---|---|---|---|---|---|
| Nmi | **0.64** | | | | | |
| Nbf | 0.62 | **1.00** | | | | |
| Sa | 0.58 | 0.14 | 0.11 | | | |
| MT | 0.43 | -0.15 | -0.16 | **0.73** | | |
| Ch | -0.50 | **-0.65** | **-0.66** | 0.19 | 0.11 | |
| De | -0.60 | **-0.70** | **-0.69** | **-0.67** | -0.29 | 0.21 |
| Second sampling date | La | Nmi | Nbf | Sa | MT | Ch |
| Nmi | 0.40 | | | | | |
| Nbf | 0.36 | **1.00** | | | | |
| Sa | 0.53 | 0.36 | 0.34 | | | |
| MT | 0.04 | -0.35 | -0.35 | 0.28 | | |
| Ch | -0.08 | **-0.67** | **-0.69** | -0.05 | 0.26 | |
| De | -0.41 | **-0.69** | **-0.68** | **-0.73** | -0.02 | 0.42 |

concentrations of chlorophyll a (10 %). The second axis discriminated sites according to the temperature (34 % contribution to axis 2) and opposed sites 0 and 8, site 0 (Penzé estuary), being the warmest location. Similar results were obtained for the second sampling date (data not shown).

### G.4.4 Relationship between size structure, adult characteristics and environmental descriptors

Length-frequency histograms generated for each site sampled during the last date differed according to their location (Figure G.4). Inner sites displayed significantly lower median values with a dominance of larvae belonging to small size classes (sites 8 and 9). Site 0 shared the same characteristic but a higher proportion of larger larvae was observed. In the outer sites, the smallest larvae were absent (site 4) or represented a low proportion of the total number of larvae (e.g. sites 2 and 7). This reflected a shift from small size classes to larger ones from the inner to the outer sites of the bay.

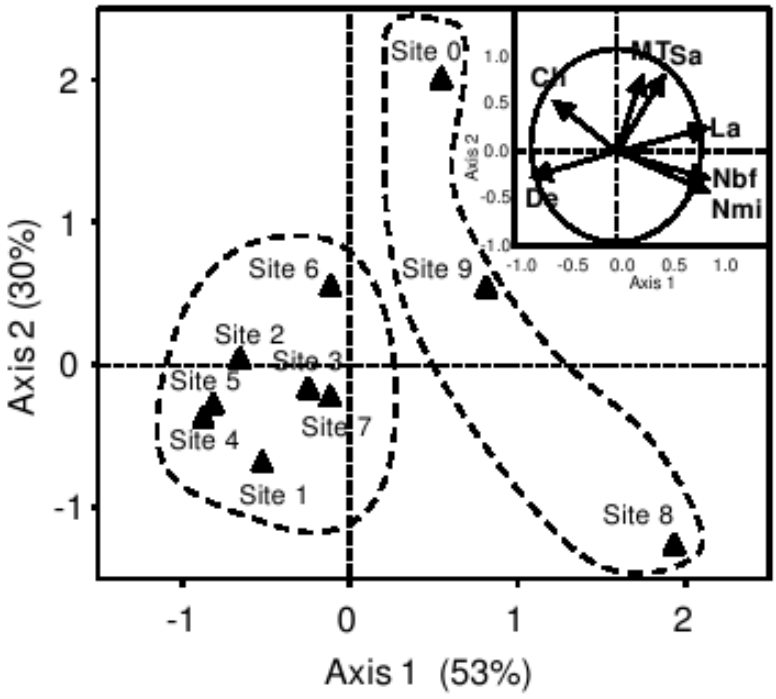


Figure G.3: Ordination of the 10 sites for the 1st sampling based on the principal component analysis. Correlation circle is represented in the upper part of the figure in order to present the contribution of each variable to the first two axes. La = larval abundance (larvae.m$^{-3}$), Nmi = number of mature individuals, Nbf = number of brooding females, Sa = salinity, MT = mean temperature (°C), Ch = chlorophyll a concentration ($\mu$g.l$^{-1}$), De = depth (m).

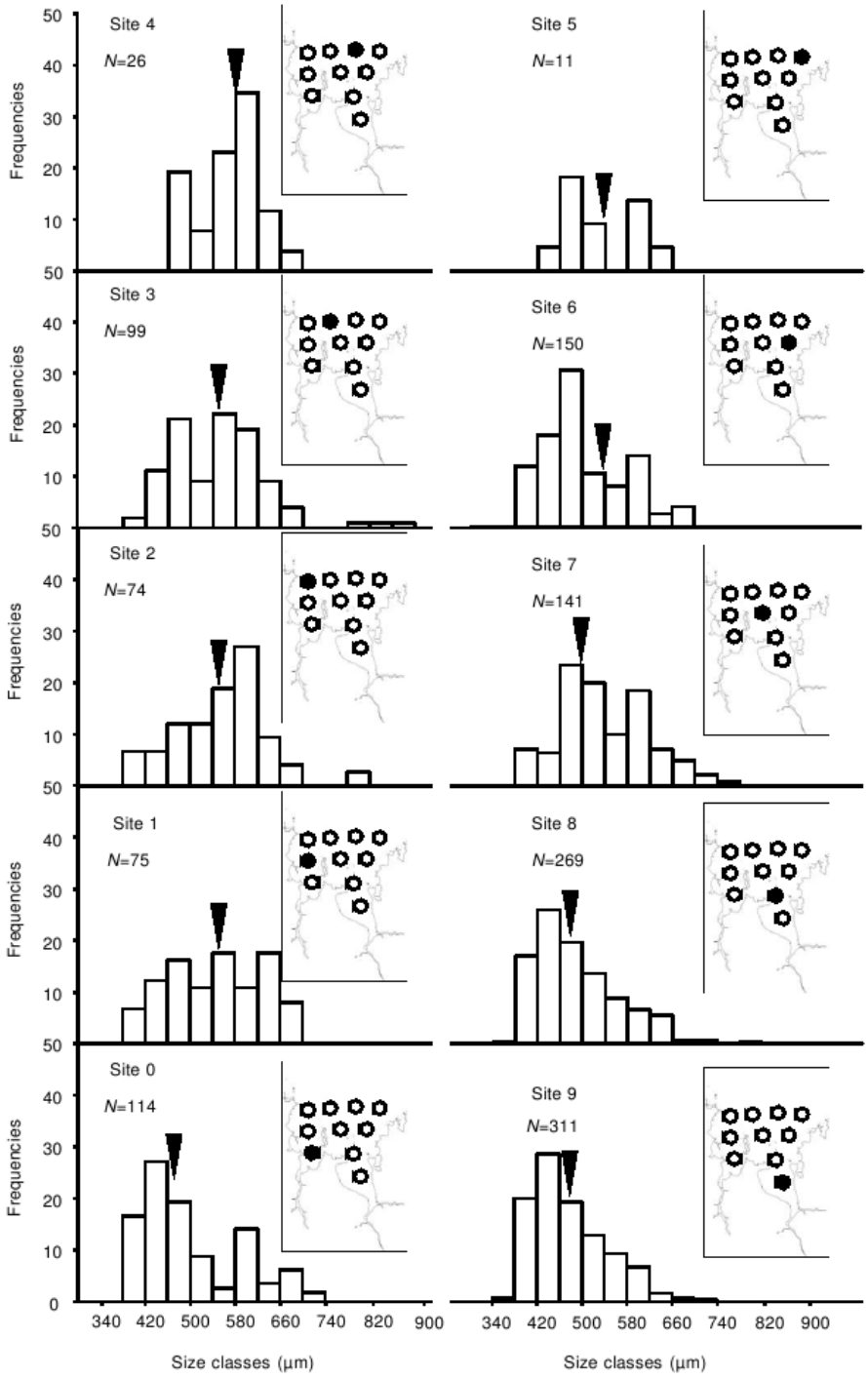


Figure G.4: Length-frequency histograms of larvae collected at the ten sites sampled during the 3rd date. Arrows indicate the median of the distributions. Inserted maps indicate site location. N is the number of larvae measured.

Taking advantage of the large sampling size obtained during the third sampling, the size structure has been examined in relation to the environmental and adult descriptors using a canonical redundancy analysis (RDA). Among the 7 explanatory variables, 3 were found significant after the forward selection procedure: the latitude (latitude only, p=0.002), the longitude (latitude × longitude, p=0.096) and the mean temperature (latitude × longitude × temperature, p=0.143). Using these three variables, the RDA was significant (p=0.005). The first two axes were significant (RDA1, p=0.001; RDA2, p=0.02) and explained 69 and 23 % of the total variance, respectively (Figure G.5). Only the latitude contributed significantly to the variability of the overall larval dataset (p=0.005), reflecting the size gradient between the inner and outer sites. Along RDA1, two clusters were separated. The cluster composed of the inner sites (0, 6, 8 and 9) was characterized by the highest values of mean temperature and lowest latitude and was dominated by small size classes. In the opposite, the cluster composed of the outer sites (1-5 and 7) was characterized by larger size classes and highest latitude.

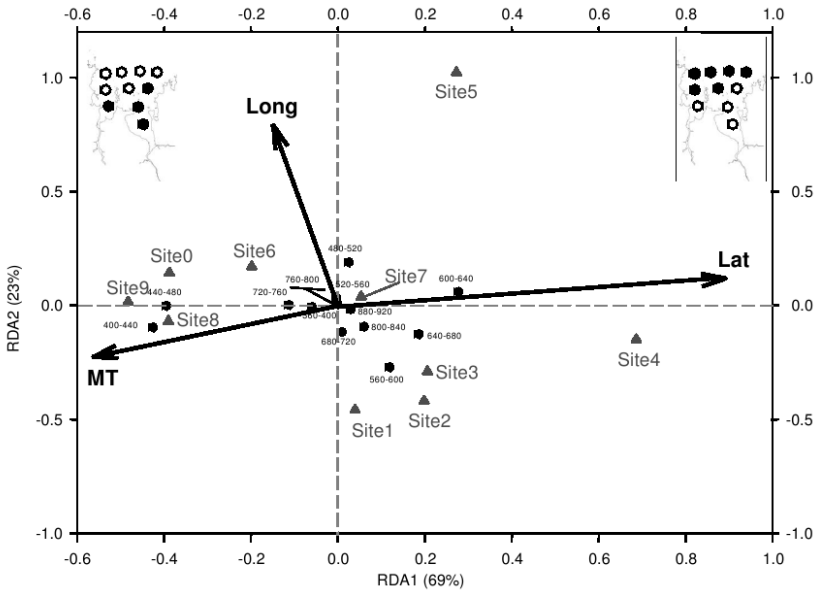


Figure G.5: RDA ordination biplot based on the RDA analysis. Maps indicate the location of the sites included in each group discriminated along the 1st RDA axis. MT = mean temperature (°C), Long = longitude, Lat = latitude. Arrows indicate the variables selected after the forward selection procedure, triangles indicate sites and dots the size classes ($\mu$m).

### G.4.5 Tidal influence on the larval transport

Our analytical model took into account both the instantaneous tidal current within the bay and an offshore residual current to simulate the larval transport, and allowed us to calculate the larval retention rate within the bay for several spawning locations and hydrodynamic scenarios. In all simulations, the number of larvae retained within the bay oscillated according to the tidal cycle and decreased due to the loss of a proportion of larvae by the offshore residual current (Figure G.6a). As an example, in spring tide conditions and with an offshore residual current U = 3 cm.s$^{-1}$, 91 % of the larvae released from the main adult population (site 8) were lost after 15 days of simulation (Figure G.6a). For a given offshore residual current, larvae released more upstream (i.e. higher values of distance within the bay) were more likely to be retained within the bay (Figure G.6b). However, for a realistic residual current in this area (U = 3 cm.s$^{-1}$), the retention rate never exceeded 20 %, whatever the spawning site.

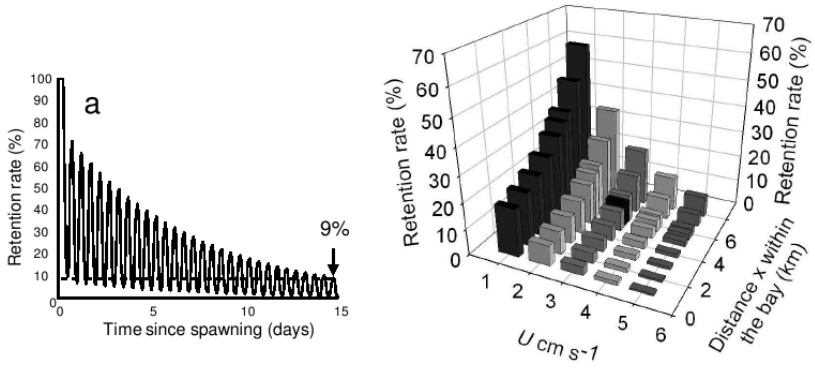


Figure G.6: (A) Evolution of the simulated retention rate (%) within the region $B$ calculated with $U$ = 3 cm.s$^{-1}$ and larvae released above the main adult population. (B) Final retention rate (%) in the bay after 15 days calculated as a function of the offshore current $U$ and the spawning location (distance within the bay $x$, see Section G.8). Black bar represents retention rate for the case shown in A. Results are presented for a spring tide.

## G.5 Discussion

Larval supply is known to play a major role in the structure and dynamics of populations of species with a bentho-pelagic life cycle (Gaines & Roughgarden, 1985) and is expected to be involved in the success or failure of invasions by non-indigenous species (Byers & Pringle, 2006; Cameron & Metaxas, 2005; de Rivera , 2007). In particular, the amount of larvae produced and their further dispersal or retention have been shown to be crucial for the establishment and spread of introduced populations in coastal ecosystems (Byers & Pringle, 2006).

In the bay of Morlaix, larval abundances of the introduced mollusc *Crepidula fornicata* were low, ranging from less than 1 to 34 larvae.m$^{-3}$, as compared to the concentrations that had been observed in other bays or estuaries of its European distribution range. This low larval abundance might be related to the overall low adult abundance in the bay (mean: 20 individuals.m$^{-2}$, maximum: 200 individuals.m$^{-2}$; Dupont, 2004). As a comparison, high concentrations of *C. fornicata* larvae (up to 2,000 larvae.m$^{-3}$) were reported in the summer months in other European bays such as the bay of Mont Saint Michel (Lasbleiz and Comtet, unpublished data) where the local adult densities reached 2,000 individuals.m$^{-2}$ (mean: 200 individuals.m$^{-2}$ ; Viard , 2006). Similarly, in the bay of Brest where adult densities reached 500 individuals.m$^{-2}$, Coum (1979) reported larval concentrations of more than 500 larvae.m$^{-3}$ in summer. At a regional scale, our observations thus suggested the occurrence of a positive relationship between summer larval abundances and adult stock.

Despite such low concentrations, our results clearly showed that the abundance and size structure of *Crepidula fornicata* larvae were spatially heterogeneous at the bay scale, exhibiting a gradient from the inner to the outer sites of the bay. In the inner sites, characterized by lower depths, higher temperatures and lower chlorophyll a concentrations, larval abundances were higher and small size classes were dominant, while in the outer sites, deeper, colder, and with higher chlorophyll a concentrations, lower abundances were observed and larger larvae occurred. The spatial structure of both larval abundance and size distribution was also linked to the distribution of benthic reproductive adults which was the most important factor explaining the observed pattern of larval abundance (PCA,

Figure G.3). Adults, and especially brooding females, were mainly located in the inner part of the bay (84 % of the adults and 83 % of the brooding females were sampled at sites 8 and 9, Table G.3), where higher larval abundances were observed. In addition, mean larval size was positively related to the distance from the major spawning area (sites 8 and 9), with the smallest larvae collected close to the adults. The mean larval size at these locations was close to the size-at-hatching (ca. 400 $\mu m$, Pechenik & Lima, 1984) which suggested that larvae were probably recently released by the reproductive females. The high abundance of small larvae in the innermost sites might thus reflect the location of the release sites.

*Crepidula fornicata* settles gregariously by responding to ecologically relevant cues which may be released by sessile conspecific adults (McGee & Targett, 1989; Pechenik & Heyman, 1987). Due to such aggregative behaviour towards adults we expected to sample large larvae (close to the size at competence, i.e. 800-1,000 $\mu m$, Pechenik & Heyman, 1987) above adult beds. This was not what we observed, only 3 larvae at this size were sampled and none of them were above the main adult beds (sites 8 and 9). This low number of large larvae likely reflected the strong developmental bottleneck due to mortality occurring during larval development (Pedersen , 2008; Rumrill, 1990; Schneider , 2003). In addition, late developmental stages were expected to be found close to the bottom, looking for available substrate, making these larvae more difficult to sample with vertical tows. Moreover, when larvae find a suitable habitat (e.g. conspecific adults for *C. fornicata*), settlement processes run fast (Todd, 1998), decreasing the opportunity to sample large larvae in the field.

If larval supply depends in part on the location of spawning adults, it is also influenced by local hydrodynamics and their interactions (Dunstan & Bax, 2007). The presence of the largest larvae in low abundance at sites distant from the main broodstock, as well as the overall low larval abundances, might be explained by the transport of larvae outside the bay, which might be expected given the shape of the bay (V-shaped, gradually deeper and widening towards the mouth) (Dame & Allen, 1996). As suggested by Geyer & Signell (1992) in other bays and estuaries, larval exportation might be due to tidal currents, known to be a major component of the prevailing hydrodynamics regime in the English Channel

(Ellien , 2000; Salomon & Breton, 1991). Outputs of our analytical model agreed with this assumption, and showed that retention rates after 15 days were low for larvae released from the main known spawning locations (sites 8 and 9). For an offshore residual current typical of this area (U = 3 $cm.s^{-1}$, Salomon & Breton, 1991), the retention rate never exceeded 20 % after 15 days, whatever the spawning site and the tidal conditions. This approach however suggested that higher retention rates might be observed in some cases with larvae released more upstream in the estuary (Figure G.6). More recent sampling revealed that larvae occurred upstream (authors' personal observations), and few adults were observed more upstream (L. Lévêque, pers. comm.), which might be in favour of higher retention. These results evidenced the importance of the interactions between spawning location and hydrodynamics at a fine scale (about 1 km), thus extending the results of Edwards (2007) who investigated the role of such interactions in shaping dispersal kernels at a broader, regional scale. More complex bio-physical models have to be specifically designed to ascertain our hypothesis of larval exportation.

Despite the strong tidal export of its larvae, *C. fornicata* is now well established in the bay, which implies that efficient recruitment occurs in the population. The size-frequency analysis done on the whole dataset revealed 2 groups of larvae (with a mean size of 474±40 $\mu m$ and 602±60 $\mu m$, respectively; Figure G.7), whose mean ages can be calculated according to a relationship between size, growth rate and temperature (Rigal , *submitted*). These mean ages were estimated to be 2.5 to 3.8 days old at high temperature (maximum field temperature: 18.4°C) and 5.2 to 8.2 days old at low temperature (minimum field temperature: 15.6°C) and suggested that rather old larvae (one week-old) may be found in the bay. However, whether these larvae were produced locally or came from adjacent bays is not known. Due to the low retention rates we estimated, self- recruitment would probably be limited and recruitment from larvae originating from distant populations might be involved in population maintenance. This assumption is supported by previous genetic assignments between 6 bays of the English Channel which suggested that the bay of Morlaix displayed the lowest levels of self-recruitment (less than 30 % of individuals from the bay were assigned to this bay), which further suggested that this population might also rely on exchanges with other populations (Dupont , 2007).

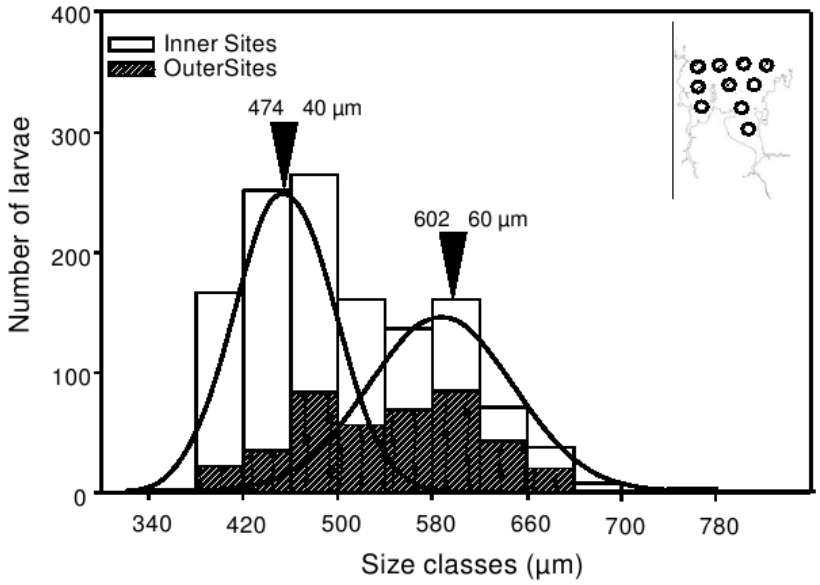


Figure G.7: Length-frequency distribution of *Crepidula fornicata* larvae at the bay scale. Curves represent the age groups identified with the Normsep software. White and dashed histograms represent the contribution of larvae from the two groups of sites discriminated by the RDA analysis according to the first RDA axis (see Figure G.5), as shown on the inserted map.

Occurring since more than 50 years along the European coasts, *C. fornicata* has particularly proliferated in sheltered areas such as bays or estuaries, with some noticeable exceptions as failure or low success (Blanchard, 1997). For instance, *C. fornicata* failed to invade the bay of Arcachon, which was explained by the scarcity of suitable habitats and absence of trawl fishing (de Montaudouin , 2001). In this case, only 30 % of the water mass is removed after 15 days in the inner part of the bay where *C. fornicata* population occurs (Plus , 2006), which suggests that the hypothesis of larval exportation could not be responsible for the failure. Conversely, our study evidenced the role of (1) adult distribution and (2) local hydrodynamics as key factors modulating larval supply. Comparisons with bays where *C. fornicata* became highly proliferative may further highlight the role of larval supply in the invasion success. Thus, the bay of Mont Saint- Michel displays high adult biomasses with 170,000 tons estimated in the western part of the bay where tidal residual currents may promote larval retention in a large and permanent anticyclonic gyre (Dubois , 2007). Similarly, the bay of Brest (10,000 tons of *C. fornicata* estimated in the inner part; Blanchard, 1995) is a semi-enclosed marine system favouring larval retention.

## G.6 Conclusion

Managing non-indigenous species requires understanding the factors which lead to the success or failure of each step of the invasion process. Our study provided an example of factors which may explain the failure of the transition between sustainable establishment and proliferation of an invasive species, by showing that limitation in larval supply due to local hydrodynamics features may impede the proliferation of a species which nevertheless has been well established since more than 50 years.

## G.7 Acknowledgements

We are grateful to our colleagues from Service Mer et Observation at the Station Biologique de Roscoff for their help in field sampling. We particularly acknowledge Laurent Lévêque who provided us with parameters forcing the analytical model. We are grateful to Pr. Pierre Legendre for his help in statistical analyses. F. Rigal and S.-D. Ayata acknowledge a PhD fellowship from the Ministère de la Recherche et de l'Enseignement Supérieur. This work was supported by the Agence Nationale de la Recherche (program ANR-05-BLAN-0001, project MIRAGE contract n°NT05-3-42438).

## G.8 Appendix

The descriptions and the values of the parameters used in the analytical model are given in Table G.1. See Figure G.2 for the schematic representation of the study bay used in the analytical model. Two regions are considered. The region $B$ is delimited in the north by a section of surface $s_1(t)$. The adult population is located within the region $B$ at a distance $x$ of the section $s_1(t)$. The region E is defined as the area outside the bay where the larvae released from the adult population can be exported by the tide: its width $L$ is equal to $x_T - x$, where $x_T$ is the maximal tidal excursion. The surface $s_1(t)$ of the section separating the regions $B$ and $E$ varies with the tidal cycle and is given by:

$$s_1(t) = W \times (h + \epsilon(t)) \qquad \text{(Eq. G.3)}$$

with $W$ the length of the region $E$, $h$ the mean depth of the bay, and $\epsilon(t)$ the free surface elevation.

The section of surface $s_2(t)$ is the other section of the region $E$. By this section, larvae are exported outside $E$ by the offshore residual current $U$. Hence, $s_2(t)$ also varies with the tidal cycle following:

$$s_2(t) = L \times (h + \epsilon(t)) = (x_T - x) \times (h + \epsilon(t)) \qquad \text{(Eq. G.4)}$$

The volume $V_B(t)$ of the region $B$ is calculated from the surface of the bay $S$, the mean depth of the bay $h$, and the free surface elevation $\epsilon(t)$ following the equation:

$$V_B(t) = S \times (h + \epsilon(t)) \qquad \text{(Eq. G.5)}$$

and the volume $V_E(t)$ of the region $E$ is calculated from:

$$V_E(t) = W \times s_2(t) \qquad \text{(Eq. G.6)}$$

The volume $V_1(t)$ exchanged between the regions $B$ and $E$ according to the tidal current $u(t)$ through the section of surface $s_1(t)$ and during a time step $\delta t$ is defined by:

$$V_1(t) = u(t) \times s_1(t) \times \delta t \qquad \text{(Eq. G.7)}$$

and the volume $V_2(t)$ removed from region $E$ by the residual current $U$ through the section of surface $s_2(t)$ during a time step $\delta t$ is defined by:

$$V_2(t) = U \times s_2(t) \times \delta t \qquad \text{(Eq. G.8)}$$

Using those equations, the final equations of the analytical model are:

During ebb:

$$\begin{cases} N_B(t+\Delta t) = N_B(t) \times \left(1 - \dfrac{u(t) \times W \times \Delta t}{S}\right) \\ N_E(t+\Delta t) = N_E(t) \times \left(1 - \dfrac{U \times \Delta t}{W}\right) + N_B(t) \times fracu(t) \times W \times \Delta t S \end{cases} \qquad \text{(Eq. G.9)}$$

During flow:

$$\begin{cases} N_B(t+\Delta t) = N_B(t) + N_E(t) \times \dfrac{u(t) \times \Delta t}{x_T - x} \\ N_E(t+\Delta t) = N_E(t) \times \left(1 - \dfrac{U \times \Delta t}{W} - fracu(t) \times \Delta t x_T - x\right) \end{cases} \qquad \text{(Eq. G.10)}$$

# Bibliographie


Ådlandsvik, B. (2008). Marine downscaling of a future climate scenario for the North sea. *Tellus A*, 60:451–458.

Aiken, C., Navarrete, S., Castillo, M. et Castilla, J. (2007). Along-shore larval dispersal kernels in a numerical ocean model of the central chilean coast. *Marine Ecology Progress Series*, 339:13–24.

Albaina, A. et Irigoien, X. (2007). Fine scale zooplankton distribution in the Bay of Biscay in spring 2004. *Journal of Plankton Research*, 29:851–870.

Allain, G., Petitgas, P., Lazure, P. et Grellier, P. (2007). Biophysical modelling of larval drift, growth and survival for the prediction of the anchovy (*Engraulis encrasicolus*) recruitment in the Bay of Biscay (NE Atlantic). *Fisheries Oceanography*, 16:489–505.

Almany, G., Connolly, S., Heath, D., Hogan, J., Jones, G., McCook, L., Mills, M., Pressey, R. et Williamson, D. (2009). Connectivity, biodiversity conservation and the design of marine reserve networks for coral reefs. *Coral Reefs*, 28:339–351.

Andrewartha, H. et Birch, L. (1954). *The distribution and abundance of animals.* University of Chicago Press, Chicago.

Andrews, J., Gurney, W., Heath, M., Gallego, A., O'Brien, C. M., Darby, C. et Tyldesley, G. (2006). Modelling the spatial demography of Atlantic cod (*Gadus morhua*) on the European continental shelf. *Canadian Journal of Fisheries and Aquatic Sciences*, 63:1027–1048.

André, C., Lindegarth, M., Jonsson, P. et Sundberg, P. (1999). Species identification of bivalve larvae using random amplified polymorphic DNA (RAPD) : differentiation between *Cerastoderma edule* and *C. lamarcki*. *Journal of Marine Biological Association of the United Kingdom*, 79:563–565.

Anger, K., Spivak, E. et Luppit, T. (1998). Effects of reduced salinities on development and bioenergetics of early larval stone crab *Carcinus maenas*. *Journal of Experimental Marine Biology and Ecology*, 220:287–304.

Arnold, W., Hitchcock, G., Frischer, M., Wanninkhof, R. et Sheng, P. (2005). Dispersal of an introduced larval cohort in a coastal lagoon. *Limnology and Oceanography*, 50:587–597.

Auad, G., Miller, A. et Di Lorenzo, E. (2006). Long-term forecast of oceanic conditions off California and their biological implications. *Journal of Geophysical Research-Oceans*, 111:C09008, doi :10.1029/2005JC003219.

Ayata, S.-D., Ellien, C., Dumas, F., Dubois, S. et Thiébaut, E. (2009). Modelling larval dispersal and settlement of the reef-building polychaete *Sabellaria alveolata* : role of hydroclimatic processes on the sustainability of biogenic reefs. *Continental Shelf Research*, 29:1605–1623.

Ayata, S.-D., Lazure, P. et Thiébaut, E. (xxxx). How does the connectivity between populations mediate range limits of marine invertebrates ? a case study in the NE Atlantic. *Soumis à Progress in Oceanography*.

Bachelet, G. (1990). Recruitment of soft-sediment infaunal invertebrates : the importance of juvenile benthic stages. *La Mer*, 28:199–210.

Bailly du Bois, P. et Dumas, F. (2005). Fast hydrodynamic model for medium- and long-term dispersion in seawater in the English Channel and southern North Sea, qualitative and quantitative validation by radionuclide tracers. *Ocean Modelling*, 9:169–210.

Bakun, A. (1990). Global climate change and intensification of coastal ocean upwelling. *Science*, 247 (4939):198–201.

Banse, K. (1986). Vertical distribution and horizontal transport of planktonic larvae of echinoderms and benthic polychaetes in an open coastal sea. *Bulletin of Marine Science*, 39:162–175.

Barnay, A., Ellien, C., Gentil, F. et Thiébaut, E. (2003). A model study on variations in larval supply : are populations of the polychaete *Owenia fusiformis* in the English Channel open or closed ? *Helgoland Marine Research*, 56:229–237.

Batten, S., Clark, R., Flinkman, J., Hays, G., John, E., John, A., Jonas, T., Lindley, J., Stevens, D. et Walne, A. (2003). CPR sampling : the technical background, materials and methods, consistency and comparability. *Progress In Oceanography*, 58:193–215.

Baums, I., Paris, C. et Chérubin, M. L. (2006). A bio-oceanographic filter to larval dispersal in a reef-building coral. *Limnology and Oceanography*, 51:1969–1981.

Beaugrand, G. (2004). Continuous plankton records : Plankton atlas of the North Atlantic ocean (1958-1999). I. introduction and methodology. *Marine Ecology Progress Series*, Proceedings of the National Academy of Sciences of the United States of America:3–10.

Becker, B., Levin, L., Fodrie, F. et McMillan, P. (2007). Complex larval connectivity patterns among marine invertebrate populations. *Proceedings of the National Academy of Sciences of the United States of America*, 104:3267–3272.

Belgrano, A., Legendre, P., Dewarumez, J. et Frontier, S. (1995a). Spatial structure and ecological variations of meroplankton on the Belgian-Dutch coast of the North Sea. *Marine Ecology Progress Series*, 128:51–59.

Belgrano, A., Legendre, P., Dewarumez, J. et Frontier, S. (1995b). Spatial structure and ecological variations of meroplankton on the French-Belgian coast of the North Sea. *Marine Ecology Progress Series*, 128:43–50.

Bellier, E., Planque, B. et Petitgas, P. (2007). Historical fluctuations in spawning location of anchovy (*Engraulis encrasicolus*) and sardine (*Sardina pilchardus*) in the Bay of Biscay during 1967-1973 and 2000-2004. *Fisheries Oceanography*, 16:1–15.

Bentley, M. et Pacey, A. (1992). Physiological and environmental control of reproduction in polychaetes. *Oceanography and Marine Biology : an Annual Review*, 30:443–481.

Bhaud, M. (2000). Two contradictory elements determine invertebrate recruitment : dispersion of larvae and spatial restrictions on adults. *Oceanologica Acta*, 23:409–422.

Bird, R., Stewart, W. et Lightfoot, E. (2001). *Transport phenomena, 2nd edition.* John Wiley, New York.

Black, K., Gay, S. et Andrews, J. (1990). Residence times of neutrally-buoyant matter such as larvae, sewage or nutrients on coral reefs. *Coral Reefs*, 9:105–114.

Blanchard, M. (1995). Origine et état de la population de *Crepidula fornicata* (Gastropoda Prosobranchia) sur le littoral français. *Haliotis*, 24:75–86.

Blanchard, M. (1997). Spread of the slipper limpet *Crepidula fornicata* (L.1758) in europe : current state and consequences. *Scientia Marina*, 61:109–118.

Bode, M., Bode, L. et Armsworth, P. (2006). Larval dispersal reveals regional sources and sinks in the great barrier reef. *Marine Ecology Progress Series*, 308:17–25.

Bonhomme, F. et Planes, S. (2000). Some evolutionary arguments about what maintains the pelagic interval in reef fishes. *Environmental Biology of Fishes*, 59:365–383.

Borcard, D., Legendre, P. et Drapeau, P. (1992). Partialling out the spatial component of ecological variation. *Ecology*, 73:1045–1055.

Botsford, L., Hastings, A. et Gaines, S. (2001). Dependence of sustainability on the configuration of marine reserves and larval dispersal distance. *Ecology Letters*, 4:144–150.

Botsford, L., Moloney, C., Hastings, A., Largier, J., Powell, T., Higgins, K. et Quinn, J. (1994). The influence of spatially and temporally varying oceanographic conditions on meroplanktonic metapopulations. *Deep Sea Research I*, 41:107–145.

Botsford, L., White, J., Coffroth, M.-A., Paris, C., Planes, S., Shearer, T., Thorrold, S. et Jones, G. (2009). Connectivity and resilience of coral reef metapopulations in marine protected areas : matching empirical efforts to predictive needs. *Coral Reefs*, 28:327–337.

Bradbury, I. et Snelgrove, P. (2001). Contrasting larval transport in demersal fish and benthic invertebrates : the roles of behaviour and advective processes in determining spatial pattern. *Canadian Journal of Fisheries and Aquatic Sciences*, 58:811–823.

Butman, C. (1987). Larval settelment of soft sediment invertebrates : spacial of pattern explained by active habitat selection and the emergig role of hydrodynamical processes. *Oceanography and Marine Biology Annual Review*, 25:113–165.

Byers, J. et Pringle, J. (2006). Going against the flow : retention, range limits and invasions in advective environments. *Marine Ecology Progress Series*, 313:27–41.

Cabal, J., González-Nuevo, G. et Nogueira, E. (2008). Mesozooplankton species distribution in the NW and N Iberian shelf during spring 2004 : Relationship with frontal structures. *Journal of Marine Systems*, 72:282–297.

Cabioch, L. (1968). Contribution à la connaissance des peuplements benthiques de la Manche occidentale. *Cahiers de Biologie Marine*, 5:488–720.

Cabioch, L. et Douvillé, J.-L. (1979). La circulation des eaux dans la baie de morlaix et ses abords : premières données obtenues par suivis de flotteurs dérivants. *Travaux de la Station Biologique de Roscoff*, 26:11–20.

Cabioch, L., Gentil, F., Glaçon, R. et Retière, C. (1977). *Biology of benthic organisms*, Chapitre Le macrobenthos des fonds meubles de la Manche : distribution générale et écologie, pages 115–128. Pergamon Press, Oxford. Éditeurs : Keegan, B.F., O'Cedigh, P., Boaden, P.J.S.

Caley, M., Carr, M., Hixon, M., Hughes, T., Jones, G. et Menge, B. (1996). Recruitment and the local dynamics of open marine populations. *Annual Review of Ecology and Systematics*, 27:477–500.

Cameron, B. et Metaxas, A. (2005). Invasive green crab, *Carcinus maenas*, on the Atlantic coast and in the Bras d'Or Lakes of Nova Scotia, Canada : larval supply and recruitment. *Journal of Marine Biological Association of the United Kingdom*, 85:847–855.

Carlton, J. et Geller, J. (1993). Ecological roulette : the global transport of nonindigenous marine organisms. *Science*, 261:78–82.

Carroll, M. (1996). Barnacle population dynamics and recruitment regulation in the southcentral alaska. *Journal of Experimental Marine Biology and Ecology*, 199:285–302.

Cazaux, C. (1964). Développement larvaire de *Sabellaria alveolata* (Linné). *Bulletin de l'Institut Océanographique de Monaco*, 62:1–15.

Cazaux, C. (1970). *Recherches sur l'écologie et le développement larvaire des Polychètes de la région d'Arcachon*. Thèse de doctorat. Université de Bordeaux.

Chassé, C. et Glémarec, M. (1976). *Atlas du littoral français : atlas des fonds meubles du plateau continental du golfe de Gascogne : cartes bio-sédimentaires. Produit numérique REBENT Ifremer-Université-CNRS, 2009, http ://www.rebent.org*. Chassé, C. and Glémarec, M. avec le concours du CNEXO.

Chen, Y.-H., Shaw, P.-T. et Wolcott, T. (1997). Enhancing estuarine retention of planktonic larvae by tidal currents. *Estuarine, Coastal and Shelf Science*, 45:525–533.

Chérubin, L. et Richardson, P. (2007). Caribbean current variability and the influence of the Amazon and Orinoco freshwater plumes. *Deep-Sea Research Part I-Oceanographic Research Papers*, 54:1451–1473.

Chia, F.-S., Buckland-Nicks, J. et Young, C. (1984). Locomotion of marine invertebrate larvae : a review. *Canadian Journal of Zoology*, 62:1205–1222.

Chiswell, S. et Booth, J. (2008). Sources and sinks of larval settlement in *Jasus edwardsii* around New Zealand : Where do larvae come from and where do they go ? *Marine Ecology Progress Series*, 354:201–217.

Christensen, J., Hewitson, B., Busuioc, A., Chen, A., Gao, X., Held, I., Jones, R., Kolli, R., Kwon, W.-T., Laprise, R., Magaña Rueda, V., Mearns, L., Menéndez, C., Räisänen, J., Rinke, A., Sarr,

A. et Whetton, P. (2007). *Climate change 2007 : the physical science basis. Contribution of working group I to the fourth assessment report of the Intergovernmental Panel on Climate Changes*, Chapitre Regional climate projections, page 296. Cambridge University Press, Cambridge, United Kingdom and New York, NY, USA.

Cohen, A. et Carlton, J. (1998). Accelerating invasion rate in a highly invaded estuary. *Science*, 279:555–558.

Comtet, T., Jollivet, D., Khripounoff, A., Segonzac, M. et Dixon, D. (2000). Molecular and morphological identification of settlement-stage vent mussel larvae, *Bathymodiolus azoricus* (Bivalvia : Mytilidae), preserved in situ at active vent fields on the mid-Atlantic ridge. *Limnology and Oceanography*, 45:1655–1661.

Coum, A. (1979). *La population de crépidules Crepidula fornicata (L. 1758) en rade de Brest : écologie et dynamique*. Thèse de doctorat. Université de Bretagne Occidentale, Brest, France.

Cowan, J. J. et Houde, E. (1992). Size-dependent predation on marine fish larvae by ctenophores, scyphomedusae, and planktivorous fish. *Fisheries Oceanography*, 1:113–126.

Cowen, R. (2002). *Coral Reef Fishes*, Chapitre 7 : Oceanographic influences on larval dispersal and retention and their consequences for population connectivity, pages 149–170. Academic press.

Cowen, R., Gawarkiewicz, G., Pineda, J., Thorrold, S. et Werner, F. (2007). Population connectivity in marine systems : An overview. *Oceanography*, 20:14–21.

Cowen, R. et Sponaugle, S. (2009). Larval dispersal and marine population connectivity. *Annual Review of Marine Science*, 1:443–446.

Cowen, R. K., Lwiza, K. M., Sponaugle, S., Paris, C. B. et Olson, D. (2000). Connectivity of marine populations : Open or closed ? *Science*, 287(5454):857–859.

Cowen, R. K., Paris, C. B. et Srinivasan, A. (2006). Scaling of connectivity in marine populations. *Science*, 311(5760):522–7.

Cox, B. et Moore, P. (2000). *Biogeography : An Ecological and Evolutionary Approach*. Blackwell Scientific Publications : London, 6ème édition.

Cunningham, P., Hawkins, S., Jones, H. et Burrows, M. (1984). The biogeography and ecology of *Sabellaria alveolata*. *Nature Conservancy Council CSD report*, 535.

Cury, P., Shin, Y.-J., Planque, B., Durant, J. M., Fromentin, J. M., Kramer-Schadt, S., Stenseth, N. C., Travers, M. et Grimm, V. (2008). Ecosystem oceanography for global change in fisheries. *Trends in Ecology and Evolution*, 23:338–346.

Cushing, D. (1975). *Marine ecology and fisheries*. London.

Dame, R. et Allen, D. (1996). Between estuaries and the sea. *Journal of Experimental Biology and Ecology*, 200:169–185.

Dauvin, J.-C. (1992). Cinétique du recrutement et croissance des juvéniles d'*Owenia fusiformis* Delle Chiaje en baie de Seine (Manche orientale). *Oceanologica Acta*, 15:187–196.

Davis, A. et Butler, A. (1989). Direct observations of larval dispersal in the colonial ascidian *Podoclavella moluccensis* Sluiter : evidence for closed populations. *Journal of Experimental Marine Biology and Ecology*, 127:189–203.

Dawirs, R. (1985). Temperature and larval development of *Carcinus maenas* (Decapoda) in the laboratory ; predictions of larval dynamics in the seas. *Marine Ecology Progress Series*, 24:297–302.

de Montaudouin, X., Labarraque, D., Giraud, K. et Bachelet, G. (2001). Why does the introduced gastropod *Crepidula fornicata* fail to invade Arcachon Bay (France) ? *Marine Biological Association of the United Kingdom*, 81:97–104.

de Rivera, C., Hitchcock, N., Teck, S., Hines, A. et Ruiz, G. (2007). Larval development rate predicts range expansion of an introduced crab. *Marine Biology*, 150:1275–1288.

deCastro, M., Gomez-Gesteira, M., Alvarez, I. et Gesteira, J. (2009). Present warming within the context of cooling-warming cycles observed since 1854 in the Bay of Biscay. *Continental Shelf Research*, 29:1053–1059.

Dekshenieks, M., Hofmann, E., Klinck, J. et Powell, E. (1996). Modeling the vertical distribution of oyster larvae in response to environmental conditions. *Marine Ecology Progress Series*, 136:97–110.

Dekshenieks, M., Hofmann, E., Klinck, J. et Powell, E. (1997). A modelling study of the effects of size- and depth-dependent predation on larval survival. *Journal of Plankton Research*, 19:1583–1598.

Delhez, E., Damm, P., De Goede, E., de Kok, J., Dumas, F., Gerritsen, H., Jones, J., Ozer, J., Polhmann, T., Rasch, P., Skogen, M. et Proctor, R. (2004). Variability of shelf seas hydrodynamic models : lessons from NOMADS2. *Journal of Marine Systems*, 45:39–53.

Demarcq, H. (2009). Trends in primary production, sea surface temperature and wind in upwelling systems (1998-2007). *Progress in Oceanography*, 83 (1-4):376–385.

Denman, K., Brasseur, G., Chidthaisong, A., Ciais, P., Cox, P., Dickinson, R., Hauglustaine, D., Heinze, C., Holland, E., Jacob, D., Lohmann, U., Ramachandran, S., da Silva Dias, P., Wofsy, S. et Zhang, X. (2007). *Climate Change 2007 : The physical science basis. Contribution of working group I to the fourth assessment report of the Intergovernmental Panel on Climate Change*, Chapitre Couplings between changes in the climate system and biogeochemistry. Cambridge University Press, Cambridge, United Kingdom and New York, NY, USA.

DiBacco, C. et Levin, L. (2000). Development and application of elemental fingerprinting to track the dispersal of marine invertebrate larvae. *Limnology and Oceanography*, 45:871–880.

DiBacco, C., Sutton, D. et McConnico, L. (2001). Vertical migration behavior and horizontal distribution of brachyuran larvae in a low-inflow estuary : implications for bay-ocean exchange. *Marine Ecology Progress Series*, 217:191–206.

Dinter, W. (2001). *Biogeography of the OSPAR Maritime Area.* Federal Agency for Nature Conservation. Bonn, Germany.

Duarte, C. (2007). Marine ecology warms up to theory. *Trends in Ecology and Evolution*, 22:331–333.

Dubois, S. (2003). *Ecologie des formations récifales à Sabellaria alveolata (L.) : valeur fonctionnelle et patrimoniale.* Thèse de doctorat. Muséum National d'Histoire Naturelle, Paris.

Dubois, S., Commito, J., Olivier, F. et Retiere, C. (2006). Effects of epibionts on *Sabellaria alveolata* (L.) biogenic reefs and their associated fauna in the Bay of Mont Saint-Michel. *Estuarine, Coastal and Shelf Science*, 68:635–646.

Dubois, S., Comtet, T., Retière, C. et Thiébaut, E. (2007). Distribution and retention of *Sabellaria alveolata* larvae (Polychaeta : Sabellariidae) in the Bay of Mont-Saint-Michel, France. *Marine Ecology Progress Series*, 346:243–254.

Dubois, S., Retière, C. et Olivier, F. (2002). Biodiversity associated with *Sabellaria alveolata* (Polychaeta : Sabellariidae) reefs : effects on human disturbances. *Journal of Marine Biological Association of United Kingdom*, 82:817–826.

Dunstan, P. et Bax, N. (2007). How far can marine species go ? influence of population biology and larval movement on future range limits. *Marine Ecology Progress Series*, 344:15–28.

Dupont, L. (2004). *Invasion des côtes françaises par le mollusque exotique Crepidula fornicata : contribution de la dispersion larvaire et du système de reproduction au succès de la colonisation.* Thèse de doctorat. Université Pierre et Marie Curie, Paris, France.

Dupont, L., Ellien, C. et Viard, F. (2007). Limits to gene flow in the slipper limpet *Crepidula fornicata* as revealed by microsatellite data and a larval dispersal modes. *Marine Ecology Progress Series*, 349:125–138.

Dupont, L., Jollivet, D. et Viard, F. (2003). High genetic diversity and ephemeral drift effects in a successful introduced mollusc (*Crepidula fornicata* : Gastropoda). *Marine Ecology Progress Series*, 253:183–195.

Eckert, G. (2003). Effects of the planktonic period on marine population fluctuations. *Ecology*, 84:372–383.

Eckman, J. (1996). Closing the larval loop : linking larval ecology to the population dynamics of marine benthic invertebrates. *Journal of Experimental Marine Biology and Ecology*, 200:207–237.

Edwards, K., Hare, J., Werner, F. et Blanton, B. (2006). Lagrangian circulation on the Southeast US Continental Shelf : Implications for larval dispersal and retention. *Continental Shelf Research*, 26:1375–1394.

Edwards, K., Hare, J., Werner, F. et Seim, H. (2007). Using 2-dimensional dispersal kernels to identify the dominant influences on larval dispersal on continental shelves. *Marine Ecology Progress Series*, 352:77–87.

Edwards, M. et Richardson, A. J. (2004). Impact of climate change on marine pelagic phenology and trophic mismatch. *Nature*, 430:881–884.

Ellien, C., Thiébaut, E., Barnay, A., Dauvin, J.-C., Gentil, F. et Salomon, J.-C. (2000). The influence of variability in larval dispersal on the dynamics of a marine metapopulation in the Eastern Channel. *Oceanologica Acta*, 23:423–442.

Ellien, C., Thiébaut, E., Dumas, F., Salomon, J.-C. et Nival, P. (2004). A modelling study of the respective role of hydrodynamic processes and larval mortality on larval dispersal and recruitment of benthic invertebrates : example of *Pectinaria koreni* (Annelida : Polychaeta) in the Bay of Seine (English Channel). *Journal of Plankton Research*, 26:117–132.

Engler, R. et Guisan, A. (2009). MIGCLIM : Predicting plant distributionand dispersal in a changing climate. *Diversity and Distributions*, 15:590–601.

Fach, B. et Klinck, J. (2006). Transport of Antarctic krill (*Euphausia superba*) across the Scotia Sea. Part I : Circulation and particle tracking simulations. *Deep-Sea Research Part I-Oceanographic Research Papers*, 53:987–1010.

Farcy, S. (2003). Analyse de la structure génétique des populations de *Sabellaria alveolata* (L.) dans la baie du Mont-Saint-Michel à l'aide de marqueurs microsatellites. Mémoire de D.E.S.S. Gestion de la biodiversité, Université Pierre et Marie Curie - Paris 6.

FIelds, P. A., Graham, J. B., Rosenblatt, R. H. et Somero, G. N. (1993). Effects of expected global climate change on marine faunas. *Trends in Ecology & Evolution*, 8:361–367.

Fiksen, O., Jørgensen, C., Kristiansen, T., Vikebø, F. et Huse, G. (2007). Linking behavioural ecology and oceanography : larval behaviour determines growth, mortality and dispersal. *Marine Ecology Progress Series*, 347:195–205.

Fogarty, M. et Botsford, L. (2007). Population connectivity and spatial management of marine fisheries. *Oceanography*, 20:112–123.

Folmer, O., Black, M., Hoeh, W., Lutz, R. et Vrijenhoek, R. (1994). DNA primers for amplification of mitochondrial cytochrome C oxidase subunit I from diverse metazoan invertebrates. *Molecular Marine Biology and Biotechnology*, 3:294–299.

Fortier, L. et Leggett, W. (1982). Fickian transport and the dispersal of fish larvae in estuaries. *Canadian Journal of Fisheries and Aquatic Sciences*, 39:1150–1163.

Franklin, C. et Seebacher, F. (2009). Adapting to climate change. *Science*, 323:876–876.

Frontier, S. (1972). Calcul de l'erreur sur un comptage de zooplancton. *Journal of Experimental Marine Biology and Ecology*, 10:121–132.

Frontier, S. (1986). Studying fronts as contact ecosystems. *In Marine interfaces ecohydrodynamics*, pages 55–66. Elsevier, Amsterdam. Nikoul, J.C.J. (Ed).

Frontier, S. et Pichod-Viale, D. (1991). *Écosystèmes : structure, fonctionnement, évolution.* Masson, Paris.

Gaines, S. et Bertness, M. (1992). Dispersal of juveniles and variable recruitment in sessile marine species. *Nature*, 360:579–580.

Gaines, S., Gaylord, B., Gerber, L., Hastings, A. et Kinlan, B. (2007). Connecting places : The ecological consequences of dispersal in the sea. *Oceanography*, 20:90–99.

Gaines, S., Gaylord, B. et Largier, J. (2003). Avoiding current oversights in marine reserve design. *Ecological Applications*, 13:32–46.

Gaines, S. et Roughgarden, J. (1985). Larval settlement rate : A leading determinant of structure in an ecological community of the marine intertidal zone. *Proceedings of the National Academy of Sciences of the United States of America*, 82:3707–3711.

Garland, E. et Zimmer, C. (2002). Techniques for the identification of bivalve larvae. *Marine Ecology Progress Series*, 225:299–310.

Garland, E., Zimmer, C. et Lentz, S. (2002). Larval distributions in inner-shelf waters : The roles of wind-driven cross-shelf currents and diel vertical migrations. *Limnology and Oceanography*, 47:803–817.

Gawarkiewicz, G., Monismith, S. et Largier, J. (2007). Observing larval transport processes affecting population connectivity : Progress and challenges. *Oceanography*, 20:40–53.

Gaylord, B. et Gaines, S. (2000). Temperature or transport ? Range limits in marine species mediated solely by flow. *American Naturalist*, 155:769–789.

Gentil, F., Dauvin, J.-C. et Ménard, F. (1990). Reproductive biology of the polychaete *Owenia fusiformis* Delle Chiaje in the Bay of Seine (eastern English Channel). *Journal of Experimental Marine Biology and Ecology*, 142:13–23.

Gerber, L., Botsford, L., Hastings, A., Possingham, H., Gaines, S., Palumbi, S. et Andelman, S. (2003). Population models for marine reserve design : a retrospective and prospective synthesis. *Ecological Applications*, 13:S47–S64.

Geyer, W. et Signell, R. (1992). A reassessment of the role of tidal dispersion in estuaries and bays. *Estuaries*, 15:97–108.

Gilg, M. et Hilbish, T. (2003a). The geography of marine larval dipersal : coupling genetics with fine scale physical oceanography. *Ecology*, 84:2989–2998.

Gilg, M. et Hilbish, T. (2003b). Patterns of larval dispersal and their effect on the maintenance of a blue mussel hybrid zone in southwestern England. *Evolution*, 57:1061–1077.

Glémarec, M. (1969). *Les peuplements benthiques du plateau continental Nord-Gascogne.* Thèse de doctorat d'état. Faculté des Sciences de Brest.

Gómez-Gesteira, M., deCastro, M., Alvarez, I. et Gómez-Gesteira, J. L. (2008). Coastal sea surface temperature warming trend along the continental part of the Atlantic arc (1985-2005). *Journal of Geophysical Research-Oceans*, 113:doi :10.1029/2007JC004315.

Gray, J. (1997). Marine biodiversity : patterns, threats and conservation needs. *Biodiversity and Conservation*, 6:153–175.

Grimm, V., Reise, K. et Strasser, M. (2003). Marine metapopulations : a useful concept ? *Helgoland Marine Research*, 56:222–228.

Gros, P. et Cochard, J.-C. (1978). Biologie de *Nyctiphanes couchii* (Crustacea, euphasiacea) dans le secteur Nord du Golfe de Gascogne. *Annales de l'Institut Océanographique de Paris*, 54:25–46.

Gruet, Y. (1982). *Recherches sur l'écologie des 'récifs' d'Hermelles édifiés par l'Annélide Polychète Sabellaria alveolata (Linné).* Thèse de doctorat. Université de Nantes, France.

Gruet, Y. (1986). Spatio-temporal changes of sabellarian reefs built by the sedentary polychaete *Sabellaria alveolata* (Linné). *Marine Ecology*, 7:303–319.

Gruet, Y. et Lassus, P. (1983). Contribution à l'étude de la biologie reproductive d'une population naturelle de l'annélide polychète *Sabellaria alveolata* (Linné). *Annales de l'Institut Océanographique de Paris*, 59:127–140.

Guichard, F., Levin, S., Hastings, A. et Siegel, D. (2004). Toward a metacommunity approach to marine reserve theory. *Bioscience*, 54:1003–1011.

Guillou, J. (1980). *Les peuplements de sables fins du littoral Nord-Gascogne.* Thèse de 3ème cycle. Université de Bretagne Occidental.

Guizien, K., Brochier, T., Duchêne, J.-C., Koh, B.-S. et Marsaleix, P. (2006). Dispersal of *Owenia fusiformis* larvae by wind-driven currents : turbulence, swimming behaviour and mortality in a three-dimensional stochastic model. *Marine Ecology Progress Series*, 311:47–66.

Hall, T. . (1999). Bioedit : a user-friendly biological sequence alignment editor and analysis program for Windows 95/98/NT. *Nucleic Acids Symposium Series*, 41:95–98.

Hannah, C. (2007). Future directions in modeling physical-biological interactions. *Marine Ecology Progress Series*, 347:301–306.

Hansen, B. et Larsen, J. (2005). Spatial distribution of velichoncha larvae (Bivalvia) identified by SSNM-PCR. *Journal of Shellfish Research*, 24:561–565.

Hanski, I. (1999). *Metapopulation Ecology.* Oxford University Press, Oxford.

Hare, M., Palumbi, S. et Butman, C. (2000). Single-step species identification of bivalve larvae using multiplex polymerase chain reaction. *Marine Biology*, 137:953–961.

Harley, C., Hughes, A., Hultgren, K., Miner, B., Sorte, C., Thornber, C., Rodriguez, L., Tomanek, L. et Williams, S. (2006). The impacts of climate change in coastal marine systems. *Ecology Letters*, 9:228–241.

Harrison, S. (1991). Local extinction in a metapopulation context : an empirical evaluation. *Biological Journal of the Linnean Society*, 42:73–88.

Hastings, A. et Botsford, L. (2006). Persistence of spatial populations depends on returning home. *Proceedings of the National Academy of Sciences of the United States of America*, 103:6067–6072.

Hastings, A., Byers, J. E., Crooks, J. A., Cuddington, K., Jones, C. G., Lambrinos, J. G., Talley, T. S. et Wilson, W. G. (2007). Ecosystem engineering in space and time. *Ecology Letters*, 10:153–64.

Hawkins, S., Southward, A. et Genner, M. (2003). Detection of environmental change in a marine ecosystem ? Evidence from the western English Channel. *Science of the Total Environment*, 310:245–256.

Heath, M., Kunzlik, P., Gallego, A., Holmes, S. et Wright, P. (2008). A model of meta-population dynamics for north sea and west of scotland cod - the dynamic consequences of natal fidelity. *Fisheries Research*, 93 (1-2):92–116.

Hedgecock, D., Barber, P. et Edmands, S. (2007). Genetic approaches to measuring connectivity. *Oceanography*, 20:70–79.

Hellberg, M., Burton, R., Neigel, J. et Palumbi, S. (2002). Genetic assessment of connectivity among marine populations. *Bulletin of Marine Science*, 70:273–290.

Hill, A. (1991a). A mechanism for horizontal zooplankton transport by vertical migration in tidal currents. *Marine biology*, 111:485–492.

Hill, A. (1991b). Vertical migration in tidal currents. *Marine Ecology Progress Series*, 75:39–54.

Hill, A. (1994). Horizontal zooplankton dispersal by diel vertical migration in S2 tidal currents on the northwest European continental shelf. *Continental Shelf Research*, 14:491–506.

Hily, C. (1976). *Ecologie benthique des pertuis Charentais*. Thèse de 3ème cycle. Université de Bretagne Occidental.

Hollowed, A., Bond, N., Wilderbuer, T., Stockhausen, W., Teresa A'mar, Z., Beamish, R., Overland, J. et Schirripa, M. (2009). A framework for modelling fish and shellfish responses to future climate change. *ICES Journal of Marine Science*, 66:1584–1594.

Holt, T., Rees, E., Hawkins, S. et Seed, R. (1998). Biogenic reefs (volume IX). an overview of dynamic and sensitivity characteristics for conservation management of marine SACs. Rapport technique, Port Erin Marine Laboratory, University of Liverpool.

Hosoi, M., Hosoi-Tanabe, S., Sawada, H., Ueno, M., Toyohara, H. et Hayashi, I. (2004). Sequence and polymerase chain reaction-restriction fragment length polymorphism analysis of the large subunit rRNA gene of bivalve : simple and widely applicable technique for multiple species identification of bivalve larvae. *Fisheries Science*, 70:629–637.

Houde, E. (1974). Effects of temperature and delayed feeding on growth and survival of larvae of three species of subtropical marine fishes. *Marine Biology*, 26:271–285.

Houde, E. (1988). Fish early life dynamics and recruitment variability. *American Fisheries Society Symposium*, 2:17–29.

Houde, E. (1989). Comparative growth, mortality, and energetics of marine fish larvae : Temperature and implied latitudinal effects. *Fisheries Bulletin*, 87:471–495.

Houde, E. et Zastrow, C. (1993). Ecosystem- and taxon-specific dynamic and energetics properties of larval fish assemblages. *Bulletin of Marine Science*, 53:290–335.

Hsieh, C.-H., Kim, H., William, W., Di Lorenzo, E. et Sugihara, G. (2009). Climate-driven changes in abundance and distribution of larvae of oceanic fishes in the southern California region. *Global Change Biology*, 15:2137–2152.

Hughes, T., Baird, A., Dinsdale, E., Moltschaniwskyj, N., Pratchett, M., Tanner, J. et Willis, B. (2000). Supply-side ecology works both ways : the links between benthic adults, fecundity, and larval recruits. *Ecology*, 81:2241–2249.

Hunter, J., Craig, P. et Phillips, H. (1993). On the use of random walk models with spatially variable diffusivity. *Journal of Computational Physics*, 106:366–376.

Huret, M., Petitgas, P. et Woillez, M. (xxxx). Dispersal patterns of anchovy (*Engraulis encrasicolus*) early life stages in the Bay of Biscay captured with a 3D hydrodynamic model and spatial indices. *Soumis à Progress in Oceanography.*

Huret, M., Runge, Jeffrey, A., Chen, C., Cowles, G., Xu, Q. et Pringle, J. M. (2007). Dispersal modeling of fish early life stages : sensitivity with application to Atlantic cod in the western gulf of maine. *Marine Ecology Progree Series*, 347:261–274.

Incze, L. et Naimie, C. (2000). Modelling the transport of lobster (*Homarus americanus*) larvae and postlarvae in the Gulf of Maine. *Fishery Oceanography*, 9:99–113.

Intergovernmental Panel on Climate Change (2007). *Climate change 2007 : the physical science basis.* Cambridge University Press, Cambridge.

Irisson, J.-O. (2008). *Behavioural approach to larval dispersal in marine systems.* Ecole doctorale de l'Ecole Pratique des Hautes Etudes.

Irisson, J.-O., Levan, A., De Lara, M. et Planes, S. (2004). Strategies and trajectories of coral reef fish larvae optimizing self-recruitment. *Journal of Theoretical Biology*, 227:205–218.

Irlinger, J.-P., Gentil, F. et Quintino, V. (1991). Reproductive biology of the polychaete *Pectinaria koreni* (Malmgren) in the Bay of Seine. *Ophelia Suppl*, 5:343–350.

James, M., Armsworth, P., Mason, L. et Bode, L. (2002). The structure of reef fish metapopulations : modelling larval dispersal and retention patterns. *Proceedings of the Royal Society B*, 269:2079–86.

Jensen, R. A. et Morse, D. E. (1990). Chemically induced metamorphosis of polychaete larvae in both the laboratory and ocean environment. *Journal of Chemical Ecology*, 16:911–930.

Jollivet, D., Empis, A., Baker, M., Hourdez, S., Comtet, T., Jouin-Toulmond, C., Desbruyères, D. et Tyler, P. (2000). Reproductive biology, sexual dimorphism, and population structure of the deep sea hydrothermal vent scale-worm, *Branchipolynoe seepensis* (Polychaeta : Polynoidae). *Journal of the Marine Biological Association of the United Kingdom*, 80:55–68.

Jolly, M., Guyard, P., Ellien, C., Gentil, F., Viard, F., Thiébaut, E. et Jollivet, D. (2009). Population genetics and hydrodynamic modelling of larval dispersal dissociate contemporary patterns of connectivity from historical expansion into European shelf seas in the polychaete *Pectinaria koreni*. *Limnology and Oceanography*, 54:2089–2106.

Jolly, M., Jollivet, D., Gentil, F., Thiébaut, E. et Viard, F. (2005). Sharp genetic break between Atlantic and English Channel populations of the polychaete *Pectinaria koreni*, along the north coast of France. *Heredity*, 94:23–32.

Jolly, M., Viard, F., Gentil, F., Thiébaut, E. et Jollivet, D. (2006). Comparative phylogeography of two coastal polychaete tubeworms in the Northeast Atlantic supports shared history and vicariant events. *Molecular Ecology*, 15:1814–1855.

Jolly, T. (2005). *Structures génétiques et histoires évolutives de polychètes inféodées aux sédiments fins envasés dans l'Atlantique Nord Est : les genres Pectinaria sp. et Owenia sp.* Thèse de doctorat de l'université de Paris 6.

Jones, C., Lawton, J. et Shachak, M. (1997). Positive and negative effects of organisms as physical ecosystem engineers. *Ecology*, 78:1946–1957.

Jones, G., Almany, G., Russ, G., Sale, P., Steneck, R., van Oppen, M. et Willis, B. (2009a). Larval retention and connectivity among populations of corals and reef fishes : history, advances and challenges. *Coral Reefs*, 28:307–325.

Jones, G., Planes, S. et Thorrold, S. (2005). Coral reef fish larvae settle close to home. *Current Biology*, 15:1314–1318.

Jones, G., Russ, G., Sale, P. et Steneck, R. (2009b). Theme section on "larval connectivity, resilience and the future of coral reefs". *Coral Reefs*, 28:303–305.

Jones, G., Srinivasan, M. et Almany, G. (2007). Population connectivity and conservation of marine biodiversity. *Oceanography*, 20:100–111.

Jones, M. et Epifanio, C. (1995). Settlement of brachyuran megalopae in delaware Bay : a time series analysis. *Marine Ecology Progress Series*, 125:67–76.

Kelly-Gerreyn, B., Hydes, D., Jégou, A., Lazure, P., Fernad, L., Puillat, I. et Garcia-Soto, C. (2006). Low salinity intrusions in the western English Channel. *Continental Shelf Research*, 26:1241–1257.

Kinlan, B. et Gaines, S. (2003). A comparative analysis of dispersal scales in marine and terrestrial systems. *Ecology*, 84:2007–2020.

Kinlan, B., Gaines, S. et Lester, S. (2005). Propagule dispersal and the scales of marine community process. *Diversity and Distributions*, 11:139–148.

Kirby, R., Beaugrand, G., Lindley, J., Richardson, A., Edwards, M. et Reid, P. (2007). Climate effects and benthic-pelagic coupling in the North Sea. *Marine Ecology Progress Series*, 330:31–38.

Kirby, R. et Lindley, J. (2005). Molecular analysis of continuous plankton recorder samples, an examination of echinoderm larvae in the North Sea. *Journal of the Marine Biological Association of the United Kingdom*, 85:451–459.

Koutsikopoulos, C. et Le Cann, B. (1996). Physical processes and hydrological structures related to the Bay of Biscay anchovy. *Scientia Marina*, 60:9–19.

Kritzer, J. et Sale, P. (2003). Metapopulation ecology in the sea : from Levin's model to marine ecology and fisheries science. *Fish and Fisheries*, 4:1–10.

Lagadeuc, Y. (1992a). Répartition verticale des larves de *Pectinaria koreni* en baie de Seine orientale : influence sur le transport et le recrutement. *Oceanologica Acta*, 15:109–118.

Lagadeuc, Y. (1992b). Transport larvaire en Manche. Exemple de *Pectinaria koreni* (Malmgren), annélide polychète, en baie de Seine. *Oceanologica Acta*, 15:383–395.

Lagadeuc, Y. et Retière, C. (1993). Critères d'identification rapide des stades de développement des larves de *Pectinaria koreni* (Malmgren) (annélide polychète) de la Baie de Seine (Manche). *Vie et milieu*, 43:217–224.

Largier, J. (1993). Estuarine fronts : how important are they ? *Estuaries*, 16:1–11.

Largier, J. (2003). Considerations in estimating larval dispersal distances from oceanographic data. *Ecological Applications*, 13:71–89.

Larsen, J., Frischer, M., Ockelman, K., Rasmussen, L. et Hansen, B. (2007). Temporal occurrence of planktotrophic bivalve larvae identified morphologically and by single step nested multiplex PCR. *Journal of Plankton Research*, 29:423–436.

Larsen, J., Frischer, M., Rasmussen, L. et Hansen, B. (2005). Single-step nested multiplex PCR to differentiate between various bivalve larvae. *Marine Biology*, 146:1119–1129.

Lawrence, A. et Soame, J. (2004). The effects of climate change on the reproduction of coastal invertebrates. *Ibis*, 146:29–39.

Lazure, P. et Dumas, F. (2008). An external-internal mode coupling for a 3D hydrodynamical Model for Applications at Regional Scale (MARS). *Advances in Water Resources*, 31:233–250.

Lazure, P., Garnier, V., Dumas, F., Herry, C. et Chifflet, M. (2009). Development of a hydrodynamic model of the Bay of Biscay : Validation of hydrology. *Continental Shelf research*, 29:985–997.

Lazure, P. et Jégou, A.-M. (1998). 3D modelling of seasonal evolution of Loire and Gironde plumes on Biscay Bay continental shelf. *Oceanologica Acta*, 21:165–177.

Le Boyer, A., Cambon, G., Daniault, N., Herbette, S., Le Cann, B., Marié, L. et Morin, P. (2009). Observations of the Ushant tidal front in September 2007. *Continental Shelf Research*, 29:1026–1037.

Le Bris, H. (1988). *Fonctionnement des écosystèmes benthiques côtiers au contact d'estuaires : la rade de Lorient et la baie de Vilaine.* Thèse de doctorat, Université de Bretagne Occidentale, Brest.

Le Cann, B. et Pingree, R. (1995). Circulation dans le Golfe de Gascogne : une revue des travaux récents. *Actes du IVe colloque international d'océanographie du Golfe de Gascogne*, pages 217–234.

Le Fèvre, J. (1986). Aspects of the biology of frontal systems. *Advances in Marine Biology*, 23:163–299.

Le Fèvre, J., Le Corre, P., Morin, P. et Birrien, J.-L. (1983). The pelagic ecosystem in frontal zones and other environments off the west coast of Brittany. *Oceanologica Acta*, 4:125–129.

Le Goff-Vitry, M., Chipman, A. et Comtet, T. (2007a). *In situ* hybridization on whole larvae : a novel method for monitoring bivalve larvae. *Marine Ecology Progress Series*, 343:161–172.

Le Goff-Vitry, M.-C., Jacquelin, S. et Comtet, T. (2007b). Towards tracking marine larvae with in situ hybridization. *Journal of the Marine Biological Association of the United Kingdom*, 87:1077–1080.

Lefebvre, A., Ellien, C., Davoult, D., Thièaut, E. et Salomon, J. (2003). Pelagic dispersal of the brittle-star *Ophiothrix fragilis* larvae in a megatidal area (English Channel, France) examined using an advection/diffusion models. *Estuarine, Coastal and Shelf Science*, 57:421–433.

Legendre, P. et Fortin, M. (1989). Spatial pattern and ecological analysis. *Vegetatio*, 80:107–138.

Legendre, P. et Gallagher, E. (2001). Ecologically meaningful transformations for ordination of species data. *Oecologia*, 129:271–280.

Legendre, P. et Legendre, L. (1998). *Numerical Ecology, 2nd English Edition*. Amsterdam, Elsevier Science BV.

Legendre, P. et Trousselier, M. (1988). Aquatic heterotrophic bacteria : modeling in the presence of spatial autocorrelation. *Limnology and Oceanography*, 33:1055–1067.

Lehane, C. et Davenport, J. (2006). A 15-month study of zooplankton ingestion by farmed mussels (*Mytilus edulis*) in Bantry Bay, Southwest Ireland. *Estuarine, Coastal and Shelf Science*, 67:645–652.

Leis, J. (2006). Are larvae of demersal fishes plankton or nekton ? *Advances in Marine Biology*, 51:57–141.

Leis, J. (2007). Behaviour as input for modelling dispersal of fish larvae : behaviour, biogeography, hydrodynamics, ontogeny, physiology and phylogeny meet hydrography. *Marine Ecology Progress Series*, 347:185–193.

Leppäkoski, E. et Olenin, S. (2000). Non-native species and rates of spread : lessons from the brackish Baltic Sea. *Biological Invasions*, 2:151–163.

Lester, S., Ruttenberg, B., Gaines, S. et Kinlan, B. (2007). The relationship between dispersal ability and geographic range size. *Ecology Letters*, 10:745–758.

Lett, C., Ayata, S.-D., Huret, M. et Irisson, J.-O. (xxxx). Biophysical modelling to investigate the effects of climate change on marine populations dispersal and connectivity. *Soumis à Progress in Oceanography*.

Lett, C., Rose, K. et Megrey, B. (2009). *Climate change and small pelagic fish*, Chapitre Biophysical models. Cambridge University Press.

Lett, C., Verley, P., Mullon, C., Parada, C., Brochier, T., Penven, P. et Blanke, B. (2008). A lagrangian tool for modelling ichthyoplankton dynamics. *Environmental Modelling and Software*, 23:1210–1214.

Levin, L. (2006). Recent progress in understanding larval dispersal : new directions and digressions. *Integrative and Comparative Biology*, 46:282–297.

Levin, L. et Bridges, T. (1995). *Ecology of marine invertebrate larvae*, Chapitre Pattern and diversity in reproduction and development, pages 1–48. CRC Press, Bocca Raton. McEdward, L.(éditeur).

Levins, R. (1969). Some demographic and genetic consequences of environmental heterogeneity for biological control. *Bulletin of the Entomological Society of America*, 15:237–240.

Levitan, D., Sewell, M. et Chia, F.-S. (1992). How distribution and abundance influence fertilization success in the sea urchin *Strongylocentrotus franciscanus*. *Ecology*, 73:248–254.

Lewin, R. (1986). Supply-side ecology. *Science*, 234:25–27.

Limouzy-Paris, C. et al (1997). Translocation of larval coral reef fishes via sub-mesoscale spin-off eddies from the florida current. *Bulletin of Marine Science*, 60:966–983.

Lobel, P. et Robinson, A. (1986). Transport and entrapment of fish larvae by ocean mesoscale eddies and currents in hawaiian waters. *Deep Sea Research*, 33:483–500.

Lorenzen, C. (1966). A method for the continuous measurement of *in vivo* chlorophyll *a* concentration. *Deep-Sea Research*, 13:223–227.

Lorenzo-Abalde, S., Gonzáles-Fernández, A., de Miguel Ville-gas, E. et Fuentes, J. (2005). Two monoclonal antibodies for the recognition of *Mytilus spp.* larvae : studies on cultured larvae and tests on plankton samples. *Aquaculture*, 250:736–747.

Luyten, P., Deleersnijder, E., Ozer, J. et Ruddick, K. (1996). Presentation of a family of turbulence closure models for stratified shallow water flows and preliminary application to the Rhine outflow regions. *Continental Shelf Research*, 16:101–130.

Lyard, F., Lefevre, F., Letellier, T. et Francis, O. (2006). Modelling the global ocean tides : modern insights from FES2004. *Ocean Dynamics*, 56:394–415.

MacKenzie, B. et Schiedek, D. (2007). Daily ocean monitoring since the 1860s shows record warming of northern European seas. *Global Change Biology*, 13:1335–1347.

Maguer, J.-F., L'Helguen, S., Waeles, M., Morin, P., Riso, R. et Caradec, J. (2009). Size-fractionated phytoplankton biomass and nitrogen uptake in response to high nutrient load in the North Biscay Bay in spring. *Continental Shelf Research*, 29:1103–1110.

Manel, S., Gaggiotti, O. et Waples, R. (2005). Assignment methods : matching biological questions with appropriate techniques. *Trends in Ecology and Evolution*, 20:136–142.

Manel, S., Schwartz, M., Luikart, G. et Taberlet, P. (2003). Landscape genetics : Combining landscape ecology and population genetics. *Trends in Ecology and Evolution*, 18:189–196.

Mariette, V. et Le Cann, B. (1985). Simulation of the formation of the Ushant frontal systems. *Continental Shelf Research*, 4:637–660.

Marinone, S., Ulloa, M., Parés-Sierra, A., Lavín, M. et Cudney-Bueno, R. (2008). Connectivity in the northern gulf of California from particle tracking in a three-dimensional numerical model. *Journal of Marine Systems*, 71:149–158.

Marta-Almeida, M., Dubert, J., Peliz, A. et Queiroga, H. (2006). Influence of vertical migration pattern on retention of crab larvae in a seasonal upwelling system. *Marine Ecology Progress Series*, 307:1–19.

McCarthy, D., Young, C. et Emson, R. (2003). Influence of wave-induced disturbance on seasonal spawning patterns in the sabellariid polychaete *Phragmatopoma lapidosa*. *Marine Ecology Progress Series*, 256:123–133.

McGee, B. et Targett, N. (1989). Larval habitat selection in *Crepidula* (L.) and its effect on adult distribution patterns. *Journal of Experimental Marine Biology and Ecology*, 131:195–214.

Medeiros-Bergen, D., Olson, R., Conroy, J. et Kocher, T. (1995). Distribution of holothurian larvae determined with species-specific genetic probes. *Limnology and Oceanography*, 40:1225–1235.

Meehl, G., Stocker, T., Collins, W., Friedlingstein, P., Gaye, A., Gregory, J., . Kitoh, A., Knutti, R., Murphy, J., Noda, A., Raper, S., Watterson, I., Weaver, A. et Zhao, Z.-C. (2007). *Climate change 2007 : the physical science basis. Contribution of working group I to the fourth assessment report of the Intergovernmental Panel on Climate Change*, Chapitre Global climate projections. Cambridge University Press, Cambridge, United Kingdom and New York, NY, USA.

Meier, H., Kjellstrø m, E. et Graham, L. (2006). Estimating uncertainties of projected Baltic sea salinity in the late 21$^{st}$ century. *Geophysical Research Letters*, 33:doisI :10.1029/2006GL026488.

Ménesguen, A. et Gohin, F. (2006). Observation and modelling of natural retention structures in the English Channel,. *Journal of Marine Systems*, 63:244–256.

Metaxas, A. (2001). Behaviour in flow : perspectives on the distribution and dispersion of meroplanktonic larvae in the water column. *Canadian Journal of Fisheries and Aquatic Sciences*, 58:86–98.

Metaxas, A. et Saunders, M. (2009). Quantifying the "bio-" components in biophysical models of larval transport in marine benthic invertebrates : Advances and pitfalls. *Biological Bulletin*, 216:257–272.

Miller, K., Jones, P. et Roughgarden, J. (1991). Monoclonal antibodies as species-specific probes in oceanographic research : examples with intertidal barnacle larvae. *Molecular Marine Biology and Biotechnology*, 1:35–47.

Miller, T. (2007). Contribution of individual-based coupled physical-biological models to understanding recruitment in marine fish populations. *Marine Ecology Progress Series*, 347:127–138.

Mitarai, S., Siegel, D. et Winters, K. (2008). A numerical study of stochastic larval settlement in the California current system. *Journal of Marine Systems*, 69:295–309.

Mora, C. et Sale, P. (2002). Are populations of coral reef fish open or closed ? *Trends in Ecology and Evolution*, 17:422–428.

Morgan, T. et Rogers, A. (2001). Specificity and sensitivity of microsatellite markers for the identification of larvae. *Marine Biology*, 139:967–973.

Morin, P., Le Corre, P., Marty, Y. et L'Helguen, S. (1991). Evolution printanière des éléments nutritifs et du phytoplancton sur le plateau continental armoricain (Europe du Nord-Ouest). *Oceanologica Acta*, 14:263–279.

Mouquet, N. et Loreau, M. (2002). Coexistence in metacommunities : the regional similarity hypothesis. *American Naturalist*, 159:420–426.

Mullon, C., Cury, P. et Penven, P. (2002). Evolutionary individual-based model for the recruitment of anchovy (engraulis capensis) in the southern benguela. *Canadian Journal of Fisheries and Aquatic Sciences*, 59:910–922.

Munday, P., Leis, J., Lough, J., Paris, C., Kingsford, M., Berumen, M. et Lambrechts, J. (2009). Climate change and coral reef connectivity. *Coral Reefs*, 28:379–395.

Muths, D., Jollivet, D., Gentil, F. et Davoult, D. (2009). Large-scale genetic patchiness among North East Atlantic populations of the brittle-star *Ophiothrix fragilis*. *Aquatic Biology*, 5:117–132.

Ménard, F., Gentil, F. et Dauvin, J.-C. (1989). Population dynamics and secondary production of *Owenia fusiformis* Delle Chiaje (Polychaete) from the Bay of Seine (eastern English Channel). *Journal of Experimental Marine Biology and Ecology*, 133:151–167.

Natunewicz, C. et Epifanio, C. (2001). Spatial and temporal scales of patches of crab larvae in coastal waters. *Marine Ecology Progress Series*, 212:217–222.

Natunewicz, C., Epifanio, C. et Garvine, R. (2001). Transport of crab larval patches in the coastal ocean. *Marine Ecology Progress Series*, 222:143–154.

Naylor, R., Williams, S. et Strong, D. (2001). Aquaculture-a gateway for exotic species. *Science*, 294:1655–1656.

Nehring, S. (2006). Four arguments why so many alien species settle into estuaries, with special reference to the German river Elbe. *Helgoland Marine Research*, 60:127–134.

Nelson, K. et Fisher, C. R. (2000). Absence of cospeciation in deep-sea vestimentiferan tube worms and their bacterial endosymbionts. *Symbiosis*, 28:1–15.

Neumann, T. (2010). Climate-change effects on the baltic sea ecosystem : A model study. *Journal of Marine Systems*, 81(3):213–224.

Newman, M. (2003). The structure and function of complex networks. *SIAM Review*, 45:167–256.

North, E., Hood, R., Chao, S.-Y. et Sanford, L. (2006). Using a random displacement model to simulate turbulent particle motion in a baroclinic frontal zone : A new implementation scheme and model performance tests. *Journal of Marine Systems*, 60:365–380.

North, E., Schlag, Z., Hood, R., Li, M., Zhong, L., Gross, T. et Kennedy, V. (2008). Vertical swimming behavior influences the dispersal of simulated oyster larvae in a coupled particle-tracking and hydrodynamic model of Chesapeake Bay. *Marine Ecology Progress Series*, 359:99–115.

O'Connor, M., Bruno, J., Gaines, S., Halpern, B., Lester, S., Kinlan, B. et Weiss, J. (2007). Temperature control of larval dispersal and the implications for marine ecology, evolution, and conservation. *Proceedings of the National Academy of Sciences of the United States of America*, 104:1266–1271.

Oksanen, J., Kindt, R., Legendre, P., O'Hara, B., Simpson, G., Solymos, P., Stevens, M. et Wagner, H. (2008). Vegan : Community ecology package. R package version 1.16-8. http ://vegan.r-forge.r-project.org/.

Ólafsson, E. B., Peterson, C. H. et Ambrose, W. G. (1994). Does recruitment limitation structure populations and communities of macro-invertebrates in marine soft sediments : the relative significance of pre- and post-settlement processes. *Oceanography and Marine Biology Annual Review*, 32:65–109.

Olive, P. (1984). Environmental control of reproduction in Polychaeta. *In Polychaete reproduction : progress in comparative reproductive biology.*, pages 17–38. Gustav Fisher Verlag, Stuttgart. Éditeurs : Fischer, A., Pfannenstiel, H-D.

Olive, P. (1992). The adaptative significance of seasonal reproduction in marine invertebrates : the importance of distinguishing between models. *Invertebrate Reproduction and Development*, 22:165–174.

Olive, P. (1995). Annual breeding cycles in marine invertebrates and environmental temperature probing the proximate and ultimate causes of reproductive synchrony. *Journal of thermal biology*, 20:79–90.

Olive, P., Clark, S. et Lawrence, A. (1990). Global warming and seasonal reproduction : perception and transduction of environmental information. *Advances in Invertebrate Reproduction*, 5:265–270.

Olivier, F., Desroy, N. et Retière, C. (1996). Habitat selection and adult-recruit interactions in *Pectinaria koreni* (Malmgren) (Annelida : Polychaeta) post-larval populations : results of flume experiments. *Journal of Sea Research*, 36:217–226.

Olson, R. (1985). The consequences of short-distance larval dispersal in a sessile marine invertebrates. *Ecology*, 66:30–39.

Orbi, A. et Salomon, J.-C. (1988). Tidal dynamics in the vicinity of the channel islands. *Oceanologica Acta*, 11:55–64.

Palumbi, S. (1994). Genetic divergence, reproductive isolation, and marine speciation. *Annual Review of Ecology and Systematics*, 25:547–572.

Palumbi, S. (2004). Marine reserves and ocean neighborhoods : The spatial scale of marine populations and their management. *Annual Review of Environmental Resources*, 29:31–68.

Palumbi, S., Gaines, S., Leslie, H. et Warner, R. (2003). New wave : high-tech tools to help marine reserve research. *Frontiers in Ecology and the Environment*, 1:73–79.

Palumbi, S., Martin, A., Romano, S., McMillian, W., Stice, L. et Grabowski, G. (1991). The simple fool's guide to PCR. Department of Zoology, University of Hawaii, Honolulu.

Paris, C., Chérubin, L. et Cowen, R. (2007). Surfing, spinning, or diving from reef to reef : effects on population connectivity. *Marine Ecology Progress Series*, 347:285–300.

Paris, C., Clement, A. et Cowen, R. (2008). Influence of projected temperature changes in the caribbean on the pelagic phase and population networks of a common reef fish. Abstract, session 071, Ocean Sciences Meeting, Orlando, USA.

Paris, C. et Cowen, R. (2004). Direct evidence of a biophysical retention mechanism for coral reef fish larvae. *Limnology and Oceanography*, 49:1964–1979.

Pawlick, J. (1988). Larval settlement and metamorphosis of Sabellariid Polychaetes, with special reference to *Phragmatopoma lapidosa*, a reef building species, and *Sabellaria floridensis*, a non-gregarious species. *Bulletin of Marine Science*, 43:41–60.

Pawlick, J. et Butman, C. (1993). Settlement of a marine tube worm as a function of current velocity : Inteacting effects of hydrodnamics and behavior. *Limnology and Oceanography*, 38:1730–1740.

Pechenik, J. (1999). On the advantages and disadvantages of larval stages in benthic marine invertebrate life cycles. *Marine Ecology Progress Series*, 177:269–297.

Pechenik, J. et Heyman, W. (1987). Using KCl to determine size at competence for larvae of the marine gastropod *Crepidula fornicata* (L.). *Journal of Experimental Marine Biology and Ecology*, 112:27–38.

Pechenik, J. et Lima, G. (1984). Relationship between growth, differentiation, and length of larval life for individually reared larvae of the marine gastropod, *Crepidula fornicata*. *Biological Bulletin*, 166:537–549.

Pechenik, J., Rittschof, D. et Schmidt, A. (1993). Influence of delayed metamorphosis on survival and growth of juvenile barnacles *Balanus amphitrite*. *Marine Biology*, 115:287–294.

Pedersen, O., Aschan, M., Rasmussen, T., Tande, K. et Slagstad, D. (2003). Larval dispersal and mother populations of *Pandalus borealis* investigated by a lagrangian particle tracking models. *Fisheries Research*, 65:173–90.

Pedersen, O., Nilssen, E., Jørgensen, L. et Slagstad, D. (2006). Advection of the red king crab larvae on the coast of North Norway - A lagrangian model study. *Fisheries Research*, 79:325–336.

Pedersen, T., Hansen, J., Josefson, A. et Hansen, B. (2008). Mortality through ontogeny of soft-bottom marine invertebrates with planktonic larvae. *Journal of Marine Systems*, 72:185–207.

Peliz, A., Marchesiello, P., Dubert, J., Marta-Almeida, M., Roy, C. et Queiroga, H. (2007). A study of crab larvae dispersal on the Western Iberian shelf : Physical processes. *Journal of Marine Systems*, 68:215–236.

Perry, A., Low, P., Ellis, J. et Reynolds, J. (2005). Climate change and distribution shifts in marine fishes. *Science*, 308:1912–1915.

Pfeiffer-Herbert, A., McManus, M., Raimondi, P., Chao, Y. et Chai, F. (2007). Dispersal of barnacle larvae along the central Californian coast : a modeling study. *Limnology and Oceanography*, 52:1559–1569.

Pierce, D., Barnett, T., Santer, B. et Gleckler, P. (2009). Selecting global climate models for regional climate change studies. *Proceedings of the National Academy of Sciences of the United States of America*, 106:8441–8446.

Pineda, J., Hare, J. et Sponaugle, S. (2007). Larval transport and dispersal in the coastal ocean and consequences for population connectivity. *Oceanography*, 20:22–39.

Pingree, R., Forster, G. et Morisson, G. (1974). Turbulent convergent tidal fronts. *Journal of Marine Biological Association UK*, 54:469–479.

Pingree, R. et Le Cann, B. (1989). Celtic and armorican slope and shelf residual currents. *Progress in Oceanography*, 23:303–338.

Pingree, R. et Maddock, L. (1977). Tidal residual in the English Channel. *Journal of the Marine Biological Association of the United Kingdom*, 57:339–354.

Pingree, R., Mardell, D. et Maddock, L. (1985). Tidal mixing in the Channel Isles region derived from the results of remote sensing and measurements at seas. *Estuarine, Coastal and Shelf Science*, 20:1–18.

Pingree, R., Mardell, G., Holligan, P., Griffiths, D. et J. Smithers, J. (1982). Celtic sea and Armorican current structure and the vertical distributions of temperature and chlorophyll. *Continental Shelf Research*, 1:99–116.

Pingree, R., Pugh, P., Holligan, P. et Forster, G. (1975). Summer phytoplankton blooms and red tides along the tidal fronts in the approaches of the English Channel. *Nature*, 258:672–677.

Planes, S., Jones, G. et Thorrold, S. (2009). Larval dispersal connects fish populations in a network of marine protected areas. *Proceedings of the National Academy of Sciences of the United States of America*, 106:5693–5697.

Planque, B., Beillois, P., Jégou, A.-M., Lazure, P., Petitgas, P. et Puillat, I. (2003). Large-scale hydroclimatic variability in the Bay of Biscay : the 1990s in the context of interdecadal changes. *ICES Marine Science Symposium*, 219:61–70.

Planque, B., Lazure, P. et A.M., J. (2006). Typology of hydrological structures modelled and observed over the Bay of Biscay shelf. *Scientia Marina*, 70:43–50.

Plus, M., Dumas, F., Stanisière, J. et Maurer, D. (2009). Hydrodynamic characterization of the Arcachon Bay, using model-derived descriptors. *Continental Shelf Research*, 29:1008–113.

Plus, M., Maurer, D., Stanisière, J.-Y. et Dumas, F. (2006). Caractérisation des composantes hydrodynamiques d'une lagune mésotidale, le Bassin d'Arcachon. Rapport technique, n°RST/LER/AR/06.007, IFREMER, Arcachon, France.

Populus, J., Laurentin, A., Rollet, C., Vasquez, M., Guillaumont, B., Bonnot-Courtois et C. (2004). Surveying coastal zone topography with airborne remote sensing for benthos mapping. *Journal of Remote Sensing and Photogrammetry*, 3:105–117.

Pörtner, H. et Farrell, A. (2008). Physiology and climate change. *Science*, 322:690–692.

Puillat, I., Lazure, P., Jégou, A., Lampert, L. et Miller, M. (2006). Mesoscale hydrological variability induced by northwesterly wind of the French continental shelf of the bay of Biscay. *Scientia Marina*, 70:15–26.

Puillat, I., Lazure, P., Jégou, A.-M., Lampert, L. et Miller, P.-I. (2004). Hydrographical variability on the french continental shelf in the Bay of Biscay during the 1990s. *Continental Shelf Research*, 24:1143–1163.

Pérez, D., Lorenzo-Abalde, S., González-Fernández, A. et Fuentes, J. (2009). Immunodetection in *Mytilus galloprovincialis* larvae using monoclonal antibodies to monitor larval abundance on the Galician coast : optimization of the method and comparison with identification by morphological traits. *Aquaculture*, 294:86–92.

Qian, P.-Y. (1999). Larval settlement of polychaetes. *Hydrobiologia*, 402:239–253.

Queiroga, H., Cruz, T., dos Santos, A., Dubert, J., González-Gordillo, J., Paula, J., Peliz, A. et Santos, A. (2007). Oceanographic and behavioural processes affecting invertebrate larval dispersal and supply in the western Iberia upwelling ecosystems. *Progress in Oceanography*, 74:174–191.

R Development Core Team (2005). R : A language and environment for statistical computing, reference index version 2.6.2. ISBN 3-900051-07-0, http ://www.r-project.org. R Foundation for Statistical Computing, Vienna, Austria.

Reise, K., Olenin, S. et Thieltges, D. (2006). Are aliens threatening European aquatic coastal ecosystems ? *Helgoland Marine Research*, 60:77–83.

Reitzel, A., Miner, B. et McEdward, L. (2004). Relationships between spawning date and larval development time for benthic marine invertebrates : a modelling approach. *Marine Ecology Progress Series*, 280:13–23.

Reynaud, T., Legrand, P., Mercier, H. et Barnier, B. (1998). A new analysis of hydrographic data in the Atlantic and its application to an inverse modelling study. *International WOCE Newsletter*, 32:29–31.

Richardson, A., Walne, A., John, A., Jonas, T., Lindley, J., Sims, D., Stevens, D. et Witt, M. (2006). Using continuous plankton recorder data. *Progress in Oceanography*, 68:27–74.

Riera, P., Montagna, P., Kalke, R. et Richard, P. (2000). Utilization of estuarine organic matter during growth and migration by juvenile brown shrimp *Penaeus aztecus* in a South Texas estuary. *Marine Ecology Progress Series*, 199:205–216.

Rigal, F. (2005). Barrières biogéographiques et processus historiques chez les invertébrés marins : définition des unités taxonomiques et populationnelles chez *Sabellaria alveoloata*. Mémoire de Master Gène, Cellule, Développement et Evolution. Université Paris Sud-Orsay, Paris 11.

Rigal, F. (2009). *Dynamique spatio-temporelle du nuage larvaire du gastéropode introduit Crepidula fornicata au sein d'une baie mégatidale, la baie de Morlaix (France).* Thèse de doctorat de l'Université Pierre et Marie Curie - Paris 6.

Rigal, F., Comtet, T. et Viard, F. (xxxx). Invasion in a changing world : can increase in temperature promote connectivity in a marine invader ? *Soumis à Ecology Letters*.

Rijnsdorp, A., Peck, A., Engelhard, G., Möllman, C. et Pinnegar, J. (2009). Resolving the effect of climate change on fish populations. *ICES Journal of Marine Science*, 66:1570–1583.

Roberts, C. (1997). Connectivity and management of caribbean coral reefs. *Science*, 278(5342):1454–7.

Rogers, A. (2001). *Environment and animal development : genes, life histories and plasticity*, Chapitre Molecular ecology and identification of marine invertebrate larvae, pages 29–69. Oxford : BIOS Scientific Publishers Ltd. Éditeurs : Atkinson, D. et Thorndyke, M.

Ronce, O. (2007). How does it feel to be like a rolling stone ? ten questions about dispersal evolution. *Annual Review of Ecology, Evolution, and Systematics*, 28.

Ross, O. et Sharples, J. (2004). Recipe for 1- D lagrangian particle tracking models in space-varying diffusivity. *Limnology and Oceanography : Methods*, 2:289–302.

Roughgarden, J., Gaines, S. et Possingham, H. (1988). Recruitment dynamics in complex life cycles. *Science*, 241:1460–6.

Rousset, F. (1997). Genetic differentiation and estimation of gene flow from F-statistics under isolation by distance. *Genetics*, 145(4):1219–1228.

Rumrill, S. (1990). Natural mortality of marine invertebrate larvae. *Ophelia*, 32:163–198.

Runge, J., Franks, P., Gentleman, W., Megrey, B., Rose, K. A., Werner, F. et Zakardjian, B. (2005). *The Sea, Vol. 13 : The Global Coastal Ocean : Multiscale Interdisciplinary Processes*, Chapitre Diagnosis and prediction of variability in secondary production and fish recruitment processes : developments in physical-biological modelling, pages 413–473. Harvard University Press.

Russell, J., Stouffer, R. et Dixon, K. (2006). Intercomparison of the Southern Ocean circulations in IPCC coupled model control simulations. *Journal of Climate*, 19:4560–4575.

Salomon, J. et Breton, M. (1993). An atlas of long-term currents in the Channel. *Oceanologica Acta*, 16:439–448.

Salomon, J.-C. et Breton, M. (1991). Courants résiduels de marée dans la Manche. *Oceanologica Acta, Special Volume*, 11:47–53.

Salomon, J.-C., Garreau, P. et Breton, M. (1996). The lagrangian barycentric method to compute 2D and 3D long term dispersion in tidal environments. *In Mixing in estuaries and coastal seas*, pages 59–76. American Geophysical Union, Washington D.C. Pattiaratchi, C. (éditeur).

Scheltema, R. (1986). On dispersal and planktonic larvae of benthic invertebrates : an eclectic overview and summary of problems. *Bulletin of Marine Science*, 39:290–322.

Schneider, D., Stoeckel, J., Rehmann, C., Douglas Blodgett, K., Sparks, R. et Padilla, D. (2003). A developmental bottleneck in dispersing larvae : implications for spatial population dynamics. *Ecology Letters*, 6:352–360.

Schwiderski, E. (1983). Atlas of ocean tidal charts and maps. *Marine Geodesy*, 6:219–265.

Selkoe, K., Henzler, C. et Gaines, S. (2008). Seascape genetics and the spatial ecology of marine populations. *Fish and Fisheries*, 9:363–377.

Sentchev, A., Forget, P. et Barbin, Y. (2009). Residual and tidal circulation revealed by VHF radar surface current measurements in the southern Channel Isles region (English Channel). *Estuarine, Coastal and Shelf Sciences*, 82:180–192.

Shanks, A. (2009). Pelagic larval duration and dispersal distance revisited. *Biological Bulletin*, 216:373–385.

Shanks, A., Grantham, B. et Carr, M. (2003a). Propagule dispersal distance and the size and spacing in marine reserves. *Ecological Applications*, 13:159–169.

Shanks, A., Largier, J., Brink, L., Brubaker, J. et Hooff, R. (2002). Observations on the distribution of meroplankton during a downwelling event and associated intrusion of the Chesapeake Bay estuarine plume. *Journal of Plankton Research*, 24:391–416.

Shanks, A., Largier, J. et Brubaker, J. (2003b). Observations on the distribution of meroplankton during an upwelling event. *Journal of Plankton Research*, 25:645–667.

Shanks, A., McCulloch, A. et Miller, J. (2003c). Topographically generated fronts, very nearshore oceanography and the distribution of larval invertebrates and holoplankters. *Journal of Plankton Research*, 25:1251–1277.

Siegel, D., Kinlan, P., Gaylord, B. et Gaines, S. (2003). Lagrangian descriptions of marine larval dispersion. *Marine Ecology Progress Series*, 260:83–96.

Siegel, D., Mitarai, S., Costello, C., Gaines, S., Kendall, B., Warner, R. et Winters, K. (2008). The stochastic nature of larval connectivity among nearshore marine populations. *Proceedings of the National Academy of Sciences of the United States of America*, 105:8974–8979.

Slatkin, M. (1993). Isolation by distance in equilibrium and non-equilibrium populations. *Evolution*, 47:264–279.

Smedbol, R., McPherson, A., Hansen, M. et Kenchington, E. (2002). Myths and moderation in marine 'metapopulations'? *Fish and Fisheries*, 3:20–35.

Solidoro, C., Cossarini, G., Libralato, S. et Salon, S. (2010). Remarks on the redefinition of system boundaries and model parameterization for downscaling experiments. *Progress in Oceanography*, 84(1-2):134–137.

Sponaugle, S., Cowen, R., Shanks, A., Morgan, S., Leis, J., Pineda, J., Boehlert, G., Kingsford, M., Lindeman, K., Grimes, C. et Munro, J. (2002). Predicting self-recruitment in marine populations : biophysical correlates and mecanisms. *Bulletin of Marine Science*, 70:341–375.

Sponaugle, S. et Grorud-Colvert, K. (2006). Environmental variability, early life-history traits, and survival of new coral reef fish recruits. *Integrative and Comparative Biology*, 46:623–633.

Starr, M., Himmelman, J. et Therriault, J.-C. (1990). Direct coupling of marine invertebrate spawning with phytoplankton blooms. *Science*, 247:1071–1074.

Stouffer, R., Clim, R., Yin, J., Gregory, J., Dixon, K., Spelman, M., Eby, M., Flato, G. et Hasumi, H. (2006). Investigating the causes of the response of the thermohaline circulation to past and future climate changes. *Journal of Climate*, 19:1365–1387.

Strathmann, R., Fenaux, L. et Strathmann, M. (1992). Heterochronic developmental plasticity in larval sea urchins and its implications for evolution of non-feeding larvae. *Evolution*, 46:972–986.

Suchanek, T. H., Geller, J. B., Kreiser, B. R. et Mitton, J. B. (1997). Zoogeographic distributions of the sibling species *Mytilus galloprovincialis* and *M. trossulus* (Bivalvia : Mytilidae) and their hybrids in the North Pacific. *Biological Bulletin*, 193:187–194.

Swearer, S., Caselle, J., Lea, S. et Warner, R. (1999). Larval retention and recruitment in an island population of a coral-reef fish. *Nature*, 402:179–802.

Thiébaut, E. (1996). Distribution of *Pectinaria koreni* larvae (Annelida : Polychaeta) in relation to the Seine river plume front (eastern English Channel). *Estuarine, Coastal and Shelf Science*, 43:383–397.

Thiébaut, E., Dauvin, J.-C. et Lagadeuc, Y. (1992). Transport of *Owenia fusiformis* larvae (Annelida : Polychaeta) in the Bay of Seine. I. vertical distribution in relation to water column stratification and ontogenic vertical migrations. *Marine Ecology Progress Series*, 80:29–39.

Thiébaut, E., Dauvin, J.-C. et Lagadeuc, Y. (1994). Horizontal distribution and retention of *Owenia fusiformis* larvae (Annelida : Polychaeta) in the bay of Seine. *Journal of the Marine Biological Association of the United Kingdom*, 74:129–142.

Thiébaut, E., Dauvin, J.-C. et Wang, Z. (1996). Tidal transport of *Pectinaria koreni* postlarvae (Annelida : Polychaeta) in the Bay of Seine (eastern English Channel). *Marine Ecology Progress Series*, 183:63–70.

Thiébaut, E., Lagadeuc, Y., Olivier, F., Dauvin, F. et Retière, C. (1998). Does hydrodynamic affect the recruitement of marine invertebrates in a macrotidal area ? *Hydrobiologia*, 375:165–176.

Thiercelin, N. (2007). Recherche de critères morphologiques diagnostiques entre les lignées génétiques des complexes d'espèces *Owenia fusiformis* et *Pectinaria koreni* et tests d'hypothèses sur la vicariance des lignées intertidales et subtidales. Mémoire de Master Sciences de l'Univers, Environnement et Ecologie, spécialité Océanographie et Environnements Marins, Université Pierre et Marie Curie - Paris 6.

Thorrold, S., Jones, G., Hellberg, M., Burton, R., Swearer, S., Neigel, J., Morgan, S. et Warner, R. (2002). Quantifying larval retention and connectivity in marine populations with artificial and natural markers. *Bulletin of Marine Science*, 70:291–308.

Thorrold, S., Jones, G., Planes, S. et Hare, J. (2006). Transgenerational marking of embryonic otoliths in marine fishes using barium stable isotopes. *Canadian Journal of Fisheries and Aquatic Sciences*, 63:193–197.

Thorrold, S., Latkoczy, C., Swart, P. et Jones, C. (2001). Natal homing in a marine fish metapopulation. *Science*, 291:297–9.

Thorson, G. (1946). *Reproduction and larval development of Danish marine bottom invertebrates*. C.A. Reitzels Forlag, Copenhagen, Denmark.

Thorson, G. (1950). Reproduction and larval ecology of marine bottom invertebrates. *Biological Review*, 25:1–45.

Todd, C. (1998). Larval supply and recruitment of benthic invertebrates : do larvae always disperse as much as we believe ? *Hydrobiologia*, 375:1–21.

Travers, M., Shin, Y., Jennings, S. et Cury, P. (2007). Towards end-to-end models for investigating the effects of climate and fishing in marine ecosystems. *Progress in Oceanography*, 75:751–770.

Treml, E., Halpin, P., Urban, D. et Pratson, L. (2008). Modeling population connectivity by ocean currents, a graph-theoretic approach for marine conservation. *Landscape Ecology*, 23:19–36.

Troost, K., Kamermans, P. et Wolff, W. (2008). Larviphagy in native bivalves and an introduced oyster. *Journal of Sea Research*, 60:157–163.

UNESCO (1968). *Zooplankton Sampling*. Monographs on oceanographic methodology, UNESCO, Paris.

UNESCO (1983). Algorithms for computation of fundamental properties of seawater. *UNESCO Techical Papers in Marine Science*, 44:1–53.

Verdier-Bonnet, C., Carlotti, F., Rey, C. et Bhaud, M. (1997). A model of larval dispersion coupling wind-driven currents and vertical larval behaviour : application to the recruitment of the annelid *Owenia fusiformis* in Banyuls bay, France. *Marine Ecology Progress Series*, 160:217–231.

Viard, F., Ellien, C. et Dupont, L. (2006). Dispersal ability and invasion success of *Crepidula fornicata* in a single gulf : insights from genetic markers and larval-dispersal model. *Helgoland Marine Research*, 60:144–152.

Vikebø, F., Jørgensen, C., Kristiansen, T. et Fiksen, O. (2007). Drift, growth and survival of larval Northeast Arctic cod with simple rules of behaviour. *Marine Ecology-Progress Series*, 347:207–219.

Vikebø, F., Sundby, S., Ådlandsvik, B. et Fiksen, O. (2005). The combined effect of transport and temperature on distribution and growth of larvae and pelagic juveniles of Arcto-Norwegian cod. *Ices Journal of Marine Science*, 62:1375–1386.

Visser, A. W. (1997). Using random walk models to simulate the vertical distribution of particles in a turbulent water column. *Marine Ecology Progress Series*, 158:275–281.

Voisin, M., Engel, C. et Viard, F. (2005). Differential shuffling of native genetic diversity across introduced regions in a brown alga : aquaculture vs. maritime traffic effects. *Proceedings of the National Academy of Sciences of the United States of America*, 102:5432–5437.

Vorberg, R. (1995). On the decrease of Sabellarian reefs along the German North Sea coast. *Publications du Service géologique de Luxembourg*, 24:87–93.

Wang, M., Overland, J. et Bond, N. (2010). Climate projections for selected large marine ecosystems. *Journal of Marine Systems*, 79(3-4):258–266.

Waples, R. et Gaggiotti, O. (2006). What is a population ? An empirical evaluation of some genetic methods for identifying the number of gene pools and their degree of connectivity. *Molecular Ecology*, 15:1419–1439.

Warner, R. et Cowen, R. (2002). Local retention of production in marine populations : Evidence, mechanisms, and consequences. *Bulletin of Marine Science*, 70:245–249.

Werner, F., Cowen, R. et Paris, C. (2007). Coupled biological and physical models : Present capabilities and necessary developments for future studies of population connectivity. *Oceanography*, 20:54–69.

Werner, F., MacKenzie, B., Perry, I., Lough, G., Naimie, C., Blanton, B. et Quinlan, J. (2001a). Larval trophodynamics, turbulence, and drift on georges bank : A sensitivity analysis of cod and haddock. *Scientia Marina*, 65:99–115.

Werner, F., Quinlan, A., Lough, R. et Lynch, D. (2001b). Spatially-explicit individual based modeling of marine populations : A review of the advances in the 1990's. *Sarsia*, 86:411–421.

Wilson, D. (1932). On the mitraria larva of *Owenia fusiformis* Delle Chiaje. *Philosophical Transactions of the Royal Society of London. Series B, Containing Papers of a Biological Character*, 221:231–334.

Wilson, D. (1968a). The settlement behaviour of the larvae of *Sabellaria alveolata* (L.). *Journal of the Marine Biological Association of the United Kingdom*, 48:387–435.

Wilson, D. (1968b). Some aspects of the development of eggs and larvae of *Sabellaria alveolata* (L.). *Journal of the Marine Biological Association of the United Kingdom*, 48:367–386.

Wilson, D. (1970). Additional observations on larval growth and settlement of *Sabellaria alveolata*. *Journal of the Marine Biological Association of the United Kingdom*, 50:1–31.

Wilson, D. (1971). Sabellaria colonies at Duckpool, North Cornwall, 1961-1970. *Journal of the Marine Biological Association of the United Kingdom*, 51:509–580.

Wilson, J., Dormontt, E., Prentis, P., Lowe, A. et Richardson, D. (2009). Something in the way you move : dispersal pathways affect invasion success. *Trends in Ecology and Evolution*, 24:136–144.

Wing, S., Botsford, L., Ralston, S. et Largier, J. (1998). Meroplanktonic distribution and circulation in a coastal retention zone of the northern California upwelling system. *Limnology and Oceanography*, 43:1710–1721.

Wing, S., Largier, J., Botsford, L. et Quinn, J. (1995). Settlement and transport of benthic invertebrates in an intermittent upwelling regions. *Limnology and Oceanography*, 40:316–329.

Woodson, C. et McManus, M. (2007). Foraging behavior can influence dispersal of marine organisms. *Limnology and Oceanography*, 52:2701–2709.

Wright, S. (1940). Breeding structure of populations in relation to speciation. *American Naturalist*, 74:232–248.

Xie, H., Lazure, P. et Gentien, P. (2007). Small scale retentive structures and Dinophysis. *Journal of Marine Systems*, 64:173–188.

Xue, H., Incze, L., Xu, D., Wolff, N. et Pettigrew, N. (2008). Connectivity of lobster populations in the coastal Gulf of Maine. Part I : Circulation and larval transport potential. *Ecological modelling*, 210:193–211.

Zacherl, D., Gaines, S. et Lonhart, S. (2003). The limits to biogeographical distributions : Insights from the northward range extension of the marine snail, *Kelletia kelletii*. *Journal of Biogeography*, 30:913–324.

Zarauz, L., Irigoien, X., Urtizberea, A. et Gonzalez, M. (2007). Mapping plankton distribution in the Bay of Biscay during three consecutive spring surveys. *Marine Ecology Progress Series*, 345:27–39.

# Remerciements

Ce travail de thèse n'aurait pu être réalisé sans l'aide préciseuse de nombreuses personnes que je voudrais remercier ici.

En premier lieu, je tiens à remercier chaleureusement mes directeurs de thèse, Éric Thiébaut et Dominique Davoult, pour leur encadrement et leur soutien pendant ces trois années et demie de thèse. Merci beaucoup Éric d'avoir accepté de m'encadrer en thèse, de m'avoir guidée et de m'avoir fait confiance tout au long de ma thèse, de m'avoir soutenue et encouragée dans les moments de doute, et de t'être rendu disponible et attentif malgré ton emploi du temps bien rempli. Merci aussi Éric pour m'avoir initiée aux statistiques, à l'océanographie biologique, et aux campagnes de terrain[c], tout ceci bien avant ma thèse. Merci Dominique de m'avoir accueillie au sein de l'ancienne équipe Écologie Benthique et d'avoir accepté la responsabilité officielle de ma thèse.

Je remercie également les membres de mon jury de thèse, Jean-Marc Guarini, Claire Paris, François Carlotti, Xabier Irigoien et Pierre Petitgas d'avoir accepté d'évaluer ce travail de thèse. J'espère que vous prendrez plaisir à lire ce manuscrit et qu'il suscitera votre intérêt.

Je tiens aussi à remercier toutes celles et ceux dont la collaboration scientifique a participé à la réalisation de ce travail de thèse. Merci tout d'abord à Céline Ellien pour m'avoir permis de réaliser un de mes stages de Master 2 à l'interface de l'océanographie biologique et de la modélisation et pour m'avoir initiée à la modélisation de la dispersion larvaire. C'est grâce à ce stage que cette thèse a pu naître. Merci à Pascal Lazure pour

[c] C'est lors de la campagne PECTOW06 que j'ai rencontré pour la première fois *Pectinaria koreni* et *Owenia fusiformis*, si j'avais su à l'époque que ma thèse porterait en partie sur ces deux espèces !

sa disponibilité, son aide et nos discussions sur l'utilisation du modèle MARS3D. Merci Pascal d'avoir toujours répondu très rapidement à mes questions concernant le modèle et d'avoir porté ton regard de physicien océanographe et modélisateur sur les problèmes auxquels j'ai pu être confrontée. Merci aussi à ceux dont l'aide, à distance, a été précieuse pour le développement et l'utilisation du modèle bio-physique : Valérie Garnier, Franck Dumas, Marina Chifflet, et Martin Huret. Merci à tous ceux qui m'ont aidée au cours des campagnes d'échantillonnage du méroplancton lors des missions DEVIL et LARVASUD, en particuler aux membres d'équipage du navire de recherche *Côtes de la Manche* et à ceux qui ont accepté de participer aux campagnes LARVASUD : Céline, Thierry, Renaud, Kévin, Vincent et Jihane. Un grand merci à Thierry Comtet pour m'avoir initiée à la biologie moléculaire. Merci Thierry pour ta disponibilité, ta rigueur et ton aide. Merci à Robin Stolba, que j'ai en partie encadré au cours de son stage Master 2. Merci Robin pour ton aide dans le tri et le comptage des échantillons planctoniques, merci pour ta collaboration sur l'analyse des données d'abondances larvaires. Merci également à Christophe Lett, Martin Huret et Jean-Olivier Irisson. Merci pour votre collaboration et votre réflexion sur l'impact potentiel des changements climatiques sur la dispersion larvaire. Merci à Stanislas Dubois pour sa disponibilité et son aide sur la biologie de *Sabellaria alveolata*. Merci aussi à François Rigal pour m'avoir sollicitée pour la mise en place d'un modèle analytique du transport larvaire en Baie de Morlaix. Merci François pour ta persévérance, ta curiosité scientique et ton intérêt pour notre travail en collaboration. Merci également à Frédérique Viard pour son enthousiasme sientifique face à mes travaux de thèse et pour son regard acéré et objectif. Un grand merci aussi Fred pour tes corrections et remarques pertinentes sur une première version de l'introduction générale de cette thèse. Merci à Pascal Morin, Grégory Beaugrand, Franck Gentil, Caroline Broudin, et Météo France pour avoir mis à notre disposition un certain nombre de données (données climatiques, du CPR, ou du suivi Rebent). Enfin, merci à Jean-Marc Guarini et Katell Guizien, pour avoir participé pendant trois ans à mes comités de thèse et pour avoir pointé du doigt quelques points plus délicats et pour en avoir discuté ensemble.

Je voudrais aussi remercier le personnel scientifique, technique et administratif de la Sation Biologique de Roscoff pour leur aide et leur disponibilité. Merci en particulier aux

membres des équipes Divco et Retroprod pour l'aide au quotidien et pour leur bonne humeur si appréaciable ! Merci au service bioinformatique de la Station Biologique de Roscoff, et en particulier à Thierry Descombes, Gildas Le Corguillé et Erwan Le Corre, pour leur aide, leur patience et la mise à disposition des ressources informatiques de la SBR. Merci au service Genomer de la Station Biologique de Roscoff et au service laverie pour le séquençage et les manip. de biologie moléculaire. Merci au service d'accueil, et en particulier à Nicole Sanséau, pour avoir facilité mon logement pendant une partie de ma thèse. De manière générale, merci à tout le personnel de la Sation Biologique de Roscoff grâce à qui la station est un environnement de travail formidable.

Enfin, je remercie Michel Volovitch pour m'avoir conseillée dans mon choix de sujet et de laboratoire de thèse : c'est sans doute grâce à ses conseils que je me suis retrouvée en thèse à la Sation Biologique de Roscoff, un cadre de travail riche et motivant et un endroit magnifique et agréable à vivre.

Merci aussi aux enseignants avec qui j'ai travaillé au cours de mon monitorat, que ce soit sur le campus de Jussieu ou à Roscoff. Merci pour l'autonomie que vous m'avez donnée et pour votre bonne humeur.

Je voudrais aussi remercier tous mes amis, collègues, et/ou colocataires qui ont rendu ces trois années et demi de labeur une période agréable et riche en souvenir. Tout d'abord un énorme merci à Joe pour m'avoir soutenu dans les coups durs et pour voir accepté une co-locatrice plutôt absente. Merci aux copains parisiens et lillois pour tous ces bons moments passés ensembles : Vianney, Arvind, Anne-Laure, Laurent, Julie, Axelle, Chewie, Lucie, Fabienne, Vaurien, Bachus, et Akshai.

Merci aux copains roscovites pour avoir rendu mon séjour à Roscoff un si bon souvenir et pour avoir toujours accepté d'aller boire un café ou un verre pour parler vie de thèsard et autre : Marjolaine, Jihane, Gauthier, François R., Vincent, Claire, Laure, Fanny, Robin, Kévin, François T., Thomas S., Manue B., Sabrina, Régis, et Florentine. En particulier, merci Marjo, pour tout ce que tu m'as apporté au cours de ces années, j'espère avoir prochainement l'occasion de te rendre visite au pays des Caribou !

Enfin, un énorme merci aux copains bretons, Clarisse, Nico, Nathalie, Baptiste et Anne, qui, par leur présence, ont participé au bon déroulement de cette thèse, merci pour les bons moments passés ensemble à Rennes, Vannes, Paris, ou Barcelone ! Merci beaucoup Cla pour ton soutien, merci Nico de m'avoir accueillie à plusieurs reprises dans ton camion, et merci à vous deux pour les si bons moments passés en votre companie.

Merci également à Rachida pour sa bonne humeur qu'elle sait si bien partager.

Je tenais aussi à remercier ma famille qui m'a toujours soutenue au cours de mes études. Merci à mes parents, Danielle et Slimane : Maman, Papa, j'espère que vous serez fière de votre fille et que vous continuerez à me soutenir dans mes choix, comme vous avez pu le faire au début de mes études. Un grand merci à mes frères, Samir et Sélim : merci beaucoup Samir pour ton soutien dans les coups durs et merci d'avoir toujours su être présent lorsque j'en ai eu besoin ; merci Sélim pour tes encouragements, j'espère que tu seras fier de ta grande sœur.

Enfin, je voudrais remercier celle dont la présence ces derniers mois a été un rayon de soleil quotidien, à Paris, à Roscoff, ou en Islande ! Merci Laurène pour ta présence, ta patience et ton soutien inconditionnel, merci pour tous ces bons petits plats que nous as préparés tandis que la rédaction de ma thèse m'a éloignée des fourneaux (je m'y remets dès à présent !), merci pour tes relectures attentives et pointilleuses de ce manuscrit, et enfin merci pour tout ce que tu m'apportes.

Document mis en page par LaTeX — 19 janvier 2011

**Résumé**

En assurant la **dispersion**, la **phase larvaire** joue un rôle fondamental dans la dynamique des populations d'invertébrés marins à cycle de vie bentho-pélagique et détermine la **connectivité** au sein des **métapopulations marines**. La connectivité en milieu marin influence ainsi directement la dynamique des métapopulations et la persistance des populations locales, les potentialités d'expansion des espèces en réponse à des changements des conditions environnementales ou les limites biogéographiques d'aire de distribution des espèces. Dans ce contexte, le but du présent travail a été de mieux comprendre les rôles relatifs joués par les **processus hydrodynamiques et hydroclimatiques**, et les **traits d'histoire de vie** des invertébrés sur la dispersion larvaire et la connectivité en milieu côtier dans le Golfe de Gascogne et la Manche occidentale. Pour répondre à cette question, une **approche couplée** a été mise en œuvre, alliant l'**observation *in situ*** et la **modélisation biologie-physique** à deux échelles spatiales : régionale et locale.

Dans le Nord du Golfe de Gascogne, la description de la distribution larvaire de trois espèces côtières de polychètes (*Pectinaria koreni*, *Owenia fusiformis*, et *Sabellaria alveolata*) a mis en évidence le rôle prépondérant de l'organisation spatiale des **structures hydrologiques à méso-échelle** (*i.e.* plumes estuariennes) dans la variabilité de la distribution des abondances larvaires. À l'échelle régionale du Golfe de Gascogne et de la Manche occidentale, la simulation lagrangienne de la dispersion larvaire en conditions hydroclimatiques réalistes a souligné l'importance de la variabilité saisonnière des conditions hydroclimatiques et des traits d'histoire de vie (mois de ponte, durée de vie larvaire, comportement natatoire) dans le transport larvaire et la connectivité entre populations. Ces résultats ont suggéré de possibles échanges larvaires depuis les populations côtières du Golfe de Gascogne vers celles de la Manche occidentale, *i.e.* à travers une **zone de transition biogéographique**. Ils ont aussi permis de tester plusieurs hypothèses sur les conséquences possibles du **changement climatique** sur la dispersion et la connectivité entre populations marines, *i.e. via* une période de ponte précoce et une durée de vie larvaire raccourcie. À l'échelle locale du Golfe Normand-Breton, un modèle eulérien de dispersion a permis d'estimer la connectivité entre les récifs biogéniques construits par une espèce à forte valeur patrimoniale, *Sabellaria alveolata*. Ce modèle a permis de déterminer les influences relatives de la variabilité intra- et inter-annuelle des conditions hydroclimatiques sur la connectivité, dans un contexte de gestion et de **conservation d'un patrimoine naturel**.

**Mot-clés :** Océanographie biologique, écologie, dynamique des populations, métapopulation, connectivité, dispersion larvaire, modélisation couplée biologie-physique.

**Abstract**

By ensuring the **dispersal**, the **larval phase** plays a fundamental role in the population dynamics of benthic invertebrates with a complex life cycle and determines the **connectivity** within **marine metapopulations**. Hence, the connectivity influences directly the dynamics of metapopulations and the persistence of local populations, the expansion abilities of species in response to changes in environmental conditions or biogeographic range limits. In this context, the aim of the present work was to better understand the relative roles played by **hydrodynamics and hydroclimatic processes** and **life history traits** of coastal invertebrates on the larval dispersal and the connectivity in the Bay of Biscay and in the western English Channel. To answer this question, a **coupled approach** was used, joining ***in situ* observation** and **bio-physical modelling** at two spatial scales, a regional one and a local one.

In the northern Bay of Biscay, the description of larval distribution of three coastal species of polychaetes (*Pectinaria koreni*, *Owenia fusiformis*, and *Sabellaria alveolata*) highlighted the major role of the spatial organization of the **mesoscale hydrological structures** (*i.e.*, river plumes) in the variability of larval abundance distributions. At the regional scale of the Bay of Biscay and the western English Channel, the Lagrangian simulation of the larval dispersal under realistic hydroclimatic forcing underlined the importance of the seasonal variability of the hydroclimatic conditions and the life history traits (spawning month, planktonic larval duration, larval swimming behaviour) in the larval transport and connectivity between populations. These results suggested possible larval exchanges from the Bay of Biscay to the western English Channel, *i.e.* through a **biogeographic transition zone**. They allowed to test several hypotheses about the potential consequences of **climate change** on the dispersal and connectivity of marine populations, *i.e.* through an earlier spawning period and a shortened planktonic larval duration. At the local scale of the Gulf of Saint-Malo, western English Channel, an Eulerian dispersal model permitted to estimate the connectivity between the biogenic reefs built by *Sabellaria alveolata*, a species with a high patrimonial value. This model allowed to determine the relative influences of the intra- and inter-annual variability of the hydroclimatic conditions on connectivity, in a context of management and **conservation of natural heritage**.

**Key-words:** Biologic oceanography, ecology, population dynamics, metapopulation, connectivity, larval dispersal, bio-physical modelling.